Integrated Design and Manufacturing in Mechanical Engineering

Edited by
Patrick Chedmail
Gérard Cognet
Clément Fortin
Christian Mascle
Joseph Pegna

Springer-Science+Business Media, B.V.

INTEGRATED DESIGN AND MANUFACTURING IN MECHANICAL ENGINEERING

INTEGRATED DESIGN AND MANUFACTURING IN MECHANICAL ENGINEERING

PROCEEDINGS OF THE THIRD IDMME CONFERENCE HELD IN MONTREAL, CANADA, MAY 2000

Edited by

Patrick Chedmail
Ecole Centrale de Nantes, Nantes, France

Gérard Cognet
Ecole de Genie Industriel de Grenoble, Grenoble, France

Clément Fortin
Ecole Polytechnique de Montréal, Montréal, Canada

Christian Mascle
Ecole Polytechnique de Montréal, Montréal, Canada

and

Joseph Pegna
Ecole Polytechnique de Montréal, Montréal, Canada

Springer-Science+Business Media, B.V.

A C.I.P. Catalogue record for this book is available from the Library of Congress.

ISBN 978-90-481-6157-7 ISBN 978-94-015-9966-5 (eBook)
DOI 10.1007/978-94-015-9966-5

Printed on acid-free paper

All Rights Reserved
© 2002 Springer Science+Business Media Dordrecht
Originally published by Kluwer Academic Publishers in 2002.
Softcover reprint of the hardcover 1st edition 2002

No part of this work may be reproduced, stored in a retrieval system, or transmitted in any form or by any means, electronic, mechanical, photocopying, microfilming, recording or otherwise, without written permission from the Publisher, with the exception of any material supplied specifically for the purpose of being entered and executed on a computer system, for exclusive use by the purchaser of the work.

TABLE OF CONTENTS

Preface xi
Acknowledgements xiii
List of contributors xv

Chapter 1 : DESIGN THEORY : METHODOLOGY 1

Confrontation of viewpoints in a concurrent engineering process 3
G. MARTIN, F. DÉTIENNE, E. LAVIGNE

A concurrent engineering experience based on a Cooperative and Object Oriented Design Methodology 11
S. GOMES, J.C. SAGOT

A Method and a Support for a Better Integration of Mechanical Simulation in the Design Process 19
F. POURROY, N. TROUSSIER, M. TOLLENAERE

Representation of Design Activities Using Neural Networks: Application to Fuzzy Dimensioning 27
F. BENNIS, P. CHEDMAIL, O. HELARY

Quantitative constraints in integrated design 35
X. FISCHER, J.-P. NADEAU, P. SÉBASTIEN, P. JOYOT

Handling imprecision in pairwise comparison 43
F. LIMAYEM, B. YANNOU

Funtional and Manufacturing Specifications - Part 1: Geometrical Expression by Gauge with Internal Mobilities 53
J.-Y. DANTAN, F. THIEBAUT, A. BALLU, P. BOURDET

Funtional and Manufacturing Specifications - Part 2: Validation of a Process Plan 61
J.-Y. DANTAN, F. THIEBAUT, A. BALLU, P. BOURDET

Robust design and statistical tolerances analysis 69
F. BENNIS

Development and Feedbacks of a New Communication Tool to Harness

Information and Knowledge and Know-How in Integrated Engineering - Case Study at EADS 77
M. GARDONI, M. SPADONI, F. VERNADAT

A knowledge-based environment for modelling and computer-aided process planning of rapid manufacturing processes 85
A. DEGLIN, A. BERNARD

Evaluation of Decisions Considering the Choice of Actors in Product Design Processes 93
J. STAL-LE CARDINAL, M. MEKHILEF, J.-C. BOCQUET

Chapter 2 : DESIGN THEORY : MODELS 103

A Declarative Approach to a 2D Variational Modeler 105
D. LESAGE, J.-C. LÉON, P. SERRÉ

Copying of Free-Forms from Digitized Data 113
A. CONTRI, C. LARTIGUE, G. OSTY

Flexible Parts Modelling for Virtual Reality Assembly Simulations 121
J.-C. LÉON, U. GANDIAGA

A rectification algorithm for manifold Boundary representation models 129
G. SHEN, T. SAKKALIS, N. M. PATRIKALAKIS

Information Support in an Integrated Product Development System 139
R.I.M. YOUNG, O. CANCIGLIERI JNR., C.A. COSTA, J.M. DORADOR, J. ZHAO, W.M. CHEUNG

A methodology for modeling process information 147
R. BACHA, B. YANNOU

A Set of New Tools for the Automatic Meshing and Remeshing of Mechanical Parts 157
J.-C. CUILLIÈRE, V. FRANÇOIS

A Control Criterion Dedicated to Detail Removal for F.E.A. Geometry Adaptation 165
L. FINE, L. RÉMONDINI, J.-C. LÉON

Feature Recognition and Remeshing by Local Hermite Diffuse Interpolation.. 173
A. RASSINEUX, P. VILLON, P. BREITKOPF, J.-M. SAVIGNAT, O. STAB, C. CHAPPUIS

Chapter 3 : CONTROL, MEASUREMENT AND TOLERANCING 181

Tight fit design taking into account form and surface defects 183
J.F. FONTAINE, G.M. YANG, J.C. COQUILLE, M. LAMBERTIN

Calculation of virtual and resultant part for variational assembly analysis........ 193
L. PINO, F. BENNIS, C. FORTIN

3D quantification of machining defects 201
F. VILLENEUVE, O. LEGOFF, F. GEISKOPF

Formal Definition of Tolerancing in CAD and Metrology 211
P. SERRÉ, A. CLÉMENT, A. RIVIÈRE

Quality Measurement on CMM 219
J.M. LINARES, P. BOURDET, J.M. SPRAUEL

Toward the Use of Statistical Analysis in Positional Tolerancing.................... 227
F. BENNIS, P. CASTAGLIOLA, L. PINO

Chapter 4 : MANUFACTURING AND MODELLING 235

Prediction and Simulation of Milling Burr Formation for Edge-Precision Process Planning 237
C.H. CHU, D. DORNFELD, C. BRENNUM

Optimal workpiece localization for machining applications 247
J.-F. CHATELAIN, C. FORTIN

Analysis and Mapping of the Dynamic Performance of High-Precision Motion Systems 255
E.V. BORDATCHEV

Integration of Laser Material Processing into the Computer-Aided Product and Process Development 263
M. GEIGER, A. KACH

Investigation of Sheet Metal Blanking Process 271
M. RACHIK, J.M. ROELANDT, A. MAILLARD

The Concept of the Machining Surface in 5-Axis Milling of Free-Form Surfaces 279
C. TOURNIER, E. DUC, C. LARTIGUE, A. CONTR

High Speed Milling - Solid Simulation and Machine Limits 287
A. DUGAS, J.-J. LEE, J.-Y. HASCOËT

Design of Process Parameters in Deep Drawing of Sheets to Improve Manufacturing Feasibility 295
J.-L. BATOZ, H. NACEUR, A. DELAMÉZIERE, Y.Q. GUO, C. KNOPF-LENOIR

From the Predimensioning Approach to the Optimisation of Forming Processes
of Thin Fabric Composite Parts 303
J.L. BILLOET, H. BOROUCHAKI, A. CHEROUAT

Chapter 5 : MANUFACTURING AND PROCESS PLANNING 311

Design Process Modelling of Process Planning for Flexible Lines Based on Conceptual Graphs and Design Rules - Applied to Cylinder Head Machining. 313
A. LEFEBVRE, L. SABOURIN, G. GOGU, J. RENAUD

Determination of virtual means for the integrated design 323
K. MAWUSSI, V.-H. DUONG, R. PONSONNET

Selecting material handling equipment with PROMETHEE 331
P. DE LIT, T. L'ÉGLISE, J. DANLOY, B. REKIEK, A. DELCHAMBRE

A Methodology for Cost and Quality Optimization in a Design System by Linking Quality Methods 339
G. DRAGOI, D. BRISSAUD

Disassembly Sequencing Using Technological Data 347
N. REJNERI, J.-C. LÉON, G. DEBARBOUILLÉ

Application of fuzzy logic for an assembly methodology 355

A. SINZINKAYO, C. MASCLE, M. BALAZINSKI

Chapter 6 : OPTIMAL DESIGN OF MACHINES, STRUCTURES AND COMPONENTS 363

Design of Closed Planar Mechanisms of Grippers to Clutch Flat Parts 365
L. SLUTSKI

Interaction of Gear Epicyclic Planets and the Effect of Web for Internal Gears 373
J.-P. DE VAUJANY, M. GUINGAND, D. PLAY

Kinematics of Robots with Roller-Constrained Ball-Wheels 381
S. OSTROVSKAYA, J. ANGELES

Structural Synthesis of Kinematic Chains and Mechanisms 391
L. NOTASH, J. ZHANG

General Manipulators synthesis for a given workspace 399
S. GUERRY, F.B. OUEZDOU, S. RÉGNIER

Object Manipulation and Mannequin Driving Based on Multi-Agent Architecture 407
P. CHEDMAIL, C. LE ROY, B. MAILLÉ

Isotropic design of a parallel machine-tool mechanism 415
D. CHABLAT, P. WENGER, J. ANGELES

Application of the Design of Experiments Method to a Transversely Loaded Cylindrical Assembly 423
A. DAIDIÉ, H. LAKISS, D. LERAY, J. GUILLOT

Determination of the Mode Dominance for Model Reduction 431
K. LIU, X. SUN

Development of a New Methodology for Delamination Detection in Laminated Structures 439
J.C. WALRICK, D. COUTELLIER, P. GEOFFROY

Search of Contact in Dynamic Finite Element Code: Presentation of an Analytical Method 447

E. ARNOULT, B. PESEUX, J. BONINI

Recent Progress in Preliminary Design of Mechanical Components with Topology Optimisation 457
P. DUYSINX, M. BRUYNEEL

Finding the Optimal Stock Spring from Optimal Spring Design Characteristics 465
M. PAREDES, M. SARTOR, C. MASCLET

Design Process and Optimisation of an Integrated Electromechanical Battery. 473
C. KERZREHO, J.-Y. COGNARD

A Hybrid Calculation Model for Bolted Assemblies Used for Slewing Bearings 481
A. VADEAN, D. LERAY, H. LAKISS, J. GUILLOT

PREFACE

The integration of manufacturing constraints and their optimization within the design process of mechanical products and systems are now an industrial priority. Following the first two IDMME conferences in Nantes in 1996 and Compiègne in 1998, the purpose of the IDMME'2000 conference was to present recent developments in these areas and new areas within the product and process development theme.

The original initiative of the conference is mainly due to the efforts of the French AIP-PRIMECA group (Pool of Computer Resources for Mechanics). The organizing committee and the local organizing institutions (Concordia University, Ecole Polytechnique de Montreal, and McGill University) contributed to the success of the conference.

The presentation of 190 papers and the presence of more than 225 researchers coming from more than 20 countries demonstrate the success of the initiative.

This book contains 57 of these papers selected by an International Scientific Committee :

Chairman: C. Fortin (Canada)
Co-chairmen: P. Chedmail (France), G. Cognet (France),
C. Mascle (Canada), J. Pegna (Canada)

J. Angelès (Canada)
J.L. Batoz (France)
J.C. Bocquet (France)
A.- Bernard (France)
P. Bourdet (France)
A. Clément (France)
D. Cochran (USA)
D.Coutellier (France)
A.- Dalsky (Russia)
D.A. Dornfeld (USA)
D. Deneux (France)
G. Gogu (France)
C. Gosselin (Canada)
J. Guillot (France)
H. Hagen H. (Germany)
H.I.J. Kals (The Netherlands)
F. Kimura (Japan)
T. Kjellberg (Sweden)
F.L. Krause (Germany)
F. Le Maître (France)

P. Martin (France)
C. McMahon (U.K.)
M. Mantylä (Finland)
J.L. Maxwell (USA)
N.M. Patrikalakis (USA)
J.P. Pelle (France)
B. Peseux (France)
D. Play (France)
M. Pratt (USA)
B. Ravani (USA)
A. Rivière (France)
C. Rouchon (France)
R. Soenen (France)
S.H. Suh (Korea)
S. Tichkiewitch (France)
M. Tollenaere (France)
H. Van Brussel (Belgium)
A.F. Van Houten (Netherland)
M. Véron (France)

The above specialists cover a large spectrum in computer science applied to analysis, design and manufacturing in mechanical engineering problems.

The integration of manufacturing constraints and their optimization in the design process is becoming more and more widespread in the development of mechanical products or systems. There is a clear industrial need for these kinds of methodologies. Important - but still unsolved - problems are related to the definition of design processes, the choice of optimal manufacturing processes and their integration through coherent methodologies in adapted environments.

Four main topics are addressed in this book :

- design theory : process and modeling,
- control, measurement and tolerancing,
- manufacturing : modeling and planning,
- optimal design of machines, structures and components.

By the end, apart from giving a thorough theoretical background, a very important theme is the relation between research and industrial applications.

The editors hope that they contributed to the development of the challenging research domain of Integrated Design and Manufacturing in Mechanical Engineering. We hope that this book will be of interest for engineers, researchers and Ph.D. students who are involved in the optimization of design and manufacturing processes. It will be a mine of examples and ideas, and we wish that it will contribute to the improvement and the development of concurrent engineering.

The editors
Patrick Chedmail, Gérard Cognet, Clément Fortin, Christian Mascle and Joseph Pegna

ACKNOWLEDGEMENTS

The Third IDMME Conference held in Montreal in may 2000. It received the scientific support of the AFM-AUM (French Association for Mechanics), the ASME (American Society for Mechanical Engineering), the CCToMM (Canadian Committee for the Theory of Machines and Mechanisms), the CNRS agency (French National Agency for Scientific Research), the CIRP (International Institution for Production Engineering Research) the CSME forum committee (Canadian Society for Mechanical Engineering), the IFToMM (International federation for the Theory of Machines and Mechanisms), the MESR (French Ministry of Higher Education and Research).

We are grateful to the members of the organizing committee and the local organizing institutions (Ecole Polytechnique de Montreal, Centre Prototech, Concordia University and McGill University) who contributed to a successful conference.

We particularly thank the French AIP-PRIMECA group (the former PRIMECA group, *i.e.* French Pool of Computer Resources for Mechanics) for his constant support and the MESR which provided the financial support for the edition of this selected papers book.

We thank the members of the scientific committee for their helpful participation.

LIST OF CONTRIBUTORS

Angeles 381, 415
Arnoult 447
Bacha 147
Balazinski 355
Ballu 53, 61
Batoz 295
Bennis 27, 69, 193, 227
Bernard 85
Billoet 303
Bocquet 93
Bonini 447
Bordatchev 255
Borouchaki 303
Bourdet 53, 61, 219
Breitkopf 173
Brennum 237
Brissaud 339
Bruyneel 457
Canciglieri Jnr. 139
Castagliola 227
Chablat 415
Chappuis 173
Chatelain 247
Chedmail 27, 407
Cherouat 303
Cheung 139
Chu 237
Clément 211
Cognard 473
Contri 113, 279
Coquille 183
Costa 139
Coutellier 439
Cuillière 157
Daidié 423
Danloy 331
Dantan 53, 61
De Lit 331
De Vaujany 373
Debarbouillé 347
Deglin 85
Delaméziere 295
Delchambre 331
Détienne 3
Dorador 139
Dornfeld 237
Dragoi 339
Duc 279
Dugas 287
Duong 323
Duysinx 457
Fine 165
Fischer 35
Fontaine 183
Fortin 193, 247
François 157
Gandiaga 121
Gardoni 77
Geiger 263
Geiskopf 201
Geoffroy 439
Gogu 313
Gomes 11
Guerry 399
Guillot 423, 481
Guingand 373
Guo 295
Hascoët 287
Helary 27
Joyot 35
Kach 263
Kerzreho 473
Knopf-Lenoir 295
Lakiss 423, 481
Lambertin 183
Lartigue 113, 279
Lavigne 3
Le Roy 407
Lee 287
Lefebvre 313
L'Église 331
Legoff 201
Léon 105, 121, 165, 347
Leray 423, 481
Lesage 93
Limayem 43
Linares 219
Liu 431
Maillard 271
Maillé 407
Martin 3
Mascle 355
Masclet 465
Mawussi 323
Mekhilef 93
Naceur 295
Nadeau 35
Notash 391
Ostrovskaya 381
Osty 113
Ouezdou 399
Paredes 465
Patrikalakis 129
Peseux 447
Pino 193, 227
Play 373
Ponsonnet 323
Pourroy 19
Rachik 271
Rassineux 173
Régnier 399
Rejneri 347
Rekiek 331
Rémondini 165
Renaud 313
Rivière 211
Roelandt 271
Sabourin 313
Sagot 11
Sakkalis 129
Sartor 465
Savignat 173
Sébastien 35
Serré 105, 211
Shen 129
Sinzinkayo 355
Slutski 365
Spadoni 77
Sprauel 219
Stab 173
Stal-Le Cardinal 93
Sun 431
Thiebaut 53, 61
Tollenaere 19
Tournier 279
Troussier 19
Vadean 481
Vernadat 77
Villeneuve 201
Villon 173
Walrick 439
Wenger 415
Yang 83
Yannou 43, 147
Young 139
Zhang 391
Zhao 139

Chapter 1
DESIGN THEORY : METHODOLOGY

Confrontation of viewpoints in a concurrent engineering process..................... 3
G. MARTIN, F. DÉTIENNE, E. LAVIGNE

A concurrent engineering experience based on a Cooperative and Object Oriented Design Methodology 11
S. GOMES, J.C. SAGOT

A Method and a Support for a Better Integration of Mechanical Simulation in the Design Process 19
F. POURROY, N. TROUSSIER, M. TOLLENAERE

Representation of Design Activities Using Neural Networks: Application to Fuzzy Dimensioning.. 27
F. BENNIS, P. CHEDMAIL, O. HELARY

Quantitative constraints in integrated design.. 35
X. FISCHER, J.-P. NADEAU, P. SÉBASTIEN, P. JOYOT

Handling imprecision in pairwise comparison 43
F. LIMAYEM, B. YANNOU

Funtional and Manufacturing Specifications - Part 1: Geometrical Expression by Gauge with Internal Mobilities.. 53
J.-Y. DANTAN, F. THIEBAUT, A. BALLU, P. BOURDET

Funtional and Manufacturing Specifications - Part 2: Validation of a Process Plan 61
J.-Y. DANTAN, F. THIEBAUT, A. BALLU, P. BOURDET

Robust design and statistical tolerances analysis.. 69

F. BENNIS

Development and Feedbacks of a New Communication Tool to Harness Information and Knowledge and Know-How in Integrated Engineering – Case Study at EADS 77
M. GARDONI, M. SPADONI, F. VERNADAT

A knowledge-based environment for modelling and computer-aided process planning of rapid manufacturing processes 85
A. DEGLIN, A. BERNARD

Evaluation of Decisions Considering the Choice of Actors in Product Design Processes 93
J. STAL-LE CARDINAL, M. MEKHILEF, J.-C. BOCQUET

GÉRALDINE MARTIN, FRANÇOISE DÉTIENNE, ELISABETH LAVIGNE

CONFRONTATION OF VIEWPOINTS IN A CONCURRENT ENGINEERING PROCESS

Abstract. We present an empirical study aimed at analysing the use of viewpoints in an industrial Concurrent Engineering context. Our focus is on the viewpoints expressed in the argumentative process taking place in evaluation meetings. Our results show that arguments enabling a viewpoint or proposal to be defended are often characterized by the use of constraints. One result involved the way in which the proposals for solutions are assessed during these meetings. We have revealed the existence of specific assessment modes in these meetings as well as their combination. Then, we show that, even if some constraints are apparently identically used by the different specialists involved in meetings, various meanings and weightings are associated with these constraints by these different specialists.

1. PURPOSE

In new design and production organizations, design is often the work of a multi-speciality, multi-location team, manoeuvring, according to the moment, with the same aim (co-design) or different aims (distributed design). In the collective design process, co-design phases are specifically devoted to the assessment of the global solution, integrating the solutions produced by the different designers at time t, or to the assessment, by his/her peers, of a solution produced by one designer at time t.

A first study was focused on the coordination processes in distributed design (Martin, Détienne & Lavigne, 1999). The aim of the study presented in this paper is to analyse the viewpoints brought into play in co-design. The chosen design context is a Concurrent Engineering process. This framework seemed to us to be the most relevant for studying the topic of " viewpoint ", as the simultaneousness and confrontation of viewpoints during the development of the solution are assumed to be favoured by working in Concurrent Engineering (Darses, 1997).

Aerospatiale Matra Airbus has conducted the re-engineering of its design processes in a Concurrent Engineering procedure, in order to better master costs, schedules and quality in the design of its products. This industrial development is assisted by cognitive ergonomics research work, which is the framework of this study. We are analysing this setting up of a Concurrent Engineering methodology. The industrial aim is to derive ergonomic recommendations at software level (digital mock-up, technical database) and organizational level (meeting methodology, definition of roles) in order to assist the confrontation and integration of viewpoints in multi-speciality design.

After a brief presentation of our theoretical framework and working hypotheses, we present an empirical study aimed at analysing the use of viewpoints in an

P. Chedmail et al. (eds.), Integrated Design and Manufacturing in Mechanical Engineering, 3-10.
Copyright © 2002 by Airbus France SAS published by Kluwer, with permission.

industrial Concurrent Engineering context. Our approach is strongly oriented by cognitive ergonomics work on the notion of constraint, and linguistics work on argumentation.

2. THEORETICAL FRAMEWORK AND WORKING HYPOTHESES

The confrontation of knowledge and the integration of viewpoints is at the heart of the cooperative mechanisms implemented in co-design. A new research topic is to characterize the viewpoints of the various players involved in collective design (designers themselves, and production and maintenance specialities) and the cooperative modes that enable these different viewpoints to be integrated.

During the design process, different viewpoints are implemented. On the basis of the work performed in different disciplines - Artificial Intelligence (Wenger, 1987), cognitive ergonomics (Rasmussen, 1979; Darses, 1997), ethnomethodology (Bucciarelli, 1998), Computer- Supported- Cooperative Work (Schmidt, 1994), an initial general definition of the notion of "viewpoint" would be : " for a person, a particular, personal, representation of an object to be designed". We are now going to develop this definition further.

In the representation of the object to be designed, and also of its design, design constraints seem to us to play a predominant part. For design problems, the solutions are not unique and correct but various, and more or less satisfactory according to the constraints that are considered. The designers develop and assess design solutions partly according to their own specific constraints, which reflect their own specific viewpoints, in relation with the specificity of the tasks they perform and their personal preferences (Eastman,1969; Falzon et al,1990).

Constraints are cognitive invariants which intervene during the design process. The notion of constraints has been understood from different angles (1) according to their origin - prescribed constraints, constructed constraints, deduced constraints, (2) according to their level of abstraction, and (3) according to their importance – validity constraints and preference constraints (Bonnardel,1999, Eastman, 1969). Futhermore, Bonnardel distinguishes various relationships between constraints.

The use of particular combination of constraints, characterizing a viewpoint, will also determine the level of abstraction at which the design object is represented. The representation of the object to be designed is characterized according to an abstract-concrete line or abstraction hierarchy (Rasmussen,1979). The different levels of abstraction are integrated into each state of the solution. This can reflect functional, structural or physical representations all along the design process (Darses,1997; Darses & Sauvagnac, 1997). Factors such as the field of expertise and specific technical interest play a role in this representation. Indeed, several participants see the design object differently according to the specificities and constraints specific to their speciality. In addition, for the same speciality, the representation will be variable according to the problem to be solved.

So, our approach is based on the following assumption: a viewpoint is (1) specific to each speciality ; (2) dependent on the problem to be solved ; 3) characterized by a level of abstraction, i.e., functional, structural or physical, (4) characterized by the implementation of a certain combination of constraints.

Our working hypothesis is that viewpoints are expressed, more or less explicitly, in multi-speciality meetings, aimed at co-design, in particular, the assessment of solutions. It is thus on the analysis of these meetings that we have focussed our empirical work.

In design activities, the assessment intervenes (1) to appreciate the suitability of partial solutions to the usual state of resolution of the problem, and (2) to select one of the solutions envisaged (Bonnardel,1999). The finality of this assessment is to make the decision to change one of its components, or to pursue the design if the assessment is positive (Darses, 1994). It is in assessment meetings that we should observe the confrontation of the viewpoints of the various participants in design. Owing to the collective nature of the activity, viewpoints should be expressed, more or less explicitly, through argumentation (Plantin, 1996). In the argumentative dialogue, a proposer will express a viewpoint that will be argued about by presenting a certain amount of information substantiating the initial proposal.

3. METHODOLOGY

3.1 Context

We conducted this study during the definition phase of an aeronautical design project, lasting three years, in which the participants work in Concurrent Engineering to design the centre section of an aircraft. These participants use Computer Assisted Design (CAD) tools and a technical Data Management System (PDM). About 400 people with 10 different specialities are involved. These specialities are the traditional design office specialities (structure, system installation, stressing), specialities that used to intervene further downstream (maintainability, production) and new specialities that have appeared with the introduction of CAD and PDM tools..

3.2 Collection of data

All the specialities work on the same part of the aircraft but each person according to his technical competence. “Informal” inter-speciality meetings are organized, as needed, to assess the integration of the solutions of each speciality into a global solution. We took part in 7 of these meetings as observers:

- Five meetings involved upstream design office players (designers from structure and systems installation specialits);
- Two meetings involved upstream-design office and dowstream players (from production or maintenance specialities).

On the basis of audio recordings and notes taken during the meeting, we retranscribed the full content of the meetings. Each meeting involved 3 to 6 players.

We conducted interviews afterwards with the various participants of meetings to validate the coding we had made and make explicit a certain amount of information that was implicit in the meetings.

Our second concern was to identify what representation each specialist had about constraints: in particular the representation of the meaning assigned to a constraint expressed a certain way and the ordering between constraints. For each meeting, we collected the constraints used (either explicitly or implicitly) and presented the list to each participant of this meeting. Our question concerned:

- for each constraint: to give their meaning;
- for all constraints: to order them as a function of their importance in this design-problem-situation.

3.3 Coding scheme

The protocols resulting from the retranscriptions were broken down according to the change of locuters. Each individual participant statements correspond to a "turn". Each turn was coded according to the following coding scheme and broken down again as required to code finer units. Our coding scheme comprises two levels, a functional level and an argumentative level.

- The functional level highlights the way in which collective design is performed. Each unit is coded by a mode (request/assertion), an action (e.g., assess) and an object (e.g., solution n). At this level, a turn can be broken down into finer units according to whether there is a change in mode, activity or object.
- The argumentative level brings out the structure of the speech on the basis of a dialogue situation. We coded the proposals for solutions made and the different types of arguments used by the speakers during the meetings.

4 RESULTS

Our results concerns the assessment modes, their temporal organization and the involvement of constraints in the viewpoints expressed through the argumentation process.

4.1 Assessment modes and temporal organization

On the basis of the coding of arguments, we have revealed the existence of analytical, comparative or analogical assessment modes in these meetings. This type of result is similar to the assessment modes analysed in individual design (Bonnardel, 1999). In addition, we have highlighted combined assessment modes, e.g. analytical/analogical.

We found that different assessment modes are used in the order shown in Figure1, whatever the meeting:

- Step1: Analytical assessment mode of the current solution;
- Step 2: if step 1 has not led to a consensus, comparative or/and analogical assessment is involved;

- Step 3: if step 2 has not led to a consensus, one (or several) argument(s) of authority is (are) used.

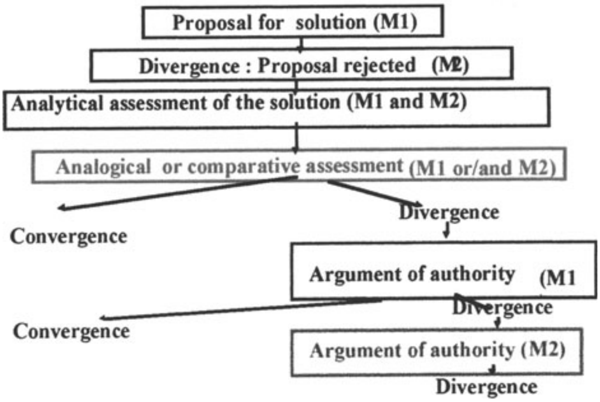
Proposal for solution (M1)
Divergence : Proposal rejected (M2)
Analytical assessment of the solution (M1 and M2)
Analogical or comparative assessment (M1 or/and M2)
Convergence
Divergence
Argument of authority (M1
Convergence
Divergence
Argument of authority (M2)
Divergence

Figure 1. The argumentation process

Firstly the current solution is assessed. This is made using an analytical assessment mode. Arguments used by the two (or more) specialities may use more or less explicit design constraints. Specialists M1 use arguments to convince specialists M2 and M2 does the same thing. Based on this analytical assessment, a consensus is rarely found.

If no consensus has been found, then M1 and M2 use either an analogical assessment mode or a comparative assessment mode of the solution or both. The two types of assessment may also be combined. This can lead again to a consensus toward the initial solution or toward a proposed alternative solution.

Arguments used are arguments by comparison and arguments by analogy. An argument by comparison compares several objects in order to assess them. This is typically the case in the comparative assessment mode. The current solution is compared to one or several alternative solutions in function of the way they meet constraints.

An argument by analogy makes use of a precedent which is a typical case used as a model for the current case. This is typically the case in the analogical assessment mode. The current solution is compared to an analogous solution developed and already assessed in the past, either in the same project or in another project. By referring to a model of analogous reasoning the current solution is considered to be the target and the analogous solution is considered to be the source.

If no consensus has been found, either M1 or M2 propose one or several arguments of authority. Any argument can take the status of argument of authority depending on specific factors of the situation. This argument is presented as inconstestable and therefore it has a particularly strong weight in the negotiation process. We have found that an argument can take the status of argument of authority depending on :

- the status, recognised in the organisation, of the speciality that expresses it.
- the expertise of the proposer. The argument is going to make reference to a person recognized by all to be an expert in the speciality. It will be something like " It's Alphonse who said it would be more logical like that to pick up on these parts of the stringers".
- the "shared" nature of the knowledge to which it refers.

This generally leads to a consensus.

4.2 Contraints involved in the argumentation processs

Constraints used in the argumentation process to express viewpoints are of two kinds:

- Prescribed constraints independent of the speciality or skill-independent constraints: those constraints are prescribed in the design specification and, *a priori*, shared by all the players of the design process;
- Derived constraints specific to a speciality or skill-dependent constraints.

We found that, even though some constraints used by different players in a meeting are the same at a surface level (same terminology), these constraints may have different meanings in the viewpoints expressed by players from different specialities. Also, the level of refinement selected may be different according to the speciality.

Selection of a meaning for a skill-independent constraint

We observed that the same constraint (the same terms are used by different players in a meeting) can have different meanings according to the speaker's speciality.

In this case it is necessary to distinguish the two slopes of the sign, the signifier and the meaning. The meaning can have the same generic seme for different speakers but a very different functional seme. For example, a cost constraint can, for one speciality, mean "production cost" and, for another speciality, mean "design cost". It seems particularly true for general constraints prescribed for all the players of the design process (e.g., the cost) as opposed to constraints derived by a speciality (e.g., structure).

Selection of a refinement level in a hierarchical network of a skill-dependent constraint

We found that some constraints expressed in the argumentation process may be organized hierarchically along different levels of refinement. For example, a maintenance constraint may be refined as three constraints: accessibility constraint, dismounting constraint and mounting constraint. However, when we analysed the skill-dependent constraints used for expressing the viewpoints of different players, we identified some gaps between the level of refinement selected and used in the argumentation process according to the speaker's speciality. For a constraint specific to a skill, the level of refinement is more detailed for the speciality which represents this skill and more general for the other speciality.

Constraints weighting

Constraints used and their weighting, which also founds the viewpoint of the participants, depend on several factors.

- The participant's speciality;
- The interlocutors;
- The design-problem situation.

The selection of constraints depends on speaker speciality and on the interlocutors. In general, constraints taken into account in a particular meeting are those constraints specific to the specialities involved in the meeting in addition to the prescribed constraints. However skill-dependent-constraint weighting depends on speaker speciality. Whereas we found a high intra-speciality agreement on constraint weighting, we found disagreement between specialities.

For exemple, in a meeting involving Hydraulic system intallation specialists and Structure specialists, we observed that the constraints which are specific to Hydraulic system intallation specialists are : system installation and frontier. The constraints which are specific to Structure specialists are : structure and stress. Even if most of these constraints are used by the two specialities involved in the meeting, the way each speciality orders those constraints by importance is different. Each specialist ranks his/her own constraints as more important than the constraints of his/her interlocutors.

Constraints weighting also depends on the problem in hand. For example, we observed for the same speciality, air system installation, that constraint weighting varied between two problems processed sequentially in a meeting : the maintainability constraint was ranked as being of average importance for problem A and as being of high importance for problem B. Furthermore the production constraint was evoked only for problem A.

5 DISCUSSION AND IMPLICATIONS

This paper presents an initial empirical study of viewpoints expressed through the argumentation process in design. Our results have two kinds of implication.

We have shown that the argumentation process involves knowledge on the current solution, i.e., the solution to be assessed, but also on other solutions, i.e., alternative solutions or source solutions. This is involved in comparative assessment modes and analogical assessment modes. This result highlights the importance of documenting the design rationale for the current solutions but also those for the other solutions evoked.

We have also shown that viewpoints involve constraints which may be skill-independent or skill-dependent. The meaning and weighting of these constraints greatly depends on the multi-speciality context. This result should also be taken into account so as to better support and document the decision process in design.

6 REFERENCES

Bonnardel, N. (1999) L'évaluation réflexive dans la dynamique de l'activité du concepteur. In J. Perrin (Ed) : *pilotage et évaluation des processus de conception*. L'Harmattan.

Bucciarelli, L.L (1988) An ethnographic perspective on engineering design. *Design studies, 9* (3), 159-168.

Darses, F. (1994) *Gestion des contraintes dans la résolution de problèmes de Conception*. PhD Dissertation, University Paris 8, France.

Darses, F. (1997) L'ingénierie concourante : Un modèle en meilleure adéquation avec les processus cognitifs de Conception. In P. Bossard, C.Chanchevrier & P.Leclair (Eds) *: Ingénierie concourante de la technique au social.* Economica. Paris.

Darses, F., & Sauvagnac, C. (1997) Représentations cognitives de l'objet à concevoir : construction collective dans une situation de Conception continue. *Proceedings of 01 Design 97*, Théoule-sur-mer, 24-26 septembre. Europia: Paris.

Eastman, C. M. (1969) Cognitive processes and ill-defined problems: a case study from design. In D.E. Walker & L. M. Norton (Eds*): Proceedings of the First Joint International Conference on Artificial Intelligence*. Bedford, MA: MITRE

Falzon, P., Bisseret, A., Bonnardel, N., Darses, F., Détienne, F., & Visser, W. (1990) Les activités de conception: l'approche de l'ergonomie cognitive. *Actes du Colloque Recherches sur le design. Incitations, implications, interactions*, Compiègne, 17-19 octobre 1990.

Martin, G. , Détienne F. & Lavigne E. (1999) Le processus de conception en ingénierie concourante : une étude ergonomique. *Proceedings of MICAD 99*, Edition Hermes Science, p 215-222.

Plantin, C. (1996) *L'argumentation*. Seuil.

Rasmussen, J. (1979) *On the structure of knowledge" a morphology of mental models in a Man-Machine System context.* Technical report Riso-m-2192, Riso national laboratory, DK-4000 Roskilde, Denmark.

Schmidt, K. (1994) *Modes and Mechanisms of interaction in Cooperative Work : outline of a conceptual framework* . Technical report Riso National Laboratory, DK-4000 Roskilde, Denmark.

Wenger, E. (1987) *Artificial intelligence and tutoring systems: computational and cognitive approaches to the communication of knowledge*. Morgan Kaufman Publishers. Californy, US.

7 AFFILIATIONS

Françoise Détienne and Géraldine Martin,
EIFFEL Research Group "cognition and cooperation in design", INRIA
Domaine de Voluceau, Rocquencourt, BP 105, 78153 Le Chesnay, France.
Géraldine Martin and Elysabeth Lavigne
EADS AIRBUS-SA BTE/SM/GDT-CAO M0101/9 316 route de bayonne31060
Toulouse cedex 03, France.

S. GOMES, J-C. SAGOT

A CONCURRENT ENGINEERING EXPERIMENT BASED ON A CO-OPERATIVE AND OBJECT ORIENTED DESIGN METHODOLOGY

Abstract : Designing a new product progresses from needs and function specifications to a detailed description of its physical components. The design activity involves many contributors throughout the life cycle of the product, which starts with its specification and ends with its destruction. This paper presents an object oriented design methodology integrated into a human based and co-operative design life cycle. In order to apply this methodology to industrial design projects, we defined two software environments using human motor activity modelling and simulation linked to a Computer Supported Collaborative Workshop in Design (CSCW). This methodology and the software tools are now applied to student design projects in the field of concurrent engineering.

1. INTRODUCTION

Concurrent engineering methods and tools are increasingly being integrated into industrial organisations to reduce costs and design time, but also to improve product quality and value. These new organisations tend to introduce, very early in their design projects, various dimensions such as the technical, human, organisational, social, and economic points of view [1] [2]. Our research in this field has focused on integrating human factors, based on input from product users, manufacturing operators, etc., into the concurrent engineering design process [3]. Particular attention was paid to product and process usability, but also to co-operation between all those involved in the concurrent design process. This paper firstly reviews a human based co-operative design process representing our own experience of integrating human factors into concurrent engineering design projects before going on to present an operational methodology based on object oriented concepts and distributed design theory. Section 4 presents ACSP, a Computer Supported Co-operative Workshop in Design (CSCW) environment developed to apply this methodology to industrial projects. Section 5 will present some project results extracted from ACSP design activity analyser module. Our results show how this design methodology and the software tools can be applied to real industrial projects. Finally, section 6 concludes the paper with a brief summary of the main points and looks at what could lie ahead for research in this field.

2. HUMAN BASED AND CO-OPERATIVE DESIGN LIFE CYCLE

Working on various design projects associating product, process and activity aspects, we have tested a pragmatic human based design methodology integrated

P. Chedmail et al. (eds.), Integrated Design and Manufacturing in Mechanical Engineering, 11-18.
©2002 *Kluwer Academic Publishers.*

into the concurrent engineering design life cycle [4] [5]. This design life cycle includes the traditional phases of a design project such as the feasibility study, and preliminary and detailed studies [6] [7]. Each phase interacts with the others through feedback loops in order tevaluate, validate and optimise the results obtained.

The particularity of this design life cycle is that it is centred on co-operation between all the design contributors involved in industrial projects (marketing, design, ergonomics, engineering, manufacturing, users, operators, etc.). According to Sagot [8], this co-operation can be difficult to manage in current design projects because of differences in culture, language, knowledge, methods and tools specific to each profession. With this in mind, we set out to develop new methods and tools including new mediating objects [9] [10] in order to promote the above-mentioned human based and co-operative design life cycle. These new mediating objects, which describe the global Human-Product-Environment interaction in different real-life situations (use, manufacturing, recycling, etc,), have been defined to complete traditional technical data such as CAD files, technical sheets and specifications describing the properties of products These co-operation supports include video recorded data extracted from user activities on current products and processes, virtual animated pictures presenting predicted usability of the future product in various future uses, manufacturing, recycling and other situations.

3. OBJECT ORIENTED DESIGN METHODOLOGY

Modelling and simulation of complex systems before their actual design has proven to be a valuable approach in mechanical system engineering. Modelling produces an abstract representation of the system being studied which is then used as a basis for simulation. Such representation requires a modelling approach to describe the functional, structural and dynamic aspects of the system. Various other complementary aspects are also considered in design projects, such as the physical or geometrical aspects [11] [6].

The model we proposed in this paper is based on the “design worlds” method developed by SOLHENIUS [12], which is divided into "domains" that we refer to as "design domains" divided into "aspects". This model is also based on recent design approaches such as distributed design methodology, mechanical systems engineering, and object oriented concepts as applied in computer science [13]. Situated in a connectionist paradigm, distributed design methodology can be described as a modular approach, where modules are connected in a network and where communication plays a major role, allowing the solution to emerge [14] [15]. Each module seeks to achieve its own local objective and needs its own tools. It is also necessary to exchange information between the different modules (interactions) in order to reach the solution. Practical experience in modelling has taught us that complex systems can be modelled and analysed provided we adhere to certain sound principles such as modularity and abstraction [16]. Object-oriented approaches adhere to these principles and provide a good support for building models that are closer to real-world complex systems [17].

Based on these different observations, we chose to follow object oriented concepts to build our systemic and global design methodology situated in a concurrent engineering field. This methodology considers that a design project, in mechanical system engineering, is a network of various interacting design domains such as project, product, process, activities, etc. (Figure 1).

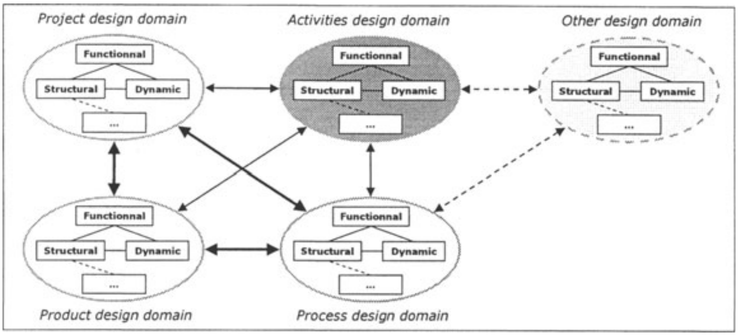

Figure 1 : The design domain network. Functional, structural and dynamic aspects considered in each design domain

Each of these design domains can be examined from several aspects (or models) in interaction, as defined in the previous approach. In accordance with object oriented concepts, we chose to develop three aspects in each design domain :

- a functional aspect, which describes the main objectives and goals of the system,
- a structural aspect, defining the system elements and architecture,
- a dynamic aspect, which describes the chronological behaviour of the system.

In this configuration, other design aspects such as physical or geometrical models are directly linked to the structural aspect of the system. For example, applied to the product design domain, this kind of association generates functions commonly found in PDM (Product Data Management) systems.

Concerning the interactions between each module, two levels can be differentiated : internal interactions in each design domain and external interactions between design domains. For the internal interactions, they are carried out with well-known current design methods such as F.A.S.T. (Functional Analysis System Technique) diagrams for structural/functional interactions and Statechart diagrams for structural/dynamic interactions. A Statechart is a structured and hierarchical formalism based on finite state automata which describes the dynamic behaviour of the system. External interactions are also defined between design domains. For example, in a design project, it is very useful to link a part of a manufacturing process to the corresponding elements of the manufactured product (structural aspect of the product / structural aspect of the process interaction).

The particularity of this design methodology is that it treats human activities (the activities of users, manufacturers, designers, etc.) as an effective design domain linked to the other product, process and project domains. This activity dimension is integrated into our object oriented design methodology in order to integrate ergonomics in the human based and co-operative design life cycle shown above.

In order to test industrial projects using this human based concurrent engineering design methodology, we specified two software environments : MANERCOS (Module d'ANalyse pour l'ERgonomie et la COnception des Systèmes [18]) and

ACSP (Atelier Coopératif de Suivi de Projet [19]), which represents the main subject of this paper.

4. ACSP: A COMPUTER SUPPORTED CO-OPERATIVE WORKSHOP

ACSP is a web-based environment, which employs the object oriented methodology and organises the co-operative activities of the design contributors. This web-based application, supporting the previously mentioned concurrent engineering design life cycle, has been defined as a Human Computer Co-operative Workshop system HCCW, and is also termed Computer Supported Co-operative Workshop environment CSCW [20]. The ACSP exploitation module is divided into four main sub-modules managing data from the project, product, process and activity design domains. Each design domain includes various design data describing functional, structural and dynamic aspects. For example, various types of data integrated into the ACSP environment can be displayed :

- project data, such as human and material resources (structural aspect) or task planning (dynamic aspect),
- product data, such as product assembly including the different product elements (structural aspect) linked to CAD files (geometrical aspect) or functional specifications (functional aspect) available in different situations in the product's life cycle (Figure 2),
- process data, such as process architecture including the different machines (structural aspect) linked to CAD files (geometrical aspect) or process dynamic sequences describing various manufacturing, maintenance, recycling, etc. operations (dynamic aspects).
- activities data, such as various Human-Machine-Environment interactions in different life situations (structural aspect), multimedia documents describing dynamic sequences like video-recorded data from human work activities or virtual films extracted from MANERCOS simulations, as illustrated in Figure 2 (dynamic aspect).

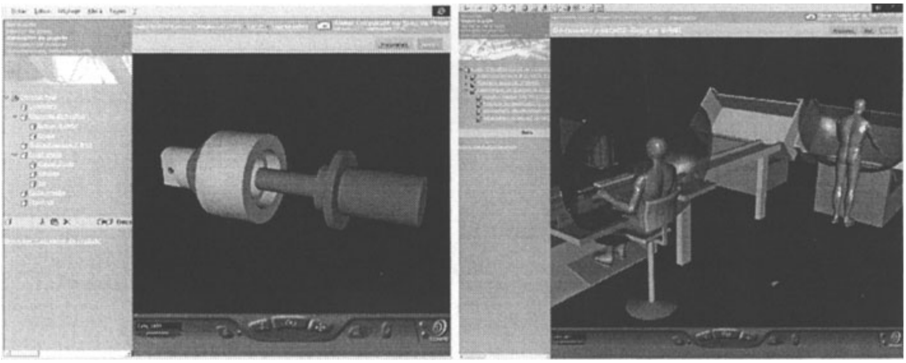

Figure 2 : ACSP interface describing a geometric model linked to an element of the product structural decomposition and an example of activity data integrated into the ACSP environment

These data are completed with internal and external interactions in the design domains and even communication features (email, forums, etc.).

This exploitation module is also completed with an administration and a designer activity analyser module.

The administration module includes several features for managing projects, design contributors, specific company needs, etc., such as creating, modifying, deleting, storing and archiving data with the Data Base Management System included in ACSP.

The designer activity analyser module has been defined to perform research activities in contextual design process modelling within the field of concurrent engineering, using designer activity traceability when designing with this CSCW environment. Traceability analysis features, showing how designers are applying the proposed methodology, are available in the ACSP environment.

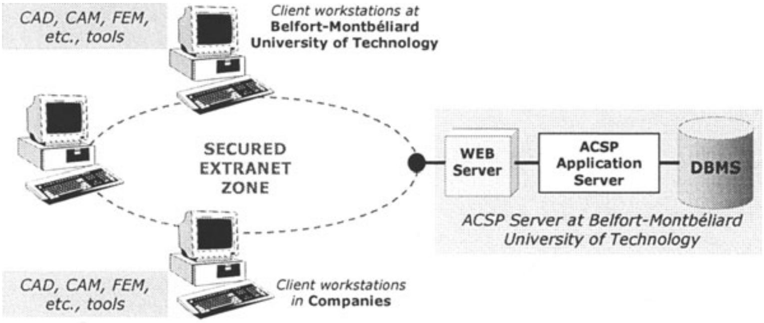
CAD, CAM, FEM, etc., tools
Client workstations at Belfort-Montbéliard University of Technology
SECURED EXTRANET ZONE
WEB Server
ACSP Application Server
DBMS
ACSP Server at Belfort-Montbéliard University of Technology
CAD, CAM, FEM, etc., tools
Client workstations in Companies

Figure 3 : ACSP client-server architecture connected to a database through a Web Server

From a technical point of view, ACSP can be defined as an asynchronous CSCW including a Data Base Management System connected to various Computer Aided tools : CAD/CAM tools, Finite Element Method Processors, etc. (Figure 3).

Around 50% of ACSP features have been implemented. ACSP is available as a Web Server with security layers managing user access. The system has a client-server architecture available for heterogeneous environments (NT, Unix, Mac, etc.).

5. APPLICATION IN DESIGN PROJECTS

The object oriented design methodology based on the human and co-operative design life cycle through the MANERCOS and ACSP environments have been applied to six student product-process design projects. Among these six projects, only one is centred on designing a manufacturing process. The five other projects are traditional mechanical system design projects linked to their manufacturing processes. Around 60 design contributors were involved in these projects. The average number of design contributors in a project group is 10 :

- 6 or 7 engineering students, including a project manager,
- 1 or 2 teachers in mechanical systems engineering,
- 1 or 2 engineers from companies.

The engineering students are all beginners to the aforementioned design methodology. They are also involved in a three-week training course with a fictive project before working on their own industrial projects.

During these industrial projects, for a period of four months, design contributors share, exchange, capitalise and re-use project, product, process and activity design data in a concurrent engineering context.

To manage research activities in concurrent engineering design process modelling, we use ACSP as an experimental research tool to analyse designer activity in the above mentioned design projects. The first quantitative and qualitative results from the ACSP designer activity analyser module relative to these projects are now available.

For example, as illustrated in Figure 4, it is possible to analyse the time evolution of the designers' actions on design data (creating, modifying, and deleting actions) compared to the number of connections to the projects.

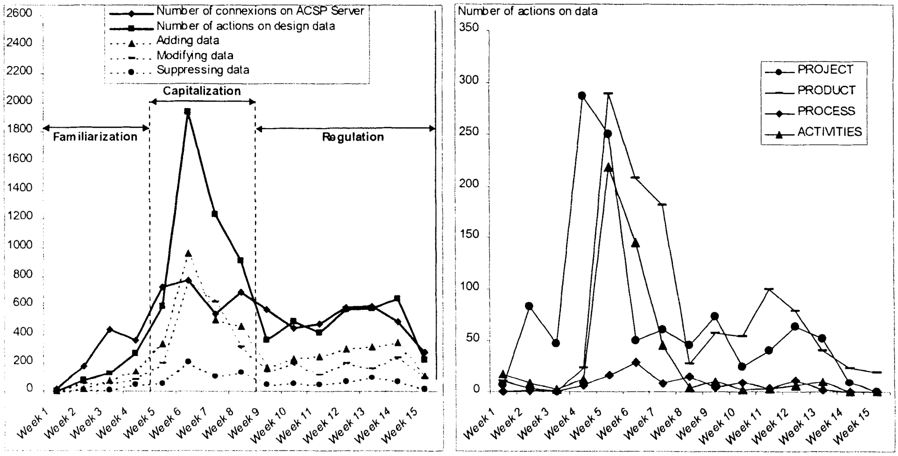

Figure 4 : Evolution of designers' actions on design data (create, modify and delete / project, product, process and activity data) compared to the number of connections to the projects

Through this diagram describing our first quantitative results on designer activity analysis using the ACSP experimental tool, it is possible to identify three steps in the project development cycle :

- a familiarisation step, in which design contributors discover at the same time the purpose of the project and the detailed ACSP functionalities. This step can be considered as a observation step where designers make more connections to their project than actions on data. We can observe a high level of deleting and modifying operations compared to the creating actions,
- a capitalisation step, in which design contributors create and modify a high number of design data per connection on their project. This step can be considered as a period of intensive activitywhere designers contribute to filling the ACSP database. This intense activity period also introduces a significant number of deleting actions on data, but still a low percentage compared with the number of data creation and modification activities,

- a regulation step, in which design contributors manage the design data capitalised previously. They make some adjustments to data, integrating the interactions between the design domains to achieve the final goal of the project. During this step, designers usually connect to gather information and perform less actions on design data than in the previous capitalisation step. They also have more creation action than modification and suppression actions.

After this global overview of these first results, it is now interesting to have a look at the distribution of actions in the various design domains. For example, as illustrated in Figure 4, it is also possible to analyse the time evolution of the designers' actions (creating, modifying, and deleting actions) in relation to the project, product, process and activity design data. This Figure shows that design contributors work on project design domain data during the entire period of their project. We can also observe an intensive period of activity from the beginning of the project until the 5th week, corresponding to the previously explained capitalisation step. It is significant to specify that all these actions on project design data are only carried out by the project managers, which corresponds to six designers out of 10.

Concerning the product and activity design data, we can observe a significant level of actions from week 5 to week 7. From week 8 to the end of the project, these actions decrease to less than 15 actions per week for activity data and a mean level of 50 actions per week for product data.

Concerning the process data, a low level of activity throughout the project can be observed. This can be explained by the low rate of projects involving the design of manufacturing processes.

6. CONCLUSIONS

All these items illustrate our first global results extracted from ACSP designer activity analyser module when managing projects in an academic context involving engineering students, teachers in mechanical systems engineering and professional engineers. The next step will consist in introducing the ACSP environment to industry in order to manage the same actions with professional designers.

This experience with the ACSP environment, using specific human factor features, shows that users browsed among activity data with new co-operative supports based on product usability functions and on human activities, manufacturing activities, recycling activities, etc. These new co-operative supports, such as structured data (life situations, usability functions, etc.) and documents (video films and human virtual simulations) generated with MANERCOS and shared through ACSP, seem to ensure co-operation in the design process. Supports such as these would also appear to assist the design participants to collect information, identify problems, search for new solutions, evaluate concepts, etc. during creativity sessions.

This set of results, combined with greater emphasis being placed on agent concepts, an extension of the object oriented approach, could open up challenging new ways forward for research in this field.

7. ACKNOWLEDGEMENTS

The authors would like to thank Prof. Abder KOUKAM (Laboratoire SET-UTBM) for his help and contributions to this research and for his help on this paper.

A part of this work was funded by PRéCI, i.e. Pôle Régional de Conception et d'Innovation, IRéCI, 90000 Belfort Cedex, FRANCE.

8. REFERENCES

[1] Tichkievitch, S., Chapa Kasusky, E., & Belloy, P. (1995). Un modèle produit multi-vues pour la conception intégrée. *Congrès international de Génie Industriel de Montréal, 3*, 1989-1998,.

[2] Bossard, P., Chanchevrier, C., Leclair P. (1997). *Ingénierie concourante - De la technique au social, Edition Economica*, 166.

[3] Gomes, S. (Janvier 1999). Contribution de l'analyse de l'activité à la conception de produits innovants - Application à la conception de systèmes de contrôle-commande automobiles, *Thèse de doctorat en Génie des Systèmes industriels, INPL Nancy*, 220.

[4] Gomes., S., Sagot, J.C., & Koukam A. (1998, june). Ergonomic approach based on modeling and simulation, *11th European Simulation Multiconference (ESM'98), Manchester*, 661-665.

[5] Sagot, J.C., Gomes, S., & Zwolinski P., (1998). Vers une ergonomie de conception : gage de sécurité et d'innovation, *International Journal of Design and Innovation Research, 2*, 22-35.

[6] Bocquet, J.C., Gabriel, M., Geury, M., Jean A., & Noël, J. (1996). Maîtriser la conception des produits et des systèmes - Conception en mécanique industrielle. *Les référentiels DUNOD.*

[7] Quarante D. (1995). *Eléments de design industriel, Editions Masson.*

[8] Sagot, J.C. (Mai 1999). Ergonomie et conception anthropocentrée. *Document présenté en vue d'obtenir l'Habilitation à Diriger des Recherches, INPL Nancy*, 267.

[9] Vinck, D., & Jeantet, A. (1995). Comissioning or mediating objects in the sociotechnical process of product design : a conceptual approach. *COST Social Sciences Serie, CCE.*

[10] Boujut, J-F., & Jeantet, A. (*Octobre* 1998). Les entités de coopération dans les nouvelles organisations de la conception. *Performances Humaines & Techniques, 96*, 38-44.

[11] Suh, N.P. (1988). Basic Concepts in Design for Productibility. *Annals of the CIRP, (37) 2.*

[12] Solehnius, G. (1992). Concurrent engineering. *Annals of the CIRP, (41) 2.*

[13] Rumbaugh, J. (1995). Modélisation et conception orientées objet - Object Modeling Technique (OMT). *Editions Masson.*

[14] Garro, O., Salaü, I., & Martin, M., (1995). Distributed design theory and methodology. *International Journal of Concurrent Engineering : research and applications, 3, n°1*, 43-54.

[15] Brissaud, D., & Garro, O. (1996). An approach to concurrent engineering using distributed design methodology. *International Journal of Concurrent Engineering : research and applications, 4, n°3*, 303-311.

[16] Koukam, A., & Tarby, J.C., (1996). An integred model for interactive systems. *Human Interaction with complex systems : Conceptual principles and design practice by C.A. NTUEN & E.H. PARK, Kluwer Academic Publisher*, 3-11.

[17] Kolsky, C. (1997). Interfaces Homme-Machine, *Editions Hermès.*

[18] Gomes, S., Sagot, J.C., Koukam, A., & Leroy, N., (1999, April). MANERCOS, a new tool providing ergonomics in a concurrent engineering design life cycle. *4th Annual Scientific Conference on Web Technology, New Media, Communications and Telematics - Theory, Methods, Tools and Applications, EUROMEDIA 99, Munich*, 237-241.

[19] Gomes, S., Sagot, J.C., Koukam, A., & Leroy, N. (1999, April). ACSP, an intranet forum supporting a concurrent engineering design life cycle. *6th European Concurrent Engineering Conference, ECEC'99, Erlangen-Nuremberg*, 249-251.

[20] Erceau, J., & Bourgine P. (1994). Complexité et ergonomie cognitive : vers une Ingénierie des Systèmes Complexes. *XXIXème Congrès de la SELF, Paris, Editions Eyrolles*, 75-87.

9. AFFILIATIONS

Equipe de recherche en ERgonomie et COnception (ERCO) – Université de Technologie de Belfort-Montbéliard (UTBM) 90010 BELFORT Cedex, France.

F. POURROY, N. TROUSSIER, M. TOLLENAERE

A METHOD AND A SUPPORT FOR A BETTER INTEGRATION OF MECHANICAL SIMULATION IN THE DESIGN PROCESS

Abstract. World wide competition in industry has dramatically increased the use of computational mechanics techniques which are nowadays a key factor of the design process. Nevertheless, the use of the simulation techniques in a more systematic way and in the early stages of the design process gives rise to numerous problems. Even the state-of-the-art "integrated" CAD software tools are unable to give efficient solutions to these problems.

Following a brief bibliographical revue of different research works related to this subject, the present paper proposes, through the SG3C software, a working methodology and a supporting software tool in order to provide some elements of solution to the different problems related to integrating computational mechanics in the design processes. The conceptual model is first presented. A simple example of a design situation is then used to show why the SG3C system is interesting for the numerical simulations efficiency. Some particular features such as modelisation guidelines, process tracking, knowledge management and co-operative work are underlined.

1. INTRODUCTION

World wide competition in industry has dramatically increased the use of computational mechanics techniques in the early stages of the design process of products and systems. The industrial stakes expressed in terms of cost, schedules, quality and capitalisation issued from simulation are essentials but the arising difficulties still remain important. An efficient implementation of these numerical techniques supposes more particularly a high level of integration of computational activities in the design process. This integration should not be based only on the tools, but also on technical know-how and industrial organisations.

Concerning with the area of computational mechanics, a new issue in some industrial companies is to transfer some simulation activities from structural analysis department to design offices in order to achieve the required level of integration. In this case, design technicians are trained to computational mechanics techniques and have to support the most classical problems required by their design activity (linear problems for example). In this scheme, the traditional specialists of computational mechanics are in charge of scientific support of technicians activities while they still keep the responsibility of the more complex studies. This support consists mainly in technical assistance or supervision either in the definition of more adequate calculation models according to the objectives and context of simulation, and in the critical analysis of computational results.

During the 90's, a lot of research work has been done to provide solutions to these difficulties of integrating computational simulation in engineering design.

P. Chedmail et al. (eds.), Integrated Design and Manufacturing in Mechanical Engineering, 19-26.
©2002 *Kluwer Academic Publishers.*

Some works propose software environments which enable more or less automatic idealisation of the product geometry to make it ready for a simulation process. In that way, Shephard [1] describes the computational mechanics process as a succession of idealisation steps and presents a framework of an automated analysis idealisation control system in an engineering design context. Other works based more particularly on geometric criterions (for example [2,3]…) have similar purposes.

The area of artificial intelligence seems to be another way of integrating computational mechanics in the design process. In this manner, some research works try to provide modelling and analysis assistants. Dym [4] describes a computer system based on symbolic representation of knowledge involved in engineering modelling and computation. Model-based reasoning (MBR) techniques are used to represent structure, function and behaviour explicitly. In [5], Turkiyyah proposes a knowledge-based framework for assisting users in setting up, interpreting, and hierarchically refining finite element models in a structural engineering domain. An expert system defines an appropriate mathematical model for the structural mechanics problem and performs interpretation operations, leading to model refinements. The research presented in [6] develops a multilevel product model that supports Simulation-Based Design (SBD) of mechanical systems, from preliminary to detailed design stages. A global database is used to support both CAD and simulation data. This database is accessed by the different actors for defining simulation models.

Those research works carry out interesting contributions to some specific aspects of the problem of integrating computational mechanics in the engineering design process. Nevertheless, none of them takes into account the whole problem. From our viewpoint, three main issues are not fully answered :

- Integration is generally considered as a problem of data transfer from the design process environment (CAD systems) to simulation software tools. The information feedback from simulation to design is poorly achieved.
- All along the design process, many models are created to simulate the product behaviour. This multiplicity of models is a source of difficulties in managing models and ensuring consistency of the whole process. Very few research works take this problem into consideration.
- The crucial question of capitalising and reusing both simulation and design knowledge is more or less present but does not receive satisfying answers.

The present research work has been driven to give solution elements to the three above mentioned problems. A design organisation and a supporting tool are defined in order to provide a satisfying level for integrating computational mechanics in the design process of products. Our research also provides practical answers to capitalisation and reusing questions.

2. CONCEPTUAL MODEL

The definition of a conceptual model is a necessary stage to reach the above mentioned objectives. This conceptual model has been created from structuring and formalising computational mechanics present practices [7]. The first step is to identify and to define the different entities handled by designers and analysts. The second step is to provide different links between the entities, in order to capture and to express rationale and consistency of the integrated analysis process.

2.1. Identification of level dependent entities

At the very global level of a simulation process, two different classes of entities are distinguished : the Project entity and the Instructional Case entity. A Project entity consists in the whole of design models and simulation data explicitly associated with a particular product in the context of a particular design project. An Instructional Case entity (see [8]) includes one or more complete simulation process related to a particular problem. This problem should be sufficiently general to allow the Instructional Case to be separated from any Project entity. The so-defined Instructional Cases should answer either modelisation problems (for example, a simulation process drawn to define a model well adapted to represent the stiffness of a bolted assembly) or design problems (for example, a sensitivity analysis driven to get the influence of a fillet radius on a stress concentration factor).

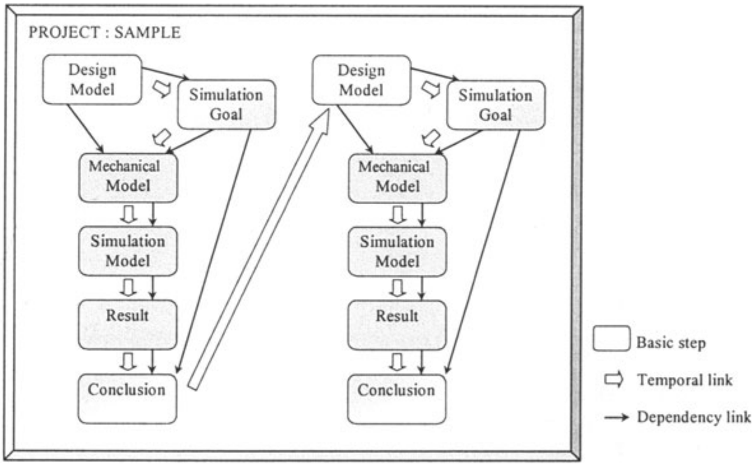

Figure 1. Representation of the project "Sample"

The distinction between these two high level entities is interesting from a strategic point of view insofar as it is a support for identification and capitalisation of knowledge provided by mechanical simulation.

Going to a higher detail level in the conceptual model, the Project, as well as the Instructional Case can be broken down into one or several simulation Cycles. A Cycle corresponds to one complete simulation phase, that means a process starting from the definition of a particular goal for simulation, continuing with constructing a calculation model, obtaining numerical results and analysing these results. A Project is made of numerous cycles corresponding to the different product specifications.

Refining the conceptual model and structuring the Cycle contents, six different Steps are identified [7] and briefly described below :

- The Design Model contains at once geometrical (CAD data), technological and functional descriptions of the product. It represents the whole set of information usually handled by designers and required for computation.
- The Simulation Goal explicitly defines the objectives of the running simulation Cycle. It also describes the situation of the product in its environment from which loads and boundary conditions will be deduced, and some specifications on the context in which the Cycle will be created (cost constraints, time limits, required accuracy…).
- The whole set of mechanical assumptions are gathered in the Mechanical Model which is a representation of the product from a mechanical behaviour point of view, without any consideration about the numerical method and software tool to be used for computation.
- The Result contains all data provided by the calculation tools sufficient and necessary for the analyst interpretation.
- The Conclusion is made of two parts. The first one includes an estimation of the computation results credibility. The analyst has first to put trust in the simulation Cycle. The second part consists in interpreting the Result and drawing meaningful conclusion for the designer.

Finally, several attributes aim at describing and structuring more precisely the contents of each step. However, it is to be noticed that the Steps still remain semi-structured entities, preventing from excessive locking of the simulation process.

2.2. Links between entities

Links are necessary to represent progress and consistency of the simulation process. They occur at each of the four levels of the conceptual model. Two kind of links may be distinguished : Temporal links and direct Dependency links.

Temporal links express the approach of constructing the simulation process. They also represent the logical connection in the definition of Steps attributes, Steps themselves, Cycles, or ways between Project and Instructional Cases. This kind of link is of great interest for tracking and capitalising the computational mechanics process. In fact, it allows capturing and preserving a process for solving problems at a more or less global level, depending on the considered detail level.

Direct Dependency links have their advantage in the maintainability of the simulation process when engineering changes occur. Following the modification of an entity (functional requirement, geometrical data, computational mode, etc.), they allow to track the other entities open to be affected by the modification. The decision of propagating modification remains in the users responsibility. So, these dependency links are a kind of support to prevent simulation process from consistency loss, all along the design evolution. Figure 1 shows an example of the project “sample” viewed throughout the presented conceptual model. This small project consists in two analysis cycles.

3. USER GUIDE OF THE METHODOLOGY

The previously described conceptual model has been implemented in a software tool named SG3C (in French "Système de Gestion des Connaissances Calcul en Conception"). This tool can be viewed as a support for the presented working methodology. Some principles for implementing and using the tool and the methodology in a design process will be now explained. An example of a design situation involving computational mechanics activity is used to illustrate the subject.

The example describes the design progress of an industrial system : an hydraulic press for stamping of small mechanical parts. The list of functional and technical requirements has been drawn up in order to guide the designer who has to carry out the study. The evolution of the design process has led to a first solution for a part of the frame of the press : the supporting beam (see figure 2).

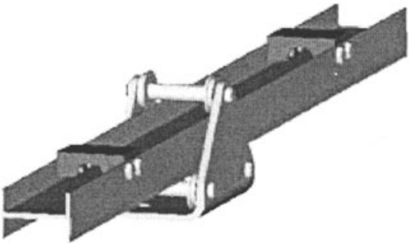

Figure 2. First CAD model of the supporting beam.

The designer has now to check if its solution fits the technical requirements, and more particularly those concerning the rigidity of the device. The conceptual model previously described will help him to achieve this task. Starting with the existing Design Model (CAD model of the beam, technical requirements, materials definition,…) the designer has first to define precisely a Simulation Goal for this problem. In this case, the Simulation Goal could be the following small text : "verify that the deflection of the beam is less than 1 mm under the maximum load due to the hydraulic device. The beam is supposed to be clamped to the frame of the press. High confidence in the calculation is required."

From this point, the mechanical analysis process can be started. Using the data contained in the Design Model and in the Simulation Goal, mechanical assumptions can be made. For example, even if a good accuracy is required, a beam model can be adopted because of the geometry of the part, and considering that only a global result (displacement) has to be calculated. Some guidelines can be proposed to help the designer to achieve the modelisation tasks. The whole of the resulting mechanical assumptions constitute the Mechanical Model, as illustrated in figure 3.

All is now defined for choosing a resolution method and a software tool adapted to the problem. Some additional parameters can be required to carry out the simulation of behaviour such as the finite element type, the discretisation level,…). The parameters can be adjusted according to the data contained in the Design Model, in the Simulation Goal and in the Mechanical Model. In the example no particular parameter is needed : this very simple mechanical problem can be solved with basic tools, well adapted to the design office context. All the input data of the simulation software constitute de Simulation Model. Once the Result have been obtained, the designer can draw up his conclusion : "the calculation seems to be OK. Deflection of the only beam under maximum load exceeds the required total value of one millimeter. The supporting beam has to be rigidified".

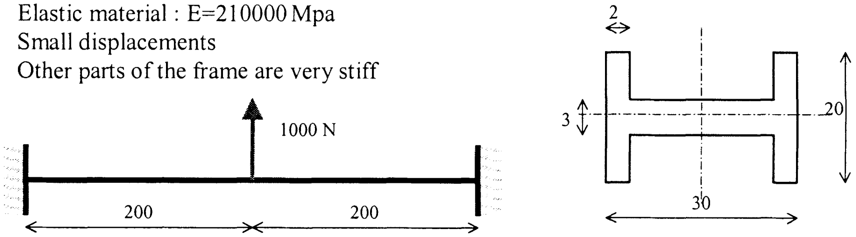
Elastic material : E=210000 Mpa
Small displacements
Other parts of the frame are very stiff

Figure 3. A Mechanical Model for the supporting beam.

This first part of the example shows that the decomposition and structuring of the calculation process into several well defined steps can be a helpful means of carrying out an efficient mechanical analysis in an industrial design context. Some other features of the presented conceptual model are introduced now in the continuation of the example.

The designer choose to add ribs to the supporting beam in order to get a more rigid behaviour. This decision implies the definition of new design parameters such as a number of ribs, a location and an orientation for each of them. The designer can connect to the SG3C software system in order to get some help for defining the design parameters values. SG3C database contains a description of the different processes of analysis previously carried out by the designers and mechanical engineers of the company. These processes are easy to understand as they are structured in several cycles, described themselves as a succession of the six basic steps presented in the conceptual model. The user can access to any step of any cycle by the way of requests based on a few keywords.

In the case of the press, the keywords lead the designer to the conclusion of a previous calculation which aimed at determining the optimum orientation of a rib in order to increase the flexural stiffness of a U-sectional beam by means of a sensitivity analysis. This previous calculation was identified as an Instructional Case because of a certain level of generic knowledge. The Instructional Case is considered to be close enough to the designer own problem, so the conclusion can be directly reused for the supporting beam design. It is to be noticed that in some situations the previous models could be partially reused to get new results for the rib orientation problem. Modifications of these old models are intended to make them fit the new problem. Finally, in other situations only the way in which the old problem was approached (i.e. sensitivity analysis on a basic structure geometry) could be interesting to reuse.

Helped by the Instructional Case, the designer now defines a new solution for the supporting beam and needs to check it again. But the new geometry gives rise to some modelisation problems and the designer is not skilled to achieve this task. So he decides to get some help from a specialist in mechanical analysis and contacts an engineer at the calculation office of the company.

In their discussion, they define together the new Simulation Goal which can be nearly the same as the first one. Only the parameters which characterise the context of analysis might have changed. Indeed, some time has gone by since the first cycle of the process and the forthcoming analysis cycle has to be carried out within two days. It's now the turn of the engineer to connect to the SG3C software system and to consult the same Instructional Case the designer did. The specialist wants to find out some useful information for the model definition. Once the Mechanical Model and the Simulation Model have been defined, the Result is obtained.

As it was done for the Simulation Goal, the Conclusion is drawn up in co-operation between the designer and the calculation specialist to ensure the efficiency of the analysis process : with this new design, the deflection of the beam is less than the required limit. So, the design process of the hydraulic press can be continued.

This second part of the example explained how the conceptual model and the SG3C tool can support a co-operative process between a designer and a calculation engineer. It was also pointed out that SG3C can be a useful tool for solving modelisation problems or design problems by means of the Instructional Cases stored in the database.

During their work, the designer and the calculation engineer have defined several steps described below. These steps can be stored in the SG3C system database so that the related information can become available for all design actors of the company. Some other features are also available such as the possibility to get an automated simulation report, which is possible when all necessary data are available from the database. This feature also contributes to have a defined level of standardisation and document structuring at the company level.

4. CONCLUSIONS

Nowadays, some commercial software try to give solutions to the crucial problem of integrating calculation in the design process. Unfortunately, the proposed integration level is dramatically low. Only a few well formalised data such as geometry or some material descriptions could be concerned by a process reduced to a more or less automated data transfer operation.

This integration problem is of socio-technical order and appears to be very complex. The arising difficulties also concern working methodologies, organisational dynamics, education and training. Moreover, they are beyond the analysis area and should probably concern the whole of the design actors. So, the solution cannot only be a software tool.

The presented work was initiated from this point of view and consists in a first contribution to the addressed problem. A structuring of the analysis process into six well defined steps has been proposed in order to provide guidelines to the analysts and to make a capitalisation of this process possible. Among the six steps, the Design Model is the responsibility of the designer, while the Mechanical Model, the

Simulation Model and the Result are the responsibility of the analyst. The Simulation Goal and the Conclusion are particular steps as they have to be defined by both the designer and the analyst in a co-operative way.

To complete the structuring, some links have been defined in order to catch the logic of the analysis process and to prevent from consistency loss.

The methodology is supported by a software tool whose database is used to store all the processes of analysis at the company level. Some of them, more generic, gain the status of Instructional Case. An automated calculation report is also available from the software.

All this framework makes possible some important features for the design project such as tracking of the processes, guidelines for non specialists and also for specialists in case of complex situations, some means of knowledge management, and reusing capabilities of results, models or resolution processes.

In the forthcoming months, this work will be implemented in the design offices of a company. Based on an analysis of the methodology and supporting tool in use, some very interesting conclusions are expected.

5. REFERENCES

1. Shephard M.S., Wentorf R. Toward the Implementation of Automated Analysis Idealization Control. Applied Numerical Mathematics 1994; 14 : 105-124.
2. Armstrong C., Douaghi R., Bridgett S. Derivation of an Appropriate Idealisations in Finite Element Modeling. Advances in Finite Element Technology, 1996.
3. Remondini L., Leon J.C., Trompette P. Generic Data Structures Dedicated to the Integrated Structural Design. Finite Elements in Analysis and Design 1996; 22 : 281-303.
4. Dym C., Levitt R. Toward the Integration of Knowledge for Engineering Modeling and Computation. Engineering with Computers 1991; 7 : 209-224.
5. Turkiyyak G., Fenves S. Knowledge-Based Assistance for Finite-Element Modeling. AI in Civil and Structural Engineering. IEEE Expert 1996 : 23-32.
6. Chang K., Choi K., Wang J., Tsai C., Hardee E. A Multilevel Product Model for Simulation-Based Design of Mechanical Systems. Concurrent Engineering 1998; 6 : 131-143.
7. Troussier N., Pourroy F., Tollenaere M., Trebucq B. Mechanical models management in engineering design. Proceedings of IDMME; 1998 : 1087-1094; Compiègne, A.G.I.R.
8. Troussier N., Pourroy F., Tollenaere M., Trebucq B. Information structuring for use and reuse of mechanical calculations models in engineering design. Journal of Intelligent Manufacturing 1999; 10 : 61-72.

5. AFFILIATIONS

Franck Pourroy, Laboratoire 3S, BP 53, 38041 Grenoble cedex 9, France.

Nadège Troussier, Laboratoire CQP2, BP 60319, 60203 Compiègne cedex, France.

Michel Tollenaere, Laboratoire GILCO, 46 av. F. Viallet, 38031 Grenoble, France.

F. BENNIS, P. CHEDMAIL, O. HELARY

REPRESENTATION OF DESIGN ACTIVITIES USING NEURAL NETWORKS:

Application to fuzzy dimensioning

Abstract: This paper deals with the problem of product mechanical design within the framework of integrated design. It proposes a technique based on the fuzzy logic approach. The design process is divided in several sub-problems (professions or points of view : Pov). Fuzzy approach allows the comparison of the PoV to each other and the final solution emerges through a global compromise. This approach allows the design process to be distributed in parallel tasks. The neural network (NN) tool is used in order to encapsulate data and the analysis of each design PoV. So it allows a flexible decision making in design process. Numerical advantage of this approach is discussed.

1. INTRODUCTION

Decision making during the conceptual design stage has a significant influence on factors such as cost, performances, reliability, safety and environmental impact of a product. However, knowledge of all the design requirements and constraints during this early phase of product life cycle is usually imprecise, approximate or unknown [1]. In this paper, the complex problem of mechanical design is solved using the fuzzy logic approach, especially during the dimensioning phase.

Several authors study the mechanical design problems. Pahl *et al* proposed a sequential approach [2]. Wooldridge used the multi-agent method [3]. Other works tempted to solve this problem by using the fuzzy logic approach ([4-7]).

The fuzzy logic methods take into account the vague and imprecise nature that often arises during the specifications stage as well as in the data choice, system boundaries choice, unsatisfactory formulation of design objectives and constraints, and the relative importance of the points of view. We use also neural networks (NN) to learn and represent the complex data input-output mappings of each PoV. NN has been found to be useful in performing nontrivial mapping function [8].

This paper is organized as the follows. First, the fuzzy logic and neural network methods are presented. An industrial application corresponding to the study of an aeronautic cladding system is presented.

2. FUZZY LOGIC OPTIMIZATION METHOD

The fuzzy logic approach has been introduced by Zadeh in 1965 [9]. Since that time, several authors contributed to the improvement of this concept, with theoretical contributions as well as with applications [4-7]. Feraille and Chedmail [6] proposed a parallel process to solve conflicts in design process. This model is described in

P. Chedmail et al. (eds.), Integrated Design and Manufacturing in Mechanical Engineering, 27-34.

©2002 *Kluwer Academic Publishers.*

Figure 1. Every PoV formulates the problem in terms of optimization of objective function subjected to constraints. Hence, this problem is fuzzified and an aggregation of the results of the whole PoV is performed. The crisp design problem **P**, corresponding to a given PoV is formulated as the following:

$$\begin{aligned} &\text{min. } F(\mathbf{x}) \\ &\text{subject to the constraints : } \mathbf{G}(\mathbf{x}) \leq 0, \end{aligned} \qquad (1)$$

where **x** is the design variables vector. **G**(**x**) is the vector of constraints defining the admissible domain, G_i is the i^{th} component of **G**(**x**). F is the criterion function.

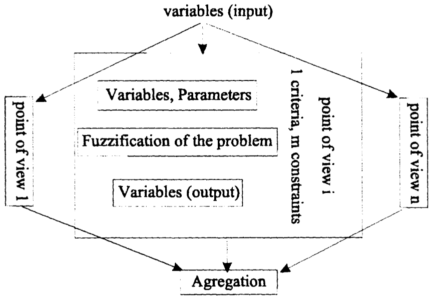

Figure1. Parallel design process from [6].

The transformation of the crisp problem **P** in a fuzzy one ***P*** is achieved in two stages, namely "Fuzzy action" and "aggregation".

2.1. Fuzzy action

The first stage consists in fuzzifying the criterion and the constraints. A membership function $\mu_F(F)$ chosen beforehand is associated to the criterion function F. This membership function is described with a continuous range of values between zero and one, according to the degree of satisfaction that one assigns to every value of F independently of **x**. Knowing $\mu_F(F)$, it is possible to calculate for every value of **x**, the corresponding value of $\mu_F(F(\mathbf{x}))$ and therefore to get μ according to **x**. This function will be denoted $\mu_F(\mathbf{x})$. We apply the same procedure for every constraint G_i From $\mu_{Gi}(G_i)$, we calculate $\mu_{Gi}(\mathbf{x})$. The fuzzy constraints is defined as follows:

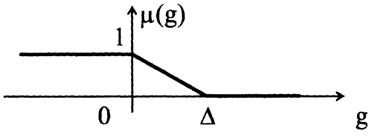

$$\tilde{G} : \forall \mathbf{x} \in IR \text{ and } G(\mathbf{x}) \in IR \rightarrow \mu_G(\mathbf{x}) \in [0;1]$$

$$\mu_{Gj}(\mathbf{x}) = \begin{cases} 1 & Gj(\mathbf{x}) \leq 0 \\ (\Delta_j - Gj(\mathbf{x}))/\Delta_j & 0 < Gj(\mathbf{x}) < \Delta_j \\ 0 & Gj(\mathbf{x}) \geq \Delta_j \end{cases} \qquad (2)$$

Figure 2 : Satisfaction function of g.

The coefficient Δ allows the relaxation of the definition domain of $\mu_{Gj}(\mathbf{x})$ (Figure 2).

Δ is not the same for all the constraints and its value may be chosen by the designer. In order to approximate faithfully the behavior of the satisfaction function, a strategy of sampling points is necessary. This set of points needs to be as full as possible. Indeed, upper and lower values of each design variable have to be defined.
Assuming that $\mathbf{x} = (x_1, x_2, \ldots, x_n)$ represents the design variables vector and x_i the i^{th} component of $\mathbf{x}$. n is the number of design variables involved in the studied point of view. We assume that $\mathbf{x}^i$ is a particular value of $\mathbf{x}$, sampled between $\mathbf{x}_{Low}$ and $\mathbf{x}_{upp}$: where: $\mathbf{x}^i=(x_1^i, x_2^i, \ldots, x_n^i)$, $\mathbf{x}_{Low} = (x_{low1}, x_{low2}, \ldots, x_{lown})$, $\mathbf{x}_{upp} = (x_{upp1}, x_{upp2}, \ldots, x_{upp,n})$
The set $\mathbf{X}$ of all the sampled points in the domain ($\mathbf{x}_{Low}$, $\mathbf{x}_{upp}$) is defined as the following : $\mathbf{X}= \{\mathbf{x}^1, \mathbf{x}^2, \ldots, \mathbf{x}^r\}$ in $R^r = R^{p1} \times R^{p2} \times \ldots \times R^{pn}$ where pk is the number of components of the design variable x_k; and $r = p1 \times p2 \times \ldots \times pn$. For each value $\mathbf{x}^i$, and for each constraints G, we have to calculate $G(\mathbf{x}^i)$ and then $\mu_G(\mathbf{x}^i)$. Let's assume that the global problem of mechanical design is divided in v sub-problems or point of view. When it is necessary, the index j (or J) will be added to each one of the parameters above, it designates the point of view number $j= 1,\ldots, v$. For example $X_J =\{\mathbf{x}_J^1, \mathbf{x}_J^2, \ldots, \mathbf{x}_J^r\}$. We observe that this calculation process is time and memory consuming especially when n and r increase. This problem can be resolved by using Neural Network (NN). We apply the same method to the fuzzy action of criterion function. The membership function for the criterion is defined as :

$$\tilde{F} : \forall \mathbf{x}\in R,\ F(\mathbf{x})\in R\rightarrow\mu_F(\mathbf{x})\in [0;1] \text{ that:}$$

$$\mu_F(\mathbf{x}) = \begin{cases} 0 & \text{for } F> F^{max} \\ \dfrac{F^{max}-F}{F^{max}-F^{min}} & \text{for } F^{min} <F< F^{max} \\ 1 & F<F^{min} \end{cases} \qquad (3)$$

R represents the real domain, with $F^{max} = F(\mathbf{X}^{max})$ and $F^{min} = F(\mathbf{X}^{min})$. $\mathbf{X}^{max}$ respectively $\mathbf{X}^{min}$ represents the vector of values of the design variables that maximizes, respectively minimizes, $F(\mathbf{x})$ subjected to the constraints. The research of $\mathbf{X}^{max}$ and $\mathbf{X}^{min}$ is done in a relaxed domain D'. Figure 3 depicts a comparative analysis of membership functions of criterion [4-6]. Regarding the other methods, ours permits to find solutions with independence between all the points of view [10].

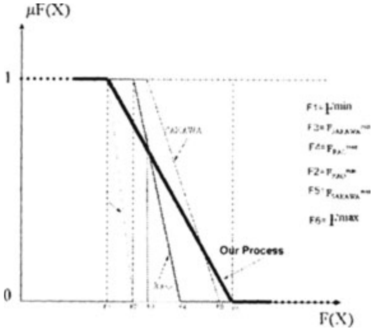

Fig. 3: Comparison of the satisfaction criterion.

2.2. Aggregation

The second stage consists in aggregating all the membership functions corresponding to the criterion and the constraints. The result of the fuzzy problem $\tilde{P}$ is gotten by associating a new aggregation criterion, φ, chosen beforehand:

$$\mu_{\tilde{P}}(\mathbf{x}) = \varphi(\mu_F, \mu_{G1}, \mu_{G2}, \ldots, \mu_{Gn}) \tag{4}$$

μ_F and μ_{Gi} are function of **x**. $\mu_{\tilde{P}}(\mathbf{x})$ is the satisfaction function for the PoV **P**. The aggregation of all the points of view, can be described by the following equation:

$$\mu_{glob}(x) = \psi(\mu_{\tilde{P}1}, \mu_{\tilde{P}2}, \ldots, \mu_{\tilde{P}n}) \tag{5}$$

It is achieved with a function ψ that represents the ability of every PoV to globally satisfy the problem. Methods of aggregation are generally distinguished by the choice of ψ and φ. In our approach, we use the same criterion for the two aggregation phases. Namely the "*min*" operator as proposed by Dubois in [10]. From (4) and (5) we obtain the following relations:

$$\mu_{PVj}(\mathbf{x}) = \min(\mu_F(\mathbf{x}), \ \mu_{G1}(\mathbf{x}), \ldots, \mu_{Gn}(\mathbf{x})) \tag{6}$$
$$\mu_{glob}(\mathbf{x}) = \min(\mu_{PV1}(\mathbf{x}), \mu_{PV2}(\mathbf{x}), \ldots, \mu_{PVv}(\mathbf{x})) \tag{7}$$

Relation (6) is evaluated for every particular value $\mathbf{x}^i_.$ in **X.** We assume that, for a given point of view J, $\mathbf{x}_{JLow}$ and $\mathbf{x}_{Jupp}$ are identical for the criterion and for all the constraints. Equation (7) is also evaluated for every $\mathbf{x}^i_.$ of **X.** Numerically, this phase requires $\mathbf{x}_{Low}$ and $\mathbf{x}_{upp}$ to be identical for all points of view. Moreover, the set **X** must be the same for all points of view. In reality, these numerical constraints are not necessary in the parallel design approach. We propose to overcome these difficulties by using the neural network tools.

3. NEURAL NETWORKS

In the previous sections, techniques of calculation of the satisfaction function of each point of view (PoV), and the global satisfaction function have been presented. We also presented the aggregation process of all these points of view. For a given PoV **P** and for a given point $\mathbf{x}_i$ in the extended space of design variables, the previous method permits to calculate $\mu_P(\mathbf{x}_i)$. Selecting n points in the design variable space gets the global satisfaction function and all the results. Theoretically the discretisation step (size) can be chosen according to the PoV and according to the extended interval size of each variable. In addition, the global aggregation did not require having the same discretisation step and therefore the same vector **X** for all points of views. It is necessary to develop a tool in order to encapsulate the intermediate calculations. We propose a method based on the Neural Networks technique (NN). We use this heuristic tool in order to identify the satisfaction functions of every point of view. A net topology, node characteristics and training rules specify the NN model [11]. The goal of NN training is to produce a network which produces small errors on the training set, but which will also respond properly to novel inputs. The network generalises well if it is able to perform as well on novel inputs, as on training set inputs [11].

The NN of each point of view are performed at the end of the internal process analysis. For a given reference data and a given net topology, a bayesien learning technique is used to identify the efficient neurons [13]. At the training stage, we evaluate pj values of $\mu_J(\mathbf{x}_{Ji})$ $(i=1,\ldots pj)$. Input vectors and the corresponding output vectors are used to train a network until it can approximate a function. The following input and output couples are used $(\mathbf{x}_{Ji}, \mu_J(\mathbf{x}_{Ji}))$. The approximation of the satisfaction function is performed until the difference between the target output $\mu_J(\mathbf{x}_{Ji})$ and the network output $\mu_{JN}(\mathbf{x}_{Ji})$ corresponding to $\mathbf{x}_{Ji}$ is minimum. We minimize the average of the sum of these errors.

$$\text{mse} = \frac{1}{r_J} \sum_{k=1}^{r_J} [\mu_{JN}(\mathbf{x}_J^k) - \mu_J(\mathbf{x}_J^k)]^2 \qquad (8)$$

$r_J = p_{J1} \times p_{J2} \times \ldots \times p_{Jn}$, r_J is the number of sampled point $\mathbf{x}$ in the point of view PV_J. p_{Ji} is the number of sampled values corresponding to the design variable x_{Ji} of $\mathbf{x}_J$.

The obtained network N_J allows to estimate the value of the satisfaction function $\mu_J(x)$ for any points $\mathbf{x}$. These points don't necessarily belong to X_J. Furthermore, the network does not need to evaluate neither the intermediates value of the constraints nor the values of the criterion. We also observe that the size of the networks file is generally very small in comparison with the size of storage of the set $\mathbf{X}$ and the corresponding values of the satisfaction function. Hence the networks coefficients are memorized. The project manager receives the networks results N_J of every point of view PoV. Then, he can calculate the global satisfaction function at each point.

$$\mu_{N\text{global}}(\mathbf{x}) = \min(\mu_{JN}(\mathbf{x}))\ (J = 1,\ldots v) \qquad (9)$$

By using neural network, it is not at all necessary to have the same set X for all points of views. Moreover, the chosen set, **X,** by the project manager may integrate supplementary information or constraints.

4. DESIGN OF AN ACCESS TRAP DOOR IN AN AIRPLANE COCKPIT

In this section, fuzzy approach is applied in the design phase. The industrial application consists in studying an aeronautic cladding system. It is composed of a door and a framework. This cladding system allows a manipulator to place a pressurized oxygen bottle in an aircraft *cockpit*. We distinguish two systems: the cladding system (S1) and a door (S2) as shown on figure 4. The cladding and the door are modeled with equivalent stiffened beams. L3 and L4 are the dimensions of the trap door, e_1 the thickness of beams and e_2 the thickness of the door.

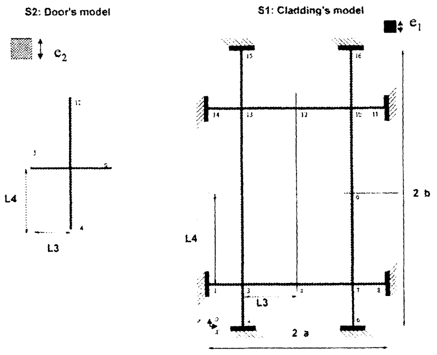

Figure 4: Structural model of the systems S1, S2.

Among many aspects, we study the geometric, structural and mass PoV of S1 and S2. Four sub-problems corresponding to three different PoV (mass, structural and geometric) are used. A functional and structural analysis allows establishing the following 5 specification tasks:

- a human operator must be able to put down in the cockpit a pressurized bottle.
- The door must insure the tightness of the cockpit.
- S1 and S2 elements must be light (aeronautic criterion).
- The deformations of S1 and S2 are limited.

Table 1 gives all the parameters and variables used by each point of view.

Table 1: Design parameters

Points of view	Parameters	dependent variables	independent variables
PV1 : S1/mass	a, b, ρ		e_1
PV2 : S1/geometric	a, b, r	L_1, L_2	L_3, L_4
PV3 : S 1/structure	a, b, E, ν, f,σ	L_1, L_2	L_3, L_4, e_1
PV4 :S2/mass	ρ		L_3, L_4, e_2

Dependent variables may be obtained explicitly from the independent variables. The hole dimensions are limited by three parameters a, b and r.

Mass point of view for the system S1 PV1 : Figure 5 represents the membership function $\mu_{PV1}(e_1)$ corresponding to the mass PoV S1. Figure 6, depicts the output of the difference $(\mu_{PV1}(e_1) - \mu_{NPV1}(e_1))$.

Geometric point of view for the system S1 PV2 : Figure 7 depicts the membership function corresponding to the geometric PoV PV2 depending of the variables L_3 and L_4. The relative error is little than 0.01.

Structural point of view for the system S1 PV3: This PoV studies the deformation of the elements of the system S1. The chosen criterion consists in minimizing the strain energy of the structure. We use the finite elements method to calculate the displacements of the structure defined by figure 4. The NN topology is defined as (3-10-8-1). The error is smaller than 0.03.

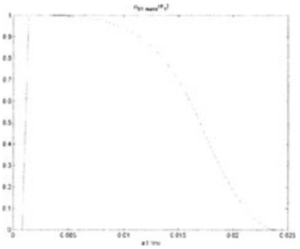

Figure 5 : Mass PV1/S1.

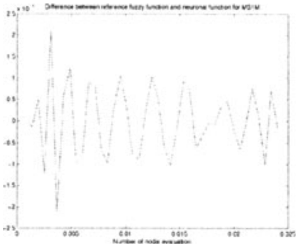

Figure 6 : Relative error for PV1/S1.

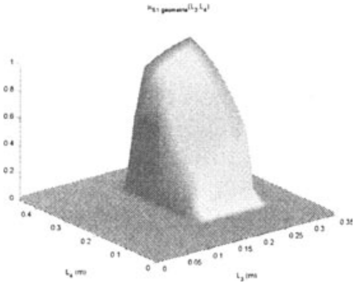

Figure 7: Geometric PV2/S1.

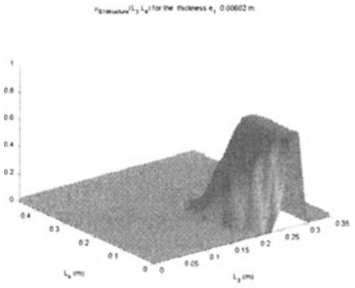

Figure 8 : Structural PoV /S1 (e_1 = 6mm)

Mass point of view for the system S2 PV4 : This PoV leads to the minimisation of the mass of the door. This door insures the tightness of the cockpit. Figure 9 depicts the best tendency that a candidate (L_3, L_4, e_2) has to satisfy the mass PoV of the system S2. The error is smaller than 0.01.

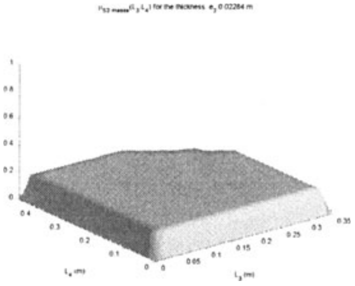

Figure 9 : Mass PoV S2 (e_2= 22.8 mm)

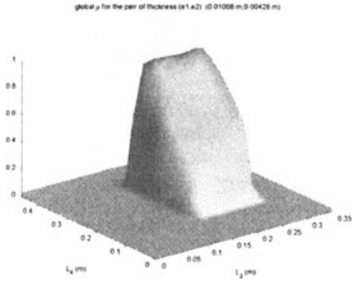

Figure 10 : Global membership function

Aggregating all Points of view : The global function of satisfaction μ_{glob} gives the global performance according to the design variables. At this stage, the network results of all the PoV are gathered, and aggregated according to relation (9). Figure 10 depicts the tendency of the global satisfaction function (e1=10 mm, e2 =4.2mm).

5. CONCLUSION

The global design problem is broken down in several sub-problems corresponding to every PoV or tasks. Our process succeeds in finding a solution domain with a global satisfaction of all the points of view. One can notice the ability of our approach to consider each aggregated satisfaction function as a macro point of view. It becomes a component of a new macro problem. We have proposed to solve this problem by using NN tools. Numerical results are obtained and compared to the sweep technique.

F. BENNIS, P. CHEDMAIL, O. HELARY, IRCCyN - U.M.R. CNRS 6597, ECN, 1 rue de la Noë, B.P. 92101 - 44321 Nantes Cedex 3 – France.

6. REFERENCES

[1] W. Hsu and I.M.Y. Woon, "Current research in the conceptual design of mechanical products", Computer Aided design, Vol 30, No 5, pp 377-389, 1998.
[2] G.Pahl & W.Beitz, "Engineering Design", The Council – London, Springer, 1995.
[3] M.Wooldridge, "Agent-based software Engineering", IEEE Proceeding in Software Engineering", 144(1): 26-37, Feb.1997.
[4] S.Rao, " Mutli-objective fuzzy optimization techniques for engineering design ", Computers & Structures, vol.42,n°.1,pp. 37-44, 1992.
[5] M.Sakawa, "Fuzzy sets and interactive multi-objective optimization", Plenum Press,New York, 1993.
[6] F. Féraille, P. Chedmail, "Concurrent Engineering : use of fuzzy logic », IDPT'96, 2nd World Conference on Integrated Design & Process Technology, 1-4 1996, Austin, Texas.
[7] E.K.Antonsson, "Imprecision in engineering design", Journal of mechanical design, vol.117 B, pp.25-32, 1995.
[8] K. E. Zanganeh and P.C. Hughes, "Fast Estimation of the Kinematics of the parallel Modules of a Variables-Geometry-Truss Manipulator Using Neural Networks", IEEE, Int. Conf. On Robotics and Automation, pp. 1665-1670, May 1999.
[9] L.A. Zadeh, " Fuzzy sets ", Information and Control, vol.8, pp.338-353, 1965.
[10] D.Dubois & M.Grabish, "Aggrégation multicritère et optimisation", Masson Paris, pp.179-199, 1994.
[11] Matlab "Optimization Toolbox and Neural Networks Toolbox", mathworks Inc., 1998.
[12] R.P. Lippman, An introduction to computing with neural nets, IEEE, ASSP Magazine, pp.4-22, 1987.
[13] F. D. Foresee & M. T. Hagan, Gauss-Newtown approximation to bayesian learning, Journal of International Conference on Neural Networks, vol. 8, pp. 1930-1935, 1997
[14] F.Bennis, P.Chedmail, O.Hélary, 1999, "Towards the Use of Fuzzy Approach in Mechanical Design", 3^{th} IEEE International conference on Intelligent Engineering Systems, Stara Lesna, Slovakia, November 1-3, pp. 363-368, 1999.

X. FISCHER, J.P. NADEAU, P. SEBASTIAN, P. JOYOT

QUALITATIVE CONSTRAINTS IN INTEGRATED DESIGN

Design support system in mechanical design

Abstract: Designers use mechanical calculus and their technical knowledge to give, propose and validate technical choices. Product perception and design reasoning are modeled using graphs. The knowledge used is defined through fuzzy-logic rules, qualitative analysis, analytical forms and reasoning is represented as a system of constraints. We give an example which aims at defining the technological choices of a lattice work of beams.

1. INTRODUCTION

Our objective is to lay the foundations of a mechanical design support system, from physical laws, expertise and know-how. In order to provide support for product design, we propose the concerted and simultaneous use of rules relating to:
- physical laws,
- design objectives,
- the knowledge of the state of the art,
- professional habits.

A number of studies detail a similar problem. First, some methods make it possible, from a formalisation of product perception, to find again already validated solutions. They integrate an expertise linked to computational principles. Next, they will make it possible to characterise the problem and match validated solutions. Modeling may be based on:
- a decomposition of the overall problem into substructures of local mechanical problems [1],
- a structuring of the different points of view about the product, so as to find again useful data —as regards mechanical behaviour [2]—,
- the use of characteristics identifying a specific point of view of the product (computational features [3]).

Moreover, related studies propose to use data bases to better direct computation and identify solutions, according to the behavioural objectives [4]. In all the methods proposed, only already validated design solution can be found again.

P. Chedmail et al. (eds.), Integrated Design and Manufacturing in Mechanical Engineering, 35-42.
©2002 *Kluwer Academic Publishers.*

Faltings [5] and Joskowicz [6] propose a particular formalism based on qualitative analytical principles integrating computational rules in the form of expertise. Sam [7] puts forward a different approach by only using mechanical analytical rules through a CSP method, and she obtains combinations of consistent values for product-characterising variables.

At last, some articles propose to resort to fuzzy logics, so as to use computational expertise to determine local solutions [8].

We have developed a kind of formalism enabling us to provide solutions from a system in which there are both theoretical and empirical rules.

The originality of our work lies in a double approach:

- reasoning is modeled as constraints: we can thus exploit a set of rules of diverse natures and resolve an under-constrained problem to favour creativity,
- knowledge is modeled through variables of very heterogeneous natures. We can then precisely characterise a viewpoint.

This original aspect builds up through a particular design logic corresponding to an Inverted Integrated Design (IID) [9] approach.

2. THE DESIGN APPROACH: AN INVERTED APPROACH

In a conventional design approach (figure 1), actors have at their disposal their professional habits and their knowledge of the state of the art. They thus produce a priori existing elements which enable them to generate models and results. The latter are validated according to their level of cohesion with the objectives defined in the specifications. Invalidity requires backtracking, which causes the current ponderousness of design processes. Our vision, called Inverted Integrated Design process (IID), is a design methodology defined to avoid iterative cycles in design process. Initially, we have some professional habits, our knowledge of the state of the art and behavioural objectives. We do not use the objectives at the end of the process, but as properties which combine with related rules and allow us to determine the solutions. Then, the logic developed from an expression of the knowledge and the very objectives provides models associated with the results. Confrontation with the specifications is no longer necessary since the objectives turn out to be the foundations of designing (figure 1).

IID puts forward the notion of integrated engineering. In particular, we introduce the notion of computation integration [10]. Computation intervenes as rules, at any moment in design, either to direct solutions (i.e., synthesis activity), or to avoid outlier evaluations: concepts are validated on line. Therefore, our approach differs from the conventional sequential [11] and iterative approach which requires a validation of all the concepts put forward, in particular using numerical computation.

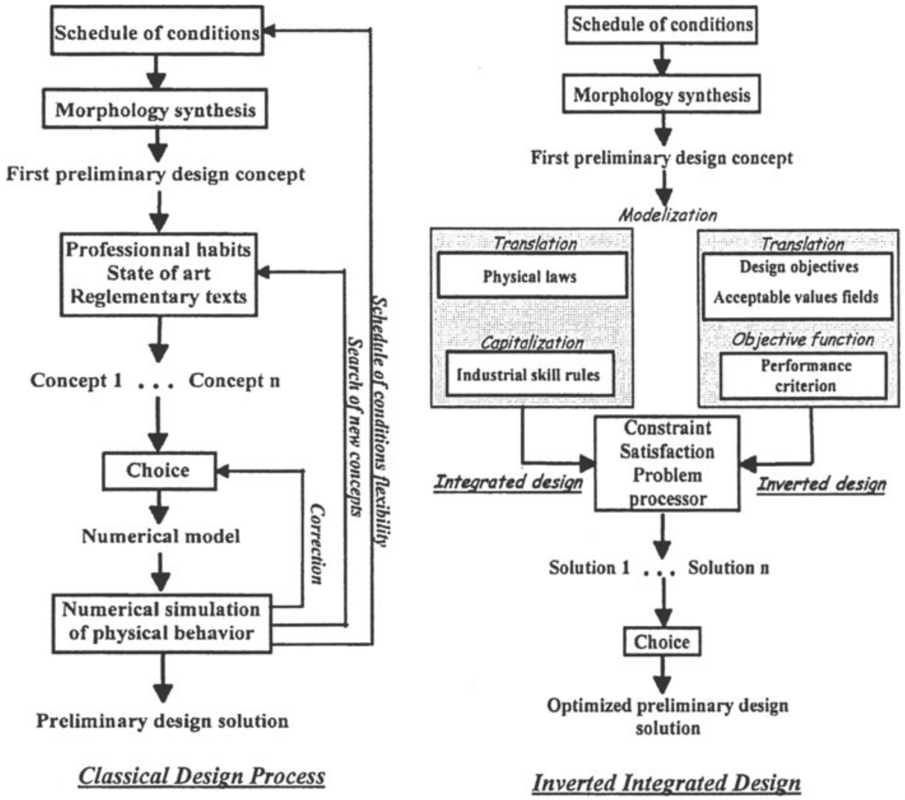
Schedule of conditions
Morphology synthesis
First preliminary design concept
Professionnal habits
State of art
Reglementary texts
Concept 1 . . . Concept n
Choice
Numerical model
Numerical simulation of physical behavior
Preliminary design solution
Correction
Search of new concepts
Schedule of conditions flexibility
Classical Design Process
Schedule of conditions
Morphology synthesis
First preliminary design concept
Modelization
Translation
Physical laws
Capitalization
Industrial skill rules
Translation
Design objectives
Acceptable values fields
Objective function
Performance criterion
Constraint Satisfaction Problem processor
Integrated design
Inverted design
Solution 1 . . . Solution n
Choice
Optimized preliminary design solution
Inverted Integrated Design

Figure 1. Inverted Integrated Design approach, in comparison with conventional approach.

3. DIFFERENT KINDS OF KNOWLEDGE FOR ADAPTED MODELING

People acting in the design process have a perception of the product. Some product-related knowledge is taken up once again through variables. Each variable value is assigned or has to be instanciated.

Problem-characterising variables may bear imposed values, relating to the functions defined by the specifications or the industrial context. Otherwise, they are to be evaluated. But the initial perception of the product may be highly incomplete, and although some values be established, this establishment cannot be precise. Furthermore, providing solutions from a kind of knowledge which is —incidentally— rather impreciSed, requires proposing a certain flexibility, as for the technological solutions put forward. Therefore, we had to establish an adapted kind of modeling which would consider this imprecise aspect, regarding both the initial values and the values to be provided.

In our modeling, four sorts of variables are considered:

- numerical-value variables: possible values for these variables are strict real values a (equation 1),

$$a \in IR \tag{1}$$

- linguistic-value variables: variables assume values a in discrete domains, in which each variable carries a linguistic notion (equation 2),

$$a \in \{characterization_1, \ldots, characterization_n\} \tag{2}$$

- qualitative-value variable [12],[13]: this kind of modeling provides a certain flexibility at the level possible values. The values a assumed by a variable is a bounded numerical interval [14] (equation 3),

$$a \in \{[a,b],\ a \in IR,\ b \in IR,\ [a,b] \subset IR\} \tag{3}$$

- fuzzy-value variables [15]: variables assume numerical values a associated to a level of membership μ_T to a variable-characterising linguistic notion T (equation 4).

$$\tilde{a} = \begin{cases} a \in IR \\ \mu_T(a)\ \%\ \text{of acceptability} \\ T = \text{'}characterization\text{'} \end{cases} \tag{4}$$

4. CONSTRAINTS OF HETEROGENEOUS NATURES FOR REASONING MODELING

Variables are linked together by elementary algebraic rules called constraints. The set of constraints makes up global design reasoning. As a result, designing boils down to assigning values to variables —when unassigned—, while satisfying all the constraints. A constraint-based problem is any problem in which

- a family of n variables $V = \{V_1, \ldots, V_n\}$ assuming their values in n continuous or discrete domains $D_1, \ldots, D_n$,
- a set of p constraints $C = \{c_1, \ldots, c_p\}$ that are continuous algebraic relations or discret relations specifying rules.

Variables are linked together by constraints. The problem is said to be consistent if the variables V_i assume values a_i which satisfy all the constraints. In order to determine consistent values, a constraint-satisfaction problem (CSP) is set up.

Three kinds of constraints have to be distinguished:

- computational constraints: a computational constraint is a (equality or inequality) continuous constraint, linking variables having values in continuous domains, or mixed constraints linking variables having values in discrete or continuous domains. Computational constraints define physical laws,

- design constraints: a design constraints is a mixed constraint or a discrete constraint, when panel of technological element have to be declared. Design constraints determine industrial skill rules, reglementary texts and design objectives,
- expertise constraints: an expertise constraint is a mixed constraint including a fuzzy value. An expertise constraint specifies the rules orientating value selection and possible value combinations. This kind of constraints boils down to a single constraint characterised by an objective function. The objective function defines the performance level of e design solution (equation 5).

$$\tilde{F}_o = \begin{cases} F_o = \sum_i k_i \frac{V_i}{V_i^0} \quad F_o \in IR \\ \mu_T(F_o) = \begin{cases} 1 - F_o \quad \text{if } F_o \in [0,1] \\ 0 \ \mathit{if} \ F_o \in [-\infty,0] \cup [1,+\infty] \end{cases} \\ T = \text{'}\mathit{performant}\text{'} \end{cases} \tag{5}$$

Implicated variables V_i evaluate the level of performance of the product, for i viewpoints. These variables are compared to reference values V_i^0. Since all the evaluation criteria cannot be equally important in design, we link an importance weight k_i ($\Sigma\ k_i=1$) to each point of view. The values of point-of-view variables must be an evolution of the reference values.

An evolution from reference values justifies that $F_0 \leq 1$. Thanks to this condition, it is possible to assign values to the design parameters; the latter will then direct other-variable assignment, through the network.

5. OUR APPROACH: AN OVERALL LOGIC, FOR THE SPECIFICATIONS TO THE DESIGN SOLUTIONS

Inverted Integrated Design approach includes a methodology that leads to the reasoning models necessary to search design solutions. This methodology is build through three steps:

- First step of the logic: product perception: it consists in identifying product perception and related knowledge,
- Second step of the logic: the second step of our approach aims at specifying constraints and their dependencies. First, industrial expressed rules are capitalized as constraints. In another hand, the translation of schedule of conditions leads to acceptable values fields specifications of several variables. Finally, we build the objective function. At this stage, an evaluation of materiality between the different

evaluation points of views is required. Weights are thus associated to each objective parameter of the design-evaluation vector. The objective function measures conceptual evolution, according to a reference case. In an optimisation phase, we take, as reference case, the best solution expected and given by engineers. We thus ensure once again to go forward in value assignment (the progression level is measured thanks to the objective function),

- Third step of the logic: generation of design solutions; once the identified kinds of knowledge and reasoning have been established, we use a particular technique, namely a constraint-satisfaction technique to obtain the consistent solutions. These solutions correspond to combinations of values satisfying all the constraints, at possibly different priority levels. Solutions are assigned a degree of satisfaction which depends on fuzzy values and relative degrees of priority between constraints.

6. THE CSP PROCESSOR

We have a particular model-building a system that sets in situation equations of very heterogeneous natures —discrete or continuous natures— implicating variables of diverse values —fuzzy, qualitative, numerical, linguistic values. The resolution method we use consists in combinatory tests. It is called a constraint-satisfaction problem or CSP. The CSP technique, which enables us to determine solutions, meets our expectations since both the use of very heterogeneous constraints and variables. Eventually, we obtain a set of solutions which correspond to combinations of values compatible between one another. Furthermore, solutions are provided with a level of satisfaction. We propose solutions in a flexible manner, thus giving free expression to creativity, as far as design is concerned: we only propose an orientation towards consistent values. This vision differs from numerical methods in the sense that not a single and unique value is proposed.

This provides reasoning with a certain modularity: modifying, removing or adding rules is made easy.

7. A SIMPLE APPLICATION: DESIGN OF A LATTICE OF BEAMS

We design a lattice of beam. We want to determine the shapes and dimensions of the beams as well as their constituting materials, while limiting the overall mass of the product, and the displacement of node 3 (figure 2).

As for the expertise criterion, we only used the overall mass M of the structure and the displacement U of node 3 (equation 6). We could have integrated other points of view such as realisation cost. The use of a catalogue of beams and cables directs the results. Two solutions have been found (table 1).

$$F_o = k\frac{U}{6.10^{-3}} + (1-k)\frac{M}{256} \qquad (6)$$

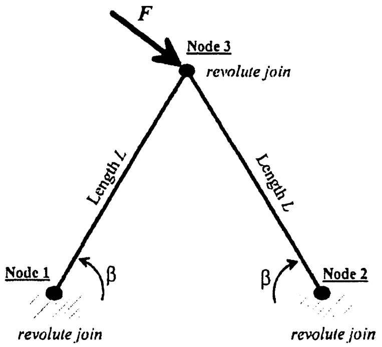

Figure 2. The lattice of beams to design.

	Reference case	*Solution 1*	*Solution 2*
Beam 1		Cable ⊘ 3110^{-3} m	IPE80 - Titanium
Beam 2		IPE180 - Titanium	IPE180 - Titanium
Displacement of node 3	6.10^{-3} m	$2.535.10^{-3}$ m	$2.462.10^{-3}$ m
Beams average strain		0.041%	0.040%
F_o		0.277	0.222
Mass	256 kg	70.917 kg	56.730 kg

Table 1. Solutions found for the design problem.

The tension beam (element 2) has very small sections (cable or IPE80). They are the smallest sections of the selection available. It is possible to lighten the system by developing the catalogue with even smaller section elements. Regarding the compression beam (element 4), in both solutions, a similar solution is obtained: an IPE180 beam. In fact, the system has selected the smallest section to prevent buckling and plasticity: design constraints have thus played their part.

8. CONCLUSION AND WAY AHEAD

We have built a specific model of knowledge and reasoning in mechanical-product designing. Through our approach, which characterises the resolution of an inverse problem, we have integrated mechanical computation as well as expert rules and design constraints. Although the problem is under-constrained, constraint-based reasoning systems have allowed us to determine solutions, from rules and kinds of knowledge both of very heterogeneous natures.

For our constraint-satisfaction problem, we resorted to the Conflex environment [16]. This environment only enables us to resolve static problems. We apply IID to pressure apparatus design [17], aeronautical systems design and snowboard design.

9. REFERENCES

1. D. Constant. Contribution à la spécification d'un modèle fonctionnel de produits pour la conception intégrée de systèmes mécaniques [Phd thesis]. Grenoble (France): Université Joseph Fourier, 1996.
2. A. Ben Amara. Contribution à l'intégration de la composante calcul dans une démarche de conception fonctionnelle intégrée [Phd thesis]. Valenciennes (France): Université de Valenciennes, 1998.
3. N. Ifaoui and D. Deneux. Conception à base de caractéristiques de calcul. Proceedings of MICAD 99, 1999 Feb 9-12; Paris . 1999.
4. N. Troussier, F. Pourroy, M. Tollenaere, and B. Trébucq. Mechanical models management in engineering design. Proceedings of IDMME 98; 1998. Compiègne (France), 1998.
5. B. Faltings. A symbolic approach to qualitative kinematics in Artificial Intelligence Journal. Elsevier 1992; 56:139–170.
6. L. Joskowicz and E. Sacks. Computational kinematics in journal of mechanical design. ASME 1995; 117.
7. D. Sam Haroud. Constraint consistency techniques for continuous domains intégrée [Phd thesis]. Lausanne: Ecole Polytechnique fédérale de Lausanne, 1995.
8. F. Féraille and P. Chedmail. Conception intégrée et logique floue. Proceedings of 5ième colloque PRIMECA sur la conception mécanique intégrée; 1997. La Plagne (France). 1997.
9. X. Fischer, P. Sébastian, J.P. Nadeau and P. Joyot. Inverted Integrated Design. Proceedings of CPI'01; 2001 Oct 24-26. Fes (Morocco), 2001.
10. F. Pourroy, L. Remondini, B. Yannou, and P. Clozel. Modèles de comportements. In M. Tollenaere, editor. Conception de produits mécaniques ; méthodes, modèles et outils. Paris: Hermés, 1998:347–396.
11. J.C. Bocquet. La capitalisation intégrée du produit, du process et de l'organisation: modèle global et outils. Proceedings of Séminaire PROSPER; 1998 Dec 17; Grenoble (France). Grenoble: INPG, 1998.
12. B.J. Kuipers. Qualitative simulation in Artificial Intelligence Journal. Elsevier 1986; 29:289–338.
13. L. Travé Massuyès, P. Dague, and F. Guerrin. Le raisonnement qualitatif. Paris: Hermés, 1997.
14. L. Granvilliers. On the combination of interval constraint solvgers in Reliable Computing. Kluwer Academic Publishers 2001; 7(6):467-483.
15. X. Fischer, J.P. Nadeau, C. Merlo and P. Joyot. Aide à la décision en conception mécanique intégrée par contraintes qualitatives. Proceedings of IDMME 2000; 2000 May 17-19. Montreal, 2000.
16. J.P. Rellier. Con'Flex Manuel de l'utilisateur [technical manual]. Toulouse (France): INRA. Laboratoire de biométrie et d'intelligence artificielle, 1998.
17. X. Fischer, P. Joyot, B. Bourseau, P. Sébastian and J.P. Nadeau. Pressure equipment design tool: application to a parallelepipedic oven. Proceedings of ESOPE'01; 2001 Oct 22-25. Paris, 2001.

10. AFFILIATIONS

Xavier Fischer, Pierre Joyot
Laboratoire en Ingénierie des Processus et des Services Industriels (LIPSI), Technopole Izarbel, 64210 Bidart –France, Tel.: 33 559 438 469, Fax: 33 559 438 401, E-mail: {x.fischer,p.joyot}@estia.fr

Jean-Pierre Nadeau, Patrick Sébastian, Laboratoire Énergétique et Phénomènes de Transfert - UMR CNRS 8508, ENSAM Esplanade des Arts et métiers, 33405 Talence cedex – France, Tel.: 33 556 845 428, Fax: 33 556 845 401, E-mail: {nadeau,sebas}@lept-ensam.u-bordeaux.fr

F. LIMAYEM, B. YANNOU

HANDLING IMPRECISION IN PAIRWISE COMPARISON

For better group decisions in weighting

Abstract. The present paper describes an original contribution to handling imprecision in multi-criteria group decision making. Based on Monte Carlo simulation, this approach allows the generalization of any deterministic pairwise comparison method. Furthermore, it extends the practical interest of the pairwise comparison concept to a wider variety of inputs. For instance, it can provide a useful aid in concurrent engineering.

1 INTRODUCTION

Most of the multi-criteria decision making approaches consist in ranking or weighting a set of n alternatives with regards to a set of m criteria. Among the existing methods, the pairwise comparison approach considers a single criterion (for the comparison) and proceeds by comparing each pair of alternatives in order to reduce the difficulty of the problem. In the context of priority theory, Saaty generalized the basic approach (limited to one criterion) to a set of m criteria in a two step method. First, the m criteria are weighted according to a principal objective. Then, the n alternatives are weighted according to each criteria. This procedure leads to global alternative weights. Furthermore, in decision making problems, imprecision is usually a key element. It can arise from different causes such as uncertainty, incomplete knowledge or choice subjectivity. The concurrent engineering environment is typically representative of such a situation since different decision makers (with different skills and knowledge) are involved at different stages of the design process in order to handle different alternatives (strategic decision criteria, costs, customer preferences, gravity of event consequences and so on).

The following work addresses the issue of imprecision assessment in multi-criteria decision making environment via the pairwise comparison approach. After a brief recall of the essential concepts and a review of several contributions to the problem, the next section is dedicated to the presentation of a Monte Carlo simulation approach. In section 4, a numerical example and comments illustrate the performances of the Monte Carlo Pairwise Comparison algorithm. Eventually, in the conclusion, future research perspectives and industrial engineering design utilities are presented.

P. Chedmail et al. (eds.), Integrated Design and Manufacturing in Mechanical Engineering, 43-52.
©2002 *Kluwer Academic Publishers.*

2 BACKGROUND

In the following paragraphs, a brief presentation of two deterministic approaches, respectively based on eigen value analysis and logarithmic least squares regression, is followed by a critical review of several generalizations in order to handle imprecision.

2.1 Deterministic[1] pairwise comparison approaches

When applied to a set of n alternatives {a1,..an} with respect to a single criterion, the basic pairwise comparison approach requires n^2 weight ratios estimation, as shown in figure 1. Furthermore, if the symmetric comparisons are inverse of each other ($c_{ij} \cdot c_{ji} = 1;\ i,j = 1..n$), only $n(n-1)/2$ pairwise comparisons are required and the pairwise comparison matrix is called reciprocal.

$$
\begin{array}{c|cccc}
 & a_1 & a_2 & \dots & a_n \\
\hline
a_1 & c_{11} & c_{12} & \dots & c_{1n} \\
a_2 & c_{21} & c_{22} & \dots & c_{2n} \\
\vdots & \vdots & \vdots & \dots & \vdots \\
a_n & c_{n1} & c_{n2} & \dots & c_{nn}
\end{array}
\quad , \quad where\ c_{ij} \approx \frac{w_i}{w_j}
$$

Figure 1. Pairwise comparison matrix.

In order to compute the weight of each alternative it is necessary to consider the consistency of the pairwise comparison matrix. A comparison matrix is called consistent if the transitivity condition $c_{ik} \cdot c_{kj} = c_{ij}$ is verified for $i,j,k = 1,..n$.

2.1.1 Approach based on eigen value analysis

When the pairwise comparison matrix is reciprocal, the maximal eigen value is real positive and the corresponding eigen vector has real positive components. Saaty's approach [6] computes the weights vector as the eigen vector associated to the maximal eigen value λ_{max}.

2.1.2 Approach based on logarithmic least squares regression

The previous method requires exactly one comparison per pair of elements. In the case of multiple decision makers or missing data in the pairwise comparison matrix, De Graan [4] and Lootsma [5] propose an approach based on logarithmic least squares regression that leads to a weight vector estimation, unless the missing data result in a non resolvable system of equations. In their contribution, they assume the non empty symmetric comparisons to be inverse of each other.

---

[1] In this chapter, a "deterministic pairwise comparison method/algorithm" is a method that does not handle imprecision.

Let c_{ijk}, $i=1,..n;\ j=i+1..n;\ k=1,..d_{ij}$, represent the comparison of the k^{th} decision maker on the pair of alternatives (i,j). The logarithmic transformation is useful to set a linear relation between the comparisons ($c_{ijk} \approx w_i / w_j$) and the corresponding weights.

Minimizing the regression function, in the least squares sense (Euclidean norm), leads to the normal equations described in equation 1.

$$\theta_i \sum_{j\neq i}^{n} d_{ij} - \sum_{j\neq i}^{n} d_{ij}\theta_j = \sum_{j\neq i}^{n}\sum_{k=1}^{d_{ij}} \ln(c_{ijk}), \quad \mathrm{i}=1,..\mathrm{n} \text{ where } \theta_t = \ln(w_t), \quad \mathrm{t}=1,..\mathrm{n}. \tag{1}$$

These normal equations are linearly dependent, since the weights can be determined up to a multiplicative factor. To eliminate this linear dependency, one weight is set to an arbitrary value (extra condition). Then the resulting weights are normalized, in order to add up to one. In the case of missing comparisons, this estimation remains possible as long as the normal equations system rank equals $n-1$. This condition is equivalent to the following: each alternative is involved in at least one comparison and no disjoint (in the transitivity sense) sets of comparisons can be identified.

For exactly one opinion (decision maker) per binary comparison, the resulting solution is equivalent to a normalized geometric mean (see equation 2).

$$w_{\mathrm{i}} = \frac{r_i}{\sum_{i=1}^{n} r_i}, \quad \mathrm{i}=1,..\mathrm{n}; \text{ where } r_i = \left(\prod_{j=1}^{n} c_{ij} \right)^{1/n} \tag{2}$$

2.2 Handling of imprecision in pairwise comparison approaches

Van Laarhoven and Pedrycz [7], presented a fuzzy extension of the logarithmic least squares approach of De Graan and Lootsma by considering each comparison as a triangular fuzzy number $\tilde{c}_{ijk}$.

The triangular membership function (see figure 2) assigns to each comparison value a membership degree that ranges in [0,1] and expresses a qualitative scale of "precision". The membership function is defined by three points: a lower value (c_{ijkl}), a modal value (c_{ijkm}) and an upper value (c_{ijku}).

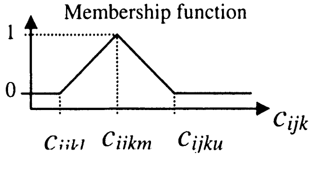

Figure 2. Triangular fuzzy number.

The corresponding least squares logarithmic regression function (to minimize) is presented in equation 3.

$$\sum_{i=1}^{n}\sum_{j=i+1}^{n}\sum_{k=1}^{d_{ij}}\left(\begin{array}{l}\left\{\ln(c_{ijkl})-\ln(w_{il})+\ln(w_{ju})\right\}^2\\+\left\{\ln(c_{ijkm})-\ln(w_{im})+\ln(w_{jm})\right\}^2\\+\left\{\ln(c_{ijku})-\ln(w_{iu})+\ln(w_{jl})\right\}^2\end{array}\right) \qquad (3)$$

The normal equations derived from triangular fuzzy algebraic operations are given by equation 4.

$$\begin{aligned}\theta_{il}\sum_{j\neq i}^{n} d_{ij}-\sum_{j\neq i}^{n} d_{ij}\theta_{ju}&=\sum_{j\neq i}^{n}\sum_{k=1}^{d_{ij}}\ln(c_{ijkl}),\quad \mathrm{i}=1,..\mathrm{m}\\ \theta_{im}\sum_{j\neq i}^{n} d_{ij}-\sum_{j\neq i}^{n} d_{ij}\theta_{jm}&=\sum_{j\neq i}^{n}\sum_{k=1}^{d_{ij}}\ln(c_{ijkm}),\quad \mathrm{i}=1,..\mathrm{m} \qquad (4)\\ \theta_{iu}\sum_{j\neq i}^{n} d_{ij}-\sum_{j\neq i}^{n} d_{ij}\theta_{jl}&=\sum_{j\neq i}^{n}\sum_{k=1}^{d_{ij}}\ln(c_{ijku}),\quad \mathrm{i}=1,..\mathrm{m}\end{aligned}$$

Boender et al. [1] proved that the normalization procedure used by Van Laarhoven and Pedrycz produces a loss of optimality and propose the procedure given by equation 5.

$$\begin{pmatrix} w_{il}\\ w_{im}\\ w_{iu}\end{pmatrix}=\begin{pmatrix}\dfrac{\exp(\theta_{il})}{\left(\sum_{j=1}^{n}\exp(\theta_{jl})\cdot\sum_{j=1}^{n}\exp(\theta_{ju})\right)^{1/2}}\\ \dfrac{\exp(\theta_{im})}{\sum_{j=1}^{n}\exp(\theta_{jm})}\\ \dfrac{\exp(\theta_{iu})}{\left(\sum_{j=1}^{n}\exp(\theta_{jl})\cdot\sum_{j=1}^{n}\exp(\theta_{ju})\right)^{1/2}}\end{pmatrix},\ \mathrm{i}=1,..\mathrm{n} \qquad (5)$$

In spite of this correction, the normalized values can violate the condition "lower value ≤ modal value ≤ upper value". This drawback is avoided by Buckley's contribution [2], which requires an analytical expression of the resulting weights. For example, when applied to equation 2 (exactly one opinion per binary comparison), his method generalizes the variables of the right part of the equation to trapezoidal fuzzy numbers. The corresponding left part terms (weight) are derived from fuzzy algebraic operators application. This approach was subject to criticism since the resulting weights were less accurate than those given by the extended logarithmic regression approach.

From the perspective of handling imprecision it does not seem obvious that providing the sharpest weights is the best way of answering the question, even if this allows for a better discrimination of the criteria. Actually, intrinsically different inference mechanisms can be used to map from the input to the output imprecision, for instance the "fuzzy regression" inference used by Boender et al. versus the fuzzy max-min extension principle used by Buckley. When two different mechanisms are compared it is important to consider the specificity of each before comparing the results.

In the following section, a probabilistic inference mechanism is presented.

3 THE MONTE CARLO PAIRWISE COMPARISON

From a probabilistic viewpoint, handling imprecision is expressed in terms of uncertainty and differs from the concept of membership degree used in the theory of fuzzy sets. Actually, it seems more difficult to express or interpret imprecision in terms of likelihood than in terms of fuzziness. For instance it is easier to say that a given comparison value has a "precision" membership degree of 0.5 than to estimate its frequency of occurrence relatively to all the possible comparison values. In order to enhance the interpretability of both input and output values, in a probabilistic approach, Wood et al. [8] propose a reversible mapping from a [0,1] scaled function to a probability density function. This transformation affects the representation of both input and output variables but not the inference mechanism which remains probabilistic.

3.1 Relevance of the Monte Carlo method

By considering each pairwise comparison as a random variable defined by its probability density function (pdf), it is possible to sample a set of input values (one from each comparison) and map to a set of output values (one for each alternative weight) by any deterministic pairwise comparison approach. This is the main idea underlying the use of a statistical approach. The conventional (analytical) assessment of such multi-dimensional integrals is computationally expensive, moreover it is restricted to specific classes of functions (sufficiently smooth). The Monte Carlo methods involve statistical process to solve various problems of computational mathematics. It is particularly efficient in estimating multi-dimensional integrals [3].

As detailed in the literature review, the extension of pairwise comparison approaches to handle imprecision is mainly based on the theory of fuzzy sets and limited to a generalization of the logarithmic least squares approach, as well as those which allow an explicit analytical expression of the solution. In the following paragraphs, a Monte Carlo based approach is proposed to extend any deterministic pairwise comparison.

3.2 Monte Carlo statistical process

The pairwise comparisons c_{ijk}, $i=1,..n$; $j=1,..n$; $k=1,..d_{ij}$, are considered as random variables (represented by a lower case letter), with possible missing or multiple data (variable number of opinions per pairwise comparison) and even non reciprocal comparison matrix.

The basic statistical process consists in sampling a value C_{ijk} (represented by a capital letter) from each available comparison c_{ijk} and mapping, by any appropriate deterministic pairwise comparison approach, to the resulting set of weights $\{W_i, i=1,..n\}$ on the corresponding random variables $\{w_i, i=1,..n\}$. After N iterations, a distribution of N points is obtained for each weight w_i. The corresponding probability density function (pdf) can be approximated by a frequency distribution.

The plausibility (probability) p of a given range $[W_{i_1}, W_{i_2}]$ on the weight w_i is expressed as the ratio of the corresponding area under the pdf (limited by $[W_{i_1}, W_{i_2}]$) to the overall area under the pdf. In order to estimate p, let "A" be the following event: "the value W_i, resulting from the statistical process, falls in the interval $[W_{i_1}, W_{i_2}]$". Among the N iterations, the occurrence frequency of event "A" is a random variable whose mathematical expectation equals p. The Monte Carlo approach provides a satisfactory approximation (in a reasonable time) when the probability p is not too small. In order to achieve a maximal relative error of r while estimating p, the required number of iterations is given by equation 6.

$$N \approx \frac{9(1-p)}{pr^2} \qquad (6)$$

3.3 MCPC algorithm

3.3.1 Global description

The Monte Carlo Pairwise Comparison algorithm applies to any deterministic pairwise comparison approach with a convergence order of $1/\sqrt{N}$, for N iterations.

Inputs :

- Pairwise comparisons defined by their pdf. If the comparison matrix is reciprocal only $n(n-1)/2$ comparisons are required.
- Monte Carlo sampling parameters: r and p.

Outputs :

- Alternative weights defined by their approximated pdf.
- Most plausible weight value of each alternative, associated to an estimation of the absolute error.
- Overall consistency estimator.
- Most inconsistent comparisons and the corresponding way of change (decrease/increase) in order to improve the overall consistency.

The Monte Carlo Pairwise Comparison algorithm consists in 4 steps :

1. random generation of N comparison matrices,

2. computation of the resulting N component weight vectors,
3. pdf approximation and smoothing of weight,
4. consistency analysis.

The first two steps are respectively illustrated in sections (3.2) and (2.1). Step 4 is not detailed in this chapter, while step 3 is briefly described in the following.

3.3.2 pdf approximation and smoothing of weight

The pdf approximation and smoothing of the weight is achieved by a kind of moving average. Within the set of N values obtained for a given alternative weight, let a window represent a subset of consecutive weight values corresponding to a certain density. Each point of the approximated pdf curve, defined by its x and y coordinates, is representative of a window whose density equals p (the Monte Carlo estimated probability). The x-coordinate of a point on the estimated pdf curve is computed as the average weight in the corresponding window (with relatively great accuracy according to the Central Limit Theorem). The y-coordinate is computed as the ratio of the density (p) of the corresponding window to the window width. The resulting value represents the window average ordinate. This measure is given with a maximal relative error of r (the Monte Carlo relative error). For a tight enough window and a smooth enough pdf portion, the computed y-coordinate is a satisfactory/reliable estimate of the x-coordinate pdf image.

For given parameters p and r, equation 6 helps in estimating the required weight sample size N.

The modal weight value estimation (most plausible value) is exposed to two main error types: the relative error r on the y-coordinate and the absolute error on the x-coordinate. The absolute error is dominated by half the corresponding window width if no other maximums exist within the same window, which is usually the case for sufficiently small p values. This assumption holds for any p if the comparison pdf accepts only one maximum (i.e. triangular comparison pdf). Low y-coordinate points are estimated with less accuracy than high ones. Indeed, for a given p, the corresponding window is larger than that of the modal value, which leads to low accuracy estimation for the reasons mentioned above. Hence, the extremities of the weight distribution, corresponding to the null y-coordinate, cannot be estimated. The same problem occurs for a wide weight distribution since a given p corresponds to a larger window than that of a narrow distribution. Consequently, a given accuracy level is more time consuming for low y-coordinates or wide distributions. This can be considered as the main limitation of such an approach.

4 NUMERICAL RESULTS

For the MCPC approach, the results presented in this section correspond to a maximal relative error (r) of 5% and different values of the Monte Carlo estimated probability (p).

The computations were performed on a Pentium III PC with a double 350 Mhz processor. For 1000 sampling on one comparison pdf, the required computational time is about 2 cpu seconds. This value is not steady. It slowly increases as a function of the sample size *N*. Still, this value is over estimated and can be decreased with a better optimization of the algorithm computational time.

4.1 Comparison with existing methods

First, the Monte Carlo pairwise comparison is tested on an example from the literature, published by Boender et al. [1] in the context of ranking three candidates for a professorship in operations research. The procedure involves both multiple decision makers and triangular imprecision handling functions. Only one comparison matrix (out of four in the original problem), respectively related to the criteria "Mathematical creativity" (see figure 3) is considered in this section.

	a_1	a_2	a_3
a_1	(1,1,1)	$(\frac{2}{3},1,\frac{3}{2})$ $(\frac{2}{3},1,\frac{3}{2})$	$(\frac{2}{3},1,\frac{3}{2})$ $(\frac{2}{5},\frac{1}{2},\frac{2}{3})$
a_2	$(\frac{2}{3},1,\frac{3}{2})$ $(\frac{2}{3},1,\frac{3}{2})$	(1,1,1)	$(\frac{2}{5},\frac{1}{2},\frac{2}{3})$
a_3	$(\frac{2}{3},1,\frac{3}{2})$ $(\frac{3}{2},2,\frac{5}{2})$	$(\frac{3}{2},2,\frac{5}{2})$	(1,1,1)

Figure 3. "Mathematical creativity" comparison matrix.

The MCPC extension of the deterministic Logarithmic Least Squares approach (MCLLS) is compared to the fuzzy logic based extension proposed by Boender et al. (BLLS). The results are detailed in table 1. The Monte Carlo algorithm provides a sound estimation of the weights imprecision. Its results are inherently less accurate and computationally more expensive than those of the approach based on the fuzzy sets theory. Nevertheless, acceptable accuracy levels can be attained within a reasonable time on the modal value. The weight distribution extremities have very low accuracy (as discussed in 3.3.2). The differences observed on the modal weight values, between the approach based on "fuzzy regression" and that based on "probabilistic regression", arise from the conceptual differences underlying both inference mechanisms. Similar differences can be observed between the probabilistic inference and the fuzzy max-min extension principle, as explained by Wood et al. [8].

The next example illustrates the robustness of the probabilistic approach for its ability to handle a wide variety of inputs. None of the methods described in the literature review can deal with such an example, though it is inspired from a realistic decision making context.

4.2 Experimentation of an original comparison matrix

The second example involves a comparison matrix with missing data and histogram imprecision representation. Such inputs can easily be obtained in practice from Group decision making methods, such as the DELPHI approach. The computation corresponds to a maximal relative error (*r*) of 5% and a Monte Carlo estimated probability (*p*) of 10%. The comparison matrix is presented in figure 5 while the resulting weights and consistency analysis are illustrated in figure 6. Both figures are captures of an existing MCPC tool developed on MATLAB® 5.3.

Table 1. *Comparison with existing methods.*

	MCLLS (r=5%,p=20%)	MCLLS (r=5%,p=10%)	BLLS
a1	(24.05 , 30.15±0.53 , 39.40)	(23.53 , 30.10±0.29 , 39.93)	(22.87 , 28.91 , 36.97)
a2	(21.78 , 26.90±0.40 , 34.62)	(21.51 , 26.86±0.23 , 33.99)	(22.70 , 26.51 , 31.58)
a3	(31.77 , 42.66± 0.66, 50.01)	(32.40 , 42.71±0.37 , 50.03)	(40.16 , 44.58 , 48.10)
time	202 cpu seconds	539 cpu seconds	0.016 cpu seconds
N	16000	32000	

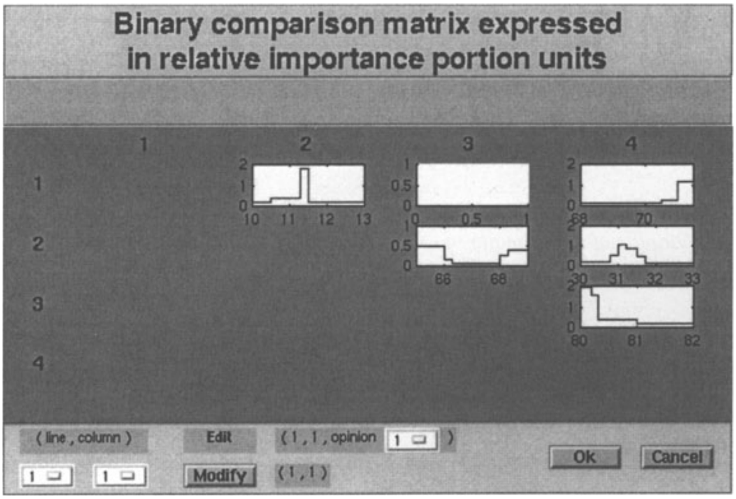

Binary comparison matrix expressed
in relative importance portion units

Figure 4. *Original comparison matrix.*

5 CONCLUSION

The MCPC algorithm presented in this paper allows the weighting of a set of alternatives in a multi-criteria decision making context.

The algorithm is suitable to easily extend any existing deterministic pairwise comparison approach in order to handle imprecision from a probabilistic inference angle. Compared to existing methods it can handle a wider variety of inputs.

Furthermore, it offers simple but interesting interactive utilities that help in reducing inconsistency, in group decision making, by pointing to the most inconsistent comparisons. Such utilities can be very useful in team oriented engineering design (i.e. concurrent engineering, value analysis).

A more general application of the Monte Carlo approach, to handle imprecision in engineering design is currently studied. The approach extends some aspects of Value Analysis in order to assess the adequacy between needs and design alternatives since the earliest stages of the design process [9].

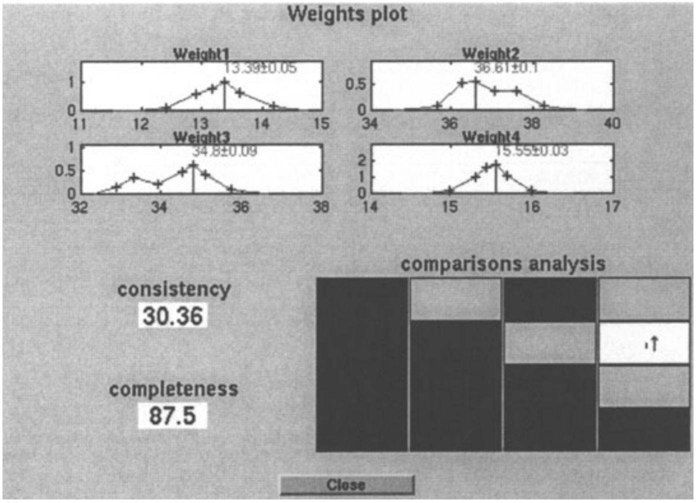

consistency
30.36

completeness
87.5

Figure 5. *Outputs of the example "experimentation of an original comparison matrix".*

6 REFERENCES

[1] C. G. E. Boender, et al., "Multi-criteria decision analysis with fuzzy pairwise comparisons," *Fuzzy Sets and Systems*, vol. 29, pp. 133 - 143, 1989.

[2] J. J. Buckley, "Fuzzy hierarchical analysis," *Fuzzy sets and systems*, vol. 17, pp. 233-247, 1985.

[3] N. P. Bushlenko, et al., *The Monte Carlo Method - The Method of Statistical Trials*, vol. 87, 1966.

[4] J. G. De Graan, "Extensions to the multiple criteria analysis of T. L. Saaty," Report National Institute of Water Supply, The Netherlands, 1980.

[5] F. A. Lootsma, *Performance evaluation of nonlinear optimization methods via multi-criteria decision analysis and via linear model analysis*, vol. 1, M.J.D. Powell ed. London, 1982.

[6] T. L. Saaty, "A scaling method for priorities in hierarchical structures," *Journal of Mathematical Psychology*, vol. 15, pp. 234-281, 1977.

[7] P. J. M. van Laarhoven and W. Pedrycz, "A fuzzy extension of Saaty's priority theory," *Fuzzy sets and systems*, vol. 11, pp. 229-241, 1983.

[8] K. L. Wood, et al., "Comparing fuzzy and probability calculus for representing imprecision in preliminary engineering design", presented at Design Theory and Methodology, Montreal, CANADA, pp 99-105, 1989.

[9] B. Yannou et al, "La méthode SPEC : suivi de performances en cours de conception", accepted at the 3rd International Conference on Integrated Design and Manufacturing in Mechanical Engineering, Montreal, CANADA , May, 16-19, 2000.

J.Y. DANTAN, F. THIEBAUT, A. BALLU, P. BOURDET

FUNCTIONAL AND MANUFACTURING SPECIFICATIONS

Part 1: Geometrical expression by Gauge with Internal Mobilities

Abstract: During all steps of product life cycle, especially at the design level and manufacturing level, a coherent model for functional geometry of the product is required. The inherent imperfections of manufacturing processes involve a geometrical deterioration of functional geometry of the product, and therefore of its quality.

This paper introduces a model by Gauge with Internal Mobilities that allows representing

- the standard geometrical specifications of a part,
- the manufacturing process capabilities.

The approach by Gauge with Internal Mobilities establishes the domain of acceptable variations of the non-ideal geometry, starting from two concepts:

- the interface gauge / part defining the relative position between the ideal features of the gauge and the non ideal features of the part,
- the gauge structure modeling the environment of the part.

The main interest of this approach is that the same description model is proposed for both the standard geometrical specifications and the manufacturing process capabilities. In the companion paper, the validation of the process plan is proposed, the validation method consists in comparing the manufacturing capabilities to the standard geometrical specifications.

1. INTRODUCTION

In this paper, we introduce a model allowing the geometrical specification representation and the manufacturing process representation with the same specification model: the Gauge with Internal Mobilities (G.I.M.).

In the tolerancing community, many ways have been presented to describe geometrical specifications; they do not always permit the description of standard geometric specifications.

Requicha introduced a new theory for geometrical tolerances based on offsetting the boundary of a nominal solid model. Srinivasan and Jayaraman showed that functional geometrical specifications could be stated in terms of Virtual Boundary Requirement like virtual gauge. In 1997, Mathieu and Ballu presented a model of expression of geometrical specifications, and they showed the possibilities of their model of expression in the case of geometrical specifications with virtual gauge. Robinson presented the interest of gauges as regards assembly tolerancing.

The issue is that these two complementary approaches do not usually use the same description tool to study the two points of view, and that involves difficulties to valid a process plan and even to know the capability of a machining process to realize right parts according to the geometrical specifications. In order to establish the comparison, the usual way consists in depreciating the two models used during

P. Chedmail et al. (eds.), Integrated Design and Manufacturing in Mechanical Engineering, 53-60.
©2002 *Kluwer Academic Publishers.*

the design and manufacturing stages and to use one directional tolerance chains in order to validate the process plan.

To contribute to the resolution of this issue, we propose a three dimensional model which uses G.I.M. to describe:

- the standard geometrical specifications
- the manufacturing process capabilities.

We will define the semantics of the specification model by G.I.M..

In order to illustrate our approach, we will use the simple part presented in figure 1. The standard geometrical specifications are supposed to be known, then we will define the mathematical expression of these functional specifications.

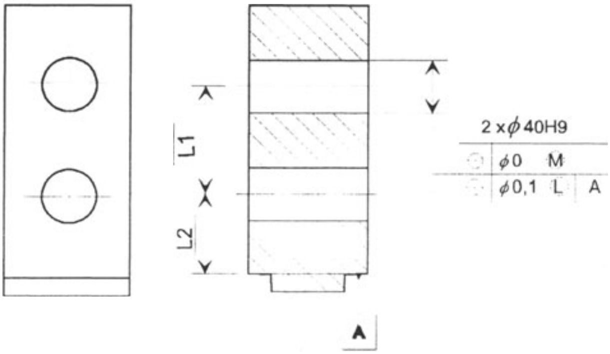

Figure 1: Definition drawing of a bearing

In order to comply with the functional specifications, we define a process plan (figure 2). This process plan is constituted of two phases. During the first phase, the groove S.a is machined. The part is located using two perpendicular planes PL.e and PL.f. The two bores are realized during the second phase. The part is located using three perpendicular planes PL.a, PL.e and PL.g.

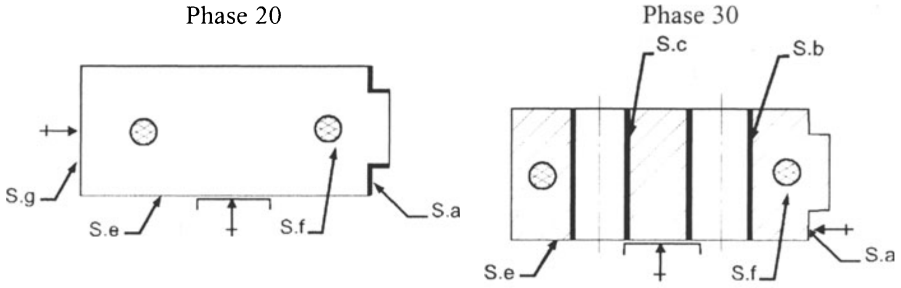
Phase 20

Phase 30

Figure 2: Process plan.

2. GEOMETRICAL SPECIFICATION BY G.I.M.

In this paper, we propose a new concept of gauge allowing a geometrical specification, which give a better approach of the design intent. For that, two concepts are introduced, the concept of interface gauge / part and the concept of internal mobilities. The following paragraphs present these two concepts.

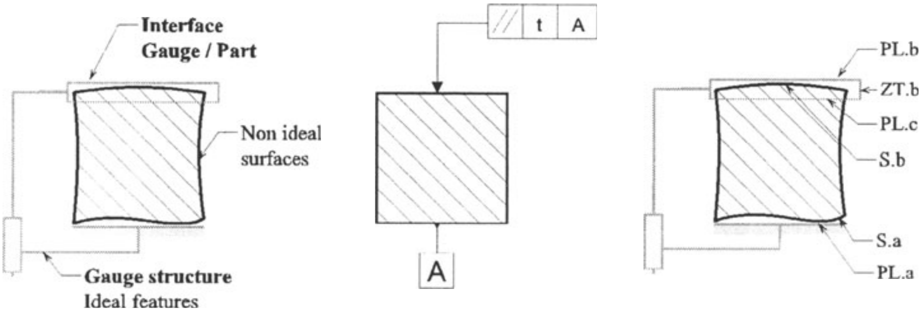

Figure 3: G.I.M. definition

2. 1 Interface gauge / part

The interface gauge/part defines the relative position between the ideal features of the gauge and the non ideal features of the part. The mathematical expression of the interface gauge / part is defined by a whole of geometrical constraints on the parameters describing the position between non ideal features and ideal features of G.I.M.. We define three types of geometrical constraints for interface gauge/part : association, virtual boundary and tolerance zone.

- An association identifies one or more ideal surfaces of the gauge from one or more non-ideal surfaces of the part. An association depends on criteria which are function of the technological constraints. This criteria give an objective on a characteristic and can fix constraints.
- A virtual boundary constrains a non-ideal surface in a half space which is limited by one ideal surface of the gauge. A virtual boundary limits the permissible variation of a non ideal surface inside a hull.
- A tolerance zone constrains a non-ideal feature in an area of space which is constructed by two offsetting on gauge surface, or by one offsetting on gauge line or point. A tolerance zone limits the permissible variation of a non ideal surface inside a hull.

2.2 Gauge structure

The gauge structure modelizes the environment of the part. It includes several features with relative mobilities, which are ideal surfaces or situation features.
The geometrical expression of the gauge structure comprises:

- statement of features (ideal surfaces, situation features),
- a whole of geometrical constraints on the parameters describing the position between the features of G.I.M.

The tolerance zone location or the virtual boundary location could be entirely defined with respect to the datum system, but there could be also freedom degrees.

In such a case, internal mobilities in the gauge are used to take into account these freedom degrees.

Example of GIM (Figure 3) : A simple example of parallelism between two planes permits to illustrate the construction of the gauge. Let us consider a geometrical specification of parallelism between two planes. This specification does not locate the position of the tolerance zone. It just specifies that the non ideal plane has to be included between two parallel ideal planes distant of the tolerance value and parallel to an ideal plane which is associated to the reference surface, which is not ideal. From this definition, the gauge is defined using an ideal plane representing the simulate reference and two ideal planes distant of the tolerance value representing the tolerance zone. The prismatic pair joining these features represents the degree of freedom between the reference and the tolerance zone.

- Interface gauge/part
  - Association
    - Interface feature: One plane PL.a
    - Constraints: PL.a exterior of the material
    - Objective to minimize: The largest distance between PL.a and S.a
  - Tolerance zone
    - Interface feature: Tolerance zone
    - Two planes PL.b and PL.c
    - Constraints: S.b $\subset$ TZ.b

- Gauge structure
  - Constraints:
  - Angle (PL.a, PL.b) = 0°
  - Angle (PL.b, PL.c) = 0°
  - Distance (PL.b, PL.c) = t

3. FUNCTIONNAL STANDARD SPECIFICATION:

The functional specifications are represented on a drawing using the standard specification.

3.1 Standard representation

The formalization of the standard specification is being processed by the ISO community through the definition of a model for geometric specification as a part of the Geometrical Product Specification (GPS). The main interest of this work is that the main concepts of current standards are kept and that the mathematical definition of the specification is given.

Among the two ways permitting the specifications, by dimensions or by zones, only the second one is concerned in the paper. The specification by zone limits the non-ideal features of a workpiece into a space. This space is limited by ideal features that can be characterized:

- by intrinsic characteristics of the ideal features
- by situation features of the ideal features

3.2 Representation by Gauge with internal mobilities

The non ideal geometry of the part is assembled on the gauge. This gauge represents the datum system, the location of the tolerance zone, and the location of the virtual boundary.
The gauge consists in locating the non ideal surfaces of the part. The definition of the gauge uses :

- sequential associations of the non-ideal surfaces on the ideal surfaces of the gauge representing the datum system,
- tolerance zone definition or virtual boundary definition, for which the specified feature is included in,
- gauge structure construction which allows to define the location of the tolerance zones or the location of the virtual boundary.

Example: Concerning the example, the definition of the gauge includes :

- an interface gauge / part (an association which represents the datum A, two virtual boundaries which represents the worst geometry of two cylinders. The diameter of these cylinders is defined thanks to extreme value of the permissible diameter of the specified features),
- a gauge structure which defines two cylinders and the datum plane in exact relative location.

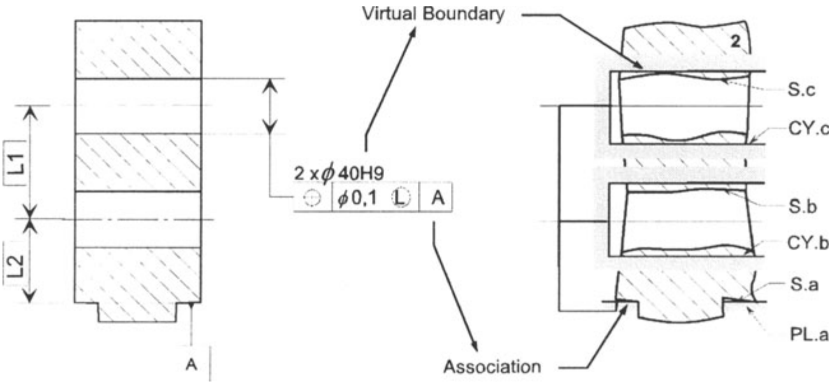

Figure 4: Functional specification of the least material requirement

Interface gauge/part
Association
Interface feature: One plane PL.a
Constraint:PL.a exterior of the material
Objective to minimize:The largest distance between PL.a and S.a
Virtual boundary
Interface feature: One cylinder CY.b
Constraint: CY.b interior of the material (S.b)
Virtual boundary

Gauge structure
Structure feature: One plane PL.d
Constraints:
Radius of CY.b = ϕDmax +0.1
Radius of CY.c = ϕDmax +0.1
Angle (PL.a, PL.d) = 90°
Angle (axis CY.b, PL.a) = 0°
Angle (axis CY.c, PL.a) = 0°
Angle (axis CY.b, PL.d) = 0°
Angle (axis CY.c, PL.d) = 0°
Distance (axis CY.b, axis CY.c) = L1

Interface feature: One cylinder CY.c
Constraint: CY.c interior of the material (S.c)

Distance (axis CY.b, PL.a) = L2
Distance (axis CY.b, PL.d) = 0
Distance (axis CY.c, PL.d) = 0

4. MANUFACTURING SPECIFICATION

The same model should be used to describe the manufacturing process of a part. In such a case, the environment of the part corresponds to the different entities of the manufacturing process and the interface corresponds to the pairs that are used to locate the part relative to the machining process.

For the manufacturing specifications, the main idea of the gauge is to limit the geometrical variation of the part compared to the worst geometry of its environment. The environment is the geometrical model of manufacturing processes. The gauge structure admits some geometrical deviations and some relative mobilities, these deviations and mobilities simulate gaps and mobilities of manufacturing processes.

Once the machining process is known, the pairs that assure the relative movements between the tool and the part are also known.

The non ideal part is assembled on the machining process which is represented by ideal features of the gauge. The contacts between the non ideal surfaces of the part and the fixture are modelized by sequential association. The part is located on the reference frame using this sequential association.

The constitutive parts of the gauge correspond to the mobile entities and the frame of the machine tool. Internal mobilities are used to take into account the relative movements of the machine tool parts. The gauge structure admits some geometrical deviations that simulate gaps of manufacturing processes.

The deviation values could be determined locally for each pair or globally between the frame and the tool of the manufacturing process. In the case of a milling operation using a three axes machine tool, the gauge is constituted of five distinct entities and four pairs representing the three movement axes and the spindle rotation axis.

Example: Concerning the phase 30, the machining process is a three axis milling machine. The part is located using three perpendicular planes PL.a, PL.e and PL.g.. This definition of the part location permits to define a sequential association. This association is defined using the same way than the one described during the standard specification study, ie by the definition of the interfaces between the part and its environment.

The structure of the gauge modelizes the machine tool, the internal mobilities of the gauge represent the movements of the machine tool. The definition of gaps of manufacturing processes is more difficult to apprehend.

The two holes are realized with two different locations of the spindle relative to the frame of the machining process.

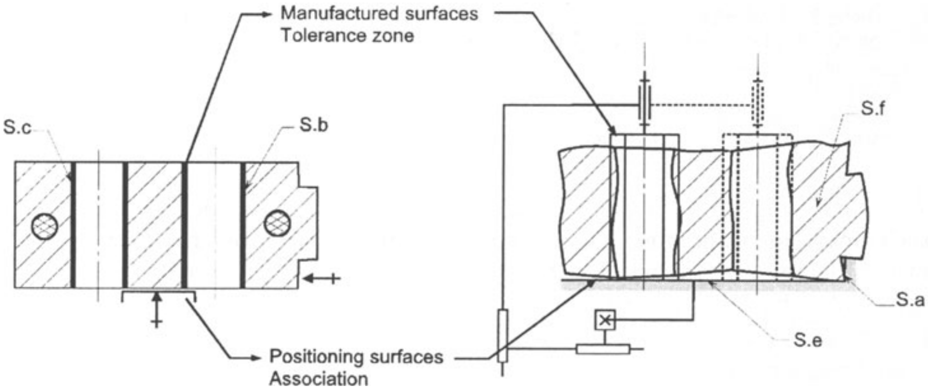

Interface gauge/part

Association

Interface feature: Three planes PL.e, PL.f and PL.a

Constraints: PL.e, PL.f, PL.g exterior of the material

Objective to minimize:

The largest distance between PL.e and S.e

The largest distance between PL.f and S.f

The largest distance between PL.a and S.a

Tolerance zone

Features: Two cylinders CY.b and CY.c

Constraints: S.b $\subset$ TZ.b and S.c $\subset$ TZ.c

Gauge structure

The gauge structure is constituted of all entities of manufacturing process.

Figure 5: Manufacturing specification of phase 30

5. CONCLUSION

In this paper, we have shown that the same model may be used to specify both the machining process and the standard geometrical specification.

This common approach is possible by the use of the same operations to describe the location of the non-ideal workpiece on ideal feature representing the environment.

This coherence in the representation of the two complementary approaches and their mathematical definition is a first step in the definition of a common language and common tools. We believe that such common approaches are necessary in order to predict the whole behavior of a mechanism during all the steps of his life. The companion paper shows a kind of geometrical model that may be used to describe the geometry of the parts for both the specification and process specification. The definition of this model and the use of G.I.M. permits to compare the capability of the machining process to the geometrical specifications.

6. REFERENCES:

1. Anselmetti B. ; TOLERANCING METHOD FOR FUNCTION AND MANUFACTURING; In: proc. of ILCE 95; Paris; France; Fevruary 1-3; 1995.

2. Ballot E., Bourdet P., Thiebaut F. ; CONTRIBUTION OF A MATHEMATICAL MODEL OF SPECIFICATIONS OF A PART TO THEIR COHERENCE ANALYSIS, In: proc. of 6th CIRP Seminar on Computer Aided Tolerancing; University ofTwente; Enscede; Netherlands; March 22-24; 1999.
3. Ballu A. and Mathieu L. ; VIRTUAL GAUGE WITH INTERNAL MOBILITIES FOR VERIFICATION OF FUNCTIONAL SPECIFICATIONS; In: proc. of 5rd CIRP Seminar on Computer Aided Tolerancing; Toronto; Canada; April 27-29; 1997.
4. Clement A., Rivière A., Serre P. and Valade C. ; THE TTRS : 13 CONSTRAINTS FOR DIMENSIONING AND TOLERANCING; In: proc. of 5rd CIRP Seminar on Computer Aided Tolerancing; Toronto; Canada; April 27-29; 1997.
5. Dantan J.Y. and Ballu A. ; FUNCTIONAL AND PRODUCT SPECIFICATION BY GAUGE WITH INTERNAL MOBILITIES; In: proc. of 6th CIRP Seminar on Computer AidedTolerancing; University of Twente; Enschede; Netherlands; March 22-24; 1999.
6. Requicha A.A.G. ; TOWARD A THEORY OF GEOMETRIC TOLERANCING; The International Journal of Robotics Research; Vol.2; n°4; pp.45-60; 1983.
7. Rivest L., Fortin C. and Morel C. ; TOLERANCING A SOLID WITH A KINEMATIC FORMULATION; Computer Aided Design; Vol.26; n°6; pp.465-476;1994.
8. Robinson D.M. ; GEOMETRIC TOLERANCING FOR ASSEMBLY; PhD Thesis; Cornell University; May 1998.
9. Srinivassan V. and Jayaraman R. ; CONDITIONAL TOLERANCES; IBM Journal of Research and Development; Vol.33; n°2; pp.105-124; 1989.

7. AFFILIATIONS

DANTAN Jean-Yves
LGIPM - CER ENSAM de Metz
4, rue A. Fresnel
57070 METZ, France
Email: jean-yves.dantan@metz.ensam.fr

BALLU Alex
LMP – UMR 5469 CNRS – Université Bordeaux 1
351, Cours de la Libération
33405 TALENCE Cedex, France
Email: ballu@lmp.u-bordeaux.fr

THIEBAUT François & BOURDET Pierre
LURPA - E.N.S. de Cachan
61 av. du Président Wilson
94235 CACHAN Cedex, France
Email: thiebaut@lurpa.ens-cachan.fr

J.Y. DANTAN, F. THIEBAUT, A. BALLU, P. BOURDET

FUNCTIONAL AND MANUFACTURING SPECIFICATIONS

Part 2: Validation of a process plan

Abstract: After the study of geometrical specifications by Gauge with InternalMobilities G.I.M. in part 1, we propose to analyze the functional and manufacturing specifications in order to valid the process plan. The purpose is to compare functional specifications to manufacturing specifications. When a manufacturing process plan is being set up, it is essential to verify the geometrical consistency between functional and manufacturing specifications.

Our tolerancing analysis model uses a variational approach, the real geometry of parts is apprehended by a variation of the nominal geometry. Three dimensional dimension chains are characterized by n-hulls (compatibility hull: relations between displacements of surfaces of part and gauge, interface hull: geometrical constraints between part surfaces and gauge surfaces, structure hull: geometrical constraints between gauge entities) expressed in n-affine spaces such each axis corresponds to a parameter of geometrical description (geometrical deviations and gaps). Our method allows us to express formal relations between n-hulls and specification (or manufacturing) hull which limits the deviations of part. So that the process plan is acceptable, the manufacturing hull must be included in the specification hull.

1. INTRODUCTION

The inherent imperfections of manufacturing processes involve a degradation of functional characteristics and a degradation of the quality of the product. Our objective is to valid the process plan of parts. The permissible geometrical variations ensure a certain level of quality, which is defined by functional geometrical requirements. After, when a manufacturing process plan is being set up, it is essential to verify the geometrical consistency between functional and manufacturing specifications. The aims of our tolerancing analysis model are :

- to anticipate the geometrical behavior of the manufacturing process which is modelized by a Gauge with Internal Mobilities,
- to describe the functional and manufacturing specifications with the same model,
- to complete by comparing specifications for design and specifications resulting from manufacturing model.

The resolution of the analysis is based on the expression of geometrical behavior relations between part and gauge.

The same example is developed during this part (Part 1, Fig.1); We will study :

- the maximum material requirement,
- the manufacturing specification of phase 30 (Figure 1).

P. Chedmail et al. (eds.), Integrated Design and Manufacturing in Mechanical Engineering, 61-68.

©2002 *Kluwer Academic Publishers.*

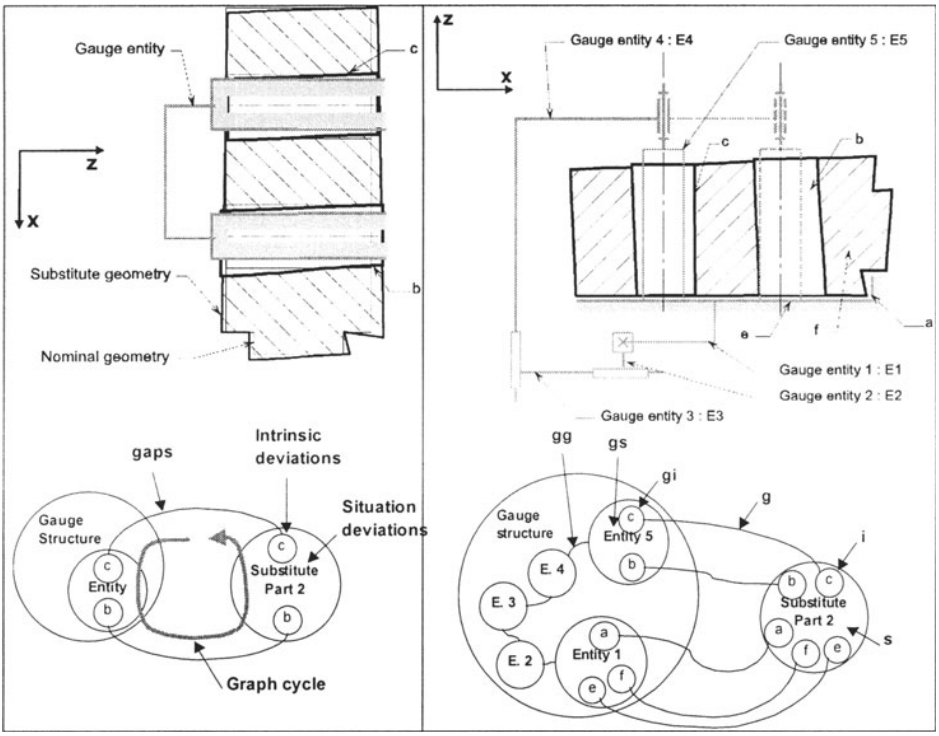
Gauge entity
c
z
x
Substitute geometry
b
Nominal geometry
gaps
Intrinsic deviations
Situation deviations
Gauge Structure
c
Entity
b
c
Substitute Part 2
b
Graph cycle
z
x
Gauge entity 4 : E4
Gauge entity 5 : E5
c
b
a
e
f
Gauge entity 1 : E1
Gauge entity 2 : E2
Gauge entity 3 : E3
gg
gs
gi
g
i
Gauge structure
c
Entity 5
b
E. 4
E. 3
E. 2
a
Entity 1
e
f
b
c
Substitute Part 2
a
f
e
s

Figure 1 : Maximum material requirement & Manufacturing specification of phase 30

2. VARIATIONAL GEOMETRY

The geometrical definition of parts requires the use of several geometrical models. During the design - manufacturing - metrology cycle, the geometry takes various forms (Figure 1): non ideal geometry, nominal model, substitute geometry.
It is impossible to completely capture the variation of non ideal surface. The non ideal surfaces are modelized by substitute surfaces, a substitute surface is an ideal surface (conservation of the typology of the nominal surface). Compared with the nominal model, each substitute surface has position variations, orientation variations and intrinsic variations.

2.1 Mathematical formulation of fine positioning

The incorporation of simulated manufacturing variations in tolerance analysis requires a mathematical formulation of fine positioning. Relative substitute surface positioning is described by a mathematical formulation. The position of a geometrical element in a coordinate system is completely specified by a 4×4 transformation matrix. The manufacturing variations are relatively small compared to the nominal size, the requisite rotations for positioning the surfaces are small, the rotation elements can be linearized. Consequently, at each point M in Euclidian space, small displacements can be described by two vectors : **r** and **t**. The **t** vector represents three translations along perpendicular directions, two by two. The **r** vector represents to three small rotations along perpendicular directions, two by two.

$$\{d\} = \begin{Bmatrix} \mathbf{r} \\ \mathbf{t} \end{Bmatrix} \qquad \mathbf{r} = \begin{bmatrix} \alpha \\ \beta \\ \gamma \end{bmatrix} \qquad \mathbf{t} = \begin{bmatrix} u \\ v \\ w \end{bmatrix}$$

2.2 Characteristics

In the following, we distinguish two types of deviation: the situation deviation (orientation and position variation between a substitute surface and the nominal geometry) and the intrinsic deviation. And we associate a gap transformation to each couple of substitute surface of the part and ideal surface of the gauge potentially in contact to modelize the displacement in joints.

2.2.1 Situation deviation

There are two types of deviation : the situation deviation and the intrinsic deviation. The situation deviation defines the variation (position and orientation) between a substitute surface ia and the nominal geometry i. A transformation $\{d_{ia/i}\}$ is associated to each substitute surface ia of part i. The transformation $\{d_{ia/i}\}$ represents the small displacement between substitute surface ia and nominal geometry i.

2.2.2 Intrinsic deviation

The intrinsic deviation of substitute surface are specific for a type of surface itself. It defines the surface variations. For instance, the intrinsic variation of a substitute cylinder is radius variation Δr between the substitute cylinder and the nominal cylinder .

2.2.3 Gap

A transformation $\{\mathrm{d}_{\mathrm{ia/ja}}\}$ is associated to each substitute surface ia and ja of part i and gauge entity j. This transformation $\{\mathrm{d}_{\mathrm{ia/ja}}\}$ represents the small displacements between two substitute surfaces of part and gauge.

2.3 N-space geometrical description

The deviation of part, the deviation of gauge entities, the gaps between part and gauge and the gaps between gauge entities have been just described by parameters.

Thereafter, the geometrical behavior of part and gauge will be defined in spaces whose each axis corresponds to a parameter. We distinguish six types of space :

space name	vector	designation
Situation	**s**	situation deviation space of the specified part
Intrinsic	**i**	intrinsic deviation space of the specified part
Gap	**g**	space of all gaps between the part and the gauge
Gauge situation	**gs**	situation deviation space of gauge entities
Gauge intrinsic	**gi**	intrinsic deviation space of gauge entities
Gauge gap	**gg**	space of all gaps between gauge entities

For each specification, the N-Space geometrical description are defined, because this description depends on the gauge morphology.

Example: N-Space description of manufacturing specification of phase 30

$$\mathbf{s}=\begin{bmatrix}\alpha_{2a/2},\beta_{2a/2},w_{2a/2},\alpha_{2b/2},\beta_{2b/2},u_{2b/2},v_{2b/2},\\ \dots,\alpha_{2f/2},\gamma_{2f/2},v_{2f/2}\end{bmatrix}\qquad \mathbf{i}=\left[\,\Delta r_{2b/2},\Delta r_{2c/2}\right]$$

$$\mathbf{g}=\begin{bmatrix}\alpha_{E1a/2a},\beta_{E1a/2a},\Gamma_{E1a/2a},U_{E1a/2a},V_{E1a/2a},w_{E1a/2a},\\ \dots,\alpha_{E1f/2f},\mathrm{B}_{E1f/2f},\gamma_{E1f/2f},U_{E1f/2f},v_{E1f/2f},W_{E1f/2f}\end{bmatrix}$$

$$\mathbf{gs}=\begin{bmatrix}\alpha_{E1a/E1},\beta_{E1a/E1},w_{E1a/E1},\\ \alpha_{E5b/E5},\beta_{E5b/E5},u_{E5b/E5},v_{E5b/E5},\\ \dots,\alpha_{E1f/E1},\gamma_{E1f/E1},v_{E1f/E1}\end{bmatrix}\qquad \mathbf{gi}=\left[\,\Delta r_{E5b/E5},\Delta r_{E5c/E5}\right]$$

$$\mathbf{gg}=\begin{bmatrix}\alpha_{E1/E2},\beta_{E1/E2},\gamma_{E1/E2},u_{E1/E2},V_{E1/E2},w_{E1/E2},\\ \dots,\alpha_{E4/E5},\beta_{E4/E5},\Gamma_{E4/E5},u_{E4/E5},v_{E4/E5},w_{E4/E5}\end{bmatrix}$$

3. GEOMETRICAL BEHAVIOR

The tolerancing analysis model is based on the expression of the geometrical behavior of the mechanism, we define various hulls limiting the geometrical behavior of the mechanism.

In the first stage, the relations between small displacements of surfaces of part and gauge are defined. To do so, we develop the composition of small displacements in all cycle of the graph (part + gauge). These relations define the compatibility hull (Dcompatibility).

In the second stage, the approach by Gauge with Internal Mobilities establishes the domain of permissible deviations of the substitute geometry. We express these constraints by two hulls : Dinterface (the interface gauge/part defines the relative position between the ideal features of the gauge and the substitute features of the part) and Dstructure (the gauge structure modelizes the environment of the part). We define all hulls of each specification (manufacturing and functional).

3.1 Compatibility hull

The geometrical behavior of the mechanism (part + gauge) is expressed by the composition relations of small displacements in the various cycles of the graph, these relations rest on the property of the mathematical tool (4×4 transformation matrix): the relation of Chasles.

These composition relations define compatibility equations between the situation deviations and the gaps of the part and the gauge. The set of compatibility equations, obtained by the application of composition relation to the various cycles, makes a system of linear equations. So that the system of linear equations admits a solution, it is necessary that compatibility equations are checked. We define the compatibility equations for each specification. These compatibility equations characterize some hyperplans in the Situation×Gap×Gauge_situation×Gauge_gap space. $D_{\text{compatibility}}$ is the compatibility hull.

Example : compatibility equations of maximum material requirement (Fig.1)

$$\begin{cases} \alpha_{2/2b} + \alpha_{2b/Eb} + \alpha_{Eb/E} + \alpha_{E/Ec} + \alpha_{Ec/2c} + \alpha_{2c/2} = 0 \\ \beta_{2/2b} + \beta_{2b/Eb} + \beta_{Eb/E} + \beta_{E/Ec} + \beta_{Ec/2c} + \beta_{2c/2} = 0 \\ \Gamma_{2b/Eb} + \Gamma_{Ec/2c} = 0 \\ u_{2/2b} + u_{2b/Eb} + u_{Eb/E} + u_{E/Ec} + u_{Ec/2c} + u_{2c/2} = 0 \\ v_{2/2b} + v_{2b/Eb} + v_{Eb/E} + v_{E/Ec} + v_{Ec/2c} + v_{2c/2} = 0 \\ W_{2b/Eb} + W_{Ec/2c} = 0 \end{cases}$$

3.2 Interface hull

The concept of the interface gauge / part defines the relative position between the ideal surfaces of the gauge and the non-ideal surfaces of the part. The interface hull is the mathematical expression of interface gauge / part. The interface constraints limit the gap between the part and the gauge. These constraints define the interface hull in Gap×Intrinsic×Gauge_intrinsic space. $D_{\text{interface}}$ is the interface hull.

In the first part, we define three types of constraints for interface gauge/part :

- association operation, it identifies one or more ideal surfaces from one or more non-ideal surfaces, it depends on criteria which is defined by the semantic of the specification, it results in equations defined in Gap×Intrinsic×Gauge_intrinsic,
- virtual boundary, it characterizes non-interference constraint between an ideal surface of the gauge and an non-ideal surface of the part, it results in inequations defined in Gap×Intrinsic×Gauge_intrinsic
- tolerance zone, it constraints a non ideal surface of the part in a tolerance zone, the position of the tolerance zone depends on the gauge, tolerance zone results in inequations defined in Gap×Intrinsic×Gauge_intrinsic

Example : A constraint of interface hull of manufacturing specification of phase 30

The association between surface e of the part and plane e of the gauge modelizes the fixture, it implies identical displacements according to degrees of contact:

$$\alpha_{E1e/2e} = \beta_{E1e/2e} = w_{E1e/2e} = 0$$

Example : A constraint of interface hull of maximum material requirement (Fig.1) For the virtual boundary between surface b of the part and cylinder b of the gauge, the gap is limited by the non interference constraint.

$$\mathbf{t}_{\mathbf{Eb/2b,M}} \cdot \mathbf{n}_{\mathbf{M}} \le \Delta r_{2b/2} - \Delta r_{Eb/E} + r_{2b} - r_{Eb} \cdot$$

3.3 Structure hull

For the functional specifications, the gauge structure represents the datum system and the location of the tolerance zone. And for the manufacturing specifications, the gauge structure represents the geometrical model of manufacturing processes. The gauge structure admits some geometrical variations and some relative mobilities, these variations and mobilities simulate gaps and mobilities of manufacturing processes.

The gauge structure is composed of geometrical entities also having mobilities with gap. It defines the relative position between the ideal surfaces of gauge entities and between gauge entities. The structure hull is the mathematical expression of gauge structure. The structure constraints limit the gap between gauge entities and the deviation between ideal surface of gauge entity and gauge entity. These constraints define structure hull in Gauge_situation×Gauge_gap space. $D_{\text{structure}}$ is the structure hull.

Example : The machine structure is constituted by four subassemblies which are in serial prismatic pairs. These three prismatic pairs are along x-axis, y-axis and z-axis. There are inaccuracies in manufacturing processes, because the machine structure have position and orientation variations. The limits of these variations can be measured and characterize the structure hull.

4. SPECIFICATION AND MANUFACTURING HULLS

The mathematical expressions of each geometrical specification are defined in various spaces. Indeed Gap, gauge situation, gauge intrinsic and gauge gap spaces depend on the gauge morphology. We distinguish the functional gauge and the manufacturing gauge by an index (s, m). To study the feasibility of the process plan, we must express all specifications in a same space: deviations space of the part.

Our objective is to define the permissible (or manufacturing) geometrical deviations of the part ensuring the assembly requirement between the gauge and the part. This assembly requirement between the gauge and the part is constrained by the compatibility hull, the interface hull and the structure hull. To do so, for each specification, we build a Gauge with Internal Mobilities and we define a compatibility hull, a interface hull and a structure hull.

4.1 Specification hull

For functional specification, all parts that respect the assembly requirement with the gauge, satisfy the functional specification. Therefore, for a part that satisfies the functional specification, it must exist at least a gauge that verifies the constraints of the compatibility hull, the interface hull and the structure hull.

The functional constraints that limit the permissible deviations, characterize the specification hull. These constraints are equivalent to : the acceptable configurations between part and gauge are defined by all permissible states of gauge. The mathematical expression of this equivalence is

$$(\mathbf{s}, \mathbf{i}) \in \mathrm{Ds}$$

$$\Leftrightarrow \exists\ (\mathbf{gs}_s, \mathbf{gg}_s) \in \mathrm{Dstructure}_s$$

$$: (\mathbf{s}, \mathbf{g}_s, \mathbf{i}, \mathbf{gs}_s, \mathbf{gi}_s, \mathbf{gg}_s) \in \mathrm{Dcompatibility}_s \cap \mathrm{Dinterface}_s$$

4.2 Manufacturing hull

In the same way, we define the manufacturing constraints. For manufacturing specification, all parts that respect the assembly requirement with the gauge, satisfy the manufacturing specification. Therefore, for a part that satisfies the manufacturing specification, it must exist at least a gauge that verifies the constraints of the compatibility hull, the interface hull and the structure hull.

The manufacturing constraints that limit the manufacturing deviations, characterize the manufacturing hull. These constraints are equivalent to : the acceptable configurations between part and gauge are defined by all acceptable states of gauge. The mathematical expression of this equivalence is

$$(\mathbf{s}, \mathbf{i}) \in \mathrm{Dm}$$

$$\Leftrightarrow \exists\ (\mathbf{gs}_m, \mathbf{gg}_m) \in \mathrm{Dstructure}_m$$

$$: (\mathbf{s}, \mathbf{g}_m, \mathbf{i}, \mathbf{gs}_m, \mathbf{gi}_m, \mathbf{gg}_m) \in \mathrm{Dcompatibility}_m \cap \mathrm{Dinterface}_m$$

4.3 Validation of a process plan:

To valid the process plan, we compare functional specifications to manufacturing specifications. The manufacturing deviations must be smaller than the functional deviations. So that the process plan is acceptable, the following constraint must be respected : $\mathrm{Dm} \subset \mathrm{Ds}$

5. CONCLUSION

After the study of geometrical expression by Gauge with Internal Mobilities of functional and manufacturing specifications in part 1, we study the validation of a process plan. A model of geometrical variations allows us to express functional constraints (or manufacturing constraints) and geometrical behavior of the gauge and the part. We identify relations between the geometrical expression and the mathematical expression :

- interface gauge / part – interface hull,
- gauge structure – structure hull.

This mathematical expression is characterized by n-hulls. To define the permissible deviations (or manufacturing deviations) of a part, we formalize relations between n-hulls (compatibility hull, interface hull and structure hull) and specification hull

(or manufacturing hull). This formal approach enables us to write the constraints between the permissible deviations and the manufacturing deviations.
This approach applies in tolerancing synthesis model for all functional requirements take into account the assembly process.

6. REFERENCES:

1. Ballot E., Bourdet P., Thiebaut F. ; CONTRIBUTION OF A MATHEMATICAL MODEL OF SPECIFICATIONS OF A PART TO THEIR COHERENCE ANALYSIS, In: proc. of 6th CIRP Seminar on Computer Aided Tolerancing; University ofTwente; Enscede; Netherlands; March 22-24; 1999.
2. Ballot E., Bourdet P. ; A COMPUTATION METHOD FOR THE CONSEQUENCES OF GEOMETRIC ERRORS IN MECHANISMS, CIRP Seminar on Computer Aided Tolerancing, Toronto, Canada, April 1997.
3. Clément A., Desrochers A., Rivière A. ; THEORY AND PRACTICE OF 3D TOLERANCING FOR ASSEMBLY, CIRP Seminar on Computer Aided Tolerancing, Penn State University, USA, May 1991.
4. Giordano M., Duret D., CLEARENCE SPACE AND DEVIATION SPACE, APPLICATION TO THREE-DIMENSIONAL CHAIN OF DIMENSIONS AND POSITIONS, CIRP Seminar on Computer Aided Tolerancing, ENS Cachan, May 1993.
5. Guilford J., Turner J.U. ; ADVANCED TOLERANCE ANALYSIS AND SYNTHESIS FOR GEOMETRIC TOLERANCES, International Forum on Dimensional Tolerancing and Metrology, CRTD-Vol.27, pp.187-198, 1993.
6. Gupta S., Turner J.U. ; VARIATIONAL SOLID MODELING FOR TOLERANCE ANALYSIS, IEEE Computer Graphics & Application, Vol.13, n°3, pp.64-74, 1993.
7. Rivest L., Fortin C., Morel C. ; TOLERANCING A SOLID WITH A KINEMATIC FORMULATION, Computer Aided Design, Vol.26, n°6, pp.465-476, 1994.
8. Roy U., Li B. ; REPRESENTATION AND INTERPRETATION OF GEOMETRIC TOLERANCES FOR POLYHEDRAL OBJECTS, Computer Aided Design, Vol.31, n°4, pp.273-285, 1999.
9. Sodhi R. ; ASSEMBLY MODELING FOR DESIGN ANALYSIS, PhD Thesis, Rensselear Polytechnic Institute, March 1995.
10. Teissandier D., Couétard Y., Gérard A. ; THREE DIMENSIONAL FUNCTIONAL TOLERANCING WITH PROPORTIONED ASSEMBLIES CLEARENCE VOLUME : APPLICATION TO SETUP PLANNING, CIRP Seminar on Computer Aided Tolerancing, Toronto, Canada, April 1997.
11. Turner J.U ; THE M_SPACE THEORY OF TOLERANCES, Advanced in Design Automation, ASME, Vol.23, n°1, pp.217-226, 1990

7. AFFILIATIONS

DANTAN Jean-Yves
LGIPM - CER ENSAM de Metz
4, rue A. Fresnel
57070 METZ, France
Email: jean-yves.dantan@metz.ensam.fr

BALLU Alex
LMP – Université Bordeaux 1
351, Cours de la Libération
33405 TALENCE Cedex, France
Email: a.ballu@lmp.u-bordeaux.fr

THIEBAUT François & BOURDET Pierre
LURPA - E.N.S. de Cachan
61 av. du Président Wilson
94235 CACHAN, France
Email: thiebaut@lurpa.ens-cachan.fr

F. BENNIS

ROBUST DESIGN AND STATISTICAL TOLERANCE ANALYSIS

Abstract: Product variation is a key piece of information that flows from the design function to manufacturing function in an enterprise. Every, engineering design is subject to variation that can arise from a variety of sources, including manufacturing operations, variation in material properties, and at the operating environment. Engineers must deal with variations in the products they design and manufacture. They have to produce robust designs by assessing the expected size of variation and determining the risk of failure. The best time to reduce the impact of variation is in the early stages of design process. Variation analysis in mechanical design becomes an essential practice.

This paper presents a review of statistical tolerance analysis and the robust design approaches. The main objective of tolerance analysis and robust design domains is to control the geometrical and operational variation of product. Tolerance analysis and robust design methods are based on several precise hypotheses and conditions.

1. INTRODUCTION

Engineering design is subject to variation that can arise from a variety of sources, including manufacturing operations, variation in material properties, and at the operating environment. Variation of geometrical parameters of mechanical products is usually specified in terms of tolerances. The tolerance design process determines the most economical and tolerable deviations that minimise the cost of the product. This approach only controls the geometrical parameters. The robust design objective is to minimise the variation impact of the variables and parameters on the system performance by reducing the cost associated to the control of the variation sources. This approach deals with all the parameters of the mechanical product.

Several reasons justify the use of statistical analysis tools. These reasons are technical as well as economic. Indeed, inspection-level is based on sampling plan (part lot acceptance) rather than 100% sampling. It is nearly improbable to manufacture all the entities of all the parts of the assembly at the worst limits. Moreover the resultant variation is likely to be compensated between the parts at the assembly-stage. In the other hand, the actual manufacturing processes do not allow the respect of the so tight value of the functional tolerance of some products. Finally, the tolerance process aims to predict the impact of the random manufacturing variations [1, 2].

This paper start out by looking at some definitions, hypothesis and applications related to the statistical tolerance approach and the robust design one. Firstly, the statistical tolerance analysis method is presented. Then, in the third section, the robust design is presented as an extension of the statistical tolerance concept. The paper aims for a unifying abstraction to deal with variation in a product of an engineering enterprise.

P. Chedmail et al. (eds.), Integrated Design and Manufacturing in Mechanical Engineering, 69-76.
©2002 *Kluwer Academic Publishers.*

2. STATISTICAL TOLERANCE ANALYSIS

In the last decade, the statistical tolerance analysis received particular attention of several authors. Many papers and states-of-the-art, with complementary points of view, were presented in this field [3-6]. As far as we know, all the authors only address traditional tolerances (plus/minus) in statistical analysis. They generally suggest translating geometrical tolerances to statistical parametric tolerances. Thus, the analysis is based on this type of equation:

$$y = f(x_1, x_2, \ldots, x_n) \tag{1}$$

Where y represents the functional tolerance of the assembly (gap or distance between two parts). It depends on the n dimensional variables x. During the tolerance design process, a designer has to evaluate the risk of failure by identifying all the properties of the resultant component. The identification of statistical distribution of the component y is generally based on several hypotheses related to the components x_i and to the function f. The variables x_i are assumed to be random, independent and normal. In addition, the function $f(x_1,\ldots,x_n)$ is approximated by a linear function and the distributed of the component y is assumed to be normal [7-11]. Tolerance analysis uses either "*worst case*" or statistical models.

2.1. Worst case analysis

"*Worst-case*" analysis is based on a complete interchangeability of parts in an assembly. It leads to expensive tight parts tolerances especially when the number of features, parts or sub-assemblies increases. The worst case analysis assumes that all the components of all the parts are manufactured at their worst limits.
Interchangeability is allowed if all the combinations $f(x_i \pm T_i)$ are into the tolerance interval of y. $[x_i - T_i, xi + T_i]$ is the tolerance interval of the dimension x_i. If the function defined in equation (1) is linear, then it can be written as the following:

$$y = f(\mathbf{x}) = a_0 + \sum a_i x_i \tag{2}$$

Equation (2) leads to the following inequality:

$$|a_0| + \sum |a_i| T_i \le T_y \tag{3}$$

If the function f is not linear then relation (3) is not satisfied. This is the case of geometrical tolerances. In the general case, we have to compute $\{l_y = \min f(x_1, x_2,\ldots, x_n)\}$ and $\{u_y = \max f(x_1, x_2,\ldots, x_n)\}$ for every x_i in the interval $[x_i - T_i, x_i + T_i]$ $i=1,\ldots,n$. The functional specification is guarantee, if the interval $[l_y, u_y]$ is included in $[y - T_y, y + T_y]$. According to the number of the parts in the assembly and the number of variables, the tolerance interval of each variable x_i may be dramatically reduced [12]. The worst case analysis assumes that manufacturing process only produces perfect parts at the furthest dimensions. This condition is in complete contrast with the tolerance concept. "*Worst-case*" method gives overly pessimistic results because of the simultaneous occurrence of such "*worst-case*" part-level events is rather rare. In the following section, the statistical method is presented. It is more effective and gives better results.

2.2. Statistical Hypotheses

Statistical models make the assumption that a reasonable percentage of non-conforming parts may occur. In statistical tolerance inspection, one needs a population of parts before deciding whether the whole population is acceptable or not. Thus, contrary to the worst case approach, the decision for a single part is not allowed. The literature related to statistical tolerance has been reviewed by several authors [2, 16, 17, 18]. A careful study from the preview researches indicates three categories of statistical tolerance approaches. The first one assumes that each component tolerance spans a 6σ range distribution with its mean at the midpoint of the range. The second category relaxes the previous constraint and accepts shifts and drifts of the distribution. The last category takes advantage of the results of the second category researches and works on the best industrial practices. They participate to the clarification, harmonization and consolidation of the statistical tolerancing standard. Two possible interpretations of statistical tolerancing were provided [19, 17, 15].

Statistical methods applied to the tolerances analysis are based on precise hypotheses and conditions. It is necessary to verify the validity of these conditions before an effective application of these methods. These hypotheses are summarised in the following section.

The expectance and standard deviation of $y = f(x)$ *are* written as the following

$$\mu_y = a_0 + a_1\,\mu_1 + a_2\,\mu_2 + \ldots + a_n\,\mu_n \tag{4}$$

$$\sigma_y^2 = a_1^2\,\sigma_1^2 + a_2^2\,\sigma_2^2 + \ldots + a_n^2\,\sigma_n^2 \tag{5}$$

where μ_i and μ_y are the expectances of the random variable x_i and y respectively. σ_i and σ_y are the standard deviations of x_i and y respectively. Thanks to its simplicity, the relation between standard deviations is very popular. However, relation (5) is not applicable when the variables x_i are dependent.

2.2.1 Hypothesis of Normal Distribution with its Mean at the Midpoint of the Range

In order to estimate the probability of success or the risk of failure of the assembly, several information related to the distribution of the resultant *y* have to be collected. Thanks to its simplicity, the most popular hypothesis assumes that each component tolerance spans a 6σ range. Besides, the distribution is supposed to be normal with its mean at the midpoint of the range. According to this hypothesis, the equality of the *Root Sum Square* method is derived from equations (5) and $(2T_i = 6\sigma_{i},)$:

$$\sum_{i=1}^{n} a_i^2 T_i^2 \leq T_y^2 \tag{6}$$

Since the actual distributions of the process are rarely normal, this method leads to optimistic results. Whether the distribution is normal, its mean is probably not at the midpoint of the range. This hypothesis is somewhat equivalent to the worst case approach. It assumes that all the produced lots have equal values (μ, σ) for a given component x_i.

In order to take into account these contradictions and to solve this problem, industrials used several heuristic solutions. By the end, this leads to the introduction of the capability indices and the Statistical Tolerance Zone based approach [1, 5, 6 and 12].

2.2.2 Statistical Tolerance Zone Approach

The statistical tolerance zone approach results from several recent works [13, 14]. The ISO standard deliberation about Statistical Tolerancing leads to the following definition [1, 2 and 6]:

$$C_p = \frac{\tau}{3\,\sigma} \; ; C_{pk} = \frac{\tau - |m-\mu|}{3\,\sigma} \quad \text{et} \quad C_c = \frac{|\mu - m|}{\tau} \tag{9}$$

2τ is the tolerance range and m the midpoint of the range of the component x_i. According to the used process and the tolerable risk of failure, industrials use the constants P, K and F to define the limits of the indices defined in equation (9) :

$$P \leq C_p \, , K \leq C_{pk} \;\text{ et } C_c \leq F \tag{10}$$

Equation (10) defines the statistical tolerance zones in the plane (μ, σ) [1]. Figures (1) and (2) depict two particular shapes of these zones.

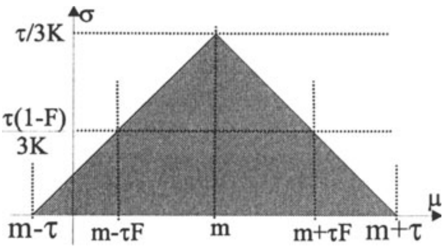

Figure 4 : 3Kσ –τ+m≤ μ ≤ –3Kσ+τ+m

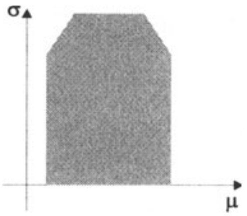

Figure 5 : statistical tolerance zone for $1.5 \leq C_p$, $1.0 \leq C_{pk}$ et $C_c \leq 0.5$

3. ROBUST DESIGN

The precursor researchers who used an optimisation formulation in the robust design context are [16,19-21 and 24].
The traditional design problem is generally formulated as the following:

Problem ***P***:

Minimise the criterion : $y=f(\mathbf{x}, \mathbf{p})$
Subject to the constraints: $\mathbf{g}(\mathbf{x},\mathbf{p}) \leq 0$

where:
$\mathbf{x} = (x_1, x_2, ..., x_u)$ is the design variables vector of dimension u.
$\mathbf{p} = (p_1, p_2, ..., p_v)$ is the design parameters vector of dimension v.
$\mathbf{g}(\mathbf{x},\mathbf{p}) = (g_1(\mathbf{x},\mathbf{p}), g_2(\mathbf{x},\mathbf{p}), ..., g_w(\mathbf{x},\mathbf{p}))$ is the vector of constraints defining the admissible domain, g_i is the i^{th} component of $\mathbf{g}(\mathbf{x})$. w is the number of **g** components, $f(\mathbf{x},\mathbf{p})$ is the criterion function. The functions **g** and f depend on **x** and **p**.
This crisp formulation did not take into account probable variations of the variables and parameters. Thus, if the theoretical optimal solution is on the boundary of the admissible domain defined by the components of **g**, the actual components of the parts of the product may be out of this domain. The following relation represents the probabilistic formulation of the admissible crisp domain:

$$\mathbf{D} = \{ (\mathbf{x}, \mathbf{p}) \in R^u \times R^v \,|(\mathrm{Prob}(g_i(\mathbf{x},\mathbf{p}) \leq 0) = 1), \ (i=1, ..., u+v) \}$$

In the other hand, the theoretical optimal solution of the performances may be very sensitive with respect to the variation of the components.
The robust design aims to minimise the variation of performances around the theoretical optimal solution. The components of **x** and **p** are assumed to be random variables with known expectance and standard deviation.
Let μ_i be the expectance value and σ_i the standard deviation of the components of **x** and **p** (with i= 1 ..., u+v). From the hypotheses presented in the first section of this paper, the expectance and the standard deviation of the criterion f and the components of the vector **g** can be to computed. Thus the robust design is obtained from the following:

Problem P_Robust:

Minimise the criterion $(\mu_y(\mathbf{x}, \mathbf{p}), \sigma_y(\mathbf{x}, \mathbf{p}))$
Subject to the constrains: $\mu_{gi}(\mathbf{x}, \mathbf{p}) + k_i\, \sigma_{gi}(\mathbf{x}, \mathbf{p}) \leq 0$, i= 1, ..., u+v.

Designer chooses the value of the constant k_i according to tolerable risk of failure. In the most general case k_i is equal to three.
Let's observe that σ_y is dependent on μ_i and on σ_i. Thus, it is possible to reduce the variation of the performance by only adapting the choice of the expectance values of **x** and **p** and without necessarily reducing the variation range of each component. This is the preliminary step of the robust design approach.

The following relation represents the probabilistic formulation of the robust domain:

$$\mathbf{D}_S = \{ (\mathbf{x}, \mathbf{p}) \in R^u \times R^v \mid (\mathrm{Prob}(g_i(\mathbf{x},\mathbf{p}) \leq 0) \geq P_i), (i=1, \ldots, u+v) \}.$$

where $k_i = \frac{\mu_{gi}(\mathbf{x}, \mathbf{p})}{\sigma_{gi}(\mathbf{x}, \mathbf{p})} = \Phi^{-1}(P_i)$, and Φ is the cumulative function of the normal distribution. For instance, $\Phi^{-1}(0.9987) = 3$.

In literature about robust design, μ_{gi} and σ_{gi}^2 are generally obtained from the following approximations:

$$\mu_{gi} = g_i(\mu_x, \mu_p)$$

$$\sigma_{gi}^2 = \sum_{i=1}^{u} \left(\frac{\partial g(\mathbf{x},\mathbf{p})}{\partial x_i} \right)^2 \sigma_{xi}^2 + \sum_{i=1}^{v} \left(\frac{\partial g(\mathbf{x},\mathbf{p})}{\partial p_i} \right)^2 \sigma_{pi}^2$$

The worst case formulation use the following approximation:

$$g_i(\mu_x, \mu_p) + \sum_{i=1}^{u} \left| \frac{\partial g(\mathbf{x},\mathbf{p})}{\partial x_i} \Delta_{xi} \right| + \sum_{i=1}^{v} \left| \frac{\partial g(\mathbf{x},\mathbf{p})}{\partial x_i} \Delta_{pi} \right| \leq 0$$

Thanks to its simplicity, the previous inequality is very popular notwithstanding the risk occurring in the case of very small dimensions.

In the general case, it would be better to use the equations (12) and (14).

Recent works about robust design can be found in the following references [17, 22, 23 and 25].

Let's observe that the majority of the proposed methods are time and memory consuming. In addition, the number of variables of the examples proposed in literature is relatively small compared with the number of variables of industrial applications.

4. COMPUTATION OF THE FIRST TWO MOMENTS

The previous methods are based on the linearity of the function f. Several works of Chase and Turner [4, 5, 8, 10, 11, 15] indicate that, the second order terms must be taken into account. This section gives the main relations needed to compute the first two moments μ and σ.

The Taylor expansion approximation at the 3rd order leads to the following relation:

$$y = f(\mu) + \mathbf{h}^T (\mathbf{x} - \mu) + \frac{1}{2} (\mathbf{x} - \mu)^T \mathbf{H} (\mathbf{x} - \mu) + O(\mathbf{x} - \mu)^3$$

where $\mathbf{x} = (x_1, x_2, \ldots, x_n)^T$, $\mu = E(\mathbf{x}) = (\mu_1, \mu_2, \ldots, \mu_n)^T$, $\mathbf{h}^T = (h_1, h_2, \ldots, h_n)$ and $\mathbf{H}$ is the (nxn) matrix of components h_{ji} (the partial derivatives are computed at point $\mathbf{x} = \mu$):

$$h_i = \left(\frac{\partial f(\mathbf{x})}{\partial x_i}\right)_{\mu},\ h_{ii} = \left(\frac{\partial^2 f(\mathbf{x})}{\partial x_i^2}\right)_{\mu} \text{ et } h_{ij} = h_{ji} = \left(\frac{\partial^2 f(\mathbf{x})}{\partial x_j \partial x_i}\right)_{\mu} \text{ for } i \neq j.$$

The expectance of y might be computed by omitting all the 3rd order terms:

$$\mu_y = E(y) = f(\mu) + \frac{1}{2} \sum_{i=1}^{n} h_{ii}\, \sigma_i^2 \qquad (12)$$

This relation assumes that the variables x_i are independent. We remark that the second term depends on the standard deviation σ_i of the variables x_i.
The computation of the standard deviation $\sigma_y^2 = E(y-\mu_y)^2$ of y is more complex :

$$\sigma_y^2 = E\left(\left\{\mathbf{h}^T(\mathbf{x}-\mu) + \frac{1}{2}(\mathbf{x}-\mu)^T \mathbf{H}\, (\mathbf{x}-\mu)\right\}^2\right)$$

Indeed the calculation of $(y-\mu_y)^2$ leads to an exorbitant number of terms. Several approximations are then necessary. Thus, the second order is generally neglected:

$$\sigma_y^2 = E\,[\mathbf{h}^T(\mathbf{x}-\mu)]^2 = \sum_{i=1}^{n} \left(\frac{\partial f(\mathbf{x})}{\partial x_i}\right)^2 \sigma_i^2 \qquad (13)$$

We can also take into account, at least partially, some second order terms by applying the following approximation [15]:

$$\sigma_y^2 = \sum_{i=1}^{n} [\, h_{ii}\sigma_i^2 + h_i h_{ii}\, m_{3i} + 1/2\, h_{ii}\, m_{4i}] + \sum_{i=1}^{n-1} \sum_{j=i+1}^{n} [\, 1/2\, h_{ii} h_{jj} + h_{ij}]\, \sigma_i^2 \sigma_j^2 \qquad (14)$$

m_{3i} and m_{4i} are the 3rd and 3rd moments of x_i [5, 15].

5. CONCLUSIONS

The state-of-the-art about tools and methods used in the statistical tolerance analysis and in the robust design approaches is presented in this paper. These two approaches deal with the variation of the design variables and parameters at different stages of the design process. They generally use the same statistical hypotheses.
This paper emphasises on the validity of the statistical hypotheses. In order to improve the proposed methods for industrial problems with a large number of variables and parameters, further developments are necessary.

Fouad BENNIS, IRCCyN, UMR. CNRS 6597, Ecole Centrale de Nantes, 1, rue de la Noë, B.P. 92101, 44321 Nantes cedex France.

6. REFERENCES

[1] Srinivasan V., "ISO Deliberates Statistical Tolerancing". Proc. of the 5th CIRP International Seminar on Computer Aided Tolerancing, Toronto, Canada.1997, pp:25-35.

[2] Srinivasan V., "Role of Statistics in Achieving Global Consistency of tolerances", Proc. of he 6th CIRP International Seminar on Computer Aided Tolerancing, The Netherlands, 22-24 March 1999, pp 395-404.

[3] Bjorke O. "Computer Aided tolerancing", ASME Press, second edition 1989.

[4] Chase K. W. et Parkinson A. R., "A Survey of Research in the Application of Tolerance Analysis to the Design of Mechanical Assemblies". Research In Engineering Design, 3:pp:23-37, 1991.

[5] Nigam S. D. et Turner J. U., "Review of statistical approaches to tolerance analysis". Computer-Aided Design, 27(1):6-15, 1995.

[6] Srinivasan V., O'Connor M. A. et Scholz F.W., 'Techniques for composing a Class of Statistical Tolerances Zones". IBM Research Division. Report n°20254, 1996.

[7] Zhang W., "Sensitive factor for position tolerance". Int. Jour. Of Research In Engineering Design, (9), pp:228-234, 1997.

[8] Greenwood W.H and Chase K.W, " Root sum squares tolerance analisysis with nonlinear problems", Transaction of the ASME Journal of Engineering for Industry, Vol 112, Nov. 1990, pp:382-384.

[9] Whitney D. E. et Gilbert O.L., and M. Jastrzebski, "Representation of geometric variations using matrix transforms for statistical tolerance analysis in assemblies". Inter. Jour. Of Research In Engineering Design, (6), pp:191-210, 1994.

[10] Skowronski V.J and Turner J.U, "Estimating gradients for statistical tolerance synthesis", Computer Aided Design, Vol 28, n° 12, 1996,pp 933-941.

[11] Skowronski V.J and Turner J.U , "Using Monte-Carlo variance reduction in statistical tolerance synthesis", Computer Aided Design, Vol 29, n° 1, 1997, pp 63-69.

[12] Taylor W.A, "Process tolerancing: A solution to the dilemma of worst-case versus statistical tolerancing", Fall technical conference, 1995.

[13] Kane V. E, "Process Capability indices", Jour. Qual. Technol., 18(1), 1986, pp: 41-52.

[14] Harry M.J and Stewart R, "Six sirma mechanical design tolerancing" , Tech. Report 6sigma 2-10/88 Motorola Corporation (1988).

[15] Glancy C.G and Chase K. "A second-order method for assembly tolerance analysis", Proc. of ASME Design Engineering Tech. conf. Las vagas Nevada, Sept. 12-15, 1999. DETC99/DAC-8707.

[16] Sundaresan S. Ishii K and Houser D.R, " A robust optimization procedure with variations on design variables and constraints", DE-Vol 65-1 Advances in design Automation, Vol 1, ASME 1993, pp379-387.

[17] Kaisi M. Hacker K. And Lewis K, "A comprehensive Robust Design Approach for decision Trade-offs in comlex systems design". Proc. of ASME Design Engineering Tech. conf. Las vagas Nevada, Sept. 12-15, 1999. DETC99/DAC-8589.

[18] Srinivasan V. "On interpreting key characteristics", Proc. of ASME Design Engineering Tech. conf. Las vagas Nevada, Sept. 12-15, 1999. DETC99/DAC-8701.

[19] Parkinson A., Sorensen C. and Pourhassan N. "A general Aproach for robust optimal design", Transaction of ASME Journal of Mechanical Design, Vol. 115, June 1993, pp:74-80.

[20] Parkinson A. "Robust Mechanical Design using engeneering models", Transaction of ASME Journal of Mechanical Design, Vol. 117, June 1995, pp 48-54.

[21] Gadallah M.H. and ElmaraghyH.A. "Desing for robust performance : a concurent engineering approch", Adances in Manufacturing systems 1994R.S. Sodhi (editor), 1994, pp 269-277.

[22] Parkinson A, Chase K. Rogers M. "Robust design via tolerance analysis in the conceptual design stage", Proc. of ASME Design Engineering Tech. conf. Las vagas Nevada, Sept. 12-15, 1999. DETC99/DAC-8577.

[23] Chen Li, "A coordination based approach to robust product design", Proc. of ASME Design Engineering Tech. conf. Las vagas Nevada, Sept. 12-15, 1999. DETC99/DAC-8558.

[24] Yu J.C and , Ishii K. "Design for robustness based on manufacturing variation patterns",Transaction of The ASME Journal of Mechanical Design, Vol 120, June 1998, pp 196-202

[25] Du. X and Chen W, "Towards a better understanding of modeling feasibility robustness in engineering design". Proc. of ASME Design Engineering Tech. conf. Las vagas Nevada, Sept. 12-15, 1999. DETC99/DAC-8565.

GARDONI M., SPADONI M., VERNADAT F.

DEVELOPEMENT AND FEEDBACKS OF A NEW COMMUNICATION TOOL TO HARNESS INFORMATION AND KNOWLEDGE AND KNOW-HOW IN INTEGRATED ENGINEERING - CASE STUDY AT EADS

Abstract. Concurrent Engineering approaches heavily rely on reliable and efficient shared information among people involved in the design, engineering, industrialization and even manufacturing of products. In a context of an integrated design methodology, the nature of information exchanged by the design team evolves and enterprises tend to support this information through co-operative technology (CSCW). Thus, Non-Structured-Information becomes increasingly important within Integrated-Teams. Pieces of information flowing in this kind of teams are hardly controlled. Although informational aspects become more and more strategic, they are barely controlled. Indeed, it could be difficult to structure, share and access pieces of information to enhance Integrated-Team working and to capitalize knowledge and know-how to learn from past experiences and to avoid doing the same mistakes twice.

In this paper, an approach is proposed and a simple groupware tool working on a network is proposed. The tool supports informal message exchange among users. It also provides facilities to structure and archive knowledge learned during this process. The tool has been developed and evaluated at EADS, especially to feed back design teams with manufacturing knowledge in the context of product change requests. Then a method to capitalize knowledge and know-how contents in relation with the tool is proposed.

1. EVOLUTION OF ENGINEERING INFORMATION REQUIREMENTS

Several organizational strategies have been deployed by many enterprises over the century to face evolving economical constraints (standardized production, economy of scale, economy of scope). Traditionally, engineering activities are performed in a sequential order. Over the last ten years, strong market pressures have forced manufacturing companies to drastically reduce the time-to-market of their products. This is why companies tend to apply the Concurrent Engineering approach (CE) [1]. Most of the information exchanged in sequential engineering are the results of the different tasks. In CE, actors of the design have to exchange conjectures that allow the others to work simultaneously. However, Non-Structured-Information, i.e. free format information, becomes increasingly important within Integrated-Teams [2] and appears to be poorly controlled. Indeed, it could be difficult to structure, share and access pieces of information to enhance operations of Integrated-Teams and to capitalise knowledge and know-how to learn from past experiences. To this aim, we propose to characterize information by means of a taxonomy related to information structuring.

2. TAXONOMY RELATED TO INFORMATION STRUCTURING

To meet the needs of rigor of the companies without going to a too detailed level of granularity, an instructional design of the significance of information has been

P. Chedmail et al. (eds.), Integrated Design and Manufacturing in Mechanical Engineering, 77-84.
©2002 *Kluwer Academic Publishers.*

chosen. Exchanged information is then an abstracted entity, a theoretical object, which consists of linguistic components and components rhetoric (Fig. 1) [3]:

- The linguistic components build the significance of information starting from instructions. They are characterized by the clearness of their formalism.
- The rhetoric components bring a meaning to information by addition of contextual information. This construction is characterized by the facility to identify information context.

The properties of this structuring enable to define *Structured-Information* (*SI*), *Semi-Structured-Information* (*SSI*), and *Non-Structured-Information* (*NSI*) [4].

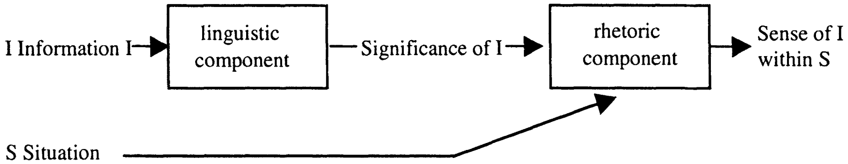

Figure 1. Instructional design of the significance of information.

Characteristics of the *SI*:

- Linguistic components of the *SI* are generally imposed (example: an industrial design).
- Rhetoric components of the *SI* are also imposed (example: an industrial design is associated with the name of the designer, the product, the part, the date, etc.).

The emission of a *SI* is, in general, an integral part of the work of the transmitter. This generates uniformity of the *SI* within an entity.

Characteristics of *SSI* :

- Linguistic components of the *SSI* are weakly formalized (for instance: graphs without keys, drawing without industrial formalism, etc.).
- Rhetoric components are few (example: meeting reports are often not easily understandable by a person who did not take part in the meeting).

The *SSI* are stored less longer than the *IS* because the context is not always associated with information, they can thus quickly become useless.

Characteristics of *NSI* :

- The *NSI* are very poorly formalized, they are open to a multitude of interpretations.
- The rhetoric components can be very light if they ensure a sufficient degree of relevance for the comprehension of information by the receiver (example: 'we do as we said').

The *NSI* are essentially volatile, because even if it is possible to preserve a piece of information of a talk, they are seldom recorded.

However, this kind of information is important in industrial context because it relates to reactivity and agility. Moreover, it increases the product knowledge. Knowledge is thus not static but dynamic, it is in constant evolution [3].

In a Concurrent Engineering context, the *Non-Structured-Information* exchanges are favored. Thus, the knowledge acquisition is carried out by simple successive steps, which improves decision coherence. The product knowledge is in turn enhanced. So, the time-to-market is cut down, the cost is reduced and the quality is improved.

These *Non-Structured-Information* exchanges thus improve the product development process. This is why some enterprises promote the exchanges among design teams, and CE relies on so-called *Integrated Teams*.

Exchanges of NSI are mainly performed verbally during face-to-face talks or on the phone. Unfortunately, this information is therefore poorly controlled. This term "control" can be characterized in terms of four criteria: structuring, sharing, access, and capitalization [5]. Therefore, it appeared interesting to the authors to study modern ways of communication to phase a CE project by using Groupware tools [6].

3. GROUPWARE AND CHARACTERIZATION OF MODERN ENGINEERING INFORMATION SYSTEMS

Groupware tools are computer support tools for collaborative work. The terminology concerning Groupware has not been stabilized yet. Nevertheless, it is usually admitted that Groupware comprises seven types of tools, namely: e-mail, public files, electronic forms, shared files, shared agendas, forums and workflow.

To assess relevance of Groupware tools to CE information system requirements, an evaluation matrix has been proposed (Fig. 2). This matrix intends to highlight three of the axes of a firm's information requirements.

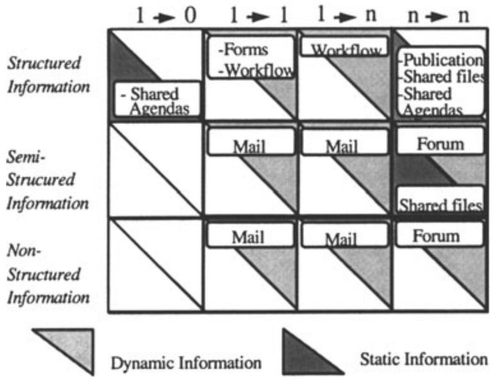
1 → 0
1 → 1
1 → n
n → n
Structured Information
Semi-Strucured Information
Non-Structured Information
- Shared Agendas
-Forms
-Workflow
Workflow
-Publication
-Shared files
-Shared Agendas
Mail
Mail
Forum
Shared files
Mail
Mail
Forum
Dynamic Information
Static Information

Figure 2. Information Requirements Fulfilled by each Groupware Tool.

Dynamics axis: Concerns static versus dynamic information

Destination axis:

1 to 0: Information is stored on one computer and is only used by its owner
1 to 1: Information is send to a selected person
1 to n: Information is send to several selected persons
n to n: Information is send to a group of people

Characterization axis: Information type as *Structured Information*, *Semi-Structured Information*, *Non-Structured Information*

The matrix shows that no single tool can fulfill all information requirements. Especially, *NSI*, which plays an important role in CE, can hardly be structured, accessed, shared, and capitalized in means such as mail or forum.

4. INTERACTIVE MESSAGING SYSTEM FOR AEROSPATIALE MATRA CONCURRENCY (M.I.C.A.)

As argued earlier, neither current means of communication (oral and paper) nor groupware tools fully answers the specifications of CE communication requirements. It was therefore decided to develop a new type of tool at EADS [7]. The purpose of M.I.C.A. is to provide a computerized assistance for engineering problem monitoring and to support capitalization of the trade knowledge from manufacturing backwards to design (Fig. 3).

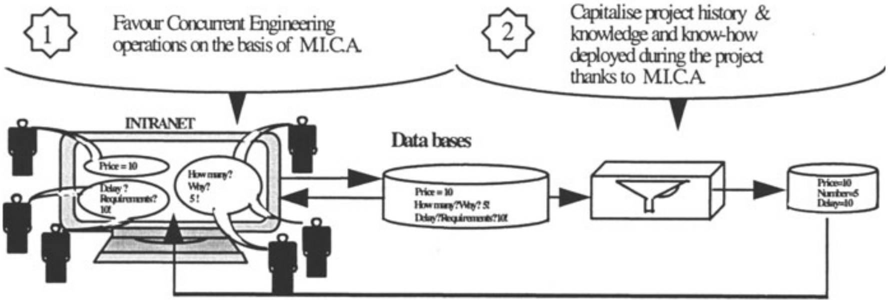
1
Favour Concurrent Engineering operations on the basis of M.I.C.A.
2
Capitalise project history & knowledge and know-how deployed during the project thanks to M.I.C.A.
INTRANET
Price = 10
Delay ? Requirements? 10!
How many? Why? 5 !
Data bases
Price = 10 How many?Why? 5! Delay?Requirements?10!
Price=10 Number=5 Delay=10

Figure 3. Principles of M.I.C.A. Tool.

4.1. M.I.C.A. Information Structuring

To formalize non structured information aspects in M.I.C.A. (at the rhetoric and linguistics levels), we have considered various enterprise modeling methods such as CIMOSA [8]. Especially, we preserved various CIMOSA concepts, for instance the concept of modeling views. which can be represented by a meta-model. The objective of this meta-model is to be at the same time generic, exhaustive, and representative in a certain context. A modeling language based on the oriented object concepts of UML (Unified Modeling Language) is used. Four main views have been defined in M.I.C.A.: the *Co-operative View*, the *Resource View* , the *Product View,* and the *Process View*. All these *Views* can be related to the description of a design "context". They are part of the contextual information, which should be associated with the *NSI* to facilitate the understanding of their meaning.

Co-operation View

The co-operation view attempts to model interactions between the members of the Integrated Team. We model the rhetoric aspects and the linguistic aspects separately. For the rhetoric aspects, we make use of the general outline of the Baker's negotiation model (Fig. 4) [9].

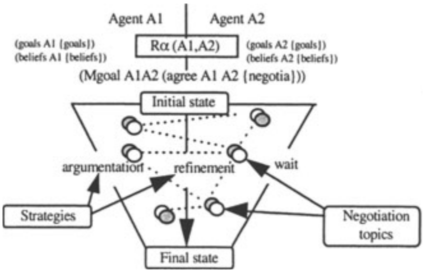
Agent A1
Agent A2
(goals A1 {goals})
(beliefs A1 {beliefs})
Rα (A1,A2)
(goals A2 {goals})
(beliefs A2 {beliefs})
(Mgoal A1A2 (agree A1 A2 {negotia}))
Initial state
argumentation
refinement
wait
Strategies
Negotiation topics
Final state

Figure 4. General Scheme of Baker's Negotiation Model.

This modeling enabled us to choose a grouping of the *NSI* involved in a negotiation for problem solving in product design. It was decided to gather all the *NSI* concerning the same negotiation in the same form (Fig. 5). A form is made of three paragraphs symbolizing "the initial state", "the final state", and "the current state of negotiation" (Fig. 5). These paragraphs are made of:

- pre-defined fields containing contextual information resulting from the *Resource, Product, and Process Views*,
- free fields containing the *NSI*.

Because our goal is to build a computer-based application as a support to the *NSI*, the contextual information will take the practical form of pre-defined data fields in the M.I.C.A. forms containing the characteristic elements of the context.

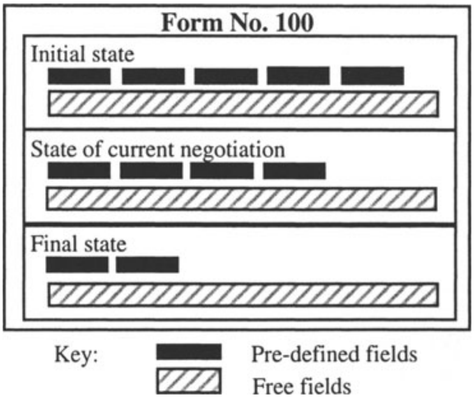
Form No. 100
Initial state
State of current negotiation
Final state
Key:
Pre-defined fields
Free fields

Figure 5. Schematic Example of a M.I.C.A. Form.

4.2. M.I.C.A. Information Sharing

All the Department Representatives can have access to all *INS* of the computer application.

4.3. M.I.C.A. Information Access

Various means of access can be used: search from the words contained in the predefined fields, use of a search engine for specified fields, etc.

4.4. M.I.C.A. Capitalization of knowledge and of know-how

Thanks to the M.I.C.A. software, *Non-Structured Information* exchanged between the members of the team can be traced. Thus, software packages applying data analysis techniques can then be used [10]. The goal is to propose a practical solution to derive expert rules from the corpus of M.I.C.A. based on the suggestions of a software tool. The analysis of linguistic data (using data-mining techniques) can be divided into two main families : factorial analysis and hierarchical classification. Hierarchical classification techniques have been selected because they were previously used at EADS.

Three main methodological phases are identified to perform a data-mining search:

- Constitution of the corpus: In our case, we select a set of forms of M.I.C.A.
- Automatic indexation: automatic phase to build a lexical index representative of the corpus.
- Automatic classification: There are two kinds of hierarchical classification algorithms: top-down and bottom-up hierarchical classification. A tool based on bottom-up classification has been chosen because this kind of tool goes into the detail of the associations of terms constituting the text

After several iterations on the data contained in M.I.C.A., four clusters of terms can be obtained. These clusters (modeled as graphs) can be completed by an expert giving a meaning to connections (arcs of the graphs) with semantic terms.

Finally, these graphs can be translated in the form of if-then rules. For instance, examples 1 and 2 of cluster parts of Fig. 6 can be translated into IF-THEN rules as shown on the figure.

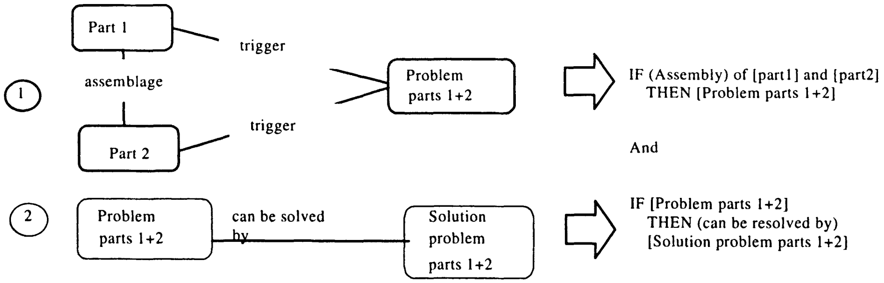
Part 1
trigger
① assemblage
Problem parts 1+2
IF (Assembly) of [part1] and [part2] THEN [Problem parts 1+2]
trigger
Part 2
And
② Problem parts 1+2
can be solved by
Solution problem parts 1+2
IF [Problem parts 1+2] THEN (can be resolved by) [Solution problem parts 1+2]

Figure 6. Examples of IF-THEN rules derived from term clusters.

The objective assigned seems to have been achieved because we have a way to derive expert rules from the suggestions of a data-mining tool. Nevertheless, to be more exhaustive in terms of elaboration of possible rules, it would be advisable to use a tool based on top-down hierarchical classification to edit more significant classes [11]. Further research needs to be done in this way.

5. PATTERNS

Thanks to data-mining tools, we are able to elaborate IF-THEN rules. We now tackle the problem of information use with the pattern concept [12]. Our objective is to adapt the pattern approach according to target, i.e. to exploit IF-THEN rules. We have used the Gamma formalism by retaining and adapting only the six headings that were judged essentials. These headings are listed in Fig. 7 [14].

Name: Name of the pattern.
Classification : relating to a predefined field in the M.I.C.A. form.
Intention : problem to which the pattern addresses.
Context : context of the problem characterize with predefined field of M.I.C.A forms.
Motivation : a scenario of application of the pattern describing particular problems.
Semi-formal description: solution suggested by the pattern.

Figure 7. Example of pattern headings.

6. EXPERIENCE FEEDBACK

Currently, without the M.I.C.A. software, members of the Integrated-Team are in a difficult communication mode which is based on a rumor phenomenon. Conversely, with the M.I.C.A. approach, the members can write (which implies a contractual connotation) informal information that is not validated at 100%. Therefore, errors can be visible to all. A suspicion phenomenon can result. However, this should be balanced by the individual observation of the M.I.C.A. advantages in terms of structuring, sharing, and accessing information. These advantages lead to project consolidation anticipation. To be effective, M.I.C.A. has to be based on some confidence within the Integrated Team, it can indeed support this fact. By defining exactly what can be shared by M.I.C.A., this would contribute to unify the Integrated-Team around M.I.C.A. acting as a shared knowledge base.

7. PERSPECTIVES

The experimentation of the M.I.C.A. approach appears to be successful. However, at least seven major topics should be further investigated:

1. Identification of the *NSI* captured by M.I.C.A.
2. Identification of the knowledge and know-how capitalized by M.I.C.A.
3. Genericity of the M.I.C.A. approach and potential application to other contexts
4. Connections between *Structured*, *Semi-Structured,* and *Non-Structured Information* systems
5. Aggregation of various tools of communications to propose a homogeneous communication environment.
6. Use of new information technologies to favor the use of the M.I.C.A.
7. Generalization to large engineering teams.

This list is not exhaustive. These are topics that should be taken into account to undertake other experiments and before a generalization of the M.I.C.A. approach can be made. The M.I.C.A. approach thus opens new perspectives in collaborative work.

8. CONCLUSION

The paper argues that actual means of communication used in engineering can hardly support *Non-Structured Information*. This is the reason why a tool called M.I.C.A. has been implemented and tested in industry. At the beginning of the design cycle and product development, M.I.C.A. intervenes as a communication tool using forms on screens which crystallizes the efforts of the Integrated Team members and thus facilitates work in a Concurrent Engineering environment. Afterwards, M.I.C.A. can be used to capitalize the knowledge and the know-how deployed during the project. This tool is also able to structure, share, have access, and capitalize information through an Intranet infrastructure. It has been implemented and put into operation in an engineering team of twenty people in May 1998 at EADS. Improvements have been identified and are being taken into account in the framework of other experiments.

REFERENCES

[1] Prasad, B. (1996) "Concurrent Engineering Fundamentals - Integrated product and process organisation", Vol. 1, Prentice Hall, Englewood Cliffs, NJ.

[2] Bocquet, J.C., Ingénierie Simultanée, conception intégrée, Conception de produits mécaniques (méthodes, modèles et outils), coord. Tollenaere, M., Editions Hermès, Paris, 1998

[3] Moeschler, J. Modélisation du dialogue (représentation de l'inférence argumentative), Editions Hermès, Paris, 1989

[4] Gardoni, M., Spadoni, M., & Vernadat, F.B. (1999) Requirements analysis for enhanced information support in Concurrent Engineering Environments. 5th Int. Conf. on Industrial Engineering and Production Management, Glasgow, Scotland, July 12-15

[5] Barthes, J.P., Grundstein, M., "Discussion Summary", 3rd International Symposium on the Management of Information and Corporate Knowledge (ISMICK'95), Institut International pour l'Intelligence Artificielle, Compiègne, France, October 23-24 1995

[6] Gardoni, M., Spadoni, & M.,Vernadat, F., "Information and Knowledge Support in Concurrent Engineering Environments", 3rd International Conference on Engineering Design and Automation, EDA'99, Vancouver, B.C., Canada, August 1-4, 1999

[7] Gardoni, M., Maîtrise de l'information non structurée et capitalisation du savoir et du savoir-faire en Ingénierie Intégrée - Cas d'étude Aérospatiale Matra, PhD thesis of Metz University 1999

[8] Vernadat, F.B., "Enterprise Modeling and Integration: Principles and Applications", Chapman & Hall, London, 1996

[9] Baker, M. A model for negociation in Teaching-Learning Dialogues, *Journal of Artificial Intelligence in Education*, n.5.(2), pp.199-254, 1993

[10] Benzécri, J.P. (1973) "L'Analyse de données : L'analyse des correspondances" , Tome 2, Editions Dunod

[11] De Looze, M.A., Roy, Has., Reinert, Mr., Jouve, & O., Copronini, R. "Analyse de données et analyse de mots associés, comparaison d'algorithmes différents sur un corpus concernant la prise en compte du risque dans le développement des OGM dans le domaine des végétaux, Veille Stratégique Scientifique et Technologique", Toulouse, 19 au 23 octobre 1998 , pp.241-255

[12] Spadoni, M., Youssef, A., & Gardoni, M., "Adaptative shop-floor control : Distributed approach based on know-how", 1st International Federation of Automatic Control (IFAC) on Multi-Agent-Systems in Production, Vienna, december 2nd -4th , 1999

[13] Gzara, L., Rieu, & D., Tollenaere, M., "An Approach for Building Product Models by Reuse of Patterns", 7th ISPE International Conference On Concurrent Engineering CE2000, Lyon, France, 17-20 juillet 2000

A. DEGLIN, A. BERNARD

A KNOWLEDGE-BASED ENVIRONMENT FOR MODELLING AND COMPUTER-AIDED PROCESS PLANNING OF RAPID MANUFACTURING PROCESSES

Abstract. *This paper introduces a knowledge-based environment dedicated to the choice of rapid manufacturing processes. Rapid manufacturing processes are not limited to layer-manufacturing machines, but they also integrate CAD, reverse engineering, indirect methods for metallic and plastic part manufacturing, etc…*

Due to short delays, people have no time to test and compare different solutions of rapid manufacturing. Tests are also money consuming and it is very difficult for someone to know all about industrial technologies and to be able to evaluate a multi-criteria choice at a time.

The aim of the presented knowledge-based environment is to propose, from the client requirement, different alternatives of rapid manufacturing processes, which can be ordered and optimised when considering a combination of different specification criteria (cost, quality, delay, aspect, material, etc…).

At present a first version of the conceptual model has been implemented on Kadviser platform and validation tests are ongoing based on industrial case studies.

1. INTRODUCTION

Currently, in the field of rapid prototyping, a great number of new technologies joined already more conventional ones, and they did not have of cease to progress. This is why today the possibilities are multiple and varied to obtain a prototype, tools, a series of part... But, considering the number of processes, materials, machines, subcontractors..., there are means more or less judicious to obtain the desired results (AFPR, 2001 ; Bernard, Taillandier, 1998 ; Wolhers, 2001).

In this number of solutions of processes, of possible subcontractors, a system of assistance to the choice of the various processes of rapid manufacturing should thus allow many services of the companies to share the knowledge and the solutions delivered by the technologies.

Due to the short life cycle of products, companies have to adapt their development and industrialisation organisation in order to reduce time-to-market, based on numerical information that has become the reference for the product. In fact, new challenges concern the capability to manufacture the just necessary number of products at a given price. The main consequence is flexibility for tool manufacturing with low-price and consumable tools, instead of very cost-consuming ones. This is possible because of numerical information, used along the complete development of the product, and due to new materials. But, consequently, it is necessary to validate product and process concepts very early during the design stage. Some recent developments in rapid manufacturing allow such possibilities (Bernard, 1998 ; Xu, Wong, Loh, 1999 ; Zhang, Ajmal, Yang, 1995).

P. Chedmail et al. (eds.), Integrated Design and Manufacturing in Mechanical Engineering, 85-92.
©2002 *Kluwer Academic Publishers.*

These examples show that the dynamic evolution of technologies is not easy to take into account in real time. This is why it is strategic to find the just necessary process for given specifications.

What is proposed in this paper is an approach dedicated to knowledge and know-how modelling for computer-aided process planning (CAPP) from given specifications (type of part, material, delay, quality, colour, etc…).

2. CAPTION AND MODELLING OF KNOWLEDGE

Knowledge is defined in a general way as being the unit of the know, the experiments, the rules and the expertise (Kassel, 1995).

Three categories of knowledge have been distinguished:

- Knowledge relating to knowing: it is descriptive, static, directly usable and is acquired while being informed, information is thus the privileged vector of this type of knowledge.
- Knowledge relating to making: it is dynamic and generally corresponds to methods or procedures, the privileged vector of this type of knowledge is the training.
- Knowledge relating to understanding: it results from the enrichment of knowledge relating to knowing and making obtained through the experience sharing lived by different people, in more or less close contexts. This knowledge is not directly transferable, the communication is the privileged vector of this type of knowledge.

The capture and modelling of knowledge suppose a step of identification of relevant pertinent knowledge in order to allow its management.

Knowledge formalisation and management are significant elements, which for these ten last years have worried many industrialists.

Today, the field of rapid prototyping, and even more rapid manufacturing, come within domains where each actor represents his technologies, and its competencies represent only one small part of the complete field. The interest for a company to model technologies and the knowledge of the field, is to pre-empt the future needs, to capture and model in a field without being tributary of the expert, who can leave to the retirement, competition or to even be sick... In fact makes it capitalise the field of rapid manufacturing by means of computer, makes reliable, makes safe, and perpetuates the knowledge and know-how (Perpen, 2000).

With the objective of computerisation, it is necessary to give a physical and static representation of the field in order to make it possible to limit and know the various values to be handled and intervening in the field. It is the first work of analysis, it makes it possible to include/understand, then to generalise the mechanisms in order to draw a certain number of concepts, principles and heuristic governing the field. Once this work is carried out, it is used as a basis for the system.

The processing of knowledge capture and modelling can be broken up into several categories:

- The acquisition of knowledge is specific to the fields and to the problems to be treated. This knowledge, primarily symbolic, often expresses relations between objects, but also formal or numerical calculations on these objects.
- The representation of knowledge according to models; as general as possible, as independent of the processing as possible and sufficiently semantic so that the acquisition of knowledge is easy.
- The implementation of the reasoning on this knowledge which results in models of handling of knowledge more or less general, related to the models of representation translating the principles of reasoning by the absurdity, recurrence, or by analogy.
- The control of the reasoning and its implementation on specific problems to reduce the space of search for solution.
- The explanation of the reasoning in two objectives:
    - to leave a detailed trace of the reasoning undertaken with the developer of the system
    - to give a concise explanation to the user of the system
- The revision of knowledge must determine up to what point one can modify in the established knowledge as a preliminary and consider an automatic revision of knowledge (maintenance of coherence).

3. MODELLING OF KNOWLEDGE

The problem of the representation of knowledge consists in finding a correspondence between an external world and a symbolic system. Knowledge that the computers usually handle is of a numerical nature. The expert system of assistance to the choices of the various processes of rapid prototyping, has as a principal objective, to answer a need capturing and modelling of the knowledge and know-how in the field of rapid manufacturing (Bernard, 1999). This is like restoring a relevant orientation in term of process solution to the case imposed to the various actors (Rechenmann, 1995 ; Rechenmann, 1999). The schedule of conditions of the application emphasises two great phases of use of the environment to be set up:

- The capture and modelling of knowledge, which represents the whole of the parameters, the behaviours and the variables to be integrated in the expert system, in order to be representative of the field. This has to be introduced into the system by the experts and by the knowledge engineers.
- Extraction and exploitation of knowledge, represents the service accessible by the users, this service results in a solution in terms of processes, technologies, subcontractor... according to the various specification of the part that the user defines.

Modelled knowledge should represent the processes and the technologies used in rapid manufacturing. The models representing the processes and the technologies are representative of the significant aspects and criteria of decision. The criteria indicated by the user in the schedule of specification have similarities with the criteria of the processes figure 1 and meta-technology figure 2, so then allowing a correlation making it possible to generate a solution.

Knowledge is of type capacitating, behavioural and environmental. In other terms capacitate material, type of machine, minimal thickness of realisation, dimensions... Knowledge of the behavioural type results in the difference between the input and output states of the process. Environmental knowledge defines the context of manufacture, the parameters of delivery (time, cost, quality,…).

The modelling of knowledge will be carried out within a system, which will make it possible to store various knowledge classified by processes and by technologies (SME, 1999).

The cognitive model of process (given on figure 1) represents the structure making it possible to the experts to model examples of processes (case studies) and technologies used in the field of the rapid manufacturing of products.

The cognitive model of specification makes it possible to the user to inform the various constraints associated with its need, and on which the system will base its reasoning.

The model of specification is a significant element of structure, because it allows the user transcribing its need of a formal manner, and allows then the system working on the stored objects (technologies and process). One of the possible solutions for reasoning should be the comparison of the user specification with the stored technologies, processes and meta-technologies which allow of define the procedure of solution.

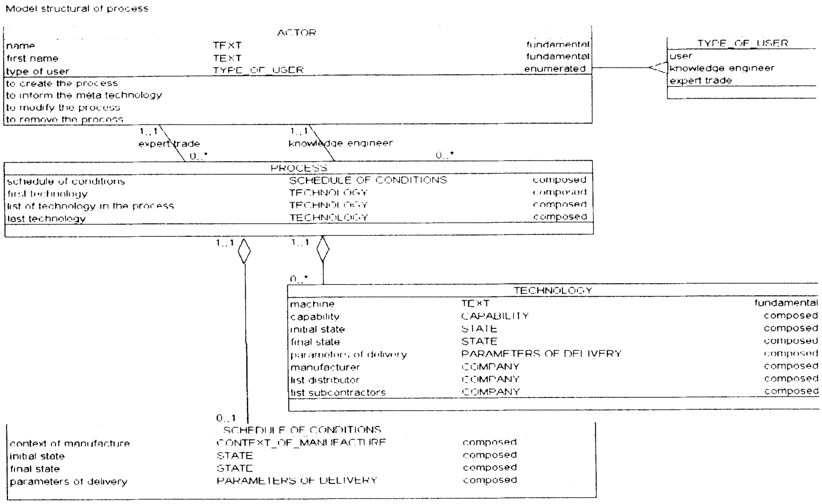
Model structural of process
ACTOR
name TEXT fundamental
first name TEXT fundamental
type of user TYPE_OF_USER enumerated
to create the process
to inform the méta technology
to modify the process
to remove the process
TYPE_OF_USER
user
knowledge engineer
expert trade
1..1
expert trade
0..*
1..1
knowledge engineer
0..*
PROCESS
schedule of conditions SCHEDULE OF CONDITIONS composed
first technology TECHNOLOGY composed
list of technology in the process TECHNOLOGY composed
last technology TECHNOLOGY composed
1..1
1..1
0..*
TECHNOLOGY
machine TEXT fundamental
capability CAPABILITY composed
initial state STATE composed
final state STATE composed
parameters of delivery PARAMETERS OF DELIVERY composed
manufacturer COMPANY composed
list distributor COMPANY composed
list subcontractors COMPANY composed
0..1
SCHEDULE OF CONDITIONS
context of manufacture CONTEXT_OF_MANUFACTURE composed
initial state STATE composed
final state STATE composed
parameters of delivery PARAMETERS OF DELIVERY composed

Figure 1. Part of the process cognitive model.

The third major element in the system is the model of knowing of technical manufacture and represented by the model of meta-technology (given on figure 2) and by the model of technology. A meta-technology is the generic class of technology having as common point a given technology of fabrication. For example:

- stereolithography meta-technology gathering SLA 3500 technology type,
- powder sintering meta-technology gathering EOSINT P350 technology type.

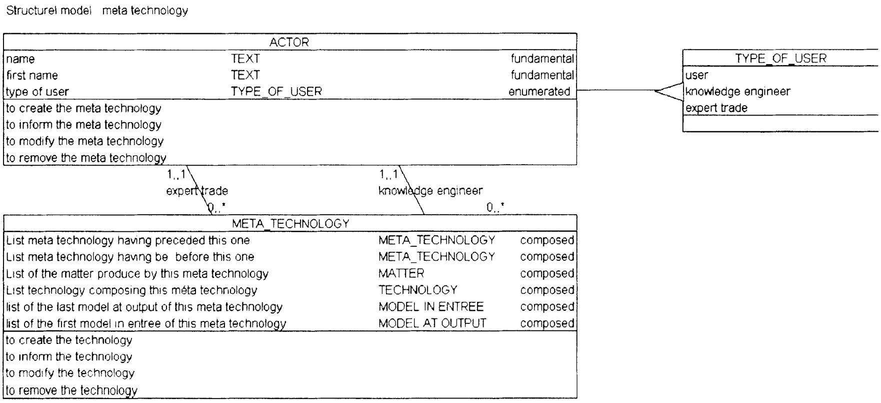
Structurel model meta technology
ACTOR
name TEXT fundamental
first name TEXT fundamental
type of user TYPE_OF_USER enumerated
to create the meta technology
to inform the meta technology
to modify the meta technology
to remove the meta technology
TYPE_OF_USER
user
knowledge engineer
expert trade
1..1
expert trade
0..*
1..1
knowledge engineer
0..*
META_TECHNOLOGY
List meta technology having preceded this one META_TECHNOLOGY composed
List meta technology having be before this one META_TECHNOLOGY composed
List of the matter produce by this meta technology MATTER composed
List technology composing this méta technology TECHNOLOGY composed
list of the last model at output of this meta technology MODEL IN ENTREE composed
list of the first model in entree of this meta technology MODEL AT OUTPUT composed
to create the technology
to inform the technology
to modify the technology
to remove the technology

Figure 2. Part of the cognitive meta-technology model.

The meta-technology and the technology are elements that constitute the knowing, these two models are defined and introduced in the system only by people having the technical knowledge; these are thus the experts as well as the knowledge engineers who have the privilege to implement the base of new technologies.

4. USE OF THE CAPP EXPERT SYSTEM

For the utilisation of the CAPP system we set up two types of reasoning allowing to bring different functionalities, closely connected to give a real efficiency in order to satisfy the various user's needs (figure 3).

Based on these kinds of reasoning the user has to fill the various fields of the specification form. All these parameters do not require to be informed because some are not known and are not of primary importance for the treated case. This form includes all the parameters relevant for the definition of the user needs.

During the description of the various parameters of the user specification, the system makes the first reasoning, making it possible to simplify the tree structure of the various meta-technologies as well as technologies.

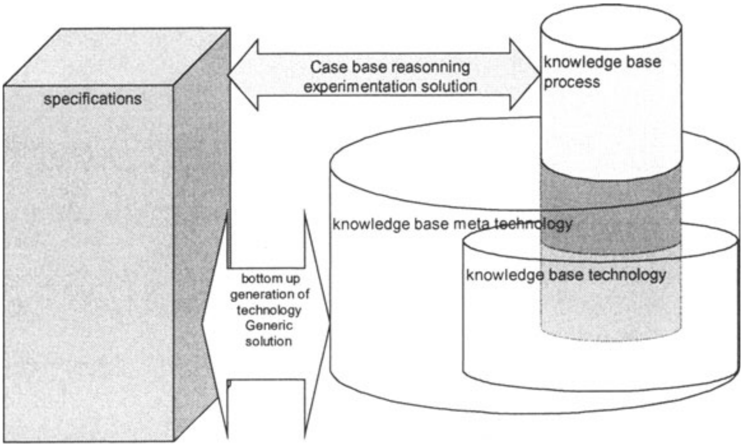
specifications
Case base reasonning
experimentation solution
knowledge base
process
knowledge base meta technology
knowledge base technology
bottom up
generation of
technology
Generic
solution

Figure 3. Schema representing the two types of reasoning applied in the CAPP system.

To allow a rapid and efficient simplification and a fast reasoning, an example of criteria making it possible to create the first outline of process solution is:

- Type of model in input
- Typology of the material for the final desired part

The type of model in input makes it possible to define all the processes and the meta-technology having the same type of model in input as that by the user.

The typology of the material of the final part makes it possible to define the meta-technology as well as the processes potentially capable to produce a part in a coherent state compared to the specification, or potentially able to be the final process of the required solution.

Then the system analyses if a process has the two both elements (typology of the material and type of model of input). In this case, the process is made up only of one meta-technology, and in consequence of one technology. Then, if the system does not find any type of process having the typology of the material and the model in input, it generates a solution by bottom-up output generation of process. It starts from the final meta-technology and see for a meta-technology such as its material typology is coherent with the one in input of the final meta-technology. This is repeated for all the final processes, and then gradually in order to determine the complete solutions archived when finding the first possible processes, corresponding to the type of model in input given by the user.

It is clear that the various criteria making it possible to select the proposed solutions between the various processes constituting each one a potential solution are more numerous than the two ones used for the example.

5. ACPIR CAPP APPLICATION

Some part of CAPP system screen is presented bellow (figure 4).

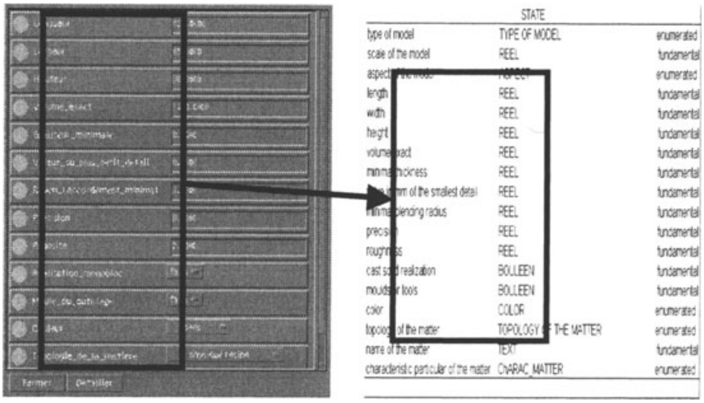

STATE		
type of model	TYPE OF MODEL	enumerated
scale of the model	REEL	fundamental
aspect of the model	ASPECT	enumerated
length	REEL	fundamental
width	REEL	fundamental
height	REEL	fundamental
volume exact	REEL	fundamental
minimal thickness	REEL	fundamental
[illegible] of the smallest detail	REEL	fundamental
minimal bending radius	REEL	fundamental
precision	REEL	fundamental
roughness	REEL	fundamental
cast solid realization	BOLLEEN	fundamental
moulds or tools	BOLLEEN	fundamental
color	COLOR	enumerated
topology of the matter	TOPOLOGY OF THE MATTER	enumerated
name of the matter	TEXT	fundamental
characteristic particular of the matter	CHARAC_MATTER	enumerated

Figure 4. Part of screen and corresponding attributes of the model of state.

To model the knowledge and know-how of the field, we chose to use an industrial expert environment, a system containing knowledge, Kadviser (CEGOS KADETECH, 1999), which allows from its intrinsic construction:

- An object based representation.
- The modularity of the base of knowledge.
- A communication with external applications , using DBMS standard (Data Base Management System), geometrical modeller...
- An easy and user-friendly interface with the various actors using this system.

Kadviser is a generator of expert system including an inference engine for constraint propagation based on the mathematical logic of command 1, allowing the non-monotonous reasoning by management of assumptions on the objects which are handled through typified and quantifiable variables. The mechanism of inference and the principle of resolution are non-monotonous and based on a non-configurable logic by the user. Because of this mode of reasoning, Kadviser knows the opposite of any rule and includes the deductive non-complete. Its capacities of simulation of reasoning, as well as the potential for the processing of overstrained problems (without precise solution), under constrained (multiple precise solutions) or even complete (single precise solution) confer the possibility of treating expert applications in different fields.

The global application menu is used as command interface with to the user, making it possible for him to interact with the CAPP system (specification definition, solution collection). The model in input makes it possible to define which are the various processes, which have the same starting state.

6. CONCLUSIONS

In conclusion, the ACPIR CAPP expert system for the assistance to the choices of processes of rapid manufacturing makes it possible to model the knowledge and know-how of the field. Its main objective is to make it possible to the various users of the system to find, whatever their need, a solution through the system.

The first phase carried out at the time of this project was the census of technologies, the processes, the criteria, the procedures and behaviours, the uses and habits of this field. This stage of cognition allowed highlighting and implementing the structures and functions to be integrated into the CAPP expert system. In parallel search and analysis of a great number of fast case studies in the field of rapid manufacturing has been carried out.

With this stage followed the phase of formalisation and object modelling of the specifications representative of the need, processes representative of the case studies, and meta-technologies and processes representing technology used for the various stages of prototype part manufacturing.

7. REFERENCES

AFPR (2001). *Proceedings of EURO RP 2001 Conference.* Ed AFPR, Paris. France.

Bernard A., Taillandier G. (1998). *Le prototypage rapide.* ISBN 2866016734, Ed Hermès. Paris. France.

Bernard A. (Coordinator) (1998). *Développement rapide de produit.* International Journal of CADCAM and computer graphics. Vol. 13, n°4-5-6. N° ISSN 0298-0924.

Bernard A. (1999). Computer-aided process planning for rapid prototyping. *Solid Freeform Fabrication Symposium.* Austin. USA. pp 39 – 45.

CEGOS-Kadetech (1999). Technical documentation on Kadviser. Kadviser is a trademark of CEGOS-Kadetech. 17 chemin du Petit Bois - 69130 Lyon-Ecully - France

Kassel G. (1995). Contribution à la représentation des connaissances pour les Systèmes Experts de Seconde Génération : projet AIDE. *Habilitation à diriger les recherches.* Université de Compiègne.

Perpen J. L. (2000). Définition et réalisation d'une application orientée objet pour la maitrise du processus de coupe. *PhD dissertation.* Université de Bordeaux. France.

Rechenmann F. (1988). SHIRPA : système de gestion de bases de connaissances centrées objet. *INRIA/ ARTEMIS.* Grenoble. France.

Rechenmann F. (1995). Les catégories de connaissances et leur modélisation, proceedings of 2nd rencontres Théo Quant sur "décision spatiale". Besançon. France.

SME (1999). *Proceedings of Rapid Prototyping and Manufacturing (RP&M'99).* USA.

Wolhers T. (2001). Rapid Prototyping and Manufacturing *State of Industry report.*

Xu F., Wong Y. S., Loh H. T. (1999). A Knowledge-based Decision Support System for RP&M Process. *Solid Freeform Fabrication Symposium.* Austin. USA. pp 9 –18.

Zhang S. G., Ajmal A. and Yang S. Z. (1995). Reverse engineering and its application in rapid prototyping and computer integrated manufacturing. *Proceedings of Computer Applications in Production and Engineering (CAPE'95).* Beijing. Chine. pp. 171 - 178.

Alexandre DEGLIN, Research Centre for Automatic Control of Nancy (CRAN)
BP 239 – 54506 VANDOEUVRE Cedex – FRANCE
+ 33 3 83 90 51 07 ; + 33 3 83 90 51 01 ; aipl@aipl.uhp-nancy.fr
Alain BERNARD, Professor, Research Institute for Communications and Cybernetics of Nantes (IRCCyN),
1 rue de la Noë BP 92101 44321 – NANTES Cedex 3 – FRANCE
+ 33 2 40 37 69 53 ; + 33 2 40 37 69 30 : Alain.Bernard@irccyn.ec-nantes.fr

EVALUATION OF DECISIONS CONSIDERING THE CHOICE OF ACTORS IN PRODUCT DESIGN PROCESSES

Julie Stal-Le Cardinal
Ecole Centrale Paris, Laboratoire Productique-Logistique
92295 Châtenay-Malabry, France
stalj@pl.ecp.fr

Mounib Mekhilef
Ecole Centrale Paris, Laboratoire Productique-Logistique
92295 Châtenay-Malabry, France
mekhilef@cti.ecp.fr

Jean-Claude Bocquet
Ecole Centrale Paris, Laboratoire Productique-Logistique
92295 Châtenay-Malabry, France
bill@pl.ecp.fr

Abstract Optimization of quality, cost, and time is still one of the industry's general objectives. We present here a malfunction approach for decision making processes. This allows the evaluation of decisions and then, the optimization of decision making processes. We introduce the concept of Decision Time Line (DTL) which models the decision process from the request to the answer. In addition to this temporal description of malfunctions, we highlight that it is possible to give a characterization of these malfunctions. Then, we focus our research works more particularly on decisions considering the choice of actors in product design processes. We propose, on one hand, an evaluation of malfunctions appearing in such decisions and, on the other hand, a methodology that helps to find appropriated recommendations to avoid them.

Keywords: DTL, decision, project, malfunction, evaluation.

P. Chedmail et al. (eds.), *Integrated Design and Manufacturing in Mechanical Engineering*, 93-102.
©2002 *Kluwer Academic Publishers.*

1. Introduction

The aim of any firm is to make profit. Firms reach this objective by designing products which fulfill consumers' needs. In order to help firms in that direction, first of all, products have been optimized by methods such as Value Analysis, Quality Function Deployment, Robust Design... Then a reflection about the design process has been conducted to reduce cost and time and to improve quality.

The problem that interests us here concerns the study of malfunctions in decision making processes. Questions which directly arise from this are about the definition of a malfunction, the criteria to characterize it, and also the way to define a typology for the malfunctions representation. Moreover, in this research work, we are trying to build two kinds of tools: tools to detect malfunctions, and tools to evaluate their impacts on the process. At the very end of this study, we hope that we will be able to propose methodologies that give recommendations "at the earliest" in a decision making process so as to avoid malfunctions.

2. Field of inquiry

Industrial projects provide a frame of potential malfunctions. Indeed, teamwork, material means and resources sharing, concurrent and simultaneous engineering can lead to different kinds of difficulties: lack of a particular resource, objective or environment bad understanding, actor's state of mind... These breakdowns within processes appear quite often but seem to be hazardous. Their origin can sometimes be identified but nothing is done to make their detection possible and to try to reduce them. However, a study realized by *the Standish Group International* [5] highlights that, among 8,380 computer applications, only 16% of projects had respected the objectives in terms of cost and time, and offered only 42% of the initially specified functions. Moreover, 53% of projects cost more than 189% of initial budget and 31% of computer projects never finished.

A functional analysis of process modeling has led us to four characteristics of a sufficient representation model: **i-** the development process is a decision making process in which questions are conceived, accepted, and answered, **ii-** time appears as an evolution parameter, **iii-** the human factor has an impact on the processes, and **iv-** the interactions between resources are important for such a systemic based model (human or inanimate, concrete or conceptual). To further focus on the modeling approach, we have chosen a "dysfuntions" analysis of the decision making process. According to *Bana e Costa* [1], such a study does not consist in the quest for the optimum as the only solution, but as a help for decision making.

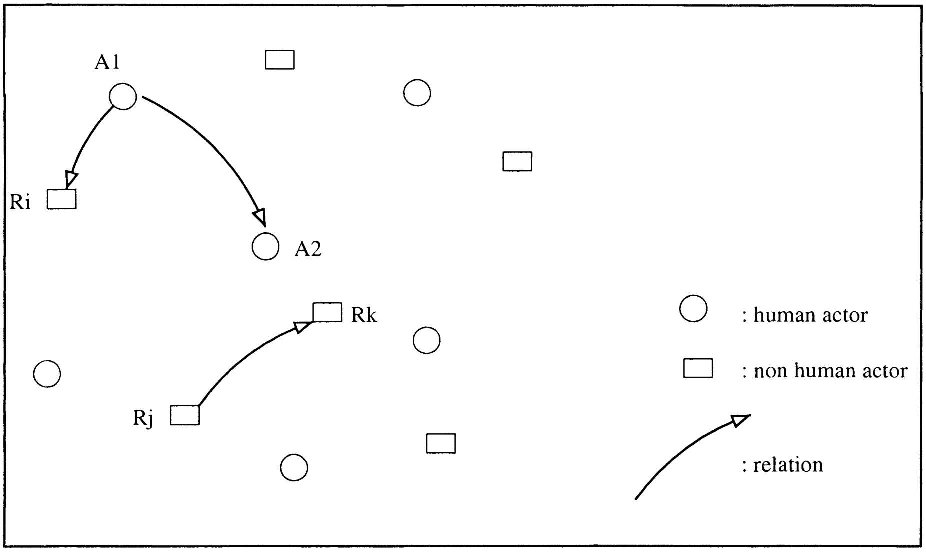

Figure 1.1. A network of actors and resources.

A capitalization database provides a mean for malfunction prediction, by capturing the firm's experience from prior decision making tasks. Software, accessing the capitalization database, and the decision making model, can give an early warning to a decision maker when an action or decision making strategy is likely to lead to a known malfunction, and consequently to a problem in cost, time, or quality. Such a capitalization database can also be used to conduct a statistical study of malfunctions within the firm. A set of examples involving malfunctions observed in industry will be presented, and analyzed using our methodology.

3. Presentation

Our purpose is to study malfunctions within a network of actors, which represents the firm. The main idea is that any organization can be viewed as a graph, as shown in Figure 1.1, where the nodes represent firm resources or competencies, and arcs the existence of potential relations between resources.

Actors and resources belong to the firm means. But, whereas an actor can make decisions, a resource cannot make any. According to *Kolodner* [6], decision makers elaborate their own personal reasoning process thanks to their experience. An expert decision maker, for *Shanteau* [12], is "someone who can make sense out of chaos". The assembly of actors represents the available competencies for the firm. Competence is the capacity for an actor to execute an elementary task within a project. Particular competencies are essential for a given task in order to reach the objective. Actors are chosen according to their competencies, and availability. Two steps in the process are fundamental:

- the competencies identification: issued from the analysis of the necessary technologies (with as much uncertainties as new technologies are concerned) considering Quality, Cost, and Time constraints,
- the actors identification: issued from the analysis of the available actors who have the competencies identified previously.

Three kinds of relations can be drawn on the network:

- $r(A_1, A_2)$: A_1 knows the competencies (and their levels) of the actor A_2,
- $r(A_1, R_i)$: A_1 has the competence to use R_i. However, his levels of competencies may not match with those required by A_1,
- $r(R_j, R_k)$: R_j needs R_k to perform some tasks.

In this article, we are interested in the relation $r(A_1, A_2)$ between two human actors within a decision making process. We study more particularly decisions that concerns the choice of an actor (illustrated by Figure 1.2) among all the potential actors of a firm to perform a given task. We call hereafter DECISION MAKER (A_1 in $r(A_1, A_2)$) the actor who is making the choice, and ACTOR the one who is chosen. With respect to *Simon* [11], we believe that it is possible to model human reasoning processes, and information treatment, and that each decision has, as a starting point, the projection of the real expected situation, and the objectives.

So as to describe this process, we propose a decomposition of the Decision Time Line (DTL) into six phases (Apprehending, Identification, Negotiation, Analysis, Capitalization, Transmission). Among these six phases, the Identification phase is where a given objective can be decomposed into sub-objectives. If an actor does not have the competencies to perform a task completely, the global objective is decomposed, and, at least, an additional actor is chosen to reach some of the sub-objectives. Once the objective is decomposed, the DECISION MAKER has to identify the ACTORS having the competencies (*Durand* [4]) to reach the sub-objectives, and to choose among them the best with regards to Quality, Cost, and Time. The objective of the study is to analyze malfunctions which may create disorder in such decision making processes.

4. Definitions

A **project** is a process engaged to satisfy a need defined with specifications. An **objective** is the translation, at different levels of the project (strategic, tactic,

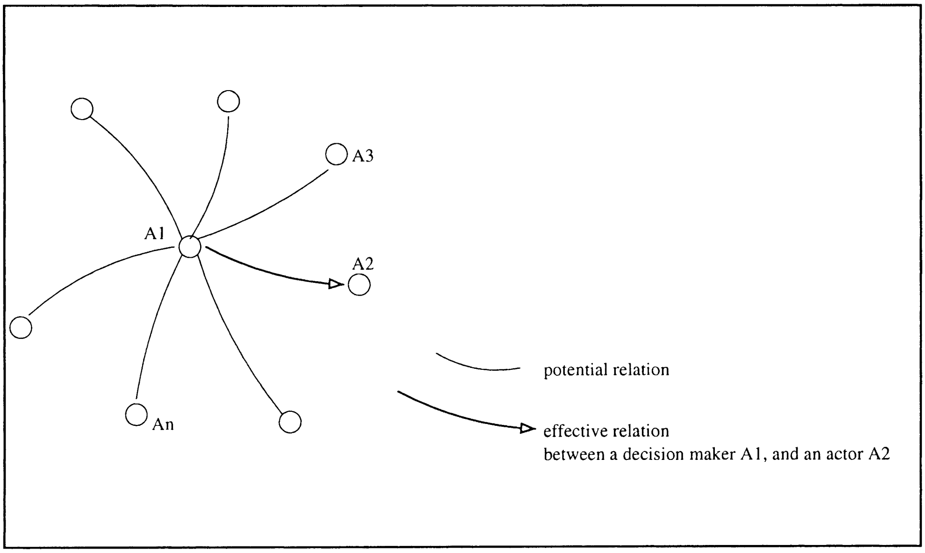

Figure 1.2. The choice of an actor in a network.

and operational), of the need written in the specifications. A project is implemented to reach an assembly of objectives. A **decision process** is a route of decisions over a network of actors to reach a fixed objective, limited in time, and value. Then an **elementary task** is the realization of an objective by an ACTOR who is supposed to have the level of competencies required by the task.

As far as there is no balance between what we want, and what we get, there is, according to us, **malfunction** in the decision making process. As said by *Rees* [10], "Failure is related to purpose". So, the importance of a malfunction is measured by the gap between the result expected before the realization of an action, and the result really obtained once the action is done. This gap can be positive or negative. For instance, choosing an actor with a level of competence higher than required is considered as a malfunction.

At last, a **decision** is an action which can have an effect on resources, actors, constrains, and/or objectives. According to us, a decision is a process that leads an actor to answer a given question. Referring to *Crowley* [3], a decision, to be rational, must mirror the actor's state of mind. Each decision induces a change of state. The kind of decisions that we consider here is the choice of an actor within the strategic, and tactical levels of the decision making process. Such decisions can be made from the Executive Office at the strategic level up to the Drawing Office at the tactical level.

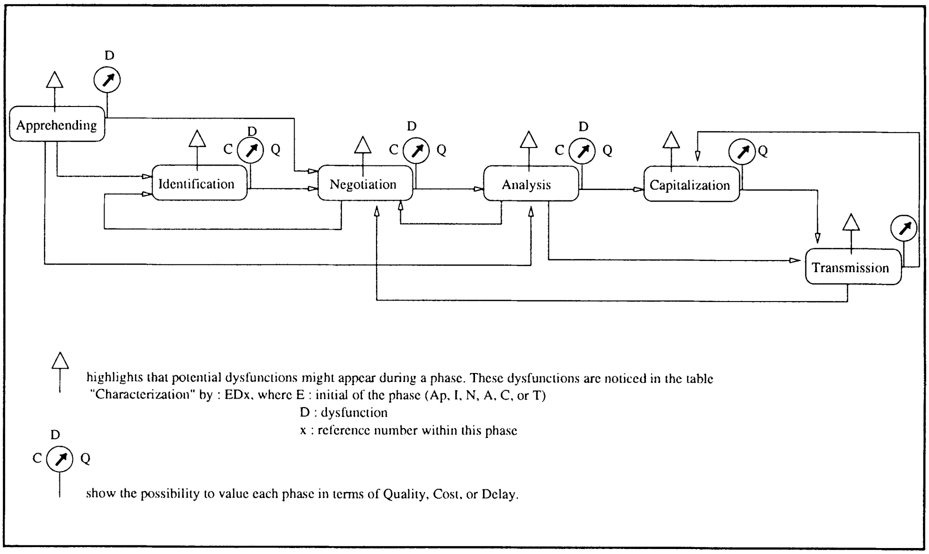
D
Apprehending
D
C Q
Identification
D
C Q
Negotiation
D
C Q
Analysis
Q
Capitalization
Transmission
highlights that potential dysfunctions might appear during a phase. These dysfunctions are noticed in the table "Characterization" by : EDx, where E : initial of the phase (Ap, I, N, A, C, or T)
D : dysfunction
x : reference number within this phase
D
C Q
show the possibility to value each phase in terms of Quality, Cost, or Delay.

Figure 1.3. Scheme of decision making process.

5. Decision Time Line

Working on decision process, we illustrate its various aspects with the help of the *Decision Time Line* (DTL). The DTL is constructed in concert with the conceptual architecture for identifying potential malfunctions. The time line includes four main phases, some of which are not connected. The figure 1.3 brings out a general scheme of this dynamic representation: the DTL covers indeed the decision making process from initial request (question formulation) to final chosen solution (answer).

The first phase regards the primary DECISION MAKER in the sub-process of considering a request for a decision, followed by a **negotiation** phase which represents the interaction between the primary actor, and other actors in order to build together the environment of the request (i.e. ground rules in terms of time, resources, and type of decision required).

If this initial negotiation leads the primary actor to consider the request, then this one is **identified**. The identification includes decomposition of the request into sub-requests when necessary, and the identification of the competencies needed for each task.

The next phase, which we call **analysis** phase in this paper, deals with coordination/synthesis (if the request has been handled, at least in part, by others) or problem resolution/decision making (if the request is handled directly by the ACTOR).

When ready, the decision/answer and its request environment are documented, **capitalized** (*Lewkowicz* [9], *Stal-Le Cardinal* [13]) in a database, and the results returned to the actor who made the request.

This graph may be developed for each phase, and for different levels of decision making within a single phase. Using this representation, we can examine the evolution of a request in network-space from several perspectives or *schemes*. That kind of dynamic relations can highlight how actors are chosen to give answers/participate in decision making, or why non-human resources such as software are used.

A unique evaluation tool (to identify, and characterize malfunctions) is associated with each of these phases. Using our model, it is possible to give a temporal characterization of malfunctions as well as a functional characterization that allows classification of various malfunction types. The various stages in the DTL are delineated so that important malfunctions are emphasized because we do not intend to represent all malfunctions in design processes.

6. Evaluation

The malfunction evaluation method is motivated by the typical Quality, Cost, and Time trio applied on the DTL (the decision process itself), its result (the choice of actors), and its effect on the product. For instance, the evaluation of the cost aspect for a given malfunction considers the cost of the decision process, the cost of the chosen actor, and the cost of the chosen technical solution.

The DTL is here used to solve management process problems. Our field of observation is the decision process, and its results. The particular decision, we are interested in, is the choice of an actor to accomplish a task. This is the source of potential "project" malfunctions.

7. An analysis pattern

Our analysis pattern is, on the one hand, based on a systemic representation of malfunction, and, on the other hand, enhanced by a decomposition into sub-criteria defined by an analogy with failure in maintenance. A comprehensive treatment of maintenance concepts may be found in the book by *Boucly* [2]. Figure 4 is a graphical representation of the characterization of a malfunction.

The *Ontological*, *Genetic*, and *Functional* axis, defined by *Le Moigne* [8] within the systemic, are the basement of the characterization of malfunctions, as shown in figure 4.

The *Ontological* axis defines what a malfunction is: it is due to a partial or complete non-respect of the DTL, and appears in one phase or more of this decision making process. A malfunction is also characterized by its stochastic aspect, i.e. its speed of appearance, its fugitive aspect (or not), and its frequency.

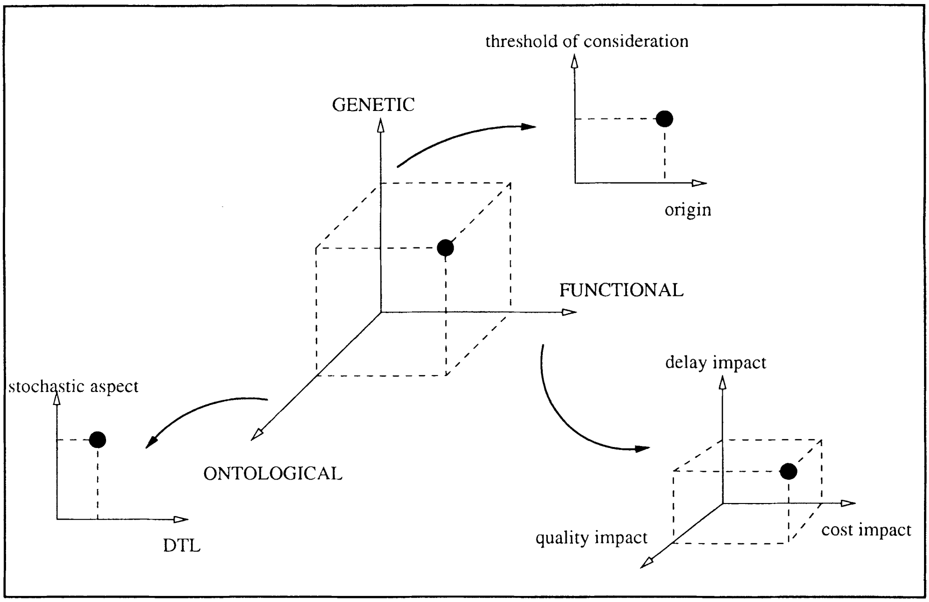
threshold of consideration
GENETIC
origin
FUNCTIONAL
delay impact
stochastic aspect
ONTOLOGICAL
DTL
quality impact
cost impact

Figure 1.4. A characterization of malfunctions.

The *Genetic* axis defines the evolution of a malfunction. Two notions are concerned here: its origin (inner or external) within a project, and its threshold of consideration.

The *Functional* axis defines how damaging a breakdown is, what a malfunction generates, and what is the gravity of its impacts.

In fact, the *Functional* axis is the quantitative evaluation of malfunctions, and also the link between a malfunction, and recommendations.

8. Recommendations

As said previously, the gap between an objective and its realization can be measured by three different but additive ways: Quality, Cost, and Time. For each of them, we also have three factors: the Decision process, its Result, and the result on the Product. That leads to three relations:

$$Gap_{time} = Gap_{timeDTL} + Gap_{timeDTLresult} + Gap_{timeTech.Sol.} \tag{1.1}$$

$$Gap_{cost} = Gap_{costDTL} + Gap_{costDTLresult} + Gap_{costTech.Sol.} \tag{1.2}$$

$$Gap_{quality} = Gap_{qualityDTL} + Gap_{qualityDTLresult} + Gap_{qualityTech.Sol.} \tag{1.3}$$

Whereas for Time, and Cost relations we have only one unit (time or money), we have to face up to different units for the Quality evaluation (competencies, technical characteristics...) that makes it much more complicated. A complete decision making process for the choice of actor is proposed to evaluate Quality aspects. The quality criterion is satisfied only if the six stages that constitute this process are respected. The first three steps correspond to the decomposition of the Identification phase of the DTL, and the last three ones, of the Analysis phase. This decomposition is used to fulfill two objectives. First of all, it leads to a plan of action to reduce risks of malfunctions during a decision making process (preventative action). Then, for the analysis of a past malfunction, it gives some help to find recommendations to avoid future malfunctions (corrective action). A malfunction is often a combination of problems referring to Quality, Cost, and Time all together. We therefore elaborate a Gravity Function, that determines the gravity level of a malfunction. Recommendations, obtained here, are specific recommendations elaborated with respect to the firm, its culture, its strategy, and the way resources are managed. Their purpose is to annihilate the gap created by the malfunction between the objective, and the result of the task. We are currently in the validation process of our models, methods, and recommendations in an industrial context. Results will be presented in the final paper.

9. Conclusion and future prospects

So, at this stage of our study, we are able to identify a malfunction in a decision that consists in the choice of an actor. Then, we analyze and evaluate it so as to estimate its relative gravity level. At first, only priority malfunctions can be taken into account so as to look for their causes, and then give recommendations. We have elaborated three main dependency trees (for Quality, Cost, and Time) that represent links between a malfunction, and causes. But it is important to notice that recommendations are context dependent. Even if it is always possible to give a list of actions to avoid a malfunction, the pertinence lies in the capacity to elaborate a strategy of actions so as to always avoid such problem.

References

[1] Bana e Costa, C.A., "Les problématiques dans le cadre de l'activité d'aide à la décision.", Les cahiers du LAMSADE, Paris, n^o80, 1993.

[2] Boucly, F., "Maintenance : coûts de la non-efficacité des équipements.", AFNOR gestion, 1988.

[3] Crowley, J., "Pratique de l'analyse de risque.", ECP, Paris, 1998.

[4] Durand, T., "L'alchimie de la compétence.", p.1-38, Paris, 1998.

[5] Janiaux, Ph., "Développement de projets. Les clés de la réussite.", Informatiques magazine, p.30-35, Paris, 1997.

[6] Kolodner, J.L., "Toward an understanding of the role of experience in evolution from novice to expert.", Development in expert systems, p.95-116, 1984.

[7] Le Moigne, J.-L., "Les systèmes de décision dans les organisations.", Presses Universitaires de France, 1974.

[8] Le Moigne, J.-L., "La théorie du système général, théorie de la modélisation.", Presses Universitaires de France, 1977.

[9] Lewkowicz, M., Zacklad, M., "La capitalisation des connaissances tacites de conception à partir des traces des processus de prise de décision collective.", Actes d'ingénierie des connaissances, Pont-à-Mousson, France, 1998.

[10] Rees, R., "What is a failure?", IEEE - Transactions on Reliability, Woodinville, USA, Vol.46, p.163, 1997.

[11] Simon, H.A., "Models of bounded rationality.", Tome 2, MIT Press, Cambridge, 1982.

[12] Shanteau, J., "Psychological characteristics and strategies of expert decision makers.", Acta Psychologica, n^o68, p.203-215, 1988.

[13] Stal-Le Cardinal, J., Mekhilef, M., Bocquet, J.-C., 1998. "A bijective user's profile oriented model for design action capitalization", Third Biennal World Conference on Integrated Design and Process Technology, Berlin, Germany, Vol.3, p.48-55, 1998.

Chapter 2
DESIGN THEORY : MODELS

A Declarative Approach to a 2D Variational Modeler 105
D. LESAGE, J.-C. LÉON, P. SERRÉ

Copying of Free-Forms from Digitized Data 113
A. CONTRI, C. LARTIGUE, G. OSTY

Flexible Parts Modelling for Virtual Reality Assembly Simulations................ 121
J.-C. LÉON, U. GANDIAGA

A rectification algorithm for manifold Boundary representation models 129
G. SHEN, T. SAKKALIS, N. M. PATRIKALAKIS

Information Support in an Integrated Product Development System 139
R.I.M. YOUNG, O. CANCIGLIERI JNR., C.A. COSTA, J.M. DORADOR, J. ZHAO, W.M. CHEUNG

A methodology for modeling process information 147
R. BACHA, B. YANNOU

A Set of New Tools for the Automatic Meshing and Remeshing of Mechanical Parts.. 157
J.-C. CUILLIÈRE, V. FRANÇOIS

A Control Criterion Dedicated to Detail Removal for F.E.A. Geometry Adaptation.. 165
L. FINE, L. RÉMONDINI, J.-C. LÉON

Feature Recognition and Remeshing by Local Hermite Diffuse Interpolation .. 173

D. LESAGE, J.-C. LEON, P. SERRE

A DECLARATIVE APPROACH TO A 2D VARIATIONAL MODELER

Abstract. The goal of this paper is to present the interest to define a geometric declarative modeler according to the needs of the associated solver. The modeler presented will seem, in a first view, of a complex architecture. A more detailed description of the modeler allows the presentation of the geometric constraints management. The interest of such approach is finally illustrated by the solver presentation. This solver, divided in three modules, allows a reliable and fast resolution of the geometric problems. Indeed, each module has been defined to optimize the resolution in terms of time and robustness.

1. INTRODUCTION

For few years, CAD systems have been oriented toward a parametric approach. This technological choice has been motivated by user requests. Indeed, a product is designed to come up to its specifications. Unfortunately, the initial needs are rarely defined from a geometric point of view. The geometric constraints are essentially the consequences of the functional constraints. So, the geometric representation of a product evolves continuously to conform to the user specifications. The CAD systems have to allow the designer to modify/update rapidly a model to satisfy the user constraints. To this end, few variational or parametric geometric solvers have appeared. Furthermore, some approaches, initially defined to solve geometric problems, are not able to include engineering constraints (for example: equations between the dynamic equilibrium of a part and some shape parameters). Some other approaches, based on a powerful mathematical solver, have been deviated from their initial aim: solving a geometric problem generally badly defined, i.e. locally over and under-constrained, and finding an intuitive solution for the user.

This article shows how, with an original geometric modeler, a promising geometric solver can be worked out. The modeler originality comes from its perfect compatibility with the solver (at the opposite to the current technology in which a variational or parametric solver has been added rather than integrated). The following section describes the modeler approach. The subsequent section presents the integration of the constraint information in the modeler. The last section details the main treatments performed in the solver.

2. MODELER PRINCIPLE

In case of a B-Rep approach, a geometric object is defined by a set of elementary geometric elements linked together with topological relationships. A way to define an elementary geometry is to place a set of characteristic points in the user workspace and for some of them, to add complementary characteristics (for

P. Chedmail et al. (eds.), Integrated Design and Manufacturing in Mechanical Engineering, 105-112.
©2002 *Kluwer Academic Publishers.*

example: a circle is defined by its centre point, its radius, ...). Generally, the position of a point is known by its coordinates in a reference frame. So, the position of a point is an absolute position in a particular frame. This frame is absolutely useless to an intrinsic definition of the object. The significant information of geometry is the relative position between each elementary geometric element. Indeed, the main idea of this modeler is to describe the position of each element in a natural way: an element is known only with its dimensions and/or its position with regard to other elements. There, the relative position of each characteristic point is sufficient to define the relative position of the geometric elements of a part. This set of points and relationships is called the skeleton.

To add data about the geometry, a skin is attached to the skeleton. The skin defines the surface geometry. It is a set of elementary entities linked together by topological relationships. Each skin element is defined by its characteristic points, which are localized in the workspace by the skeleton. A geometric object is entirely defined by the set skeleton/skin (see Figure 1a).

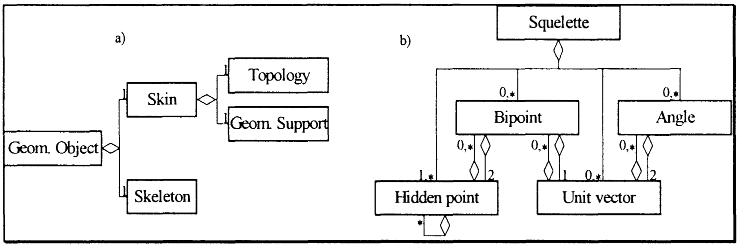

Figure 1 .a) UML representation of a geometric object. b) UML representation of a skeleton.

The proposed modeler is a declarative modeler, i.e. each object is solely described with a set of relationships with other objects and by its intrinsic properties.

The skeleton: The skeleton has to contain all the necessary data to position its attached set of points in space. It defines a rigid structure on which a skin is attached. The parts, which make up this robot, are beams of variable length and connections that define the angle between two adjacent beams. According to the connections, the nacelle can be positioned at every point of the 2D space.

The skeleton positions the set of characteristic points of the geometry with the same approach. Each characteristic point is linked to the extremity of a bipoint i.e. a hidden point. The bipoints represent the beams of the elevator. A hidden point is used as a connection to link the bipoints together. The second function of a connection, i.e. to define the angle between two beams, is performed by two other entities: the unit vector and the angle. By definition, a bipoint is associated with a unit vector. So, the angle between two bipoints is defined by the angle between two unit vectors.

Starting from these four elements, a data structure (Figure 1b) has been defined to store the necessary information about a skeleton. It is important to note that the position of the point obtained with this formalism is a relative position.

With a declarative approach, a point is known as soon as it is created. There is no reason to position it as long as it is alone (Figure 2a). The necessary information for two points is the distance between the two points. This distance is defined in this formalism by the modulus of the associated bipoint (Figure 2b). A bipoint is created with a unit vector defining the direction and the orientation of a bipoint. The position of a third point according to the first two ones is known by the characteristics of the bipoints, the vectors and the angle which are needed to describe these points (Figure 2c). If their points are aligned, the unit vectors are collinear. According to a specification configuration, both bipoints can be carried either by only one unit vector (Figure 2d) or two collinear unit vectors (Figure 2e).

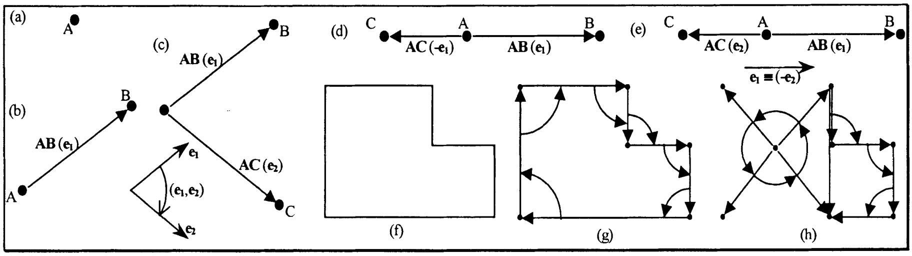

Figure 2 .a, b, c, d, e) few simple examples of skeletons. f) a simple geometry. g, h) two skeletons for the same skin geometry.

The great point of this approach is its ability to define an object geometry according to the user design intent and to the geometric specifications. Indeed, the skeleton of a geometries object is not unique. It is built in real time during the sketch definition according the user actions. The user design intent is captured according the operations he (or she) has conducted. For example, the Figure 2f represents a simple geometry. A skeleton (Figure 2g) was obtained by the definition of the geometry with a polyline tool while another one (Figure 2h) conveys the user design intent to position the four points with respect to a fifth one.

The skin: The skin contains all the information about a B-rep object:

- a set of elementary geometric objects to define the geometric support of the skin,
- a set of topological relationships.

The main difference with respect to current approaches is that the geometric elements are defined only by their intrinsic properties. For example, a NURBS is defined by its control points, homogeneous coordinates and knot sequence.

The most frequently used elementary geometric objects in CAD software are points and segments. A "real point" is simply attached to a hidden point. A segment, which is a finite part of a line, is defined by its extremities. Each extremity is linked to a hidden point. The circle, the conics, the parametric curves and surfaces are the other entities used in CAD/CAM. All these entities can be described by a set of points and by some other characteristics. For example, a centre point and a radius define a circle and its position is defined by the hidden point linked to its centre.

The approach to the representation of parametric curves and surfaces is similar, i.e. each control point of a NURBS is linked to a hidden point. A current representation of the set of control points is a net conform to the representation of the first formulation of the Bézier curves [3].

The specifications: The skeleton has to express the geometric constraints defined by the user. A polyhedral object can be entirely specified with 13 elementary geometric constraints: the TTRS and a set of topologic constraints [4, 5]. All the dimensional constraints can be defined by a set of two elementary constraints: the distance between two points and the angle between two segments. Two skeleton objects define both constraints: the bipoint and the angle. These objects may have a prescribed measure. In case a skeleton object defines a constraint, its measure becomes a prescribed value. Thus, the measure is called a *specification*. In the other case the measure is called a *variable*, its value has to be deduced from the set of constraints. The logical constraints like the point – point coincidence are defined by logical information in the skeleton. To illustrate these concepts, few constraint skeletons are presented. A full example is detailed later.

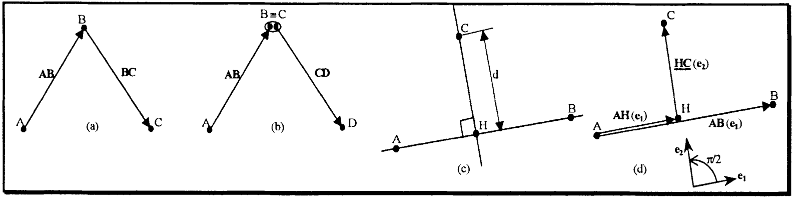

Figure 3. a, b) two ways to specify a point – point coincidence. c, d) formal representation of a constrained bipoint.

Point – point coincidence: This elementary logical constraint is defined by two ways according to its end. Either this constraint is temporary, so it is defined with “an assembly coincidence”, or it is permanent, so it is defined with an “absolute coincidence”. Two points are absolutely coincident if they are carried by only one hidden point (for example, both bipoints of the Figure 3a have an absolute coincidence at one of their extremities). When the coincidence is specified temporarily, it is interpreted as a logical coincidence of the hidden points: a hidden point has a set of coincident points (Figure 1b and 3b).

Distance point – line: The distance between a point C and a straight line (AB) is equivalent to the distances between points C and H, the orthogonal projection of C onto (AB) (Figure 3c). The skeleton of this constraint is defined by the constraint skeletons (Figure 3d): “point – straight line coincidence” (of H with (AB)), “point – point distance” (between C and H) and “straight line – straight line angle” (between (AB) and (CH)).

3. THE SOLVER APPROACH

The global approach of the solver is classical to geometric solver dedicated to a CAD/CAM system and is based on a top-down solver approach. Firstly, the geometric problem is considered as a whole before a sequence of construction steps is derived. Secondly, the construction steps are carried out to derive a solution [12]. To this end, the solver is decomposed into three modules: a generative, an analyzing and a solving modules. The solving module will not be described.

To understand the interest of this approach, the solver is under focus. Indeed, the modeler has been defined for the solver. Thanks to the solver declarative approach, solving a geometric problem is simplified. The position of the various geometric elements is only relative to the other elements. So, the geometry is solved locally without paying attention to the final position of the set of geometric elements treated. Moreover, thanks to the skeleton structure, the geometric equations (which need to be solved) are obtained easily and an efficient choice of equations allows to derive a solution equivalent to construction steps with " a rule and a compass".

Generally, the generative module uses the modeler data added to the set of the user's constraints to write the set of data under a structured form. Many approaches use a graph, for example Owen and Fudos [9, 12] use a "constraint graph".

The graphs are highly used in this approach too. Unlike the constraint graph, the geometries and the constraints are represented by the same entities in the graphs. The skeleton is divided into two graphs. The first one represents the links between the "hidden points" and the bipoints. The second one links the unit vectors and the angles. A set of equations is generated from these graphs. The equations represent the relationships between the various geometric elements of the skeleton.

Afterwards, the analyzing module subdivides the global equation system into subsystems. The system is composed of the generative module equations completed by some possibly complementary equations (engineering equations, specific equations of the NURBS, etc). This analysis is carried out using a bipartite graph [1, 11]. The result of this analysis is a resolution scheme, i.e. an ordered set of subsystems to solve.

Finally, the resolution module computes solutions for each subsystem according to the resolution scheme in order to obtain the expected result. This module has some solver agents. Each agent is a specific mathematical solver dedicated to a particular system i.e. linear/non-linear problems, etc. The rule of this module is to choose for each subsystem the fastest agent. This approach in three modules has the advantage to reduce the initial problem into a set of sub-problems easier to solve.

Generator: The skeleton is a way to store the geometric information about the position of a set of points as well as the geometric specifications with the same formalism, in the same database. This forms the basis of the geometric equation identification. The skeleton has two categories of dimensional elements. Their measure is either specified by the user or defined in the initial sketch. The resolution of a geometric problem consists in getting the measure of the non-specified elements coherent with the measure of the specified elements. It is based on the geometric relationships between the various elements of the skeleton. In the context of a 2D problem, two types of relationships can be identified in the skeleton: the vectorial closed loops and the angular closed loops. From these relationships, a necessary equation system can be derived. The sufficient system is obtained, for a well constrained problem, with a maximal set of independent loops. In the case of an under-constrained problem, some complementary equations will be necessary to add to reduce the solutions to a finite number.

The vectorial loop: A vectorial loop is a sequence of bipoints such that each bipoint of the sequence has an extremity in common with the previous one and the other extremity in common with the next one. A loop is known as open (respectively closed) if the two ends nodes of the loop are different (respectively coincide). A closed vectorial loop is strictly equal to the null vector. From the information contained in the database, a maximum set of independent vectorial loops is identified. In 2D, starting from a closed loop, two equations are obtained by projecting this loop on two non-collinear vectors (preferably orthogonal). Each projection gives the equation $\sum_i d_i \cos(e_i, e_k) = 0$ where d_i is the modulus of the i^{th} bipoint, e_i the unit vector which defines the direction of the i^{th} bipoint, e_k the projecting vector, (e_i, e_k) the oriented angle between the vectors e_i and e_k.

In order to obtain simpler equations, the vectorial loops are projected onto two orthogonal axes. The first one is defined by a vector chosen using heuristics. The second one is orthogonal to the first one. In this way, the equation system obtained has the following advantages:

- the numerical error is minimized. Indeed, we assumed that the numerical error depends on of the angle between projection vectors and the minimum error is obtained with two orthogonal vectors,
- there is no need to select a second vector,
- the second equation of projection is straightforwardly obtained. Indeed, if e_h is a vector such that $(e_k, e_h) = +\pi/2$, therefore $\cos(e_i, e_h) = \sin(e_i, e_k)$.

After the choice of the projection vectors has been performed, the missing angles are created. Indeed, the projection of a vectorial closed loop onto a vector generally uses some angles, which are still not defined. To be able to create the equations, it is necessary to define these angles. Such an example will be detailed after the presentation of the angular loops.

The angular loops: The angular graph, part of the skeleton containing the vectors and the angles, incorporates only the angles necessary to the resolution, i.e. the angles allowing the modeler to draw the non specified geometry, the angles used by the constraints and the angles used in the projection of vectorial loops. From this graph, a maximal set of independent angular closed loops is identified. Each closed loop represents the Chasles relation. The interest in using this approach is to find the existing geometric relationships between different angles.

Example: In order to illustrate these remarks, the first stage of the resolution of an example is proposed. Figure 4a presents a well-constrained geometry. Figure 4b shows the corresponding skeleton without the angles. Three independent closed loops are identified. The graph of Figure 4c shows the angles/vectors defining a subset of the skeleton. The angle (e_i, e_j) is noted on the graph, "A i-j". The set of angles {A 1-2, A 2-3, A 3-4, A 4-5, A 5-6, A 1-6} has been created from the sketch. This set is the minimal one needed to "redraw" the geometry from the initial values. The A 1-6 angle has been created with the sketch but its type has been modified during the specification stage. Indeed, the angle constraint α_1 (Figure 4a) is defined in the skeleton by the specification of this angle.

Analyzer: The analysis module is based on a bipartite graph [1]. A bipartite graph is a graph where the set of vertices can be divided into two subsets. Two vertices from the same set are never linked together. This graph is interesting to model an equation system: the first set of vertices gathers the equations and the second one the unknowns. A bond links an unknown parameter to an equation if and only if this unknown parameter appears in that equation (Figure 5a). The graph allows a qualitative study of equation systems. In the general case, this graph is sufficient enough to decompose the equation system into three parts: well-constrained, over-constrained and under-constrained subsystems. From the

Dulmage-Mendlsohn algorithm [6, 7, 8], the irreducible subsystems and their dependency are identified. The Figure 5b shows the result of the decomposition of the graph of Figure 5a. The algorithm has identified an over-constrained system which has to be solved first and an under-constrained system which has to be solved afterwards. This approach is only a logical one: a system is said well constrained if it is composed by *n* equations matched by *n* unknowns. A more subtle analysis could be performed for each irreducible subsystem using a numerical approach (to analyze the jacobian of each subsystem for example).

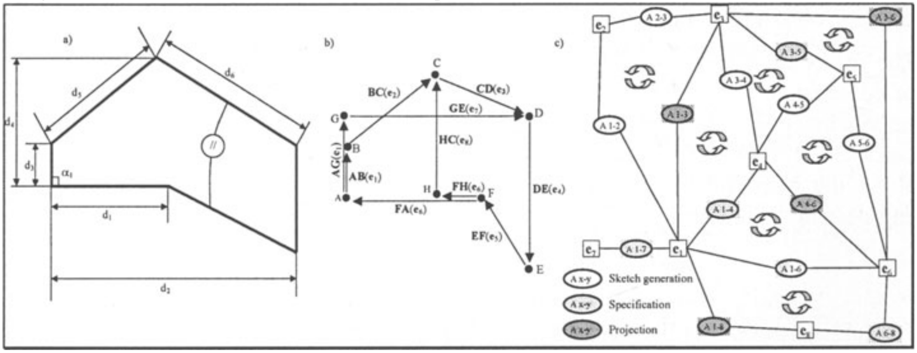

Figure 4. a) A well-constrained geometry. b) The corresponding skeleton (without angles) of a. c) Angular graph corresponding to a subset of the skeleton of Figure 4a.

The use of this approach gives a useful result only if the different equations express the geometric problem into a natural way. This remark is originated by the approach chosen to generate the equation system. In fact, each angular loop or vector loop used is typical of a construction using a rule and a compass.

The advantage of this approach is that its allows the user to add to the system of equations all kinds of equations like engineering equations which link geometric unknown parameters to engineering ones. The bipartite graph allows the analyzer to localize the over-constrained subsets of equations. An over-constrained set is, from a mathematical point of view, a subsystem containing too many equations compared with the number of unknowns. From a geometric point of view, two configurations can lead to such a subsystem: either a specification is locally redundant, i.e. some subsets of user's constraint are equivalent, either some subsets of constraints are contradictory. The user expects the system to produce useful information about the configuration leading to an over-constrained subset and the identification of the subset of constraints responsible of that configuration. With the approach proposed, a geometric object is defined by a set of specifications. Therefore, the equation system is obtained from these specifications. Hence, for a given over-constrained subsystem, coming back to the subset of initial constraints is straightforward.

The processing of an under-constrained subsystem is meaningful. Indeed, different ways to solve them can be chosen according to the configuration of the subsystem. Thus, the resolution can express different behaviours according to the user's preferences.

Manager: The solver module is a manager rather than a solver. It receives a set of organized subsystems from the analyzer module.

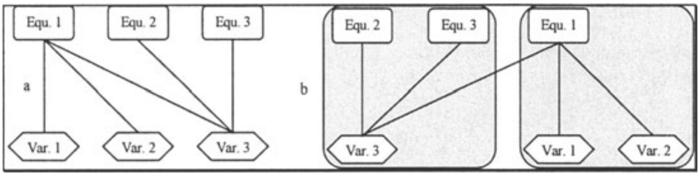

Figure 5. a) an example bipartite graph. b) Irreducible subsystems and their dependencies.

4. CONCLUSION AND PERSPECTIVES

The first step of validation of this approach has been achieved with success for a set of coplanar points and lines so that they satisfy a set of given relative dimensions. Interesting points have been highlighted which can produce a solution of under-constrained problems while expressing different behaviours, informing the user about the over-constrained origin and its type, and allowing the designer to add engineering equations.

5. REFERENCES

1. Ait-Aoudia S., Jegou R., and Michelucci D. Reduction of constraint systems, Compugraphic, Alvor, Portugal, 1993: 83-92.
2. Bouma W., Fudos I., Hoffman C., Cai J. and Paige R. Geometric constraint solver, CAD, vol. 27 (6), 1995: 487-501.
3. Bézier P. Courbes et Surfaces, Mathématiques et CAO, tome 4, Hermès, 1987.
4. Clément A., Rivière A., Serré P., Valade C. The TTRS: 13 Constraints for Dimensioning and Tolerancing, 5th CIRP Seminar on Computer Aided Tolerancing, Toronto, Canada, April 27-29, 1997.
5. Clément A., Rivière A., Serré P. Geometry and topology declarative: a new paradigm for CAD-CAM systems, Proceedings of IDMME'98, 1998: 587-595.
6. Dulmage, A. L., Mendelsohn, N.S. Coverings of bipartite graphs, Canadian J. of math., n°10, 1958: 517-534.
7. Dulmage, A. L., Mendelsohn, N.S. A Structure theory of bipartite graphs of finite exterior Dimension, Trans. of the Royal soc. of Canada. Section III, Chemical, mathematical and physical sciences, no. 53, 1959: 1-13.
8. Dulmage A.L., Mendelsohn N.S., Two Algorithms for Bipartite Graphs, SIAM J, no.11, 1963: 183-194.
9. Fudos I. and Hoffmann C. Correctness proof of a geometric constraint solver, Int. J. of Comp. Geometry & Applications, vol. 6 (4), 1996: 405-420.
10. Lamure H. and Michelucci D. Solving constraints by homotopy, Proc. of the Symposium on Solid Modeling Foundations and CAD/CAM Applications, 1995: 263-269.
11. Mathis P. Constructions géométriques sous contraintes en modélisation à base topologique, Ph. D.thesis, Université Louis Pasteur, Strasbourg, 1997.
12. Owen J. C. Constraints on simple geometry in two and three dimensions, Int. J. of Comp. Geometry & Applications, vol. 6 (4), 1996: 421-434.

Jean-Claude LEON
Laboratoire Sols, Solides, Structures UMR CNRS 5521
Domaine Universitaire
BP 53X 38041 Grenoble Cedex 9
France
Jean-Claude.Leon@hmg.inpg.fr

A. CONTRI, C. LARTIGUE, G. OSTY

COPYING OF FREE-FORMS FROM DIGITIZED DATA

The voxel-space representation

Abstract. The copying of free-forms consists in the duplication of an existing object from its 3D digitizing, and from the use of NC machining or rapid prototyping. In most cases, free-form copying uses the tools of reverse-engineering through CAD modeling. In order to ensure a good concordance to the object's geometry, we propose a direct free-form copying from the digitized points. To overcome difficulties linked to the discrete representation and the large amount of data, we suggest a representation model of the data: the voxel-spaces. Several classifications may be defined linked to the future exploitation of the points. Moreover, operations and attributes are defined on the voxel-spaces to simplify the data treatment. In the paper, we present the voxel-space representation and its application to free-form copying. We especially bring out how geometric characteristics of point cloud can be obtained, and in particular how free-form copying process can be optimized.

1. INTRODUCTION

The copying of free-forms consists in the duplication of an existing object. This duplication can be performed using molding, machining or rapid prototyping [1]. The copying operation is necessary when we want to obtain a free-form from a clay model (industrial applications) or when we need a duplication to preserve the initial form (artistic or archaeological applications). Usually, the copying of free-forms is carried out by physically following the object geometry or by applying a material restoring the form such as elastomer. These methods may cause damages to the object surface due to mechanical contact. Nowadays, the use of numerical technologies is preferred for they offer non-contact digitizing of the object surface. The information given is a cloud of points which are representative of the object surface. Therefore, the copying operation of free-forms uses the tools of reverse-engineering and relies on the geometrical modeling of the point cloud using a CAD system [2]. This modeling, which is essential for simulations or other numerical treatments, is not necessary for direct copying of the free-from surface. Moreover, through such methods, the copying is no longer the copying of the real object, but the copying of the CAD model.

We suggest a direct copying method of the point cloud with no preliminary modeling (Figure 1). The calculation of the tool movements is performed using a method of cartesian type for which the digitizing gives the discretization of the surface [3]. This direct treatment of the data allows a good concordance to the initial geometry of the object. However, the direct treatment of the whole point cloud may cause problems, for the amount of data to be considered is very large, and in most cases non-organized (registration of different 3D-views necessary for the whole object). Therefore, the treatment requires a large amount of computation time and a great capacity of data storage. Moreover, a limit in the direct copying of the data is

P. Chedmail et al. (eds.), Integrated Design and Manufacturing in Mechanical Engineering, 113-120.
©2002 *Kluwer Academic Publishers.*

the loss of the neighborhood and continuity notions, generally rebuilt by meshing or CAD modeling.

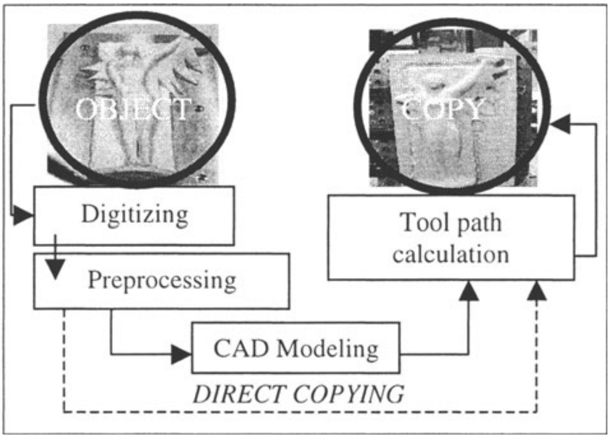

Figure 1. Direct free-form copying operation.

The method we propose is free from modeling and meshing [4]. In fact, the method relies on a discrete representation of the space in elementary volumes, the voxels [5]. The voxel (volume element) is a 3D representation of a 2D pixel (picture element) which is largely used in the 3D-imaging field. The extension we propose is, not only to consider the voxel as an elementary volume, but to take into account the information (linked to the digitized data) included in the delimited volume: the voxel-space. Each voxel-space can be characterized using attributes, and operations between voxels can be performed in function of the attributes' classes. Therefore, a voxel-space representation can be associated to the raw material, this representation evolving during the machining of the free-form.

The next section is dedicated to the definition of voxel-spaces, their attributes and associated operations. Next, the application to the copying of free-form surfaces is presented. We thus introduce the case of the finishing operation in 3-axes and show how to adapt this method for the roughing operation. In the last section, we use the voxel-space representation to define geometric characteristics from point clouds.

2. VOXEL SPACE REPRESENTATION

In the field of visualization, the voxel model has been defined to extend in 3D the notion of pixel, in particular for scene rendering and object shading [6]. A voxel can be defined as a 3D-pixel, and its usual representation is an elementary cube defining the smallest region of space. Such a model is of great interest for it gives a discrete representation of space, more adapted to the treatment of point clouds. Concerning digitized data, the information we have to consider is contained in local scale. We can thus describe the characteristics of the point cloud through its representation in voxels taking into account the information included in the delimited volume : the voxel-space (Figure 2).

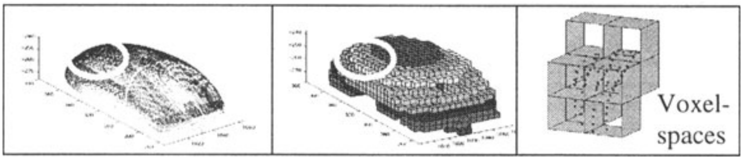

Figure 2. Voxel-space representation of a 3D digitizing

The representation by voxel-spaces adopts the properties related to the voxel model, vicinity in particular. Moreover, the whole set of points contained in the portion of space delimited by the voxel determines the characteristics of the voxel-space.
From a topological point of view, a representation by voxel allows the definition of vicinity. The p-vicinity of a voxel is defined by considering the p adjacent voxels. The nature of adjacency can be: face, edge or vertex type. We thus speak about 6-vicinity or 26-vicinity more generally of p-neighbors, according to the type of selected vicinity (Figure 3). Unlike the point cloud model, the representation by voxel-spaces inherits the notion of vicinity and allows a complete space description.

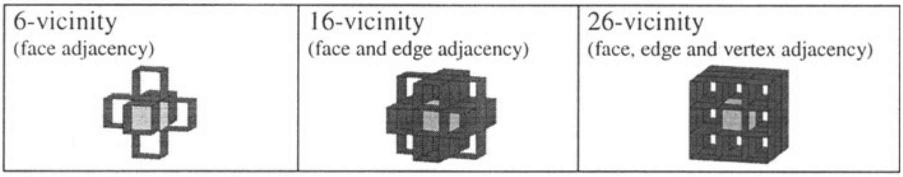

Figure 3. p-vicinity

Classifications and attributes : The concept of voxel-space allows enriching the voxel model by the contribution of specific classifications, which are function of the exploitation of the points (free-form copying, surface reconstruction, ...).
A primary classification, common to all exploitations, is defined in relation to the nature of the voxel-spaces (Figure 4):
- non-empty voxel, when its voxel-space includes a set of points,
- empty voxel, when its voxel-space does not include points,
- unknown voxel.

This last type corresponds to voxels the nature of which can not be determined. For instance, surface digitizing with 3D sensors does not allow the acquisition of the inner part of the object, and so, corresponding voxels are said unknown. From the primary classification, secondary classifications can be defined linked to the point exploitation [5]. The secondary classification characterizes the specificity of the point exploitation. For instance, if we take the example of the machining process, the exploitation allows defining whether the non-empty voxel has been machined or not (Figure 4). After the definition of classifications, the treatment of the point cloud requires the definition of attributes. Attributes locally characterize the properties of the voxel-spaces, i.e. the properties of the points within the voxel. Here again, attributes are strongly linked to the exploitation.

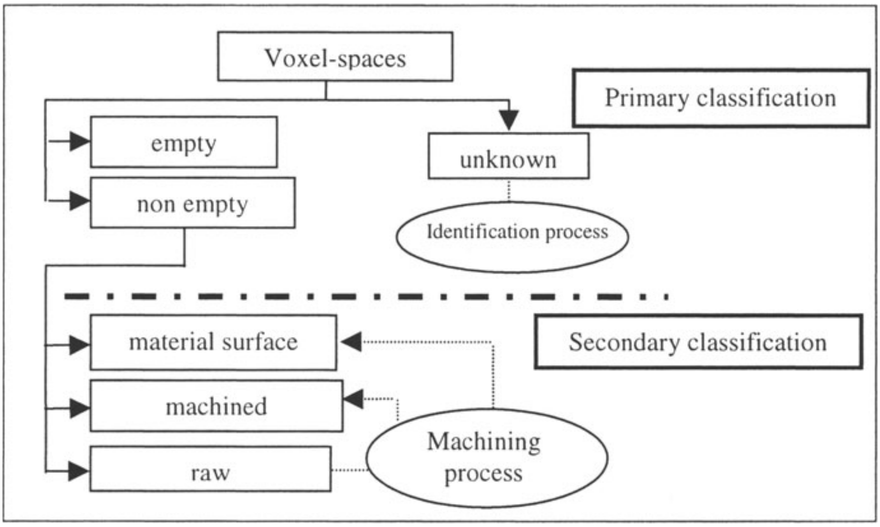
Voxel-spaces
Primary classification
empty
unknown
non empty
Identification process
material surface
Secondary classification
machined
Machining process
raw

Figure 4. Classifications

We can define for each voxel, attributes of quality, of belonging to a boundary,... The interest of these attributes is that voxel-spaces could be associated in relation with a choice of a p-vicinity, and in function of their attributes. These associations are performed through elementary operations (Figure 5) [5]:

- union, corresponding to the regrouping of voxels of common attributes,
- intersection, corresponding to the extraction of common voxels of two different voxel-space representations,
- growth, which concerns the treatment of adjacent voxels, following the adopted definition for vicinity,
- split/merge, which subdivides or gathers voxels to give multi-scale representations.

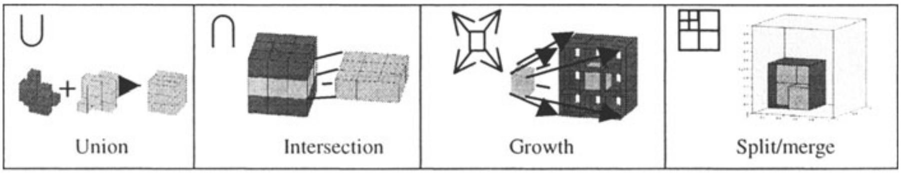
∪
+
Union
∩
Intersection
Growth
Split/merge

Figure 5. Operations

The contribution of the voxel space representation for large point clouds is multiple. The main interests are the extension of the neighborhood notion and the definition of classifications that allow the treatment by subsets of points. As a result, time of numerical treatment is largely decreased. As an example, the next section concerns the exploitation of point clouds for free-form copying taking advantage in the voxel-space representation.

3. FREE-FORM COPYING

The objective is the free-form copying from point clouds resulting from digitizing. Generally, digitizing employs non contact optical technologies such as laser sensors or structured light. It delivers a large cloud of points which is representative of the free-form surface. However, problems of shading and occultation are inherent to optics technologies, and various sensor orientations must be given to completely digitize the object. The resulting point cloud is unorganized, and presents recovery zones. Moreover, although different orientations of the sensor are given, the point cloud gives in most cases, a non-complete representation of the free-form.

We set up an algorithm that directly calculates the tool path from digitized data. This method is supplemented by the use of voxel-spaces in order to simplify numerical treatments and, then to decrease calculation time.

In 3-axis milling, the calculation method determines the tool center locations according to the machining strategy. Tool locations are calculated by minimizing the distance between points and tool center locations.

Let n_u^i be the tool axis direction, and consider M_k the k^{th} digitized point. The location of the tool center is calculated according to the following equation:

$$\left\|\mathbf{OC}_i\right\| = \min_{k=1,m} \left(\left\lfloor \mathbf{OM}_k - \lambda \cdot \mathbf{n}_u^i \right\rfloor \cdot \mathbf{n}_u^i - R_{tool} \right) \qquad (1)$$

where R_{tool} is the tool radius of a ball-end cutter tool, and λ is a real number verifying $\lambda > R_{tool}$. Note that in the general case, m is the number of digitized points.

This equation can be easily solved, but problems may appear linked to non-complete data. Indeed, unseen zones involve *gaps* in the data, and when gap dimensions are greater than the tool diameter, the calculation of the tool path cannot be carried out.

Several solutions can be supplied to overcome the lack of material: new digitizing of the gaps after detection, local densifications [7], surface reconstruction [8].

To solve this problem, the voxel-space representation constitutes a new approach. Tool path calculation generally requires elaborate data structures, particularly when the driving tool direction is not perpendicular to the digitizing lines [3]. The use of voxel-space representation may overcome this difficulty : the data structure is defined from the voxel-spaces. According to the adopted machining strategy, we can limit treatments to specific voxels, generally defined from the secondary classification. Note that the use of laser plane sensors allows the complete definition of the primary classification of the voxel [9].

For our application, let us consider the particular case of the finishing operation by parallel planes in 3-axis milling. A plaster statuette has been digitized by a plane laser sensor. Nine sensor orientations are necessary in order to restore 70 000 representative points of the form (Figure 7). We consider the case of the milling in parallel planes following the y axis. To limit treatments to points close to the machining plane, we extract points that belong to a thick slice, the thickness of which is given by the tool diameter (Figure 8).

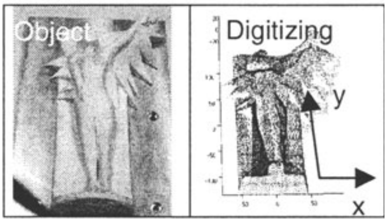

Figure 7. Initial object and its digitizing

A voxel-space representation is defined for both the cloud of points and the thick slice. From the non-empty voxels issued of the primary classification, the following attributes is defined : the voxel belongs or not to the thick slice. The intersection operation defines common voxels and the corresponding voxel-spaces of the point cloud are extracted (Figure 8).

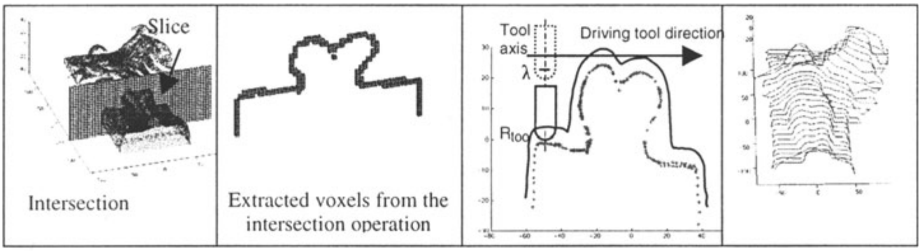

Figure 8. Intersection operation and tool path generation

Once the points are identified, the tool path is simply calculated using equation (1), where m is now limited to the number of identified points. Note that any direction of extraction can be envisaged allowing the choice of the more adapted direction to the part. Results show a significant improvement of calculation time : the calculation time is decreased by about 80%.

4. OUTLOOK OF THE MODEL

The roughing operation must remove the maximum of material from the initial raw volume. For the case of roughing operation, we suggest to calculate the tool path by sweeping the object following parallel planes. Tool path calculation relies on the voxel-space representations of the point cloud and of the raw material. The secondary classification defines the voxel machined or the voxel non-machined. These representations present multiple advantages :

- the notion of inward and outward material exists due to the primary classification obtained from to the sensor technology,

- the representation of the raw material by voxel-spaces is reactualized during the machining process; the remaining volume to be machined is then known,
- the collisions between the tool and the part are easily detected.

In order to guarantee a good concordance between the machined surface and the initial object geometry, it could be useful to link the machining strategy to geometric properties of the surface, normal to the material, principal curvatures, and to geometric singularities, discontinuities, corners, ... We thus have to be able to evaluate these geometric properties or singularities from the point cloud [4]. Methods for the determination of geometric singularities from digitized data exist and are generally used for data partitioning [10][11].

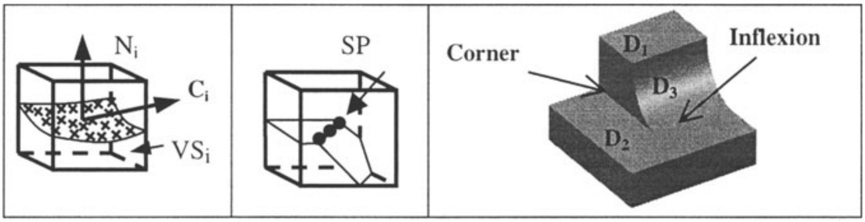

Figure 9. Singular points of a voxel-space VS_i; extracted regions using singular points

The method we develop allows the determination of singular points, such as inflexion or corner points, that characterize geometric singularities of the surface [11]. The method takes advantage of the voxel-space representation [5]. The primary classification determines the non-empty voxel-spaces VSi on which attributes are defined (Figure 9): the normal to the material, **N_i**, and the minimal curvature direction **C_i** (Figure 9). **N_i** is computed considering the hypothesis that the surface element included in VSi can be approximated by a least-square plane. **C_i** results from the cross product between **N_i** and **N_j** where **N_j** is the normal to the neighbor voxel. The search of the singular points (SP) is undertaken in each VS_i, following the perpendicular direction to **C_i**. Extracted singular points SP and attributes define singularities of the geometry object. For instance, singular points figure 9 define outlined domains where specific machining strategies can be managed. Indeed, from the attributes, the object is split into two plane regions D_1 and D. Both planes are parallel, so they can be machined with the same flat-end cutter tool. As for the region D_3, it must be machined with a ball-end cutter tool. The more appropriate machining direction must be perpendicular to the minimal curvature direction.

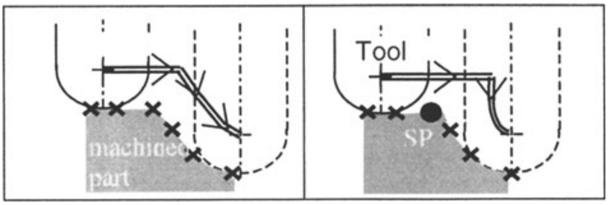

Figure 10. Change in the tool path following singularity detection

Furthermore, the detection of singular points SP provides the detection of edges. Following, the tool path calculation can be carried out in order to guarantee a good concordance to the surface geometry : the tool can withdraw from the material following the VS_i local tangent vector, and so, the local singularity is respected as shown figure 10.

5. CONCLUDING REMARKS

Usually, direct treatment of point cloud resulting from object digitizing may cause difficulties. Numerical treatments are huge and information issued from the digitizing is not sufficient to be directly used for free-form copying. The representation of data using voxel-spaces brings out a solution. It allows calculation time decrease for the treatment is limited to subsets of points. Furthermore, additional notions can be defined for discrete representations of free-forms, in particular the notion of vicinity. With the introduction of the attribute notion, some geometric characteristics can be reached. Therefore, the exploitation of the point cloud for various applications becomes easier. Among others, the case of free-form copying is developed with success. The tool path calculation from points is carried out, leading to a good concordance between the machined surface and the initial object geometry. In addition, the use of singularity detection may lead to automatic generation of machining operations in function of surface geometric characteristics.

6. REFERENCES

1. Tollenaere M., Conception de produits mécaniques, Edition Hermes, Paris 1998.
2. Varady T., Martin R., Coxt J., Reverse engineering of geometric models- an introduction, CAD, Vol. 29(4), pp 255-268, 1997
3. Lin A.C., Liu H-T., Automatic generation of NC cutter path from massive data points, CAD, Vol. 30(1), pp 77-90, 1998
4. Véron P., Léon J-C., Traitements géométriques pour l'usinage de formes complexes à partir de polyèdres issus de numérisation 3D, PRIMECA, ENS de CACHAN, 18 mars 1999.
5. Osty G., Contri A., Lartigue C., Traitements numériques et partitionnement de grands nuages de points: Préparation de la reconstruction de surface et de l'usinage, Congrès sur la Numérisation 3D, Paris 19-20 mai 1999
6. Papier L., Francon J., Evaluation de la normale au bord d'un objet discret 3D, Revue Internationale de CFAO et d'informatique graphique,Vol.13 n°2 juin 1998
7. Contri A., Numérisation et usinage de surfaces complexes, Mémoire de recherche, DEA de Production Automatisée, LURPA, ENS de Cachan, 2 juillet 1998
8. Hoppe H., Surface reconstruction from unorganised points, Computer graphics, SIGGRAPH'92, Proceedings, pp. 71-78, Chicago 1992
9. Papadopoulos-Orfanos D., Schmidtt F., Numérisation automatique avec un capteur 3D à profondeur de vue limitée, 5ème Assises Européennes du prototypage rapide, Paris, octobre 1996
10. Leonardis A., Gupta A., Bajcsy R., Segmentation of range images as the search for geometric parametric models, Int. Journal of Computer Vision, Vol. 14, pp 253-277, 1995
11. Osty G., Lartigue C., Partition of 3D Digitized Data for CAD Modelling, Revue de CFAO et d'informatique graphique, Vol. 13(4-5), pp 263-272, 1998.

LURPA, Ecole Normale Supérieure de Cachan
61 Av Pdt Wilson, 94235 Cachan cedex
tel : +33 1 47 40 29 86 - email : lartigue@lurpa.ens-cachan.fr

J.-C. LEON, U. GANDIAGA

FLEXIBLE PARTS MODELLING FOR VIRTUAL REALITY ASSEMBLY SIMULATIONS

a dual mechanical approach

Abstract. Within the scope of the simulation of assembly/disassembly operations, flexible parts modelling for virtual reality environments is described in the present paper. The study described analyzes the adequacy of various mechanical models in the specific context of oil hoses. The model behaviour is checked against experiments for validation. As an issue of this comparison, a mechanical model is proposed through the concept of a dual mechanical approach. The adequacy of this last model is deduced from the experimental data.

The mechanical model introduced is coupled with a geometric model for free-form surfaces. The deformation criterion set up uses a functional based on the external forces applied to the mechanical model..

1. INTRODUCTION

In order to reduce the maintenance costs of cars, simulations of assembly/disassembly operations should take place as soon as possible during the design process. As a result, designers will be able to integrate more effectively the maintenance criteria during the design process and adapt the architecture of the vehicle. Such simulations are based on trial and error approaches and performed under human control because of the complexity of the components trajectories and environment. Human control is also required to evaluate the effective amount of time required for assembly/disassembly operations.

To this end, virtual reality environments are well suited since they allow the user to be immersed into the digital model of a product and interact with components through haptic devices. However, virtual reality environments are currently bound to interactions between rigid parts and do not incorporate flexible part models whereas such parts play an important role during engine bay operations. Flexible part models are compulsory and need to be powerful enough to produce a minimum frame rate of 20 frames/sec.

The various modelling requirements for flexible part models can be summarized as follows:

- model the flexible part behaviour under user's interaction only,
- model the flexible part behaviour subjected to interactions with its environment (deformations due to interferences with rigid parts),
- model the control activity of the user to bind the flexible part model with a haptic device,
- model the display representation of a flexible part to fit it into the display environment.

P. Chedmail et al. (eds.), Integrated Design and Manufacturing in Mechanical Engineering, 121-128.
©2002 *Kluwer Academic Publishers.*

The work presented focuses on the generation of a mechanical model describing the flexible part behaviour under user's interactions and has been applied to parts like hoses. This work is part of a European project: DMU-VI (Digital Mock Up – Visualization) and funded by the EEC and integrated into the AIT (Advanced Information Technology) consortium.

2. WHAT MODEL FOR WHAT PURPOSES ?

In order to model the deformation behaviour of flexible parts in real time, a mechanical model is required. Either this model can be based on a finite element approach [1, 7] or a boundary element approach [5] or a simplified version of such models or some new concept or paradigm.

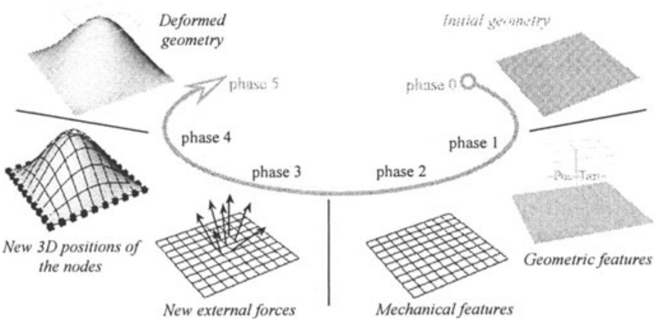

Figure 1. Free form surface model linked with a rigid bar network. The successive phases performed to achieve a surface deformation are illustrated using the example of one patch.

Because the main goal is to accurately model the force-displacement relationships, stresses and strains are not essential to the category of models set up but this aspect does not lead to specific simplifications of mechanical models. It is therefore necessary to assess the behaviour and the diversity of these models to find out if one of them fulfil the requirements. The procedure followed to evaluate a set of mechanical models incorporates:

- a qualitative analysis characterizing the deformation behaviours related to standard user's interactions (to set up a model of the real interaction between the flexible part and the user),
- a set of experiments to characterize the real behaviour of a flexible part under generic load cases. Flexible parts often exhibit complex mechanical behaviours (non linear mechanical behaviour, large displacements, anisotropic behaviour, heterogeneous material, non linear material law). Experiments produce a first reference model of reality,
- a structural analysis through Finite Element (FE) models to evaluate their adequacy to the real behaviour gained through experiments. Diverse FE models have been generated to identify their relevance with respect to the accuracy and speed requirements. These models have also helped to analyze the influence of various hypotheses as well as to provide parameters which cannot be easily measured and which helped to set up some control parameters of a dual mechanical model,

- the generation and fitting of a dual mechanical model acceptable for the virtual requirements. This model is fitted using experimental results as well as structural analysis parameters.

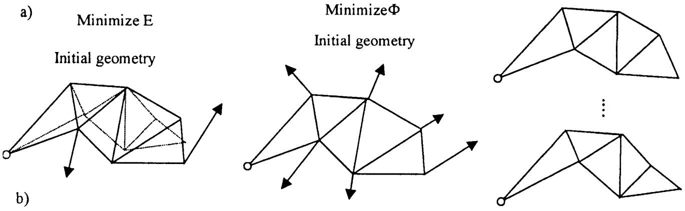

Figure 2. Illustration of the concept of dual mechanical model. a) the deformed geometry is obtained using the strain energy minimization applied to one structure. b) the deformed geometry is obtained using the functional and a series of rigid structures subjected to a dual load case.

The dual mechanical model set up is based on a free form surface model of the flexible part (here the parts studied are hoses) connected to a rigid bar network [2,6] (see Figure 1 the basic principle of this model). All the bars of the network are pin jointed without friction and the nodes of the network can be fixed, free to move in space or subjected to constraints (for example to maintain the connectivity or the continuity of a multi patch surface). The duality principle is as follows:

The strain energy functional which is minimized to produce nodal displacements of the FE model of a unique deformable structure is replaced by the minimization of an exterior forces functional to produce the static equilibrium positions of a series of rigid bar networks having a constant topology (see Figure 2).

This functional is non linear with respect to the external forces f_i and can be expressed as $\Phi_{rot}=\min\left({}^{T}\Delta F_{rot}^{[k]}.\Delta F_{rot}^{[k]}\right)$, where the forces minimized correspond to the difference between the external force $f_i^{[k-1]}$ rotated onto the direction of average normal around the i^{th} node, $N_{moy-i}^{[k-1]}$, and the force $f_i^{[k]}$ at the k^{th} iteration, i.e., $\Delta F_{rot-i}^{[k]}=f_i^{[k]}-\left\|f_i^{[k-1]}\right\|.N_{moy-i}^{[k-1]}$. Such a functional tends to preserve the intensity of the external forces while modifying their direction in order to smooth the underlying free-form surface [4] (see Figure 3c). Combined with anisotropic force densities into the bars of the networks, this criterion expresses the deformation behaviour of pipe type objects when their are subjected to bending deformations. The force density into the j^{th} bar is defined as the force/length ratio: $q_j=\left\|f_{bj}\right\|/l_j$, $q_j>0$ where f_{bj} is the force into the j^{th} bar and l_j its length. According to figure 1, these parameters form the mechanical features set by the user to express the surface deformation process.

The bar networks are associated with the free-form surface model through the concept of control polyhedron since the nodes of the bar networks are a subset of the vertices of the control polyhedrons of the free-form surfaces describing the object. Continuity conditions between surfaces dictates the vertices which are effectively used to define the nodes of the bar networks. The minimization criterion set up reflects the bending behaviour of hoses subjected to large displacements.

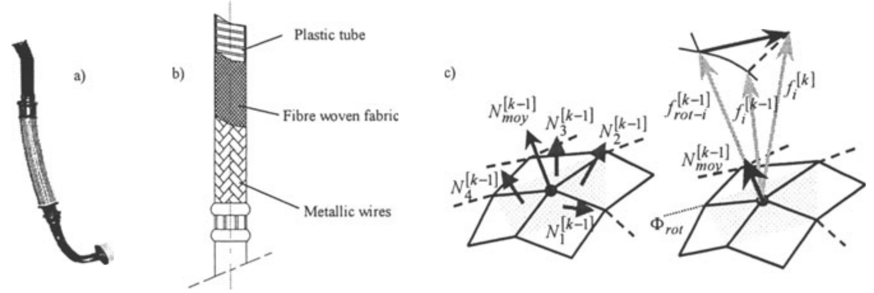

Figure 3. a) Oil hose studied with a flexible area in the centre and two rigid extremities. b) Structure of the flexible area of the oil hose. c) Minimization criterion used in dual mechanical approach.

Due to the large differences between the geometry and the constitutive material of flexible parts, it has not appeared suitable to generate a general purpose model. For these reasons, the previous procedure has focused on a specific part: an oil hose from BMW which is acting as partner in the EEC project DMU-VI (Figure 3a). This hose is placed in the engine bay of a car and is part of a maintenance scenario.

3. GENERATING A MODEL FOR AN OIL HOSE

The flexible area of interest is built around a thin cylindrical plastic pipe with variable inertia, covered with a thin layer of textile fabric which is covered itself by a metallic fabric. This flexible area is anchored at both ends into rigid metallic junctions which ensure its attachment with other components (see Figure 3b). It is assumed that no liquid pressure influences the deformation behaviour of the hose.

The qualitative analysis of the deformation behaviour has shown that under the magnitude of forces that could be applied manually during the operation, the hose could be considered as torsionally rigid as well as rigid under traction and compression load cases. The deformation model is mainly characterized by a bending behaviour. The hose exhibited also a hysteretic behaviour but due its difficulty it has not been considered in the models set up.

3.1 Experimental approach

The experiments set up were dedicated to the verification of some hypotheses, i.e. rigidity of the hose under torsion load cases, and to the characterization of the hose behaviour under bending load cases which simulates the standard action of the user (bending the hose with two hands) and the constrained behaviour when the user bends the hose which simultaneously interacts with its environment. The hose was loaded with masses like a cantilevered beam to simulate the effect of the user when bending the hose with two hands (see Figure 4a, b). The results showed that:

- large displacements (several tens of millimetres) where obtained for small loads (a few tens of Newton) justifying the non linear elastic behaviour of the structure (see Figure 5a). It is therefore not possible to simplify the model using the small displacements, small strains hypotheses of simple linear elastic models,
- the displacements obtained under two orthogonal loads applied at the free extremity of the hose justified its rigidity under torsion load cases (see Figure 5b),
- strong non linear behaviour was exhibited when the hose was subjected to two coplanar and opposite loads respectively applied at its extremity (P1) and its middle (P2), i.e. applying P1 first and P2 second gives fairly different results than the opposite (see Figures 4c and 5c). This is important to model correctly the effect of the interaction between the hose and its environment,
- no buckling of the hose has appeared for the magnitude of forces covered during the experiments.

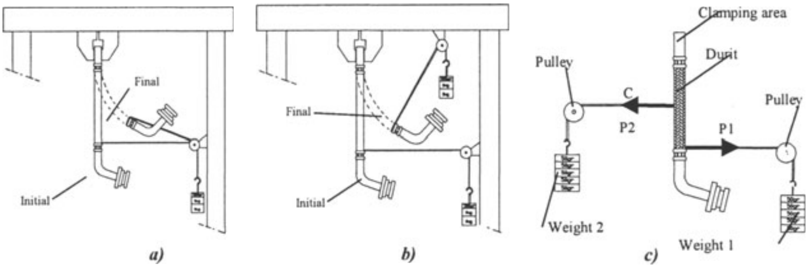

Figure 4. Loading configurations used for the experiments. Configurations a) and b) are chosen depending on the displacement amplitude applied to the hose. c)Loading configuration with two opposite forces P1 and P2.

3.2 Finite element models

Because of the dimensions of the hose, i.e. the diameter/length ratio is of the order of 1/10, two categories of FE models can be set up: beam models and shell models. For simplicity, Hooke's law and homogeneous equivalent material have been used to model the hose as a beam.

Due to the complex composition of the material, the Young's modulus of the equivalent material has been identified using the experimental displacements measured and fed into the beam model. However, to obtain the best possible fit to the experiments it has appeared that great distorsions could not be avoided if the equivalent material was behaving linearly. Since the behaviour law of the material was difficult and complex to identify, the non linear effect has been evaluated through the variation of the Young's modulus according to the intensity of the applied forces in the various load cases. As a result, the variation of the Young's modulus ranges between 3.2 N/mm^2 to 32N/mm^2. This clearly shows that the linear material behaviour cannot be used to simplify the model.

In addition, using a beam model would require further modelling treatments since the virtual reality environment needs to display the hose as a polyhedral surface. Hence, the deformed geometry of the beam has to be used as a basis to generate the polyhedral surface required for the display of the hose.

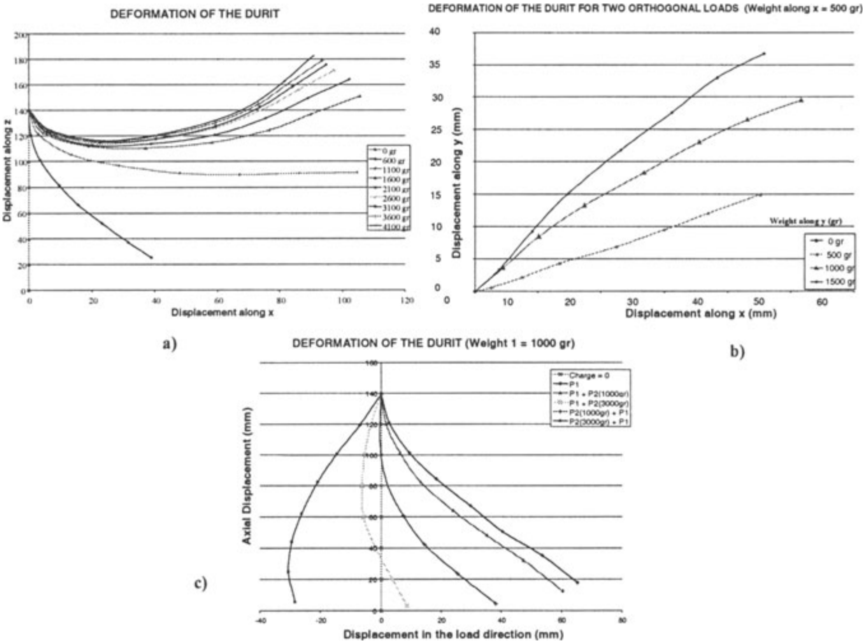

Figure 5. a) Deformed shape of the hose under bending behaviour and masses ranging from 0gr to 4100gr. One force applied at the free extremity of the hose. b) Displacement of the extremity of the hose submitted to two orthogonal loads in a plane orthogonal to the axis of the hose. The nearly linear displacement curves obtained justifies the torsionally rigid behaviour hypothesis. c) Deformed shape of the hose under two forces P1 and P2.

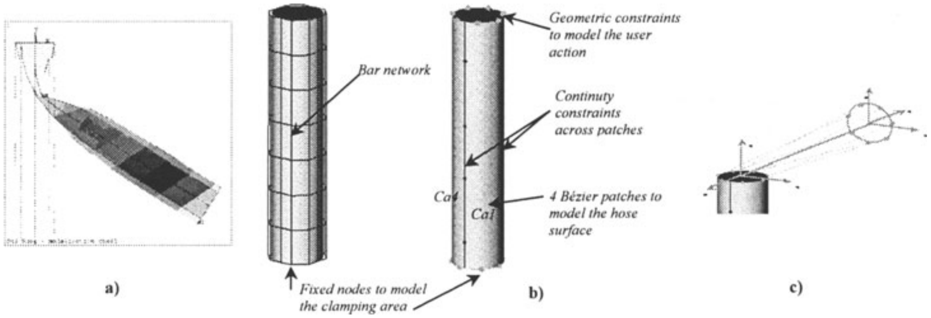
a)
Bar network
Fixed nodes to model the clamping area
Geometric constraints to model the user action
Continuity constraints across patches
Ca
Ca
4 Bézier patches to model the hose surface
b)
c)

Figure 6. a) Deformed configuration of a shell model exhibiting a buckling behaviour. b) Parameters of the free form surface model and of the bar network model. c) Example of geometric constraints used as interface parameters.

The second category of FE models that could be used is shell models. These models are based on a polyhedral surface model which could be used in the virtual environment as the representation of the hose. When generating such models with a homogeneous material, the FE model exhibited a buckling behaviour which never appeared during the experiments. To overcome this problem a model of anisotropic shell has been set up with large differences of Young's moduli in the longitudinal and the axial directions of the hose. However, the buckling effect was still existing in configurations where the experiments did not shown it (see Figure 6a). Because of the above behaviour and the computer time required to handle non linear shell models (over than 1mn CPU time for a coarse mesh using a SGI workstation with R5000 processor), shell models were not investigated further.

As a conclusion, it has appeared that a finite element model needed to use large displacements and non linear material behaviour to provide an acceptable and accurate mechanical model of the hose. The analysis of the beam finite element models has also highlighted the strong influence of the category of boundary conditions on the deformed shape of the hose in a context of non linear mechanics.

3.3 Dual mechanical model

The dual mechanical model based on the concept described at section 2 uses a CAD surface model of the hose as geometric model. The cylindrical surface is approximated using four Bézier patches whose connections ensure its G^1 continuity. The series of bar networks used to compute the static equilibrium positions are built from the control polyhedrons of the Bézier patches (Figure 6b).

The control parameters acting on the equilibrium positions of the networks are the force length ratio in each bar. These parameters are used to define an anisotropic behaviour of the surface deformation process and to prevent the surface deformation from buckling effects. In the present configuration, high force densities have been assigned to the radial bars whereas the bars oriented along the longitudinal direction have been assigned low force densities in order to preserve as much as possible the section of the hose.

The interface parameters of the model are based on geometric constraints which can be directly applied to the surface to control its deformation [2, 3] (Figure 6c). Here, the parameters set are the displacement and the rotation of the extreme section of the free end of the hose. To evaluate the accuracy and adequacy of such a model, the displacement input was based on the experimental values and the rotation of the section was based on the value provided by the beam FE model which best fits a given load case. Configuring this dual model with the above parameters produced acceptable results for all the range of deformation configurations measured experimentally under the range of masses used to load the hose, i.e., one force applied at the end of the free extremity and two opposite forces applied in the same plane (Figure 7a). The computation time required to compute a deformed configuration was of the order of 0.1sec on the same workstation as previously.

Several tests have been performed to evaluate the influence of the degrees of the Bézier patches, the surface decomposition into patches, the values of the force densities, the diameter of the hose over the deformation results (Figure 7b).

4. CONCLUSION

A new approach has been proposed to address the problem of modelling flexible parts for assembly/disassembly simulation purposes using a qualitative analysis, an experimental approach, a set of numerical models. It has been demonstrated that current FE models could not provide satisfactory results within the time scale of a virtual reality environment.

A concept of dual mechanical model has been introduced and has proved efficient both in terms of accuracy and speed to model a flexible part behaviour for assembly/disassembly purposes. Next steps of the work will focus on the extension of the dual model to incorporate the interactions between the flexible part and the surrounding rigid parts.

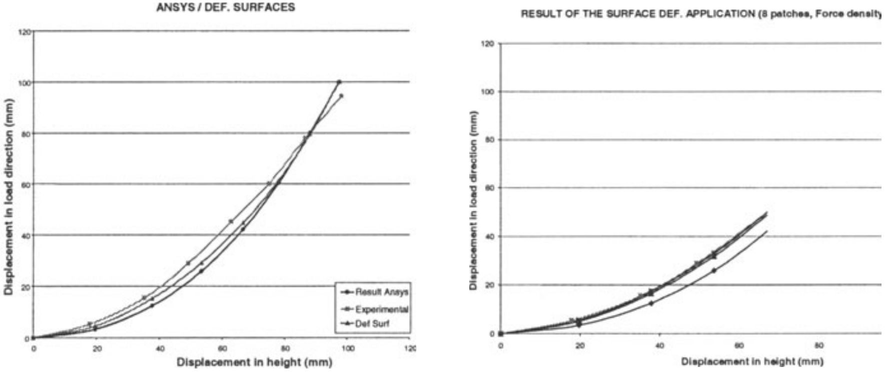

Figure 7. a) Comparison between experiments, FE beam model results, dual mechanical approach results (one load of 3000gr applied at the free extremity of the hose). The FE result (Ansys) represents the best fit to the experiment using the best possible Young modulus to minimize the fitting error. b) Influence of the polynomial degree of the surface along the axis of the hose and comparison with the FE results and experiments. Degree ranging from 5 to 8.

5. REFERENCES

1. Celniker, G. and Gossard, D., Deformable curve and surface finite elements for free form shape design, Proceedings of SIGGRAPH 91, Vol. 25 (4), 1991: 257-266.
2. Guillet, S., Modification et construction de formes gauches soumises à des contraintes de conception, Ph. D. thesis, Institut National Polytechnique de Grenoble, France, 18th january, 1999.
3. Guillet, S., Léon, J-C, Parametrically deformed free-form surfaces as part of a variational model, CAD, Vol. 30 (8), 1998: 621-630.
4. Guillet, S., Léon, J-C., Deformation criteria for the direct manipulation of free form surfaces, in Curves and Surfaces edited by L. L. Schumaker, 2000.
5. James, D. L., Pai, D.K., ArtDefo: Accurate real time deformable objects, Proceedings of SIGGRAPH 99, Los Angeles, August, 1999.
6. Léon, J-C. and Trompette, P., A new approach towards free form surface control, Computer Aided Geometric Design, Vol. 12, 1995: 395-416.
7. Qin, H. and Terzopoulos, D., D-NURBS: A physics Based framework for geometric design, IEEE Transaction on Visualization and Computer Graphics, Vol. 2 (1), 1996: 85-96.

Jean-Claude LEON
Laboratoire Sols, Solides, Structures UMR CNRS 5521
Domaine Universitaire
BP 53X 38041 Grenoble Cedex 9
France
Jean-Claude.Leon@hmg.inpg.fr

A RECTIFICATION ALGORITHM FOR MANIFOLD BOUNDARY REPRESENTATION MODELS

Guoling Shen, Takis Sakkalis and Nicholas M. Patrikalakis
Massachusetts Institute of Technology
Cambridge, MA 02139-4307, USA
guoling@rentec.com, takis@aua.gr, nmp@mit.edu

Abstract In this paper we present a boundary reconstruction methodology which builds a valid model in the neighborhood of an object described by a traditional boundary representation model with floating point specification. This method converts an erroneous model into an interval model, guaranteed to be gap-free. An example illustrates our methodology for robust conversion.

Keywords: Manifold boundary model, defects, rectification methods

Introduction

Boundary representation (B-rep) contains topological and geometric information of solid boundaries. Topological information, in general, is represented by a graph describing incidence and adjacency relations between topological boundary entities. Geometric specification involves equations for points, curves and surfaces. A B-rep model is called *valid* if it describes a solid boundary. However, as is well-known, the validity of B-rep models is not self-guaranteed [4, 10, 12].

Invalid B-rep models contain defects – representational entities that do not conform to modeling constraints due to topological errors and/or inconsistencies between topological and geometric specification. Defects often appear as gaps, inappropriate intersections, dangling entities, internal walls and inconsistent orientations [17]. Causes of defects exist throughout the entire life cycle of a model, such as computational inaccuracy stemmed from floating point arithmetic [4, 5] and approximation algorithms in model creation and inconsistent conversions in data exchange across heterogeneous modeling systems [11].

P. Chedmail et al. (eds.), Integrated Design and Manufacturing in Mechanical Engineering, 129-138.
©2002 *Kluwer Academic Publishers.*

Research on model rectification (correction) has been done mainly on triangulated models, specifically, STL models for rapid prototyping. Most algorithms [1, 9] identify erroneous triangle edges, string such edges to form hole boundaries, and then fill holes with triangles. These algorithms use local topology (incidence and adjacency) to rectify defects and are successful in the majority of candidate models, but may create undesirable global topological and geometric changes.

In our earlier work [16], we argued that the model rectification problem should be approached as a boundary reconstruction problem in order to achieve a global optimal solution, and showed that the boundary reconstruction problem is NP-hard. In order to construct gap-free B-rep models, we further developed the concept of interval solid models [15], which was first introduced by Hu et al [7, 8]. Based on these, in this paper, we develop a boundary reconstruction methodology. The objective is to reconstruct a B-rep model from a given B-rep model represented in a certain format (e.g. STEP) using interval arithmetic.

The methodology proposed in the following sections consists of three main steps: 1) construction of a graph induced by surface intersections for each surface, 2) face reconstruction, and 3) shell reconstruction. The methodology follows very closely the proof of NP-hardness of the boundary reconstruction problem in Shen et al [16]. It mainly focuses on capturing miniature numerical gaps and fills them with appropriate boxes.

In the following, we first describe the three steps of the procedure in detail. Then, we show an example to illustrate the use of interval methods in model verification and rectification.

1. Intersection-induced graph

Edges of a B-rep model are embedded on intersection curves of the underlying surfaces. On each of the surfaces, intersection curves form a geometric embedding of a graph with their intersections as nodes and the curve segments as arcs. As discussed in Shen et al [16], face boundaries must consist of arcs in this graph in order to achieve geometric consistency of all topological relations (incidence and adjacency) in which the face is involved.

In the proposed boundary reconstruction method, an intersection curve is computed using surface intersection algorithms developed by Hu et al [6], and is represented as an ordered list of non-degenerate rectangular boxes [14]. Therefore, the geometric embedding of an arc in the graph is an ordered list of boxes, called a *box curve*, and that of a node is a (unordered) cluster of boxes, called a *box point*. Whenever a new intersection curve is computed, the two graphs on the intersection surfaces need to be updated. The new curve is intersected with the geometries of all arcs and nodes in both graphs, and is subdivided into a list of box points and box curves, which are then inserted into both graphs to create new nodes and arcs.

2. Face reconstruction

Let R be the underlying surface of face f^o in model M^o, and G_f be the intersection-induced graph. As in model creation, boundary reconstruction proceeds in a bottom-up manner.

An edge e^o involved in a certain adjacency relation between f^o and another face f_1^o must be embedded in the intersection curve C of R and R_1. The reconstruction of e^o starts with its vertices v_1^o, v_2^o. The corresponding new vertices v_1^n, v_2^n are two nodes in G_f. Each of these nodes must have at least one incident arc constructed from C, i.e. the new vertices are on the intersection curve. In addition, each selected node should be the closest to the original position of the corresponding old vertex among all such nodes to minimize the geometric change in boundary reconstruction. See Figure 1 for illustration, where the dotted lines are arcs of G_f.

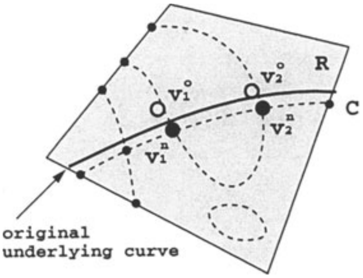

Figure 1. Reconstruction of vertices

The reconstruction of e^o amounts to finding a path between the two selected nodes in G_f. Again, the selected arcs must be constructed from the intersection curve C. If there exist multiple paths, the one with the minimum deviation from the original geometry of e^o should be selected. This often happens when C contains self-intersections or is closed, e.g. a circle. With the edge orientation given in e^o, it shall be clear which part of C belongs to an edge, unless the underlying curve of e^o in M^o is far different from C. Thus, new edge e^n is oriented in the same way as e^o.

For a loop l^o, new edges form a subgraph G_e in G_f, which may not be a simple closed curve. Though an arbitrary graph could be very complicated, the proposed method intends to resolve miniature features such as small dangling arcs and gaps. It first identifies two types of nodes in G_e: free node that has exactly one incident arc, and branch node that has more than two incident arcs. Dangling arcs are then identified by marching from a free node until another free node or a branch node is reached, and then trimmed away if the geometric change due to such actions is within a given tolerance. Large pieces of dangling arcs indicates the existence of gaps. Let v_1, v_2 be two ends of a gap. The shortest path between v_1, v_2 is then searched in G_l, where $G_l = G_f - (G_e - \{v_1, v_2\})^1$. See Figure 2 for illustration. Finding the shortest path between two nodes in a graph is a polynomial problem. Algorithms can be found in many textbooks on graph theory, such as [2]. Edges in the newly constructed loop l^n are oriented in the same way as their corresponding old edges are in l^o. Consistency can be verified by marching through these edges.

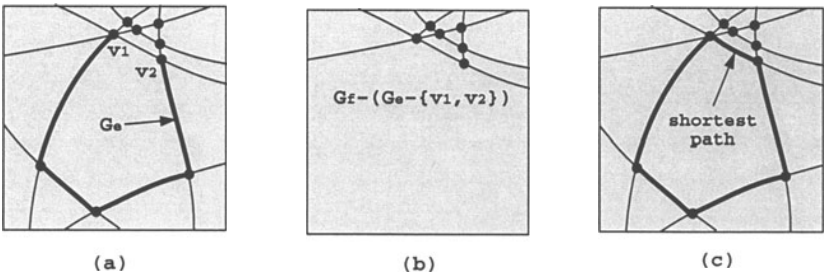

Figure 2. Gap closing in loop reconstruction

A face may have more than one loops. Loops reconstructed individually need to be modified so that together they define a valid face boundary. The modification process includes eliminating intersections between loops, verifying relative locations of loops, and orienting loops consistently. To retain the design intent of the face topology, the resulting loops should also be homeomorphic to the original face topological structure in the strong sense[2], provided that the latter is a graph consisting of simple cycles sharing at most one common node pairwise [13].

Any two loops share at most one common vertex. Assume two loops l_1^n and l_2^n share more than two vertices. We will resolve cases of two

---

[1] Here, the difference between graph $G(V, E)$ and its subgraph $G_1(V_1, E_1)$ is another subgraph consisting of nodes $V - V_1$ and arcs incident to these nodes.

[2] Two face topological structures are homeomorphic in the strong sense if they are homeomorphic and their outer loops are homeomorphic as well [16].

common vertices. Cases involving more than two common vertices may follow the same approach. Let v_1, v_2 be two common vertices of l_1^n and l_2^n. Let P_1 be the shorter path between v_1, v_2 in l_1^n, and P_2 be that in l_2^n. Also assume that the corresponding original loops l_1^o and l_2^o are topologically correct. The following is a brief description of the algorithm. See also Figure 3.

1 If both l_1^n and l_2^n are inner loops,
  (a) If P_1 is outside l_2^n, and P_2 is outside l_1^n,
    i If l_1^o and l_2^o do not have common vertices, first, delete v_1 and v_2 and their incident arcs in l_1^n, i.e. $l_1^n \leftarrow l_1^n - \{v_1, v_2\}$, and then, fill the gap in graph $G_f - l_1^n - l_2^n$. If the gap can not be filled, try the same in l_2^n.
    ii If l_1^o and l_2^o share one common vertex, first, delete v_1 and its incident arcs in l_1^n, i.e. $l_1^n \leftarrow l_1^n - \{v_1\}$, and then, fill the gap in graph $G_f - l_1^n - l_2^n$. If the gap can not be filled, try the same in l_2^n, or by deleting v_2.
    iii If l_1^o and l_2^o share one common edge, delete P_1, P_2 and merge l_1^n, l_2^n.
  (b) If P_1 is inside l_2^n, and P_2 is inside l_1^n, switch P_1 and P_2 and do the same as Step 1(a).
  (c) If P_1 is inside l_2^n while P_2 is outside l_1^n, delete P_1, P_2 and merge l_1^n, l_2^n.

2 If one, say l_1^n, is the outer loop,
  (a) If l_2^n is inside l_1^n, do the same as Step 1(a).
  (b) If one part of l_2^n is outside l_1^n, delete P_1, P_2 and merge l_1^n and l_2^n.

In Step 1(a) of the above algorithm, if l_1^n and l_2^n can not be modified in accordance with the topological structure of l_1^o and l_2^o, topological changes are then necessary. For example, if Step 1(a)i fails, we may try Step 1(a)ii by ignoring the topological structure. For two loops sharing a common edge, if the feature exists in the original topological structure, the two loops should be merged by trimming the edge; otherwise, the edge should be deleted from one of the loops and the induced hole needs to be closed as above.

Whether a part or an entire loop l_1^n is inside another loop l_2^n, can be verified by checking a box of l_1^n which does not intersect l_2^n. The ray casting algorithm should be applied to the pre-images in the parameter domain of the underlying surface. Let $\mathbf{R}_b$ be a horizontal or vertical

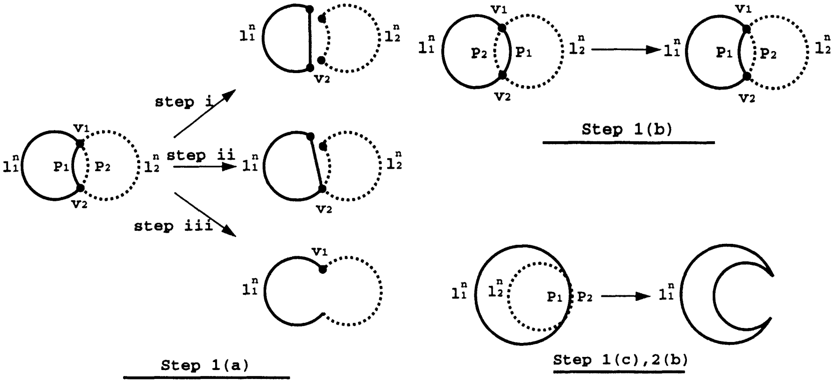

Figure 3. Loop modification

ray from a box b. Compute the intersections between $\mathbf{R}_b$ and boxes in l_2^n. The intersections are intervals, representing coordinate values in the direction of the ray. Merge all intersecting intervals. The number of remaining intervals is then the number of intersections. The same algorithm is also used to verify the relative locations of the loops. All inner loops must be inside the outer loop, and no inner loop is inside another inner loop.

The orientation of a loop can be determined by computing the rotation index [3] of its pre-image in the parameter domain. Select an arbitrary point $\mathbf{c}$ inside a loop. Let $\{\mathbf{c}_i\}$ be centers of boxes in the loop. Then, the rotation index is

$$r = \frac{1}{2\pi} \sum_i \angle(\mathbf{cc_{i-1}}, \mathbf{cc_i}), \tag{1}$$

where $\angle$ denotes the positive angle between two vectors. This number should be close to ± 1 if box sizes are small. A loop is positively oriented if $r \approx 1$, and is negatively oriented if $r \approx -1$. The outer loop must be positively oriented, and all inner loops must be negatively oriented.

3. Shell reconstruction

A shell consisting of faces reconstructed individually may have dangling patches, internal walls and holes, and may be inconsistently oriented. Similar to algorithms for STL model rectification, shell reconstruction identifies those edges shared by only one or more than two faces, and string them together to form simple closed curves. Such a simple closed curve may bound a hole if each of its edges has exactly one incident face, and bounds an internal wall if each of its edges has more than two incident faces. If it consists of two connected pieces, one having edges with one incident face and the other having edges with three incident faces, then, the closed curve bounds a piece of dangling patch. More complex situations similar to what were studied by Bohn and Wozny [1] could happen. Heuristic rules could help in such situations, but user assistance is frequently needed in resolving certain ambiguities. Here, we only deal with the above mentioned three situations, and leave other cases to user resolution.

Dangling patches with very small sizes shall be trimmed away first. The boundary of an internal wall actually bounds three connected pieces, each of which is an open shell. The one inside the shell formed by the other two is the internal wall and shall be deleted. Whether an open shell is inside a closed shell can be verified by a ray-casting algorithm in a similar manner as in loop reconstruction. In the following, we present a method for filling holes using surface patches constructed from the underlying surfaces by surface intersections. Let $\{e_i\}$ be the edges in a hole boundary and already sorted in order. The method fills the hole progressively by attaching new patches to the boundary and computing the new hole boundary. This is a trial-and-error process. It tests all possible combinations of patches until one is found to fill the hole. In the selection of patches, those with small sizes are preferable so as to minimize the geometric change. For an edge e in $\{e_i\}$, a patch shall be selected first if it is embedded on the same surface as the face sharing e. This patch can then be merged to the face, so that no new face is introduced and the change to the topological structure is minimized. See Figure 4 and the following description:

1 Start with e_0. Find a patch of small size and incident to e_0. Denote the new patch by f'_0.

2 Let e_i be the current edge, v_i be the common vertex of e_{i-1} and e_i, and e'_i be the edge on f'_{i-1} incident to v_i.

3 Find a patch f'_i of small size and incident to e_i and e'_i.

4 If no such patches exist, go back to edge e_{i-1} and select a different patch as f'_{i-1}. It may be necessary to search further back.

5 Repeat Step 2 to 4 until the process reaches e_0 again.

6 Update the hole boundary $\{e_i\}$.

7 If $\{e_i\}$ is not empty, repeat Step 1-6.

Shells constructed individually may share vertices, edges and/or faces. Such features should be detected and eliminated. Similar actions to

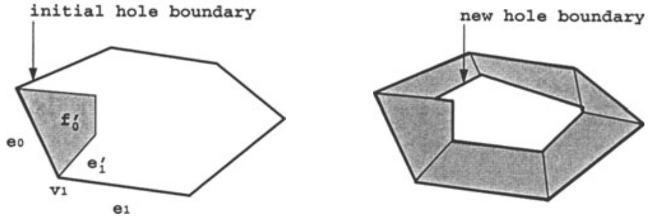

Figure 4. Hole filling in shell reconstruction

those of loop modification should be taken to achieve topological validity and retain design intent. For instance, if two shells share one common face and the face is in the original topological structure, then, it should be deleted and the two shells should be merged, because such a face is likely to be an internal wall left by improperly implemented regularized Boolean operations. However, if it is a face introduced to fill a hole, it should be trimmed away, together with all of its adjacent faces, and the induced hole must be closed.

4. Example

The model shown in Figure 5 is one part of a shaver handle, and created using a commercial CAD system. The size of the model is roughly $0.04m \times 0.06m \times 0.14m$. The underlying surfaces of the model consist of 16 integral and rational B-spline surfaces, 3 cylindrical surfaces and 5 planes. The global uncertainty measure is given by the designer as $10^{-6}m$. The model has $V = 40$ vertices, $E = 62$ edges, $F = 24$ faces, no inner loop, and one shell. The topological structure satisfies the sufficient conditions presented in Sakkalis et al [13]. Therefore, from the Euler-Poincaré formula $V - E + F = 2(1 - G)$, we can deduce that the model has genus $G = 0$ and thus it is homeomorphic to a ball.

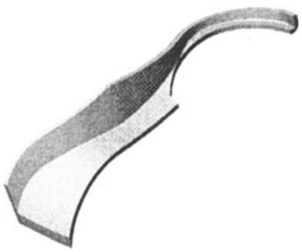

Figure 5. Part of a shaver handle

We convert this model into an interval solid model. Because edges in the original model are reasonably computed, initial conversion of each face is performed by growing the width of underlying curves of its edges by a given resolution. If such growth gives a valid face, the conversion of the face is finished, unless adjacency relations with neighboring faces are violated. For the latter cases, the reconstruction process using the proposed methodology is then performed.

The experiment starts with resolution $10^{-6}m$, given in the original STEP file. Eight faces have edges not on their underlying surfaces. Figure 6 shows one face with 2 edges partially on the underlying surface and one edge not overlapping the surface at all. Further computation reveals that the original face becomes valid at resolution $2 \times 10^{-4}m$. Figure 7 shows the valid face boundary. Overall, the model becomes valid at resolution $5 \times 10^{-4}m$.

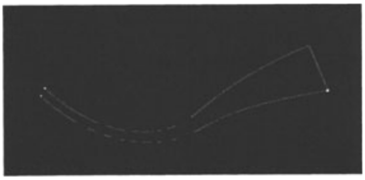

Figure 6. An invalid face with resolution $10^{-6}m$

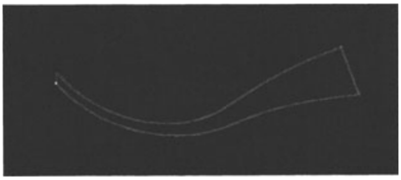

Figure 7. The same face as in Figure 6 becomes valid resolution $2 \times 10^{-4}m$.

We now test whether it is possible to reconstruct an interval model at the given resolution $10^{-6}m$, i.e. when all the surfaces in the model become interval surfaces with width $10^{-6}m$. For the face in Figure 6, because its underlying surface, now an interval surface, does not intersect one of the surfaces on which its adjacent faces are embedded, no valid face boundary can be constructed from surface intersections. If we further grow the width of all the surfaces to $10^{-5}m$, the face can then be reconstructed. The remaining seven invalid faces can be rectified at various resolutions, and an interval model can be constructed at resolution $5 \times 10^{-5}m$.

Acknowledgments

Funding for this work was obtained in part from NSF grant DMI-9215411, ONR grant N00014-96-1-0857 and from the Kawasaki chair endowment at MIT.

References

[1] J. H. Bohn and M. J. Wozny. A topology-based approach for shell-closure. In P. R. Wilson, M. J. Wozny, and M. J. Pratt, editors, *Geometric Modeling for Product Realization*, pages 297–318. Elsevier Science Publishers BV, 1993.

[2] N. Deo. *Graph Theory with Applications to Engineering and Computer Science.* Prentice-Hall, Englewood Cliffs, NJ, 1974.

[3] P. M. do Carmo. *Differential Geometry of Curves and Surfaces.* Prentice-Hall, Inc., Englewood Cliffs, New Jersey, 1976.

[4] C. M. Hoffmann. *Geometric and Solid Modeling: An Introduction.* Morgan Kaufmann Publishers, Inc., San Mateo, California, 1989.

[5] C. M. Hoffmann. The problems of accuracy and robustness in geometric computation. *Computer*, 22(3):31–41, March 1989.

[6] C.-Y. Hu, T. Maekawa, N. M. Patrikalakis, and X. Ye. Robust interval algorithm for surface intersections. *Computer Aided Design*, 29(9):617–627, September 1997.

[7] C.-Y. Hu, N. M. Patrikalakis, and X. Ye. Robust interval solid modeling: Part I, Representations. *Computer Aided Design*, 28(10):807–817, October 1996.

[8] C.-Y. Hu, N. M. Patrikalakis, and X. Ye. Robust interval solid modeling: Part II, Boundary evaluation. *Computer Aided Design*, 28(10):819–830, October 1996.

[9] I. Mäkelä and A. Dolenc. Some efficient procedures for correcting triangulated models. In *Proceedings of Solid Freeform Fabrication Symposium*, pages 126–134. University of Texas at Austin, 1993.

[10] M. Mäntylä. *An Introduction to Solid Modeling.* Computer Science Press, Rockville, Maryland, 1988.

[11] T. J. Peters, N. F. Stewart, D. R. Ferguson, and P. S. Fussell. Algorithmic tolerances and semantics in data exchange. In *Computational Geometry '97*, Nice, France, 1997.

[12] A. A. G. Requicha. Representations of solid objects - theory, methods and systems. *ACM Computing Surveys*, 12(4):437–464, December 1980.

[13] T. Sakkalis, G. Shen, and N. M. Patrikalakis. Representational validity of boundary representation models. *Computer Aided Design*, 32(12):719-726, October 2000.

[14] G. Shen, T. Sakkalis, and N. M. Patrikalakis. Interval Methods for B-Rep Model Verification and Rectification. In *Proceedings of the ASME 26th Design Automation Conference*, Baltimore, MD, September 2000. p. 140 and CDROM. NY: ASME, 2000.

[15] T. Sakkalis, G. Shen, and N. M. Patrikalakis. Topological and Geometric Properties of Interval Solid Models *Graphical Models*, 63(3):163-175, May 2001.

[16] G. Shen, T. Sakkalis, and N. M. Patrikalakis. Boundary Representation Model Rectification *Graphical Models*, 63(3):177-195, May 2001.

[17] S. Wolfe. Fixing bad CAD data. *Computer Aided Design Report*, 17(1):4–7, January 1997.

R.I.M. YOUNG, O.CANCIGLIERI-JNR, C.A.COSTA, J.M. DORADOR, J.ZHAO, W.M.CHEUNG

INFORMATION SUPPORT IN AN INTEGRATED PRODUCT DEVELOPMENT SYSTEM

Abstract. Computer-aided design systems require a comprehensive information interaction capability in order to support team-based design. This paper focuses on research concerned with providing this level of support through the use of a number of related information models. The provision of a common sharable information environment plays a critical role in an integrated product development process. Whilst the need for information models is well known, the problems of how they should be structured and the relationships and interactions between them have yet to be understood. In this paper we identify three information models as important: a product model, a manufacturing model and a product range model. The structure of these models is discussed and an approach is offered to some of the information interaction problems.

INTRODUCTION

Whilst the understanding of the organisational needs of the concurrent engineering philosophy have advanced significantly over recent years [1], the computational tools to support team based design have yet to show the same level of development. Typically Computer-aided design systems are geometric modelling systems and do not provide the comprehensive information interaction capability which team-based design requires [2]. This paper focuses on research concerned with overcoming this problem through the use of a number of related information models to support design decision making.

The provision of a common sharable information environment plays a critical role in an integrated product development process[3]. Whilst the research needed to achieve such an environment is substantial, the successful achievement of such an environment offers significant potential benefits to system users.

Product models have been recognised for many years now to be a means to the provision of a common source of product information to support integration and data sharing [4]. However in this paper we recognise three information models as important: a product model, a manufacturing model and a product range model. Product models provide a source and repository for information concerning a

P. Chedmail et al. (eds.), Integrated Design and Manufacturing in Mechanical Engineering, 139-146.
©2002 *Kluwer Academic Publishers.*

product under development. A Manufacturing model by comparison represents the capability of a manufacturing facility and can therefore provide manufacturing related input to design decision making [5]. A product range model provides a historical perspective on the design of particular product types [6]. The problems of how information models should be structured and the relationships and interactions between them have yet to be clearly understood [7]. This paper discusses the issues involved in information model support for product development and offers an approach to overcoming some of the information interaction problems.

INFORMATION MODEL ISSUES IN PRODUCT DEVELOPMENT

A wide range of information is needed to support product development decision making. Given the global nature of many modern companies this information must be communicated at a global level as individuals in a design team are likely to be based in different locations throughout the world. An illustration showing an example of some information types needed to support product development is provided in figure 1.

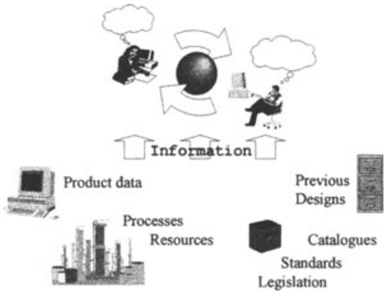

Figure 1: Example information inputs to product development

There is a distinct difference between information that is provided as text for user interpretation and information that is sufficiently structured that it can be interpreted by software applications. It is assumed that all information models provide sufficient structure to provide software support. The issues to be resolved in information model support for product development can be raised through two simple questions:

1. What information contexts are needed to support product design and manufacture in a global design and manufacture environment?
2. How can information be shared across these multiple contexts?

Finding the answers to these questions is not easy as is evident from the wide range of international research and the efforts of the ISO STEP groups over recent years [3,4,5,7,8]. Figure 2 provides a general view of an information supported integrated product development system. This highlights the separation of the applications which support design from the information which they use. This is an essential aspect of integrated information systems support and offers the potential advantages of complete data integrity, rapid flexibility, maintainability, vendor independence and life cycle support.

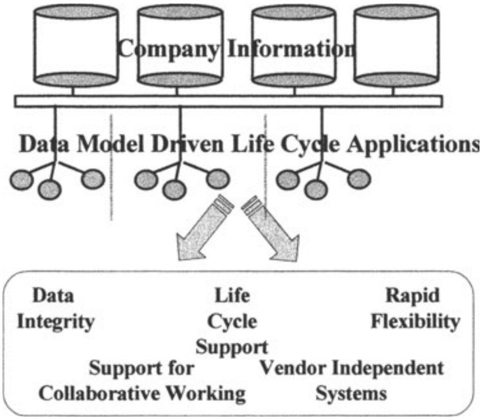
Company Information
Data Model Driven Life Cycle Applications
Data Integrity
Life Cycle Support
Rapid Flexibility
Support for Collaborative Working
Vendor Independent Systems

Figure 2: Information Supported Integrated Product Development

The pursuit of an information supported integrated product development system raises a number of issues as follows:

1. What functions in the product development process should be supported?
2. What types of information model are needed to support each function?
3. What information structures are needed to support the input and output of each function?
4. What information needs to be shared between functions and how can this be achieved?
5. How can flexible information systems be achieved which can be readily maintained and updated?
6. Do information models just capture information or are some of them knowledge models?
7. What characterises a useful set of information systems design tools?

THE FUNCTIONAL REQUIREMENTS OF DATA MODEL DRIVEN PRODUCT DEVELOPMENT SYSTEMS

The functions to be supported will depend on the particular development process to be supported. In order to explore the issues in information model supported integrated product development this work has focused on the interaction between design for manufacture and manufacturing planning in a global environment. An example of interacting functions involved in the design of an injection moulded product is illustrated in figure 3. In this example the plastic product and the mould provide the key product information contexts for the design and manufacturing functions. However there are many sub-contexts to be supported each of which has its own information requirements.

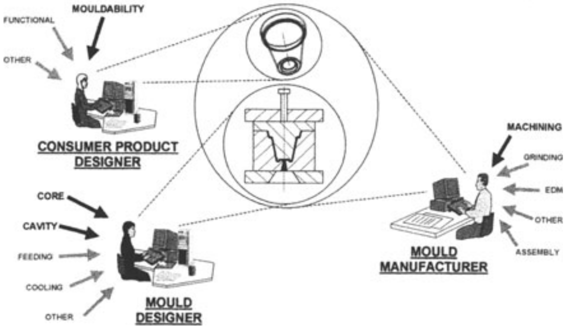
MOULDABILITY
FUNCTIONAL
OTHER
CONSUMER PRODUCT DESIGNER
MACHINING
GRINDING
EDM
OTHER
ASSEMBLY
MOULD MANUFACTURER
CORE
CAVITY
FEEDING
COOLING
OTHER
MOULD DESIGNER

Figure 3: An example of multiple functions in product development

The basic concept of information model supported product development is that any software function that is involved in supporting product development will draw on the information models for information inputs and will supply its outputs into the information models. Figure 4 shows three example applications to support the development of an injection moulded product. Each of these applications draws product information from a product model and manufacturing information from a manufacturing model.

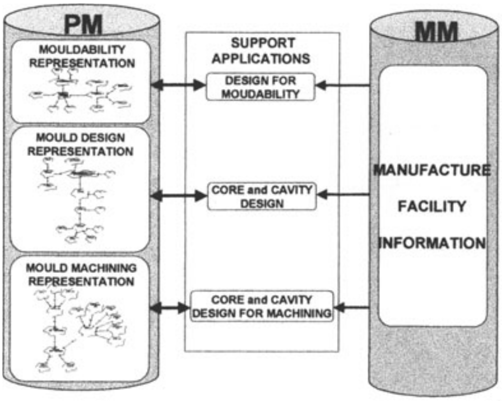
PM
MOULDABILITY REPRESENTATION
MOULD DESIGN REPRESENTATION
MOULD MACHINING REPRESENTATION
SUPPORT APPLICATIONS
DESIGN FOR MOUDABILITY
CORE and CAVITY DESIGN
CORE and CAVITY DESIGN FOR MACHINING
MM
MANUFACTURE FACILITY INFORMATION

Figure 4: Different information contexts to support specific applications.

The product information for each application is specific to that context. Hence the design for mouldability application has a mouldability context, core and cavity design have a mould design context and core and cavity machining have a mould machining context. Necessary manufacturing information concerning injection moulding machines and machining processes are drawn from the manufacturing model. The significance of these information structures is that interactions between applications are handled via the information models. The only constraint on the action of an application is the availability of information in the information model. Interactions between applications must therefore be dealt with via interactions between the information in the models.

A further necessary information model is one which can provide information concerned with previous designs and support design re-use. This can be achieved in variant and adaptive design through the use of a product range model which captures sets of product functions and maps these to a sets of possible solutions. Specific solutions can then be identified for a particular design situation, dependent on the constraints and pre-conditions which apply in that case. A product range model, while having some similarity with a product model in that it is concerned with a product type, is substantially different in that it is concerned with capturing information concerning previous designs. The aim of the product range model is that the information which it contains should be re-used to support new product development.

THE STRUCTURE OF THE INFORMATION MODELS

The three models explored in this research are product models, manufacturing models and product range models. While further information models are likely to be needed to support the full product life cycle, these three are believed to be of particular importance.

As explained in the previous section, a product model must be able to support multiple information contexts if it is to be of real value in an integrated product development system. Such a model is considered to be at the heart of any such system as it must maintain all the key information related to the product which is under development. Figure 5 shows a UML class diagram of the general product data structure that has been defined into which multiple information contexts can be constructed. This is achieved through the *views* class, which can support a range of design views of a product, or manufacturing views of a product, or other views as necessary.

A Manufacturing Model is somewhat different in that it is concerned with manufacturing facilities rather than products. Its aim is to capture a representation of the manufacturing capability of a global facility. A general representation to capture this in terms of resources, processes and strategies has already been defined and reported [9]. However the relationships between resources, processes and strategies have not, until now, been clearly specified. Figure 6 provides an illustration of a manufacturing data model showing the dependencies between resources processes and strategies.

The product range model, at a simple level, captures links between the functional needs of a product type and possible design solutions. However, to be of value, the product range model must capture the interactions which occur between possible design solutions as well as being aware of the constraints which any existing design decisions may place on remaining options. A class structure for a product range model has also been defined in a similar way to product and manufacturing data models.

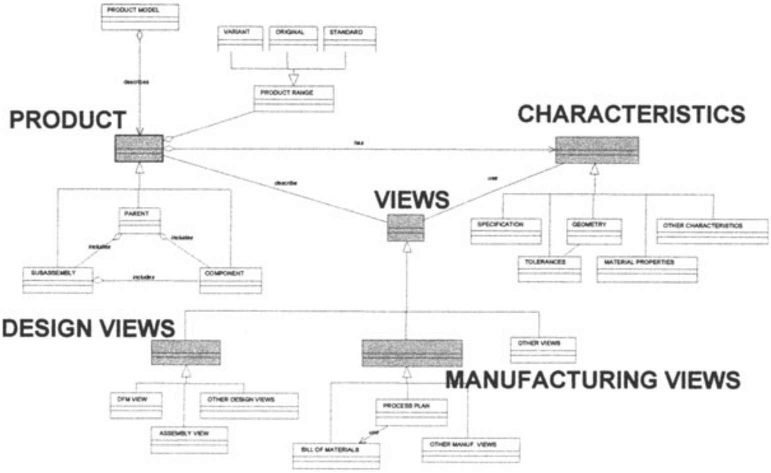
PRODUCT MODEL
VARIANT
ORIGINAL
STANDARD
describes
PRODUCT RANGE
PRODUCT
CHARACTERISTICS
has
describe
use
VIEWS
PARENT
includes
includes
SPECIFICATION
GEOMETRY
OTHER CHARACTERISTICS
TOLERANCES
MATERIAL PROPERTIES
SUBASSEMBLY
includes
COMPONENT
DESIGN VIEWS
OTHER VIEWS
MANUFACTURING VIEWS
DFM VIEW
OTHER DESIGN VIEWS
PROCESS PLAN
ASSEMBLY VIEW
use
BILL OF MATERIALS
OTHER MANUF. VIEWS

Figure 5: A product data structure to support multiple contexts.

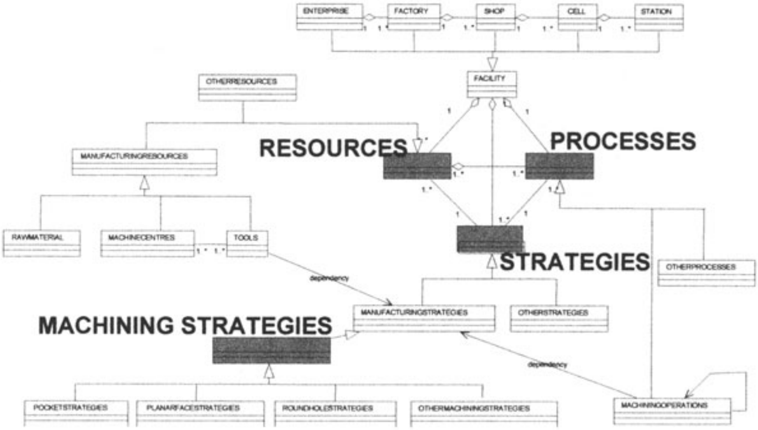
ENTERPRISE
FACTORY
SHOP
CELL
STATION
1
1..*
FACILITY
OTHERRESOURCES
RESOURCES
PROCESSES
MANUFACTURINGRESOURCES
RAWMATERIAL
MACHINECENTRES
TOOLS
STRATEGIES
OTHERPROCESSES
dependency
MANUFACTURINGSTRATEGIES
OTHERSTRATEGIES
MACHINING STRATEGIES
dependency
POCKETSTRATEGIES
PLANARFACESTRATEGIES
ROUNDHOLESTRATEGIES
OTHERMACHININGSTRATEGIES
MACHININGOPERATIONS

Figure 6: A Manufacturing Data Model showing dependencies between resources, processes and strategies.

INTERACTIONS BETWEEN INFORMATION MODELS

Although a manufacturing model is very different from a product model, there is a need for links between these models to be maintained to support interactions between product information and manufacturing capability information. This can be achieved through the use of common contexts. For example machining features in many research papers are considered to be part of a product model which provides input to a process planning application. In this research the alternative manufacturing routes for a particular feature are held in the *strategies* class of a manufacturing model. The product model captures a sufficient understanding of a machining feature, within the *dfm view* class to enable access to the information in the manufacturing model.

In order that chosen resources and processes from a manufacturing model can then be captured in a product model, parts of the same information structures can be used in both models. In this way design for manufacture and process planning applications can interrogate the information models to gain information and input results of decisions into the product model.

In a similar way a product range model can capture historical evidence of the alternative ways in which the functionality of a particular type of product can be achieved. Again this must be captured in such a way that a link between product model contexts and product range model information can be maintained. For example the data structures for particular design solutions in the product range model should match the data structures in the product model which must capture the design results.

INTERACTIONS WITHIN INFORMATION MODELS

The three information models of product model, manufacturing model and product range model all have information interactions which take place within the respective model. These interactions must be supported and maintained if a successful information support system is to be produced.

Given the central role which product models have in an integrated product development system, it is clear that maintaining information interactions within a product model are also central to the successful implementation of a product development system which can support multiple design contexts. If each application requires its own product data structure to maintain the relevant context as was illustrated in figure 4, then there is a need to develop interaction routines that maintain the relationships between the information within these contexts. This is highly significant for future integrated product development systems, as this need to understand and define relationships between views is critical to the future success of such systems.

CONCLUSIONS

This paper illustrates the potential for information model supported design and manufacture to offer a new approach to team based design support. Routes to solving some of the problems of information contexts and information sharing are highlighted. The need for a number of information models which go beyond the general approach of product modelling has been shown as has the need for the relationship between these models to be clearly defined within their information structures.It has been argued that mechanisms for the support of multiple contexts must be clearly specified before information supported integrated product development systems can be of real value to design teams.

Authors affiliation: Loughborough University, Loughborough, Leicestershire, UK

REFERENCES

[1] Maylor, H, Gosling R, "The reality of concurrent new product development" Integrated Manufacturing Systems, vol. 9/2, pp. 69-76, 1998.

[2] Brown D.C, "Which way to KIC" in Knowledge Intensive CAD volume 2, pub. Chapman & Hall, pp. 292-295, 1997.

[3] Fowler J, "STEP for data management, exchange and sharing". (UK, Technology Appraisals), ISBN 1871802369, 1995.

[4] Krause, F. – L., Kimura, F., Kjellberg, T. and Lu, S. C. – Y. "Product Modelling", Annals of CIRP, Vol. 42/2, pp. 5-12, 1993.

[5] Ellis T, Molina A, Young R.I.M. and Bell R. "An information sharing platform for concurrent engineering", in Integrated Manufacturing System Engineering (ed. P. Ladet and F. Vernadat), Chapman & Hall pp. 262-15, 1995.

[6] Costa, C.A, Young, R I M, "Product Range Models: Linking Functional Design to the Reuse of Manufacturing Information". Design Reuse, Engineering Design Conference, Professional Engineering Publishing, pp. 621-630. 1998.

[7] Guarino N., "Formal Ontology and information systems", in N. Guarino (ed) Formal Ontology in Information Systems (Amsterdam, IOS Press), 1998.

[8] Price D., ISO TC184/SC4/WG10 N284, SC4 Product Structures Ad Hoc Group/ WG10 STEP Modularization, 1999-09-21/23

[9] Molina A, Bell R, "A Manufacturing Model Representation of a Flexible Manufacturing Facility", Proceedings of the Institution of Mechanical Engineers, Vol 213, Part B, pp225-246. 1999.

R. BACHA, B. YANNOU

A METHODOLOGY FOR MODELING PROCESS INFORMATION

Towards a process technical data management

Abstract. Often, the development of Computer Aided Process Engineering (CAPE) for Manufacturing Engineering Departments (MED) leads to isolated Databases (DB) because of the past vertical orientation of system design (one database - one application). This usually caused a tremendous amount of data redundancy, heterogeneous manufacturing DB and, as a result, a configuration of manufacturing design that was far from optimal. Our objective here is to overcome those difficulties, by proposing a new Information System scheme, based on the construction of two models with interactions in two directions: the "Business Model" is a representation of business processes according to different views of the company: Function, Activity, Milestone... and at different levels of detail: Conceptual, Logical and Physical. The second one consists in modeling the trade objects (common and specific) with their mutual interactions. Eventually, this project should lead to a standardization of process specification (resource and operation stated references) with special emphasis on the data handled during the engineering stage.

1 INTRODUCTION

The issue of Technical Data Management (TDM) is not new. Number of research projects [1] have tackled several aspects of the implementation of an integrated Information System (IS) for an integrated interprise. Let us mention: information exchange standards (STEP, PDM Enablers), techniques of company data and process modeling, the role of information technologies, and so on. However, we did not hear about any attempt to formalize a process data management procedure for a specific company. Such a methodology should address all the aspects of the engineering and the production stages, and should also address the evolution and maintenance of process data management itself.

The Design Departments (DD) were probably the first to be confronted with issues related to TDM. The Manufacturing Engineering Departments (MED), in turn, are confronted with an informational process patrimonial to manage, with databases distributed by activities without connections and with associated problems such as documentation and management of product/process diversity. Table 1 summarizes such an issue from the DD and MED viewpoints.

P. Chedmail et al. (eds.), Integrated Design and Manufacturing in Mechanical Engineering, 147-155.
©2002 *Kluwer Academic Publishers.*

The Renault French car manufacturer started its questioning during the "digital factory"[1] project to evolve towards proposals of TDM solutions compatible with CAPE tools along the stages of a new vehicle project (see figure 1).

Table 1. Needs in TDM in DD and MED: some comparisons.

	Product Logic	Process Logic
Modeled object	Product and product design process	Product engineering process: associated operations and resources
Potential clients	Essentially, the engineers of DD	The MEDs (engineering and production)
Aimed technology	Product-oriented TDM	Process activity oriented TDM
Digital mock-up	The object studied is the product	The object studied is the industrial system
Standard/Reference frameworks	Product (bill of materials, components dictionary, etc)	Tools and operations bills of materials. Functional graph of the production factory…
Diversity	Product (product diversity)	Process and resources scenarios
Exchanges with softwares	CAD and dimensioning in DD	CAPE[2] : simulation, production plant layout

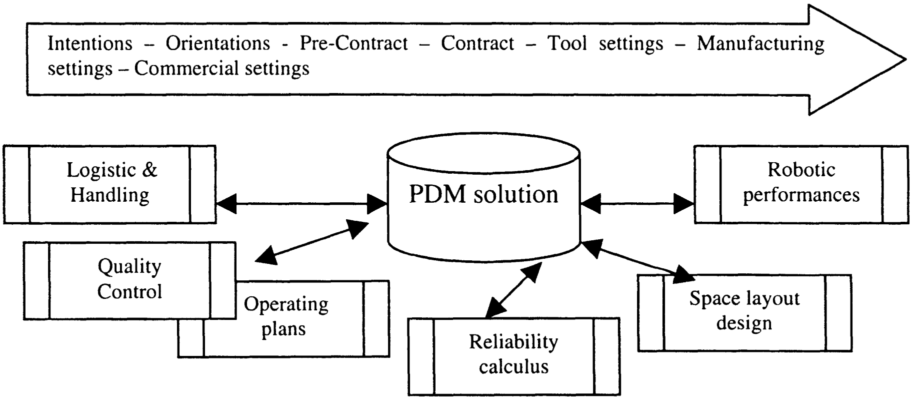
Intentions – Orientations - Pre-Contract – Contract – Tool settings – Manufacturing settings – Commercial settings
Logistic & Handling
PDM solution
Robotic performances
Quality Control
Operating plans
Reliability calculus
Space layout design

Figure 1. Integration of the existing IS: towards a TDM solution.

2 OBJECTIVES OF THE TDM

The functions of the TDM have been described in numbers of references [9]. Let us quickly mention them:

- Configuration management and Product/Process diversity considerations.

---

[1] The purpose was to build models of production flow simulation in the Renault factories and to get a tool allowing the project review and the process numerical data stating.

[2] Computer Aided Process Engineering

- Documentation storage and management.
- Transverse integration with existing IS and CAPE tools and time integration (from the project to the factory).
- Management of procedures and processes requiring the visualization of the activity along the vehicle project stages (from preliminary project to production stage), at different levels of abstraction (from the most generic processes to the elementary ones), and presented with a strategic, functional or organizational viewpoint.
- Standardization of the process specifications in the form of a functional and structural grouping of plant layout, elements of the process classifying (operation types) and resources (machines, tools, operators).

Outer specifications for TDM needs are currently assessed by Renault shop managers in partnership with potential providers of PDM softwares. We had to work on the inner part, i.e. the structure of process data, identifying the data needs in the preliminary project stage of the process activity and the merging of the existing databases. In this chapter, we further state the design methodology for the new integrated IS scheme with the principles and tools suggested.

3 DESIGN METHODOLOGY

Our new IS is built on two models : the "Business" and the "Data" models with interactions in both directions. The systemic approaches [3,7] exhibit a particular interest for the "Business Model" and proceed in a top-down mode along the modeling phase/stage. Conversely, works inspired by CASE tools (Computer-Aided Software Engineering) [2] proceed in a bottom-up mode when first modeling the company objects and then declining the use cases of the object.

Our suggested approach reconciles both visions (bottom-up and top-down). Then, it is possible to detect for each agent, process, project milestone, what the concerned IS are and how they have to be developed or improved to modify the current situation. Conversely, for any existing IS or IS development project, all the possible strategic advantages may be determined without being limited by an operational or local use (see figure 2).

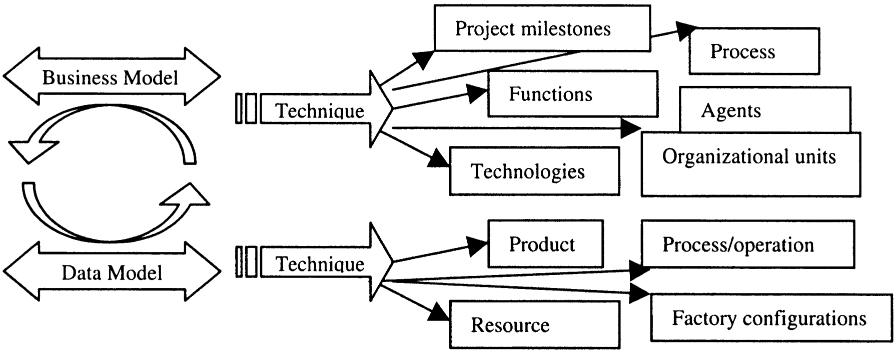

Figure 2. New approach of an IS design methodology.

3.1 Business Model

Stage 1 : Listing of all the activities able to intervene in the long engineering process and the different company entities currently represented by the questions: who? (agents), what? (data), how? (function and process), when? (project milestones), where? (locations) and why? (motivations and objectives, see figure 3).

Stage 2 : refining the model with the aid of standards specification diagrams while identifying the links between the components. With Business Engineering techniques [5], redundancies are studied and the activity logic scheme is redefined for a better optimization.

We submitted our specification diagrams to shop managers who validated them and proposed some new reengineering solutions.

3.2 Data model

Stage 1 : Enumeration of activity objects classified on axes Product – Process – Resources and a fourth axis "project/factory configurations" in which entities featuring specifically a project or a factory are classified. These are elements which cannot be standardized (see figure 4).

Stage 2 : Analysis of the potential objects similarities in order to determine the common and the specific objects for the activities and then global object classes.

Stage 3 : Refining data classes by data modeling techniques [14]. Figure 5 illustrates the main types of interaction between objects.

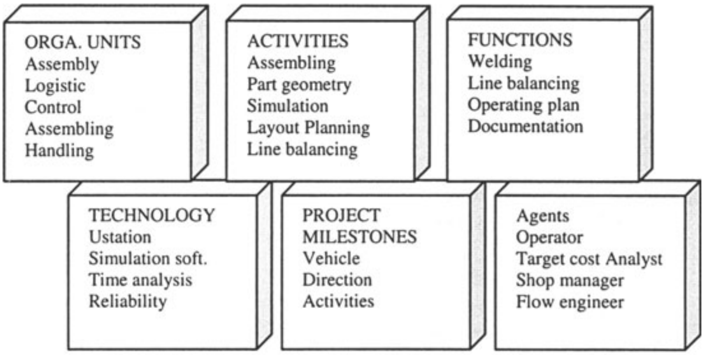
ORGA. UNITS
Assembly
Logistic
Control
Assembling
Handling
ACTIVITIES
Assembling
Part geometry
Simulation
Layout Planning
Line balancing
FUNCTIONS
Welding
Line balancing
Operating plan
Documentation
TECHNOLOGY
Ustation
Simulation soft.
Time analysis
Reliability
PROJECT
MILESTONES
Vehicle
Direction
Activities
Agents
Operator
Target cost Analyst
Shop manager
Flow engineer

Figure 3. *The Business Model components.*

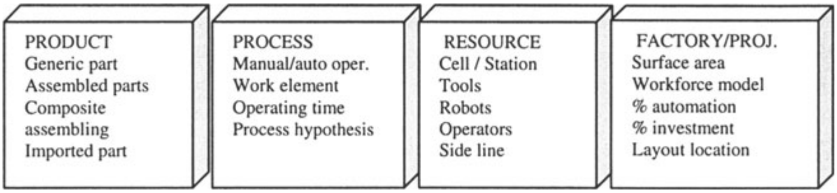
PRODUCT
Generic part
Assembled parts
Composite
assembling
Imported part
PROCESS
Manual/auto oper.
Work element
Operating time
Process hypothesis
RESOURCE
Cell / Station
Tools
Robots
Operators
Side line
FACTORY/PROJ.
Surface area
Workforce model
% automation
% investment
Layout location

Figure 4. Brainstorming on the handled activity objects.

3.3 *Function to data mapping*

Declining use cases between the Business Model and the Data Model is a crucial issue. In order to avoid resorting to functional approaches, some authors [4,6] propose a second level of modeling allowing to reconcile the two models. For each function (participating to one or several processes), the principle is to define the required data for documenting the appropriate function. Figure 6 illustrates a simple example of such a mapping.

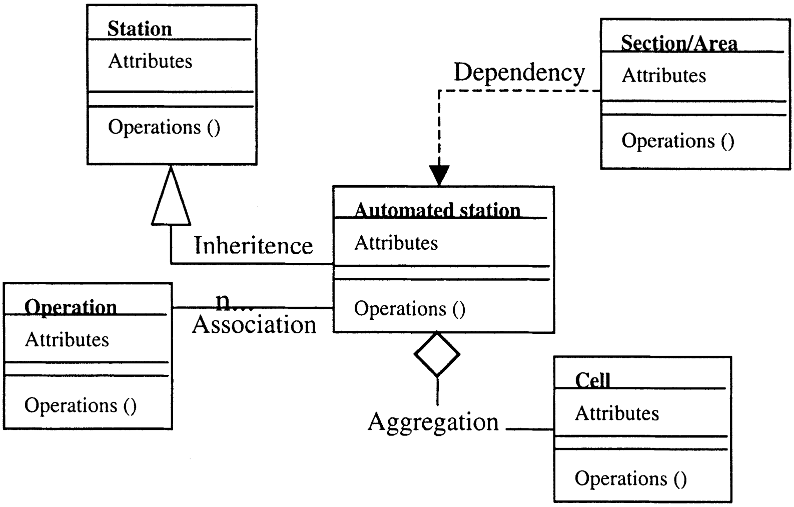
Station
Attributes
Operations ()
Dependency
Section/Area
Attributes
Operations ()
Automated station
Attributes
Operations ()
Inheritence
Operation
Attributes
Operations ()
n...
Association
Aggregation
Cell
Attributes
Operations ()

Figure 5. *Main interactions between data classes.*

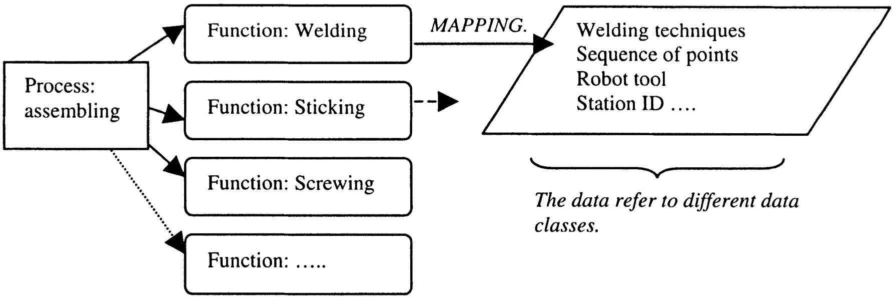
Process: assembling
Function: Welding
Function: Sticking
Function: Screwing
Function: .....
MAPPING.
Welding techniques
Sequence of points
Robot tool
Station ID ....
The data refer to different data classes.

Figure 6. Function to data classes mapping.

4 PRINCIPLES AND TOOLS

4.1 Zachman Metamodel

In the literature, there are numerous company architectures [13]. Among them, we chose the Zachman[3] reference frame for our modeling work. It proposes to cover all the company views at different levels of details thanks to standard modeling methods belonging to the following categories:

- Process modeling: Catalyst[4] method
- Data modeling :Entity-Relation
- Object modeling: UML
- Structured Methods: Gane/Sarson, Ward/Mellor…
- And other useful diagrams : Flow Chart

The detailed rules of this framework are not given here. The reader is invited to refer to the copious literature on the subject [11].

4.2 Bottom-up and top-down approaches

We implemented an exhibition platform representing the automatic building of the assembly shop simulation models. We collected and modeled the minimal amount of data for the purpose of our model.

This work allowed to validate our suggested approach, i.e. combining an ascending approach and a descending approach in the design of an IS. Our approach does not necessarily comply to the classical scheme of new ISs design: from conceptualization to implementation ignoring the existing solutions. Indeed, as can be seen in figure 8, we simultaneously worked on the existing databases that we rebuilt with the aid of reverse engineering techniques and that we enriched with data from needs perceived at a contextual level[5].

---

[3] This conceptual framework is described by a 36-cells matrix covering the company views represented by the questions: "Who, What, Where, When, Why, How". These views are divided into six dimensions representing the abstraction levels of the models. John Zachman, author of these concepts, collaborates, through the Zachman Institute (www.zifa.com), with end-users and software editors for promoting and deploying this architecture.

[4] By CSC (Computer Sciences Corporation, http://www.csc.com/france/solutions/solutions_domaines.htm). Due to its recent existence, there is no book on the subject.

[5] The needs are mainly macro-data handled in a preliminary project stage and initially non formalized.

5 CONCLUSION AND PERSPECTIVES

Some expert studies and specialist thoughts showed the advantages to integrate technical Information Systems of industrial companies. The Renault company, as all car manufacturers today, has decided to question the architecture of its process technical ISs and to start an important project for this purpose. Our contribution concerns the inner features of a PDM addressed to the Manufacturing Engineering Departments, that is the structuring of process data. The methodology and the associated principles and tools are illustrated in this chapter. A software platform is under implementation with a PDM solution, in order to model different kinds of data handled within the numerous activities of the Manufacturing Engineering Department. We showed that the existing databases can be re-used and enriched with the needs perceived after being modified by Reverse Engineering. Besides, the formalization of the logic scheme of the process activity is performed with the collaboration of the different shop managers who considered that such a capitalization was indispensable. We are now currently carrying out the second level of modeling that aims at representing the semantic links between the "Business Model" and the "Data Model". We also intend to introduce a "Technology" view for the identification of the different software components used by the different activities. Finally, we intend to use the "CRUD" matrix[6] in order to locate the place where the information has been created and to define the rights of modification and access to the new database. We should converge to a generic reference framework for process data (operations and resources) in order to build a common dictionary for all vehicle projects.

6 REFERENCES

[1] AIT for European Manufacturing Industry, "Integration Platform Specification 1.0 "Consortium Distribution, Décembre 1998 www.ait.org.uk/projects

[2] J.E. Bailey, R. H. Rucker, "Automated Management of Design Data : Product, Process and Resource structures- International Journal of Industrial Engineering 5 (1), 7-16, 1998

[3] J-A Bartoli, J-L Le Moigne, "Organisation intelligente et Système d'Information Stratégique" Economica, 1996

[4] Melissa A. Cook "Building Enterprise Information Architecture –Reengineering Information Systems" Hewlett-Packard Professional Books, 1996

[5] M. Hammer, J. Champy, "Reengineering the Corporation : A manifest for business revolution" Harper Business, New York 1993

[6] I. Jacobson, E. Ericsson, A. Jacobson, "The Object Advantage : Business Process Reengineering with Object Technology" Addison Wesley Publishing Company, 1995

[7] B. Kalpic, A. Polajnar, "Model of the holistic Information Integration of an enterprise" Strojarstvo 39(6), 275-280, 1997

[8] B. Morand, "Trois arguments et trois propositions pour concevoir des systèmes d'information organisationnels" Ingénierie systémique : de la conception orientée objet à la conception orientée projet GRASCE, URA CNRS 935, 1994

---

[6] Acronym of Create Read Update Delete: Concept currently used by IS designers.

[9] J.M. Randoing, "Les SGDT", Hermès, 1995

[10] C. Roland, "Reformuler les démarches de conception des systèmes d'information", Ingénierie des Systèmes d'Information Vol 2 n°6, p 719-741, 1994

[11] J.F. Sowa, J.A. Zachman, "Extending and formalising the framework for Information Systems Architecture" IBM sytems Journal, vol. 31 n° 3, 1992

[12] Y. Tabourier, "Propositions for changing the methodological perspective of organisational information systems design" Autour et alentour de Merise. Les méthodes de conception en perspectives. CERAM 1993

[13] F. Vernadat, "Techniques de modélisation en entreprise. Application aux processus opérationnels" Economica, 1999

[14] "Modeling Systems with UML", A Popkin Software White Paper , Version 1.1, 1998, www.popkin.com

7 ANNEXES

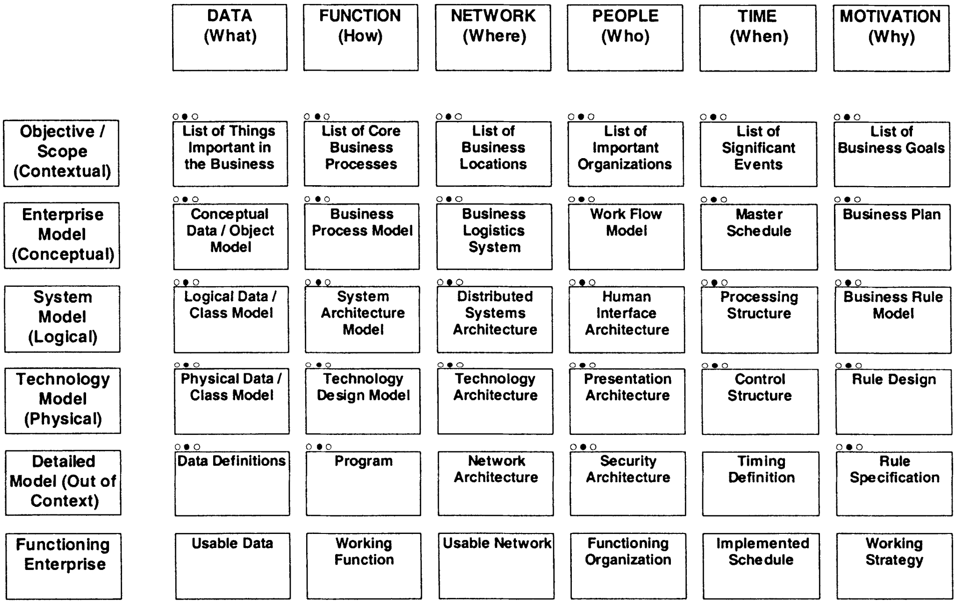

	DATA (What)	FUNCTION (How)	NETWORK (Where)	PEOPLE (Who)	TIME (When)	MOTIVATION (Why)
Objective / Scope (Contextual)	○●○ List of Things Important in the Business	○●○ List of Core Business Processes	○●○ List of Business Locations	○●○ List of Important Organizations	○●○ List of Significant Events	○●○ List of Business Goals
Enterprise Model (Conceptual)	○●○ Conceptual Data / Object Model	○●○ Business Process Model	○●○ Business Logistics System	○●○ Work Flow Model	○●○ Master Schedule	○●○ Business Plan
System Model (Logical)	○●○ Logical Data / Class Model	○●○ System Architecture Model	○●○ Distributed Systems Architecture	○●○ Human Interface Architecture	○●○ Processing Structure	○●○ Business Rule Model
Technology Model (Physical)	○●○ Physical Data / Class Model	○●○ Technology Design Model	○●○ Technology Architecture	○●○ Presentation Architecture	○●○ Control Structure	○●○ Rule Design
Detailed Model (Out of Context)	○●○ Data Definitions	○●○ Program	○●○ Network Architecture	○●○ Security Architecture	○●○ Timing Definition	○●○ Rule Specification
Functioning Enterprise	Usable Data	Working Function	Usable Network	Functioning Organization	Implemented Schedule	Working Strategy

Figure 7. Zachman framework for the company architecture.

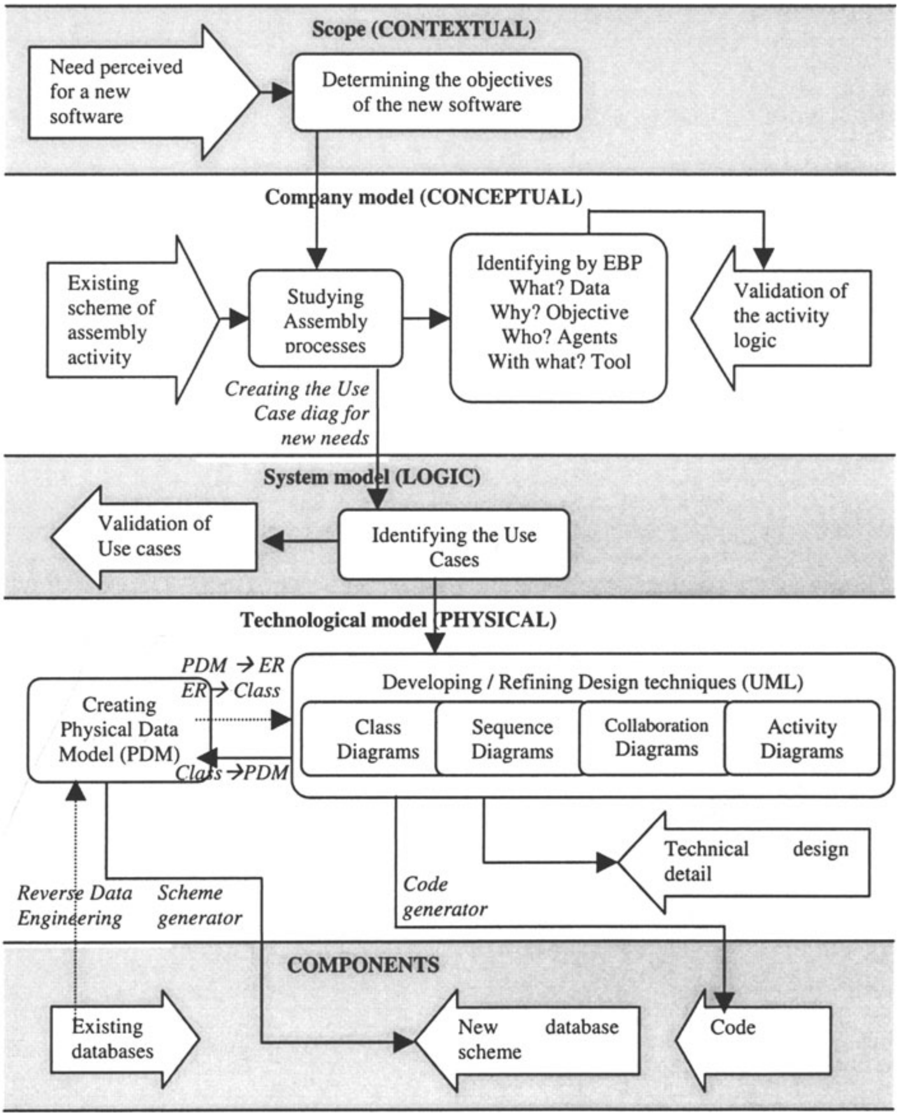
Scope (CONTEXTUAL)
Need perceived for a new software
Determining the objectives of the new software
Company model (CONCEPTUAL)
Existing scheme of assembly activity
Studying Assembly processes
Identifying by EBP
What? Data
Why? Objective
Who? Agents
With what? Tool
Validation of the activity logic
Creating the Use Case diag for new needs
System model (LOGIC)
Validation of Use cases
Identifying the Use Cases
Technological model (PHYSICAL)
PDM → ER
ER → Class
Class → PDM
Creating Physical Data Model (PDM)
Developing / Refining Design techniques (UML)
Class Diagrams
Sequence Diagrams
Collaboration Diagrams
Activity Diagrams
Technical design detail
Reverse Data Engineering
Scheme generator
Code generator
COMPONENTS
Existing databases
New database scheme
Code

Figure 8. *Followed scenario for the design of a new database from the existing databases and assembly simulation needs.*

JEAN-CHRISTOPHE CUILLIERE
VINCENT FRANÇOIS

A SET OF NEW TOOLS FOR THE AUTOMATIC MESHING AND REMESHING OF MECHANICAL PARTS

Abstract : We are proposing here an approach of the automatic three-dimensional mesh generation problem featuring a pre-optimization scheme based on the discretization error and on the "a priori" evaluation of a Brep model in order to identify, directly (without FE calculations) and automatically, geometric features causing stress concentration. Also, the design process usually implies modifications of an initial solution. We are also proposing here an original approach allowing the automatic remeshing of 3D parts in the case of geometric and/or topologic modifications.

1. INTRODUCTION

Today, Finite Element Methods and CAD/CAM are still two distinct fields. There are only a few solutions that present a efficient link between the FE and the whole CAD/CAM process. For a 3D solid part, building the FE model is the most tiresome step. In commercial FE software, this operation is made using tools borrowed from the CAD. Nevertheless, these tools are often simplified compared to those existing in CAD systems. The data transfer between CAD systems and other applications remains another problem that engineers have to overcome frequently. The main objective of the work presented here is to make the use of FE methods easier through a better and more efficient integration between CAD and FEA.

The major problem in the achievement of this integration remains automatic mesh generation even if some major improvements have been obtained in this field in the last ten years. We have developed [4] in order to improve the FE and CAD/CAM integration:

- a nodal spacing pre-optimization process based on the discretisation error and on geometric features recognition techniques.
- two automatic remeshing procedures in the case of geometric and/or topologic modifications of the part's solid model.

2. MESH PRE-OPTIMIZATION

The aim of this process is to translate automatically Brep features [7][9] into a nodal spacing nodal function E_n [1][2]. After this, the automatic mesh generator must be able to produce a mesh respecting this function as closely as possible. In our work, we use this concept in order to control the discretization error and to generate mesh

P. Chedmail et al. (eds.), Integrated Design and Manufacturing in Mechanical Engineering, 157-164.
©2002 *Kluwer Academic Publishers.*

density increases around geometric features causing stress concentrations.

2.1 Mesh pre-optimization based on the discretization error

The whole process starts with the input of two parameters ε and Eng. ε represents the maximal distance between the true and discretized geometries. Eng represents the maximal distance between two connected nodes. In fact, Eng could be defined as a constant nodal spacing constraint in non-refined zones. Our mesh generation process follows three main steps (edge mesh, face mesh, solid mesh) and, by the way, three types of nodal spacing functions are defined.

A new method has been developed for the edge discretization. It is a direct method, which consists in distributing the discretization error on all the elements [1][4].

The triangulation method used is an advancing front process. It is based on a classic scheme with an adaptation in order to take into account the riemannian metric [2] [3] [10]. The automatic volume mesh generation (tetrahedra) is also achieved using an advancing front process [6][8]. Applying this process, we are able to mesh a 3D solid model automatically and using a proper element distribution.

2.2 Mesh pre-optimization based on feature recognition techniques

The automatic identification of form features [14] [15] which will eventually be the source of high gradients is feasible and we are going to demonstrate in what way it is possible to use this information in order to refine the discretization around those features by applying the next process [12] [17]:

- morphological analysis of the object
- identification of zones with potential high solution gradients.
- analytical determination of a nodal space value function that is suitable to these zones.

These geometric features have been defined as analysis features [12] [17]. An analysis feature is a feature as defined by Shah [11] with an engineering significance related to the physical analysis context. Therefore, the process consists in integrating to the product model, a density functional based on the part's analysis features in terms of mechanical strength for example. This integration is in fact done quite naturally as the high density zones are extrapolated from the geometric model itself instead of being extrapolated from discrete spatial positions like in classical approaches. Moreover, we can emphasize that during the design process the identification of high stress gradients zones via feature recognition has to be done only once. Indeed, the high density zones are integrated to the geometric model through the B-Rep topological entities so that in the case of a geometric model refinement, if the object's topology is unchanged, these zones can be extrapolated without further geometric analysis.

In the case of 3D linear elastic stress analysis, we have identified, as a first approximation, three types of form features with a potential major influence on the stress field calculated during the analysis step [17]:

- material withdrawals: this group of features includes various shapes such as topological holes, pockets, slots, ...
- concave edges: this case corresponds to an edge formed by the intersection of two surfaces with a material angle that is superior to π.
- concave fillets: these are joining surfaces between two surfaces forming a material angle that is superior to π.

We have also used this approach in order to identify machining features for process planning purposes [13].

3. MODEL MODIFICATION

The modification of the solid model can take different forms. Depending on the operations carried out we distinguish two different types of modifications of an initial solid model:

- geometric modifications: the initial solid is modified without changing its Brep topological structure.
- topologic modifications: the topologic structure and/or geometric parametrers can change.

By considering these different types of modification, two remeshing strategies have been developed :

- the first one only applies when the solid modification is geometric. It is a very fast and efficient process but it is restrained to cases for which the topologic structure of the mesh can be kept constant.
- the second one applies for all types of modifications (topologic and/or geometric). It is a general purpose procedure.

3.1 Remeshing strategy 1

As the topologic structure of the Brep remains the same, we can apply the same mesh topology. Thus, the initial mesh is directly fitted to the new solid by a set of changes in the nodal locations [4]. The nodal fitting algorithm is based on a nodal chaining scheme. This process takes place following three steps (edge remeshing, face remeshing, volume remeshing).

3.2 Remeshing strategy 2

The basic principle used in this second approach is to identify zones where the initial solid model has been modified, to destroy elements inside these zones and to remesh these zones [4]. For 3D solids, it is very difficult to identify these zones explicitly like in the case of 2D planar domains [5]. The solution that we have developed is to isolate blocks of tetrahedra.

The algorithm consists in suppressing tetrahedra in modified zones without identifying explicitly these zones in order to minimize the CPU time.

4. RESULTS

We present, in the following paragraphs, a set of results with statistics associated about CPU times and about the respect of the imposed nodal spacing functions. Examples 1 to 4 illustrate mesh pre-optimisation based on feature recognition techniques, although examples 5 to 8 illustrate mesh pre-optimization based on the discretization error as well as automatic remeshing in the case of model modifications.

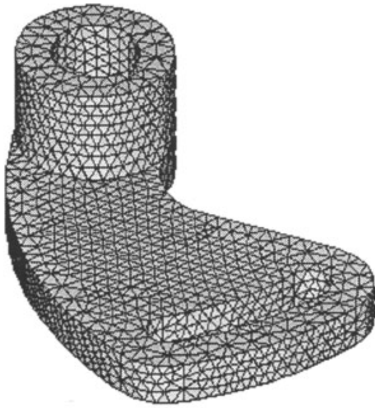

Example 1a :
Command lever (constant density)
Number of triangles : 3758
Number of tetrahedra : 10571

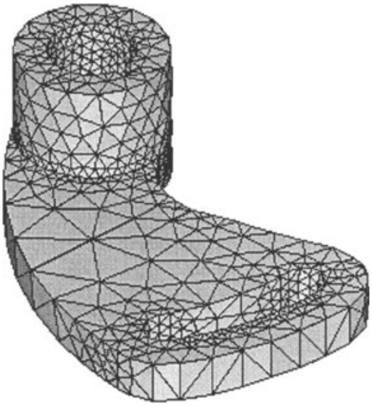

Example 1b:
Command lever (pre-optimized)
Number of triangles : 1944
Number of tetrahedra : 6013

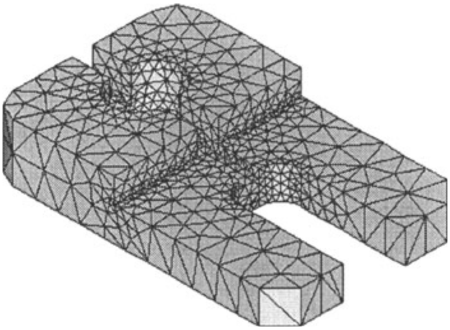

Example 2:
Sample part
Number of triangles : 1982
Number of tetrahedra : 5900

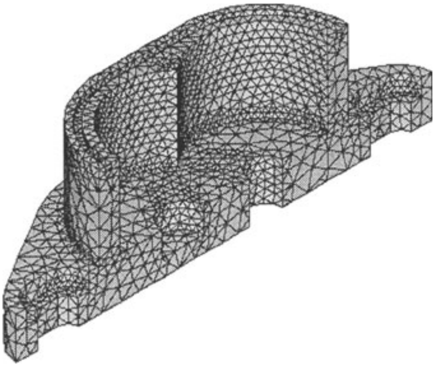

Example 3:
Pump body
Number of triangles : 4010
Number of tetrahedra : 14056

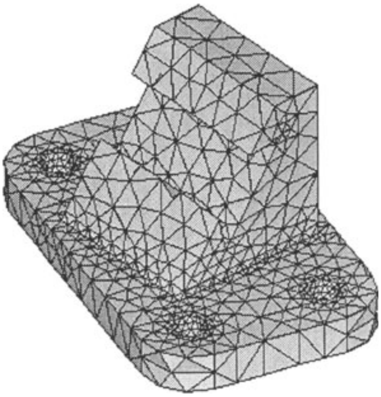

Example 4:
Tool holder
Number of triangles : 3142
Number of tetrahedra : 6899

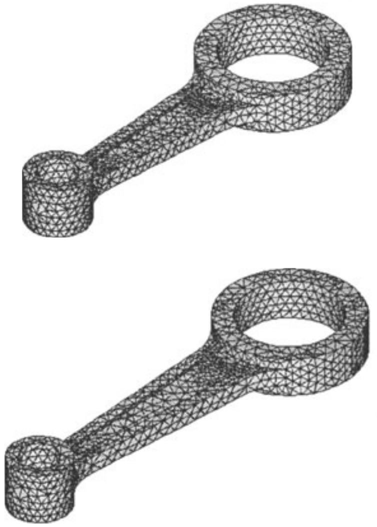

Example 5. *Geometric type modification: extension of the central part of the crank arm.*
Number of triangles : 3370
Number of tetrahedra : 8529
maximum ε value : 0.25
CPU time initial mesh : 486
CPU time modified mesh : 4

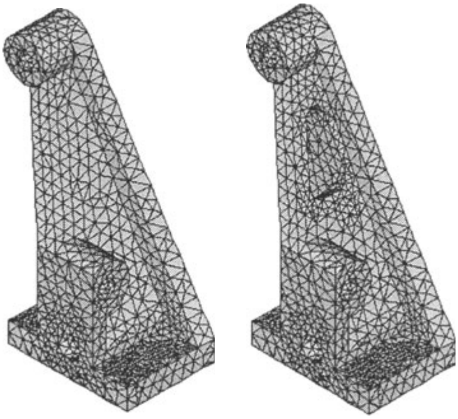

Example 6. *Topologic type modification : addition of a hole in a base ejector. (ε=1 Eng=15)*
Number of triangles : 4874
Number of tetrahedrons : 15453
ε calculated value maximal : 0.9
CPU time initial mesh : 1356
CPU time modified mesh : 137

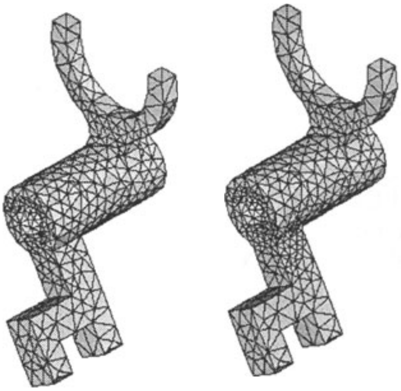

Example 7. *Topologic type modification : a chamfer is replaced by a fillet in a shifter fork (ε=0.5 Eng=10)*
Number of triangles : 1734
Number of tetrahedrons : 5598
ε calculated value maximal : 0.5
CPU time initial mesh : 538
CPU time modified mesh : 132

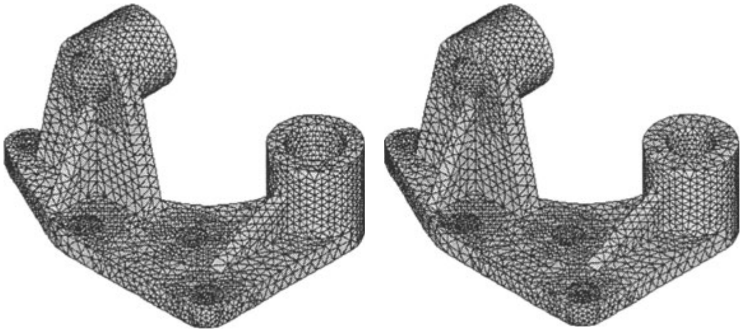

Example 8. *Geometric type modification : modification of the holes radius values in a lever bracket (ε=0.25 Eng=10)*
Number of triangles : 9686
Number of tetrahedrons : 27376
maximum ε value: 0.25
CPU time initial mesh : 1709
CPU time modified mesh : 12

5. CONCLUSION

We have presented here a work aiming to integrate in a better way FE methods in the whole CAD/CAM process. It is first achieved calculating nodal spacing functions based on the discretization error and on geometric features identification.
This is one of the strategies that can be used in order to produce more intelligent element distributions. The integration between FE and CAD/CAM has also been improved by the introduction of automatic remeshing functions. With these completely original techniques, an initial mesh can be partially or totally fitted to a new geometry. The overall CPU time gains can be very substantial when using the pre-optimization and the automatic remeshing.
Of course, in some cases the complete remeshing of the part still has to be used in order to obtain efficient enough meshes. These tools have to be seen as an additional set of automatic tools aiming at the improvement of CAD systems in the field of mechanical design.

6. ACKNOWLEDGMENTS :

This work was carried out in a project supported by research funding from the *Université du Québec à Trois-Rivières* and the *Natural Sciences and Engineering Research Council of Canada.*

7. REFERENCES

[1] J.C Cuillière « A direct method for the automatic discretization of 3D parametric curves. » Computer-Aided Design, Vol 29, pp 639-647, 1997.

[2] J.C Cuillière « An adaptive method for the automatic triangulation of 3D parametric surfaces. » Computer-Aided Design, Vol 30, pp 139-149, 1998.

[3] M.P. Do Carmo « Differential geometry of curves and surfaces. » Prentice-Hall, Englewood Cliffs, New Jersey ,1976.

[4] V. François « Méthodes de maillage et de remaillage automatiques appliquées à la modification de modèle dans le contexte de l'ingénierie simultanée.» Thèse Université Henri Poincaré, Nancy 1. 1998.

[5] V. François, J.C Cuillière, M. Gueury., «Automatic meshing and remeshing in the simultaneous engineering context. », Research in Engineering Design Vol 11 (1999), pp 55-66 .

[6] R. Lohner, P. Parikh « Generation of three-dimentional unstructured grids by the advancing-front method. » Int J. Num. Meth. Fluids ,Vol 8, pp 1135-1149, 1988.

[7] M.E. Mortenson « Geometric modeling. » John Wiley & Sons, New York, 1985.

[8] A. Rassineux « 3D mesh adaptation. Optimisation of tetrahedral meshes by advancing front technique. » Comput. Methods Appl. Mech. Engrg. 141 pp 335-354, 1997.

[9] A. A. G. Requicha, H. B. Voelker « Solid modeling : current status and research directions. » IEEE Comput. Graph. Appl. Vol 3 No 7 pp 25-37, 1983.

[10] J. R. Tristano, J. O. Steven, A. C. Scott « Advancing front surface mesh generation in parametric space using a riemannian surface definition. » Proceedings 7th International Meshing Roundtable, Dearborn, MI, Octobre 1998.

[11] Shah, J J 'Assessment of features technology ', Comput.-Aided Des. Vol 23 No5 (1991) pp 331-343

[12] Cuillière, J C, Maranzana, R and Gueury, M '*A direct approach to automatic three-dimensional finite element mesh refinement*' 7th International Conference on CAD/CAM, Robotics and Factories of the future, 17-19 Aug 92, Metz, France.

[13] Deneux, D, Buczkowski, E, Maranzana, R '*PLANET: Towards a new solution for CAD/CAM integration*', UPCAEDM 92, Tenessee Technological University, Aug 16-19, Cookeville, Tenessee, USA.

[14] Joschi, S and Chang, T C '*Graph-bases Heuristics for recognition of machined features from a 3D solid model*' Comput.-Aided Des. Vol 20 No 2 (1988) pp 58-66

[15] Sakurai, H and Gossard, D C '*Recognizing shape features in solid models*' IEEE computer graphics and applications, 1990

[16] Mantyla, M '*An introduction to solid modeling*' Computer science press, 1988

[17] J.C Cuillière, R. Maranzana 'Automatic and a priori refinement of three-dimensional meshes based on feature recognition techniques' Advances in Engineering Software, Vol 30 (1999), pp 563-573.

8 . AFFILIATIONS

JEAN-CHRISTOPHE CUILLIERE : Laboratoire Interdisciplinaire de Recherche en Imagerie et en Calculs Scientifiques. Département de Génie Mécanique. Université du Québec à Trois Rivières. Trois Rivières. Québec. Canada. G9A 5H7. E-mail : cuillier@uqtr.ca. Tél : (819) 376 5011 poste 3923.

VINCENT FRANÇOIS : Laboratoire Interdisciplinaire de Recherche en Imagerie et en Calculs Scientifiques. Département de Génie Mécanique. Université du Québec à Trois Rivières. Trois Rivières. Québec. Canada. G9A 5H7. E-mail : francois@uqtr.ca. Tél : (819) 376 5011 poste 3957.

L. FINE, L. REMONDINI, J.-C. LÉON

A CONTROL CRITERION DEDICATED TO DETAIL REMOVAL FOR F.E.A GEOMETRY ADAPTATION

Abstract. This paper presents the integration of simplification and idealisation of the geometry definitions of FE (Finite Element) models during the various steps of a FEA (Finite Element Analysis). This integration is performed using a polyhedral representation of a part which allows the engineer to perform all transformations required to adapt the geometric support of the model. These transformations are carried out through a vertex removal process which is monitored using geometrical and mechanical criteria. These criteria based on the analysis of the FE model provide interactive (through an *a priori* user definition) or automatic (through an *a posteriori* error estimator) management of geometry transformations. This approach is illustrated through two examples: the first one is based on an interactive a priori adaptation, and the second one is based on an automatic *a posteriori* adaptation.

1. INTRODUCTION

Today, the Finite Element Method (FEM) is among the most efficient numerical tools for many problems of structural mechanics, mechanical design, fluid mechanics, ... Even if this method provides valuable and dependable information regarding the analysis, successful use of this technique still requires significant expertise, time and expense. Because of the complexity of mathematical models associated with practical problems in the mechanical design process, analysis steps in the design cycle are often restricted to validation phases. One of the most time-consuming and expertise-intensive task faced by analysts is the discretization of a general geometric definition into a valid geometric support to process a FEA. Indeed, the original geometry definition is sometimes too detailed and complicated for analysis purposes. Thus, the analyst may choose to modify the input geometric model in order to generate a model easier to mesh and less expensive to compute.

Recent developments of software and hardware allow to provide tools able to increase the automation of this task. But, as M. Halpern [1] shows it, the state-of-art in CAO-FEA integration is not yet able to satisfy the requirements of the early design practice. Therefore, significant advances are still required. The approach developed here focuses on the integration of simplification and idealisation of the geometry definitions of a FE model during the various steps of a FEA process. It is based on the use of polyhedral representations acting as intermediate models able to provide significant freedom for shape modification controlled by a mechanical criterion.

2. DETAIL REMOVAL INTO F.E.A PROCESS

In the field of finite element models generation, the need of geometry simplification and idealisation is a topic increasingly presented in the state-of-art. Indeed, even if

P. Chedmail et al. (eds.), Integrated Design and Manufacturing in Mechanical Engineering, 165-172.
©2002 *Kluwer Academic Publishers.*

large progress have been obtained in the mesh generation field (a priori mesh optimisation, a posteriori mesh adaptation, ...), features of the geometry (as high curvature area, holes, ...) still largely constrain a mesh definition. Thus, geometry adaptation has become a step required to improve mesh generation. Few solutions have already been proposed. Sheffer [2] uses virtual topology to develop a scheme for detail removal and geometry clean up. Drake[3] uses a technique based on heuristic knowledge to detect and to remove features from C.S.G models. Dey [4] has developed local mesh modification operators to perform the automated features identification and elimination. These operators are mainly based on the detection of small edges. Mobley[5] presented two general categories of defeaturing: geometry-based defeaturing and finite element model-based defeaturing. He used an object oriented approach for C.A.D. geometry defeaturing. Armstrong [6] uses the analysis of the object skeleton produced by the M.A.T. (Medial Axis Transform) for determining what simplification and what idealisation to process on the geometry. Lee[7] uses Fourier Transform to build a metric system to characterise features size. This metric system allows to determine, according to the sizes computed, a classification of features. Under these conditions, a user can choose a size value as the maximum size of "details" and remove all features which have a smaller size.

All these approaches propose automated or interactive tools for geometry transformation (either on CAD models or FEA models) but details identification is still based on the analysis of the geometry of the part whereas in FE models the meaning of “details” is not only defined from geometry attributes but also from the mechanical behaviour of the part. Indeed, geometric details of a part (small holes, thin ribs,...) may be the location of critical stress concentration under specific load cases and may have negligible effect in other configurations.

To this aim, our approach is based on the use of a mechanical criterion (defined in section 3) able to monitor automatically the geometry adaptation. This criterion ensures that all geometric simplifications or idealisations applied to the part do not significantly change the result of the desired analysis.

3. AN APPROACH TO MANAGE GEOMETRY ADAPTATION

Why using a polyhedral geometry ? The approach proposed here is based on the use of polyhedrons as geometric definition for the meshing step of a FE model generation (see step 1 in the following sub-section). Polyhedral geometry has been chosen because of its significant freedom for shape modification. Indeed, compared with B-rep or CSG models which use high order mathematical definitions of the geometry (splines, cylinders...), polyhedrons are only defined as a set of vertices, edges and faces. Hence, such a geometric definition allows an object to be modified without any shape constraints whereas it is difficult to work out functions to transform a cylinder into a complex free-form surface for example.

To keep a link between the C.A.D model and FE one, a polyhedral model is used as an intermediate model. On one side, a link between C.A.D. and polyhedral models can be ensured by mean of a concept of classification of the entities (vertices, edge, faces) forming a polyhedron [8]. On the other side, a polyhedral model is a geometric representation able to cope with all data required for the definition of FEA models: it is able to describe all different shapes required for a FEA model (open or closed surfaces, non-manifold geometries) and to incorporate data used to define the boundary conditions.

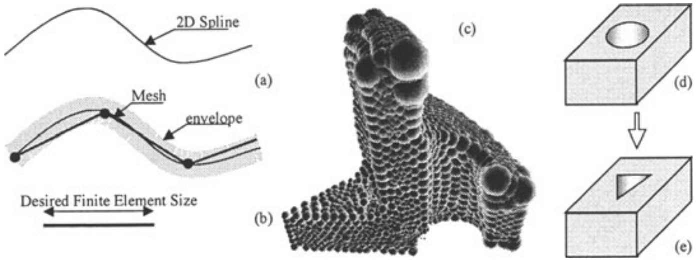

Figure 1 .a, b) An example of envelope around a 2D geometry (a) the initial 2D Spline, (b) mesh elements lying into the envelope. c) An example of envelope around a 3D geometry. d, e) (d) initial hole lying on the input polyhedron , (e) basic polyhedral model obtained after simplification.

How to manage geometry adaptation ? To ensure that geometry adaptation does not significantly modify the mechanical behaviour of the part studied, all geometric modifications are managed by a mechanical criterion defined according to the desired analysis (see step 2).

Tools for geometry adaptation are defined from the approach developed by Véron [9]. Geometric operators developed by Véron use an iterative vertex removal process and local remeshing operators to produce a simplified geometry. Compared to other approaches [10, 11], Véron's approach has the advantage to ensure, using an "error zone" concept, the control of the distance between initial and simplified polyhedrons. The use of this "error zone" concept allows the user to define, around the geometry, a discrete geometric envelope able to bound shape transformations (see step 3).

On the basis of these operators, new operators have been developed in order to process all transformations required for the adaptation of the geometry of a FEA model (see steps 4 and 5).

The following sections list the successive steps required to carry out a geometry adaptation during a Finite Element Analysis process:

1- *Generation of the polyhedral geometry.* The basic description of a polyhedron (vertices, edges, faces) allows software to generate it easily from the most common geometric descriptions. Thus, it can be generated from all C.A.D. models and even directly from an existing FEA model. Once this polyhedral geometry has been obtained, specific data (Boundary conditions, data from C.A.D,...) can be transferred onto it,

2- *Identification of the mechanical behaviour of the part.* To ensure that the new model defined after a geometry adaptation process has the same mechanical behaviour than the initial part, it is necessary to monitor the geometry adaptation through a mechanical criterion. This criterion must allows the user to characterise each area of the part that can be identified as a "detail" for the F.E.A., i.e. areas which can be removed without producing significant modifications of the stress field. Hence, criteria used must be defined for a given part in the context of a desired structural analysis (load case, objective of the analysis,…).

The concept chosen for this criterion, is a “map of finite element sizes”. This map represents, for a given analysis, the specification (sizes of elements) used to build from the initial geometry a mesh which allows to reach the desired accuracy for the analysis and which model correctly the strain energy distribution in the part.

Two directions have been considered to build this map :

- an interactive a priori approach : during the pre-processing step of a FEA During this step no new task for the analyst has been added. All data required to build this map are extracted from the initial step of the FEA analysis in which the analyst defines an appropriate initial mesh, i.e able to ensure a given accuracy of the analysis of the part,
- an automated a posteriori approach : during loops of FEA computation. In this case, the map of element sizes is obtained automatically from a previous analysis computation by an a posteriori error estimator [12, 13]. Such estimators have been designed to provide, from an initial computation, data (map of element sizes) used to redefined at each computational loop of the analysis, a new mesh able to give more accurate results.

In each approach (a priori and a posteriori), each size of element of this map is directly linked with the stress field and thus with the mechanical behaviour of the part. Thus this map of element sizes allows the adaptation to define, for a given analysis, a minimum level of discretisation for the part. Therefore, if meshes generated from an adapted geometry are able to respect this level of discretisation, then the result of FEA is kept unchanged compared with the initial model (according to the desired accuracy). This level of discretisation is then well suited to monitor geometry transformations.

3- *Definition of a geometric envelope restricting geometric transformations*. The problem of geometry adaptation is to be sure that adapted geometry stays compatible with the level of discretisation defined by the map of element sizes, i.e. to be sure that adaptation operators do not generate inadequate transformations. This monitoring of geometry transformations is achieved using an extension of the "error zone" concept developed by Véron.

The geometric envelope, defined from this concept, is computed from data of the map of element sizes according to geometric characteristics of the part (local discrete curvature,…). Taking into account these characteristics of the initial part ensures that the coarsest geometry lying within this envelope is still an adequate representation to perform the desired analysis.

Figure 1a, b shows a 2D example of an envelope definition. This envelope was generated according both to the target size of finite elements and to the curvature of the spline. Figure 1c shows an example of a 3D envelope. On this figure, the envelope has a discrete representation. The value of the distance between the part and the envelope in each area of the part has been assigned to each vertex of the input polyhedron and is displayed as a sphere.

4- *"Details" identification*. In our approach "details" are areas which would need high mesh density because of their geometric shape. So details identification lead to determine edges, vertices and faces of the polyhedron which characterise these areas. As far geometric adaptation is performed through a vertex removal process, the order in which vertices are removed has a great influence on the transformations carried out. Under these conditions, a strategy of vertices selection has been developed. This strategy requires the identification of three kinds of details:

- the "geometric" details. These details are geometric features defined on the surface of the part (thin ribs,...). They are identified using an analysis of the discrete curvatures of the input geometry. This analysis leads to the identification of vertices laid on "geometric" details.
- the "topological" details. The "topological" details are the holes of the part. They are identified using an analysis of the topology of the polyhedron. In this case, the analysis leads to identify sets of vertices, edges and faces defining holes. This analysis uses a first polyhedron simplification (vertex decimation, see step 5) to reduce holes to their basic shape, i.e. a prism with triangular bases (see Figure 1d, e). This identification is easily performed for convex holes. For non-convex holes (for example : holes with T or L shapes), the use of the vertex decimation process requires to define a characteristic size (global size or thickness of each branch of the hole) for a "detail hole" identification.
- the "dimensional" details: These details are subsets of the object geometry that may be "idealised", i.e. specific areas of the initial 3D geometry that may be represented by 2D or 1D geometry (such as surfaces or lines). The identification of such details requires a geometric analysis of the object to identify each of these subsets. At present, implementation of criteria performing this analysis are under focus.

5- *Adaptation operators*. For each category of details, a specific operator has been defined:

- Simplification operator: This operator only deals with vertex removal and local remeshing processes,
- Topological operator: This operator is able to perform hole removal through a vertex, edge and face removal processes, and changes the genus of the object.
- Idealisation operator: Compared with the two other operators, this one must deal with the generation of medial axes or surfaces of polyhedron subsets. Therefore, this operator must be able to remove, move and create entities (vertices, edges and faces). The characteristics of such an operator have been identified and its implementation is going to be inserted into our adaptation process.

Using these operators, each "detail" of the initial geometry can be removed but geometry adaptation must only be performed on "details" that can be removed without significantly modifying the FEA results. Hence, the geometric envelope defined from the map of element sizes is used to monitor adaptation operators. Indeed, geometric transformations are only applied if they lie into this envelope. This way, simplification and topological operators can be applied through an automatic process.

In the context of idealisation operators, maps of element sizes do not provide data able to monitor such transformations. To apply this transformation on a subset of the polyhedron, it is necessary to estimate its specific behaviour (shell behaviour, beam behaviour,...). For this reason, an interactive idealisation process, using the analyst expertise, is planned. Specific data from a FEA model (boundary conditions,...) can also require specific monitoring of the adaptation operators. As an example, an area of the input polyhedron subjected to pressure must still exist on the adapted geometry. So during the adaptation process such data are transferred from the initial geometry to the adapted one.

6- *Mesh generation.* After the adaptation process has taken place, the adapted polyhedron is used as a geometric representation for a mesh generation step. During this step, the map of element sizes (used during the adaptation process) is used to monitor the mesh generation in order to obtain an adapted mesh.

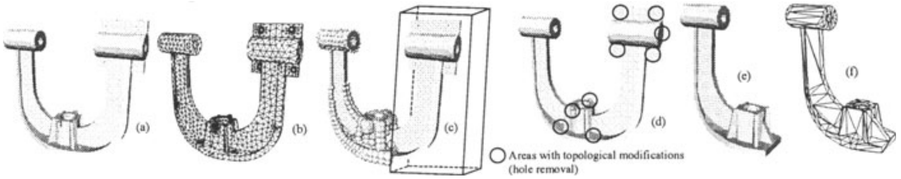

Figure 2 . a) the example part, b) the initial polyhedron (initial mesh), c) map of element sizes applied to the example part, d) result of the hole removal phasis, e, f) the adapted part (e) shaded representation , (f) wireframe representation.

3. RESULTS

An example of interactive adaptation. In the following example (Figure 2a, b), the map of element sizes has been defined a priori by the user based on his (her) expertise. This map is shown Figure 2c. In this Figure, the discrete envelope has been drawn only on the left area of the part. The right area (identified by the box) is not considered as useful by the user, so the envelope around it has been set as infinite. Figure 2d shows the intermediate step where holes, considered as details (according to the envelope) have been removed. Figures 2e, f present the adapted geometry generated from the user specification. This geometry is defined using a polyhedral representation that becomes the new geometric model used during the step of mesh generation.

This example shows how, using an interactive process, a user can easily (defining only the discrete envelope, i.e. the map of element sizes) manage large geometric transformations (like holes or sub-parts removals).

An example of automatic (a posteriori) adaptation. The example of geometry adaptation developed here is based on the structural analysis of the part presented on Figure 3a, b, c. The map of element sizes is presented in Figure 1c.This map is the result of an *a posteriori* error analysis led by the LMT [13] (Laboratoire de Mécanique et de Technologie, Cachan, France). According to the element sizes map and to the boundary conditions defined for this analysis, a geometry adaptation has been carried out. The result of this adaptation is shown in Figure 3e. The adaptation process has significantly modified the top of the part (holes and geometric details) and all the blending areas of the part has become coarser than the initial one. On this new geometry, the boundary conditions have been transferred by the adaptation operators during the adaptation process (Figure 3d).

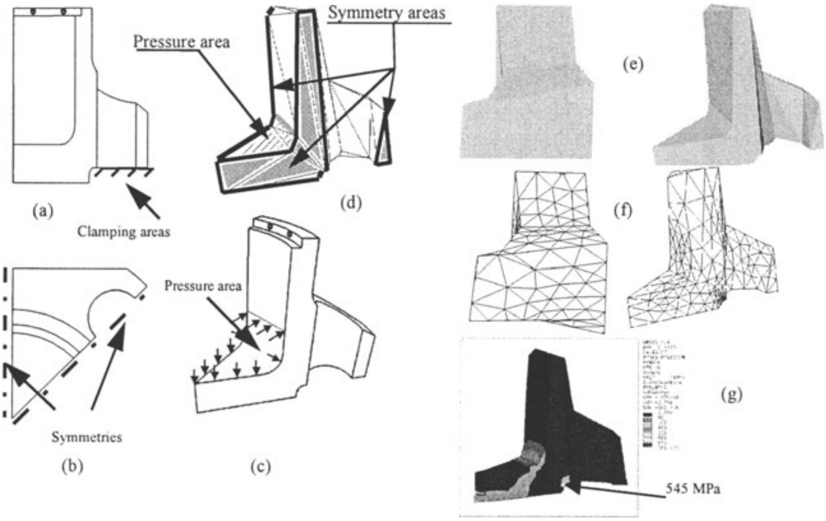

Figure 3. a, b, c) case of study, d) adapted geometry with the B.C., e) the adapted geometry, f) adapted mesh on the adapted geometry, g) map of von Mises equivalent stresses onto the adapted geometry.

To improve the efficiency of the adaptation, a FE analysis has been conducted for both the initial and the adapted geometry. For each geometry, a mesh was generated according to the map of element sizes defined above. Figure 3f depicts the mesh generated from the adapted geometry. Compared with the mesh generated with the initial geometry, the mesh generated from the adapted one has a better adequation to the element sizes map. Indeed, for the initial geometry, a high density of elements is required to mesh the areas where the two holes are located. With the adapted geometry these holes have been removed and the geometry has become coarser, then the mesh generation is easier to perform because the finite elements generated have a size smaller or at most equivalent to the size of the faces issued from the geometry adaptation process.

Figure 3g illustrates the FEA results computed from the adapted geometry. The map of Von Mises stresses of the FEA computations shows that stress values in highly stressed areas stay close for both models (564 MPa and 545 MPa). Hence, the adapted model is able to provide an acceptable representation of the mechanical behaviour of the part. The differences between the two models comes from the fact that the boundary conditions slightly differ since the adaptation process performed keeps track of the areas of the boundary conditions but does not perform the required approximations over the mechanical data attached to these faces.

4. CONCLUSIONS

In this paper we have described the various steps and tools used to implement a geometry adaptation into a FEA process. This adaptation process managed using as input data a map of element sizes offers significant advantages: on one hand it can be used as an automatic process using maps from an *a posteriori* error estimators and on an other hand it lets analysts perform their own transformations on the model. Such a map used as a mechanical criterion ensures that the new model generated by the adaptation process stays compatible with the analysis foreseen. Such a process reduce the complexity of the FE models and avoids to wasting resources (time and hardware) required to perform the analysis. So, they add flexibility to FEA tools and they improve their integration into the design process.

The next step of this work will be to implement, again from polyhedral representation, tools and criteria for dimensional reduction. Such tools have already been tested on simple shapes (plates, pipes,...).

Polyhedral representation, more than only been well suited for geometric transformations is also adapted to support hierarchical representation. This ability offers the possibility from an initial model to represent various analyses, each with an adapted model keeping links with the initial one. Such potentiality could be useful for example to handle multi-physics analysis (thermal, mechanical, …).

5. REFERENCES

1. M. Halpern, Industrial requirements and practices in finite element meshing: a survey of trends, Proc. of 6th International Meshing Roundtable, Sandia Nationnal Laboratories, 1997: 399-411.
2. A. Sheffer, T. D. Blacker, M. Clustering, Automated detail suppression using virtual topology, Trends in Unstructured Mesh Generation, ASME, AMD-Vol. 220, 1997: .57-64.
3. P. Dabke, V. Prabhakar and S. Sheppard, Using features to support Finite Element idealisation, International ASME conference, Minneapolis, volume 1, 1994: 183-193.
4. S. Dey, M. S. Shephard, M. K. Georges, Elimination of the adverse effects of small model features by the local modification of automatically generated meshes, Eng. with Computers, 1997: 134-152.
5. Anton V.Mobley, Michael P.Carroll, Scott A.Canann, An object oriented approach to geometry defeaturing for Finite Element Meshing, Proc. of 7th Int. Meshing Roundtable, Sandia Nationnal Laboratories, 1998.
6. C.G. Armstrong, R.J. Donaghy and S.J. Bridgett, Derivation of appropriate Idealisations in Finite Element Modelling, the Third Int. Conf. on Comp. Structures technology, Budapest, 1996.
7. Lee Yong-Gu and Kunwoo Lee, Geometric detail suppression by the Fourier transform, CAD, Vol. 30 (9), 1998: 677-693.
8. F. Noel, J.C. Léon and P. Trompette, A data structure dedicated to an integrated free-form surface meshing environment, Computers & Structures, Vol. 57 (2), 1995: 345-355.
9. P. Véron, J-C. Léon, Static polyhedron simplification using error measurements, CAD 29, 1997: 287-298.
10. H. Hoppe, Progressive Meshes, Computer Graphics, SIGGRAPH'96 Proceedings, 1996: 99-108.
11. J. Rossignac, P. Borrel, Multi-resolution 3D approximations for rendering of complex scenes, Modeling in Computer Graphics, Springer-verlag, 1993: 455-466.
12. O.C. Zienkiewicz, J.C. Zhu, Adaptivity and mesh generation, Int. J. For Num. Methods in Eng., 32, 1991 : 783-810.
13. P. Coorevits, P. Ladeveze, J.P Pelle, An automatic procedure with a control of accuracy for finite element analysis in 2D elasticity, Comp. meth. in appl. mech and engng., 121, 1995: 91-120.

Jean-Claude LEON
Laboratoire Sols, Solides, Structures UMR CNRS 5521
Domaine Universitaire
BP 53X 38041 Grenoble Cedex 9
France
Jean-Claude.Leon@hmg.inpg.fr

A. RASSINEUX*, P. VILLON*, P. BREITKOPF *
J-M. SAVIGNAT**, O. STAB**, C. CHAPPUIS*

(*)Laboratoire Roberval, UMR UTC-CNRS 6066
Université de Technologie de Compiègne ,
BP 20529 - 60205 Compiègne Cedex, France
(**) CGES, Ecole des Mines de Paris
33, rue Saint-Honoré, 77305 Fontainebleau, France
alain.rassineux@utc.fr

FEATURE RECOGNITION AND REMESHING BY LOCAL HERMITE DIFFUSE INTERPOLATION

Abstact. We propose a method to adapt a three-dimensional surface mesh. The data needed to optimize the mesh have been reduced to an initial mesh. The building of the geometrical model is based on a local Hermite interpolation calculated from the nodes of the initial mesh and from the normal vectors to the surface calculated from the mesh. The determination of an interpolating local surface equation, however continuous over the domain, enables us to locate nodes on the surface with respect to the curvature during a refinement process. It also allows us to control the coarsening of the mesh. The local surface equation is used to compute the principal curvatures on the surface for two main purposes, error estimation and feature recognition. .The remeshing procedures are used to refine or coarsen the mesh but also in a final step to enhance the shape quality of the elements.

1. INTRODUCTION

The generation of a three-dimensional surface mesh of an object with an imposed density while meeting "acceptable" shape quality requirements is a difficult and time-consuming task. Without pretending to be exhaustive, surface mesh adaptation techniques can be classified into two different categories according to the use or the non-use of the parametric space. The first group of techniques makes use of the parametric surfaces provided by a modeler. The most frequently used method to generate a surface mesh consists of using a mapping technique between the two-dimensional parameter space of each patch and another parameter space suitable for meshing [1]. Techniques of the second type are based on the polyhedral representation of the object by the mesh itself and therefore do not use the parameter space. These techniques can also be gathered into two groups. Techniques of the first group work on the mesh itself and no secondary geometrical model is built to achieve the adaptation. The basic idea of these techniques is to use a high density mesh on which simplification tools are performed. Among the techniques which do not use parametric space, the main idea of the second group consists of using the mesh to create a geometrical underlying model. Such approaches allow not only

P. Chedmail et al. (eds.), Integrated Design and Manufacturing in Mechanical Engineering, 173-180.
©2002 *Kluwer Academic Publishers.*

mesh coarsening but also mesh refinement. The model we build is not a global model nor a model based on surface patches and no use is made of the mapping provided by a CAD modeler. Moreover, the work presented here shows that the use of the meshfree methods is not only limited to problems that cannot be solved easily by a finite element method.

2. DIFFUSE INTERPOLATION

The diffuse approximation method has been first introduced by Nayroles *et al.* [2] and recently discussed by Breitkopf *et al.*[3]. The diffuse approximation is equivalent to the standard Moving Least Squares (MLS) introduced by Lancaster [4] based on polynomial approximation but is more general in the sense that additional constraints may be easily introduced. The MLS method is local: at any arbitrary evaluation point x, only the closest nodes x_i are taken into account. The influence of a node x_i is governed by decreasing weight functions $w_i = w(||x_i - x||)$ which vanishes outside the domain of influence of the node. We present the details of a Moving Least Square Hermite version further in the paper.

Here, we note only that in a general case, the MLS approximation does not interpolate data. This property is achieved by introducing singular weight functions w which take an infinite value at the node. The new weights may be obtained by scaling the original weight functions in the way to give a unit value at a node $w_i(x_i)=1$ and then by applying the following substitution

$$[w(x_i,x)] \rightarrow \left[\frac{w(x_i,x)}{1-w(x_i,x)}\right]$$

In our approach, the diffuse approximation has been transformed in order to take into account derivative entities provided from the surface equation. We experienced that the criterion based on normal colinearity enables a more accurate computation of the curvature than a fitting method based on the single set of nodes (as diffuse interpolation does if normal vectors are not taken into account).

3. COMPUTING THE GEOMETRICAL MODEL

The objective is to determine a local surface equation using the nodes of the initial mesh and the normal vectors to the surface. A local surface is determined for each evaluation point. Therefore, the coefficients of the surface depend on the evaluation point. However, the method guarantees that the coefficients vary in a continuous way with respect to the location of the point. Once we have determined the geometry on which the points must be located, the surface equation can be used to compute the principal curvatures of the surface. In order to provide a significant way to evaluate our work, we have decided to propose a remeshing criteria based on principal curvature computation by which both refinement process and coarsening of the mesh are controlled. During the remeshing process, feature lines of the geometry which cannot be detected with a basic geometrical angle criterion may not be respected. Also, we propose a method based on principal curvature evaluation to decompose the surface mesh into usual surfaces (plane, cylinder, cone, sphere, torus) and therefore to detect intersection lines between theses surfaces. The goal is to provide a final mesh which fits the initial geometry.

3.1 Monge patch

The form of surface suited to the local diffuse interpolation is denoted as Monge patch of equation z=f(x,y) where f is a C^2 function defined on a planar domain as shows in figure 1.

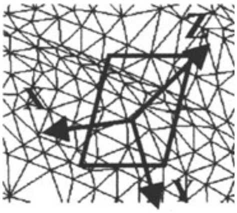

Figure 1. Determination of a Monge patch

In order to construct a surface equation on which we plan to evaluate curvatures, we have decided to evaluate the surface equation through a second order expression

$$z = f(x,y) = < 1, x, y, x^2, xy, y^2 > \alpha = P^T \{\alpha\}$$

where α is a 6 coefficient vector. In order to recover a bilinear surface equation over the patch, there must be at least 6 nodes in the patch.

The different ways to determine the local Monge patch depend on the choice of the interpolation set, on the computation of the weights, on the local coordinate system with which the surface equation is expressed and finally on the locality of the interpolation criterion. These topics are fully discussed in reference [5].

3.2 Computation of the weighting functions

In its usual form, the set of nodes which constitutes the basis of the diffuse interpolation can be determined by the k nearest nodes and the computation of the weights is given by

$$w(xi,x) = w_{ref}\left(\frac{\|xi - x\|}{R(x)}\right)$$

where $R(x)$ is the distance to the $(k+1)$ nearest node. k is the number of terms in the polynomial basis ($k=6$ for a complete second order basis).
w_{ref} has the following properties : $w_{ref}\gamma\, C^{m}(-1,1)$, $w_{ref}(0)=1$ and $0\ P w_{ref}(x)\ P 1$
In our implementation, we have used the function $w_{ref}(x)=(1-x^{2})(1+2x)$
where x denotes the ratio given by the distance to the evaluation node and the distance to node $k+1$ in the list. The method can be implemented easily and the performance is very good. However, we can notice that a selection based on nothing but a distance criterion may lead to a bad representation of the initial model. In order to avoid these problems we decided to control the neighborhood of the node while taking into account the local variation of the normal vector. We discovered that the reliability could be greatly improved.

3.3 Determination of the projection plane

During the adaptation process, edges of the successive meshes are split and the new points must be projected on the surface. Different approaches can be used to define a local coordinate system suitable for projection.

- The system can be built from the nearest triangle to the evaluation point.
- The plane can be determined by least square fit. In this case, the interpolation set can be based on a neighborhood criterion,
- Finally, the diffuse approximation can be applied to determine a plane whose coefficients vary continuously with respect to the evaluation point.

We experienced that numerical problems due to ambiguous configurations were solved when the last method was used.

3.4 Determination of the interpolation set

Nodes are selected with respect to a neighborhood criterion. Once sharp edges and singular nodes have been identified on the initial (using an angle criterion for instance), sub-domains can be identified on the initial mesh (the 6 faces of a cube for instance). This decomposition prevents us from choosing nodes which belong to different areas. As shown figure2, nodes belonging to lateral faces of the cube are rejected while nodes belonging to the upper face are selected.

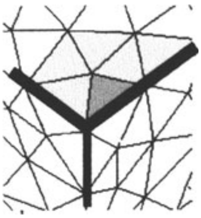

Figure 2. Local domain decomposition

4. HERMITE VERSION OF MOVING LEAST SQUARE INTERPOLATION

The diffuse approximation leads to the minimization of a criterion $J_x(\alpha)$ composed of two terms $J_{1x}(\alpha)$ and $J_{2x}(\alpha)$. All entities described below are expressed in the local coordinate system associated with each patch. We consider a set of n interpolation nodes.

Let $M_i(x_i,y_i,z_i)$ be a node belonging to the set.

The criterion suggesting the interpolating condition can be written as

$$J_{1x}(\alpha) = \sum_{i=1}^{i=n} w(x_i,x) \times \left(p^T(x_i - x)\alpha - z_i\right)^2$$

where w_i are interpolating weight functions associated to each node M_i of the set.

The normal vector to the surface mesh is defined as $\vec{n} = n_i\vec{x} + n_i\vec{y} + \vec{z}$.

The normal vector to the Diffuse Monge patch is given by

$$\vec{n}_{diff} = \frac{\partial M}{\partial x} \times \frac{\partial M}{\partial y} = -\frac{\partial P}{\partial x}\vec{x} - \frac{\partial P}{\partial y}\vec{y} + \vec{z}$$

It can be concluded that the criterion based on the colinearity of normal vectors is

$$J_{2x}(\alpha) = \sum_{i=1}^{i=n} w(x_i,x) \times \left\{ \left(\frac{\partial p^T(x_i - x)}{\partial x}\alpha - n_{ix} \right)^2 + \left(\frac{\partial p^T(x_i - x)}{\partial y}\alpha - n_{iy} \right)^2 \right\}$$

Finally, the final criterion which take into account both condition can be expressed as follows

$$J_x(\alpha) = (1-t) \times J_{1x}(\alpha) + t \times J_{2x}(\alpha) \textit{ where } t \in [0,1]$$

The above criterion can be rewritten as $J_x(\alpha) = (P^T\alpha - r)^T W (P^T\alpha - r)$

where $P^T = [P(x_1 - x), P(x_2 - x), \ldots, P(x_n - x)]$, $r = (r_1, r_2, \ldots, r_n)$

with

$$r_i = (z_i, n_{ix}, n_{iy})^T \text{ and } P(x_i - x) = \begin{bmatrix} 1 & x_i - x & y_i - y & (x_i - x)^2 & (x_i - x)(y_i - y) & (y_i - y)^2 \\ 0 & 1 & 0 & 2(x_i - x) & y_i - y & 0 \\ 0 & 0 & 1 & 0 & x_i - x & 2(y_i - y) \end{bmatrix}$$

W denotes the diagonal by blocks matrix of the weights.
The minimization of the quadratic error criterion $J_x(\alpha)$ leads to the 6×6 system

$$\left(PWP^T\right)\alpha = PWr$$

5. CONTROL OF THE MESH SIZE

In order to measure the accuracy with which the mesh describes the geometry, an error estimator inspired from Bonet's work [6] and proposed by Rodriguez-Villa [7] has been used. The estimator provides a relationship between the length L of an edge of the mesh and the smallest principal curvatures radius of the model R. The error ε is estimated with the following formula

$$\varepsilon = \xi^2 \sqrt{1 + \frac{1}{\left(1 - \frac{\xi^2}{4}\right)^2}} \quad \text{with } \xi = \frac{L}{R}$$

6. REMESHING PROCESS

The adaptation technique involves local modification of the mesh in order to satisfy an *a priori* given error. These techniques are based on optimum mesh size evaluated from an error estimator [8]. A list of edges is constituted. Every edge from the list is examined to determine whether the edge must be kept, split or removed from the triangulation in order to satisfy the criterion. The decision is made by evaluating the error criterion at the middle of the edge. The optimization procedures involve extracting from the surface mesh sets of triangles sharing the same node or the same edge and then remeshing the outer contour to a higher criterion (size or shape). The process is repeated as long as the mesh can be enhanced. The procedure are known as edge swapping, vertex removing, edge removing, edge splitting and edge collapsing.

7. FEATURE DETECTION

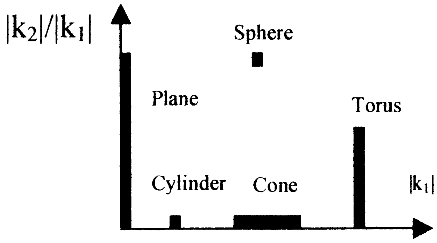

Figure3. Surface identification

During the remeshing process, feature lines of the geometry which cannot be detected with a basic geometrical angle criterion may not be respected. Also, we propose a method based on principal curvature evaluation to decompose the surface mesh into usual surfaces (plane, cylinder, cone, sphere, torus) and therefore to detect intersection lines between theses surfaces. The goal is to provide a final mesh which fits the initial geometry. Figure 3 shows that elementary surfaces have simple representation in the graph ($|k_1|,|k_2|/|k_1|$) where k_1 and k_2 denote respectively the maximum and the minimum curvature. This enables us to classify the nodes of the mesh with local and punctual operators.

8. RESULTS

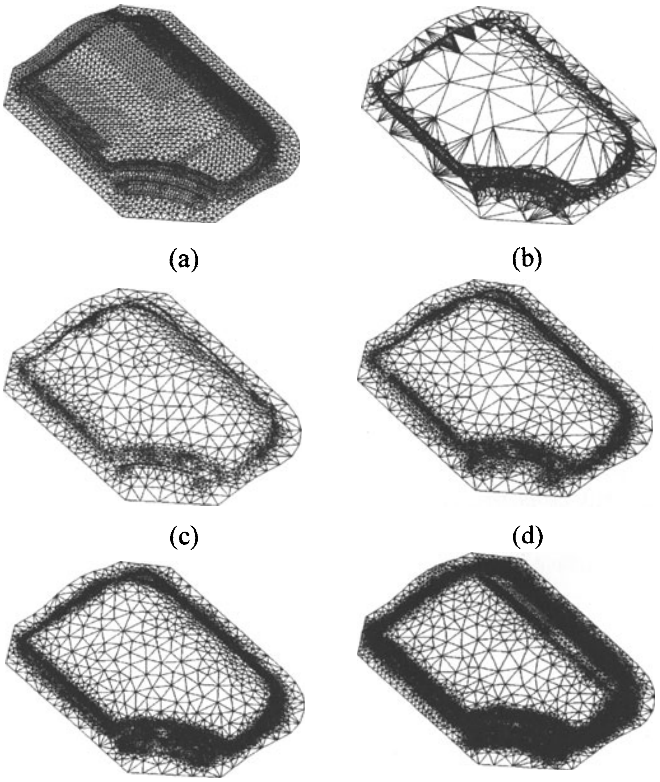

(a) (b)

(c) (d)

(e) (f)

Figures 4. Front door of a car (Numisheet99 benchmark): (a) Initial mesh; (b) Mesh at ε = 0.01. No size smoothing procedure has been applied; (c) Mesh at ε = 0.05; (d) Mesh at ε = 0.02 ; (e) Mesh at ε = 0.01 ; (f) Mesh at ε = 0.001

In order to validate our method, we have decided to adapt meshes used for numerical sheet forming simulation. A front door of a car is shown figures 4 (Numisheet'99 Benchmark). We can see (figures 4, top right) the mesh when no size smoothing procedure is applied.

The following example demonstrates the ability of the Hermite Diffuse Approximation technique to respect the geometry and to capture the variations of curvature while meeting good shape quality requirements. The CPU time of the process on a PC Pentium III 1GHz is less than one minute for models composed of hundred thousand elements.

9. REFERENCES

1. Frey P-J, George P-J, Maillages, applications aux éléments finis, ed. Hermès, 1999.
2. B. Nayroles B., G. Touzot, P. Villon, L'approximation diffuse, C.R.Acad. Sci, Paris, 1991, 313, II: 293-299.
3. P. Breitkopf, A. Rassineux, G. Touzot, P. Villon, Explicit form and efficient computation of MLS shape functions and their derivatives, Int. J. Num. Meth., 48, 2000: 451-466.
4. P. Lancaster, K. Salkauskas, Surfaces generated by Moving Least Squares Methods, Mathematics of Computation, 1981, 155, 37:141-158.
5. A. Rassineux, P. Breitkopf, , P. Villon, Apport des techniques sans maillage au maillage surfacique tridimensionnel, maillage et adaptation, collection MIM, ed. Hermès, 2001.
6. J. Bonet, Error Estimators and Enrichment Procedures for the Finite Element Analysis of Thin Sheet Large Deformation Processes, Int. J. Num. Meth., 1994; 37, 9: 1573-1591.
7. Rodriguez Villa, Etude théorique et expérimentale de l'extrusion-soufflage de corps creux en polymères, Thèse de doctorat : ENSMP, 1997.
8. A. Rassineux, P. Villon P., J-M Savignat, O. Stab, Surface remeshing by local Hermite diffuse interpolation, Int. J. Num. Meth., 49, 2000: 31-49

Chapter 3
CONTROL, MEASUREMENT AND TOLERANCING

Tight fit design taking into account form and surface defects 183
J.F. FONTAINE, G.M. YANG, J.C. COQUILLE, M. LAMBERTIN

Calculation of virtual and resultant part for variational assembly analysis........ 193
L. PINO, F. BENNIS, C. FORTIN

3D quantification of machining defects 201
F. VILLENEUVE, O. LEGOFF, F. GEISKOPF

Formal Definition of Tolerancing in CAD and Metrology 211
P. SERRÉ, A. CLÉMENT, A. RIVIÈRE

Quality Measurement on CMM 219
J.M. LINARES, P. BOURDET, J.M. SPRAUEL

Toward the Use of Statistical Analysis in Positional Tolerancing..................... 227
F. BENNIS, P. CASTAGLIOLA, L. PINO

J. F. FONTAINE, G. M. YANG, J. C. COQUILLE, M. LAMBERTIN

TIGHT FIT DESIGN TAKING INTO ACCOUNT FORM AND SURFACE DEFECTS

Abstract: ***Tight interference fit is applied extensively in industry, but, in all current models of calculation, is the supposition that the contact interfaces are always perfect. This is not only contrary to the grip principle but it greatly increases production costs. This paper offers model that takes into account the macro and micro-geometrical defects for calculating the contact pressure. We show that it is possible to predict the interface pressure and determine the fit resistance. Form defect can be integrated in FEM codes and the surface texture can be represented by a loss of interference due to the plastic strains of the asperities. This method is valid for a simple geometry, but it can be introduced in FEM code for solving industrial cases***

1. INTRODUCTION

Among different assembly processes of hub and shaft, tight interference fit is a simple method. It is easy to implement (it is not necessary to use liaison part like keys, welding,...) and strength increases because there are no stress concentrations due to geometry variations or thermal effects. The assembly cohesion is obtained by the combined action of pressure, due to an interference between shaft and hub, and friction at the contact surface level. But the accurate geometrical specifications given by the standard limits their your cant end a sentence with this possessive it has to have reference. Standards stipulate that cylindricity defect must be less than a quarter diameters tolerance and that the contact surfaces must be smooth (Ra < 0,8 μm) [1], so, a super-finishing process must be used. Standard specifications do not allow for the fact that roughness increases friction. However, if form defect and roughness are included, it is necessary to predict their influence on assembly contact strength. So interface pressure needs to calculated in taking into account both macro and micro-geometrical features.

This study shows that tight interference fit can be fully optimised for production and thus eliminate expensive time consuming manufacturing steps.

First, we introduce the general case with the complete defect and resolution methodology. Then we present the case where form defects are negligible, with the model being applied to an industrial example. Lastly, we conclude on the possibility of implementing the model in a concurrent engineering process.

P. Chedmail et al. (eds.), Integrated Design and Manufacturing in Mechanical Engineering, 183-191.
©2002 *Kluwer Academic Publishers.*

2. MODEL OF TIGHT INTERFERENCE FIT DESIGN.

2.1. general schema

Today, tight interference fit method is underpins international standards. It is a theoretical way of guaranteeing assembly strength. The method relies on the interference (shaft and hub diameters difference) that induces the contact pressure. For perfect cylindrical parts, the pressure is calculated by resolution of Lamé's equations.

$$p_n = \frac{(k^2-1)}{(a_h - a_s) + k^2(a_h + b_h)} \frac{\Delta}{d} . \qquad (1)$$

Where p_n is the nominal contact pressure, Δ, the interference, k, a geometrical constant, d, the nominal fit diameter and a_h, a_s, b_h, material constants characteristics of hub and shaft.

Minimum interference must guarantee the fit strength, the maximum interference does not cause plastic strains.

In the case where the considered surfaces are not perfect, interference is not constant, so contact pressure depends on the localisation of the considered point. So it is possible to define interference in several ways: the first consists in determining a mean interference based on the mean line (Δ_m), the second is given by the envelop line concept and called here peak to peak interference (Δ_{pp}). (see Figure 1).

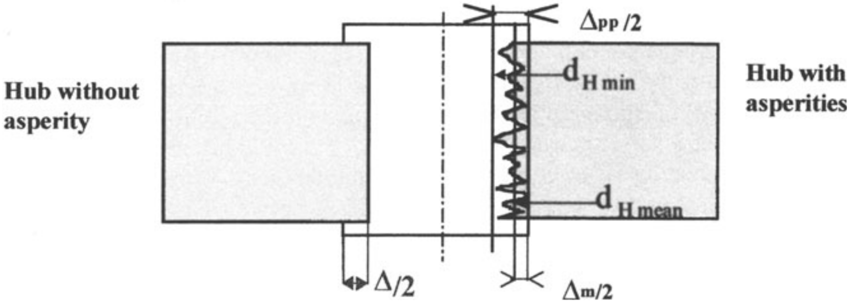

Figure 1. different definitions of interference:
Δ standard interference, Δ_m mean interference, Δ_{pp} peak to peak interference

The second definition is better because the roughness asperities contribute to the clamping. So the concept of maximum matter known in the form defect case can be extended for the roughness [2,3].

2.2. taken into account the macro-geometrical defects.

The macro-geometrical defects are the first order defect: dimension, position, form. The dimensional defect (diameters gap) being already counted in the standard model, only the form defect will be considered here. Form defect modifies the behaviour near the interface. In a cylindrical case, like figure 2, it is possible to take into account the form defect and to calculate the pressure, in solving Neuber-Papcovitch's equation [4].

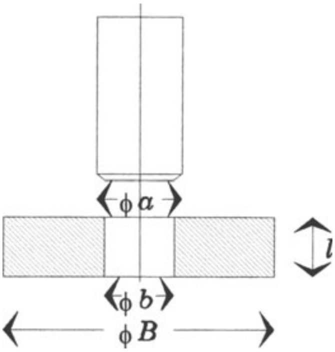

Figure 2. shaft and hub schema

The pressure can be expressed in double Fourier's series. A software called FRET3D has been developed to calculate the real pressure from the real form of shaft and hub.[5]. Figure 3 shows the real pressure calculated from the real form defect given by Figure 4 in axi-symetrical case.

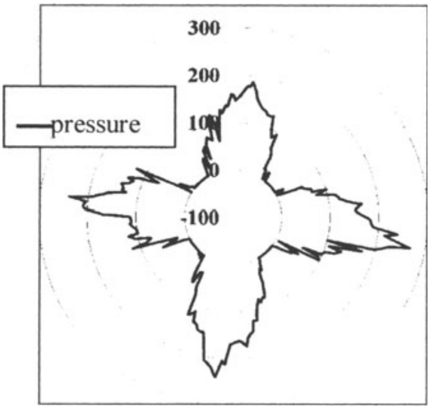

Figure 3. contact pressure (Mpa) calculated with FRET3D

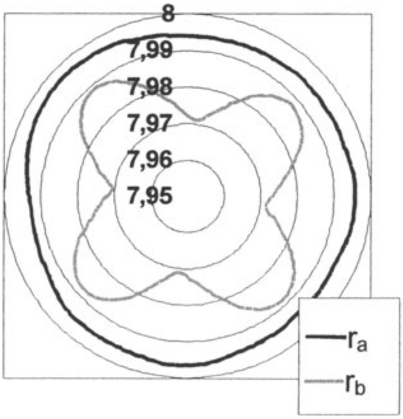

Figure 4. circularity defect of axis in steel (r_a) and of hub in duralumain (r_b)

In a previous paper [6], the authors have shown the influence of the form defect on the fit characteristics, notably the defect amplitude, but also the period and the skewness. In the case of perfect surface the pressure is constant and Von Mises's stress is maximum at the interface level. Contrary to this, when there is a form defect Von Mises' stress is reduced because a phase difference between radial stress and ortho-radial stress [5]. In conclusion, it is possible to increase the form tolerances without decreasing the assembly strength. The model is limited to simple geometry cases. For industrial cases, it is necessary to employ numerical methods.

2.3. Taken into account the micro-geometrical defects:

Several researchers have studied the asperities behaviour, notably in the case of the indentation of a rough surface by a flat smooth punch [7,8,9]. The subsurface stress state has a great influence on the evolution of the real contact area in the solid. A lateral compression delays the asperity crushing contrary to a lateral tension that speeds it up.

A Previous paper had for an object, the study of roughness asperities behaviour in the case of cylindrical fits [3]. The principal results are the following:

As it has been stated above, the peak to peak interference is a better criterion than the mean interference. For standard cases where relative interference Δ/d is less than $0{,}16.10^{-3}$, the roughness does not influence the assembly strength. The asperities contribute to strength but the roughness peaks can become partially plastic. So, there is a clamping or interference loss (L_Δ). It is possible to see a first loss $(L_{\Delta o})$ due to the crushing of local peak from a second loss $(L_{\Delta p})$ due to increases of plastic domain on all the peaks.

To calculate with a good precision nominal pressure, interference loss can be introduced in the equation (1):

$$p_n = \frac{(\lambda^2 - 1)}{(a_H - a_S) + \lambda^2(a_H + b_H)} \, \frac{(\Delta_{pp} - L_{\Delta o} - L_{\Delta p})}{d} \qquad (2)$$

In the cases of standard fits, loss is determined from the isolated peaks. It can be expressed relatively to the roughness and waviness by:

$$L_{\Delta o} = 2[(R_p - R_{pm}) + (W_p - W_a)] \qquad (3)$$

Where R_{pm} is the maximum height of the roughness peak, R_{pm}, the mean height of the roughness peak, W_p is the maximum height of the waviness peak. The mean height of Waviness peak is not a standard parameter, it is replaced by the arithmetic waviness (W_a) . $L_{\Delta o}$ represents the difference between maximum height and mean height of the total surface profile peaks.

When the interference is more important, it is necessary to consider the asperities plastic behaviour. For his, real pressure must be calculated. To do that, it is necessary to know the real contact area. It is assumed that the surface profile is regular and the pressure is distributed uniformly on all peaks. So, the authors suggest to replace the complex real surface by an equivalent surface given by the bearing area ratio curve.

Figure 5 shows the principle of substitution of real contact area by equivalent perfect and reduced area.

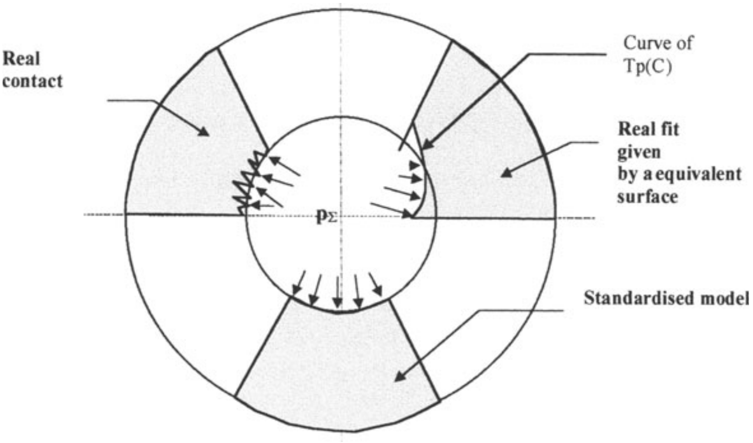

Figure 5: the rough surface can be replaced by a smooth bearing surface.

The plastic interference loss ($L_{\Delta p}$) is calculated with the following iterative schema:

- Determination of real area (A_r) with the bearing area ratio, height is given by $L^{i-1}_{\Delta p}$. (initially $L^0_{\Delta p}=0$).
- Calculation of the predicted real pressure in elasticity with the relation

$$p_r = \frac{A_n}{A_r}.p_n \tag{4}$$

- calculation of Von Mises' stress and test of plasticity in introducing a coefficient (α) depending of the texture topology.
- Plastic correction in using Neuber's method with hardening behaviour ($\sigma_{eq} = \sigma_o + K\varepsilon_p{}^n$).
- Calculation of radial displacement (u_{rp}) of a point P_p located on the elastic and plastic domains boundary.
- Calculation of radial displacement (u_{ri}) of a point P_i located on the equivalent contact interface that is assumed perfect.
- Calculation of the plastic interference loss $L^i_{\Delta p}$.= $2(u_{rp} - u_{ri})$. Elastic strains are assumed negligible before plastic strains.
- Determination of the remainder $r^i = L^i_{\Delta p}.- L^{i-1}_{\Delta p}$.
- The solution is obtained if the remainder is less than a previous value.

In the present paper, the parameter α has been determined by finite element modelling and it corresponds to take into account the asperities behaviour. A new study has been started for verifying this assumption.

3. APPLICATION TO AN INDUSTRIAL CASE.

3.1. description of the experimentation

The method has been applied to the insertion of video-recorder drums axis. These one are cylinders of diameter equal to 6 mm. They are machined with a centerless grinding process and are assumed perfect. The drums are axi-symetric with complex geometry.

The tolerances of geometrical specifications are globally less than 0,01 mm. A previous modelling of the insertion in assuming the part without defect has been made for take into account to complex boundary limits. For group of fifty samples (T1, T2, T3, T4) have been machined on precision CNN lathe with a variation of turn step for having different roughnesses and in respect of same peak to peak interference.

3.2. modelling with the proposed method

Extracting test have been made to determine the assembly strength. Table 1 gives the different parameters after and before interference loss correction. One can observe that, for the three first groups (T1,T2,T3), the correlation is good. An initial interference loss correction is sufficient but for the last group (T4) all the asperities become partially plastic and it is necessary to introduce a plastic interference loss.

Table 1: principal characteristics of samples d_{Hmin} minimum diameter of the hub, R_a arithmetic roughness, $F_{extra\text{-}exp}$ experimental extracting load,

group	d_{Hmin} (mm)	R_a (μm)	Δ_m (μm)	Δ_{pp} (μm)	$F_{extra\text{-}exp}$	$L_{\Delta o}$ (μm)	$\Delta_{pp} - L_{\Delta o}$ (μm)
T1	5,981	0,51	10,5	14,2	4197	1,96	12,3
T2	5,982	1,20	13	13,7	3681	3,38	10,3
T3	5,987	2,65	-0,6	17,3	4533	3,58	13,7
Correlation coefficient with $F_{extra\text{-}exp}$ for groups T1, T2 and T3				0,8736			0,9994
T4	5,977	4,28	-14,1	18,4	2680	4,8	13,6
correlation coefficient with $F_{extra\text{-}exp}$ for groups T1, T2, T3 and T4				0,3902			-0,0189

So, the above method is applied with the bearing area ratio given by the following Figure 6

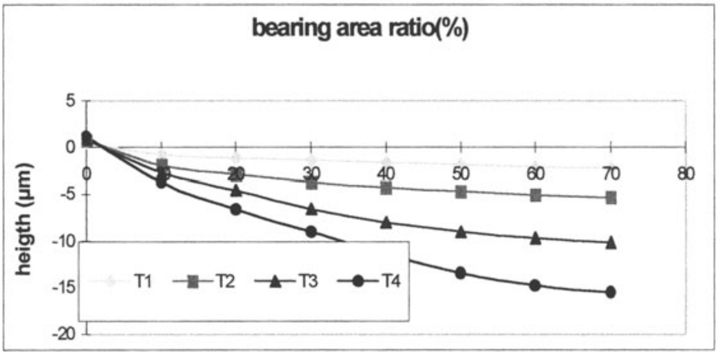

Figure 6. Bearing area curve for the different groups

The new correction calculation is presented in Table 2. The approach being macroscopic, it is assumed that classical values of elastic and hardening behaviour can be used. After calculation, the plastic displacement u_{ri} is different of zero for the group T3 and T4. The real pressure is greater than the elasticity limit (205 Mpa). The predicted extractive force is calculated from the relation (3) and integrated on the nominal area. The friction coefficient is assumed equal to 0,15. It is a classical value between steel and duralumain. The new correction gives better results that are well correlated with the experimental extractive force.

Table 2: Final results d_{Hmin} minimum diameter of the hub, R_a arithmetic roughness, $F_{extra\text{-}exp}$ experimental extracting load,

group	u_{ri} (µm)	T_p (%)	p_n (Mpa)	$p_{r\ elastic.}$ (Mpa)	Δ_{pp} (µm)	$F_{cal\cdot}$ (N)	$\Delta_{pp}cor$ (µm)	F_{exp} (N)
T1	0	100	92,25	92,5	14,2	3803	12,3	4197
T2	0	100	77,25	77,25	13,7	3211	10,3	3681
T3	0,1	50	102,75	205,5	17,3	4271	13,7	4533
T4	3,95	20	56,47	282,3	18,4	2347	5,7	2680
correlation coefficient with $F_{extra\text{-}exp}$ for all groups					0,390		0,995	

4. CONCLUSION.

The study shows that it is possible to predict the assembly strength by taking into account the form and the surface texture defects. So it is possible to increase the specification tolerances. However, the study in detail of plastic asperities behaviour is necessary notably to know if characteristic parameter like skewness or kurtosis can describe a link between the surface topology and the plastic interference loss. For both studied materials, it seems that the micro geometrical behaviour gives good results. Maybe, It will not be the case for other material, notably for thin coating.

Finally, for optimising the fit, it is necessary to model the complex form of industrial parts. So, we envisage the introduction of this method in a finite element procedure. The surface texture can be introduced by contact elements where the interference loss is the control parameter of the contact law. Currently, the contact law used in F.E.M. software does not respect Signorini's conditions. To solve numerical convergence conditions, a smoothed law is employed like that shown in Figure 7. In reality this smoothing corresponds to the interface behaviour.

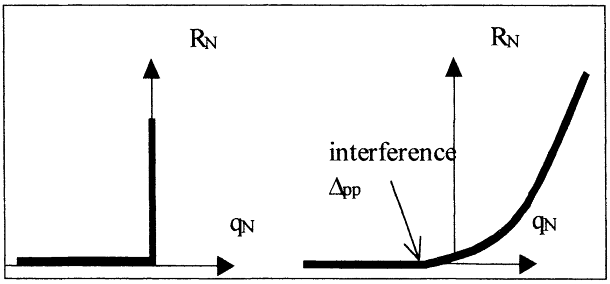

Figure 7. theoretical contact law answering to Signorini's condition and smoothed law used

5. REFERENCES

1. NF E22-621. Assemblage fretté, dimensions, tolérances et états de surface pour assemblages. AFNOR,.Paris la Défense.
2. YANG GM. Etude de l'influence de l'état de surface sur les caractéristiques d'un emmanchement fretté. Thèse de doctorat, ENSAM., France. 10 Nov. 1998
3. YANG GM, COQUILLE JC, FONTAINE JF, LAMBERTIN M . Influence of Roughness on Characteristics of Tight Interference Fit of a Shaft and a Hub. Int. J. of Solids and Struc.2001; 38; n°42-43: 7691-7701.
4. FONTAINE JF, SIALA IE,. Influence of the micro-geometry on the cylindrical fit characteristics. Proceedings of Advances in Materials and Processing Technology' 95; 1995 August; Dublin
5. FONTAINE JF, SIALA IE. Form defect influence on the shrinkage fit characteristics. Eur. J. Mech. A/ Solids. 1998; 17, n°1: 107-119,
6. FONTAINE JF, SIALA IE. Optimisation of the contact surface shape of a shrinkage fit. Journal of Materials Processing Tech. 1998;74/1-3: 96-103.
7. CHILDS THC. The persistence of roughness between surfaces in static contact. Proc. R. Soc. Lond. 1977; 353: 35-53.
8. IKE H, MAKINOUCHI A. Effect of lateral tension and compression on plane strain flattening processes of surface asperity lying over a plastically deformable bulk. Wear 1990; 140: 17-38.
9. SUTCLIFFE MPF. Surface asperity deformation in metal forming processes. Int. J. Mech. Sci. 1988; 30: 847-868.

AFFILIATIONS

JF FONTAINE
Laboratoire de Recherche en Mécanique et Acoustique,
Institut Universitaire de Technologie,
route des plaines de l'Yonne, 89 000 Auxerre, France

G.M. YANG ,
Centre de Ressources Technologique,
route de Monéteau,
89 000 Auxerre, France

J.C. COQUILLE
Etablissement National d'Enseignement Supérieur Agricole de Dijon,
21000 Quetigny , France

M. LAMBERTIN
Laboratoire Bourguignon des Matériaux et Procédés, ENSAM,
CER Cluny,
71000 CLUNY, France

L. PINO, F. BENNIS AND C. FORTIN

CALCULATION OF VIRTUAL AND RESULTANT PART FOR VARIATIONAL ASSEMBLY ANALYSIS

Abstract: Variational assembly analysis is generally a complex problem. In this paper, a method to calculate the virtual and the resultant part for assembly is presented. These two parts represent an extension of the maximum and minimum material part theory previously proposed by Robinson [13]. They may be used during the analysis of the mechanical assembly in order to reduce complexity of the analysis. For a given part, the virtual and the resultant parts are not unique. Ts paper describes the method of calculation of a virtual and a resultant part. This method takes into account datum chaining between toleranced features. A kinematic model is used.

1. INTRODUCTION

Geometric variations of mechanical assemblies are usually specified in terms of tolerances. There are three types of tolerances for several functional requirements: dimensional, form and geometric. Dimensional tolerances deal with the dimension of features of size. Form tolerances control the intrinsic shape of the considered surface. Finally, geometric tolerances define the situation of the tolerance zones of a feature of a part in relation to the other features of the same part. This relative definition uses the notion of Datum Reference Frame (DRF). Industries recognise tolerance to be a key element in all programs for improving quality, reducing overall cost, and retaining market shares. Nevertheless, a complete solution (software or tools) for tolerance analysis and synthesis is not available.

In this paper, the definitions of the mathematical standard [1] are used. They agree with the ISO Standard for this application.

In previous papers, we have presented a kinematic model in order to integrate and deal with the geometrical tolerances. These tools could be used in the geometric tolerance transfer problem [3], and for inspection of parts defined with maximum material condition modifiers [8]. In the present paper, an extension of these tools is proposed. It allows an assembly analysis based on the computation of the virtual and the resultant parts.

The notion of variational class was first introduced in the tolerance model proposed by Requicha [9]. A variational class is defined as a nominal solid associated to the tolerance specifications. Every part in the variational class is functionally equivalent and interchangeable.

The complexity of the analysis of variational assemblies comes from the simultaneous variation of the relative positions of parts in the assembly and the variation of the geometry of the parts. It is possible to analyse the variational assembly in worst cases using only two particular parts: namely the virtual part and the resultant part. The first one includes all parts of the variational class. The second

P. Chedmail et al. (eds.), Integrated Design and Manufacturing in Mechanical Engineering, 193-200.
©2002 *Kluwer Academic Publishers.*

one is included in all elements of the variational class. They represent two extreme boundaries of the material of the part. These two parts were proposed by Robinson in order to extend his work on Maximum Material Parts [13]. Robinson's major contribution is related to the reduction of the survey of the assembly based on a set of tolerance rules. It’s an inverse point of view when compared with the usual ones. He tries to answer the following question:

> What is the tolerancing that permits to achieve a functional requirement of an assembly?

As the traditional approaches try to answer the following question:

> Did a given tolerancing permits to respect a functional requirement of an assembly?

In the following sections, we give the definitions of maximum material parts, virtual parts and resultant parts. Then we present the calculation of these two parts based on the kinematics model of tolerance zones.

2. MAXIMUM MATERIAL PART

The concept of Maximum material part (MMP) was introduced in Parratt's theory of one-dimensional tolerancing for assembly [7]. Robinson has extended this theory to three dimensions and demonstrates the ability of the MMPs to simplify the analysis of assemblies using toleranced parts. MMP theory extends the concept of maximum and minimum material condition from features to entire part. He proposed a list of tolerance rules allowing the identification of a variational class with MMP. This list is not exhaustive [13]. An equivalent list of rules for Least material part (LMP) is also defined. LMP is a part that belongs to the variational class and that is enclosed by all the parts of the variational class. We emphasise that the MMP conforms to the tolerance specifications.

Figure 1 shows an example of a variational class with an MMP. The part with a diameter of 40mm and 10mm is the MMP of this variational class, indeed the actual size of the features of size are at MMC. It encloses all parts of the variational class.

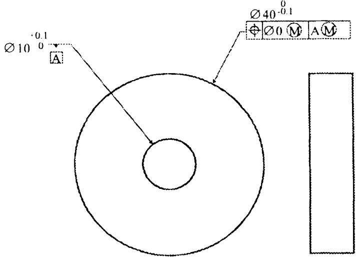

Figure 1 *: Example of Maximum Material Part [13]*

The analysis of a variational assembly is simplified by studying the MMP of each variational class. As an MMP contains all members of its variational class, it is a worst case envelope for interference checking in motion planning [13]. Moreover, because the MMP itself is within tolerance, it does not lead to overly conservative analyses. For a variational assembly comprised of parts with MMP-LMP variational classes, the configuration space regions describing the relative motion and interference between all collections of parts are bounded by the regions derived from analysing the MMP an LMP alone.

In the general case, each variational class cannot necessarily have an MMP. The set of rules proposed by Robinson does not permit to cover all the possibilities of assemblies. For example, datum chaining is not always allowed. Thus, the notion of MMP has to be extended to the virtual and resultant parts.

This paper presents a generic tool for calculating the virtual and resultant parts. Datum chaining is taken into account [4, 8].

3. DEFINITION OF THE VIRTUAL AND RESULTANT PART

According to several authors, the approaches based on the sweeping of the boundary of the part and the interference analysis between parts seems to be useful for this application [3, 11, *13*, 15]. Sweeps are regions obtained by moving a geometric object in space. In general, the motion can involve both translation and rotation.

Basically, the MMP theory aims to extend the concept of maximum and minimum material condition from features to entire part. The motivation behind the application of the virtual condition and resultant condition in current tolerancing standards is to make a direct link between the functional boundary requirement of the assembly and the tolerance specification. So we claim that equivalent tools and analysis must be used.

The analysis of parts at maximum or minimum material conditions is based on the calculation of the resultant and the virtual conditions.

The resultant condition of an internal feature is defined as the variable value corresponding to the worse case outer locus (boundary). The collective effects of size, material condition and geometrical tolerance generates the resultant condition.

The virtual condition or "neutral zone" of an internal feature is a constant value inner locus generated by the smallest feature minus the stated geometric tolerance.

Informally, we consider either the *union* or the *intersection* of all instances of parts that satisfy all applicable tolerance assertions. The *union* is used as a maximum boundary of the part. While the intersection will determine the minimum material boundary. In [15] one can find the role of sweeps and offsets in tolerancing semantics.

We saw previously that not all variational classes can have an MMP or LMP. However, for each variational class we can find some particular parts that enclose all parts of the variational class. These parts are called virtual parts. Virtual parts are an extension of MMP, but there exists two differences between MMP and virtual parts.

The first one is that a virtual part *is not a member* of the variational class.

The second one is the *non-uniqueness* of a virtual part for a given variational class.

As for LMP, we can find the "opposite" of a virtual part, the resultant part. Resultant parts are enclosed by all parts of a variational class. As virtual parts, resultant parts are not unique for a specific variational class.

4. VIRTUAL AND RESULTANT PARTS CALCULATION

In order to calculate the virtual and the resultant parts, the relative location between the features of the part needs to be calculated. The functional gage corresponding to the parts is simulated. Two tools are introduced. The first one is the ACAS calculation. The second one is the kinematic structure to simulate the relative motion of a gage in a feature.

4.1. Actual Candidate Axis Set

For an internal feature, the ACAS represents all the possible situations of the axes of a virtual gage cylinder in the actual feature with respect to datum reference frame [4, 8]. Figure 2 shows the model of an actual cylinder and figure 3 depicts the detail of the corresponding ACAS in the plane.

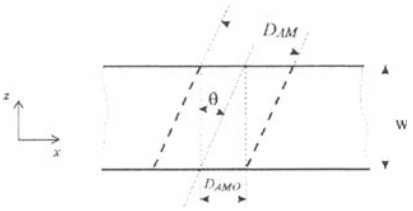

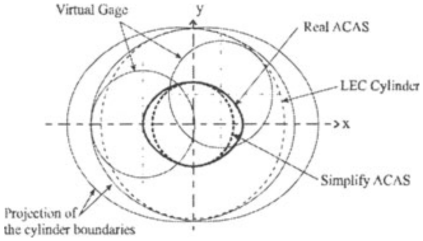

Figure 2 : *Hole model*

Figure 3 : *Definition of the ACAS*

The explicit relations of the ACAS can be found in [4], but in this paper consider only the cylindrical feature with θ=0. In this case the ACAS is a cylinder with a diameter of:

$$\text{Diameter of the ACAS} = D_{AM} - D_{CV} \qquad (1)$$

Where: D_{AM} is the diameter of the actual mating envelope. D_{CV} is the diameter of the virtual condition.

4.2. Definition and study of the kinematic mechanism

The relative situation of the Datum Reference Frame (DRF) with respect to the actual part is the result of the composition of all situations of each datum feature that define the DRF. If some datum features are MMC datum and they are manufactured away from MMC size, then multiple datum feature candidate exist, and then multiple candidate DRF exist. They are called candidate datum reference frame set [1]. In this section, a kinematic mechanism concept is used to calculate this set [3]. The mechanism is used to calculate the candidate DRF relative to an actual part.

For the internal cylindrical datum feature, the axis motion is enclosed in the ACAS of the feature. A transformation associated to each motion defines the situation axis of the virtual gage axis at virtual condition size with respect to the actual position axis of the hole (centre of ACAS) relative to a candidate DRF. This must be done for each individual datum feature. On the other hand, the feature control frame defines an explicit constraint between each individual datum feature of the DRF (datum precedence). Every constraint can be defined by a homogeneous transformation. Like in robotics, an open kinematics chain composed by joints and links can represent each homogenous transformation. The constraint transformations may close these chains. A kinematic mechanism is obtained with serial and closed chains. Rivest proposed a similar method to define tolerance zones for each individual feature using kinematics [11].

The basic situation of the axis of each toleranced hole with respect to a candidate DRF can be defined by a constant transformation. For every candidate DRF, corresponds one situation of the toleranced feature axis basically located at the DRF. This is a particular configuration of the kinematic mechanism. From the mechanism point of view, the set of all true position axis of the specified feature is the workspace of the point that simulates this axis. The properties of the determinant of the Jacobian matrix of the mechanism for a particular point are used to calculate the boundary of this workspace. As commonly known, the singularity of the Jacobian matrix corresponds to the boundary of the workspace of the studied point. This workspace represents all situations of the point of the mechanism. In the following, the study is done for the end point of the mechanism. To define the Jacobian matrix, the following relations are used.

The first one is the equation of the point relative to the base DRF that is written as:

$$ {}^{base}T_{end}(q) = U_0 \tag{1} $$

Where U_0 describes the possible situations of the end effector, and q represents the configuration parameters of the mechanism.

The second one is the equation of the closed chain of the mechanism. The product of the homogenous transformations between each closed-chain element leads to this equation.

$$ \Pi\, {}^{a(i)}T_i = I \tag{2} $$

Where $a(i)$ is the previous element of the i^{th} element of the mechanism, and I is the identity matrix. There may be more than one closed chain in the mechanism.

All these equations lead to the following system:

$$ \begin{cases} F(q_d,q_i) = 0 \\ \Psi(q_d,q_i) = U_0 \end{cases} \tag{3} $$

Where $F(q_d,q_i)$ is the equation of close chains, $\Psi(q_d,q_i)$ the equation of the task, q_d are dependent parameters, and q_i are independent parameters.

The derivative of this system leads to:

$$ dU_0 = J\, dq_i \tag{4} $$

With $J = K_d\,(J_d^{-1} J_i) + K_i$, $J_d = \dfrac{\partial F}{\partial q_d}$ $J_i = \dfrac{\partial F}{\partial q_i}$, $K_d = \dfrac{\partial \Psi}{\partial q_d}$ and $K_i = \dfrac{\partial \Psi}{\partial q_i}$

The analysis of the determinant of J gives the singularities that define the boundary of the workspace W of a particular point of the mechanism. For each toleranced feature, W is the true position set.

5. APPLICATION

The generic formulation presented in the previous section is used to calculate a virtual and a resultant part. The boundary of the sweeping movement can be calculated with the help of Jacobian matrices [8] or with an analytic method [3].

In this section, we present the development of the calculation of the virtual and resultant parts of the example defined in figure 4. The calculation is done with respect to datum ABC.

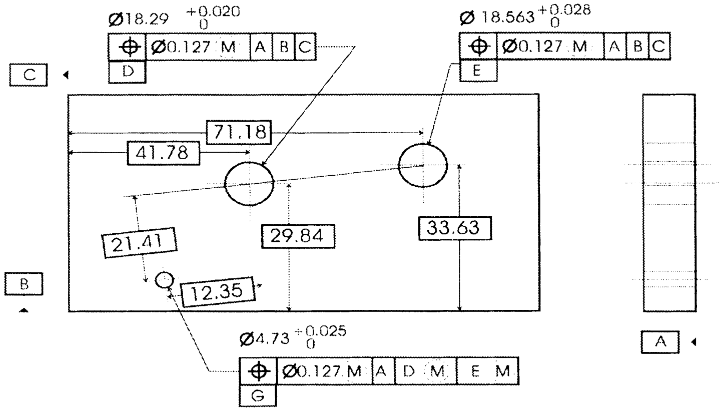

Figure 4 : *Definition of a part*

The datum chain between the axes of the D and E features and the axis of G is taken into account. The tolerance chain is represented by the kinematic structure of figure 5.

The parameters r_1, r_2 and r_3 are obtained from the tolerance specifications of the drawing of the part of figure 4.

The virtual condition of the feature D with respect to the ABC datum reference frame has a diameter of 18.163mm. The diameter of the resultant condition at LMC size of the feature D is 18.457mm.

In a same manner, the diameter of the virtual condition of the E feature is 18.436mm. The diameter of the resultant condition at LMC size of the E feature is 18.746mm.

These values will help us to calculate values of the kinematic structure parameters. These values are defined by an extension of the ACAS of the resultant LMC condition of D and E. Thus :

$$r_1 = (18.457 - 18.163)/2 = 0.147\text{mm}$$
$$r_2 = (18.746 - 18.436)/2 = 0.155\text{mm}$$
$$r_3 = 4.907/2 = 2.4535\text{ mm}$$

This value of r_3 is used to calculate the resultant part. It is associated to the LMC resultant condition of G. In this case, we calculate the union of the sweeping movement of the LMC resultant condition and we obtain the extension of the resultant condition with respect to the ABC DRF.

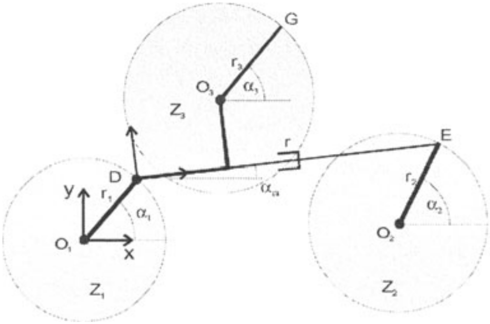

Figure 5: *Gage kinematic structure*

In order to calculate the virtual part, we use $r_3 = 4.603/2 = 2.3015\text{mm}$. This value is obtained using the virtual condition of G. In this case, we obtain the intersection of the virtual conditions of G.

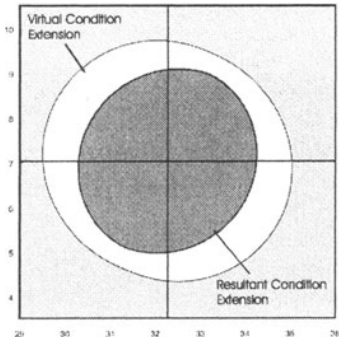

Figure 6 : *Virtual and resultant condition extension of G*

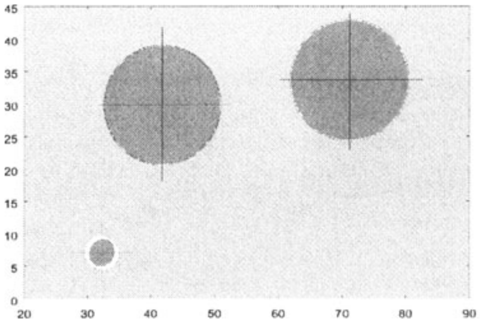

Figure 7 : *Virtual and resultant part*

Figure 6 shows the extension of the resultant condition of feature G with respect to datum ABC (in dark grey). An extension of the virtual condition of the feature G is also represented in this figure in light grey.

In figure 7 shows the virtual (dark grey) and resultant parts (light grey).

6. CONCLUSION

The virtual and resultant parts are used to simplify the analysis of variational assembly. The method used to calculate these parts using a kinematic formulation was shown. An extension of the Actual Candidate Axis Set was introduced to take into account the motion of the datum reference frame controlling features in a tolerance chain. The methodology uses Boolean union and intersection of virtual and LMC resultant conditions. These developments are an extension of Robinson's and Rivest's publications.

L. PINO, F. BENNIS* and C. FORTIN**
LI^2 – Labo Mécatronique –ENIB –29608 Brest – France
* IRCCyN – 1 Rue de la Noë, 44321 Nantes – France.
** Ecole Polythechnique de Montréal, Montréal H3C 3A7 – Canada

7. REFERENCES

[1] ASME, ASME Y14.5.1M-1994. (1994). *Mathematical definition of dimensioning and tolerancing principle.* American society of mechanical engineers..
[2] Ballot E. et Bourdet P. (1995). *Equations formelles et tridimensionnelles des chaînes de dimensions* in Les mécanismes. Séminaire tolérancement et chaîne de cotes, ENS de Cachan. 135-146.
[3] Bennis F., Pino L. et Fortin C. (1998). *Geometric tolerance transfer for manufacturing by an algebraic method.* Proceedings of the 2nd International Conference on Integrated Design and Manufacturing in Mechanical Engineering, Compiègne, France. 713-720.
[4] Bennis F., Pino L. et Fortin C. (1999). *Analysis of positional tolerance based on the assembly virtual state.* Proceeding of the 6th CIRP Seminar on Computer-Aided Tolerancing, University of Twente, The Netherlands. 415-424.
[5] Latombe J.C., Wilson R.H. and Cazals F. (1997). *Assembly sequencing with toleranced parts.* Computer Aided Design, vol. 29:2, pp. 159-174, February 1997.
[6] Pairel E. (1997). *Métrologie par calibre virtuel sur machine à mesurer tridimensionnelle.* PRIMECA. 5ème Colloque sur la Conception Mécanique Intégrée, 155-161.
[7] Parratt S. W.,(1994). *A theory of one-dimensional tolerancing for assembly.* Thesis of Cornell University. May.
[8] Pino L., Bennis F. et Fortin C. (1999). *The use of a kinematic model to analyze positional tolerances in assemblies.* Proceeding of the 1999 IEEE Conference on Robotics and Automation, Detroit, Michigan 1418-1423.
[9] Requicha A. A. G. (1983). *Toward a theory of Geometric Tolerancing.* The International Journal of Robotics Research, 2(4):45-60.
[10] Requicha A. A. G. et Whalen T. W. (1992). *Representation for assemblies.* Institute for robotics and intelligent systems. Report n°267.
[11] Rivest L., (1994). *Modélisation et analyse tridimensionnelles des tolérances dimensionnelles et géométriques.* Phd Thesis de l'Université de Montréal, Ecole Polytechnique.
[12] Rivest L., Fortin C. et Morel C. (1994). *Tolerancing a solid model with a kinematic formulation.* Computer-Aided Design 26(6), 465-476.
[13] Robinson D. M. (1998). *Geometric tolerancing for assembly.* Thesis of Cornell University. May.
[14] Srinivasan V. et Jayaraman R. (1989). *Geometric tolerancing : II. Conditional tolerance.* IBM Journal of Research an Development, 33(2):105-124.
[15] Srinivasan V. (1993). The Role of Sweeps in Tolerancing Semantics. Manufacturing Review, 6(4):275-281.

F. VILLENEUVE, O. LEGOFF, F. GEISKOPF

3D QUANTIFICATION OF MACHINING DEFECTS

A three-dimensional approach for tolerancing analysis and synthesis

Abstract. This paper is proposing to validate a three-dimensional model on manufacturing tolerancing for mechanical parts. The work presented relies on research conducted at the LURPA (Ballot and Bourdet) on the computation of three-dimensional tolerance chains for mechanisms. Models of the workpiece, the set-ups and the machining operations are provided. The concept of the Small Displacements Torsor (SDT) is used to model the process planning. The first part introduces the use of the concept of SDT in the case of manufacturing tolerancing. Then we propose, for a chosen workpiece, an experimental approach to measure and quantify the three-dimensional machining variations as torsors. At last, an analysis of the results is proposed.

1. INTRODUCTION

In the context of integrated design and manufacturing it is essential to take into account the geometrical variations of parts of a mechanism. This should allow validating the correct functioning of the mechanism during the first steps of design. These analyses have to generate an optimal tolerancing, integrating two points of view, functional point of view and manufacturing (or machining) point of view. For the manufacturing (or machining) point of view, knowing the process planning, the usual method described in papers is the following:

- Generation of minimal Manufacturing Tolerance chains: each dimension and its tolerance are modelled as a vector.
- Machining simulation: for each Manufacturing Tolerance, the expert know-how gives a realistic minimal value. These minimal values are used to check if the part can be manufactured according to Manufacturing Tolerance chains and functional tolerances.
- Optimisation: when the manufacturability has been checked it is usually possible to enlarge some tolerances in order to facilitate manufacturing.

The papers take up the whole or a part of the above fields to model [1,2], to optimise [3] or to define cost approaches [4]. They accent on process planning assistance, set-up choice or product/process integration [5,6]. They describe statistical models or worst-case models. But, in every quoted reference, the approach is unidirectional. It does not take the influence of rotation defects into account. Nevertheless, the three dimensional effects are not inconsiderable, especially when the lever arms are long.

The aim of our work is a three-dimensional approach in manufacturing tolerancing. Some works about 3D approaches of the CAT problem can be found in

P. Chedmail et al. (eds.), Integrated Design and Manufacturing in Mechanical Engineering, 201-209.
©2002 *Kluwer Academic Publishers.*

literature [7-10] and, especially, in the field of manufacturing tolerancing [11-13]. They differ in models used, just as well to describe the surfaces of the parts as to model the sum of the defects. The method we propose relies on research on the computation of three-dimensional tolerance chains for mechanisms [1]. Starting from these works, we proposed a formalisation of the problem within the more specific context of manufacturing tolerances. The main originality is to model the machining set-up as a mechanism [14,15]. This work is based on the concept of Small Displacement Torsor (SDT) [16]. It opens up the way for the three-dimensional integration product/process because of the similarities between the concepts used in both points of view. The works described in this paper concern the experimental studies carried out to valid the presented model. The first part recalls the principle of the modelling of surface variations with SDT as well as its application to the manufacturing tolerancing. The second part describes the experimental process and the results obtained on a machining job.

2. MODELING OF THE 3D MACHINING PROCESS DEFECTS

The works of E. Ballot and P. Bourdet [1] model the interactions between the parts of a mechanism, so as to predict the position and orientation variations of these parts in a three dimensional space. The variations are supposed to be small enough to use the concept of the SDT excepted for the expected movements of parts. This principle is generally verified in all mechanisms as the presence of 'unwanted' degrees of freedom goes against the working of the mechanism considering the risks of jamming, of premature wear or of shocks (vibrations) that they generate.

The main idea of the SDT consists in considering that the displacements of a rigid body or a surface, excepted for the expected movements, are supposed small as regards the other geometric dimensions (i.e. the nominal dimensions). The small rotations can then be linearized in the first order. Knowing $\mathbf{D_E}$, the small displacement vector of a point E of the element considered and $\mathbf{M}$, the small rotation matrix expressed in a frame of reference, the small displacement $\mathbf{D_{Pi}}$ of any Pi point of the element is obtained by $\mathbf{D}_{\mathrm{Pi}} = \mathbf{D}_{\mathrm{E}} + \mathbf{M} \cdot \mathbf{EPi} = \mathbf{D}_{\mathrm{E}} + \mathbf{\Omega} \wedge \mathbf{EPi}$ with $\mathbf{\Omega} = \alpha\mathbf{x} + \beta\mathbf{y} + \gamma\mathbf{z}$ where α, β and γ are the small rotations of the element, and $\mathbf{D}_{\mathrm{E}} = \mathrm{u}\mathbf{x} + \mathrm{v}\mathbf{y} + \mathrm{w}\mathbf{z}$ where u, v, w are the small translations of the point E and $\wedge$ is the cross product. The SDT of the considered element in a frame $\langle \mathfrak{R} \rangle$ is:

$$\left\{\mathbf{T}_{\text{element}}\right\}_{(\mathrm{E},\mathfrak{R})} = \begin{Bmatrix} \mathbf{\Omega} \\ \mathbf{D}_{\mathrm{E}} \end{Bmatrix} = \begin{Bmatrix} \alpha\mathbf{x} + \beta\mathbf{y} + \gamma\mathbf{z} \\ \mathrm{u}\mathbf{x} + \mathrm{v}\mathbf{y} + \mathrm{w}\mathbf{z} \end{Bmatrix} = \begin{Bmatrix} \alpha & \mathrm{u} \\ \beta & \mathrm{v} \\ \gamma & \mathrm{w} \end{Bmatrix}_{(\mathrm{E},\mathfrak{R})} \tag{1}$$

Applying this concept to 'single' surfaces such as planes, spheres, cylinders, cones, torus, requires the introduction of undetermined components in the expression of the components of the associated torsor. These undetermined components are noted *U*. They reflect the components that leave the surface invariant in its local frame. The model developed for mechanisms has been enhanced to simulate in three dimensions the behaviour of a workpiece being machined.

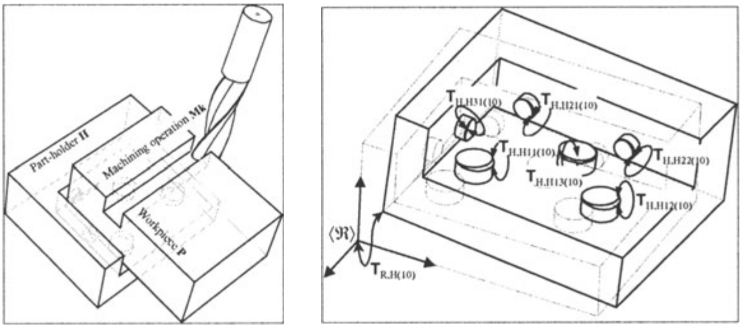

Figure 1. Components of a set-up Sj, milling of a slot and SDTs of a part-holder

The manufacturing of a part consists in creating new surfaces on a stock in a series of set-ups. Each set-up, noted Sj, is considered as a mechanism in itself made up of the following parts (figure *1*):

- The part holder H, built upon the set-up surfaces Hi.
- The part in the state it is in at the end of the set-up (called workpiece P). It is built up, on the one hand, on the previously machined surfaces (or on the stock surfaces) and, on the other hand, on machining features that result from the machining operations of the considered set-up
- The machining operations Mk built upon the surfaces Mki that result from the combination of the kinematics of the machine-tool and the geometry of the tools.

Considering that the part cannot be deformed, then the surfaces created previously to the set-up considered are invariant. Hence Pi, once it is machined, remains invariant. To makes things clearer, the part holder and the machining operations are systematically named H and Mk though they differ from one set-up to the next. They will be distinguished by their set-up number Sj. Each real surface of the part holder, the workpiece or the machining operations are modelled by a substitution surface. The substitution surface is a modelization of the real surface by a surface with a typology similar to the theoretical (or nominal) surface. It is considered that the variations of the substitution surfaces machined on the part as well as the variations of the part holder and the machining operations are of the second order relatively to the dimensions of the elements, which allows to model them thanks to a SDT. The characteristic torsors and the 3D tolerance analysis and synthesis in machining have been described in previous papers [15]. We resume hereafter some characteristic torsors and formula.

Definition of the characteristic torsors for each set-up:

Part holder (figure *1*): $\mathbf{T}_{R,H(Sj)}$: global SDT of the part holder H relatively to its nominal position in set-up j. $\mathbf{T}_{H,Hi(Sj)}$: deviation torsor of the surface Hi relatively to its nominal position on the part holder in set-up j.

Machining operation: $\mathbf{T}_{R,Mk(Sj)}$: SDT of a machining operation relatively to its nominal position in set-up j. $\mathbf{T}_{Mk,Mki(Sj)}$: deviation torsor of the surface Mki relatively to its nominal position on the machining operation Mk in set-up j.

Interface Workpiece/ Part holder: $\mathbf{T}_{Hi,Pi(Sj)}$: gap torsor that expresses the characteristics of the interface between the workpiece and the part holder at the level of the joint Hi/Pi.

Workpiece: $\mathbf{T}_{R,P(Sj)}$: SDT of the workpiece relatively to its nominal position in set-up j (positioning variations of the workpiece within the set-up). $\mathbf{T}_{R,Pi(Sj)}$: deviation torsor of the machined surface Pi relatively to its nominal position in set-up j (variations linked to the machining). This torsor is the result of the removal of matter during the machining Mk on part P. $\mathbf{T}_{P,Pi}$: deviation torsor of the surface Pi relatively to its nominal position on part P. The deviation of a surface Pi relatively to its nominal position on the part depends upon the variations of the machining operation that generates Pi within the set-up Sj ($\mathbf{T}_{R,Pi(Sj)}$) and the positioning torsor of the part within the set-up ($\mathbf{T}_{R,P(Sj)}$). $\mathbf{T}_{P,Pi}$ is obtained with $\mathbf{T}_{P,Pi} = -\mathbf{T}_{R,P(Sj)} + \mathbf{T}_{R,Pi(Sj)}$

Three-dimensional tolerance analysis and synthesis in machining

To validate a process planning, it has to be proven that each functional tolerance of the part will be respected considering the variations due to the process. The effect of these variations on the parts thus has to be calculated. It is the aim of tolerance analysis. To tolerance the workpiece at each set-up (machining tolerancing), the machining tolerances have to be increased while respecting the constraints due to the functional tolerances. It is the aim of tolerance synthesis [6]. In both contexts, the relations established can be used. Consider a functional tolerance between two surfaces Pa and Pb of part P. This functional tolerance can be expressed by means of a SDT $\mathbf{T}_{Pa,Pb}$. Consider also a process plan built up of several set-ups Sj for the machining of part P, $\mathbf{T}_{Pa,Pb}$ is $\mathbf{T}_{Pa,Pb} = \mathbf{T}_{Pa,P} + \mathbf{T}_{P,Pb} = -\mathbf{T}_{P,Pa} + \mathbf{T}_{P,Pb}$. Consider S1 (respectively S2) the set-up where the surface Pa (respectively Pb) is machined, we have $\mathbf{T}_{Pa,Pb} = -(-\mathbf{T}_{R,P(S1)} + \mathbf{T}_{R,Pa(S1)}) + (-\mathbf{T}_{R,P(S2)} + \mathbf{T}_{R,Pb(S2)})$.

The workpiece's SDT $\mathbf{T}_{R,P(Sj)}$ in set-up Sj depends on the variations of the support surfaces of the workpiece and the part-holder's surfaces opposite. It is obtained by the coupling of the torsors associated to each joint part/part-holder. Thus, for any positioning surface i in set-up Sj one gets:

$$\mathbf{T}_{R,P(Sj)} = \mathbf{T}_{R,H(Sj)} + \mathbf{T}_{H,Hi(Sj)} + \mathbf{T}_{Hi,Pi(Sj)} + \mathbf{T}_{Pi,P} = \mathbf{T}_{R,H(Sj)} + \mathbf{T}_{H,Hi(Sj)} + \mathbf{T}_{Hi,Pi(Sj)} - \mathbf{T}_{P,Pi} \quad (2)$$

Or, considering the position variations of the part-holder within the set-up $\mathbf{T}_{R,H(Sj)}$ equals to a nil torsor, $\mathbf{T}_{R,P(Sj)}$ becomes:

$$\mathbf{T}_{R,P(Sj)} = \mathbf{T}_{R,Hi(Sj)} + \mathbf{T}_{Hi,Pi(Sj)} - \mathbf{T}_{P,Pi} \quad (3)$$

The process needed to unify the different expressions of $\mathbf{T}_{R,P(Sj)}$ according to each interface between the workpiece and the part-holder is presented later on in this paper. Let us replace $\mathbf{T}_{R,P(Sj)}$ by its expression according to the positioning in the set-up considered:

$$\mathbf{T}_{Pa,Pb} = -\left\lfloor -\mathbf{T}_{R,Hi(S1)} - \mathbf{T}_{Hi,Pi(S1)} + \mathbf{T}_{P,Pi} + \mathbf{T}_{R,Pa(S1)} \right\rfloor + \left\lfloor -\mathbf{T}_{R,Hi(S2)} - \mathbf{T}_{Hi,Pi(S2)} + \mathbf{T}_{P,Pi} + \mathbf{T}_{R,Pb(S2)} \right\rfloor \quad (4)$$

The positioning surfaces Pi of the part in a set-up are machined in former set-ups, so the same calculation is used recursively as many times as necessary. It is then possible to express with a three-dimensional expression that a functional specification depends on:

- The geometric variations of the part-holder at each set-up, $\mathbf{T}_{R,H(Sj)}$, and the gap between the workpiece and the part-holder, $\mathbf{T}_{Hi,Pi(Sj)}$.
- The geometric variations of the positioning surfaces of the part, $\mathbf{T}_{P,Pi}$.
- The geometric variations of the surfaces machined at each set-up, $\mathbf{T}_{R,Pa(Sj)}$.

3. EXPERIMENTAL WORKPIECE, PART HOLDER, MACHINING PROCESS

In order to carry out tests of machining and measurements to calculate the components of the deviation torsors, we have defined a test part, its machining process and the part holder. Only one set-up of the machining process is studied. We have chosen a prismatic part. The machine tool on which were held the tests is the 4 axis milling centre of the LURPA. A series of 45 parts was produced. The other criteria taken into account are evoked hereafter.

Part: We have chosen a massive part in order to be been free from possible problems of part deformation. The workpiece material is a plain carbon steel containing 0,48% carbon.

Part holder: The part holder (figure 2) realizes an isostatic positioning of each workpiece in order to ensure an optimal repeatability of workpiece positions. This led us to design a modular assembly made up of NORELEM elements. Three grinded positioning devices, whose surface of contact with the part is a 10 mm diameter disc, carried out the main joint. The secondary support is carried out by two supports of the same type. The tertiary support is obtained by a spherical surface. Finally three flanges ensure the maintenance in position of the part (clamping). They are facing the main positioning devices in order to minimize the deformation of the part during clamping.

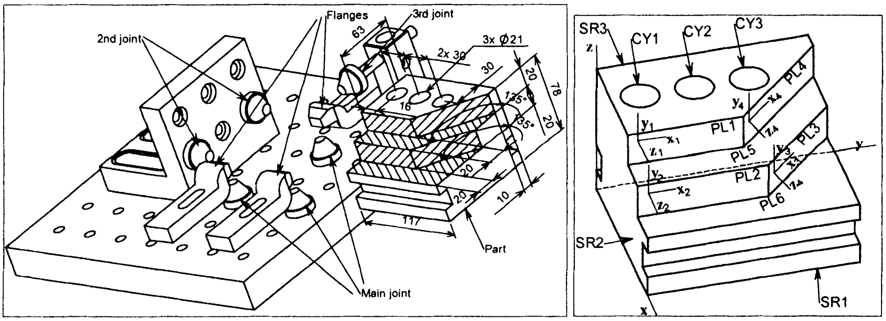

Figure 2. Part holder and workpiece (left), local coordinate frames (right)

Machining process: The machined surfaces in the considered set-up are the planes hatched on figure 2 as well as the three holes. The operations carried out before this set-up made it possible to obtain a semi-finished state compatible with the finishing operations on which we wish to make the identification.

The previous operations were: Centering, centre drill. Drilling, drill ∅ 19.6. Contourning, roughing end mill ∅ 30. Boring semi-finishing, boring bar ∅ 20.5. Contourning semi-finishing, HSS end mill ∅ 20.

So, the finishing operations in the studied set-up are: Contourning finishing, HSS end mill ∅ 21.3 (axial depth of cut = 1 mm, radial depth of cut = 0.7 mm). Boring finishing, boring bar ∅ 21 (radial depth of cut = 0.4 mm).

4. MEASUREMENTS

All the parts were measured with a Coordinates Measuring Machine with the measuring software PROMESUR. The reference coordinate frame is defined by the three datum surfaces used during machining (figure 2): SR1, SR2, SR3. For the whole of these measurements, the points were measured in the support zones of the fixture in order to minimize the effects of the form defects and perpendicularity defects. The measured surfaces are: planes PL1 to PL6, cylinders CY1 to CY3. Each measured element is automatically associated with optimized (least squares algorithm) perfect element computed from the points measured on the surface. Taking into account the identification software, it is impossible to get the coordinates of these points. It was thus essential to carry out geometrical constructions in order to extract from measurements the elements needed to calculate the deviation SDTs. Thus for each plane, three points P1, P2 and P3 belonging to the nominal plane are built in $\mathfrak{R}$ then projected onto the associated plane. Thus, we obtain a representation of the theoretical plane associated with real surface. For the cylinders, only the position of their axis is useful for calculations, so, we just need to build the intersection points between each axis with the higher plane and lower plane SR1.

5. CALCULATION OF THE DEVIATION TORSORS

Local coordinate frames: For each measured element, it is necessary to define a local coordinate frame in which calculations will be done. For the side milled planes (PL1, PL2, PL3 and PL4): the $\mathbf{z}_i$ axis is perpendicular to the plane, $\mathbf{x}_i$ axis follows the feed direction and $\mathbf{y}_i$ is parallel to the end mill axis. For the face machined planes and the holes, the reference axis **x**, **y** and **z** are used.

Deviation torsors of the planes: For any point belonging to a plane, its displacement is given by: $\mathbf{D}_{Pi} = \mathbf{D}_E + \mathbf{\Omega} \wedge \mathbf{EPi}$, where E is a chosen point on the plane. Knowing the expression of the deviation torsor of a plane in its local frame, we can write the equations associated to the plane P1, P2 and P3:

$$\left\{\mathbf{T}_{plane}\right\}_{(E,\mathfrak{R}_{plane})} = \left\{\begin{matrix} \alpha & U_u \\ \beta & U_v \\ U_\gamma & w \end{matrix}\right\}_{(E,\mathfrak{R}_{plane})} \Rightarrow \left\{\begin{aligned} x_{Ri} - x_i &= U_x + \beta(z_i - z_E) - U_\gamma(y_i - y_E) \\ y_{Ri} - y_i &= U_y + U_\gamma(x_i - x_E) - \alpha(z_i - z_E) \\ z_{Ri} - z_i &= w + \alpha(y_i - y_E) - \beta(x_i - x_E) \end{aligned}\right.$$

Where the index R indicates that they are the coordinates of the points of the theoretical plane associated with real surface, in opposition to nominal coordinates.

Let us consider now that the point E is arbitrarily chosen at the point P1 of each plane, and retain only the equations exploitable to calculate the solution (i.e. those where do not appear an undetermined). One obtains for each plane, the following system of linear equations:

$$\begin{cases} z_{R1}-z_1=w \\ z_{R2}-z_2=w+\alpha(y_2-y_1)-\beta(x_2-x_1) \\ z_{R3}-z_3=w+\alpha(y_3-y_1)-\beta(x_3-x_1) \end{cases} \Rightarrow \begin{pmatrix}\alpha\\ \beta\\ w\end{pmatrix}=\begin{bmatrix}0 & 0 & 1\\ y_2-y_1 & x_1-x_2 & 1\\ y_3-y_1 & x_1-x_3 & 1\end{bmatrix}^{-1}\begin{pmatrix}z_{R1}-z_1\\ z_{R2}-z_2\\ z_{R3}-z_3\end{pmatrix}$$

6. RESULTS AND ANALYSES

The results shown on figures are the components of the torsors resulting from calculations. The curves represent the results for the side milled planes, the face milled planes (figure 3) and holes (figure 4). These data have been putted together considering the similarities between them.

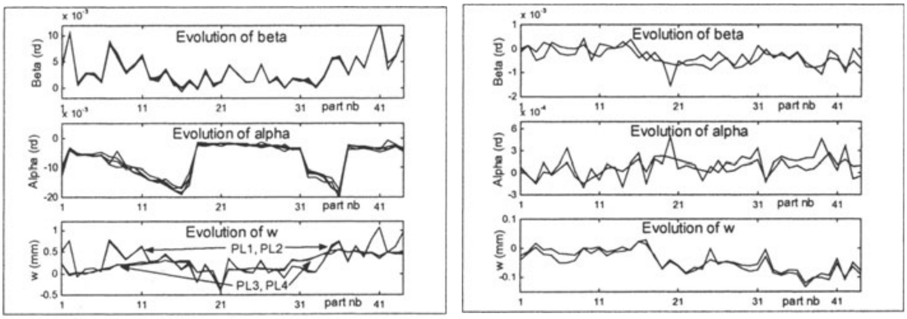

Figure 3. Results for the side milled planes (left) and face milled planes (right)

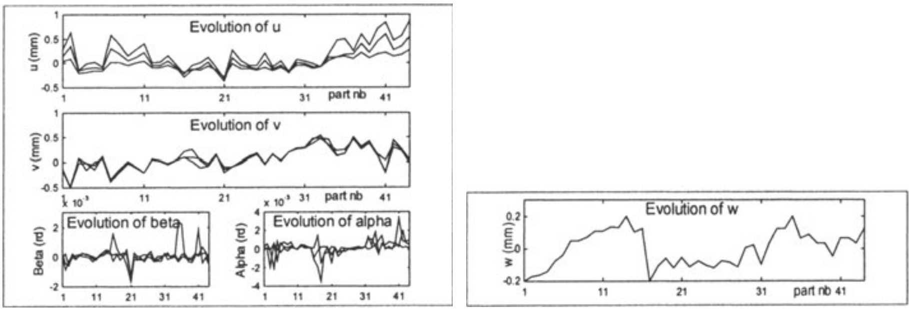

Figure 4. Results for holes (left) and w facing the tertiary joint (right)

Before analyzing of the values we have obtained, we will explain the significance of these various geometrical parameters when it is possible. For the side milled planes, α represents rotation around the feed direction, β the rotation around the milling spindle axis. Thus, excluding the defects related to "adjustable" parameters (part holder orientation and position), we can do the following assumptions: α integrates the problems involved in the deformations of the machine-tool components (particularly the cutting tool) and β integrates the defects of the machine-tool displacements during machining and the displacements from one workpiece to another one.

For the face milled planes: α is rotation around **x** and β that around **y**. Only α integrates the influence of the machining efforts. For the holes, it is more difficult to propose significance a priori for each parameter.

Analyze of the side milled planes: We clearly distinguish four distinct areas for the rotation component α. These four areas correspond to the replacements of the end mill due to wear. The evolution of α follows then a slope characteristic of the tool wear. On the other hand, we see that the values of w for the side milled planes (figure 3) are problematic. Indeed the variations from one part to another can reach up to 0.7 mm on the series of the first 16 parts where there is no tool replacement. These values are a priori much too high considering the machining process we use. Let us analyze, for plan PL1 for example, what is really measured compared to the model described before. We identify $\mathbf{T}_{Pi,PL1}$, Pi being the positioning surfaces of the workpiece. However, $\mathbf{T}_{Pi,PL1} = \mathbf{T}_{Pi,P} + \mathbf{T}_{P,R} + \mathbf{T}_{R,PL1}$ so: $\mathbf{T}_{Pi,PL1} = \mathbf{T}_{R,PL1} - \mathbf{T}_{R,Hi} - \mathbf{T}_{Hi,Pi}$.

If it is admitted that the part holder does not move from one part to another, $\mathbf{T}_{R,Hi}$ is the same for the whole series. So, the measurements we have done take into account the sum of the machining defects ($\mathbf{T}_{R,PL1}$) and the gap SDT between the part holder and the workpiece ($\mathbf{T}_{Hi,Pi}$). Considering the evolution of β (figure 4 left), we can suppose that there is a rotation from a workpiece to another around **z** but there is always contact at the tertiary joint. So, we must find smaller variations of w calculated at a point facing the support (figure 4 right).

7. CONCLUSION

An analysis process of a machining set-up in order to quantify the defects due to the setting and the machining operations was proposed. This aims to validate the three-dimensional model on manufacturing tolerancing that we proposed. After a recall of the model employed, the experimental approach to measure and quantify the three-dimensional machining variations as torsors on a mass production of parts was described. The analysis of the results proves the importance of a three-dimensional consideration of the manufacturing defects. It is shown, for example, the significant role played by the angular defects in the quality of the results. We also showed the difficulty of dissociating the effects due to the setting of those due to machining. The objective of works in progress is the improvement of the experimental protocol in order to dissociate more finely the identified components. The finality would be to specify a process of three-dimensional identification of machine-tool capabilities.

8. REFERENCES

1. Ballot E, Bourdet P. Geometrical Behavior Laws for Computer Aided Tolerancing. 4th CIRP Seminar on Computer Aided Tolerancing; 1995; Tokyo, Japan, 1995: 143-154.
2. Ji P. An algebraic approach for dimensional chain identification in process planning. International Journal of Production Research 1999; 37: 99-110.
3. Ngoi BKA, Ong, JM. A complete tolerance charting system in assembly. International Journal of Production Research 1999;37: 2477-2498.
4. He JR. Tolerancing for manufacturing via cost minimization. International Journal of Machine Tools Manufacturing 1991;31: 455-470.
5. Tseng, YJ, Terng, YS. Aternative tolerance allocations for machining parts represented with multiple sets of features. International Journal of Production Research 1999; 37: 1561-1579.
6. Zhang G. Simultaneous tolerancing for design and manufacturing. International Journal of Production Research 1996; 34: 3361-3382.
7. Mathieu L, Weill R. A model for machine-tool settings as a fonction of positionning errors. 2nd CIRP Seminar on Computer Aided Tolerancing; 1991; Jerusalem, Israel, 1991: 131-150.
8. Desrochers A, Clement A; A Dimensioning and Tolerancing Assistance Model for CAD/CAM Systems. International Journal of Advanced Manufacturing Technology 1994. 9: 352-361.
9. Teissandier D, Couétard Y, Gérard A. Three-dimensional Functional Tolerancing with Proportionned Assemblies Clearance Volume (U.P.E.L), application to setup planning. 5th CIRP Seminar on Computer Aided Tolerancing; 1997; Toronto, Canada, 1997: 113-124.
10. Laperriere L, Lafond, P. Identification of dispersions affecting pre-defined functional requirements of mechanical assemblies. IDMME'98; 1998; Compiegne, France, 1998: 721-728.
11. Kanaï S, Onozuka M, Takahashi H. Optimal Tolerance Synthesis by Genetic Algorithm under the Machining and Assembling Constraints. 4th CIRP Seminar on Computer Aided Tolerancing; 1995; Tokyo, Japan, 1995: 263-282.
12. Clément A, Le Pivert P, Rivière A. Modélisation des procédés d'usinage. Simulation 3D réaliste. IDMME'96; 1996; Nantes, France, 1996: 355-364.
13. Dupinet E, Gaudet P, Fortin C. Integrating design and manufacturing by tolerance chart analysis. IDMME'96; 1996; Nantes, France, 1996: 425-434.
14. Legoff O, Villeneuve F, Bourdet P. Geometrical Tolerancing in Process Planning : a tridimensional approach. Journal of Engineering Manufacture, section Manufacture and Design 1999; 213B:. 635-640.
15. Villeneuve F, Legoff O, Bourdet P. Three Dimensional geometrical tolerancing in process planning. 32nd International CIRP Seminar on Manufacturing Systems; 1999; Leuven, Belgique, 1999: 469-478.
16. Bourdet P, Mathieu L, Lartigue C, Ballu A. The Concept of The Small Displacement Torsor in Metrology. In: Advanced Mathematical Tools in Metrology II, Series on Advances in Mathematics for app. Sc., 40, 1996: 110-122.

9. AFFILIATIONS

François Villeneuve: *Laboratoire 3S, Domaine Universitaire; BP53, 38041 Grenoble cedex 9, France. Francois.Villeneuve@hmg.inpg.fr*

Olivier Legoff: *IRCCyN – Ecole Centrale de Nantes; 1, rue de la Noë 44321 Nantes cedex .Olivier.Legoff@irccyn.ec-nantes.fr*

François Geiskopf: *LURPA – ENS de Cachan; 61, avenue du Président Wilson 94235 Cachan cedex*

P. SERRÉ, A. CLÉMENT, A. RIVIÈRE

FORMAL DEFINITION OF TOLERANCING IN CAD AND METROLOGY

Abstract: Our aim is to unify mathematically the specification and the metrological verification of a given geometrical object. The observed differences result from the fact that strictly geometrical parameters are used in CAD systems while in mechanical engineering distances are paramount. A new mathematical concept - "Near Surfaces" - will be defined. This concept enables specifications and metrological determination to be incorporated within a unified mathematical theory.

1. INTRODUCTION

The need to unify the specification of a given geometrical object from a mathematical standpoint is based on the following 2 observations. First, The variation observed between the specification of a geometrical object by means of Euclidean geometry and its execution in a CAD software database is perfectly similar as regards its principle to the dimensional variation observed between the CAD model, taken as the specification by a NC machine tool, and its mechanical execution. A NC machine tool is actually a copying machine, which copies the CAD model errors onto the part, adding in its own uncertainties. However, these errors are currently of the same magnitude as a result of the convergence of the effect of improvements to NC machines tools and the increased complexity of the surfaces used. This variation must, therefore, be considered on a global basis, or, at the very least, its relations determined. Second, In the domain of CAD, we manipulate specifications whereas in the domain of mechanical engineering, we manipulate distances. Therefore, we need to be able to express the one in terms of the other, at least on a local basis. For example, there are 2 methods for defining the acceptable variation for a geometrical object in relation to its specification; one consists of limiting specification variation and the other of limiting the Euclidean distance from a real point to the theoretical object. The first is basically used in CAD and the second in the metrology of mechanical parts and in tolerancing.

We propose to define a new mathematical concept – "Near Surfaces" – which enables the relation between specifications and verification of geometrical objects to be amalgamated.

2. MOTIVATION

Mathematicians from time immemorial have had to contend with insufficient rational numbers for modelling the continuity properties of Euclidean geometry E^3;

P. Chedmail et al. (eds.), Integrated Design and Manufacturing in Mechanical Engineering, 211-218.
©2002 *Kluwer Academic Publishers.*

however, it was not until the 19th century that they were able to formally define the mathematical set of real numbers $\mathbb{R}$. They were probably given this name sarcastically since these numbers cannot be physically realised and can only be represented by symbols such as $\sqrt{3}$ or π! The best known example is the calculation of the number π by Archimedes who used 2 convergent series constituted by a series of 2 polygons, one inscribed and the other circumscribed to a circle with a radius of 1, with an indefinitely increasing number of sides. It will be noted that the procedure can be stopped at any moment to obtain a given precision value.

The series of mathematical tools used in CAD/CAM and engineering science is developed from the topology of the numerical straight line $\mathbb{R}$ thus created. However, this sort of model never exists, neither in computer science nor on a machine! In practice, in computer science, the set of floating numbers F is the best we have and, in mechanical engineering, we only have decimal numbers of limited accuracy. This has the following disastrous consequence: from a mathematical point of view, numerous equivalent definitions exist for the same E^3 geometric object. Unfortunately, the same is not true from a physical or numerical standpoint. Widespread belief in the practical equivalence of all mathematical definitions results in numerous trials and tribulations. In some circumstances, certain definitions are unusable but, on the other hand, they are ideal in others. It is said that the problem is or is not well conditioned for the values of the parameters under consideration.

We will call "specification" this mathematical definition: A specification is a certain mathematical definition of a geometrical object. It is always evidenced by one or several equations (implicit functions) between certain of the object's parameters. By definition, the specification variation ε is the value of the specification at measurement point M_{mes}.

$$\boxed{Equation_i(M_{nom}) = 0 \Rightarrow Equation_i(M_{mes}) = \varepsilon}$$

A point of the real object (physical or numerical) always presents a variation in relation to its specification that must be limited by a tolerance called the specification tolerance IT_{spec} : $\varepsilon < IT_{spec}$.

The standardised method consists of limiting the Euclidean distance variation between measurement point M_{mes} and the surface specified by a tolerance that we will call the standardised tolerance - $IT_{standard}$. For the same geometrical variation, we have a completely different specification variation, depending on the place where the point is located.

We propose to establish the relationship between the geometrical variation (Euclidean distance) and the specification variation.

3. SPECIFICATION AND VARIATION OF SPECIFICATION

3.1. Definitions

A surface specification is a set of constraints between the co-ordinates of the running point and its MRGEs (Minimum Reference Geometrical Element) by the intermediary of a certain number of position, orientation and dimension parameters (Clément, Rivière & Serré, 1999).

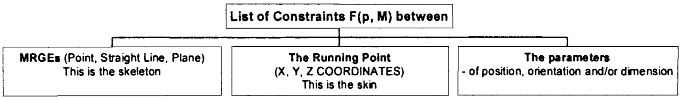
List of Constraints F(p, M) between
MRGEs (Point, Straight Line, Plane)
This is the skeleton
The Running Point
(X, Y, Z COORDINATES)
This is the skin
The parameters
- of position, orientation and/or dimension

There are also specifications which are the relative position constraints between 2 MRGEs.

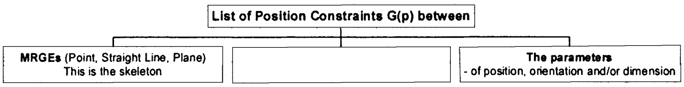
List of Position Constraints G(p) between
MRGEs (Point, Straight Line, Plane)
This is the skeleton
The parameters
- of position, orientation and/or dimension

Finally, there can be specifications which are engineering constraints resulting from the laws of physics or technology.

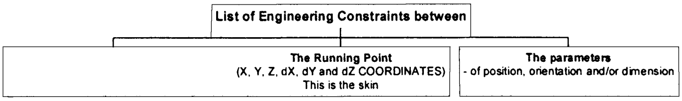
List of Engineering Constraints between
The Running Point
(X, Y, Z, dX, dY and dZ COORDINATES)
This is the skin
The parameters
- of position, orientation and/or dimension

3.2. Relative position of 2 surfaces at a finite distance

The standardised, classic method for specifying the relative positon of surface A in relation to surface B consists of using situation elements (a cylinder axis, Bézier's surface polygon, for example) which have been defined as MRGEs (Minimum Reference Geometrical Elements) in TTRS theory (Clément, Rivière, Serré & Valade, 1997) and (Srinivasan, 1999).

An example of MRGE (Fig. 1):
The parabola below can be fully defined by using either of the following as MRGEs:

- the directrix P_1P_2 and the axis of symmetry OF which constitute the axes of a Cartesian representation;
- the 2 tangents S_1S_0 and S_1S_2 at 2 points specific points M_1 and M_2 which constitute the polygon of a Bézier representation.

To position this parabola in relation to another object, we can use the relative positioning of any of either of these 2 MRGEs and, generally speaking, it always comes down to positioning points, straight lines and planes in relation to points, straight lines and planes. Justification for this method is immediate: the distance of any 2 surfaces using Hausdorff's distance, for example, is totally unusable in practice. The current method is unavoidable for the moment: the MRGEs must be used to position 2 surfaces at a finite distance.

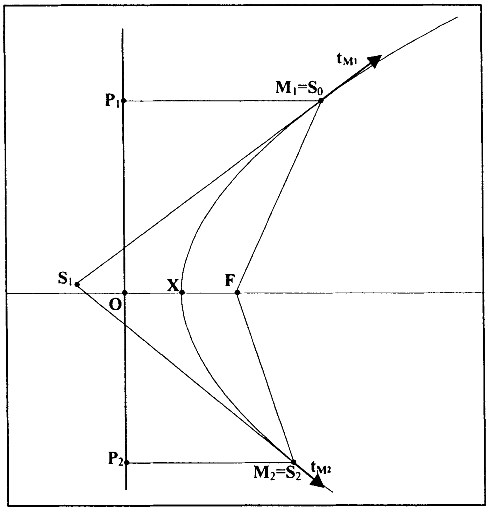

Figure 1: Declaration of a parabola with MRGE

However, the situation is different when the 2 surfaces are infinitely close to one another. We propose to show that it is possible to directly define the distance of 2 surfaces in this situation without using their MRGEs. The advantageous results of this concept will be seen in the tolerancing specifications and their metrological verification.

3.3. Relative position of 2 surfaces at a very small finite distance

We immediately notice (in the figure below for example) that not only is the specified noiminal surface positioned by means of its MRGEs but all the "acceptable" surfaces by this standardised tolerancing are also defined by the same method.

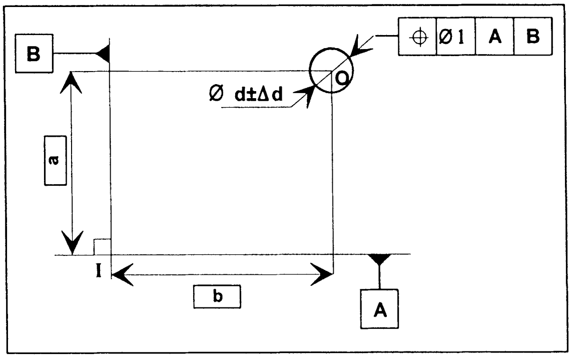

Figure 2: Standardised tolerancing

For a fully specified theoretical surface, we will not only consider **one** surface measured as being "near" but also all the surfaces specified by standardised tolerancing. We will model the actual nearness of 2 surfaces at a finite distance, albeit small, by mathematical nearness at an infinitely small distance.

4. THE CONCEPT OF NEAR SURFACES

We first of all start by defining what an objet is. A function $f(x, y)$ can be considered in 2 different ways:

- either as an application of the domain of x to the domain of y,
- or as all the couples (x, y) of the Cartesian-product of these 2 domains.

This is what is termed entity-relation duality. In computer science, this duality, known as "object-oriented programming", has had considerable success for the past twenty years or so. We say that we programme a function in a procedural manner when it is considered as a relation and that we programme a function in an "object-oriented" manner when it is considered as an entity. A solution to a set of relations is called an "instance".

4.1. Definition

A surface specification can be represented by a vectorial function of vectorial variables:

$$\begin{cases} \vec{F}\left(\vec{p}, \vec{M}\right) = \vec{0} \\ \vec{G}\left(\vec{p}\right) = \vec{0} \end{cases}$$

with the parameters denoted by $\vec{p}$ and the surface running point by $\vec{M}$.

We consider the possible displacements $d\vec{M}$ of a point $\vec{M}$ obtained by a variation $d\vec{p}$ of the parameters of the initial surface, such that point $\vec{M} + d\vec{M}$ belongs to the disturbed surface:

$$\begin{cases} \vec{F}\left(\vec{p} + d\vec{p}, \vec{M} + d\vec{M}\right) = \vec{0} \\ \vec{G}\left(\vec{p} + d\vec{p}\right) = \vec{0} \end{cases}$$

We seek the relations between the initial and the disturbed surfaces. For this, we carry out a Taylor's series development, limited to the first order (we assume here that none of the partial derivatives are equal to zero).

$$\begin{cases} \vec{F}\left(\vec{p}, \vec{M}\right) + \overrightarrow{grad_{\vec{p}}\vec{F}}\left(\vec{p}, \vec{M}\right) \cdot d\vec{p} + \overrightarrow{grad_{\vec{M}}\vec{F}} \cdot d\vec{M} = \vec{0} \\ \vec{G}\left(\vec{p}\right) + \overrightarrow{grad_{\vec{p}}\vec{G}} \cdot d\vec{p} = \vec{0} \end{cases}$$

Note: We note the derivative of the vectorial function $\vec{F}$ *in relation to the variable* $\vec{p}$*, as follows:* $\overrightarrow{grad_{\vec{p}}}\vec{F}$

And, since $\vec{F}\left(\vec{p},\vec{M}\right)=\vec{0}$ and $\vec{G}\left(\vec{p},\vec{M}\right)=\vec{0}$, we can deduce a relation between disturbance $d\vec{p}$ and variation $d\vec{M}$:

$$\boxed{\begin{cases} \overrightarrow{grad_{\vec{p}}}\vec{F}\left(\vec{p},\vec{M}\right)\cdot d\vec{p}+\overrightarrow{grad_{\vec{M}}}\vec{F}\cdot d\vec{M}=\vec{0} \\ \overrightarrow{grad_{\vec{p}}}\vec{G}\cdot d\vec{p}=\vec{0} \end{cases}}$$

4.2. Geometrical interpretation

A geometrical interpretation is made starting with a scalar function $f\left(\vec{p},\vec{M}\right)$ using the following notation:

$$\overrightarrow{grad_{\vec{M}}}f\left(\vec{p},\vec{M}\right)=\left|\overrightarrow{grad_{\vec{M}}}f\left(\vec{p},\vec{M}\right)\right|\cdot\vec{u} \quad \text{and} \quad \overrightarrow{grad_{\vec{p}}}f\left(\vec{p},\vec{M}\right)=\left|\overrightarrow{grad_{\vec{p}}}f\left(\vec{p},\vec{M}\right)\right|\cdot\vec{v}$$

with the unit vector carried by $\overrightarrow{grad_{\vec{M}}}f\left(\vec{p},\vec{M}\right)$ represented by $\vec{u}$ and the unit vector carried by $\overrightarrow{grad_{\vec{p}}}f\left(\vec{p},\vec{M}\right)$ represented by $\vec{v}$. For a given disturbance $d\vec{p}$, the displaced point $\vec{M'}=\vec{M}+d\vec{M}$ is located on a plane parallel to the plane tangent to the surface under consideration at point $\vec{M}$, at a distance equal to ξ the value of which we will now determine.

$$\left|\overrightarrow{grad_{\vec{p}}}f\left(\vec{p},\vec{M}\right)\right|\cdot\vec{v}\cdot d\vec{p}+\left|\overrightarrow{grad_{\vec{M}}}f\left(\vec{p},\vec{M}\right)\right|\cdot\vec{u}\cdot d\vec{M}=0$$

by substituting $e=\vec{v}\cdot d\vec{p}$ and $\xi=\vec{u}\cdot d\vec{M}$, we obtain:

$$\boxed{\xi=K\cdot e} \text{ with } K=-\frac{\left|\overrightarrow{grad_{\vec{M}}}f\left(\vec{p},\vec{M}\right)\right|}{\left|\overrightarrow{grad_{\vec{p}}}f\left(\vec{p},\vec{M}\right)\right|}$$

Thus, when parameters $\vec{p}$ are subject to random variation $d\vec{p}$ such that: $\vec{v}\cdot d\vec{p}<e$, then the displacement of point $\vec{M}$ extends into a zone ξ wide on either side of point $\vec{M}$. The factor K should be considered as an amplification factor of

the disturbance of parameters $\vec{p}$ on the shape of the curve at point $\overrightarrow{M}$. Moreover, it can be seen that this factor can be extremely large (for example, if the first derivatives are cancelled at a dual point) or may be zero at a specific point. Generally speaking, as we were already aware, we observe that the mathematical form of the specification can affect accuracy (Farouki & Rajan 1988).

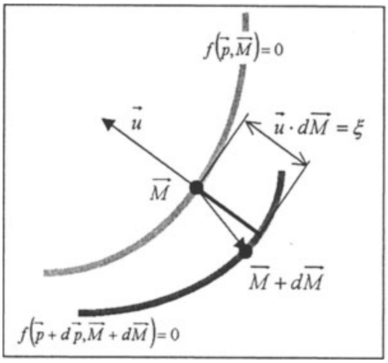
$f(\vec{p},\overrightarrow{M})=0$
$\vec{u}$
$\vec{u}\cdot d\overrightarrow{M}=\xi$
$\overrightarrow{M}$
$\overrightarrow{M}+d\overrightarrow{M}$
$f(\vec{p}+d\vec{p},\overrightarrow{M}+d\overrightarrow{M})=0$

Figure 3: Geometrical interpretation of a near surface

When the surface f is completely regular, a continuous family of vectors $\xi\cdot\vec{u}$ perpendicular to this surface can be traced for a given value of $d\vec{p}$. The ends of these vectors form a continuous surface termed the "generalised offset" of this surface. By definition, the pair of surfaces constituted by the surface and its "generalised offset" surface will be called "near surfaces". It should be noted that, although the parameters adopted are confined to position and orientation parameters, this method is the equivalent of methods using small displacements; to a certain extent, it is a sort of generalisation of the small displacements method (Bourdet & Clément 1988) and (Bourdet, Mathieu, Lartigue & Ballu, 1995).

4.3. Properties

Since we know $\vec{F}(\vec{p},\overrightarrow{M})=\vec{0}$, the "near surfaces" family is therefore a family with a vectorial parameter: $d\vec{p}$. For a given value of this parameter, we will be able to determine: $\vec{F}(\vec{p}+d\vec{p},\overrightarrow{M})$; $\vec{F}(\vec{p},\overrightarrow{M}+d\overrightarrow{M})$; $\overrightarrow{grad}_{\overrightarrow{M}}\vec{F}(\vec{p}+d\vec{p},\overrightarrow{M})$; $\overrightarrow{grad}_{\vec{p}}\vec{F}(\vec{p},\overrightarrow{M}+d\overrightarrow{M})$ and the relations between these different values.

The geometrical significance of these various parameters is illustrated below by the example of a plane curve, dependent upon 2 parameters p_1 and p_2, in 2 different planes. One is plane (x,y) of the curve and the other the parametric plane (p_1,p_2). We have also represented the gradients and numerical variation.

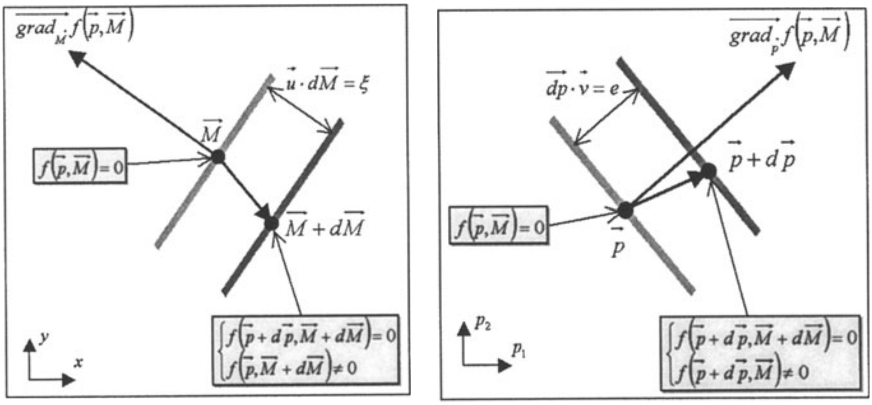
$\overrightarrow{grad}_{\vec{M}} f(\vec{p},\vec{M})$
$\vec{u}\cdot d\vec{M}=\xi$
$\vec{M}$
$f(\vec{p},\vec{M})=0$
$\vec{M}+d\vec{M}$
$f(\vec{p}+d\vec{p},\vec{M}+d\vec{M})=0$
$f(\vec{p},\vec{M}+d\vec{M})\neq 0$
y
x
$\overrightarrow{grad}_{\vec{p}} f(\vec{p},\vec{M})$
$d\vec{p}\cdot\vec{v}=e$
$\vec{p}+d\vec{p}$
$f(\vec{p},\vec{M})=0$
$\vec{p}$
p_2
p_1
$f(\vec{p}+d\vec{p},\vec{M}+d\vec{M})=0$
$f(\vec{p}+d\vec{p},\vec{M})\neq 0$

Figure 4: Illustration of the different parameters in plane (x, y) *and in plane* (p_1, p_2)

5. CONCLUSION

We have shown that a near surface of the same nature can be made to correspond to any surface, differing only with respect to the second order of the initial reference.

The symmetry of the "near surfaces" relation allows these 2 surfaces to be fully defined if we know the analytical parameters of one or the other or any combination of parameters and points belonging to one or the other. This property gives considerable flexibility to identification of the pair of near surfaces, perceived as a unique entity. This opens up the way to the resolution of extremely complex identification problems by global optimisation, which is known to be more efficient than a series of partial optimisations.

6. REFERENCES

Srinivasan V. (1999). A geometrical product specification language based on a classification of symmetry groups. *Computer Aided Design, 31,* 659-668.

Bourdet, P., & Clément, A. (1988). A study of Optima-criteria identification based on the small displacement screw model. *CIRP Annals, 37(1),* 503-510.

Bourdet, P., Mathieu, L., Lartigue, C., & Ballu, A. (1995). The concept of the small displacement torsor in metrology. In P. Ciarlini, M. G. Cox, F. Pavese & D. Richter (Eds), *Advanced Mathematical Tools in Metrology II* (pp. 110-122). Oxford, United Kingdom.

Clément, A., Rivière, A., & Serré, P. (1999). Keynote: Global Consistency of Dimensioning and Tolerancing. In F. van Houten & H. Kals (Eds), *Global Consistency of Tolerances* (pp. 1-26). Enschede, The Nederlands.

Clément, A., Rivière, A., Serré, P., & Valade, C. (1997). The TTRSs: 13 Constraints for Dimensioning and Tolerancing, In H. A. ElMaraghy (Eds), *Geometric Design Tolerancing: Theories, Standards and Applications* (pp. 122-129). Toronto, Ontario, Canada.

Farouki, R.T., & Rajan, V.T. (1988). On the numerical condition of algebraic curves and surfaces. 1. Implicit equations. *Computer Aided Geometric Design, 5,* 215-252.

J.M. LINARES, P. BOURDET, J.M. SPRAUEL

QUALITY MEASUREMENT ON CMM

Abstract. In the first section we wile discuss the sources of errors and uncertainties of the Coordinate Measuring Machine (CMM) [1]. The mastery of this process depends on a good knowledge of the initialisation methodology of the CMM.

Afterwards, we will propose a new method for calculating an A-type uncertainty on the probe system calibration. Our data-processing model provides automatically the value of uncertainties. This information enables a user to control the quality of the probe system calibration. The knowledge of these uncertainties is strategic because they will be propagated in all the other measurements.

1. MODEL OF CMM

The structure of the CMM is studied to illustrate this model [1]. This structure appears in the majority of industrial machining. This analysis should be the same for other kinds of structures. There are four main flows:

Flow 1 : Positioning or locating loop (CMM, Probe system, Part, Reference sphere).It is the central flow of the process. Other flows depend on it (acquisition flow) or influence it (flow 3 disturb it).

Flow 2 : Acquisition loop (CMM, Probe system, Pre-treating)

When the stylus ball touches a surface of the part, a front down signal is provided. That orders the treating system to acquire the position value by adding up the pulses generated by the three axes optical rulers (X, Y, Z). The result obtained is the current point position in terms of the axes of the machine (initialised to zero by contact on three stops).

Flow 3 : Mechanical Loop (CMM, Support part, Part, Sphere)

This influences flow 1 only when the system of reference of the part has not been calculated for every part. Variations in temperature should be considered as negligible.

Flow 4 : Treatment loop (Pre-treating, software)

This flow gets pre-treated data made up of the Mj point coordinates in terms of the axes of the machine. Then the loop provides the coordinates of the Mj points in terms of the axes of the part.

We can extract the central flow 1 that permits us to locate the various functional groups involved in the initialisation. First all parameters included in flow 1 are described. In figure 1, the CMM is placed on the origin of the axes of the Machine, O_M.

The application of the functional group concept to the flow 1 model permits us to bring to the fore vectors that contribute to the value of the desired vector.

The objective is to find the vector $\overrightarrow{O_P M_j}$ in the axes of the part (O_P, X_P, Y_P, Z_P).

To carry out this task we should identify the vectors that influence vector $\overrightarrow{O_P M_j}$.

P. Chedmail et al. (eds.), Integrated Design and Manufacturing in Mechanical Engineering, 219-226.
©2002 *Kluwer Academic Publishers.*

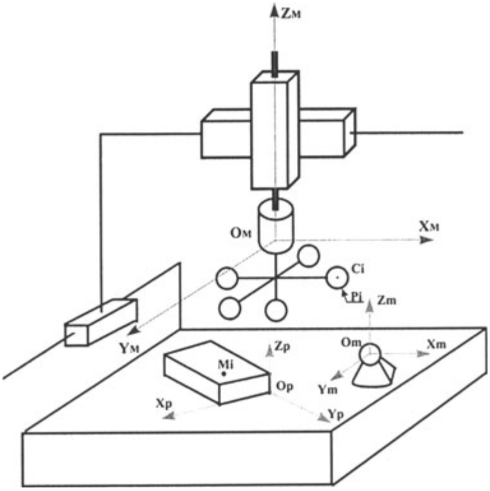

O_M: Origin of the axes of the Machine (Zero counter on the three axes)
O_m: Centre of the reference sphere
O_P: Origin of the axes of the Part
M_J : Point belonging to the measured surface j
C_i : Centre of the ruby i
P_i : contact point between the ruby i and the measured surface
Pt_{Court} : current point after displacement in terms of the axes of the Machine O_M (not pictured in Figure 1).

Figure 1. CMM model.

The measuring machine moves according to an estimated displacement in the axes of the machine (O_M, X_M, Y_M, Z_M).
By using Châles theorem we obtain the following vectorial equation written in terms of the axes of the machine (O_M, X_M, Y_M, Z_M).

$$\overrightarrow{O_PM_j}_{/RM} = (\overrightarrow{O_PO_m} + \overrightarrow{O_mO_M} + \overrightarrow{O_MPt_{Court}} + \overrightarrow{Pt_{Court}C_i} + \overrightarrow{C_iP_i} + \overrightarrow{P_iM_j})_{/RM}$$

Several hypotheses are proposed to simplify the issue. Dimensions are considered as constant between process initialisation and the Mj point acquisition (static equilibrium, no temperature variation, ...). The measuring machine kinematics is considered as perfect.
Under these hypotheses, we can identify the initialisation vectors :
$\overrightarrow{P_iM_j}$: Coordinates of the displacement vector required to put in contact P_i and M_j.
$\overrightarrow{C_iP_i}$: Projection of ruby radius along the contact normal n_j to the point M_j in the measuring reference system.
$\overrightarrow{Pt_{Court}C_i}$: Offset of the C_i ruby centre in relation to an unspecified point on the mobile system.
$\overrightarrow{O_MPt_{Court}}$: Displacement made by the current point to the origin of the axes of the machine O_M(value X,Y,Z of the counter).
$\overrightarrow{O_mO_M}$: Position of the sphere reference centre to the origin of the axes of the machine.
$\overrightarrow{O_PO_m}$: Position of the origin of the axes of the part in relation to the centre of the reference sphere.
The knowledge of all these vectors enables us to determine the vector $\overrightarrow{O_PM_j}$ in terms of the axes of the machine when vector $\overrightarrow{P_iM_j}$ is equal to zero (contact). This transformation can be written by using the formalism of matrix with homogeneous coordinates by using the values X, Y, Z of the counter as an input vector.

$$\overrightarrow{O_PM_j}_{/RM} = \begin{pmatrix} 1 & 0 & 0 & \left(\overrightarrow{O_pO_m}+\overrightarrow{O_mO_M}+\overrightarrow{Pt_{Cour}C_i}+\overrightarrow{C_iP_i}\right)\bullet\vec{X}_M \\ 0 & 1 & 0 & \left(\overrightarrow{O_pO_m}+\overrightarrow{O_mO_M}+\overrightarrow{Pt_{Cour}C_i}+\overrightarrow{C_iP_i}\right)\bullet\vec{Y}_M \\ 0 & 0 & 1 & \left(\overrightarrow{O_pO_m}+\overrightarrow{O_mO_M}+\overrightarrow{Pt_{Cour}C_i}+\overrightarrow{C_iP_i}\right)\bullet\vec{Z}_M \\ 0 & 0 & 0 & 1 \end{pmatrix} \times \overrightarrow{O_MPt_{Cour}}_{/RM}$$

A change of axes is needed to obtain $\overrightarrow{O_PM_j}$ in terms of the axes of the part.

$$\overrightarrow{O_PM_j}_{/RP} = \begin{pmatrix} \vec{X}_p\bullet\vec{X}_M & \vec{X}_p\bullet\vec{Y}_M & \vec{X}_p\bullet\vec{Z}_M & 0 \\ \vec{Y}_p\bullet\vec{X}_M & \vec{Y}_p\bullet\vec{Y}_M & \vec{Y}_p\bullet\vec{Z}_M & 0 \\ \vec{Z}_p\bullet\vec{X}_M & \vec{Z}_p\bullet\vec{Y}_M & \vec{Z}_p\bullet\vec{Z}_M & 0 \\ 0 & 0 & 0 & 1 \end{pmatrix}^{-1} \times \overrightarrow{O_PM_j}_{/RM}$$

Both transformations can be defined by only one matrix of homogeneous coordinates. That allows us to identify the desired vector easily.
After the initialisation vectors are known, the process can calculate the M_j point coordinates in terms of the axes of the part. Now our study is focusing on the preparation phase of the CMM. A flow chart of the initialisation phase for CMM is proposed by using the modelling and the vectorial equation. This flow chart could be used for any kind of CMM “Figure 2”. The counter initialisation is achieved by touching the stops. A point of the mobile part composed of the vertical sliding joint Z and the probe system is chosen as the machine origin.

Secondly it is necessary to define the reference sphere position in relation to the machine origin. The ideal sphere is associated to the measured points on the reference sphere by a least square method.

$$y_i = d_i - R$$

with

$$d_i = \sqrt{\left(x_1 - h_1\right)^2 + \left(x_2 - h_2\right)^2 + \left(x_3 - h_3\right)^2}$$

The optimisation method normally used is the least squares method.

$$\frac{\partial \sum_{i=1}^{n} y_i^2}{\partial a_j} = 0 \text{ with n the number of probed points } (1)$$

The software provides the $\overrightarrow{O_MPt_{Cour}}$ vector (Pt_{Cour} is confused with O_M if no displacement) and the associated sphere radius R_{ass}. In the set up program the software finds the real diameter R_{real} of the reference sphere. The radius of the ruby that has measured the reference sphere is immediately calculated by subtraction “Figure 3”:

$$R_{ruby} = R_{ass} - R_{real} \quad (2)$$

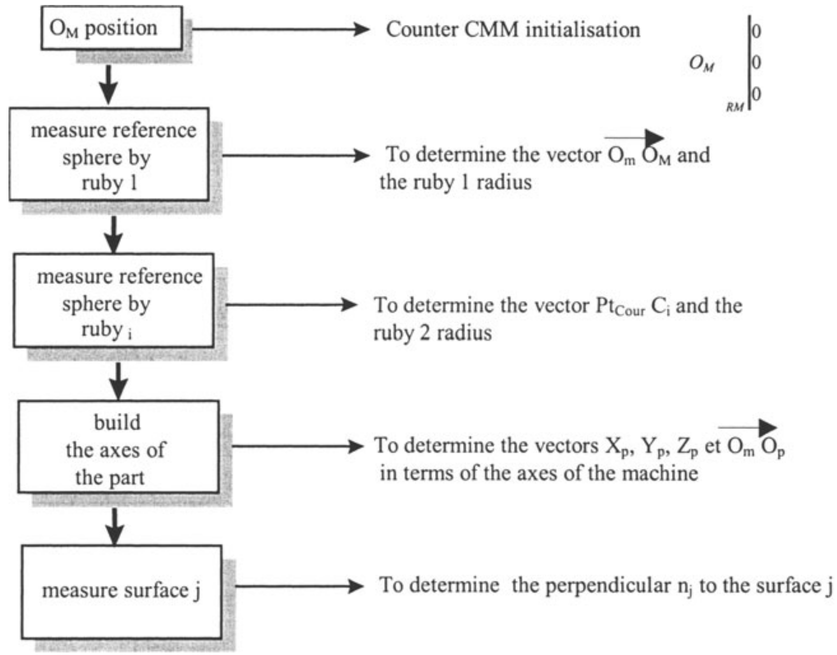
O_M position
Counter CMM initialisation
O_M 0 0 0 RM
measure reference sphere by ruby 1
To determine the vector $\overrightarrow{O_m O_M}$ and the ruby 1 radius
measure reference sphere by ruby $_i$
To determine the vector Pt_{Cour} C_i and the ruby 2 radius
build the axes of the part
To determine the vectors X_p, Y_p, Z_p et $\overrightarrow{O_m O_p}$ in terms of the axes of the machine
measure surface j
To determine the perpendicular n_j to the surface j

Figure 2. CMM initialisation procedure.

Once this operation is completed the origin of the axes of the machine is set on the first stylus ball. The same operation is repeated with the others rubies if they are involved in the checking phase. The vector $\overrightarrow{C_2O_m}$ is obtained after the optimisation phase is carried out by the software. By subtracting the vector $\overrightarrow{O_mO_M}$ from $\overrightarrow{C_2O_m}$, the $\overrightarrow{O_MC_2}$ or $\overrightarrow{Pt_{Cour}C_2}$ vector is obtained, and it is the same for the other rubies. The radius of the ruby is obtained with the same procedure "Figure 4".

$$\overrightarrow{O_MC_2}_{/RM} = \overrightarrow{O_mC_2}_{/RM} - \overrightarrow{O_mO_M}_{/RM} \quad (3)$$

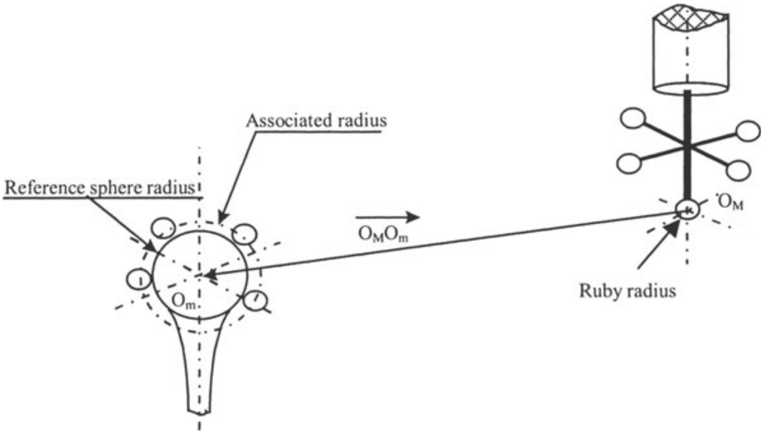
Associated radius
Reference sphere radius
$\overrightarrow{O_MO_m}$
O_M
O_m
Ruby radius

Figure 3. Acquisition of $\overrightarrow{O_mO_M}$ and ruby's radius.

$$\overrightarrow{O_MC_2}_{/RM} = \overrightarrow{O_mC_2}_{/RM} - \overrightarrow{O_mO_M}_{/RM} \quad (3)$$

The remaining tasks involve calculating the $\overrightarrow{O_PO_m}$ vector as well as filling in the axes change matrix.

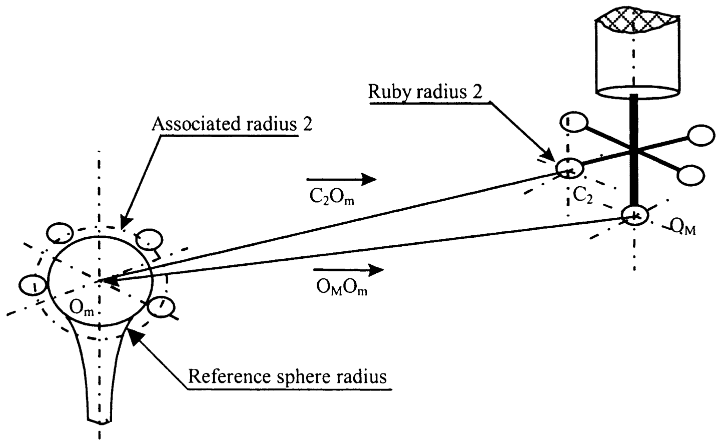

Figure 4. Determination of $\overrightarrow{OMC2}$ and radius of ruby 2.

The $\overrightarrow{O_pO_m}$ vector is obtained according to two phases :

- Geometric models built by the user.
- Its acquisition by a specific function of the software.

2. PROBE SYSTEM CALIBRATION UNCERTAINTIES

From the constructed model we have found the vectors that figure in obtaining the vector $\overrightarrow{O_PM_j}$. Uncertainties of this vector are a function of the uncertainties of the component vectors.

$$\overrightarrow{O_PM_j}_{/R_M} = (\overrightarrow{O_PO_m} + \overrightarrow{O_mO_M} + \overrightarrow{O_MPt_{court}} + \overrightarrow{Pt_{court}C_i} + \overrightarrow{C_iP_i} + \overrightarrow{P_iM_j})_{/R_M}$$

really :

$$\overrightarrow{O_PM_j}_{/R_M} = (\overrightarrow{O_PO_M} + \overrightarrow{O_MPt_{court}} + \overrightarrow{Pt_{court}C_i} + \overrightarrow{C_iP_i} + \overrightarrow{P_iM_j})_{/R_M}$$

the equation just below is the result of the precedent equation :

$$\vec{u}_{c(\overrightarrow{O_PM_j})}{}_{/R_M} = F(\vec{u}_{(\overrightarrow{O_PO_M})}, \vec{u}_{(\overrightarrow{O_MPt_{court}})}, \vec{u}_{(\overrightarrow{Pt_{court}C_i})}, \vec{u}_{(\overrightarrow{C_iP_i})}, \vec{u}_{(\overrightarrow{P_iM_j})})_{/R_M}$$

with u_c : composed uncertainty, u : elementary uncertainty

In this part of the paper we will focus on the A-type uncertainties of the probe system parameters : $\overrightarrow{O_MC_2}$ (vector) and the ruby radius (scalar). Later the other component uncertainties will be treated. The guide of uncertainties in measurement (GUM) subdivides the uncertainties into A-type and B-type [3][4][5][6]. Our proposal enables us to automatically calculate A-type uncertainties from the point coordinates (VDA file) [7]. It is not necessary to repeat repeated tests. The measurement quality is calculated on line.

During the calibration phase the vector and the ruby radius are calculated from the points file (VDA file) that has been obtained by measuring the reference sphere (see Figure 5). A software package has been created to calculate the uncertainties on the statistical vector composed of h_1, h_2, h_3 and R. The function y_i to be minimised is the gap between the acquired points and the substitution surface. In our case we will use equation (1) for the sphere.

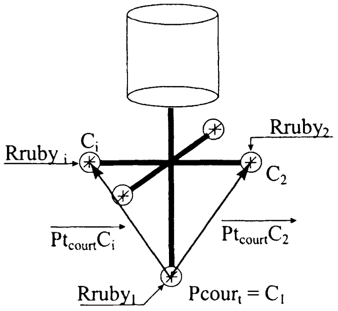
Rruby$_i$
C$_i$
Rruby$_2$
C$_2$
$\overrightarrow{Pt_{court}C_i}$
$\overrightarrow{Pt_{court}C_2}$
Rruby$_1$
Pcour$_t$ = C$_1$

Figure 5. Probe system parameters.

The uncertainties of the parameter of the substitution surface are found by the covariance matrix (4).

$$Cov(X) = \begin{pmatrix} \text{Var h1} & \text{Cov (h1, h2)} & \text{Cov (h1, h3)} & \text{Cov (h1, R)} \\ \text{Cov (h1, h2)} & \text{Var h2} & \text{Cov (h2, h3)} & \text{Cov (h2, R)} \\ \text{Cov (h1, h3)} & \text{Cov (h2, h3)} & \text{Var h3} & \text{Cov (h3, R)} \\ \text{Cov (h1, R)} & \text{Cov (h2, R)} & \text{Cov (h3, R)} & \text{Var R} \end{pmatrix} \quad (4)$$

The measurement model function is : $y = f(x_1, x_2 ... + x_n)$ (5)
with y as scalar, x_i are statistically non independent inputs.

The uncertainty of the output y is :

$$u_{2c(y)} = (J).Cov[X].(J)^T \quad (6)$$

with:

$$J = \left[\frac{\partial f}{\partial x_1} \frac{\partial f}{\partial x_2} ..... \frac{\partial f}{\partial x_n}\right]$$

$$Cov[X] = \begin{bmatrix} u^2(x_1) & u(x_1,x_2) & u(x_1,x_n) \\ u(x_2,x_1) & u^2(x_2) & u(x_2,x_n) \\ & & \ddots & \\ u(x_n,x_1) & u(x_n,x_2) & u^2(x_n) \end{bmatrix}$$

The uncertainties which come from the calibration phase can be determined from the equations (2) (3). For the vector uncertainty the equations (5) and (6) are :

$$y^{\alpha} = f^{\alpha}(x_1^{\alpha} + x_2^{\alpha} + \dots x_n^{\alpha})$$

where y^{α} is vector

$$\mathrm{Cov}[y_{\alpha}] = \left[[J]\mathrm{Cov}[X][J]^T\right]$$

$$[J] = \begin{bmatrix} \frac{\partial f_1}{\partial x_1} & \frac{\partial f_1}{\partial x_2} & \dots & \frac{\partial f_1}{\partial x_n} \\ & & \ddots & \\ \frac{\partial f_m}{\partial x_1} & \frac{\partial f_m}{\partial x_2} & & \frac{\partial f_m}{\partial x_n} \end{bmatrix}$$

J : Jacobian matrix

From the diagonal term of this covariance matrix, the variance vector can be defined by :

$$\overrightarrow{u^2}_{c(y^{\alpha})} = \mathrm{Cov}\left[y^{\alpha}\right]_{\alpha\beta} \quad \text{for } \alpha=\beta$$

In our case we find the uncertainties on the vector $\overrightarrow{O_M C_2}$ and ruby radius.

$$\overrightarrow{u^2}_{(\overline{O_M C_2})} = \overrightarrow{u^2}_{(\overline{O_M O_m})} + \overrightarrow{u^2}_{(\overline{O_M C_2})}$$

$$u^2_{(Rruby_1)} = u^2_{(R_{ass2})} + u^2_{(R_{real})}$$

and : $u_{(Rreal)} = U/k$; U extended uncertainty ; k = 2

From 6 points on the reference sphere (standard calibration) we have calibrated the 5 rubies on the CMM. These 5 files have been saved in VDA format files. The results obtained by the software show that the quality of the probe system calibration is not perfect. The uncertainties on these parameters are not negligible and are not communicated to the user, "Table 1".

Table.1 Uncertainties of calibration parameters

	J_x	J_y	J_z	R_{ruby}	$uc_{(Jx)}$	$uc_{(Jy)}$	$uc_{(Jz)}$	$uc_{(Rruby)}$
C1	0	0	0	1.9996	0	0	0	$6.22\ 10^{-4}$
C2	0.218	-26.194	28.866	0.9962	$5.61\ 10^{-4}$	$5.62\ 10^{-4}$	$5.61\ 10^{-4}$	$3.28\ 10^{-4}$
C3	26.217	-0.152	28.975	1.9981	$1.03\ 10^{-3}$	$1.01\ 10^{-3}$	$1.03\ 10^{-3}$	$9.20\ 10^{-4}$
C4	0.044	25.691	29.194	0.9983	$8.03\ 10^{-4}$	$8.01\ 10^{-4}$	$8.01\ 10^{-4}$	$6.59\ 10^{-4}$
C5	-25.986	-0.393	29.087	1.9998	$1.10\ 10^{-3}$	$1.12\ 10^{-3}$	$1.12\ 10^{-3}$	$9.94\ 10^{-4}$

With : $J_x = \overrightarrow{Pt_{court}C_i} \cdot \overrightarrow{X}_M$, $J_y = \overrightarrow{Pt_{court}C_i} \cdot \overrightarrow{Y}_M$, $J_z = \overrightarrow{Pt_{court}C_i} \cdot \overrightarrow{Z}_M$ (in mm)

3. RESULTS AND DISCUSSION

All the results situated downstream of the calibration phase are influenced by these uncertainties. Our software can calculate the uncertainties value on the probe system in real time. With this information the user can accept the proposed values or redo the stylus ball calibration. From an experimental design we have shown that a lot of parameters have an influence on calibration quality of the rubies. The number of points, the position points (position and measuring normal direction), the probe effort and the measuring speed are the most preponderant. To conclude this section, we have shown that the stylus ball calibration phase influences measurement quality to a great extent.

4. AFFILIATION

Linares J.M., EAMS[2] , Université de la Méditerranée / IUT d'Aix en Provence, Avenue Gaston berger, 13625 Aix en Provence, France.

Bourdet P., LURPA, ENS Cachan, 61 Av du Président Wilson, 94230 Cachan, France.

Sprauel J.M., EAMS[2] , Université de la Méditerranée / IUT d'Aix en Provence, Avenue Gaston berger, 13625 Aix en Provence, France.

5. REFERENCES

[1] A. Idriss, J.M. Linares, J.M. Sprauel, CMM Acquisition Chain, 33rd Internationnal MATADOR Conférence, Juillet Manchester. 2000

[2] Satori S., Colonnetti G., Zhang G.X., Geometric error measurement and compensation of machines, Annals of the CIRP, Vol.44/2,1995, pp599-602.

[3] ISO and al., Guide to the expression of uncertainties in measurement, first edition, 1993, corrected and reprinted 1995, International Organisation for Standardisation.

[4] Fanti G., A procedure to evaluate uncertainties measurement, Processing of the 9th Congress International of Metrology, 18-20 October, Bordeaux. 1999.

[5] Arri E., Cabiati F., D'Emilio S., Gonella L., On the application of the Guide to the expression of uncertainty in measurement to measuring instruments, Journal of the international Measurement , Vol.16,1995: 51-57.

[6] Kessel W., European and international standards for statement of uncertainties, Engineering Science Education Journal (ESEJ) Vol.7, October 1998: 201-207.

[7] Linares J.M., Sprauel J.M., Bourdet P., Propagation de l'incertitude d'acquisition dans la chaîne de traitement d'une MMT, Processing of the 9th Congress International of Metrology, 18-20 October, Bordeaux. 1999.

F. BENNIS, PH. CASTAGLIOLA, L. PINO

TOWARD THE USE OF STATISTICAL ANALYSIS IN POSITIONAL TOLERANCING

Abstract: In this paper, a novel method of positional tolerance analysis is discussed. These tolerances are critical in the assembly analysis. The statistical approach is introduced and its performance is evaluated on a best case study. Industries claim that statistical tolerance analysis is necessary in order to perform a a reduction of the cost of manufacturing, assembly and inspection process. Some applications are given to highlight the advantages of our statistical approach.

1. INTRODUCTION

The main objective of engineering design is to create a competitive product with high quality. Including uncertainty in engineering design decision making may help to produce robust designs by assessing the expected size of variations and determining the risk of failure. These variations are usually specified in terms of tolerances. The tolerance design determines the most economical tolerance that minimizes products cost for given tolerable deviations. Industries recognise tolerance to be a key element in all programs for improving quality, reducing overall cost, and retaining market shares [1].

Existing standards define the geometrical tolerances as zones within which the part features or their resolved geometry (centreplane, centreline, centrepoint) are constrained to lie. The effect of each assigned tolerance on global behaviour of the product must be controlled in order to respect its functional requirement and also in order to reduce the cost of manufacturing, assembly and inspection processes.

Many authors have reviewed the literature of statistical tolerancing [2-5]. Statistical models make the assumption that a reasonable percentage of non-conforming parts may occur. As far as we know, all the authors address only traditional tolerances (plus/minus) in statistical analysis. They generally suggest translating geometrical tolerances to statistical parametric tolerances. Existing tolerancing standards and industrial practices widely use geometrical tolerances because it incorporates the functionality of each feature of the part. There is a real need to set up this topic.

This paper attends to introduce a novel technique for statistical tolerance analysis in the sweeping approach.

2. GEOMETRICAL TOLERANCING

There are three types of tolerance for expressing different functional requirements: dimensional, form and geometric. Dimensional tolerances deal with the dimension of feature of size like the diameter of a cylinder or the distance between two parallel

P. Chedmail et al. (eds.), Integrated Design and Manufacturing in Mechanical Engineering, 227-234.
©2002 *Kluwer Academic Publishers.*

plans. Form tolerances control the intrinsic shape of the considered surface. Finally, geometric tolerances define the situation (position or/and orientation) of the tolerance zones of a feature of part in relation to the other feature of the same part. This relative definition uses the notion of Datum Reference Frame (DRF). In the tolerance design process, we start with the assembly definition of the mechanism, by associating theoretical datum on each part according to the order of assembly (datum precedence) and to the mating surfaces in the assembly. These datum are used to ensure the relative positioning of parts in the assembly. They also permit the analysis and the manufacturing of parts independently.

In this paper, the definitions of the mathematical standard [6] are used. They agree with the ISO Standard for this application. According to the extensive use of CAD tools some software try to integrate tolerance analysis [1]. But, up to now, all users and researchers agree that there is a real needs to set up this topic.

In the following, we deal only with cylindrical inner features, and the primary datum is a plane. Actual mating surfaces of all features are supposed to be given.

3. STATISTICAL DEFINITIONS

General definition of the expectance and variance-covariance are given in this section [7]. The application of these relations is described in the next section. It consists in the calculation of the tolerance zone of point G of the part defined in figure 1. A performance evaluation of the approximation is performed on the same case study.

Let $\hat{\mathbf{p}}_1, \ldots, \hat{\mathbf{p}}_n$ be n random points in $R^{r1}, \ldots, R^{rn}$. Let $\mathbf{p}_k$ be the expectance and Λ_k the variance-covariance matrix (r_k x r_k) of the random point $\hat{\mathbf{p}}_k$:

$$\mathbf{p}_k = E(\hat{\mathbf{p}}_k) \tag{1}$$

$$\Lambda_k = E\,[(\hat{\mathbf{p}}_k - \mathbf{p}_k)\,(\hat{\mathbf{p}}_k - \mathbf{p}_k)^T] \tag{2}$$

Finally, let $\hat{\mathbf{z}}$ be the random points in R^r, defined by the following relation:

$$\hat{\mathbf{z}} = \mathbf{f}(\hat{\mathbf{p}}_1, \ldots, \hat{\mathbf{p}}_n) \tag{3}$$

Where **f** is a non-linear function from R^{r1} x …x R^{rn} in R^r. The linear model of the function **f** near points $\mathbf{p}=(\mathbf{p}_1, \ldots, \mathbf{p}_n)$ is obtained by the following approximation for the expectance $\mathbf{z} = E(\hat{\mathbf{z}})$ and Λ for variance-covariance matrix (r x r) of the random point $\hat{\mathbf{z}}$. The Taylor expansion approximation leads to the following relation:

$$E(\hat{\mathbf{z}}) \approx \mathbf{f}(\mathbf{p}) + \frac{1}{2}\sum_{i=1}^{n}\left(\frac{\partial^2\mathbf{f}(\mathbf{p})}{\partial \mathbf{p}_i^2}\right)_{\mathbf{p}} \mathrm{Var}(\mathbf{p}_i) \sum_{j>i}^{n}\sum_{i=1}^{n}\left(\frac{\partial^2\mathbf{f}(\mathbf{p})}{\partial \mathbf{p}_i\,\partial \mathbf{p}_j}\right)_{\mathbf{p}} \mathrm{Cov}(\mathbf{p}_i,\mathbf{p}_j) \tag{4}$$

Where $\mathrm{Var}(\mathbf{p}_i)$ is the variance of $\mathbf{p}_i$ and $\mathrm{Cov}(\mathbf{p}_i,\mathbf{p}_j)$ is the covariance of $\mathbf{p}_i$ and $\mathbf{p}_j$.

Where $\partial \mathbf{f}(\mathbf{p})/\partial \mathbf{p}_k$ is the partial derivative matrix $(r x r_k)$ of function **f** with respect to $\mathbf{p}_k$. Generally all term corresponding to the second derivative are negligible with respect to the first term, thus the expectance can be approximated by the following equation:

$$\mathbf{z} = E(\hat{\mathbf{z}}) \approx \mathbf{f}(\mathbf{p}) \tag{5}$$

The same hypothesis is applied to approximate the variance-covariance matrix Λ. It leads to the following general relation:

$$\Lambda = E\,[(\hat{\mathbf{z}} - \mathbf{z})\,(\hat{\mathbf{z}} - \mathbf{z})^T] \tag{6}$$

The approximation leads to the next relation:

$$\Lambda \approx \sum_{k=1}^{n} \frac{\partial \mathbf{f}(\mathbf{p})}{\partial \mathbf{p}_k}\, \Lambda_k \left[\frac{\partial \mathbf{f}(\mathbf{p})}{\partial \mathbf{p}_k}\right]^T \tag{7}$$

4. APPLICATION TO THE CASE STUDY

4.1. Statistical definition of the parameters of the case study

The part defined in figure 1 is used in the following section in order to describe our statistical approach. Several authors studied this part [8-9]. It is used as a best case study for many models and methods. In the case of the example presented in figure 1, the non-linear function **f** is defined as the following:

$$\hat{\mathbf{z}} = \mathbf{f}(\hat{\mathbf{x}},\hat{\mathbf{y}},\hat{\mathbf{d}}) = \begin{bmatrix} \mathbf{f}_1(\hat{\mathbf{x}},\hat{\mathbf{y}},\hat{\mathbf{d}}) \\ \\ \mathbf{f}_2(\hat{\mathbf{x}},\hat{\mathbf{y}},\hat{\mathbf{d}}) \end{bmatrix} \tag{8}$$

Where:

$\hat{\mathbf{x}} = (\hat{x}_1,\hat{x}_2)^T$ is the random point corresponding to the center of the hole D in the drawing. $\hat{\mathbf{y}} = (\hat{y}_1, \hat{y}_2)^T$ is the random point corresponding to the center of the hole E in the drawing. $\hat{\mathbf{d}} = (\hat{d}_1, \hat{d}_2)^T$ is the random point defining the coordinates of the center of the hole G with respect to D and E (figures 1 and 2).

The expectance of the points $\hat{\mathbf{x}}$, $\hat{\mathbf{y}}$ and $\hat{\mathbf{d}}$ are noted **x**, **y** and **d** and their variance-covariance Λ_x, Λ_y, Λ_d respectively; with :

$\mathbf{x} = E(\hat{\mathbf{x}}) = (x_1, x_2)^T$; $\mathbf{y} = E(\hat{\mathbf{y}}) = (y_1, y_2)^T$ and $\mathbf{d} = E(\hat{\mathbf{d}}) = (d_1, d_2)^T$

The co-ordinate of the center of the hole G in the global co-ordinate system are calculated using figure 2.

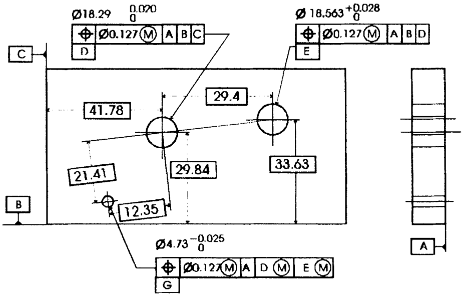

Figure 1 : Technical Drawing : best case study

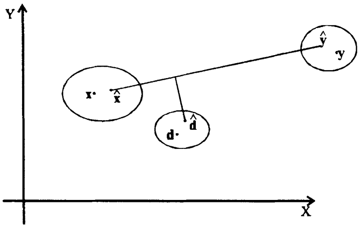

Figure 2 : Statistical definition of the parameters

We obtain the following relations:

$$\mathbf{f}_1 = \hat{x}_1 + \frac{\hat{d}_1\,[\hat{y}_1 - \hat{x}_1] - \hat{d}_2\,[\hat{y}_2 - \hat{x}_2]}{\|\hat{\mathbf{y}} - \hat{\mathbf{x}}\|} \tag{9a}$$

$$\mathbf{f}_2 = \hat{x}_2 + \frac{\hat{d}_1\,[\hat{y}_2 - \hat{x}_2] + \hat{d}_2\,[\hat{y}_1 - \hat{x}_1]}{\|\hat{\mathbf{y}} - \hat{\mathbf{x}}\|} \tag{9b}$$

The calculation of the variance-covariance matrix in equation (7) needs the development of the partial derivatives matrices:

$$\frac{\partial \mathbf{f(x,y,d)}}{\partial \mathbf{u}} = \begin{bmatrix} \dfrac{\partial \mathbf{f}_1\mathbf{(x,y,d)}}{\partial u_1} & \dfrac{\partial \mathbf{f}_1\mathbf{(x,y,d)}}{\partial u_2} \\[2ex] \dfrac{\partial \mathbf{f}_2\mathbf{(x,y,d)}}{\partial u_1} & \dfrac{\partial \mathbf{f}_2\mathbf{(x,y,d)}}{\partial u_2} \end{bmatrix} \tag{10}$$

where **u** may be substituted by x, y or d and u_1 and u_2 are the coordinates of **u**.

4.2. Performance of the suggested approximation

In this section we assume that $\hat{\mathbf{x}}$, $\hat{\mathbf{y}}$ and $\hat{\mathbf{d}}$ are three multinormal independent random points. The expectance points **x**, **y** and **d** of random points $\hat{\mathbf{x}}$, $\hat{\mathbf{y}}$ and $\hat{\mathbf{d}}$ correspond to the values indicated in figure 1:

$\mathbf{x} = (x_1 , x_2)^T = (41.78 , 29.84)^T$,
$\mathbf{y} = (y_1 , y_2)^T = (71.18 , 33.63)^T$
$\mathbf{d} = (d_1 , d_2)^T = (-12.35 ,-21.41)^T$

The corresponding matrices of variance-covariance Λ_x, Λ_y, and Λ_d are assumed to be equal and diagonal (no correlation) and the variance coefficient σ^2 is such that the tolerance 0.127 indicated on figure 1, represents six times the standard deviation:
$\sigma^2 = (0.127/6)^2 = 0.000448$,
Thus :

$$\Lambda_x = \Lambda_y = \Lambda_d = \begin{bmatrix} 0.000448 & 0 \\ 0 & 0.000448 \end{bmatrix}$$

Then Relations (5) and (7) are used to compute the expectance point **z** and the matrix of variance-covariance Λ_z of random point $\hat{\mathbf{z}}$.
We obtain the following values:

$$\mathbf{z} = (32.2687\ , 7.0267)^T \text{and : } \Lambda_z = \begin{bmatrix} 0.0015149 & -0.0005816 \\ -0.0005816 & 0.0012735 \end{bmatrix}$$

In order to evaluate the performance of the approximation presented in the previous section, we have generated *n=10000* multinormal random points $(\hat{\mathbf{x}}_1, \hat{\mathbf{y}}_1, \hat{\mathbf{d}}_1)$, ... , $(\hat{\mathbf{x}}_n, \hat{\mathbf{y}}_n, \hat{\mathbf{d}}_n)$ and we have computed the random points $\hat{z}_1, \ldots, \hat{\mathbf{z}}_n$ using relation (9a and 9b) These random points are plotted in figure 3.

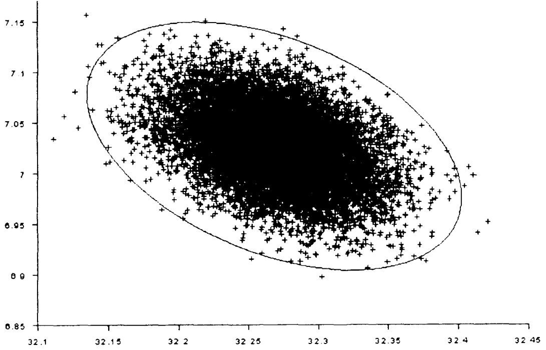

Figure 3 : Random points and theoretical ellipse

Assuming that $\hat{\mathbf{z}}$ is also a multi-normal random point we have computed an estimation $\tilde{\mathbf{z}}$ of **z** and an estimation $\tilde{\Lambda}_z$ of Λ_z :

$$\tilde{\mathbf{z}} = (32.269, 7.027)^T \text{and } \tilde{\Lambda}_z = \begin{bmatrix} 0.0015289 & -0.0005777 \\ -0.0005777 & 0.0013073 \end{bmatrix}$$

We can see that the estimations $\tilde{\mathbf{z}}$ and $\tilde{\Lambda}_z$ obtained from the simulated data are very close to the theoretical values **z** and Λ_z We have also plotted on the same figure the theoretical ellipse (computed from **z** and Λ_z) containing a probability ($1-\alpha=1-0.0027 = 0.9973$) (this probability corresponds to the six sigma case for the normal distribution). We have computed the estimation ($\tilde{\alpha} = k/n$) of α, where k is the number of random points which are outside the theoretical ellipse. In our example we found $\tilde{\alpha}=0.0026$. We can see that this estimation is very close to the expected probability $\alpha=0.0027$. We have repeated this simulation process $m=1000$ times, and computed at each time the estimation $\tilde{\alpha}$. We have computed the mean $\mu(\tilde{\alpha})=0.002708$ and the standard deviation $\sigma(\tilde{\alpha})=0.0005276$ of the $m=1000$ estimations. We can conclude that the simulated data gives an estimation $\tilde{\alpha}$ which is 95% of the time in the interval [0.001674,0.003742].

This result shows that our approach gives a very good approximation in a statistical point of view.

4.3. Applications

In this section we discuss some results corresponding to the case study defined in figure 1.

These results demonstrate the ability of the above statistical analysis method to solve the general problem of geometrical tolerancing.

Figure 4 depicts all the possible ellipses obtained by combining all the worst case size (maximum and minimum) of the three hole. These combinations are given in Table 1. The ellipse of a given combination represents statically all the situations of the axe G. We can observe that these situations are contained in the two ellipses corresponding to the combinations 1 to 8 in Table 1.

Table 1: Results for the 8 combinations

	$T_{Z,D}$	$T_{Z,E}$	$T_{Z,G}$	Λ_Z
1	0.147	0.155	0.152	$\begin{bmatrix} 0.0021109 & -0.0007958 \\ -0.0007958 & 0.0017546 \end{bmatrix}$
2	0.147	0.155	0.127	$\begin{bmatrix} 0.0019172 & -0.0007958 \\ -0.0007958 & 0.0015608 \end{bmatrix}$
3	0.147	0.127	0.152	$\begin{bmatrix} 0.0019810 & -0.0007416 \\ -0.0007416 & 0.0017320 \end{bmatrix}$
4	0.147	0.127	0.127	$\begin{bmatrix} 0.0017873 & -0.0007416 \\ -0.0007416 & 0.0015382 \end{bmatrix}$
5	0.127	0.155	0.152	$\begin{bmatrix} 0.0018386 & -0.0006358 \\ -0.0006358 & 0.0014898 \end{bmatrix}$
6	0.127	0.155	0.127	$\begin{bmatrix} 0.0016448 & -0.0006358 \\ -0.0006358 & 0.0012960 \end{bmatrix}$
7	0.127	0.127	0.152	$\begin{bmatrix} 0.0017087 & -0.0005816 \\ -0.0005816 & 0.0014672 \end{bmatrix}$
8	0.127	0.127	0.127	$\begin{bmatrix} 0.0015149 & -0.0005816 \\ -0.0005816 & 0.0012735 \end{bmatrix}$

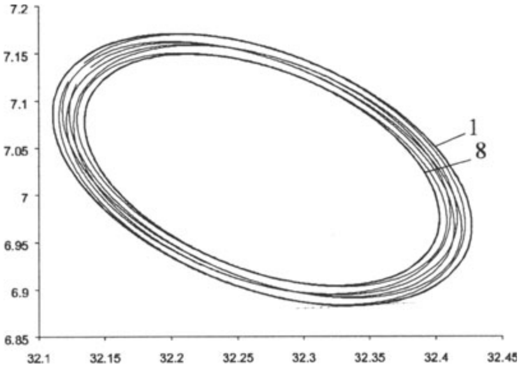

Figure 4 : Evolution of the resultant zone

Figure 5 shows the evolution of the ellipse of the axe G corresponding to the following data:

$$\sigma_x^2 = \sigma_y^2 = (0.127/6)$$

$$\text{Thus : } \Lambda_x = \Lambda_y = \begin{bmatrix} 0.000448 & 0 \\ 0 & 0.000448 \end{bmatrix}$$

σ_d^2 is variable. From the center of the figure to the exterior, the ellipses correspond to the following values :

$\sigma_d^2=0$, $\sigma_d^2=[(0.127/2)/6]$, $\sigma_d^2=[0.127/6]$, $\sigma_d^2=[(0.127*2)/6]$, $\sigma_d^2=[(0.127*4)/6]$.

Finally, Figure 6 gives the ellipse of the axe G corresponding to the following data :

$\sigma_d^2 = (0.127/6)^2 = 0.000448$,

$$\text{Thus : } \Lambda_d = \begin{bmatrix} 0.000448 & 0 \\ 0 & 0.000448 \end{bmatrix} \text{and : } \Lambda_x = \Lambda_y = \begin{bmatrix} 0.0005577 & -0.0001097 \\ -0.0001097 & 0.0005577 \end{bmatrix}$$

The situations of the axis D and E (variables **x** and **y** respectively) are chosen to be themselves ellipses. Indeed, the components x_1 and x_2 (or y_1 and y_2) are really correlated. The following numerical definitions yield the resultants situation of the axe G. This resultant is defined by Λ_z and shown in figure 6.

$$\Lambda_z = \begin{bmatrix} 0.0019796 & -0.0009176 \\ -0.0009176 & 0.0016808 \end{bmatrix}$$

Since the two tolerance zones are not circular, the last example is particularly difficult to calculate by using the worst case analysis. we notice that even if this example can be observed in the practice, tolerancing standard defines the tolerance zone as circular.

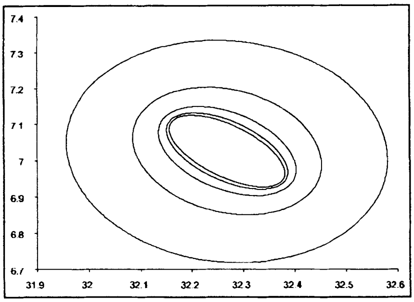

Figure 5 : Evolution of the resultant regarding to σ_d.

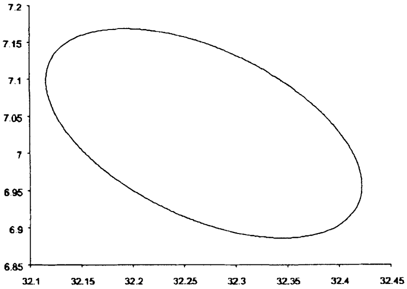

Figure 6 : Resultant zone of G when D and E are ellipses.

5. CONCLUSION

In this paper a kinematics model is applied to the calculation of the resultant zone and the neutral zone. The statistical approach is introduced and its performance is evaluated on a best case study. This is a first tentative toward a general method of statistical analysis of geometrical tolerancing.

F. BENNIS*, PH. CASTAGLIOLA**, L. PINO***
*IRCCyN UMR. CNRS 6597, ECN, 1 rue de la Noë, 44321 Nantes – France
**IRCCyN UMR. CNRS 6597, Ecole des Mines de Nantes, France
*** LI^2 – Labo Mécatronique –ENIB –29608 Brest – France

6. REFERENCES

[1] Zhang W., "Sensitive factor for position tolerance". Int. Jour. Of Research In Engineering Design, (9), pp:228-234, 1997.
[2] Chase K. W. et Parkinson A. R., "A Survey of Research in the Application of Tolerance Analysis to the Design of Mechanical Assemblies". Research In Engineering Design, 3:pp:23-37, 1991.
[3] Nigam S. D. et Turner J. U., "Review of statistical approaches to tolerance analysis". Computer-Aided Design, 27(1):6-15, 1995.
[4] Srinivasan V., O'Connor M. A. et Scholz F.W., 'Techniques for composing a Class of Statistical Tolerances Zones". IBM Research Division. Report n°20254, 1996.
[5] Whitney D. E. et Gilbert O.L., and M. Jastrzebski, "Representation of geometric variations using matrix transforms for statistical tolerance analysis in assemblies". Inter. Jour. Of Research In Engineering Design, (6), pp:191-210, 1994.
[6] ASME Y14.5.1M-1994, "Mathematical definition of dimensioning and tolerancing principle". American society of mechanical engineers. 1994.
[7] P. Castagliola and B. Dubuisson. "Simultaneous Real Robot Motion and World Estimation using Trinocular Vision", 2nd International Workshop on Sensor Fusion and Environmental Modelling, september 1991.Oxford, UK.
[8] Rivest L., Fortin C. et Morel C., "Tolerancing a solid model with a kinematic formulation". Computer-Aided Design 26(6), 465-476. 1994.
[9] Pino L., Bennis F. et Fortin C. "The use of a kinematic model to analyze positional tolerances in assemblies". Proc. of IEEE Conf. on Robotics and Automation, Detroit, Michigan pp:1418-1423. 1999.

Chapter 4
MANUFACTURING AND MODELLING

Prediction and Simulation of Milling Burr Formation for Edge-Precision Process Planning 237
C.H. CHU, D. DORNFELD, C. BRENNUM

Optimal workpiece localization for machining applications 247
J.-F. CHATELAIN, C. FORTIN

Analysis and Mapping of the Dynamic Performance of High-Precision Motion Systems 255
E.V. BORDATCHEV

Integration of Laser Material Processing into the Computer-Aided Product and Process Development 263
M. GEIGER, A. KACH

Investigation of Sheet Metal Blanking Process 271
M. RACHIK, J.M. ROELANDT, A. MAILLARD

The Concept of the Machining Surface in 5-Axis Milling of Free-Form Surfaces 279
C. TOURNIER, E. DUC, C. LARTIGUE, A. CONTR

High Speed Milling - Solid Simulation and Machine Limits 287
A. DUGAS, J.-J. LEE, J.-Y. HASCOËT

Design of Process Parameters in Deep Drawing of Sheets to Improve Manufacturing Feasibility 295

المنـــارة للاستشارات

J.-L. BATOZ, H. NACEUR, A. DELAMÉZIERE, Y.Q. GUO, C. KNOPF-LENOIR

From the Predimensioning Approach to the Optimisation of Forming Processes
of Thin Fabric Composite Parts.. 303
J.L. BILLOET, H. BOROUCHAKI, A. CHEROUAT

CHIH-HSING CHU, DAVID DORNFELD, AND
CHRISTIAN BRENNUM

PREDICTION AND SIMULATION OF MILLING BURR FORMATION FOR EDGE-PRECISION PROCESS PLANNING

Abstract. A burr prediction and simulation system is developed for edge-precision process planning in planar milling. Given workpiece geometry, cutting parameters, and tool path, this system classifies the workpiece edges according to different burr formation mechanisms obtained in experimental studies. For each type of edge, tool engagement conditions are computed for inquiry generation to corresponding database, in which burr type is predicted with different criteria. The location of each type of burr is graphically displayed along the workpiece edges. This study provides a systematic approach to the use of experimental data on milling burr formation represented in different forms. Burr prediction is integrated into the process planning stage, providing effective tools that help reduce milling burr formation and deburring cost.

1. INTRODUCTION

Burr formation is a highly complex behavior of material deformation. A number of factors influence burr formation, including material properties, workpiece geometry, surface treatment, tool geometry, tool path, and cutting parameters. It is difficult to model burr formation in 3D oblique cutting processes such as milling and drilling. Hence most previous studies employed experimental approaches. A series of experiments are first conducted in which different factors are varied in sequence; the burrs generated are then observed and analyzed to find how those factors affect the burr formation. Empirical equations have been obtained in this manner [1, 2]. More importantly, a few key factors have been identified that can effectively control burr formation [3, 4]. However, due to the particular test settings and the simplifications made in these experiment, each controlling factor can usually only be applied to a narrow range of conditions. Those empirical equations are also too over-simplified to use in real machining. On the other hand, a simple face milling operation such as straight step milling involves multiple burr formation conditions to which no single controlling factor can be applied alone. Unfortunately, there is a lack of systematic methods that utilities those different experimental findings in an integrated manner. Not surprisingly, edge-precision process planning literally has benefited little from previous experimental work on burr formation. However, recent studies [5-7] have shown that machining burr formation can be significantly reduced through process planning. As opposed to the traditional concept that deburring is the only solution, the "design for manufacturing" approach is in fact very effective in solving burr problems. Targeting on this, this paper presents a milling burr prediction and simulation system for edge-precision process planning. This system allows the input of 2D workpiece geometry, cutting parameters, tool geometry, and tool path. Edge classification is first conducted according to each burr formation mechanism obtained in experimental studies. With the input information, tool engagement is

P. Chedmail et al. (eds.), Integrated Design and Manufacturing in Mechanical Engineering, 237-246.
©2002 *Kluwer Academic Publishers.*

then computed for the inquiry generation to burr database. Burr prediction is thus accomplished with particular burr formation criteria in each database. The prediction results, including burr type and burr location, are displayed graphically on the 2D workpiece. This study establishes a framework that overcomes the limited applicability of each individual experimental finding. Distinct burr formation criteria can be employed simultaneously for the planar milling operation of 2D polygonal contours. Experimental data has been successfully integrated into the process planning stage for reducing milling burr formation.

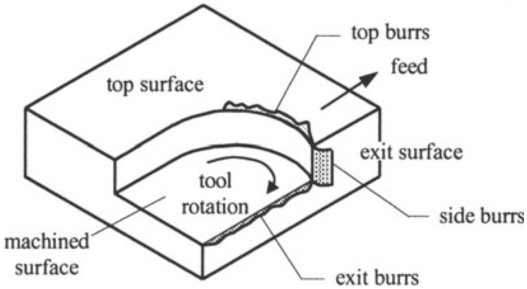

Figure 1. Burrs produced in planar milling

2. CRITERIA FOR MILLING BURR FORMATION

Planar milling operations can be distinguished between face milling and end milling. Inserts are often used in the face milling operation. Each cutting edge of an insert produces burrs as the tool follows its trajectory through the workpiece. Figure 1 shows a schematic view of three different burrs – exit burr, side burr and top burr, which occur along (1) the edge between the machined surface and the exit surface, (2) the edge between the transition surface and the exit surface, and (3) the edge between the top surface and the transition surface. Exit burr causes the most serious problem in planar milling, because side burr and top burr are only transient products. From this point of view, planar milling burrs are usually considered a two-dimensional problem taking place in the machined surface.

Milling burr formation is significantly affected by the tool engagement condition. Therefore, most experimental studies limit their work only on one single tool engagement condition. For instance, Chern [1] conducted a series of fly cutting experiments for investigation of exit burr formation occurring parallel to the tool feed direction. Link [8] considered the burr formation in slot/step milling that occurs perpendicular to the tool feed direction. Chang [9] studied the exit burr formation occurring along the edges that are neither parallel nor perpendicular to the feed direction. In this paper, these three exit burrs are denoted as exit burr in the cutting direction (Figure 2a), exit burr in the feed direction (Figure 2b), and exit burr with gradient (Figure 2c), respectively. Not only are distinct experimental settings required for each type of exit burr, but the data analysis method is also different. As a result, each burr formation criterion is represented in a different form. For the exit burr in the cutting direction, a set of empirical equations have been derived [10] that distinguish exit burrs among the primary burr, the secondary burr and the wavy burr, given a set of cutting parameters. Figure 3 shows schematic illustrations for those three types of exit burr. This set of empirical knowledge is usually represented in a 2D chart, namely a burr control chart [2].

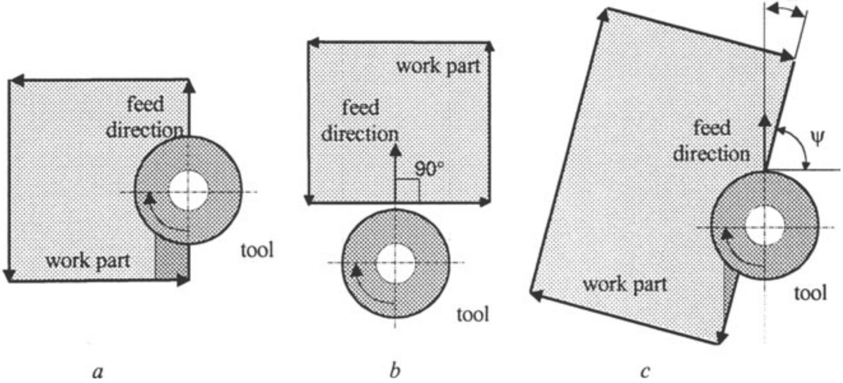
feed direction
work part
tool
work part
feed direction
90°
tool
α
feed direction
ψ
work part
tool
a
b
c

Figure 2. Exit burrs occurring in different tool engagement

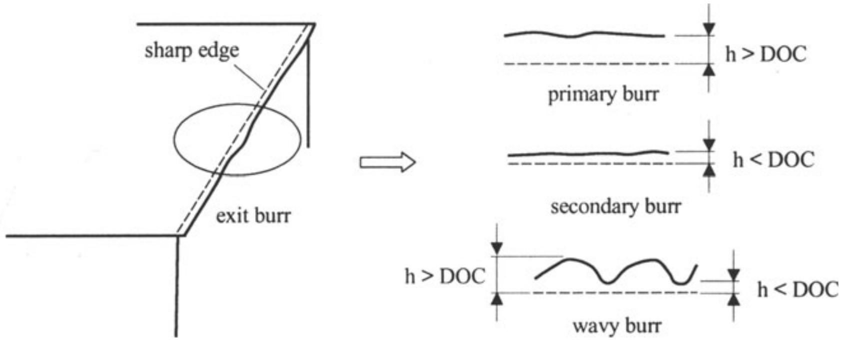
sharp edge
exit burr
h > DOC
primary burr
h < DOC
secondary burr
h > DOC
h < DOC
wavy burr

Figure 3. Schematic illustrations for three different exit burrs

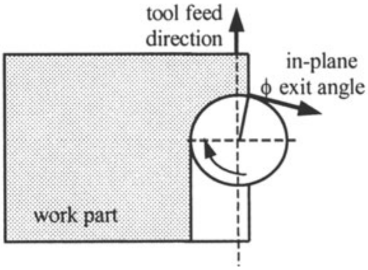
tool feed direction
in-plane
ϕ exit angle
work part

Figure 4. Definition of the in-plane exit angle

For the edges perpendicular to the feed direction, a set of simple rules is used to predict exit burr formation, such as the primary burr occurs at tool exit and entry burr occurs at tool entry. Note that the entry burr size is small, and is thus considered to be burr-free. In the exit burr formation with gradient, our previous experimental study has shown that the in-plane exit angle and its gradient are the main factors determining the transition from the primary burr to the secondary burr. The definition of the in-plane exit angle is shown in Figure 4. The typical change of burr height with the in-plane exit angle and its gradient is shown in Figure 5.

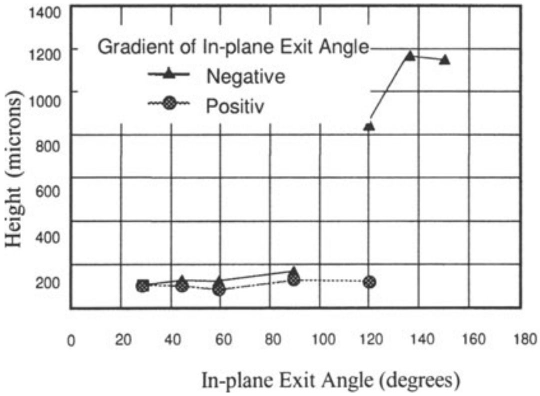

Figure 5. Burr height vs. the exit angle and its gradient

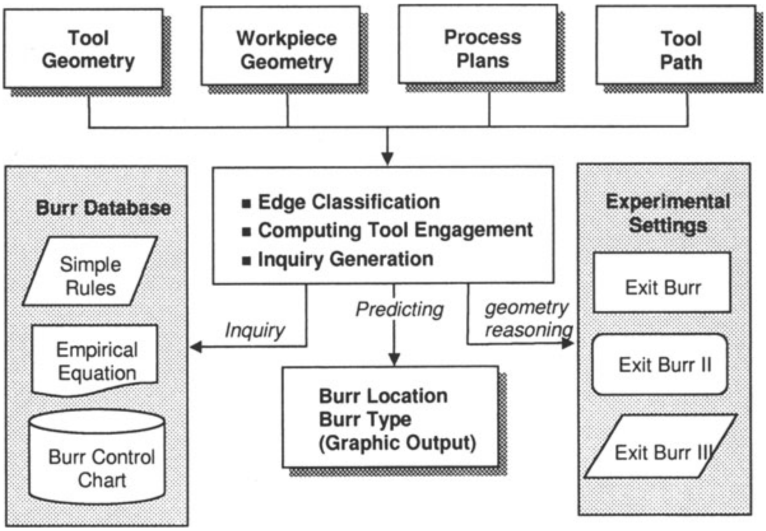
Tool Geometry
Workpiece Geometry
Process Plans
Tool Path
Burr Database
Simple Rules
Empirical Equation
Burr Control Chart
■ Edge Classification
■ Computing Tool Engagement
■ Inquiry Generation
Inquiry
Predicting
geometry reasoning
Burr Location
Burr Type
(Graphic Output)
Experimental Settings
Exit Burr
Exit Burr II
Exit Burr III

Figure 6. Framework of the burr prediction system

Table 1. Parameters for classifying tool entry and exit

u_1	+	+	0	–	–	0	–	+
u_2	+	0	+	–	0	–	+	–
Edge Type	exit	exit	exit	entry	entry	entry	entry/exit	entry/exit

3. SYSTEM FRAMEWORK

The framework of this prediction system is shown in Figure 6. Tool geometry, workpiece geometry, process plans, and tool path are generated from other software modules [5]. The workpiece geometry can be arbitrary 2D polygons with inner contours. Currently only zigzag and single direction tool paths are allowed in the burr prediction. With the input information, three main procedures are carried out: edge classification, tool engagement computation and inquiry generation to burr database systems. The burr database will estimate the burr type with the inquiry and the corresponding burr formation knowledge. A graphic module will show different burr type along with location along the workpiece edges.

3.1. Edge Classification

This procedure is to determine the type of the workpiece edge created, based on geometry and possible burr formation criteria. By classifying edge types, we are able to link previous experimental findings to corresponding tool engagement conditions, and thereby predict the burr formation. Previous research has identified that the in-plane exit angle significantly affects the type of burr formed and transition between burr types. Therefore it is essential to classify the edges in terms of the exit angle. This study proposes the edge classification scheme shown in Figure 7. One important step in the edge classification is to identify tool entry and exit regions. Assume the vertices of the polygonal part are linked in a counter clockwise sense so that the interior of the material lies on the left as each edge is traversed. Each edge $\mathbf{e}_i$ is parametrically represented as:

$$\begin{aligned} x(t) &= (1-t)\, x_i + t\, x_{i+1} \\ y(t) &= (1-t)\, y_i + t\, y_{i+1} \end{aligned} \tag{1}$$

where t is the parameter of the line equation and $t \in [0, 1]$. In addition, assume the tool rotates in a clockwise sense and the radius is r. Two parameters u_1 and u_2 are computed for classifying an edge into three categories: pure entry edge, pure exit edge, and entry-exit edge according to Table 1 [7].

$$\begin{aligned} u_1 &= (y_{i+1}-y_i)\sqrt{r^2 - x_i^2} + (x_{i+1}-x_i)\, x_i \\ u_2 &= (y_{i+1}-y_i)\sqrt{r^2 - x_i^2} + (x_{i+1}-x_i)\, x_{i+1} \end{aligned} \tag{2}$$

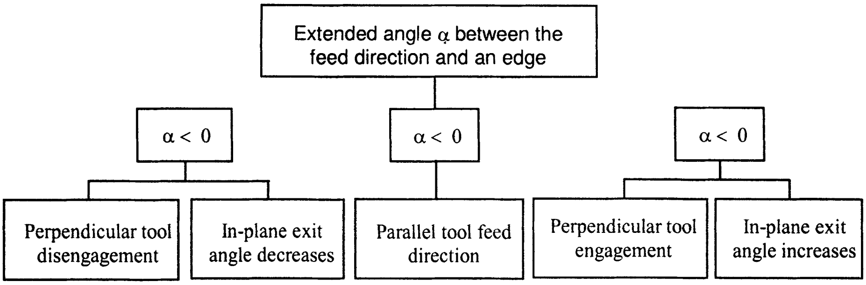
Extended angle α between the feed direction and an edge
α < 0
α < 0
α < 0
Perpendicular tool disengagement
In-plane exit angle decreases
Parallel tool feed direction
Perpendicular tool engagement
In-plane exit angle increases

Figure 7. Edge classification scheme

3.2. Tool Engagement Computation

Each burr formation criterion employs distinct parameters for burr type prediction. However, they all require tool engagement information including (1) the in-plane exit angle, (2) the initial tool contact point, and (3) undeformed chip geometry. The calculation of the in-plane exit angle is described in our previous work [11]. Given an arbitrary point (x(t), y(t)) in an edge $\mathbf{e}_i$, the corresponding in-plane exit angle Ψ at this point is expressed as:

$$\Psi = \cos^{-1}\left[\frac{(x_i - x_{i+1})\cdot\sqrt{r^2 - x(t)^2} + (x_{i+1} - x_i)\cdot x(t)}{r\cdot e}\right] \tag{3}$$

If one edge contains both an exit and an entry region, it is necessary to find the point that separates the two regions. For this to happen, the tool must touch the workpiece edge at the initial contact point **p** (Figure 8). The following geometrical equations can be used to compute the x coordinate of **p**. Once the x coordinate is obtained, the y coordinate can be calculated by using the line equation of the edge.

$$p_x = \frac{r(y_{i+1} - y_i)}{\sqrt{(x_{i+1} - x_i)^2 + (y_{i+1} - y_i)^2}} \tag{4}$$

Two parameters are necessary for describing the undeformed chip geometry: the undeformed chip thickness $C_{t,u}$ and undeformed chip width $C_{w,u}$. The undeformed chip width is identical to the depth of cut. The undeformed chip thickness can be calculated by:

$$C_{t,u} = \frac{2f\pi r}{iv_c}\cos(\Psi - 90^\circ) \tag{5}$$

where f = absolute feed rate, i = number of inserts, v_c = cutting velocity, r = tool radius, and Ψ = the in-plane exit angle

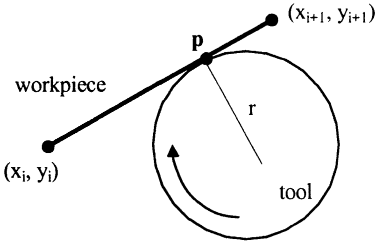

Figure 8. Initial tool contact point

3.3. Inquiry generation and burr prediction

Our previous studies found that the in-plane exit angle Ψ, the undeformed chip ratio $C_{r,u}$, and the undeformed chip area $C_{a,u}$ can be used as parameters to develop empirical equations, enabling the milling burr type prediction. Note that

$$C_{r,u} = \frac{C_{w,u}}{C_{t,u}}, \quad C_{a,u} = C_{w,u} C_{t,u} \tag{6}$$

where $C_{w,u}$ and $C_{t,u}$ have been defined in the last section. The burr control chart proposed for use here contains a two-dimensional space constructed by $C_{r,u}$ and $C_{a,u}$. Two transition curves divide the 2D space into three regions that correspond to, respectively, the presence of primary burr, the wavy burr, and the secondary burr. A typical burr control chart is shown schematically in Figure 9. Based on the experimental data, the transition curves are assumed to have the general equation:

$$C_{r,u} \sqrt[3]{C_{a,u}^2} = \rho_j(\Psi) \tag{7}$$

```
If gradient is positive
        return secondary burr
If gradient is negative
    •   calculate transition in-plane exit angles from experimental data
    •   separate the workpiece edge into
        $\Psi \in$ [0, transition angle 1]                        return secondary burr
        $\Psi \in$ [transition angle 1, transition angle 2]    return wavy type burr
        $\Psi \in$ [transition angle 2, 180°]                     return primary burr
```

Algorithm 1. Burr prediction rules in the existence of a in-plane exit angle gradient

where ρ_j is a constant determined by the in-plane exit angle. For j = 1, the above equation represents the transition curve from the primary to the wavy-type burr, whereas the transition curve from the wavy-type to the secondary burr is represented with j = 2. These transition constants are determined from the experimental data. The in-plane exit angle gradient is a crucial factor for burr formation along edges at an angle to the feed direction. Our previous experimental study [9] has shown that a negative in-plane exit angle gradient exhibits the transitions between the secondary, primary, and wavy burrs. A positive gradient, on the other hand, tends to produce just secondary burrs. Therefore, the rule used to predict the burr type in the existence of an in-plane exit angle gradient is shown as in Algorithm 1.

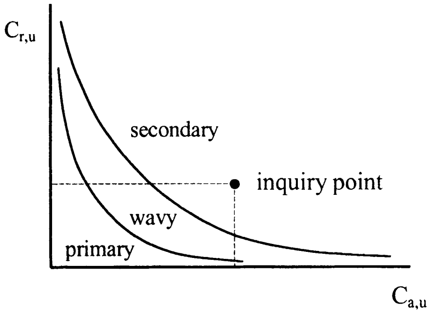

Figure 9. A typical burr control chart

```
In tool engagement
    Divide the edge into
        entry region            return entry burr
        exit region             return secondary burr

In tool disengagement
    Divide the edge into
        entry region            return secondary burr
        exit region             return primary burr
```

Algorithm 2. Burr prediction rules in tool engagement and disengagement

If the tool feed direction is perpendicular to a workpiece edge, there still exists an in-plane exit angle gradient but the value range in which the in-plane exit angle varies is so small that it is not proper to consider this case as the case with transition constants as we did in the previous section. Therefore the burr formation criterion used contains only simple rules shown in Algorithm 2

4. SIMULATION RESULTS

Figure 10 shows a test example for the burr type prediction and simulation. The circle indicates the cutting tool. The thick white parallel lines represent the tool path, and the dotted lines represents fast motion of the tool. Note that the single-direction tool path is used in this case. Different burr types are denoted with different colors along the workpiece contour, including the primary burr, the secondary burr, the wavy burr, and the entry burr. This system is implemented with C++ language, and

OpenGL is used for the graphic outputs. The burr prediction functionality can be further extended and integrated into other process planning modules for minimizing exit burr formation. For instance, Figure 11 shows the simulation result of the same example indicating how the total primary burr length varies with the depth of cut. The sudden drop in the figure represents the critical depth of cut [1]. With this simulation result, process planners can easily select appropriate cutting parameters for edge-precision planning. Automatic process planning for enhancing edge quality can be thus achieved.

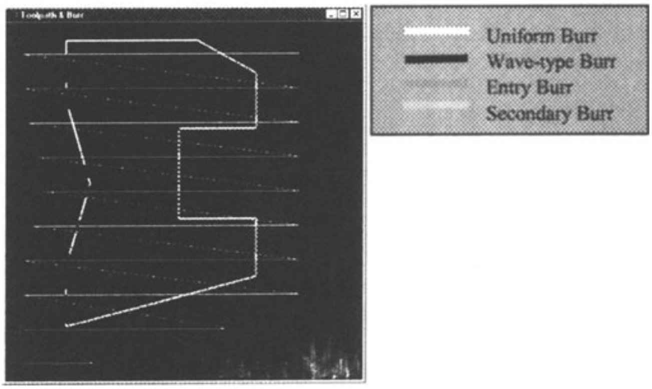

Figure 10. Burr prediction and simulation result

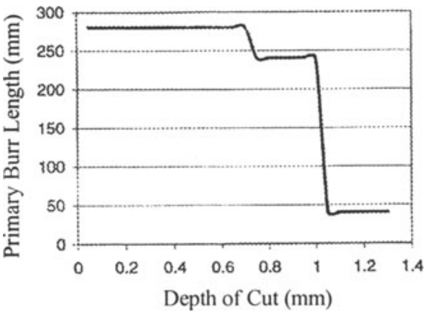

Figure 11. Influence of the depth of cut on primary burr length

5. CONCLUSIONS AND FUTURE WORK

This study has proposed a burr prediction and simulation system that estimates the burr type and burr location in planar milling. A framework has been established that links experimental data on burr formation to the process planning stage. This approach overcomes the difficulties of using experimental findings obtained with different data analysis methods and represented in various forms. A clean interface between geometric factors and material-related factors is also introduced. This study provides effect tools for edge-quality process planning. Future work is to allow quick data collection so that the estimation of burr size can be realized. The Internet technologies will be used to enable the automatic updating of the current burr formation database. In addition, interfaces with other process planning modules need to be developed, including operation, tool path, and deburring planning.

REFERENCES

[1] Chern, G.L., Analysis of Burr Formation and Breakout in Metal Cutting, Ph.D. Dissertation, University of California at Berkeley, Department of Mechanical Engineering, 1993.

[2] Park, I., Modeling of Burr Formation Process in Metal Cutting, Ph.D. Dissertation, University of California at Berkeley, Department of Mechanical Engineering, 1996.

[3] Kishimoto, W., Miyakw, T., Yamamoto, K. and Takano, K., "Study of Burr Formation in Face Milling," *Bulletin Japan Society of Precision Engineering*, Vol. 15, No. 1, March 1981.

[4] Gillespie, L.K. and Blotter, P.T., "The Formation and Properties of Machining Burr," *ASME Journal of Engineering for Industry*, Vol. 98, No. 1, Feb., 1976, pp. 66-74.

[5] Chu, C.H., "A Framework for Burr Minimization in a CAD/CAM Integrated Environment, " Research Report, LMA, University of California at Berkeley, 1999-2000.

[6] Chu, C.H. and Dornfeld, D.A., "Tool Path Planning for Avoiding Exit Burr," *Journal of Manufacturing Processes*, Vol. 2, No. 2, pp. 116-123, 2000.

[7] Narayanaswami, D. and Dornfeld, D.A., "Burr Minimization in Face Milling: A Geometric Approach," *Journal of Manufacturing Science and Engineering*, Vol. 119, 1997, pp. 170-177.

[8] Link, R., Gratbildung und Strategien zur Gratreduzierung bei der Zerspanung mit geometrisch bestimmter Schneide, Dissertation, RWTH Achen, Germany, 1992.

[9] Chang, A. "Burr Data Generation and the Effect of a Gradient In-Plane Exit Angle on End Milling Burrs in Stainless Steel 304L," M.S. Report, University of California at Berkeley, Department of Mechanical Engineering, 1997.

[10] Trommer, G., Study on Burr Formation in Milling with an Extreme Positive Axial Rake Angle, M.S. Thesis, University of California at Berkeley, Mechanical Engineering Department, 1997.

[11] Chu, C.H. and Dornfeld, D.A., "Tool Path Planning for Exit Burr Minimization by Estimating the Total Length of Primary Burrs," submitted for publication, *International Journal of Computer Integrated Manufacturing*, 2000.

Chih-Hsing Chu
Research Assistant

David Dornfeld
Professor

Laboratory for Manufacturing Automation
Department of Mechanical Engineering
University of California at Berkeley, Berkeley, CA 94720-1740

Christian Brennum
Graduate Student

Department of Production and Quality Engineering
Norwegian University of Science and Technology
Trondheim, Norway

J.F. CHATELAIN, C. FORTIN

OPTIMAL WORKPIECE LOCALIZATION FOR MACHINING APPLICATIONS

Abstract: This paper presents a new approach to the workpiece localization problem in machine tools for optimal machining. The proposed localization algorithm is based on a preferential constrained optimization problem solved at each iteration of a global process which aims to best align a sparse data set of points, representing the workpiece, with respect to a corresponding CAD solid representation of the nominal part. The simplex method of direct search is selected to minimize a logarithmic objective function formulated for the workpiece balancing problem. This function is defined to solve the problem of having insufficient stock allowance during a machining operation for complex parts. In those cases, the approach preferentially orients the lack of material during the balancing process, in order to simplify the rework operation. The technique is applied to the balancing of a turbine blade.

1. INTRODUCTION

The part setup for machining applications is one of the most important operations in the entire manufacturing process. When properly achieved, the casting or forging part localization, with respect to the machine tool reference coordinate system, ensures productivity and expected quality for the part and the manufacturing process. Such localization is particularly critical for large and complex parts for which the blank or workpiece part size and shape is specified close to the design model. In these applications, stock allowances are generally very small, because their specification directly affect the workpiece related manufacturing costs, which depends on the volume of material required, as well as the time and resources required to remove the excess material through the machining operation. In this context, even small deviations produced by the blank part manufacturing process, may result in a shortage of material during the machining of the part, if a previous balancing of the material was not performed during the setup operation. In these cases, the part is either scrapped or reworked following material addition, through an appropriate welding process for example. The balancing of a workpiece would compensate for the part's deviations by finding a proper stock distribution with respect to the part bosses or datums involved in its reference frame localization into the machine-tool fixture.

This work presents an innovative computer assisted tool for the automatic part localization process, which optimally balances workpieces such that the corresponding reference frame is properly set from machine offsets or tool path compensation to insure sufficient stock allowance, when possible. For workpieces where no feasible solution is found possible, the algorithm determines how the shortage of material can be located in order to minimize the rework costs of the part. The proposed system is

P. Chedmail et al. (eds.), Integrated Design and Manufacturing in Mechanical Engineering, 247-254.
©2002 *Kluwer Academic Publishers.*

integrated to a solid modeler, from which the parts to be machined are specified. The balancing process is expressed as a three-dimensional alignment problem of a data cloud, representing the workpiece as manufactured and inspected, with respect to its corresponding nominal part solid model.

Some research teams have already found different solutions to the alignment problem from measurement data. They are mostly related to the geometric tolerance verification rather than to the balancing of blank parts. Some solutions concern the fitting of data points to find the optimal parameters of substitute geometries of perfect form, while others best adjust the data points to given surfaces through three-dimensional alignment algorithms. Concerning the first approach of best fitting geometries, the techniques evaluate the geometric errors either from elementary geometrical substitution (plane, circle, cylinder, etc.) [1], [2], or from more complex geometries involving interpolation techniques like Kriging for example [3]. More related to the balancing problem, the alignment techniques of points over geometries interested different research teams in the same area of coordinate metrology but also in robotics for locating parts with respect to manipulators. In this field, Gunnarsson [4] developed an algorithm to align dense or sparse data to polyhedral, quadric and parametric surfaces. Sahoo and Menq [5] developed an alignment technique applicable without any limitation on the type of surface on which it applies. Bourdet and Clement [6], innovated with their complex surfaces control through the small displacement screw technique. Other research teams developed techniques specifically related to the alignment of NURBS (non-uniform rational b-spline) surfaces over data clouds [7], [8]. This latter work innovates in aligning measurement points within analytically defined tolerance zones. Jinkerson et al. [9] formulated their alignment problem in order to constrain the points to be inscribed inside a tolerance zone that is symmetrically defined on either side of a nominal surface of control. Their technique applies to the quality control of a blade for the naval industry.

Concerning the alignment techniques directly applied to the balancing of blank parts, Beshko and Bazhenov [10] developed one for the turning application of large cylindrical parts, like turbine shafts or hydraulic press columns, from forging workpieces. Their technique finds the best workpiece axis for avoiding shortage of material during machining. Li [11] and Chu [12] developed a constrained alignment technique for the localization problem of blank and in-process workpieces based on linear programming optimization. Their technique stops when no feasible solution is found.

Our proposed approach innovates in being able to preferentially orient any missing material when no feasible balancing solution exists. The technique is based on a three-dimensional alignment mechanism of a workpiece, defined through a data set of points captured from the workpiece, over the corresponding CAD nominal model.

2. THE CONSTRAINED LOCALIZATION ALGORITHM

The localization algorithm will properly answer the following question: “Given the solid model of a part, is there enough material in a corresponding workpiece for it to be completely machined within its specifications?” When found possible, this means the machining occurs with sufficient stock allowance during the complete process. Then, the algorithm will compute the best part localization, or part reference frame compensation, in order to minimize the maximum stock found on any part surface. On the other hand, if one or more areas of the workpiece is missing material, then the algorithm will balance the part in order to locate it based on a minimum rework effort.

Thus, in any case, the localization algorithm must compute a rigid transformation R^*, including three translations and three rotations, which best satisfies two objectives. First, the maximum stock allowance shall be minimized without leading to any missing material area, or “machineless” gouging, on the part surfaces. Second, when areas missing material are found to necessarily occur, they will be located to user-predefined part areas in order to ease the reworking process of the part.

This problem finds its solution through an iterative process bringing closer, at each step, a measurement data set to the corresponding nominal solid model. In fact, the model corresponds to the final part to be obtained after the completion of the machining process, while the data set is related to the coordinate measurement of the workpiece being localized. During the iterative optimization process, the points are brought closer to the model with respect to a constraint set related to the preferential distribution of missing material, when it is found to occur. The solid model definition of the part is required to discern outside points from inside points, the inside ones meaning a missing material area. This deficit of material is mathematically defined through a negative Euclidean distance measured between the transformed measurement point at a current iterative and the corresponding nominal model. The minimax criterion applied to the distances is used for the solution of the optimization problem at each iteration of the localization process. The process converges to a feasible solution, when existing, or to a solution which forces the missing material to specific areas based on the user specifications. Figure 1 shows the successive improvement of a solution for one iteration of the localization process. For each iteration “k”, “np” nominal points D_i^k are calculated to be the nearest to their corresponding transformed measurement points ($M_i^k = R^{*(k-1)} \circ M_i^{(k-1)}$). Both D_i^k and M_i^k are used in the calculation of the oriented Euclidean distance for the optimization problem to solve at the current iteration, as expressed below. The optimal transformation calculated at the previous iteration “k-1”, $R^{*(k-1)}$, as well as the measurement point $M_i^{(k-1)}$ are both involved in the calculation of the position of M_i at the current iteration “k.” At the end of the process, the transformation matrix R^* results from the concatenation of all the optimal transformations calculated at each global iteration $R^{*(k)}$.

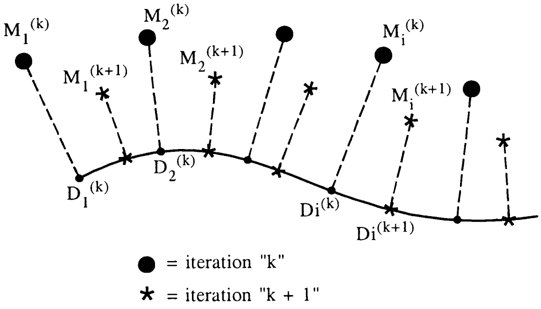

Figure 1. Global iterative improvement process of a solution

The constrained optimization problem to be solved at each iteration tries to push inside points to the outside of the solid model based on user priorities. As mentioned above, the oriented distance d_{oj} is required to discern inside (negative distance) from outside points during the alignment process. This distance is calculated based on the type of surface on which it applies. It is different whether the surface is planar, cylindrical, spherical or of free form type. The expression of this oriented distance is explained at the next section for a cylindrical surface. In order to insure a minimum stock allowance, this distance value is constrained to be higher than a predefined limit ε. In fact, these constraints applied with a different weight for each surface defines the constraint set of the optimization problems to be solved in our localization iterative process. This non-linear constrained optimization problem is solved using the simplex method of direct search. This one transforms the constrained problem into an unconstrained formulation by considering an artificial function F_{art} that severely penalizes the objective when one or more constraints are found unsatisfied. This function has no effect when all the constraints are satisfied. In this case, only the minimax real term "F_{real}" of the objective function is evaluated. The problem formulation is expressed as the following:

$$minimize\ U = F_{real} + F_{art} \tag{1}$$

$$with,\quad F_{real} = MAX[\, d_i \,],\, i = 1,\ldots,np \tag{2}$$

$$d_i = \left\| d_i \right\| = \left(d_{xi}^2 + d_{yi}^2 + d_{zi}^2 \right)^{1/2} \ and\ d_i = R \cdot M_i^{(k)} - D_i^{(k)} \tag{3}$$

$$R = \begin{bmatrix} c\varphi c\theta & (c\varphi s\varphi s\psi - s\varphi c\psi) & (c\varphi s\theta c\psi + s\varphi s\psi) & T_x \\ s\varphi c\theta & (s\varphi s\theta s\psi + c\varphi c\psi) & (s\varphi s\theta c\psi - c\varphi s\psi) & T_y \\ -s\theta & c\theta s\psi & c\theta c\psi & T_z \\ 0 & 0 & 0 & 1 \end{bmatrix} \tag{4}$$

where R is the "Roll, Pitch and Yaw" matrix definition with "s" and "c" being respectively the sine and cosine functions, and,

$$F_{art}=\sum_{j=1}^{nv}\{\ 1E(23\omega_j+3)\cdot[21+LOG(\ d_{oj}^2\ )]\ \}\ ,\ \ F_{art}=0\ if\ \ d_{oj}\geq-\varepsilon \quad (5)$$

The F_{art} value, when non-zero, depends on the oriented distance amplitude and on the violated points weight, found inside the solid model. This weight is introduced based on the importance of having a shortage of material on a specific area of the part. The logarithmic artificial function has been specially defined to force the process to satisfy the constraints under a decreasing order of priority, beginning with weight values of 9 and ending with the weight values of 0. This mean a point with weight value equal to 9, will be pushed outside the model before any other point with lower weight .

3. ORIENTED EUCLIDEAN DISTANCE d_{oj} AND THE ζ CORRECTOR

The oriented distance expression depends on the geometry. Our approach considers exact formulations for planar, cylindrical and spherical surfaces while it considers a spherical approximation for any other type of surface. The following shows the expression of the distance for a cylindrical surface, referring to Figure 2:

$$d_{oj}=SIGN[\ |\ r_{cyl}\ |\ -\ |R^{(it)}\ {}^{\circ}M_j-S_c-\zeta|\ ]\cdot|\ d_j\ |\ \ for\ a\ concave\ surface\ with\ r_{cyl}<0 \quad (6)$$

$$d_{oj}=SIGN[\ |R^{(it)}\ {}^{\circ}M_j\ -S_c-\zeta|\ -\ |\ r_{cyl}\ |\ ]\cdot|\ d_j\ |\ \ for\ a\ convex\ surface\ with\ \ r_{cyl}>0 \quad (7)$$

$$with,\ \ C_c=D_j-r_{cyl}\cdot n_j\ \ and\ \ S_c=[\ (\ R^{(it)}\ {}^{\circ}M_j-C_c\ )\cdot t\ ]\cdot t+C_c$$

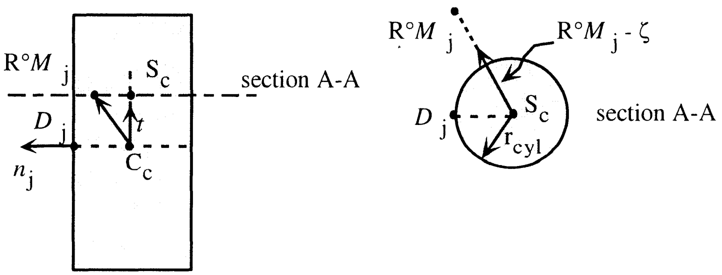

Figure 2. Oriented distance for a cylindrical surface

As shown in Figure 2, a corrector ζ is introduced in the oriented distance calculation to take into account two compensations. The first compensation relates to a minimum stock allowance possible to assign for specific part areas, when the default value ε is found inappropriate. The second compensation corrects for the workpiece lack of definition, using discrete measurement points. It is represented in Figure 3 for a cylinder using the λ_j notation. As shown in this case, the alignment of the blank with respect to the nominal part could lead to a feasible solution with sufficient stock while in fact, a shortage of material exists. When the corrector is considered, this error type is reduced or eliminated, depending on the geometry. This correction becomes more and more important as the workpiece geometry significantly differs from its corresponding nominal representation. The expression of the corrector for cylindrical surfaces is expressed below.

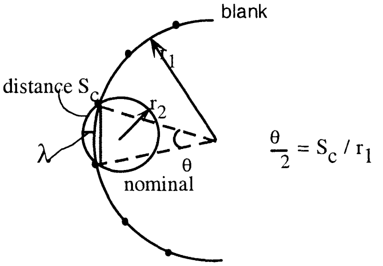

$$\lambda_j = r_1 \cdot \cos\left(\frac{\Theta}{2}\right) - \sqrt{r_2^2 - [r_1 \cdot \sin\left(\frac{\Theta}{2}\right)]^2} + r_2 - r_1 \qquad (8)$$

Figure 3. Corrector for a cylindrical blank part definition

4. EXAMPLE

To show the algorithm behavior and the effect of the weighting factors, let consider the balancing of a hydroelectric turbine blade having a bounding box size of about 4x3x1 meter (Figure 4). In this case, 26 points were simulated on face 4, 21 on face 5, 5 on the trailing edge and 3 points on the remaining faces 0 and 1. The points are simulated to have a shortage of material equal to 12.7 millimeters all around the part. In a first scenario, all points have the same weight value of zero, as a starting point of the process. As shown in Table 1, faces 1, 2 and 4 result with respectively 3, 5 and 23 inside points to the model, while faces 0 and 5 are saved from any shortage. The optimal parameters as well as the resulting minimum and maximum oriented distances are given in the table. In order to save face 4 instead of face 5, and face 1 prior to the other faces, the following weighting scenario would be required: $\omega_0 = \omega_2 < \omega_1 < \omega_5 < \omega_4$. The second column of Table 1 shows the results related to this weighting. None of the faces 0, 1 or 2 is satisfied, since those directly affect the deviations for faces 4 and 5. As required through the weighting, face 4 is a priority compared to face 5 and the stock allowance for face 4 is minimized in order to keep the shortage on opposed face 5 the smallest as possible.

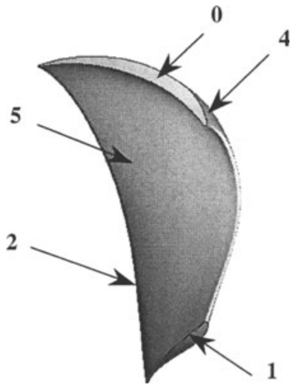

Figure 4. Turbine blade surfaces

Table 1. Two weighting scenarios

Weight	$\omega_j=0$	$\omega_0=\omega_2=0,\ \omega_1=5,$ $\omega_4=8,\ \omega_5=7$
ψ, θ, φ (deg.) T_x , T_y , T_z (mm.)	-0.03, -0.06, -0.44, 11.33, 18.09, -6.27	-0.03, -0.05, -0.44 -23.73, 29.79, 2.04
U_{real} (mm)	164.78	148.79
$(d_{e\omega})_{MAX}$ (mm)	23.28	17.51
$(d_{e\omega})_{MIN}$ (mm)	-36.39	-37.98
face /unsatisfied	4 / 23, 2 / 5, 1 / 3	5 / 20, 2 / 5, 0 / 3, 1 / 3

5. CONCLUSION

In this work, an innovative approach to the localization problem of casting or forging workpieces has been presented. The technique is unique due to its ability to orient any unavoidable shortage of material to specific areas following the user specifications. The algorithm consists of a global iterative process improving the solution at each step through the resolution of a constrained optimization problem using the simplex method of direct search. A specially developed logarithmic artificial penalty function has proven to be very efficient and compatible to the balancing problem. The approach has been applied to the balancing of a hydroelectric turbine blade to emphasize the behavior of the logarithmic function as well as the weighting factors effect. The technique developed works well for applications having a limited number of measurement points.

It has to be tested and further optimized for applications referring to a dense data representation of the workpieces.

Jean-François Chatelain, Ph.D., eng.
Professor, Department of Mechanical Engineering
École de Technologie Supérieure
1100 Notre Dame Street West, Montreal, Quebec, Canada H3C 1K3
Tel.: (514) 396-8512, fax: (514) 396-8530,
e-mail: jfchatelain@mec.etsmtl.ca

Clément Fortin, Ph.D., eng.
Professor, Department of Mechanical Engineering
École Polytechnique de Montréal
P.O. Box 6079, Station A, Montreal, Quebec, Canada H3C 3A7
Tel.: (514) 340-4711, fax: (514) 340-5867,
e-mail: clement.fortin@polymtl.ca

6. REFERENCES

[1] Fukuda, M., Shimokohbe, A., "Algorithms for Form Error Evaluation - Methods of the Minimum Zone and the Least Squares", Proc. of the Int. Symp. on Metrology for Quality Control in Production, Tokyo 1984.

[2] Elmaraghy, W.H., Wu, Z., Elmaraghy, H.A., "Evaluation of Actual Geometric Tolerances Using Coordinate Measuring Machine data", Manuf. Review, Vol.3, No.1, 1990.

[3] Nassef, A.O., Limaiem, A., ElMaraghy, H.A., "On the Accurate Evaluation of Geometric Deviations from CMM Data", Proc. of the 5th CIRP Seminar on Computer Aided Tolerancing, Toronto, Ontario, Canada, pp.277-291, 1997.

[4] Gunnarsson, K.T., Prinz, F.B., "CAD Model-Based Localization of Parts in Manufacturing", Computer, Vol.20, No.8, 1987.

[5] Sahoo, K.C., Menq, C.H., "Localization of 3-D Objects Using Tactile Sensing and Surface Description", ASM, Production Engineering, 1988.

[6] Bourdet, P., Clement, A., "A Study of Optimal-Criteria Identification Based on the Small-Displacement Screw Model", Annals of the Cirp, Vol.37, No.1, 1988.

[7] Patrikalakis, N.M., Bardis, L., "Localization of Rational B-Spline Surfaces", Engineering with Computers, Vol.7, No.4, pp.237-52, 1991.

[8] Choi, W., Kurfess, T.R., "Data Localization Algorithms and Minimum Zone Evaluation for Automated Inspection", Concurrent Product Design, DE-Vol.74, pp.39-46, 1994.

[9] Jinkerson, R.A., Abrams, S.L., Bardis, L., Chryssostomidis, C., Clement, A., Patrikalakis, N.M., Wolter, F-E., "Inspection and Feature Extraction of Marine Propellers", Journal of Ship Production, Vol.9, No.2, pp.88-106, 1993.

[10] Beshko, Y.N., Bazhenov, V.A., "Use of Gauging Robots for Marking-Out Blanks in One-Off and Small-Batch Production", Soviet Engineering Research, Vol.7, No.10, 1987.

[11] Li, Z., Gou, J., Chu, Y., "Geometric Algorithms for Workpiece Localization", IEEE Transactions on Robotics and Automation, Vol.14, No. 6, Dec. 1998.

[12] Chu, Y.X., Gou, Li, Z.X., "On the Hybrid Workpiece Localization / Envelopment Problems", Proc. of the 1998 IEEE Int. Conf. on Robotics and Automation, May 1998.

E. V. BORDATCHEV

ANALYSIS AND MAPPING OF THE DYNAMIC PERFORMANCE OF HIGH-PRECISION MOTION SYSTEMS

Integrated Manufacturing Technologies Institute
National Research Council of Canada

Abstract. The research reported in this paper aims at improving the dynamic performance of motion systems by analysing and mapping the non-uniformity of feed motion within the travel area. This paper (a) develops the real-time measuring of the feed motions through built-in position encoders, (b) considers the feed motion as a space-time random process, and (c) applies analysis in order to evaluate and map the dynamic performance. The dynamic performance as a "dynamic imprint" of the entire motion system is represented by the dynamic/statistic characteristics of feed motion. The transfer function of the motion system as a dynamic operator, which transforms prescribed motion into actual motion, is applied to model the dynamic performance. The results of the experimental investigations, analysis, and mapping of the dynamic performance indicate a wide range of industrial uses of the developed approach for certification, diagnostics, and tool path optimisation purposes to achieve highest accuracy for a particular motion system.

1. INTRODUCTION

The high-precision motion system is a complex electro-mechanical assembly consisting of a base, the electro-mechanical drives, and translation tables to provide the feed motions. The ideal motion system must provide good correlation of the actual motion attributes (tool path, feedrate, acceleration, *etc.*) to the predetermined ones. However, industrial and laboratory practice indicates that there are considerable tracking and contouring errors and variations within feed motions [1-5]. Up until now, the dynamic performance of motion systems has been associated with positional accuracy and trajectory tracking capabilities. The positional accuracy calibration is based on static measurements where the worktable is moved to a desired position several times and the distribution of the errors is analysed. This approach mainly deals with the repeatability of reaching a desired position and does not take into account the actual behaviour of motions. The accuracy of trajectory tracking is a measure of a motion system's ability to follow the prescribed trajectory [6]. Specifying trajectory-tracking accuracy is not always enough for some machining processes. For example, the laser machining process needs to synchronize the motion and laser pulses to provide constant material removal [7]. This discussion emphasizes various aspects of the motion system operation to characterize its performance. Therefore, for this paper, the dynamic performance of a motion system is understood as the ability to provide a prescribed motion, and the manner in which a motion system provides the motion. Thus, the dynamic characteristics of a motion are indicators of the system's dynamic performance.

P. Chedmail et al. (eds.), Integrated Design and Manufacturing in Mechanical Engineering, 255-262.
©2002 *Kluwer Academic Publishers.*

This paper develops a dynamic calibration approach [3-5] for analysing and mapping the dynamic performance of motion systems by means of the spatial distribution of feedrate variations within the travel area. Knowing the mapping allows us to recognize "sweet" spots with lowest non-uniformity of motion in order to optimise the workpiece location on the table to achieve the highest level of accuracy for a particular motion system. In addition, the mapping of motion is understood as a "dynamic imprint" of motion system dynamic performance and can be used for certification, diagnostics, and control purposes.

2. DEFINITION OF DYNAMIC PERFORMANCE

According to *Webster's Dictionary*, [8] performance is an ability to perform and the manner of reacting to stimuli. Applying this fundamental definition towards a motion system, the dynamic performance is the ability to provide a prescribed motion with specified attributes (tool path, feedrate, acceleration, etc.) and the dynamic manner in which the system provides the motion. To be unambiguous, the engineering meaning of the words “ability” and “manner” needs to be specified. Thus, the dynamic parameters and characteristics of a motion are suggested as indicators of system dynamic performance as shown in Figure 1. In other words, how an actual motion is similar to a prescribed one is analogous to the characterization of the system dynamic performance. In this case, the prescribed and actual motion is considered as a time-space random process; e.g., “feedrate with respect to (wrt) position” $v(x)$ or “feedrate wrt time” $v(t)$. Fundamentally, the representation of dynamic performance is based on the combined observation and analysis of position, feedrate (velocity) and acceleration as random processes. In addition, the dynamic performance can be modelled and estimated by the transfer function of the motion system. This definition is also useful if we mathematically model the motion system as a dynamic operator, which transforms prescribed motion into actual motion. The magnitude of the transfer function is commonly referred to as the gain factor wrt feedrate $|W_{v_0 v}(j\omega)|$ and is shown as follows:

$$|W_{v_0 v}(j\omega)| = \sqrt{S_{vv}(\omega)/S_{v_0 v_0}(\omega)} \tag{1}$$

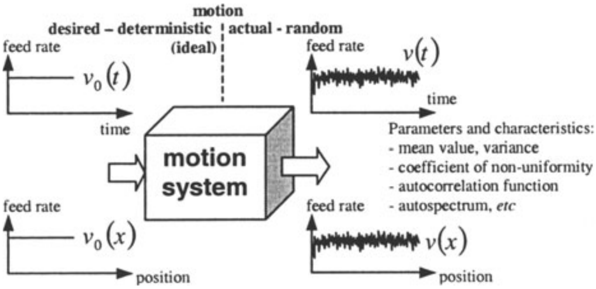
motion
desired – deterministic
(ideal)
actual - random
feed rate
$v_0(t)$
time
feed rate
$v(t)$
time
motion system
Parameters and characteristics:
- mean value, variance
- coefficient of non-uniformity
- autocorrelation function
- autospectrum, *etc*
feed rate
$v_0(x)$
position
feed rate
$v(x)$
position

Figure 1. Motion system dynamic performance.

where $S_{v_0 v_0}(\omega)$ is the autospectrum of the prescribed (ideal) feedrate v_0, $S_{vv}(\omega)$ is the autospectrum of the actual feedrate v, ω is the frequency, and $\mathrm{j} = \sqrt{-1}$.

3. EXPERIMENTAL SET-UP AND FEEDRATE ANALYSIS PROCEDURE

A multi-axis positioning system was used for signal measurements and data collection. The worktable consists of a granite base fitted with precision translation tables (with air bearings) for X and Y movements. The travel area of XY-table is 203.2x203.2 mm. The linear motors #LM210-16.80-3-AC:WD2 (Trilogy Systems Corp.) provide the feed motions and the corresponding linear encoders LS403 (HEIDENHAIN Corp., encoder resolution $\Delta\ell$ = 0.5 μm) furnish the positional feedback for the control system. The data related to linear motions was collected by using PCI-MIO-16XE-10 (National InstrumentsTM) I/O card. All measurements were carried out for 203.2 mm feed movement in X and Y directions. Data was collected during the experiments as a "feedrate wrt position" process along X-direction $v(x)$ and along Y-direction $v(y)$ with $\Delta x = \Delta y = 2.032\,mm$. The elements of matrixes $\mathrm{M}_y(x)$, $\mathbf{G}_y(x)$, $\mathrm{M}_x(y)$, and $\mathbf{G}_x(y)$, which are statistical parameters $v_{\max} - v_{\min}$ and σ_v, were calculated on length $\delta_x = \delta_y = 1.016\,mm$.

The investigations were carried out by using built-in positional encoders as a source of data for the feedrate analysis. The collected information represents a sequence of impulses, where the period of each impulse precisely corresponds to the encoder resolution $\Delta\ell = const$. The data acquisition technique consists of measurements of period for each impulse T_i, $i = 1:N$, where N is the number of measured periods. Calculations allow obtaining "feedrate wrt position" $v(x)$. This process $v(x)$ carries a significant property, such that the position scale $x = (1:N)\Delta\ell$ is even in space. This property permits the application of statistical analysis to determine the characteristics of the feed motion as a space-time random process. For the feedrate analysis the following parameters, which characterize actual dynamic performance, were calculated: highest $v_{\max}$ and lowest $v_{\min}$ values of $v(x)$; mean μ_v; coefficient of non-uniformity K_v; variance σ_v; difference $\mu_v - v_0$.

4. MOTION SYSTEM BEHAVIOUR FOR DIFFERENT FEEDRATES

The observed acceleration stage was measured for different feedrates ranging from 2.52 mm/s to 12.7 mm/s. Figure 2 illustrates the dynamic behaviour of these motions corresponding to the individual feedrates. From this data it can be seen that the "manner" of the acceleration stage characterizes the dynamic performance of the motion system kinematics and the control system. The acquired data indicates that the length of the acceleration stage λ increases with the increase in the feedrate, along with the amplitude of the feedrate variations during the motion, resulting in a decrease in the overall system performance. The calculated values of feed motion parameters such as λ, $v_{\max}$, $v_{\min}$, μ_v, K_v, σ_v, and $\mu_v - v_0$ for motion feedrates from 2.52 to 12.7 mm/s are detailed in Table 1.

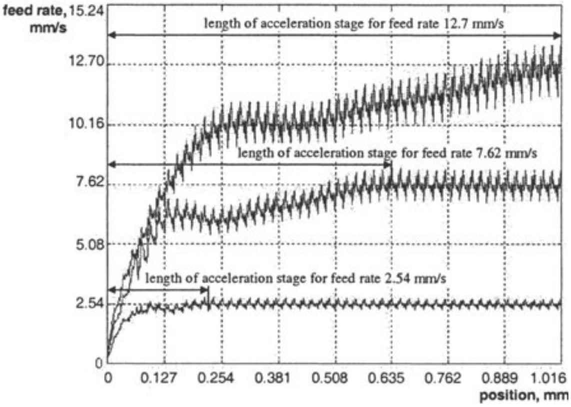

Figure 2. Actual acceleration stage of motions with different feedrates.

Table 1: Feed motion parameters

feedrate v_0, *mm/s*	2.54	7.62	12.70
length of acceleration stage, mm	0.203	0.635	1.016
$v_{\max}$, *mm/s*	2.896	8.484	14.097
$v_{\min}$, *mm/s*	2.184	6.528	11.227
$v_{\max}$ - $v_{\min}$, *mm/s*	0.712	1.956	2.870
μ_v, *mm/s*	2.54	7.62	12.70
K_v, *%*	28.301	25.456	22.472
σ_v, $(mm/s)^2$	0.01584	0.11198	0.31336

From Table 1, the following inferences can be drawn:

- Motion achieves the desired feedrate that characterizes excellent technical perfection for the motion system under consideration.
- The length of the acceleration stage increases with the increase in the prescribed feedrate, along with the amplitude of feedrate variations resulting in a decrease in the overall system performance.
- The coefficient of non-uniformity, K_v, remains relatively constant.
- The variance of the feedrate, σ_v, increases exponentially as feedrate increases.

The above analysis provides only an estimation for the non-uniformities of motion, which characterize the system dynamic performance. It does not recognize the sources and nature of disturbances which caused the non-uniformities. Comparing motion signatures at different feedrates can help to identify these disturbances. Figure 3 shows comparative motion signatures for feedrates 2.5 mm/s and 12.7 mm/s along the X axis. Although the dynamics of the motion system differs, the signature of motion does not change. Both motion signatures have uniform shape and a constant period of 20 μm; however, the amplitude of fluctuations increases wrt feedrate. Figure 3 also illustrates power spectral densities for feedrates 2.5 mm/s and 12.7 mm/s. It was observed that the source of the kinematic disturbances for the period of feedrate fluctuations of 20 μm corresponds to a dominant spatial frequency of 50 periods/mm. The calculated coherence function demonstrates a linear relationship between the two motions with a corresponding spatial frequency of 50 periods/mm and its harmonics. In addition, the spatial frequency harmonics of 2x50 periods/mm, 3x50 periods/mm, *etc.* also indicate the presence of the kinematic disturbances wrt their location.

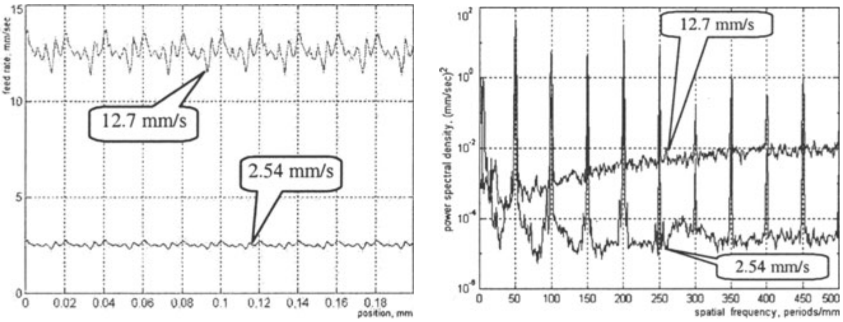

Figure 3. Spatial signatures (left) and power spectral densities (right) of different motions.

5. MAPPING PROCEDURE

Nowadays, the mapping procedure has been used as a method to reduce positional errors, such as lead-screw errors, backslash, *etc.* Based on prior measurements of the actual position of a table, the desired positions are corrected. Opposite to that static approach, the mapping of dynamic performance is based on measuring and recording the stable motion excluding the acceleration and deceleration stages. The measured data, for example, $v_{y=fix}(x)$, represents the dynamic signature of motion along the X direction for a given Y coordinate. The set of data for different $y = fixed$ shows the XY distribution of $v(x)$ for the total travel area for a prescribed feedrate v_0 and direction of movement. The data $v_{y=fix}(x)$ and $v_{x=fix}(y)$ are reorganized into matrixes $\mathbf{V}_y(x)$ and $\mathbf{V}_x(y)$, where each row $v_{k\Delta y}(1:N_x)$, $v_{\ell\Delta x}(1:N_y)$ represents the measured feedrate wrt position; Δx is the distance along the X direction between two consecutive measurements in the Y direction; Δy is the distance along the Y direction between two consecutive measurements in the X direction; $k = 0,\ldots,K$; $\ell = 0,\ldots,L$; $K+1$ is the number of measurements along the X direction, and $L+1$ is the number of measurements along the Y direction. The parameters $v_{\max} - v_{\min}$ and σ_v were calculated within the specified range of δ_x and δ_y correspondingly along Λ_x and Λ_y for each $v_{k\Delta y}(1:N_x)$, $v_{\ell\Delta x}(1:N_y)$. Afterwards, parameters were reorganized into corresponding matrixes of amplitude of feedrate variation $\mathbf{M}_y(x)$ and variance $\mathbf{G}_y(x)$ completely covering the XY travel area. The final result of mapping is the contour plot of $\mathbf{G}_y(x)$ representing the dynamic performance.

6. MAPPING OF DYNAMIC PERFORMANCE

The mapping is targeted on analysing the dynamic performance over an XY travel area that is represented by the contour plots of matrixes $\mathbf{M}(x)$ and $\mathbf{G}(x)$. Results of the XY-table mapping are presented for two different feedrates (2.5 mm/s and 12.5 mm/s) as an example of dynamic performance distribution. Figure 4 illustrates XY distribution of $\mathbf{M}_y(x)$ and $\mathbf{G}_y(x)$ for forward (+X) and backward (-X) motions. The analysis shows that the dynamic performance of a motion system represented by the dynamic behaviour of XY motions has a quite complex spatial distribution. The contours and values in the XY distribution remain the same if experiments are repeated under the same conditions. The variations in the XY distribution are caused by the system response on resistance to feed motion. The feedrate signatures represent the system response. The dynamic and kinematic disturbances form the actual resistance. The system response to resistance depends on the direction and feedrate of the motion. It follows that XY distributions have similarly shaped contours and different values; for example, compare matrixes $\mathbf{M}(x)$ or $\mathbf{G}(x)$ for the same direction of motion but with different feedrates. Direction of motion (+X or -X) significantly changes the contours and the values of the XY distributions. Experiments show that the difference in feedrate variation is higher for +X motion than for -X motion. These features characterize the dynamic performance of a motion system and provide the potential for individual tool path optimisation to achieve the highest accuracy for a particular motion system.

7. SUMMARY AND CONCLUSIONS

To improve the dynamic performance of high-precision motion systems, a new approach to analysis and mapping has been developed using a time-based technique to measure the actual motions as a “feedrate wrt position” process. The definition of dynamic performance was introduced as the technical ability to provide a prescribed motion with specified attributes (tool path, feedrate, acceleration, *etc.*) and the dynamic manner in which the system provides the motion. The parameters of motions, such as the difference between process mean value and the desired feedrate, coefficient of non-uniformity, variance, power spectrum density, and the coherence function were analysed to characterize the actual dynamic performance of the motion system.

The time-based technique was applied to measure the motion as a space-time random process. Motions with different feedrates were investigated in order to evaluate the dynamic performance. Experimental results indicate that:

- The length of the acceleration stage increases with the increase in the feedrate, along with the amplitude of prescribed feedrate variations, resulting in a decrease in the overall system performance.
- The coefficient of non-uniformity remains relatively constant for all feedrates.
- The variance of motion increases exponentially with the feedrate.
- The statistical analysis of feed motions allows separation of kinematic and dynamic disturbances and locates the respective sources.

The mapping of feedrate non-uniformity was utilized to characterize the XY distribution of dynamic performance. The obtained contoured plots of feedrate parameters show that:

- The direction of motion significantly changes the dynamics of motion.
- The resistance to motion is formed by dynamic and kinematic disturbances; is estimated by the XY distribution of feedrate variations and variance; and represents the dynamic performance of the motion system.
- The XY distribution of the motion parameters symbolizes a "dynamic imprint" of a motion system and highlights the "sweet" spots that correspond to the highest accuracy due to the lowest non-uniformity of feedrate.

In addition, the results of the experimental investigations, analysis, and mapping of dynamic performance indicate wide range of industrial uses of the developed approach for certification, diagnostics, and tool path optimisation purposes to achieve highest accuracy for a particular motion system.

8. ACKNOWLEDGEMENTS

Thanks are due to Mr. Moe Islam, Director of Research, IMTI-NRC, and Dr. Suwas Nikumb, Group Leader, for their continued support in this work. The author also appreciates the assistance of his colleagues, Mr. Hugo Reshef, Mr. Craig Dinkel, and Mr. Gary Yeung for their help in performing the experimental work.

9. REFERENCES

1. Chiu GTC Tomizuka M. Coordinated Position Control of Multi-Axis Mechanical Systems. ASME J of Dynamic Systems, Measurement, and Control 1998;120:389-393.
2. Altintas Y. Direct Adaptive Control of End Milling Process. Int Journal of Machine Tools & Manufacturing 1994;34:4:461-472.
3. Bin HZ, Yamazaki K, DeVries MF. A stochastic approach to the measurement and analysis of lead-screw drive kinematic errors. J of Engineering for Industry. 1984;106:339-344.
4. Bordatchev EV, Afanasiev AV. Software/hardware analytical complex. Russian Engineering Research. 1993;13:3:55-60.
5. Postlethwaite SR, Ford DG, Morton D. Dynamic calibration of CNC machine tools. Int J of Machine Tools & Manufacturing. 1997;37:3:287-294.
6. Vukobratovic M, Filipovic M. Dynamic accuracy of robotic mechanisms. Part 1: Parametric sensitivity analysis. Mechanism and Machine Theory, 1999;35:221-237.
7. Bordatchev EV, Nikumb SK. Laser material-removal process as a subject of automatic control. Proceedings of the ASPE Annual Meeting; 1999 Oct 31-Nov 5; Monterey, CA, USA; 236-239.
8. Webster's Dictionary, http://www.m-w.com/

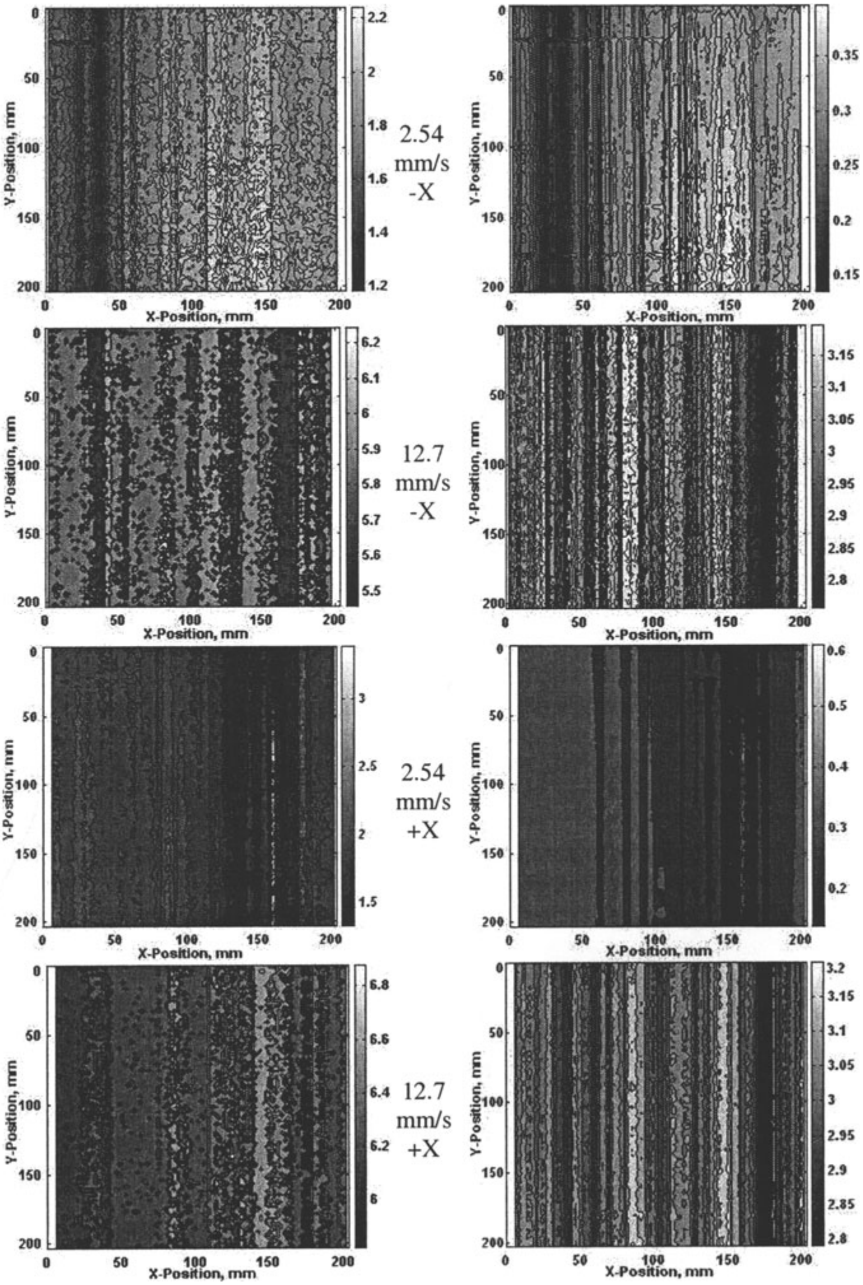

Figure 4. Variations (left) and variances (right) of different motions.

M. GEIGER, A. KACH

INTEGRATION OF LASER MATERIAL PROCESSING INTO THE COMPUTER-AIDED PRODUCT AND PROCESS DEVELOPMENT

Abstract. Many high-tech products consist of laser-manufactured products. Therefore one of the most important demands is the integration of data necessary for laser material processing into computer-aided (CA) product and process development. This paper focuses on technical data exchange to improve communication, especially in areas where simultaneous engineering is applied. The aim is the integration of CA systems providing information about processes as well as laser-manufactured products. Attention is mainly paid to laser welding, although laser beam processing can be applied to many machining methods in the manufacture of products. By using the product data technology of STEP and special laser welding features, an advanced, neutral data exchange is possible. In this paper the development of laser-manufactured products is first analyzed. Afterwards, the data integration with STEP is described.

1. INTRODUCTION

The development of laser-manufactured products puts high demands on programming robots and gantries. Therefore off-line programming (OLP) systems were developed for the generation of NC/RC programs [1][2]. However, OLP systems can only be efficiently used in combination with CAD systems. That means OLP and CAD systems must be integrated.

The integration of time and space separated development processes is usually realized by neutral data formats [3]. In the field of laser material processing the exchange of neutral data is usually restricted to geometry because of the sequential proceeding of OLP systems. The CAD model of the workpiece is a free form surface, which is described using the VDA/FS, IGES or STEP (Standard for the Exchange of Product Model Data) [1][2]. Although this data exchange seems to be sufficient for the information flow from CAD systems to OLP systems, it is no solution in the sphere of small lot or job shop manufacturing or simultaneous engineering, in which more knowledge has to be transported by data formats.

Due to the problem of vertical and horizontal data integration, this paper focuses its attention on laser welding. The communication interfaces are designed for STEP to realize international data exchange possibilities. This standard has never been used for the exchange of product model data in the field of laser material processing before. So this paper shows abilities and limits of STEP.

P. Chedmail et al. (eds.), Integrated Design and Manufacturing in Mechanical Engineering, 263-270.
©2002 *Kluwer Academic Publishers.*

2. LASER WELDING

For welding applications the well-defined monochromatic and coherent laser beam (LB), which is emitted by specific laser sources like CO_2 lasers or Nd:YAG lasers, is sharply focused to deliver high process energy to very small interaction areas. This high energy density beam leads at a focused power density in the order of 10^6 W/mm^2 to a keyhole in the workpiece. Laser welding differs from gas or arc welding due to this deep penetration effect. The keyhole movement along given contours forms weld seams with characteristic aspect ratios, weld depth in relation to width, between 2:1 and 6:1. The advantages of laser welding are welding speeds of several meters per minute, a total heat input which is lower than that achieved by arc welding, aesthetic appearance, simplified design, reduced component size and reduced post-weld machining. Furthermore, the heat-affected zone is very narrow and the workpiece has only little weld distortion. Examples for laser welding can be found in many products – electronic, medical, automotive and machine tool. [4]

3. DEVELOPMENT OF LASER-MANUFACTURED PRODUCTS

The development of laser welded products is a complex procedure which involves modifications in product and process planning during the development phases. The design department provides the geometry of the workpiece and machining contours for downstream departments like work scheduling or process planning. This vertically and sequentially oriented development can cause increasing time and cost for manufacturing, e.g. in the case of critical contour segments. These segments are characterized by the loss of constant tool centre point (TCP) velocity along the contour.

To avoid the deterioration in the areas in which the laser-velocity ratio is changed the designer can modify the curvature of his construction or he can use path-planning strategies, e.g. extending the area of the head orientation. That means the designer needs more information or restrictions in fields of knowledge which is not in his daily work.

Usually a job shop manufacturer should produce parts without changing the whole design. Therefore, it is important for the design department to know the limitations in advance. Another aspect is that the process planers want to know very early whether they have to change or order machines or tools. Consequently, the transfer of knowledge from downstream departments into upstream ones is important. However, this feedback and integration of knowledge into the product and process development of laser-manufactured products is not realized yet.

4. REQUIREMENTS FOR COMPUTER-AIDED PRODUCT AND PROCESS DEVELOPMENT

The reusage of computer applications data can minimize the time and money spent on data exchange, consistency and redundancy problems. Besides the transformation of sequential into parallel running product developments, one of the main demands is the transfer of knowledge into the early phases [3]. Therefore, this paper also defines laser welding features and associated constraints to enable designing of laser-welded products within the limits of a given manufacturing configuration, and to avoid multiple, expensive loops of design changes.

The product model for laser material processing consists of submodels. These models concerning geometry, product and resources can be used alone or in complex combinations to describe processes by using specialized technology data. The various product states are referenced by process inputs and outputs. Consequently, laser material processes can be integrated into process structures describing the complete sequence of various processes for the manufacture.

The transformation of a state is described by entities, which are called operations and operation_properties. The operations contain the technology data that precisely define the machine or tool operations which can be subdivided into positioning, clamping and manufacturing. The degree of detail of the first two operations depends on the stage of automation. The production operations, however, always have to be specified in detail. As machines allocated for the same manufacturing task may vary, due to modification in technique or change of supplier, the information is represented not only machine-dependently, but also machine-independently (fig. 1). Thus OLP systems are able to generate specific control data on the basis of already predetermined, machine-independent data.

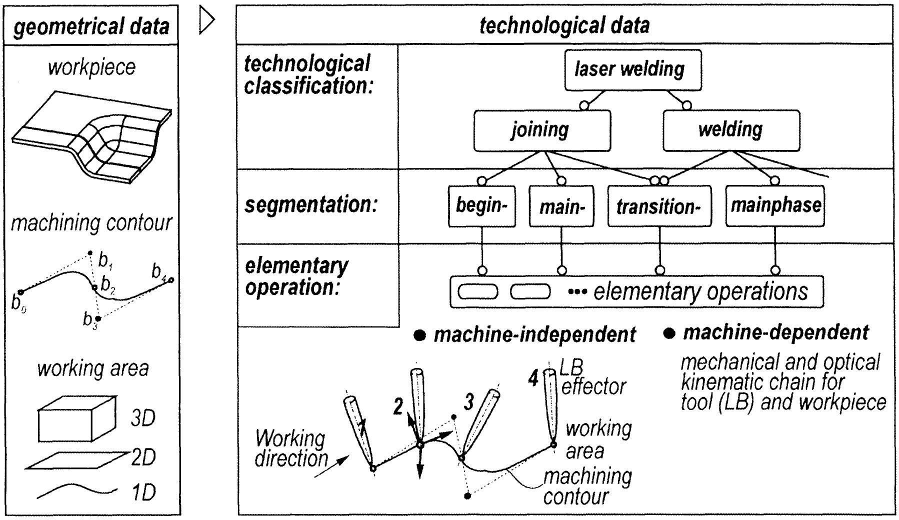
geometrical data
workpiece
machining contour
b_0
b_1
b_2
b_3
b_4
working area
3D
2D
1D
technological data
technological classification:
laser welding
joining
welding
segmentation:
begin-
main-
transition-
mainphase
elementary operation:
••• elementary operations
• machine-independent
• machine-dependent
mechanical and optical kinematic chain for tool (LB) and workpiece
Working direction
1
2
3
4
LB effector
working area
machining contour

Figure 1. Description of laser processes

There are two types of machine-independent representations: geometrical and technological ones. The geometrical description is e.g. the mathematical representation of a workpiece, machining contour and working area. Different models like non-topological surface and wireframe, manifold surfaces with topological or advanced boundary representation solids are used as a starting point for OLP activities. The models and the associated mathematical descriptions like B-splines are interpreted by the program or by the user. Hence machines, tools, clamping devices, workpieces and machining contours can be represented geometrically and linked to suitable technological data structures. The conversion of geometrical machining contours into elementary operations is saved into a technology-oriented data structure (fig. 1). An elementary operation is defined by discrete states, intermediate states are interpolated. At the fulcrums of the tool paths frames are placed in which technology points are defined. These points include information about TCP, orientation of effect and technological parameters for laser material processing like feed rate and laser power. All operations can be associated with process plans, where the machine-dependent descriptions are allocated. These descriptions contain instructions for machines involved, mainly given as NC/RC programs.

A characteristic technology property of laser material processes is the way the laser and the workpiece are moved in relation to each other. The cinematic system of the laser machine consists of mechanical and optical axes. The mechanical mechanism controls the processing head or/and the workpiece. The optical axes are used for laser beam guiding and forming so that, e.g. the focus plane and radius can be controlled.

Other parameters for laser welding to be controlled include the position of beam centerline relative to weld seam, the position of beam focal plane relative to surface, beam intensity, scan speed and ambient atmosphere at the weld site, along the trailing edge and on the underside of weld.

The linking of machine or resource models to elementary operations enables OLP systems to generate adequate NC/RC programs.

To avoid losing technological information, the elementary operations are integrated into a hierarchy including two other domains, segmentation and technological classification. The segmentation level is responsible for the reproduction of four phases, namely start-, main-, end- and transition-phase, which take short delays during NC-program processing into account; as a consequence, mandatory auxiliary tool paths like approach or departure paths are required. The technological classification domain is needed for the definition of manufacturing processes like laser welding, where the technological attribution defines joining and welding operations.

The necessity of this hierarchy can be shown by manufacturing tasks like shaft-hub joint configurations with axial welding. To obtain less distortion the process is subdivided into five segmentation phases including two main phases. In the first main phase a welding operation with minimum penetration depth is carried out to achieve a fixed part with little distortion. Afterwards, the second main phase continues welding of the whole machining path with deep penetration. Without the reproduction of the technological sequences and classifications of the individual operations a lot of process information or knowledge is lost.

Another possibility for the integration of laser material processing is the use of features to provide the developers with a set of meaningful engineering aides. In general, the features consist of restricted product areas which can be represented by geometry and semantic information. The features can be classified into horizontal and vertical ones. Moreover, constraints are allocated to features to maintain the semantic validity of feature-based models and to introduce or support modification operations on the product model [7].

In the case of laser welding, a vertical feature and its constraints are needed. Therefore, different joint configurations like butt, lap or T butt welds are analyzed. In fig. 2, an example of a lap seam (a) illustrates the characteristics of the joint and in (b) a general feature for joining is presented. The lap joint shows three joining faces and two parts, both being expressed geometrically. The lap seam is represented by the joining line. Several global or local constraints depending on the respective machine can be attached to manufacturing features, e.g. penetration depth, type of joint or range of curvature.

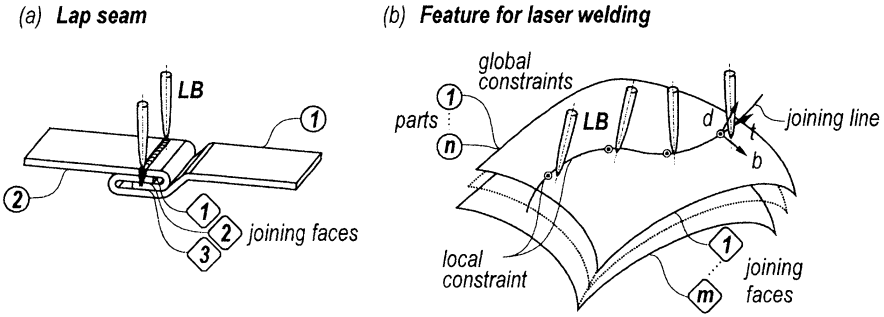
(a) **Lap seam**

(b) **Feature for laser welding**

Figure 2. Joint example (a) and a general feature for laser welding (b)

5. DATA INTEGRATION WITH STEP

After specifying the requirements for an integrated process development of laser-manufactured products these data are to be reproduced with the product data technology of STEP defined and described in the International Standard 1030. The aim of this standard is to define models and a methodology for supporting the data exchange during the whole product life cycle, independent from any particular system. STEP is suitable not only for neutral data exchange, but also for implementing and sharing product databases. A fundamental concept of STEP is defining application protocols (AP) as mechanisms for specifying information requirements and for ensuring reliable communication. An AP is a part of ISO 10303 that defines the context, scope and information requirements for applications and constructions of integrated resources. It furthermore specifies the requirements for conformance testing of AP implementations. Therefore, STEP can exchange data in compliance with standardized product models. The data specification language EXPRESS is used to specify the information which is to be represented. The documentation of an application protocol comprises an Application Activity Model (AAM), an Application Reference Model (ARM), an Application Interpreted Model

(AIM) and a set of conformance and testing requirements. There are several APs used to meet different industrial requirements within the framework of STEP like the AP 212, Electrotechnical Plants or the AP 214, Core Data for Automotive Mechanical Design Processes [5].

In order to apply STEP it must be analyzed which of the APs are more suitable for the reproduction of information requirements. The starting point of the examination is always the AAM or/and ARM. As the EXPRESS-defined ARM represents the context of the application, the successful mapping of the information requirements into the ARM leads to a suitable AP. Another mapping, specified by mapping tables of the AP leads to the AIM, used for the implementation of STEP interfaces. The definition of the AIM is provided by a set of integrated resources concerning generic information models like Part 42 of ISO 10303, Geometric and Topological Representation or application specific models like Part 105, Kinematics. The integrated resources are interpreted by the modification and addition of constraints, relationships and attributes.

6. REPRODUCTION OF INFORMATION REQUIREMENTS WITH STEP

There are three possibilities of integration with STEP product data technology. First, the development of a new application protocol helps to solve the problems of laser material processing. However, this proceeding is mainly applied for internal data exchange, e.g. in order to integrate two different information areas [8]. Secondly, an already standardized application protocol can be extended with to laser-specific data structures. But both methods face the loss of standardized and international data exchange as a consequence. Furthermore, there is no statement concerning the integratability of laser material processing in standardized and important application protocols like the AP203 (Configuration Controlled Design) or the AP214 (Core Data for Automotive Design Processes). In this paper the integration of the information requirements into standardized application protocols is presented.

To realize the potential of an international data exchange standard, existing application protocols must be analyzed to find out which one can reproduce the information needed for laser manufacturing tasks. For this reason, the AP 214 [5] was analyzed, due to its industrial importance and due to several intersections with many application protocols like the AP 207 (Sheet Metal Die Planning and Design) or the AP 213 (Numerical Control Process Plans for Machined Parts). The AP214 supports various stages of development during the design of technical products and mainly refers to the automotive industry´s requirements. The quantity of data exchange is growing in this industry because the development of subsystems is given to suppliers, so that consequently not only the geometry has to be exchangeable but also the technology data. The AP214 neutrally describes the product as well as processes and manufacturing resources/systems, in order to improve or enable communication among different data processing systems for designing, configurating and simulating the manufacturing systems. In the AP validation protocol of AP214 [6] some examples of industrial relevance are given, e.g. Machining Features for Press Die Machining or Process Plan for Equipment Design.

In general, application protocols including resource constructs of part 10303-49 (Process Structure and Properties) are suitable for technological data exchange for laser material processing requirements only on condition that the specific interpretation of the application protocols is checked. To realize the process in general part 49 defines the relationships within the process and between the processes, the efficiency of a process, the properties of a process, the resources, the properties of the resource, the representation of the process, the representation of the resource, and the relationship of the process to the product. It should be pointed out that all these elements of the process can be represented in a discrete manner. Since the abovementioned defined structure for laser material processing conforms to this constraint, the major subdivisions like method definition, process property and process property representation of part 49 can be applied. With this application reference model various process_operation entities can be instanced and assigned to products and process plans. The entity general_process_property enables the assignment of laser material process parameters, e.g. the laser power. The product forming process is represented by combining the entity process_state with item _version and design_discipline_item _definition. By using the attribute relation_type of process_operation_relationship the process operation can be structured e.g. as decomposition or series. The resources of the process can be related to the process through process_operation_resource_assignment.

As far as the Integrated Resources are concerned, the mapping of features with STEP seems to be difficult, because the part 10303-48 Form Features was cancelled. Within this form feature model the laser welding feature can be represented by using the general_feature. For the reproduction of the necessary constraints the AP214 offers no mapping.

Although the information requirements of laser material processes can be reproduced within the context of the AP214 in which the structured instanced entities for laser welding are not standardized. Therefore, interpretation problems can occur. That could be the reason why CAD system developers present only a solution for a submodel of the AP214. Up to now an AP214 interface of a CA systems offers in most implementations the same options as AP203 interfaces.

To overcome the difficulties, the gap between standardized vocabulary and symbols for laser material processing, e.g. EN ISO 11145 or EN ISO 11146 on the one side and standardized generic data structures on the other side must be closed by introducing an intermediated information level. In the following, the STEP interface is divided into levels for geometry, laser material processing and AP 214 data structures, and includes special database converters (fig. 3). The STEP data are located in databases assigned only to one application program. With the aid of database converters, the information can always be converted into the right context, e.g. geometry or laser material processes. The main advantage of this bi-level architecture is that the data exchange between CA systems is standardized and that system developers only need the implementation of the database converter between their CA system and the second level. The mapping of the laser specific data structure to the standardized application protocol is universal and must only be programmed once.

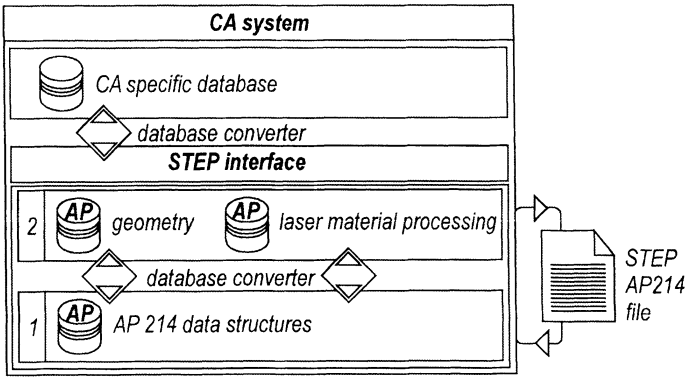

Figure 3. STEP interface architecture

Manfred Geiger, Chair of Manufacturing Technology
Andreas Kach, Bavarian Laser Center gGmbH

7. ACKNOWLEDGEMENTS

The authors gratefully acknowledge the financial support from AnySim, EDAG, Memmert and Bavarian Research Foundation for Laser Technology within the FORLAS program.

8. REFERENCES

[1] Backes, F.; Geiger, M.; Franke, V., "Technology Oriented Off-Line Programming for 3D Laser Material Processing", in: Technical Papers of the 24th North American Manufacturing Research Conference NAMRC ´96, Dearborn, Society of Manufacturing Engineers (SME), 1996, pp. 214.
[2] Geiger, M.; Pursche, L.; Backes, F., "Macro and Micro – Off-Line Programming of 3D Laser Systems in all Dimensions", in: IX. Internationales Produktionstechnisches Kolloquium PTK ´98, Berlin, IWF, 1998, pp. 255.
[3] Lincke, W., "Simultaneous Engineering", München, Carl Hanser, 1995.
[4] Dawes, C., "Laser Welding", New York, McGraw-Hill, 1992.
[5] Mohrmann, J.; Katzenmaier, "ISO/CD 10303-214 – Part 214: Core Data for automotive mechanical Design", Genf, TC184/SC4/WG3/P19 N578, 1994.
[6] Mohrmann, J.; Donges, C., "ISO/CD 10303-214 – Part 214: AP Validation report of ISO/CD 10303-214", Genf, TC184/SC4/WG3/P19 N574, 1994.
[7] Vieira, A. S.; Ovtcharova, J.; Jasnoch, U., "Consistency Management Aspects in SINFONIA", in: Modelling and Graphics in Science and Technology, Springer, Berlin, 1996.
[8] Abeln, O. (Eds.), "Innovationspotentiale in der Produktentwicklung: Das CAD-Referenzmodell in der Praxis", Stuttgart, Teubner, 1997.

M. RACHIK - J.M. ROELANDT - A. MAILLARD

INVESTIGATION OF SHEET METAL BLANKING PROCESS

Abstract. In this paper, we present a comprehensive experimental and numerical study of sheet metal blanking process. Various blanking tests with different materials and geometry are investigated and the numerical results are compared with experiments. For the numerical aspects of this study, the main discussed topics are sheet metal constitutive model, numerical integration algorithm and mesh adaptivity.

1. INTRODUCTION

The sheet metal blanking process consists in separating a blank from a sheet by a punch. It combines material plastic flow and ductile fracture. The main characteristics associated with the blanking operation are the global behavior related to the punch force versus the punch displacement curve and the cut edge shape (burr size). The force-displacement curve (figure 1) first presents an increasing evolution until a maximum corresponding to a plastic instability is reached. Then, ductile fracture is developed until the separation of the blank from the sheet. It should be noticed that the maximum punch force is an important parameter for tool dimensioning and calibration.

Given a blanking configuration defined by part material, sheet thickness and part shape, there are some relevant parameters for blanking operation like punch shape, clearance, friction.... The choice of these parameters is generally based on empirical knowledge even if several research works were devoted to the process modeling and it's numerical simulation. In this area, some analytical models based on the tension zone theory [1] were developed to estimate the maximum punch force. But such models are not suitable to study the influence of all the parameters. Moreover, their use is limited to plane strain problems. Contrary to this approach, the finite element simulation is more efficient since it is more adapted to the complex constitutive models and the general boundary conditions. The finite element approach is primarily characterized by the way of taking into account the ductile fracture, the load stepping algorithm and the mesh adaptation technique. Concerning the ductile fracture, the commonly used models are based on a critical value of a damage variable and its evolution law [4]. Among the available models, the most popular are the Rice-Tracy model based on the growth of void and its critical size [4], [5], the Gurson - Tvergaard - Needleman model based on the void volume fraction evolution [5], [6], [7] and the models that use the Katchanov's formalism like the Lemaître model [8]. Schematically, two approaches can be used to take into account the damage:

- When using the discrete approach, the fracture is modeled by the onset and the growth of a discrete crack. The fracture occurs when one or more criteria are reached. The simulation is often based on a standard elasto-plastic model while

P. Chedmail et al. (eds.), *Integrated Design and Manufacturing in Mechanical Engineering*, 271-278.
©2002 *Kluwer Academic Publishers.*

the damage variable is calculated by the integration of its evolution law along the process in an uncoupled way. This approach is combined with a mesh adaptation technique to accommodate for the crack propagation [9], [10].

- In the continuum damage approach, the damage evolution is directly taken into account in the equilibrium iterations. When the failure criteria is reached in an element, the element is deactivated or numerically eroded [11].

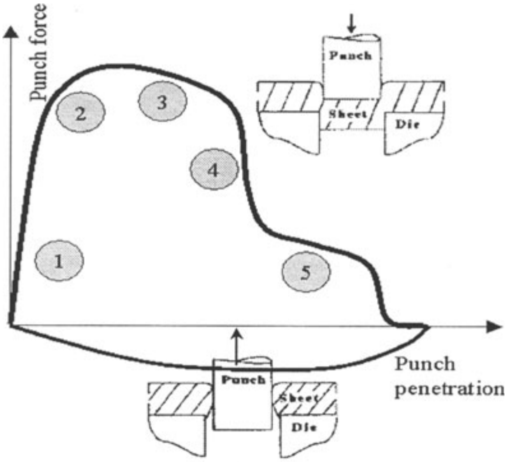

Figure1. Schematic representation of punch force - punch displacement diagram

In numerical simulation of sheet metal forming processes, the problems one can encounter are related to high kinematics non linearities, material non linearities and frictional contact. For sheet metal blanking process the damage leads to additional difficulties. To overcome these difficulties, several numerical techniques can be used (static implicit [10], [11], dynamic explicit or static explicit [13], [14], [15], [16] methods). Several commercial codes based on the previously cited techniques are available to simulate such processes. Each technique has its disadvantages: the implicit scheme is often limited by convergence problems and computational cost whereas the explicit method suffers from the stability condition and the oscillations of the solution. In addition, sheet metal blanking process involves large inelastic deformations and changing boundary conditions. The latter suggests the use of adaptive mesh techniques to guarantee the solution reliability. These methods can be classified essentially in two groups. In the first group, one encounter the Arbitrary Lagrangian Eulerian (ALE) formulations. For this class of methods, the evolutions of the mesh and material particles are uncoupled, and the mesh is moved to prevent excessive element distortion [9], [12] and [17]-[20]. The second class of methods is based on global remeshing techniques. The deformed configuration is rediscretized at certain load steps and the history dependent state variables are properly transformed from the distorted mesh to the new mesh. The main drawback of this method is the rapid increase of the total number of degrees of freedom that leads to a prohibitive computational cost. In addition, the whole domain is rediscretized and additional computational effort is required to handle boundary conditions and contact state [9], [11], [14], [21] and [22].

Our work is a comprehensive numerical and experimental study in which we evaluate the efficiency of some finite element methods that are commonly used in sheet metal blanking simulation. We have used two numerical models. The first one is based on an ALE finite element method (ABAQUS / Explicit) [23]. The second one is based on an implicit approach associated with global remeshing techniques (MARC) [24].

2. EXPERIMENTAL ASPECTS

Various blanking tests were performed with different geometries. In this work, one material is investigated (FePO4 steel). The material characteristics values of this steel are: E=210000 MPa (Young's modulus) and σ_y =223 MPa (initial yield stress). For all the tests, the sheet thickness t and the die radius R_d are hold constant (t=1.9 mm, R_d = 4.5 mm). Different punch radius (R_p) are used to examine the clearance influence on the punch force. The clearance j is usually expressed as a percent of the sheet metal thickness.

3. MODELLING AND NUMERICAL ASPECTS

From a numerical simulation point of view, three significant aspects were studied within the framework of this project, namely the sheet metal constitutive model, the load stepping algorithm and the mesh adaptivity.

3.1. Constitutive model

Concerning the sheet metal constitutive model, we compare a classical elastoplastic model with a porous plasticity model. In this section, we briefly recall the constitutive relations associated with the Gurson-Tvergaard-Needleman's model that can be considered as a generalization of the Prandtl-Reuss plasticity model to porous media. For this damaging model, schematically, ductile fracture involves four successive damage processes, namely the nucleation of voids from inclusions, the void growth, the coalescence of voids and the crack propagation. In our study, we use the Gurson's model modified by Tvergaard and Needleman [5], [6]. This model is defined by the following relations. The yielding surface is defined by:

$$\Phi = \frac{\sigma_{eq}}{\bar{\sigma}} + 2 q_1 f^* \cosh\left(-q_2 \frac{3\sigma_m}{2\bar{\sigma}} \right) - \left(1 + q_3 f^{*2} \right) = 0 \tag{1}$$

σ_{eq} is the effective equivalent stress and $\bar{\sigma}$ is the yielding stress; q_1, q_2 and q_3 are adjustable material parameters. The material capacity rapidly decreases when void coalescence occurs. This phenomenon is modeled using the parameter f*:

$$f^* = \begin{cases} f & \text{if } f \le f_c \\ f_c + \left(\bar{f}_F - f_c \right)\left(f - f_c \right) / \left(f_F - f_c \right) & \text{if } f_c \le f \le f_F \\ \bar{f}_F & \text{if } f \ge f_F \end{cases} \tag{2}$$

f_c is the critical void volume fraction, f_F is the void volume fraction at failure and $\overline{f}_F = 1/q_1$ when $q_3 = q_1^2$.

It should be noted that when the void volume fraction is zero the previously described model reduces to the classical Prandtl-Reuss plasticity model.

3.2. Numerical integration algorithm and mesh adaptivity

In numerical simulation of sheet metal forming processes, the vast majority of approaches for solving the equilibrium non linear equations are based on Newton-Raphson iterative scheme. The convergence problems of this method has motivated the development of several explicit (non iterative) algorithms. But as mentioned above, each technique has its disadvantages. In this work, the considered blanking tests were investigated using two load stepping algorithms. The first one is based on an explicit dynamic scheme associated with the Arbitrary Lagrangian-Eulerian approach to handle mesh adaptivity. The second method is based on the Newton-Raphson iterative scheme. The mesh adaptivity is ensured using a global remeshing technique. The remeshing is performed according to a user's specified frequency and maximum element size. Figure 2 gives a comparison between the two previously described approaches.

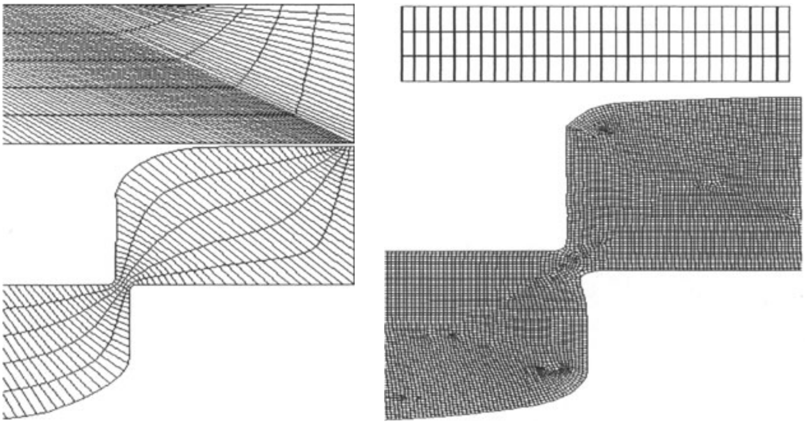

Figure 2. Initial and deformed mesh, comparison between ALE and global remeshing

4. APPLICATIONS

4.1. Constitutive model comparison

The maximum punch force, which is an important parameter in sheet metal blanking process, is strongly related to the sheet constitutive model. Most studies on numerical simulation were carried out with a damage model. In this section, we clearly show that the maximum punch force is essentially governed by the plastic instability. Figure 3 shows a comparison between a classical elastoplastic model (isotropic hardening) and a damage model for the investigated material.

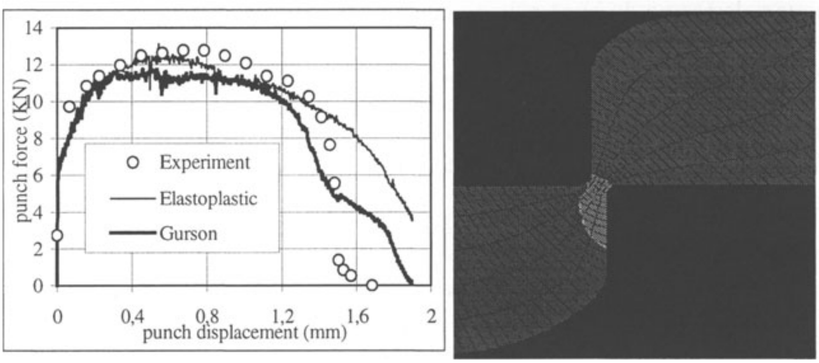

Figure 3. Elastoplastic and Gurson model – burr shape

When a standard elastoplastic model is used, one can examine the total equivalent plastic strain to have an idea on the burr shape. But it is not possible to highlight the difference between traction and compression using such quantity. On the other hand, the damage model makes possible to have a good idea on the burr shape starting from the void volume fraction . Figure 3 shows a burr shape prediction using the damage model. The numerical result is compared with an observed burr shape [10].

4.2. Load stepping algorithms and adaptivity

In this section, we compare the numerical results obtained by an implicit iterative algorithm based on the Newton-Raphson scheme with those obtained by an explicit dynamic scheme. The implicit algorithm is associated with a global remeshing method while the explicit scheme is associated with an ALE approach. It should be noted that the calculations are performed with an elastoplastic constitutive model. Figure 4 shows a comparison between the two approaches. We can notice that the two approaches give similar results.

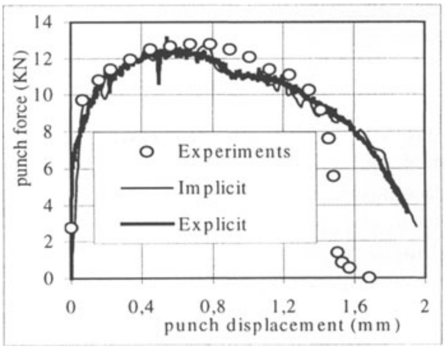

Figure 4. Implicit and explicit schemes

4.3. Clearance influence

It was experimentally shown that the maximum punch force increases when clearance decreases. In our work, numerical simulations were performed with three ranges of clearance (7.9%, 4.2% and 2.5%). Table 1 gives a comparison between experiments and numerical. The numerical results can be improved by taking into account the friction effect, as it will be discussed in the next section. In addition, it should be pointed out that for small clearance range, the simulation becomes difficult and the time step size is reduced which increases the computational cost.

Table 1. Influence of clearance on maximum punch force-FePO4 steel

Clearance	*Numerical result*	*Experiment*
7.9%	11.74 (KN)	12.77 (KN)
4.2%	12.14 (KN)	13.62 (KN)
2.5%	12.43 (KN)	14.17 (KN)

4.4. Friction effect:

In the previously presented numerical results, the friction was neglected in order to simplify the calculations. But in the real blanking process, the friction effects are important, particularly for the maximum punch force. To examine this influence, calculations are performed with different friction coefficients. The frictional contact is handled using a simple Coulomb friction law and the friction coefficient is identical for all the interfaces. Calculations were carried out for a clearance of 7.9%. It is clearly shown (table 2) that the maximum punch force increases with friction effects.

Table 2. Influence of friction on maximum punch force-FePO4 steel

Friction coefficient	*Maximum punch force (KN)*
0	11.74
0.05	12.49
0.1	12.56
0.2	12.68

5. CONCLUSION

In this work, some significant aspects of numerical simulation of sheet metal blanking process are discussed. All the numerical results are compared with experiments in order to examine their validity. The relevant conclusions relate to the sheet metal constitutive model, the load stepping algorithm and the mesh adaptivity. Concerning the constitutive model, it can be noticed that an elastoplastic model is sufficient to obtain a quite satisfactory estimation of the maximum punch force. But the results can be improved by using a damaging model. In addition, such a model is necessary to predict the shape of the cut edge and the burr size.

For the load stepping algorithm, both the implicit (iterative) Newton-Raphson method and explicit method give quite acceptable results. The implicit method is more stable than the explicit one but it suffers some convergence problems and it requires an important computational effort. The main drawback of explicit method is the stability condition that limits drastically the time step size. Some precautions are thus needed to obtain a reliable solution.

As pointed out in several studies on the subject, a mesh adaptativity procedure is required for numerical simulation of sheet blanking process. In this work, we noted that both the global remeshing procedure and the ALE approach are adapted for such a simulation. Some other significant parameters such as friction and clearance were investigated within this work.

6. REFERENCES

1. Zhou, Q. & Wierzbicki, T. (1996). A tension zone model of blanking and rearing of ductile metal plates. Int. J. of Mech. Sci., 38 (3), 303-324.
2. Atkins, A.G. (1980). On cropping and related processes. Int. J. Mech. Sci., 22, 215-231.
3. Johnson, W., & Slater, R.A.C. (1967). Survey of slow and fast blanking of metals at ambient and high temperatures. Paper presented at the Int. Conf. Manufacturing Technology, CIRP-ASTME.
4. Steinmann, P., Miehe, C., & Stein, E. (1994). Comparison of different finite deformation inelastic damage models within multiplicative elastoplasticity for ductile materials. Comp. Mech.,13,458-474.
5. Rice, J.R., & Tracey, D.M. (1969). On the ductile enlargement of voids in triaxial stress field. J. Mech. Phys. Solids, 17, 201- 217.
6. Gurson, A.L. (1977). Continuum theory of ductile rupture by void nucleation and growth: part I – yeld criteria and flow rules for porous ductile media. J. Engng. Mater. Tech., 99, 2-15.
7. Tvergaard, V., & Needleman, A. (1982). Analysis of the cup-cone fracture in a round tensile bar. Acta. Metall., 32, 157-169.
8. Lemaître, J. (1985). A continuous damage mechanics model for ductile fracture. J. Engng. Mater. Tech. Trans. ASME, 107, 83-89.
9. Brokken, D., Brekelmans, W.A.M., & Baaijens, F.P.T. (1998). Modelling ductile fracture in the metal blanking process. In J. Huétink & F. P. T. Baaijens (Eds.), Simulation of Materials Processing: Theory, Methods and Applications (pp. 967-972). Balkema: Rotterdam.
10. Golovashchenko, S.F. (1999, September). Numerical and experimental analysis of the trimming process. Paper presented at Numisheet 99, Besançon, France.
11. Morançay, L., Homsi, M., & Roelandt, J.M. (1997). Application of remeshing technics to the simulation of metal cutting by punching. In D. R. J. Owen, E. Onate & E. Hinton (Eds.), Computational plasticity (pp. 611-618). CIMNE: Barcelona.
12 Goijaerts, A.M., Stegeman, Y.W., Govaert, L.E., Brokken, D., Brekelmans, W.A.M., & Baaijens, F.P.T. (1998). A validated FEM model to improve metal blanking. In J. Huétink & F. P. T. Baaijens (Eds.), Simulation of materials processing : Theory and applications (pp. 979-984). Balkema: Rotterdam.
13. Makinouchi, P. & Ogawa, H. (1988). Simulation of sheet bending processes by elastic-plastic finite element method. Annals of the CIRP, 38 (1), 279-282.
14. Hamel, V., Roelandt, J. M., Gacel, J.N., & Schmit, F. (2000). F.E. modeling of clinch forming with automatic remeshing. Computers and Structures, 77(2), (pp. 185-200).
15. Rachik, M., & Roelandt, J.M. (1998). Schémas explicites d'ordre élevé pour les problèmes non linéaires de mécanique des structures. Revue Europ. Elém. Fin., 7 (4), 401-420.
16. Rachik, M., & Ibrahimbegovic, A. (1998, July). A solution method for non linear problems with contact. Paper presented at the 4th World Congress on Comput. Mechanics, Buenos Aires, Argentina.
17. Wisselink, H.H., & Huétink, J. (1998). Simulation of stationary sheet metal cutting process. In J. Huétink & F. P. T. Baaijens (Eds.), Simulation of materials processing : Theory and applications (pp. 985-990). Balkema: Rotterdam.
18. Atzema., E.H., & Huétink, J. (1995). Finite element analysis of forward/backward extrusion using ALE techniques. Paper presented at Numiform 95, ITHACA/New York , USA.

19. Chenot, J.L., & Bellet, M. (1995). The ALE method for the numerical simulation of material forming process. Paper presented at Numiform 95, ITHACA/New York, USA.
20. Huetink, J., Akkerman, R., Mooi, H.G., & Rekers, G. (1995). Aspect of Lagrangian-Eulerian formulation. Paper presented at Numiform 95, ITHACA/New York, USA.
21. Coupez, T. (1995). Automatic remeshing in three – dimensional moving mesh. Paper presented at Numiform 95, ITHACA /New York, USA.
22. Popat, P.B., Ghosh, A., & Kishore, N.N. (1989). Finite element analysis of the blanking process. J. Mech. Work. Technol. 18, 269-282.
23. Hibbit, Karlsson & Sorensen. (1996). ABAQUS/Explicit User Manual, vers. 5.6, Pawtucket, Rhode Island, USA.
24. MARC Analysis Research Corporation. (1998). MARC manuals, Vol. A-F, Palo Alto, California, USA.

M. Rachik – J. M. Roelandt
Universté de Technologie de Compiègne – Lab. Roberval
Centre de recherche de Royallieu
BP. 20529
60200 Compiègne, France

A. Maillard
CETIM - Service Métaux en Feuilles
52 avenue Félix Louat
BP. 80067
60304 Senlis cedex, France

C. TOURNIER, E. DUC, C. LARTIGUE, A. CONTRI

THE CONCEPT OF THE MACHINING SURFACE IN 5-AXIS MILLING OF FREE-FORM SURFACES

Abstract : The concept of the machining surface *(MS)* is an approach to the process of design and manufacturing of free form surfaces. The machining surface is the surface representation of the tool path, integrating functional design specifications and machining constraints. By definition, it is a surface including all the information necessary for the driving of the tool, so that the envelope surface of the tool movement sweeping the *MS* gives the expected free-form. In this paper, we study the building of the *MS* for 5-axis end milling with usual cutting tools, ball, flat and filleted endmill. We make so that the design and manufacturing constraints taken into account by the machining surface are completely uncoupled within the *MS*.

1. INTRODUCTION

The elaboration process of free-form surfaces must ensure the adequacy between the design intent and the produced part. The process consists of two main activities : the engineering and the manufacturing process (see Figure 1). The engineering process starts with styling and includes engineering constraints through the definition of high quality surfaces in the CAD database. The CAD model becomes the common support from the digital mock-up to the digital manufacturing. Then the CAM system computes the tool path to machine the part.

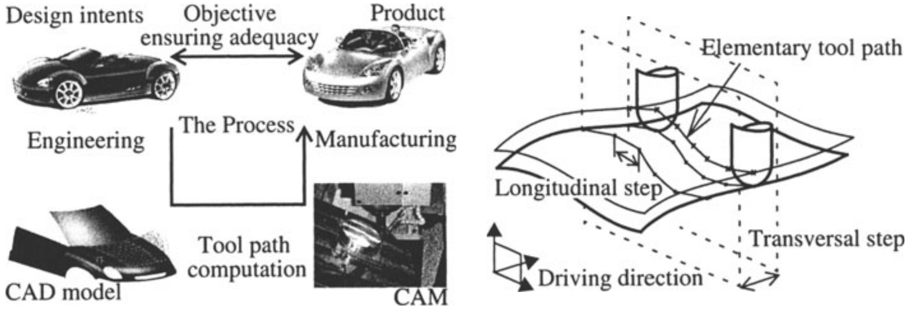

Figure 1 . Elaboration process of free-form surfaces and tool path generation

Each link of the process chain is liable to introduce errors between the final part and the design intents. First there may be a deterioration of data when functional requirements and design intents are converted into 3D CAD data. It is not always possible to obtain the expected forms by the designer as well as continuity connections between surfaces that are necessary to a precise machining. User's actions depend on the CAD

P. Chedmail et al. (eds.), Integrated Design and Manufacturing in Mechanical Engineering, 279-286.
©2002 *Kluwer Academic Publishers.*

software functionalities and the resulting shape may not fit with the user intent but is the closest shape the modeler can produce. Furthermore, styling or engineering specifications are lost: only the CAD model describes geometry. In the process, the tool path computation and the machining activities must guarantee a part that meets the geometry of the CAD model. But other errors are introduced during the tool path computation linked to approximations and discretizations and during the machining because of the dynamic behaviour of the machine tool.

The tool path computation for sculptured surfaces in 3 or 5-axis end milling relies on the choice of a tool driving direction and two discretization steps, the step length along the path (longitudinal step) and the cutter path interval (transversal step) (see Figure 1). The values of the discretization steps must be linked to the geometrical specifications of form deviation or roughness. They must also ensure the achievement of sharp edges and curvature radii specified on the part. The concept of the machining surface has been developed in order to ensure the accuracy between the machined part and the design intents and to optimize the tool path planning (Duc, 1998). We present in this paper the result of our work concerning the use of the machining surface for tool path planning in 5-axis milling. Our previous work on the adequacy between the machined part and the design intent has been presented in (Duc & al, 1999).

2. THE CONCEPT OF THE MACHINING SURFACE

By definition, the machining surface (MS) is a surface including all the information necessary for the driving of the tool, so that the envelope surface of the tool movement sweeping the MS gives the expected free-form (see Figure 2).

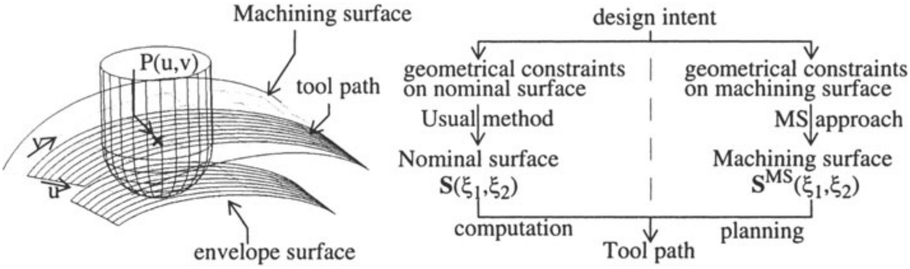
Machining surface
P(u,v)
tool path
v
u
envelope surface
design intent
geometrical constraints on nominal surface
geometrical constraints on machining surface
Usual method
MS approach
Nominal surface $S(\xi_1,\xi_2)$
Machining surface $S^{MS}(\xi_1,\xi_2)$
computation
planning
Tool path

Figure 2 . The machining surface : definition and process evolution

The MS is built on geometrical elements so that the envelope surface respects the geometrical constraints of the design intent. The machining surface is the surface representation of all the cutter locations. Then, the tool path planning only consists in the choice of curves belonging to the machining surface (see Figure 2). In usual methods of free-form design and machining, the geometrical constraints are respected by the nominal surface. The tool path is planned on the nominal surface, by the computation of the trajectory of the contact point between the surface and the tool, the C_C point (cutter contact). The sampling of the path according to the step length criterion produces successive C_C point locations. Then, the center point of the tool C_L (cutter location), which is used by the numerical controller during machining, is computed regarding to the tool geometry (see Figure 3). The tool path computation based on C_C points generally produces errors function of the used NC interpolating format : linear (Choi & al, 1988) or Nurbs (Duc, 1998).

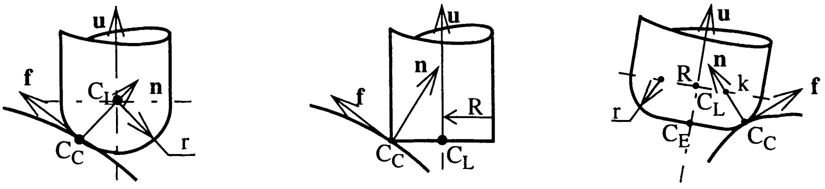

$$C_L = C_C + r \cdot \mathbf{n}$$

$$C_L = C_C + r \cdot \mathbf{n} + R \cdot \mathbf{v}$$

$$\mathbf{v} = ((\mathbf{u} \wedge \mathbf{n}) / \|\mathbf{u} \wedge \mathbf{n}\|) \wedge \mathbf{u}$$

$$C_L = C_C + r \cdot \mathbf{n} + R \cdot \mathbf{v}$$

$$\mathbf{v} = ((\mathbf{u} \wedge \mathbf{n}) / \|\mathbf{u} \wedge \mathbf{n}\|) \wedge \mathbf{u}$$

Figure 3 . Tool geometry

The sampling phase from the nominal surface to the set of discrete C_L points involves geometric deviations between the envelope of the tool movement and the expected surface (Lartigue & al, 1999). The continuous approach suggested by the machining surface helps to avoid problems previously mentioned. Our objective is to build a surface on which we can compute tool paths as curves, according to a machining strategy. The shape of the machining surface must lead to the respect of the design intents, whatever the machining strategy adopted. In 5-axis milling, the machining surface supports the positioning of the effective cutting area of the tool and the orientation of the tool axis.

3. FIVE-AXIS END MILLING TOOLPATH GENERATION

The toolpath generation in 5-axis milling consists in the computation of the cutter center location C_L and the tool axis vector **u** for each C_C point along the tool path (Choi & al, 1993) (Lee, 1997). To ensure the tangency between the tool and the machined surface and avoid gouging, the tool can be rotated around both vectors **t** and **n** of the local coordinate frame defined by (C_C,**f**, **n**, **t**), where **f** is the tool feed vector, **n** the normal to the surface and **t** the tangent vector to the surface with $\mathbf{t} = \mathbf{f} \wedge \mathbf{n}$. Initially, the tool is positioned at C_C so that the axis vector **u** is parallel to the normal vector **n**. Then, we apply the first rotation Ω_t around the vector **t,** and the second rotation Ω_n around the vector **n** (see Figure 4) (Choi & al, 1993). Nevertheless, the movement of rotation is not centered at the same point in function of the tool geometry. For the flat endmill, the rotation Ω_t is applied around the line (C_C, **t**) and the rotation Ω_n around the line (C_C, **n**). While, for the filleted endmill the rotation Ω_t must be applied arround the line (K, **t**) to prevent the tool from rolling on the surface and to keep it tangent to the surface at C_C. The second rotation Ω_n is applied around the line (C_C, **n**) passing through the point K. So, K is considered as the instantaneous rotation center for the two rotations. This remark remains valid when using a ball endmill tool that can be considered as a filleted endmill with a principal radius R equal to zero.

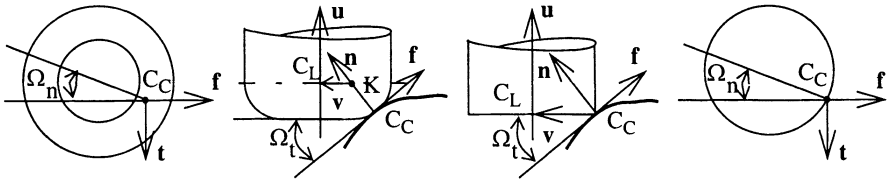

Figure 4 . Tool positioning in 5-axis milling

4. GENERATION OF THE MACHINING SURFACE IN 5-AXES

Our objective is to determine the machining surface according to the geometry of the tool and the number of axes used. The machining surface may consist of one or two surfaces. First, we show that the couple (C_L, **u**) used conventionally to locate the tool in 5-axes is not appropriate to conceive the machined surface in the case of the filleted and flat tools. Indeed, the orientation of the tool axis **u** is defined in a local coordinate system related to the normal of the surface **n**, and the cutter feed direction **f**. That means that the cutter feed direction, linked to the machining strategy, is known during the generation of successive tool positions. The resulting machined surface, defined as the locus of C_L and P so that $\mathbf{C_L P} = \mathbf{u}$, would thus be a particular case only adapted to the adopted machining strategy. Therefore, it becomes not possible to uncouple the design and manufacturing phases. On the other hand for the ball endmill, the position of the center point C_L is independent on the tool axis orientation. Thus, we preserve the couple (C_L, **u**) to locate the ball endmill tool. In order to deal with a general case, let us consider the 5-axis milling with a filleted endmill. Then we can extrapolate results to other tool geometries. Rather than using (C_L, **u**), we suggest to use the point K and the vector $\mathbf{v} = \mathbf{KC_L}$ (see Figure 4). K is defined as the offset point of C_C by a distance equal to the corner radius r. As exposed previously, K remains fixed during the rotational movements of the tool. There remains a possible rotation around the vector **v**. However, it should be noticed that the tool axis vector **u**, the vector **v** and the normal vector **n** passing through C_C remain always coplanar during both rotations Ω_t and Ω_n. Indeed, they are always coplanar, for at any C_C point, the normal to the surface passes through the torus axis. Then, both rotations around **t** and **n** leave the vectors **u, v, n** coplanar. Now, knowing points K, C_L and the normal vector **n** is sufficient to position the tool in the 3D space, and the tool axis vector is thus defined by :

$$\mathbf{u} = \mathbf{v} \wedge ((\mathbf{n} \wedge \mathbf{v})/\|\mathbf{n} \wedge \mathbf{v}\|) \text{ with } \mathbf{v} = \mathbf{KC_L} \quad (1)$$

The points K and C_L make it possible to define a unique tool position because they are located in the symmetry plane of the tool. The machining surface is thus composed of two surfaces S_1 and S_2, loci of the points K and C_L (see Figure 5).

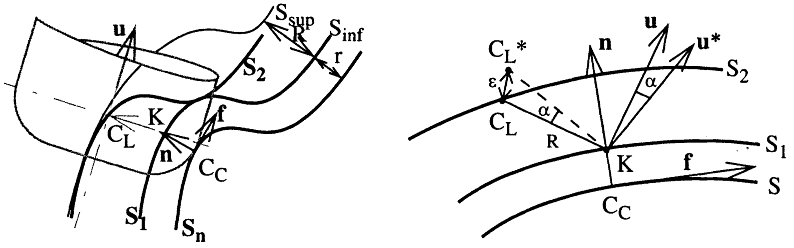

Figure 5 . MS in 5-axis milling with a filleted endmill and variation of the tool orientation

The normal vector is embedded in the equation of S_1. We call the surface S_1 the guiding surface and surface S_2 the orientation surface. The guiding surface S_1 is the offset surface of the nominal surface by the corner radius r of the tool. It is thus independent of the machining strategy. The orientation surface S_2 is the surface which gives the orientation of the tool axis according to the machining strategy.

The orientation surface S_2 is located between two limit surfaces S_{inf} and S_{sup}. Using the parametric equation $F(\xi^1, \xi^2)$ of the nominal surface S_n, we can write:

$$\begin{aligned} \Phi_{sup}(\xi^1, \xi^2) &= F(\xi^1, \xi^2) + (r+R) \cdot \mathbf{n}(\xi^1, \xi^2) \\ \Phi_{inf}(\xi^1, \xi^2) &= F(\xi^1, \xi^2) + r \cdot \mathbf{n}(\xi^1, \xi^2) \end{aligned} \tag{2}$$

The upper limit corresponds to the case for which the tool axis orientation **u** is parallel to the tool feed direction **f**. Moreover, for a given tool path *(C_1)* on surface S_1, the associated curve (C_2) on surface S_2 is included in the pipe surface of radius R and of spine curve (C_1). This condition materializes the fixed distance between K and C_L. The lower limit corresponds to the case for which the tool axis orientation **u** is parallel to the normal vector **n**. This lower limit is a condition necessary but not sufficient to avoid gouging.

Concerning the tool shape, results obtained in the case of 5-axis milling with a filleted endmill can be extended to other tool geometries. The flat endmill can be regarded as a filleted endmill for which the radius of corner r is null. The point K then coincides with the cutter contact point C_C and the surface S_1, locus of point K, is the nominal surface to be machined. In this case, the machining strategy controls the cutter contact point. As previously exposed, the ball endmill can be considered as a filleted endmill with a principal radius R equal to zero. The point K coincides with the C_L point. The adopted solution that uses points K and C_L is not valid for this type of tool, and the original configuration (C_L , $\mathbf{u}$) is used.

5. CONSTRUCTION OF THE GUIDING AND ORIENTATION SURFACES

Let us consider the nominal surface S_n of R^3 and F the map which transforms an interval of the parametric plane (O,ξ^1,ξ^2) into S_n. From the nominal surface S_n described by $F(\xi^1,\xi^2)$, one can determine the map of the guiding surface : $\Phi^{gui}(\xi^1,\xi^2)$.

$$\Phi^{gui}(\xi^1,\xi^2) = F(\xi^1,\xi^2) + r \cdot n(\xi^1,\xi^2) \tag{3}$$

The orientation surface is built according to the given orientation of the tool along the path. The axis orientation is described by $\mathbf{u}(\xi^1,\xi^2)$. One can evaluate the map of the orientation surface $\Phi^{ori}(\xi^1,\xi^2)$ followed by the center of various types of tools. For example, the orientation surface is given by the following equation, when the tool is a filleted endmill defined by the two radii R and r.

$$\Phi^{ori}(\xi^1,\xi^2) = F(\xi^1,\xi^2) + r\mathbf{n}(\xi^1,\xi^2) + R\mathbf{v}(\xi^1,\xi^2) \tag{4}$$

The following table gathers different machining surfaces according to the geometry of the tool and the number of axes used for machining.

Table 1: Various machining surfaces

	3-axis	*5-axis*	
Ball endmill	S_1 : $\mathbf{F} + r\mathbf{n}$	S_1 : $\mathbf{F} + r\mathbf{n}$	S_2 : $\mathbf{F} + r\mathbf{n} + \mathbf{u}$
Flat endmill	S_1 : $\mathbf{F} + R\mathbf{v}$	S_1 : $\mathbf{F}$	S_2 : $\mathbf{F} + R\mathbf{v}$
Filleted endmill	S_1 : $\mathbf{F} + r\mathbf{n} + R\mathbf{v}$	S_1 : $\mathbf{F} + r\mathbf{n}$	S_2 : $\mathbf{F} + r\mathbf{n} + R\mathbf{v}$

We propose to build the guiding and orientation surfaces according to the method described in (Farouki, 1986) for S_1 and S_2 are generalised offset surfaces. S_1 and S_2 are modeled by a multi-patch surface. Patches are bi-cubic interpolants connected in tangency. Each patch r(u,v) is expressed as a Ferguson tensor product surface, with C the matrix of blending function (cubic Hermite basis) and Q the Coons matrix (Faux & Pratt, 1979), where $\Phi(\xi^1,\xi^2)$ is the implicit equation of the guiding or the orientation surface. In order to keep the consistency of the surface representation in the CAD system, we use a Bezier (UNISURF) representation for patches, with M the cubic Bernstein basis matrix and B the matrix of the Characteristic Polyhedron vertices :

$$\begin{array}{l} r(u, v) = UCQC^T V^T \\ r(u, v) = UMBM^T V^T \\ B = (M^1 C) Q (M^1 C^T) \end{array} \qquad \begin{bmatrix} Q_{00} & Q_{01} & Q_{02} & Q_{03} \\ Q_{10} & Q_{11} & Q_{12} & Q_{13} \\ Q_{20} & Q_{21} & Q_{22} & Q_{23} \\ Q_{30} & Q_{31} & Q_{32} & Q_{33} \end{bmatrix} = \begin{bmatrix} \Phi 0,0 & \Phi 0,1 & \Phi_{\xi^2} 0,0 & \Phi_{\xi^2} 0,1 \\ \Phi 1,0 & \Phi 1,1 & \Phi_{\xi^2} 1,0 & \Phi_{\xi^2} 1,1 \\ \Phi_{\xi^1} 0,0 & \Phi_{\xi^1} 0,1 & \Phi_{\xi^1 \xi^2} 0,0 & \Phi_{\xi^1 \xi^2} 0,1 \\ \Phi_{\xi^1} 1,0 & \Phi_{\xi^1} 1,1 & \Phi_{\xi^1 \xi^2} 1,0 & \Phi_{\xi^1 \xi^2} 1,1 \end{bmatrix} \qquad (5)$$

The precision obtained on surfaces S_1 and S_2 is proportional to the number of patches. From a point K on S_1 one finds the corresponding point C_L on S_2 with the assumption that parameter setting of S_1 and S_2 are identical. Thus, the method generates approximations. The errors on the guiding surface S_1 must be controlled because they cause local gouging between the tool and the nominal surface. We have to use a large number of patches in the offset surface approximation to perform a precise machining. On the other hand, errors on the orientation surface S_2 present fewer disadvantages because variations of the tool axis orientation do not generate machining errors. Indeed, the controlled point is the point K which is the instantaneous center of rotation during the two rotations of the tool. The orientation of **u** does not influence the position of the active part of the tool. Moreover the tool radius R reduces the amplitude of the variations of S_2 on the orientation of the axis tool (see Figure 5). The maximum angle variation is given by $\tan\alpha_{max} = \varepsilon / R$.

6. EXAMPLE

The treated example consists in machining a surface (a Bezier patch of degree 5) with a filleted endmill ($R = 10$, $r = 4$) and with the following strategy: 5-axis milling, tool center guiding along parallel planes to yoz and $\Omega_t = 20°$, $\Omega_n = 0°$. S_1 is the offset surface of S_n with an offset distance equal to 4 mm. S_2 is the generalised offset surface ($S_2 = S_n + r\mathbf{n} + R\mathbf{v}$) with offset distance equal to $R = 10$ and $r = 4$. S_1 and S_2 are free from loops. The modeling of the kinematics of the displacement of the tool on both surfaces S_1 and S_2 make it possible to simulate the machining along the curve C_1 (see Figure 6), intersection of S_1 with the guiding plane. C is the contact curve followed by the C_C point on the nominal surface and C_2 is the curve followed by C_L on the orientation surface.

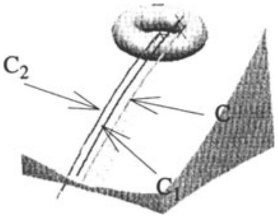

Figure 6 . Machining simulation

7. CONCLUDING REMARKS

The concept of the machining surface offers a new solution to generate tool-paths. Its construction is common for various cutting tools usually used. The guiding surface generation is only based on the corner radius of the considered tool, independently of the machining strategy. The tool path planning is initially carried out by choosing curves belonging to the guiding surface. Then, if necessary, the orientation surface makes it possible to position the tool for machining with five axes. The objective is now to use the machining surface for machining of compound surfaces. To achieve this task, we will have to introduce technical surfaces in the machining surface framework to be able to add approach, retract and linking tool movement.We are also working on another method to build the orientation and guiding surfaces. The method is based on the two fundamental forms to evaluate the local characteristics of the orientation and guiding surfaces. Nevertheless, the current approach is difficult to implement. The encountered difficulties come from several factors : the loops resulting from the offset operation, the need for synchronizing the parameter settings, the number of patches required to achieve a high quality machining.

8. REFERENCES

Duc E. (1998). Usinages des formes gauches, contribution à l'amélioration de la qualité des trajectoires d'usinage. *Thèse de Doctorat ENS Cachan.*

Duc E., Lartigue C., Tournier C., Bourdet P. (1999). A new concept for the design and the manufacturing of free-form surfaces: the machining surface. *Annals of the CIRP*, vol 48/1, 103-106.

Lartigue C., Duc E., Tournier C. (1999). Machining of free-form surfaces and geometrical specifications. *IMechE, Proceedings of the Institution of Mechanical Engineers.*Vol. 213 Part B, 21-27

Choi B.K, Lee C.S, Hwang J.S, Jun C.S (1988). Compound surface modelling and machining. *Computer Aided Design*, vol 20, no 30, 127-136.

Choi B.K, Park J.W, Jun C.S (1993). Cutter location data optimization in 5-axis surface machining. *Computer aided Design*, vol 25, no 6, 377-386.

Lee Y.S. (1997). Admissible tool orientation control of gouging avoidance for 5-axis complex surface machining. *Computer Aided Design*, vol 29, no 7, 507-521.

Farouki R.T (1986). The approximation of non degenerate offset surfaces. *Computer Aided Geometric Design*, no 3, 15-43.

Faux I.D, Pratt M.J (1979). Computional Geometry for Design and Manufacture, *Ellis Horwood Ltd*, Chistester.

Affiliation

Lurpa, Ecole Normale Supérieure de Cachan
61 av du pdt Wilson, 94235 Cachan cedex
tel 01 47 40 22 20
email : lartigue@lurpa.ens-cachan.fr

A. DUGAS – JJ. LEE – JY. HASCOET

HIGH SPEED MILLING

Solid simulation and machine limits

Abstract. The rational exploitation of the potentials of HSM (High Speed Milling) leads industrials to review their ranges of machining and especially their strategies of machining. However, the specifics imposed by HSM have not been much integrated in the actual CAD/CAM systems. The integration of the HSM specifics in CAD/CAM systems can be a powerful and efficient way to use the HSM potentials. In this paper, we will first present what are the HSM specifics in terms of the limits of cutting tools, controllers, and machine-tools. Then, we will introduce an algorithm to predict the real feed rate and tracking errors, considering the limits of the controllers and the machine tools. The real feed rate is often very lower than the programmed one. In order to analyze the milling process more precisely, the use of the real feed rate is one of the essential factors. The efficiency of the algorithm has been verified through several experiments with various tool paths. In addition, the algorithm has been already integrated into our machining simulator being developed. We will show some results obtained from the machining simulator concerning tracking errors estimation.

1. INTRODUCTION

The progress achieved by cutting materials, high-speed spindles, linear motors and high-performance controllers are the origin of some revolution in the milling area. Using the potentials of these new technologies, HSM permits to increase the quality of produced parts, and to reduce the delay and eventually the costs [9] . To reach this result, HSM machines have been changed. Cutting speeds and feed rates have been multiplied up to 10. The rigidity has been reinforced and the weight has been reduced in order to minimize inertia effects and to permit high accelerations. Fast data processing allows controllers to be able to control the machines at high speeds. Such changes offer new possibilities in metalworking industry. However, the specifics imposed by HSM have not been considered much in the actual CAD/CAM systems. To success in HSM, the specifics must be integrated within the CAD/CAM systems. We have established three axes to incorporate the HSM specifics in the CAD/CAM field. The first axis is to exploit new milling strategies satisfying HSM specifics. The second one is to make a general machining simulation tool being capable of analyzing the quality of these new milling processes. The third one is to develop optimal algorithms according to the feedback from the machining simulation tool. The complete integration of these three axes in a CAD/CAM system is our ultimate goal. he simulation part is one of key points of our gateway. While most machining simulators can simulate the material removal processor, they consider machines and controllers as perfect and cutting tools as stiff. This approach is not appropriate for giving an accurate analysis on cutting process, especially in the case of HSM. Our simulator, implemented on windows

P. Chedmail et al. (eds.), Integrated Design and Manufacturing in Mechanical Engineering, 287-294.
©2002 *Kluwer Academic Publishers.*

environment, has integrated tool deflection as considering machine and controller's limits as shown in Figure 1 [5] .

2. HSM SPECIFICS TO INTEGRATE

The difference between HSM and conventional speed machining (CSM) comes mainly from the difference of machining speed. There exist efficient roughing and finishing strategies for CSM, but these strategies are not well adapted to HSM [6] [1]. For example, the CSM strategies do not assure a constant tool engagement, which can cause a tool breakage in HSM. When milling a die and mold, the size of the part program is so large and the path length of each block is so small that it is difficult for the controller to process the blocks in real time at high feed rates [3]. Such tool paths often have so high curvatures that it is hard to keep the programmed feed rate. In addition, the format of tool path trajectories does not exploit the possibilities of new controllers such as Nurbs or B-spline interpolation [2].

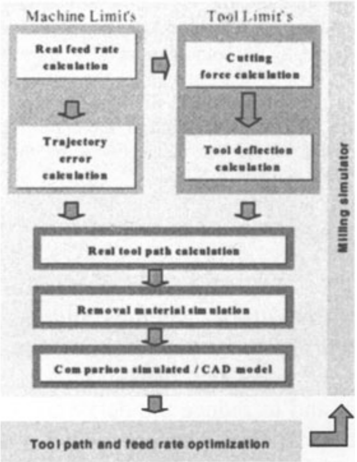
Machine Limit's
Tool Limit's
Real feed rate calculation
Cutting force calculation
Trajectory error calculation
Tool deflection calculation
Milling simulator
Real tool path calculation
Removal material simulation
Comparison simulated / CAD model
Tool path and feed rate optimization

Figure 1. Milling simulator

Fundamentally, this failure is due to the fact that the CSM strategies depend on geometric criteria (e.g. parallel plan and isoparametric tool paths) much more than machining constraints such as the limits of the cutting tool, the controller, and the machine. In order to assure the quality of machined part, the machining constraints should be considered in the CAM step.

The limits of the cutting tool : In die and mold machining, the ratio length/diameter of the cutting tool is so high (for example, sometimes it can be up to 20) that they are very sensitive to cutting force. Since the cutting force is directly affected by tool engagement volume, varying tool engagement volume can cause a variation of tool deflection and the quality of the machined surface, in the worst case a tool breakage, especially in HSM due to the high feed rate [4] .

The limits of the machine : In free form surface milling, we are limited by the most restrictive axis. In milling a curve with a radius of curvature of R, the relationship between the acceleration Ac, and the feed rate Vf is given by :

$c = Vf\,2 / R$ [1] Ac is equal to centrifugal acceleration. When this relation cannot be satisfied, the controller has to reduce the feed rate. For example, in mold milling, the real feed rate is rarely equal to the programmed feed rate because the part geometry has a high curvature. This problem is specific to HSM. If R is constant and Vf increases 10 times, Ac has to increase 100 times to preserve the required feed rate. If R is small, it will be a critical problem in HSM. For example, it is very difficult for the cutter to move at the high feed rate when the curvatures along the tool path are high. To alleviate this problem, the tool path should have as low curvatures as possible.

The limits of the controller : The controller must be able to maintain an accurate cutter path during fast displacements. The power of the control is characterized by a) the block preprocessing time, b) the size of the buffer between the preprocessor and main processor, c) the interpolation cycle time, and d) the dynamic look-ahead. As the development of high-performance processors, the computing time (block preprocessing and interpolation cycle time) is getting shorter. However, when the path length of each block is too small and the feed rate is high, the controller does not have enough time for computing the next trajectory point. To solve this problem, some controllers reduce the feed rate. The dynamic look-ahead is the function that sees the trajectory in advance and finds a maximum path velocity from which braking down into zero is guaranteed without exceeding the possible axis acceleration rates at the end of the block in the buffer between the preprocessor and the main processor. The function makes it possible to perform continuous acceleration operation and avoid unexpected overshoots [8] . While increasing the size of the buffer gives better look-ahead, it requires more memory and computation time.

3. MACHINE BEHAVIOR MODEL – DYNAMIC SIMULATION

In HSM, the real feed rate could be often very lower to the programmed feed rate, caused by machine and the controller's limits. However, to simulate the milling process and to optimize this one, the feed rate is required (Figure 1). To use programmed feed rate lead to an important error, it, there is a high curvature on the trajectory and a high programmed feed rate. Therefore, it's important to get a tool permitting to simulate the machine behavior combined to its controller. The proposed model permits to calculate the real feed rate along the milling trajectory, considering the features of machines and controllers (Figure 2). Then, this feed rate is used by tool deflections calculation module and error path calculation module (Figure 1). With these modules, we can simulate the real tool path instead of the programmed one. Because of the great diversity of commercial machines and controllers, it is impossible to describe all behavior precisely. Therefore, we have developed a generic model, to answer to the main controllers on the market.

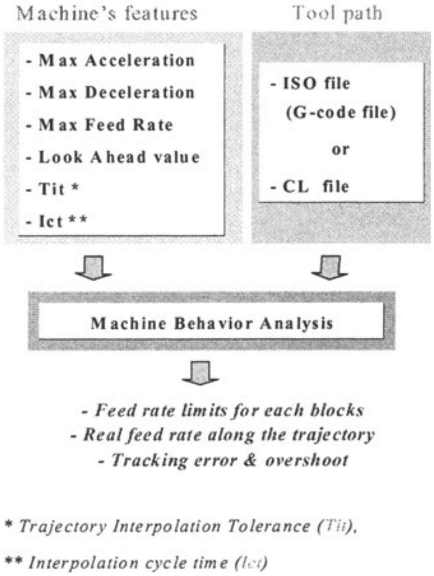
Machine's features
Tool path
- Max Acceleration
- Max Deceleration
- Max Feed Rate
- Look Ahead value
- Tit *
- Ict **
- ISO file
(G-code file)
or
- CL file
Machine Behavior Analysis
- Feed rate limits for each blocks
- Real feed rate along the trajectory
- Tracking error & overshoot
* Trajectory Interpolation Tolerance (Tit).
** Interpolation cycle time (Ict)

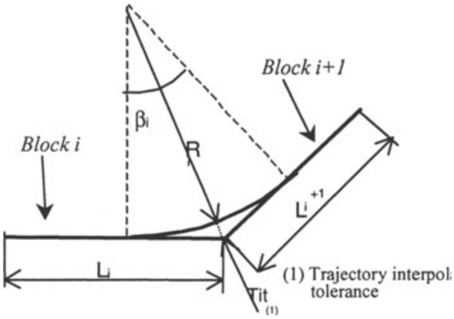
Block i+1
Block i
βi
R
Li+1
Li
Tit (1)
(1) Trajectory interpol
tolerance

Figure 2. Dynamic behavior simulator

Figure 3. Cirle arcs Interpolation

Trajectory interpolation : Generally, the tool path includes some geometrical discontinuities (the trajectory is C0 class but not G1). If we want to cross these discontinuities with an imposed feed rate Vf, it requires that the machine produce an infinite acceleration! To solve this problem, the controller calculates a trajectory G1, from the programmed tool path. The parameter Trajectory interpolation tolerance (Tit) permits to adjust the admissible distance between the programmed trajectory and the calculated one. n our model, we chose to calculate a circular arc in order to generate the trajectory G1 (Figure 3). But, it's possible to choose another kind of model to generate the trajectory G1.

Static Look Ahead calculation : At this step, the trajectory is G1 class but it still includes some areas where the feed rate can not be maintained. Indeed, when there are high curvatures, the required centripetal acceleration can be higher to the available acceleration on the different axes of the machine. In order to follow the calculated trajectory precisely, the controller limits the feed rate locally. In practice, this calculation is based on the most restrictive axis, which required more acceleration and speed then the others. n the other hand, the controller limits also the feed rate Vf to respect the interpolation cycle time limits. In practice, the feed rate is limited in order to get a bloc execution time lower than the CNC cycle of time t (Vf <L / t with L length of the block considered). herefore, the purpose of this step is to

calculate feed rate limits to be able to follow the trajectory, considering each axis features and CNC cycle of time.

Dynamic Look Ahead calculation : After the above two steps, it is necessary to calculate for each axis the exact feed rate profile with its acceleration and deceleration steps. To calculate this profile on one block, it is necessary to anticipate the trajectory. Indeed, without this anticipation we can avoid overshoots in the case of a sharp deceleration. In practice, to preserve the CNC cycle of time and block processing time, this anticipation is limited to n blocks. n is called Look Ahead value and depends on the controller's generation. The figure 4 presents several results from different look ahead value. The dotted profile corresponds to the result of the static look ahead calculation.

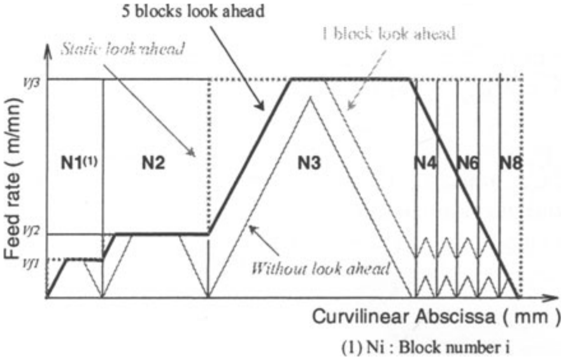

Figure 4. Example of dynamic look ahead calculation with various value

Tracking error (or Real position) evaluation : Using the feed rate profile and the tool path, the interpolation function calculates the reference position for each axis: Xc[k], Yc[k], and Zc[k], where k represents the current cycle value of the servo control loops. n order to calculate the real position on each axis with respect to the reference position (Xc,Yc,Zc), it is necessary to integrate the dynamic behavior of each axis. For analyzing the dynamic behavior, several models are available. Theses models can be classified into two approaches: a) rigid machine structure model, and b) flexible machine structure model. The second category can give more accuracy than the first one, and can consider axis vibration, but it requires much more computation time and needs a lot of parameters necessary to describe axis behavior. Up to now, two models based on the first category (rigid machine structure model) have been integrated into the machining simulator for the computational efficiency.

$$Xr[k]=\frac{1}{\frac{1}{\Delta t2\omega_0^2}+\frac{2\xi}{\Delta t\omega_0}+1}\left(Xc[k]+2\left(\frac{1}{\Delta t2\omega_0^2}+\frac{2\xi}{\Delta t\omega_0}\right)Xr[k-1]-\frac{1}{\Delta t2\omega_0^2}Xr[k-2]\right) \qquad [2]$$

The first model is based on first order model and the second one on second order model. For example, with the second model, the real X position Xr[k] at the k cycle of the position loops is given in Equation 2, where Δt represents the sampling time of the position loops, ω_0 the natural frequency and ξ the damping ratio. Thus, the tracking error on X axis is the difference between Xc[k] and Xr[k].

4. EXPERIMENTAL AND SIMULATION RESULTS

To validate our model, we measured the real feed rate profile during machining, and compared it with the results obtained from our proposed algorithm. Moreover, we compared contour errors of the both cases. The term "contour error" is to denote the component error orthogonal to the desired trajectory. Figure 5 shows the diagram of our trajectory acquisition system. For each axis, we can get the real axis positions, as acquiring the output axis encoder data during the milling. Then, the real feed rate profile can be rebuilt by derivation of the positions. igure 6 shows one of our test part and its test trajectory. We measured the real positions and the real feed rates when the programmed feed rate is 8 m/mn along all the trajectory. Figures 7 and 8 present the comparison results. Figure 7 shows the programmed feed rate, the real feed rate, and the simulated feed rate obtained by our algorithm. Figure 8 shows contour error comparison. In this figure contour errors have been magnified 40 times.

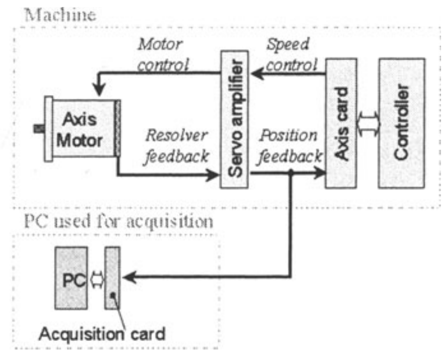

Figure 5. Trajectory acquisition diagram.

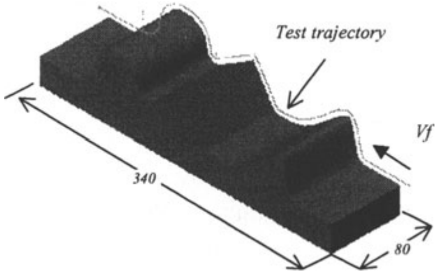

Figure 6. Tested workpiece

From the comparison results, we can see that the programmed path and feed rate are not the same with the real ones, and our algorithm can estimate the difference quite well. In addition, it is worth noting that the real feed rate is rarely equal to the programmed one (8m/mn). On figure 8, we note that geometrical discontinuity causes an important contour error.

The loop on measured profile and simulated profile is caused by magnification of the contour error. In order to validate our algorithm, others experimentations, using others CNC machines, have been realized.

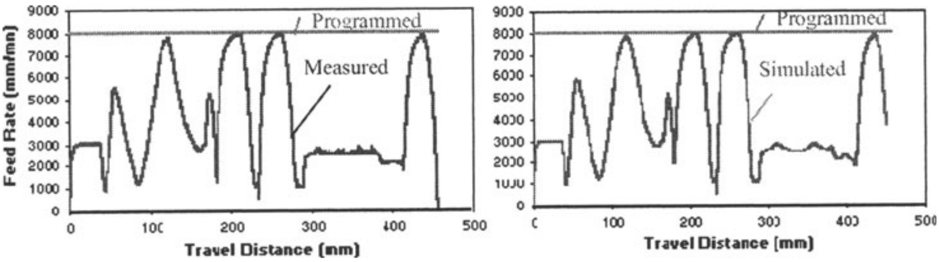

Figure 7. Feed rate, Experimentation/Simulation

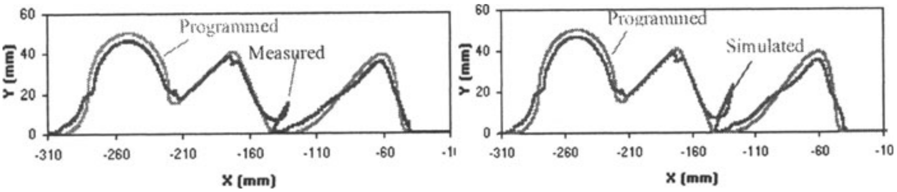

Figure8. Contour Error, Experimentation/Simulation

5. 3D SOLID MODEL MILLING SIMULATION

Figure 9 presents a 3D solid simulation result from our machining simulator concerning tracking errors. The left-half part of the workpiece is realized without considering real feed rates and tracking errors and the other part is realized by considering these factors. Without considering tracking errors, the most area of the machined surface has the same color (gray).

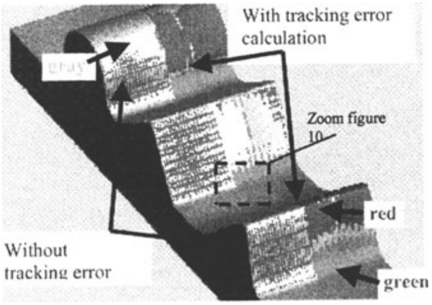
gray
With tracking error calculation
Zoom figure 10
red
green
Without tracking error

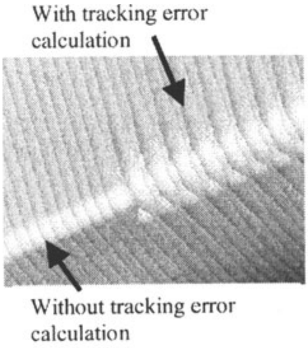
With tracking error calculation
Without tracking error calculation

Figure 9. STL Comparison

Figure 10. Scallop edge visualization

Figure 10 also shows the effect of the estimated tracking errors on scallop edges. It means that the machined surface is within the given tolerance (0.05 mm) and that the tool path is acceptable in the geometrical viewpoint. However, with tracking errors, some area is gouged (red) and some is undercut (green). Indeed, Zig Zag strategy causes this error because the axis behavior is not the same when the axis speed up and when the axis speed down. Such errors are often noted in motor industry [7]. After simulation, the errors can be easily quantified in various ways since the errors are already reflected on the solid model.

6. CONCLUSION

Specificities of the HSM must be integrated within the CAM systems. In this optics, we developed a machining simulator allowing to take into account the limits of the cutting tools and the limits machines. This simulator is thus able to simulate the part which would be really obtained after machining. The Simulation part of the Dynamic Behavior is essential. Indeed, to know the real feed rate allows to calculate the deflections tools, to calculate the error on the trajectory according to the limits machines. This simulation must be used in all the applications using the feed rate like data of input. The model developed here wants to be sufficiently generic to answer the main controllers of the field. The algorithm has been already integrated into our machining simulator, which can quantify the errors based on 3D simulation model.

7. REFERENCES

[1] BAGARD, P., "Outils coupants, conditions de coupe et stratégies en Usinage à Grande Vitesse des Outillages et formes complexes : Point de départ de la chaîne CFAO", Journées de l'usinage 1996, CETIM, 4 décembre 1996.
[2] DUC, E., BOURDET, P., "NC Toolpaths Generation With Non-Uniform B-Spline Curves for High Speed machining of Mold and Dies", 1 st French and German Conference on HSM, Metz (France), p. 240-248, 06/97
[3] LE FAUCHEUX, J.P., "Utilisation des NURBS. Point de vue du constructeur de Commande Numérique", CFAO et Usinage de formes complexes, Primeca, Ecole Normale Supérieure de CACHAN, 18 mars 1999.
[4] HASCOET, J.Y., DEPINCE, P., SEO, T.I., "Compensation of Tool Deflection in Ball-End Milling Simulation and Experimental results", proceedings of International Seminar on Improving Machine Tool Performance, CIRP, San Sebastian (Spain), 6-8 july 1998.
[5] HASCOET, J.Y., LEE, J.J., DUGAS, A., "Machining simulator with dynamic error analysis on free surface machining", IDMME'2000, Montréal (Canada), 2000.
[6] LARTIGUE, C., DUC, E., "Machining of free-form surfaces and geometrical specifications", Inter. Jour. Engineering Manufacture, vol 213, p. 21-29, 1999.
[7] Lio J.P., "L'UGV dans l'industrie automobile : les difficultés rencontrées aujourd'hui par les utilisateurs", Assises Machines et Usinage à Grande Vitesse, Senlis (France), pp 1.1-1.7, mars 2000.
[8] PAPLERNIK, W., "Architecture and Design of Modern CNC/Drive Systems", proceedings of Intelligent Motion, p. 271-280, may 1996.
[9] SCHULZ, H., "State of the Art of High-Speed Machining", 1 st French and German Conference on High Speed Machining, Metz (France), p. 1-7, june 1997.

8. AFFILIATIONS

Arnaud Dugas - Jung-Jae Lee - Jean-Yves Hascoët *- Institut de Recherche en Communications et Cybernétique de Nantes (IRCCyN) UMR CNRS 6597 - Ecole Centrale de Nantes 1, rue de la Noë, BP 92101 44321 Nantes, France*
Jean-Yves.Hascoet@irccyn.ec-nantes.fr

J.L. BATOZ[***], H. NACEUR[*], A. DELAMÉZIÈRE[***], Y.Q. GUO[**],
C. KNOPF-LENOIR[*]

DESIGN OF PROCESS PARAMETERS IN DEEP DRAWING OF SHEETS TO IMPROVE MANUFACTURING FEASIBILITY

*Université de Technologie de Compiègne, UMR 6066
BP 20529 - 60205 Compiègne Cedex, France

** Université de Reims Champagne-Ardenne,
I.U.T Génie Mécanique et Productique
BP 1035 - 51687 Reims Cedex, France

***Institut Supérieur de l'Ingénierie de la Conception
27 rue d'Hellieule – 88100 Saint-Dié-des-Vosges, France

Abstract: The aim of this investigation is to present a numerical procedure combining a simplified finite element inverse approach (I.A.) for the rapid simulation of the stamping process with mathematical programming technique (BFGS method) to optimize the stamping process design. Our objective is to optimize the quality of the final workpiece, by minimizing the risk of rupture and wrinkles. The design variables of this problem are the drawbead restraining forces, and the material parameters such as the strain hardening exponent n (Hollomon law) and the Lankford anisotropy coefficient in relation with the Forming Limit Diagram (FLD). The optimization procedure developed has been applied for the square cup of Numisheet'93 and the Renault/Twingo dashpot cup. The satisfactory results demonstrate the usefulness of this automatic optimization procedure in the preliminary design of deep-drawing process.

1. INTRODUCTION

From some recent specialized conferences (Numiform'98, Numisheet '96, '99] one can observe a clear tendency for the need and development of simplified methods (such as the ''one-step method'' and the "Inverse Approach") for the numerical simulation of sheet metal forming problems. This is mainly due to the efficiency of these kinds of procedures for the evaluation of forming difficulties in relation with the preliminary design stages of blanks and tools. The Inverse Approach (I.A.) developed by Batoz and Guo [1-4] appears to estimate efficiently the large elasto-plastic strains in thin walled structural parts obtained by deep drawing. Since 1995 the present authors have proposed a numerical procedure [5-8] which consists of a coupling between the I.A. for the simulation of sheet forming parts and a

P. Chedmail et al. (eds.), Integrated Design and Manufacturing in Mechanical Engineering, 295-302.
©2002 *Kluwer Academic Publishers.*

Sequential Quadratic Programming (S.Q.P) method for the shape optimization of blank contours. This numerical procedure has given satisfactory results on academic and industrial applications.

To control the material flow and the part quality, the drawbeads are perhaps the most important parameters, because too strong restraining forces prevent the sheet from draw-in and may cause the necking, but insufficient forces may lead to wrinkling. The aim of the present work is the determination of the optimal restraining forces and optimal material characteristics (n and $\bar{r}$) to reduce the risk of necking and wrinkling by the use of the Forming Limit Diagram (FLD) [10-12]. This optimization procedure is based on the Inverse Approach developed by the authors and a BFGS optimizer.

2. STATEMENT OF THE OPTIMIZATION PROBLEM

2.1. Objective function

We define an objective function based on the Forming Limit Diagram FLD, because it is considered as a good indicator for the failure and wrinkling criterions. In order to allow the analytical evaluation of sensitivities, we first define the Forming Limit Curve by an explicit function based on the least squares polynomial approximation defined by the function $\varphi(\varepsilon_2)$ which takes the form:

$$\varphi(\varepsilon_2) = a_0 + a_1\varepsilon_2^1 + a_2\varepsilon_2^2 + \ldots + a_{n-1}\varepsilon_2^n \qquad (1)$$

where n is the polynomial degree.

Based on this function we define also a so called *"secure FLC"* function $\psi(\varepsilon_2)$ given by:

$$\psi(\varepsilon_2) = \varphi(\varepsilon_2) - s \qquad (2)$$

where s is a *"safety"* from the FLC, this constant quantity is chosen by the user (see Figure 1). Our objective function is thus expressed by the sum of all distances from the "*secure FLC*" but only for elements where the major strain ε_2 is greater than $\psi(\varepsilon_2)$ (Figure 1). Therefore the global objective function can be given by:

$$J = \sum_{e=1}^{nelt} J_e \quad \text{with} \quad \begin{cases} J_e = (\varepsilon_1^e - \psi(\varepsilon_2^e))^{2p} & \text{if} \quad \varepsilon_1^e > \psi(\varepsilon_2^e) \\ J_e = 0 & \text{if} \quad \varepsilon_1^e \le \psi(\varepsilon_2^e) \end{cases} \qquad (3)$$

where nelt is the total number of elements, the couple ($\varepsilon_1^e, \varepsilon_2^e$) are the element principal logarithmic strains; p is an integer constant (p=1,2,3 ...) introduced in order to capture the maximal function variations by the use of higher values ($\geq$ 2).

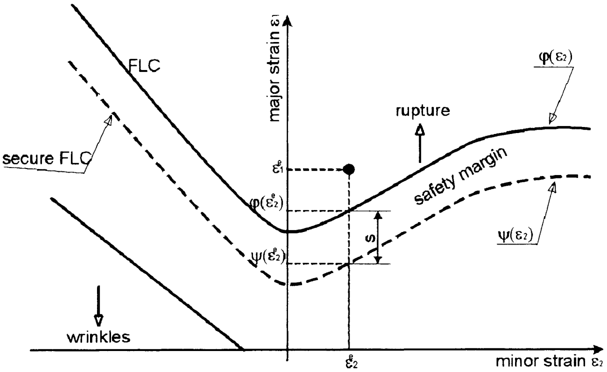
FLC
secure FLC
wrinkles
major strain ε_1
ε_1^e
$\varphi(\varepsilon_2^e)$
$\psi(\varepsilon_2^e)$
$\varphi(\varepsilon_2)$
rupture
safety margin
s
$\psi(\varepsilon_2)$
ε_2^e
minor strain ε_2

Figure 1. *Definition of the objective function*

2.2. Design variables

In the present research investigation our goal is to evaluate a numerical procedure to automatically determine optimal restraining forces while minimizing the objective function given by equation (3).

In general the problem of nonlinear optimization is stated as follows:

$$\begin{cases} min & J(v), \quad v = \langle v_1, \ldots, v_n \rangle^T \\ with & v_{il} \leq v_i \leq v_{iu}, \quad i = 1, \ldots n \end{cases} \tag{4}$$

where $J(v)$ is the objective function, v is the design variables vector. v_{il} and v_{iu} are the lower and upper bounds on the design variables. In our study two kinds of design variables are taken into account:

2.2.1 Restraining forces

The design variables can be the intensities of restraining forces on some prescribed drawbead lines. Each restraining force is uniformly distributed along the drawbead segment (Figure 2). These forces are chosen to be normal to the drawbead segment and always oriented externally.

2.2.2 Material parameters

The second kind of design variables are the material parameters. Previous simulations indicate that the sensitivity to the strength coefficient K is poor, therefore we consider only the strain-hardening exponent n and the anisotropy coefficient $\bar{r}$ as design variables. Since the FLC depends on the material we have to predict a FLC for every new couple $(n, \bar{r})$. We use the theory developed by Graf and Hosford [10] based on the growth of an imperfection described by a parameter f which is the ratio of the thickness of the imperfection to the thickness of the remaining part of the sheet. That theory can predict FLC for pre-strained materials.

The former authors adjust the parameter f to match the point $(\varepsilon_2=0,\ \varepsilon_1)$ for the experimental FLC with the predicted one.

3. SENSITIVITY ANALYSIS

The use of the finite difference method for the computation of sensitivities is very simple regarding the implementation, but it involves the need of numerous non-linear analyses and the lack of precision on the gradient values which often lead to a slow convergence.

For these reasons it is evident that analytical methods are more suitable and especially when the analysis is highly nonlinear. The "direct" nature of the static implicit I.A. is well adapted to analytical sensitivity computation because the initial and final states are only requested in the derivation of the objective function. A sensitivity analysis method for sheet metal forming problems using the I.A. has been developed on the basis of the direct differentiation of the equilibrium equations combined with the adjoint state method because generally in sheet metal forming, there are more design variables than functions to derive.

The final sensitivities equations generated by this method are only valid when the nonlinear equilibrium equations are satisfied:

$$\{R(U)\} = \{F_{int}(U)\} - \{F_{ext}\} = \{0\} \tag{5}$$

where $\{R\}$ is the global residual vector, $\{F_{int}\}$ and $\{F_{ext}\}$ are respectively the internal and external force vectors, U is the unknown variable vector representing the two displacement components.

The total derivation of the objective function $j(v)=J(v,\ U(v))$ with respect to a design variable v_i, and the partial derivation of the equilibrium equation system (5) give the following relation:

$$\frac{dj}{dv_i} = \frac{\partial J}{\partial v_i} + \langle P \rangle \left\{ \frac{\partial R}{\partial v_i} \right\} \tag{6}$$

The FLC is approximated using a least squares polynomial approximation. We use a safety distance of *0.15* and a value of *2* for the exponent p in (3). The value of the objective function before optimization was $J=6.310^{-5}$ and the maximum value of major strain was about *0.32* and is situated above the secure FLC as shown in Fig. 3.

The initial restraining forces are set equal to *100N/mm*, their lower and upper bounds are respectively *0N/mm* and *200N/mm*, the residual force norm is fixed to 10^{-6} and the objective function norm is 10^{-10} for the convergence criteria.

Convergence was achieved after *18* iterations allowing a reduction of *99.7 %* of the objective function using *153* seconds of CPU time on a PC Pentium II with 400 Mhz of frequency and 128 Mbytes of RAM. The maximum value of major strain is about *0.2* and is under the secure FLC as indicated in Fig. 4.

Table 1 gives the optimal distribution of the restraining forces obtained at the end of the optimization process. These forces mean that we should facilitate the draw-in on the drawbeads 3, 4, 5 to reduce the thinning in the punch corner and then avoid necking and we should prevent the metal flow on the drawbeads 1, 2, 6, 7 to reduce the thickening and then avoid wrinkles.

We can observe that the restraining force on the drawbead 4 has reached the lower bound (0 N/mm) since this is the zone where the sheet is strengthen at its maximum.

Drawbead	1	2	3	4	5	6	7
Rest. force (N/mm)	144.03	124.95	1.85	0	1.85	124.95	144.03

Table 1. Optimal drawbead restraining forces

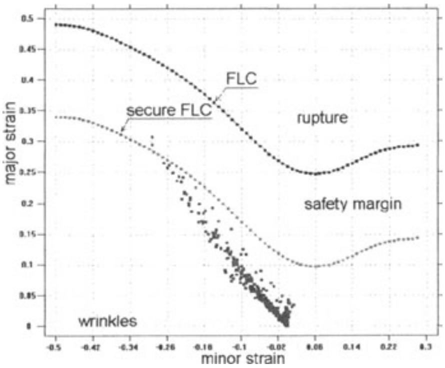

Figure 3. FLD of a 1/4 of the square box before optimization

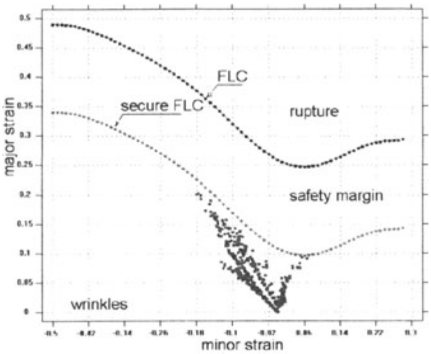

Figure 4. FLD of a 1/4 of the square box after optimization

where P is the adjoint state vector associated to the equilibrium equation (5); P is solution of the following linear system:

$$[K_T]^T \{P\} = -\frac{\partial J}{\partial U} \tag{7}$$

where $[K_T]$ is the tangential stiffness matrix. This linear resolution is carried out only one time per iteration (for all dj/dv_i) so that the computations are considerably reduced compared to a direct differentiation approach. The derivation of a constraint $g_i(v, U)$ can be performed in a similar way.

4. NUMERICAL APPLICATIONS

4.1 Optimization of restraining forces in the deep drawing of a square box

The square box of 15 mm depth which was presented in Numisheet'93 as a benchmark test [13] is considered for the optimization of restraining forces due to drawbeads (Fig. 2).

The quarter of the box is meshed with 468 nodes and 856 triangular elements. The optimization procedure exposed in sections 2 and 3 is applied to determine the optimal restraining forces minimizing the objective function given in (3). Seven segments situated about 12 mm from the die contour are taken as drawbead lines (Fig. 2).

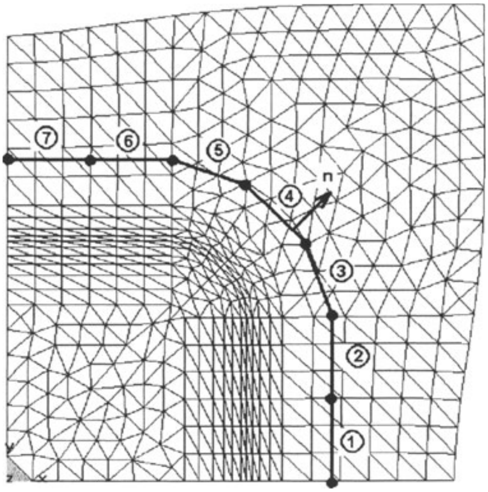

Geometrical and material data:

Dimensions of the flat blank : $150\times150\ \text{mm}^2$

Young's modulus:206000 Mpa

Initial thickness: 0.78 mm

Lankford coefficient $\bar{r} = 1.77$
Friction coefficient $\nu = 0.144$

Total blank holder force: 19600 N

Swift uniaxial stress-strain curve :
$\sigma = 567.29\,(\varepsilon^p - 0.007127)^{0.2637}$ Mpa

Figure 2. *Repartition of design variables in a 1/4 of the square box of Numisheet'93*

4.2 Optimization of material parameters in the deep drawing of the Twingo dashpot cup

The numerical simulation of the forming of the Twingo Dashpot cup was originally proposed by El Mouatassim in 1995 [9]. The nonlinear analysis by the I.A. is carried out without considering the friction effects between the sheet and the tools. The initial material characteristics of the sheet are:

- Young's modulus E= 206000 Mpa,
- Initial thickness h^0= 1.97 mm
- Lankford coefficient $\bar{r} = 0.995$
- Hollomon uniaxial stress-strain curve : $\sigma = 624\ \varepsilon^{0.176}$ Mpa

The solution of this problem shows an important thinning (-18 %), localized in the zone under the punch together with an increase of thickness in the part under the blank holder (+26 %) (see Figure 8). The finite element mesh consists of 848 nodes (1696 nonlinear equations) and 1634 triangular membrane elements (Fig. 5).

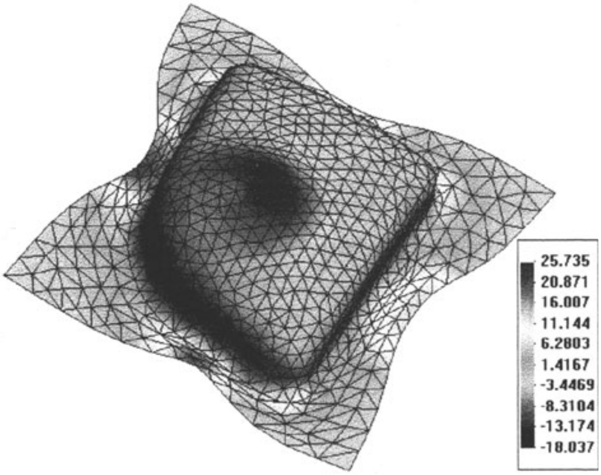

Figure 5. Thickness distribution in percentage of the Twingo dashpot cup

The optimization procedure discussed above is applied to determine the material characteristics minimizing the objective function given in equations (3).

As we do not have an experimental FLC we set the value of the parameters *f* equal to *0.975*. With this value some points of the FLD are beyond the FLC. In this application we use a coefficient s equal to *0.02*.

Table 2 shows material parameters before and after optimization. The FLD and FLC associated to this optimal material have been computed and are satisfying (all the points of the FLD are under the *secure FLC*)

	n	$\bar{r}$
Before optimization	0.176	0.995
After optimization	0.215	0.999

Table 2. Parameters values for the Twingo dashpot cup

5. CONCLUSION

An automatic optimization procedure is presented for the estimation of drawbead restraining forces and material parameters in the preliminary design of deep-drawing process. A new objective function is proposed. The procedure is obtained by combining the Simplified Inverse Approach (a one step approach) and a BFGS algorithm. Sensitivities are computed explicitly by using the Forming Limit Curve (FLC). Two examples are considered to demonstrate the application of the numerical procedure for the design of blank and dies.

The developments on the optimization procedure for other process parameters of the sheet metal forming simulations are under study.

6. REFERENCES

1. Shen SF, Dawson P. Simulation of material processing: theory, methods and applications. *NUMIFORM'95* 1995; Balkema, Rotterdam, The Netherlands.
2. Lee JK, Kinzel GL, Wagoner R. 3rd Int. Conf. on Numerical Simulation of 3D Sheet Metal Forming processes, Verification of simulations with experiments. *NUMISHEET'96;* 1996; Dearborn, USA.
3. Batoz JL, Guo YQ. Analysis and design of sheet forming parts using a simplified inverse approach. *COMPLAS V* 1997: 178-185, Barcelona, Spain.
4. Barlet O, Naceur H, Batoz JL, Knopf-Lenoir C. Shape Optimum Design Of Blank Contours Using A Simplified Inverse Approach. *NUMIFORM'98* 1998: 801-806, Enschede, The Netherlands.
5. Gelin JC, Picart P. 4th Int. Conf. Numerical Simulation of 3D Sheet Metal Forming processes. *NUMISHEET'99* ;, 1999, Besançon, France.
6. Geiger M, Bay N, Kopp R. Advanced Technology of Plasticity. *6th ICTP* 1999; Nuremberg, Germany.
7. Barlet O, Batoz JL, Guo YQ, Mercier F, Naceur H, Knopf-Lenoir C. Optimum Design Of Blank Contours using the Inverse Approach And Mathematical Programming Techniques. *NUMISHEET'96* 1996; 178-185; Michigan, USA.
8. Barlet O, Batoz JL, Guo YQ, Mercier F, Naceur H, Knopf-Lenoir C. The Inverse Approach and Mathematical Programming Techniques for Optimum Design of Sheet Forming Parts. *ASME* 1996; (3); 227-232.
9. El Mouatassim M, Thomas B, Jameux JP, Di-Pasquale E. An industrial finite element code for one step simulation of sheet metal forming. NUMIFORM'95; 1995: 761-766; Balkema, Rotterdam, The Netherlands.
10. Graf A, Hosford WF. Calculations of Forming Limit Diagrams. Met. Trans., V21A; 1990: 87-94.
11. Hosford WF, Caddell RM. Metal Forming Mechanics and Metallurgy, Second Edition, PTR PrenticeHall , Englewoods Cliffs, 1993.
12. Zhao L, Sowerby R, Sklad M.P. Int. J. Mech. Sci.; V38, No12, (1996): 1307-1317.
13. Nakamashi E. Sheet Forming Process Characterization by Static-Explicit Anisotropic Elastic-Plastic Finite Element Simulation ; Proceedings of Numisheet'93 , 1993: 109-123

FROM THE PREDIMENSIONING APPROACH TO THE OPTIMISATION OF FORMING PROCESSES OF THIN FABRIC COMPOSITE PARTS

J.L. BILLOET[1], H. BOROUCHAKI[2] & A. CHEROUAT[2]

1- LMSP-151 Bd de l'hôpital, 75013 Paris - France

2- LASMIS, UTT- B.P. 2060, 10010 Troyes - France

Abstract. An important step in the manufacturing processes of thin composite components is the laying-up of the reinforcement onto the mould surface. The prediction of the angular distorsion of the reinforcement during the laying-up and the changes in fibre orientation are essential for the understanding of the manufacture process and the evaluation of the mechanical properties of the composite structures. This paper presents an optimization based method for simulation of forming processes of woven fabric reinforced composites. Two different approaches are proposed for the simulation of the draping of woven fabric onto complex geometries : geometrical and mechanical. The geometrical approach is based on a geometrical fishnet model and the mechanical approach is based on a meso-mechanical model. Some numerical simulations of forming process are proposed and compared with the experimental results in order to demonstrate the efficiency of the proposed approaches.

1. INTRODUCTION

Composite materials with glass, carbon or aramid fibres and polymeric matrices are known to have high specific strengths and stiffnesses which on combination with automatic manufacturing processes, make possible to fabricate composite structures with high level of weight and cost efficiency. As we know, the substitution of metal alloys by composite materials, in general, reduces structure mass by 20-30%. The increase is also due to the numerous variety of products (roving, fabrics, knitted fabrics, braids pre-impregnated or not) permitting the elaboration of structures [6]. Fabrication processes, also, have undergone substantial evolution in recent years. Although the traditional hand lay-up process will remain the process of choice for some applications, new developments in resin transfer moulding, sheet moulding compound, low temperature curing pre-pregs and low pressure moulding compounds have reached new heights of sophistication, and are now being exploited in high technology areas such as aerospace industry.

Hand lay-up is the most common method of producing thin composite parts. The primary methods of automation in hand lay-up relate to computer software. Software is used to generate flat patterns from the layer surface and the ply boundary and to find the most efficient nest of cut plies to minimize the scrap. As for many other composite forming processes, the tendency of getting a more and more geometrically complicated part demands a systematic numerical simulation of the laying-up processes. This allows to "virtually" modify the process conditions in order to find the best process parameters for the final product. Thus, it gives an efficient way to reduce cost and time (Figure 1).

The composite manufacturing process involves large displacements and finite shear deformation of fibres, which can have a significant effect on the processing and on

P. Chedmail et al. (eds.), Integrated Design and Manufacturing in Mechanical Engineering, 303-310.
©2002 *Kluwer Academic Publishers.*

the structural properties of the finished product. Many studies have been devoted to the mechanical and numerical modelling of the laying-up processes using the finite element analysis [2,3,4,10], allowing the prediction of the fibre deformation during the process.

In this work, we propose two different numerical approaches to simulate the deformation of pre-impregnated woven fabrics: geometrical approach and mechanical approach. The geometrical approach is well adapted to the pre-dimensioning level. It is based on a modified "MOSAIC" algorithm, which is suitable to generate a regular quad mesh representing the lay-up of the curved surfaces. The method is implemented in the GeomDrap software [4]. This software provides a fibre quality chart (showing the fibre distortions, the rate of falling and the rate of draped surface) to predict badly impregnated regions. It can be used to optimise the draping process (with respect to the above quality measure) by improving the lay-up directions or the marker data location. The lay-up of complex curved surfaces can be made in a few seconds.

The mechanical approach is based on a meso-structural level. It permits to take into account the various dominating mechanics in the physics of the mechanical transformation of prepreg fabrics during the shaping process, namely, large angular variations of yarns, viscoelasticity of resin and evolution of possible damages in yarns. Applications are made to the simulation of the shaping of some geometrically complex parts to show the efficiency of the proposed methodology.

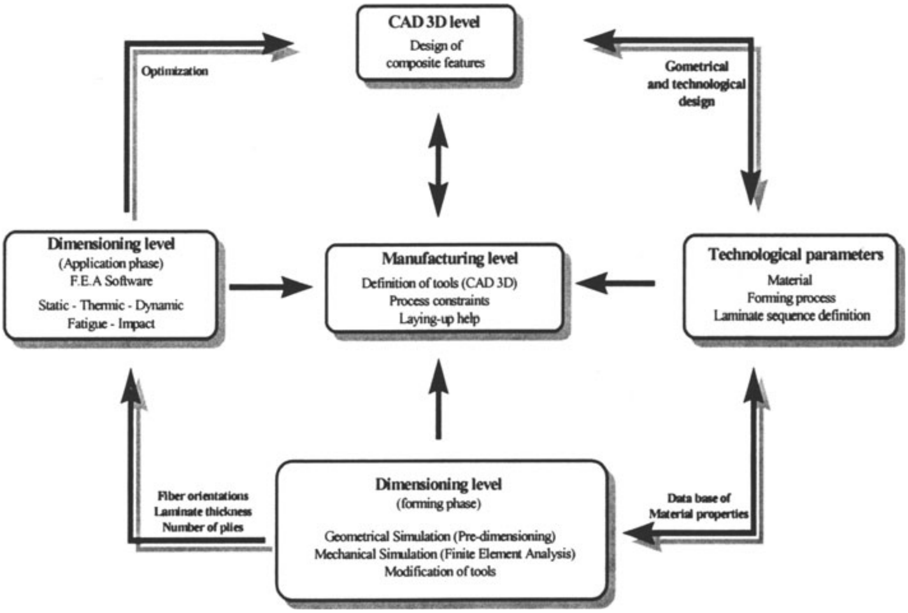
CAD 3D level
Design of composite features
Optimization
Gometrical and technological design
Dimensioning level
(Application phase)
F.E.A Software
Static - Thermic - Dynamic
Fatigue - Impact
Manufacturing level
Definition of tools (CAD 3D)
Process constraints
Laying-up help
Technological parameters
Material
Forming process
Laminate sequence definition
Fiber orientations
Laminate thickness
Number of plies
Dimensioning level
(forming phase)
Geometrical Simulation (Pre-dimensioning)
Mechanical Simulation (Finite Element Analysis)
Modification of tools
Data base of
Material properties

Figure 1. Virtual conception for design and manufacture of composite pieces

SUMMARY OF THE GEOMATRICAL APPROACH

First, we recall the mathematical formulation of the geometrical draping and we propose an algorithm to solve the draping problem. Let denote by Σ the surface to drape. Let F be the woven fabric modelled by two families of mutually orthogonal and inextensible fibre described by the co-ordinates $x = (\xi, \eta)$. These families constitute regular quad mesh T_F of the fabric F. The problem of draping of woven fabric F onto the surface Σ consists in associating each node of T_F with a point of the surface such that the lengths of the edge of the corresponding mesh T_F^Σ on the surface are preserved. This problem presents an infinity of solutions depending on the first node of T_F^Σ (called the point of impact) associated to a node of T_F^Σ and on the direction of the fabric co-ordinate axes at this node. Thus, to ensure a unique solution, we suppose that the point of impact on the surface as well as the fabric orientation at this point are known. The draping process is given by the following scheme :

1. associate a node $x_0 = (\xi_0, \eta_0)$ of T_F to the specified point of impact on the surface,
2. compute step by step the nodes of T_F^Σ, classified as α -nodes, from the point of impact, associated with nodes (ξ, η_0) of T_F,
3. compute step by step the nodes of T_F^Σ, classified also as α -nodes, from the point of impact, associated with nodes (ξ_0, η) of T_F,
4. compute cell by cell all the other nodes of T_F^Σ, classified as β -nodes, from x_0 and the nodes associated to nodes (ξ, η_0) and (ξ_0, η) of T_F.
5. the nodes of T_F^Σ associated with nodes (ξ, η_0) and (ξ_0, η) of T_F (the α -nodes) are put on the surface along the geodesic lines emanating from the point of impact.

Regarding the β -nodes, various algorithms are proposed [1,4,10]. Most of them use an analytical expression of the surface and formulate the draping problem in terms of non-linear partial differential equations. Other algorithms are also proposed to simplify these equations by using a discrete approximation of the surface by flat triangular face (i.e. a mesh of the surface).

Based on this latter approach we propose a new algorithm using a mesh of the surface. The geodesic lines on the surface are approximated by the polylines plotted on the surface using linear orthogonal transformation in $\Re^3$ to flatten the surface locally (these polylines become a straight line segment after these transformations). This allows us to determine the α -nodes. The β -nodes are computed by solving an optimisation problem corresponding to determine a vertex of an equilateral quad plotted on the surface from the data of the three other vertices. This optimisation problem formulate the direction of the geodesic lines emanating from the searched vertex.

SUMMARY OF THE MECHANICAL APPROACH

Several deformation modes may occur during the forming process of pre-impregnated reinforcements, which can have a significant effect on the finished product. The formability of composite fabric is strongly affected by the fabric waving, the properties of reinforcements and the geometry of the mould. The prediction of the fibre distorsions, the yarns and resin deformations and the final fabric shape are essential for the understanding of the forming process and the evaluation of the mechanical properties of the composite products.

Woven fabric deformation involve large geometrical transformation, but the associated strains are small. Some models are proposed to simulate the deformation of these materials by forming process [2,3,7]. These models can predict the deformations of woven fabric and evaluate the influence of different parameters on the fabric behaviour during the forming phase. However, their disadvantages are the extreme complexity for the generation of a lot of degrees of freedom and the limitation to small studies. In order to predict structural behaviour of pre-impregnated woven fabric, a new numerical model has been developed on a mesostructural level [2,3,5]. This model permits to take into account the various mechanical parameters, like, large angular variations of yarns, viscoelasticity behaviour of resin, elastic nonlinear behaviour of yarns and contact with friction between fabric and rigid tools.

The basic assumptions for the mechanical draping are that : the warp and weft yarns are assimilated as a truss which connecting points are hinged and the resin, considered as a membrane is, kinematically, coupled to the fabric at these connecting points. In this method, an initially flat fabric is first subdivided into a finite number of structured small grid which are called bi-component finite elements. A bi-component finite element contains two orthogonal elements representing the warp and the weft fibres and one membrane element representing the membrane resin. The effective cross sections of the truss and the effective thickness of the membrane are calculated by using the fibre volume fraction of the pre-impregnated fabric. The continuum motion of each connecting point, ensured by the non-sliding inter-fibre and the membrane resin, means that a nodal approximation for the displacement can be used. The global equilibrium is obtained by the total potential energy

$$\Pi(\dot{\mathrm{u}}) = \int_{\Omega^{resin}} \sigma^{m} \delta \mathbf{D}^{mR} dV + \int_{L^{fibre}} \sigma_L^f \delta D_L^{fR} ds - \int_{\Omega_c} \mathbf{f}_c \dot{\mathrm{u}} dS - \int_{\Omega_u} \mathbf{f}_s \dot{\mathrm{u}} dS + \int_{\Omega} \rho \ddot{\mathrm{u}} \dot{\mathrm{u}} dV \qquad (1)$$

Using Green-Naghdi's objective tensor stress [8], the stress rate of the fibre σ_L^f, depending on the stretching deformation D_L^f, and the stress rate tensor of the resin σ^{mR}, depending on the tensor strain rate $\mathbf{D}^{mR}$, can be written at each time t_{n+1} as

$$\left(C^f_L\right)_{n+1} = \left(\bar{\sigma}^f_L\right)_n + \int_{t_n}^{t_{n+1}} E^f_L D^f_L dt \text{ (fibres)} \quad \left(\sigma^m\right)_{n+1} = \left(\sigma^m\right)_n + \int_{t_n}^{t_{n+1}} \mathbf{C}^m : \bar{\mathbf{D}}^m dt \text{ (resin)} \qquad (2)$$

The constitutive law of fibres is non linear and is written in terms of longitudinal modulus of stretching E^f_L depending on the principal elongation of fibre λ^f_L, the elastic modulus of fibre E_f and the shrinkage factor ε_{sh}. The viscoelastiy behaviour law of resin is formulated in the time domain by the hereditary integral and using the relaxation time τ_k and the fourth order relaxation tensor C^m_{ij} :

$$E^f_L\left(\lambda^f_L\right) = E_f\left(1 - e^{\frac{-\dot{\lambda}^f_L}{\lambda^f_L \varepsilon_{sh}}}\right) \text{ (fibres)} \qquad C^m_{ij} = \left(C^m_{ij}\right)^\infty + \sum_1^k \left(C^m_{ij}\right)^k e^{\frac{-\tau}{\tau_k}} \text{ (resin)} \qquad (3)$$

The highly non-linear system (Eq. 1) expresses the mechanical dynamic equilibrium of the fabric and the tool at each time step. It can be solved either by an iterative implicit or by a dynamic explicit method. The latter is extremely robust and helpful in forming simulation since there are no iterative procedures to solve the global dynamic equilibrium problem. However, one should control, efficiently and automatically, the time step size in order to satisfy the accuracy and stability requirements (see Abaqus User's Manual [9]).

NUMERICAL EXAMPLES

Two 3-D composite forming simulations will be now presented in order to test the capability of the proposed methodologies to predict the fibre orientation and the fabric shape during the laying-up operation. These simulations are performed using the geometrical analysis computer code GeomDrap [9] and the FEA computer code Abaqus/Explicit [9]. The first example investigates the effect of the fibre orientations required to completely draping complex part without any defect (Figure 2a). The second example shows the effect of the imposed fabric orientation on the quality of stamped composite part (Figure 2b).

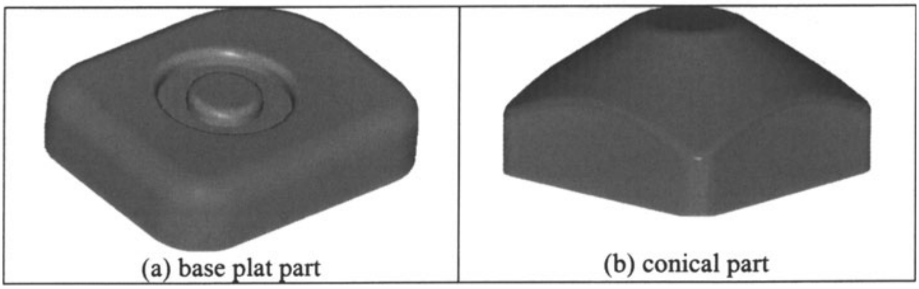
(a) base plat part

(b) conical part

Figure 2. CAD of the composite parts

Geometrical forming

The first example concerns the effect of the fibre orientations on the draped composite part using the geometrical draping of a base plate piece. The impact points is chosen at the centroid of the piece. Two different fibre orientations (0°/90°) and (-45°/45°) has been considered. Figure 3a (resp. Figure 4a) shows the resulting 3D surface lay-up for the (0°/90°) (resp. (-45°/45°)) fibre orientation, the 2D corresponding flat patterns is illustrated in Figure 3b (resp. Figure 3b). It is clearly visible that, in the considered cases, the surface of the piece is globally draped. However, in the second case, a smaller area of the flat fabric is used (cf. Table 1). These results show the effect of the fabric orientation in the draping processes.

Table 1. Numerical results of the geometrical draping

Fabric	**length of grid**	**length of fabric**	**drape quality**	**surface covering**	**speed grid/s**	**fall rate**	**CPU second**
0°/90°	2	120	51.0	96.7 %	27494	19.4 %	0.34
-45°/ 45°	2	120	58.4	95.2 %	26368	30.8 %	0.35

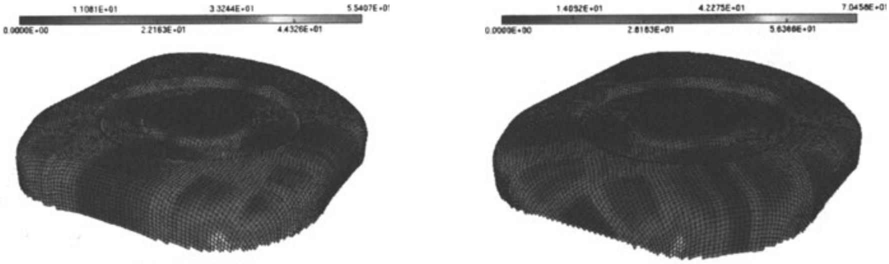

(a) (0°/90°) (b) (-45°/45°)

Figure 3. 3D surface lay-up of composite parts

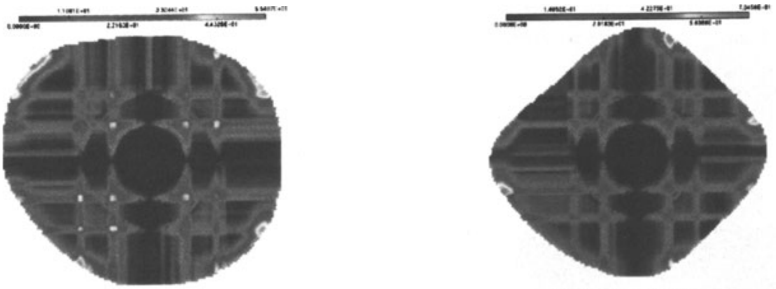

(a) (0°/90°) (b) (-45°/45°)

Figure 4. 2D Flat patterns of the composite parts

Mechanical forming

The second example is the 3D deep-drawing simulation of a conical piece by experimental and mechanical approaches. Figure 5 shows the experimental shapes with respect to (0°/90°) and (-45°/45°) fibre orientations for 100 mm displacement of the punch. Notice that, the woven fabric material is highly anisotropic and the initial directions of the fibre influence the final resulting shape. Figure 6 presents shaded contours interpolated from the map of the shear angle of (0°/90°) and (–45°/45°) fibre orientations. Figure 7a shows the variation of fibre shear angles along the diagonal lines of the final shape. The local shear angle is represented by the orientation of the deformed truss elements (warp and weft) representing the fibre behavior. From this figure, it is clear that for (0°/90°) fibre orientation, the zero shear angle corresponds to the transition zone within each of the four quarters corresponding to the four corners of the conical punch. The shear angles of deformed elements are less than 45°. For (–45°/45°) fibre orientation, the zero shear angle zone extends around the diagonal-lines of the fabric. Figure 7b shows the variation of fibre shear angles along the median axes of the final shape. The shear angles of deformed elements are less than 40° and prove the accuracy of the model.

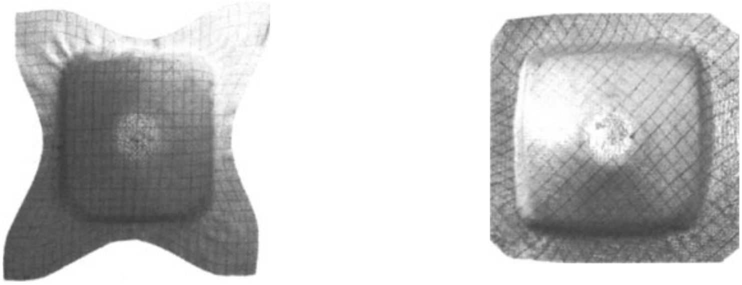

(a) (0°/90°)

(b) (-45°/+45°)

Figure 5. Experimental shapes

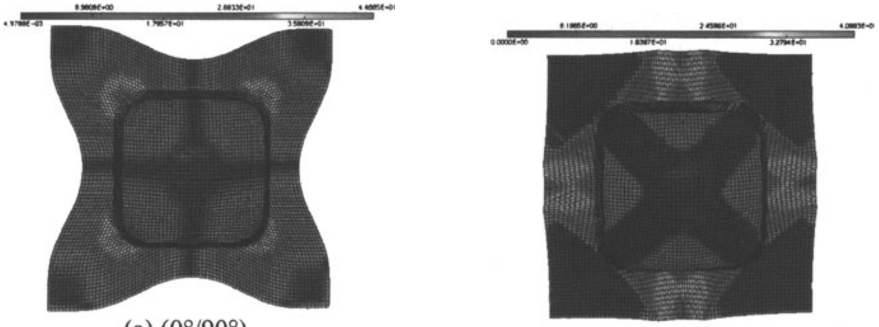

(a) (0°/90°)

(b) (-45°/45°)

Figure 6. Iso-values of the shear angles of the fibres

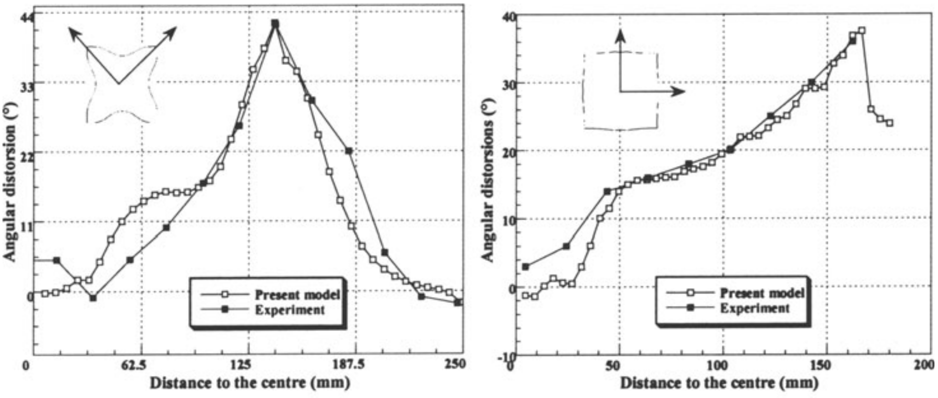

(a) (0°/90°) (b) (-45°/+45°)

Figure 7. Angular distorsions along the fabric lines

CONCLUSION

An efficient numerical approach has been presented to simulate accurately the draping of composite fabric. The numerical simulation is made up two steps : geometrical draping and mechanical draping. The geometrical approach is used to optimise the draping process by improving the lay-up orientations and the location of the point impact (pre-dimensioning step). The mechanical approach completes the dimensioning procedure.

REFERENCES

[1] Bergsma O.K. & Huisman J., Proceeding of the 2nd In. Conference On Computer Aided design in Composite Material Technology, Springer Verlag, pp. 323-333, 1988
[2] Billoët J.L. & Cherouat A., Proc. of Numisheet'99, vol. 1, pp. 567-572, 1999
[3] Blanlot. R & Billoet J.L, J.N.C. 9, pp. 761-772, 1996
[4] Borouchaki H., Cherouat A. & Billoët J.L., "GeomDrap®" New Computer Aided Design and Manufacturing for Advanced Textile Composites, Version 1, 1999
[5] Cherouat A. & Billoët J.L., Proc. of Numisheet'99, vol. 1, pp. 573-578, 1999
[6] Gay D. & Carronnier D., Revue des Composites et des Matériaux Avancés, vol 6, 1996
[7] Gelin J.C., Cherouat A., Boisse P., Sabhi H., Composites Science and Technology, 56, pp. 711-718, 1996
[8] Gilormini P. & Roudier P., Abaqus and Finite Strain, Intern report LMT Cachan n° 140 France, 1993
[9] Hibbit, Karlsson & Soresen, ABAQUS theory, User's Manual V. 5.5, 1995
[10] Van Der Ween F., Int. J. Num. Meth. Engng, 31, pp. 1415-1426, 1991

Chapter 5
MANUFACTURING AND PROCESS PLANNING

Design Process Modelling of Process Planning for Flexible Lines Based on Conceptual Graphs and Design Rules - Applied to Cylinder Head Machining. 313
A. LEFEBVRE, L. SABOURIN, G. GOGU, J. RENAUD

Determination of virtual means for the integrated design.................................. 323
K. MAWUSSI, V.-H. DUONG, R. PONSONNET

Selecting material handling equipment with PROMETHEE............................. 331
P. DE LIT, T. L'ÉGLISE, J. DANLOY, B. REKIEK, A. DELCHAMBRE

A Methodology for Cost and Quality Optimization in a Design System by Linking Quality Methods 339
G. DRAGOI, D. BRISSAUD

Disassembly Sequencing Using Technological Data... 347
N. REJNERI, J.-C. LÉON, G. DEBARBOUILLÉ

Application of fuzzy logic for an assembly methodology 355
A. SINZINKAYO, C. MASCLE, M. BALAZINSKI

A. LEFEBVRE, L. SABOURIN, G. GOGU, J. RENAUD

DESIGN PROCESS MODELING OF PROCESS PLANNING FOR FLEXIBLE LINES BASED ON CONCEPTUAL GRAPHS AND DESIGN RULES. APPLIED TO CYLINDER HEAD MACHINING

Abstract. Process planning for mass-produced parts in the manufacturing industry requires a long and critical approach as both product/process data interaction and technical and cost-effectiveness parameters are crucial. Within the RENAULT Powertrain Division, the scope of our research work is to define process plans for prismatic parts machined on flexible production lines. A process plan is the outcome of a constraints analysis based on quality, cost, lead time, strategy and innovation goals. The first step of our work consists in identifying and formalizing any constraints: manufacturing process constraints (machining, assembly, etc.), product geometry, functional constraints (camshaft bearing lines, combustion face, etc.) and production constraints (volume, mix, etc.). Using conceptual graphs associated with the *Design Rules* methodology enables us to view precisely several functional conditions to be met for a product. One of the key features of the *Design Rules* methodology is to provide feasibility areas used to assess whether a product may or not be machined on a production line. In addition conceptual models are also used to identify and set procedural rules to limit technical risks and re-use already developed practical skills.

1. INTRODUCTION

The work presented in this paper has been sponsored by RENAULT's Research Branch. The field of study includes process planning modeling for prismatic parts, and in particular cylinder heads. For about four years, the Mechanics Branch has been setting up flexible production lines that can handle variations in volume and mix (different cylinder heads).

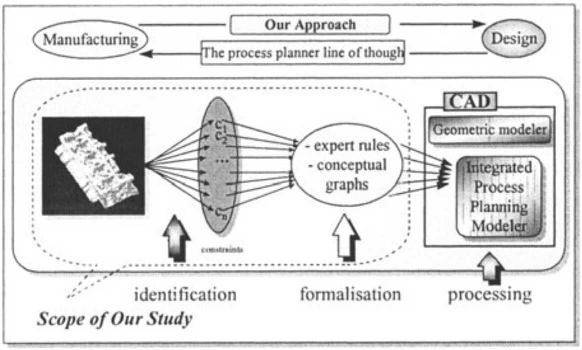
Our Approach
Manufacturing
Design
The process planner line of though
CAD
Geometric modeler
C_1
C_2
...
C_n
- expert rules
- conceptual graphs
Integrated Process Planning Modeler
constraints
identification
formalisation
processing
Scope of Our Study

Figure 1. Scope of Our Study

P. Chedmail et al. (eds.), Integrated Design and Manufacturing in Mechanical Engineering, 313-322.
©2002 *Kluwer Academic Publishers.*

Process planning is the outcome of processing various requirements (requirements handled by the process planner, but also by the project leader, machine manager, etc.). Our goal consists in identifying and modeling these requirements in order to feed them into a process modeler "Figure 1". This paper describes first the *Design Rules* approach used to capitalize and formalize craftsmanship. The second part covers product/process constraints modeling using *conceptual graphs*.

2. KNOWLEDGE CAPITALIZATION

The *Design Rules* methodology [1,2] used to capitalize and formalize craftsmanship is used here to identify constraints. One of its key features lies in the representation of validity domains associated with the product/process parameter combination. The main steps required to provide product feasibility areas are described hereafter. The following example shows the overall machining process for a cylinder head. The first step consists in building the manufacturing macro-process "Figure 2". This is the sequence of process activities with functional links added that show the mutual influence of these activities (e.g.: valve guide and seat assembly and cylinder head combustion face machining). Resources and entities to be processed are also assigned to each activity. This step consists in gathering expertise and brainstorming sessions with the department in charge of cylinder heads industrialization.

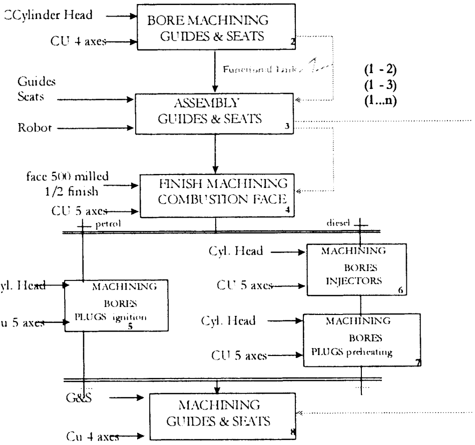
CCylinder Head
CU 4 axes
BORE MACHINING GUIDES & SEATS
2
Functional Links
(1 - 2)
(1 - 3)
(1...n)
Guides
Seats
Robot
ASSEMBLY GUIDES & SEATS
3
face 500 milled
1/2 finish
CU 5 axes
FINISH MACHINING COMBUSTION FACE
4
petrol
diesel
Cyl. Head
CU 5 axes
MACHINING BORES INJECTORS
6
Cyl. Head
Cu 5 axes
MACHINING BORES PLUGS ignition
5
Cyl. Head
CU 5 axes
MACHINING BORES PLUGS preheating
7
G&S
Cu 4 axes
MACHINING GUIDES & SEATS
8

Figure 2. Partial Macro-Process for Machining a Cylinder Head

A list of existing products matching the values of the product/process parameters is then drawn up for a given process operation "Figure 3". Only the parameters that significantly affect an operation are retained.

Blank Boring & Guide Bores Finish - ADM Seats

	PRODUCT			PROCESS											
	Cyl Head			Unit 3 axes			Tool/sing. spindle				Axe B	Cooling Unit			
	Vol.	Desc	TT	Part Position			a mm/t		N t/min		direct.	Rate		Pressure	
				x	y	z	Eb.	Fi.	Eb.	Fi.	ADM	Eb.	Fi.	Eb.	Fi.
Product A															
Product B															
Product C															

Figure 3. Component/Equipment and Product/Process Parameter Table, Applied to the Valve Guide/Intake Seat Boring Process

The third step consists in finding the functional conditions CF_i to be met for the operation and the major parameters. $CF_i = f_i(p_1, p_2, \ldots, p_n)$ models are provided, where $p_1, p_2, \ldots, p_n$ are product, process parameters or parameter combinations and f_i coupling functions. The last step consists in graphically representing the models previously determined "Figure 4". This representation features a scatter plot, where each point corresponds to an existing product manufactured on a production line. Sometimes several parameters may be consolidated in the form of 'composite parameters'; this combination, generally more typical for the experts, decreases the dimension of the CF_i model, which makes graphical representation easier.

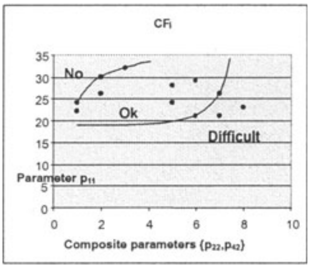

Figure 4. Product Feasibility Domain

The *Design Rules* approach is based on capitalizing on the company's craftsmanship. In an innovation context, the representation of the product feasibility domains will be used to consider integrating a new part into existing flexible lines as critical parameters outside the validity domain can be identified sooner.
The *Design Rules* approach requires that the domain entities be defined first. The obvious choice was to identify the manufacturing features; these are then classified with reference to their attributes and toleranced geometrical items.

2.1. Manufacturing Feature

The expertise breakdown approach is based on the manufacturing feature concept "Figure 5". Manufacturing features are used to provide the players [3] involved from design to manufacturing [4,5] with a better understanding of a part. These include therefore both product and process data [6,7]. The definition hereafter should be compared with the GAMA group's definition [8]: a manufacturing entity features a number of geometrical surfaces with attributes (surface condition, tolerancing, etc.) and a known sequence of operations (machining, assembly, Heat Treatment, etc.).

Figure 5. Detail of a Feature's Product Part

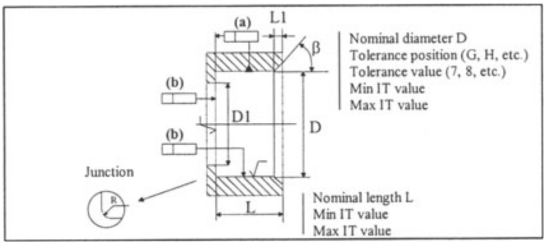

2.2. Manufacturing Feature Classification

After identifying features for the cylinder head camshaft bores function, these were classified from a product viewpoint based on their attributes (diameter, tolerances and surface condition) and toleranced geometrical items (axis, face, etc.). The information has been taken from methods oriented drawings.

2.3. Camshaft Bearing Lines Case Study

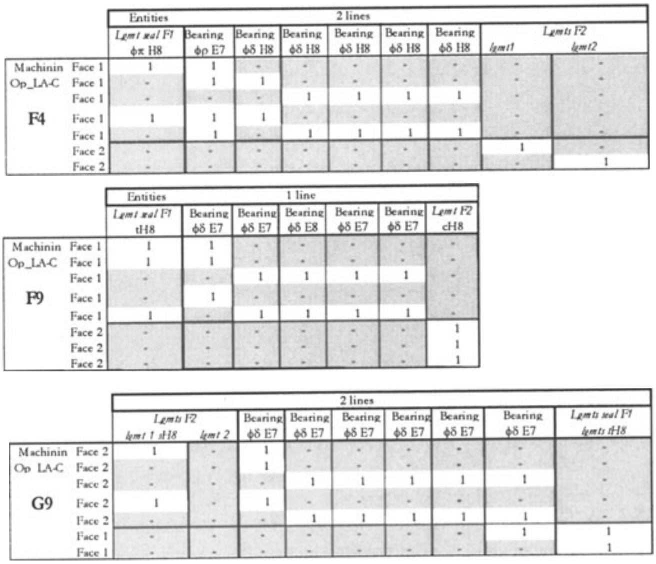

		Entities	2 lines							
		Lgmt seal F1 φπ H8	Bearing φρ E7	Bearing φδ H8	Bearing φδ H8	Bearing φδ H8	Bearing φδ H8	Bearing φδ H8	Lgmts F2 lgmt1	lgmt2
Machinin	Face 1	1	1	-	-	-	-	-	-	-
Op_LA-C	Face 1	-	1	1	-	-	-	-	-	-
	Face 1	-	-	-	1	1	1	1	-	-
F4	Face 1	1	1	1	-	-	-	-	-	-
	Face 1	-	1	-	1	1	1	1	-	-
	Face 2	-	-	-	-	-	-	-	1	-
	Face 2	-	-	-	-	-	-	-	-	1

		Entities	1 line					
		Lgmt seal F1 tH8	Bearing φδ E7	Bearing φδ E7	Bearing φδ E8	Bearing φδ E7	Bearing φδ E7	Lgmt F2 cH8
Machinin	Face 1	1	1	-	-	-	-	-
Op_LA-C	Face 1	1	1	-	-	-	-	-
	Face 1	-	-	1	1	1	1	-
F9	Face 1	-	1	-	-	-	-	-
	Face 1	1	-	1	1	1	1	-
	Face 2	-	-	-	-	-	-	1
	Face 2	-	-	-	-	-	-	1
	Face 2	-	-	-	-	-	-	1

		2 lines								
		Lgmts F2 lgmt 1 sH8	lgmt 2	Bearing φδ E7	Bearing φδ E7	Bearing φδ E7	Bearing φδ E7	Bearing φδ E7	Bearing φδ E7	Lgmts seal F1 lgmts tH8
Machinin	Face 2	1	-	1	-	-	-	-	-	-
Op LA-C	Face 2	-	-	1	-	-	-	-	-	-
	Face 2	-	-	-	1	1	1	1	1	-
G9	Face 2	1	-	1	-	-	-	-	-	-
	Face 2	-	-	-	1	1	1	1	1	-
	Face 1	-	-	-	-	-	-	-	1	1
	Face 1	-	-	-	-	-	-	-	-	1

Figure 6. Detailed Machining Process for Camshaft Bearing Line Feature per Type of Cylinder Head (F4, F9 and G9)

Cylinder head camshaft bearing line machining is a highly complex operation. Selecting the machining parameters (i.e., number of passes) requires craftsmanship know-how related to using special tools (reamers) with tight design tolerances.
The machining process "Figure 6" used by Renault is not set and this leads to process variants from one process planner to the next and to significant process differences from one type of cylinder head to the next (8 or 16 valves, number of bearings per camshaft): figure 6 shows the machining process for cylinder head camshaft bearing lines for three types of parts: F4, F9 and G9. The main differences lie in the number of passes per entity, selecting the entities to be machined and selection of tools (shouldered or not). These differences come from the design dimensioning which is different from one cylinder head to the next, the part's geometry, and are also related to the process planner know-how.
The operation is broken down as in the first step of the *Design Rules* methodology: the process activity sequence is described for each product (G9, F4, F9), and each activity is assigned resources and processed entities "Figure 7".

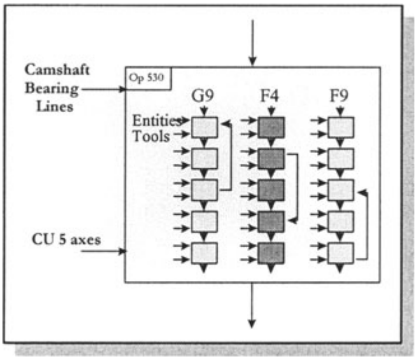

Figure 7. Machining Micro-Process for Cylinder Head Camshaft Bearing Lines

2.4. Expertise Feedback & Craftsmanship Rules

Our expertise feedback approach is based on the process planner who handles the manufacturing features and whose line of thought generates the process described in Figure 9: operation sequencing, selecting the entities to be machined per operation, selecting the tools required for the operation, etc. Identifying the bidirectional links between product/process parameters and determining the know-how rules are used to build a craftsmanship knowledge base [2].
These expertise rules are currently under review. Those already established are of the 'if, then, else' type "Figure 8". The following three types have been defined f1, f2 and f3. Figure 8 shows each of them applied to machining a coaxial seal housing on a bearing. The goal is now to be able to represent and process this set of rules with their interactions. These will include relations and constraints that will be modeled using conceptual graphs.

3 f1: if $\{\text{parameters}\}_{product}$ then $\{\text{parameters}\}_{process}$

if $\varnothing_{housing} = \varnothing\rho$ **and** $H = H\rho$ **and** $R = R\rho$ **and** $loca_{bearing}$ = loca ∅d2 **and** no restriction

then nb_passes = 2

3 f2: if$\{\text{parameters}\}_{process}$ then $\{\text{parameters}\}_{product}$

if tool_type = shouldered **and** machining_type = finish **and** nb_assembly = 1

then coax ∅d1/M-N Ok

3 f3: if $\{\text{param.}\}_{product/process}$ then $\{\text{parameters}\}_{process}$

if cycle time = tcy **and** coax ∅d1/M-N **and** M-N is $loca_{bearing}$ ∅d2

then shouldered tool finish

Figure 8. Sample Expertise Rules

3. MODELING CONSTRAINTS

This involves modeling and describing the line of thought behind the machining process, i.e., the entire product/process constraints. In order to do this, the parameters describing product industrialization, such as tool selection, type of operation, number of machining passes per entity, sequence of operations, type of assembly, etc., had to be determined.

In order to structure these data, a representation tool was required to identify any type of relation between any object and its attributes, but the objects also had to be broken down and tiered [9]; in addition, the tool must also allow model simulation using in particular external data handled by experts (tools databases). The models thus defined must be understandable by every expert from the various trades.

Conceptual graph modeling was retained as it features the following advantages:

Both static and 'dynamic' appearance of the models, in particular when concept instances change. Processes can therefore be simulated.

Ability to define specific concepts such as database or function concepts used to access data external to the model.

3.1. Conceptual Graph Modeling

A conceptual graph is an abstract representation comprising nodes called concepts and conceptual relations interlinked by arcs [ISO/IEC 10646-1].

3.1.1. Definition

A more formal definition is provided by M.-L. Mugnier [10]: a conceptual graph "Figure 9" is related to a base S which defines the basic vocabulary used to represent knowledge handled in a domain. A base is described as $S = (T_C, T_R, s, I, t)$, and includes: T_C a set of the types of concepts, T_R, a set of the types of relations, s which assigns the maximum type of each of its arguments to any type of relation, I a set of individual markers, t an application from I to T_C which assigns a type of concept t to any individual marker m.

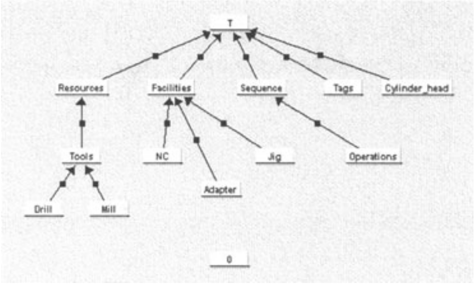
T
Resources
Facilities
Sequence
Tags
Cylinder_head
Tools
NC
Jig
Operations
Adapter
Drill
Mill
0

T_C: Partial Concept Type Lattice, I = {boring, 1231, M4, blank}, t = {(boring, entity), (1231, tool), (M4, assembly), (blank, operation)}

Figure 9. Partial Sample Base $S = (T_C, I, t)$

A basic conceptual graph "Figure 10" is a graph entered as $G = (R, C, U, label)$ where:

- R and C are two classes of nodes known as relation nodes and concept nodes (with C different from zero),
- U is a set of edges, the set of edges adjacent to a node r is fully sequenced,
- Label: Each node has a label defined as follows:

  if $r \in R$, then $label(r) = type(r) \in T_R$; if $c \in C$, then $label(c) = (type(c), ref(c))$

3.1.2. CharGer© Modeling Tool:

The modeling tool used has been developed by the University of Alabama. The conceptual graphs built with CharGer© [11] are used to:

- build animated data models upon instance changes,
- model static data (properties, etc.) and processes (database searches, function calculation, etc.) in multi-contexts and to simulate them [12,13].

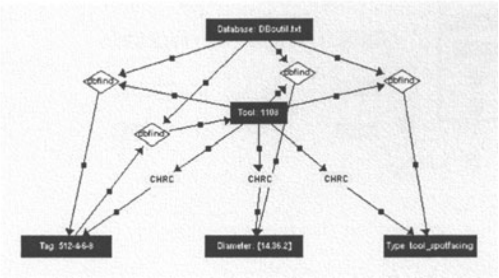
Database: DBoutil.txt
dbfind
dbfind
dbfind
Tool: 1108
dbfind
CHRC
CHRC
CHRC
Tag: 512-46-8
Diameter: [14.36.2]
Type: tool_spotfacing

Figure 10. Simple Conceptual Graph

Figure 10 shows a simple conceptual graph formalizing the relations between a tool and its characteristics. Concepts are defined by rectangles, and ellipses and diamonds define conceptual relations. The *Tool* features three attributes (*tag*, *diameter*, *type*). If the tool number is considered as system input data, a change in tool number value automatically triggers an instance update for the other three attributes via a dynamic link. The associated database is of the text type (DBoutil.txt) and contains the fields as specified in the graph from Figure 10.

3.2. Identifying product-process constraints

As to the constraints related to building a process, only the manufacturing constraints establishing links between product and process parameters have been taken into account so far. Assuming a bore with known geometrical characteristics, the simplified conceptual graph "Figure 11" of the *bore* entity features generic product (*characteristics*) and process (*operation* and *tool*) concepts. The relations between concepts are either basic links {POSS (possesses), CHRCED (characterized), SUP, INF} or mathematical relations {functions} or database searches {dbfind}. The representation tool CharGer© is also used to simulate the change in values of each concept based on the dynamic operator defined. In this example "Figure 11", the major parameters for a tool (length and diameter) have to be defined. This graph shows how selecting tool parameters is restrained by product information [14]. The bore depth and diameter tolerance determine the tool length and diameter which are read through a search in the DBCPI.txt database. Likewise, the quality and condition of the bore surface will determine the type and sequence of the operation. In this case, database searching is based on a heuristic process.

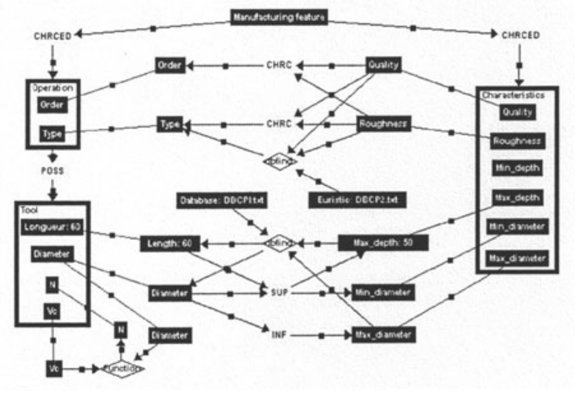
Manufacturing feature
CHRCED
CHRCED
Order
CHRC
Quality
Operation
Order
Type
Characteristics
Quality
Type
CHRC
Roughness
Roughness
dbfind
POSS
Min_depth
Database: DBCP1.txt
Euristic: DBCP2.txt
Max_depth
Tool
Longueur: 60
Length: 60
dbfind
Max_depth: 50
Min_diameter
Diameter
Max_diameter
N
Diameter
SUP
Min_diameter
Vc
N
Diameter
INF
Max_diameter
Vc
function

Figure 11. Product/Process Constraints

3.3. Expertise Modeling

Formalization, analysis and assessment of the manufacturing constraints based on experts' know-how are the main goal of our modeling work. Conceptual graphs are used to express the expertise rules in the form of relations between concepts and links, and to simulate their application.

The conceptual graph from Figure 15 shows an feature breakdown for camshaft bearing lines. Each entity *Bearing1*, *Bearing6* and *Seal_housing* from the product viewpoint features geometrical items and attributes. All of this information is detailed in the form of nested graphs [10]. The expertise rules described earlier *f1*, *f2* and *f3* (see section 2.4) are formalized according to their description "Figure 8". These represent the links between product (known) and process (to be explained) data. This is then used to establish the heuristic processes, i.e., the dynamic links assigned to *f1*, *f2* and *f3*, and to simulate lines of thought.

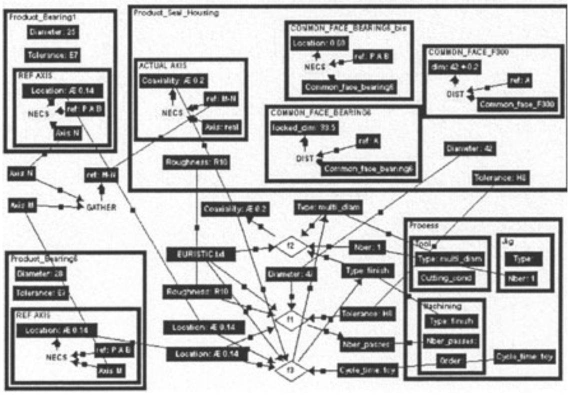
Product_Bearing1
Diameter: 25
Tolerance: E7
REF AXIS
Location: Æ 0.14
NECS
ref: P A B
Axis N
Product_Seal_Housing
ACTUAL AXIS
Coaxiality: Æ 0.2
ref: M-N
NECS
Axis: real
Roughness: R10
COMMON_FACE_BEARING6_bis
Location: 0.03
ref: P A B
NECS
Common_face_bearing6
COMMON_FACE_F300
dim: 42 +0.2
ref: A
DIST
Common_face_F300
COMMON_FACE_BEARING6
locked_dim: 33.5
ref: A
DIST
Common_face_bearing6
Diameter: 42
Tolerance: H8
Axis N
ref: M-N
Axis M
GATHER
Coaxiality: Æ 0.2
Type: multi_diam
f2
EURISTIC Ld
Nber: 1
Diameter: 42
Type: finish
Product_Bearing6
Diameter: 28
Tolerance: E7
REF AXIS
Location: Æ 0.14
NECS
ref: P A B
Axis M
Roughness: R10
Location: Æ 0.14
Location: Æ 0.14
f1
Tolerance: H8
Nber_passes
f3
Cycle_time: tcy
Process
Tool
Type: multi_diam
Cutting_cond
Jig
Type
Nber: 1
Machining
Type: finish
Nber_passes
Order
Cycle_time: tcy

Figure 12. Constraints Graph Model Defined from Expert Rules

All of these models are currently under review. They are related to camshaft bearing line functions and related functions, and will then be extended to the entire cylinder head functions. This first step will also be used to feed information into knowledge bases for a CAD/CAM tool.

4. CONCLUSIONS AND PROSPECTS

In a highly competitive and innovative context, representing expertise domains related to a set of product characteristics associated with process characteristics is a major issue. These domains must be used to consider integrating a new part into existing flexible lines as critical parameters outside the validity domain can be identified sooner. This is the first goal of the research work undertaken in cooperation with RENAULT. The approach used is based on the *Design Rules* methodology associated with *conceptual graph* constraints modeling. The long run goal is to design a computer tool built into a CAD/CAM modeler to help designing mass-production process plans for flexible machining lines for prismatic parts. This product/process data integration tool as a process engineering consolidator (man, cutting tools, machine manager, line leader, etc.), will make decision making and selecting parameters easier (adding or removing constraints), both at strategic and product detail level.

5. REFERENCES

1. Voirpin J.-M., Renaud J., Dufour M., Mutel B., Guidat C. Design Rules: a method for the modeling of technical data in the context of innovation. INCOM'98, Nancy, 1998.
2. Renaud J. Démarche de capitalisation de connaissances-métier. Thèse de Troisième Cycle, ENSGSI Nancy, 1994.
3. Salomons O. W. Computer support in the design of mechanical products: constraint specification and satisfaction in feature based design for manufacturing. Thesis, University Twente, January 1995.
4. Quichon J. Programmation Logique sous Contraintes: Application à la génération automatique de gammes d'usinage en fraisage. Thèse de Doctorat de l'Université Blaise Pascal, Clermont II, 1999.
5. Sabourin L., Machining features: integration of the machining function in the modelling of parts for automated process planning. IDMME, Kluver Academic: ISBN 0-7923-4739-0, 1997: 103-112.
6. Lutters D., Kals H.J.J. Control of design and manufacturing processes based on information content. Annals of CIRP; Enschede, 1999.
7. Irani S.A., Koo H.Y., Raman S., Feature-based operation sequence generation in capp. Int. Journal of Production Research. Vol. 33, N°1, 1995; 17-39
8. Groupe GAMA, textes réunis par Bourdet P.et Villeneuve F. La gamme automatique en usinage. Ed. Hermès: ISBN 2-86601-255-0, Paris, 1990.
9. Dieng R. Comparison of Conceptual Graphs for modelling Knowledge from Multiple Experts. Fondations of Intelligent Systems. Proc. of the 9tth Int. Symposium on Methodologies for Intelligent System; Zakopane; Pologne, 1996.
10. Mugnier M.-L., Chein M. Représenter des connaissances et raisonner avec des graphes. R.I.A., vol. 10, n°1, 1996; 7-56
11. CharGer 2000 v2.2b, Copyright 1998-1999 by Harry S. Delugach, 1999.
12. Mineau G.W. Constraints on Processes: Essential Elements for the Validation and Execution of Processes. Dept. of Computer Science, Université Laval, Québec City, 1998.
13. Mineau G.W. The Representation of Semantic Constraints in Conceptual Graph Systems. Dept. of Computer Science, Université Laval, Québec City, 1998.
14. Lefebvre A., Sabourin L., Plusquellec J.-F. Entités de réalisation, référentiel commun entre concepteur et fabriquant. Modélisation par graphes conceptuels. Colloque CPI'99; 108-115, Tanger, Maroc, 1999.

6. AFFILIATIONS

Arnaud LEFEBVRE, Laurent SABOURIN, Grigore GOGU
LaRAMA, Laboratoire de Recherches et Applications en Mécanique Avancée
Institut Français de Mécanique Avancée, Université Blaise Pascal – Clermont II
Campus des Cézeaux, BP 265, 63 175 Aubière Cedex (France)
Tel.: + 33 4 73 28 80 38 / Fax: + 33 4 73 28 81 00
E-mail: sabourin@ifma.fr E-mail: gogu@ifma.fr

Jean RENAUD
LRGSI, Laboratoire de Recherche en Génie des Systèmes Industriels
Ecole Nationale Supérieure en Génie des Systèmes Industriels, INPL Nancy
8 rue Bastien Lepage, BP 647, 54 010 Nancy Cedex (France)
Tel.: + 33 4 83 19 32 31 / Fax: +33 4 83 19 32 00
E-mail: Jean.Renaud@ensgsi.inpl-nancy.

K. MAWUSSI, V. H. DUONG AND R. PONSONNET

DETERMINATION OF VIRTUAL MEANS FOR THE INTEGRATED DESIGN

1. INTRODUCTION

Process planning of mechanical parts is mainly based on experts' know how (Vandenbrande et al., 1993). From this know how, we can extract constraints associated to the description parameters of the parts. Usually, all the shapes and geometric parameters chosen by the designer do not satisfy machining constraints, or at best, reduce the options for the manufacturing preparation stage (Gayretli et al., 1999). To overcome this situation, companies must react by abandoning traditional design and manufacturing practices for new concepts like concurrent engineering or simultaneous engineering.

Concurrent engineering is based on two mechanisms. The first one is the increase in the sharing of information since the beginning of the design project to reduce work redundancy as well as downstream work (functional participation). The second mechanism is the extension of the overlapping of the activities carried out within the various services of a company (Bhuiyan et al., 1999). In CAD/CAM the combination of both mechanisms is the basis of DFX (Design For X). The objective of DFX is to work out design decisions of products and processes simultaneously by inspecting their relations (Huang et al., 1999). This task includes the development of constraints associated to products and machining processes. There exist several constraints related to: the various shapes of parts, the relations between shapes and processes and the means (machine tools and cutting tools). By satisfying these constraints as soon as possible it is possible to ensure that the part has an intrinsic possibility to be manufactured (Brissaud et al., 1998).

This paper deals with the determination (or specification) of the virtual means. This task is a part of a general application "Virtual VIEW" (V-VIEW) which objective is to provide an assistance tool for the integrated design of mechanical parts. The means are cutting tools and machine tools.

2. CONTEXT AND APPROACH

The context in which our general application V-VIEW is used is presented in Figure 1. It brings out two universes:

- the first is the idea universe in which designers propose technical solutions ensuring functions defined by functional requirements

P. Chedmail et al. (eds.), Integrated Design and Manufacturing in Mechanical Engineering, 323-330.
©2002 *Kluwer Academic Publishers.*

- the second is the model universe which gathers the product model and the means (machine tools and cutting tools).

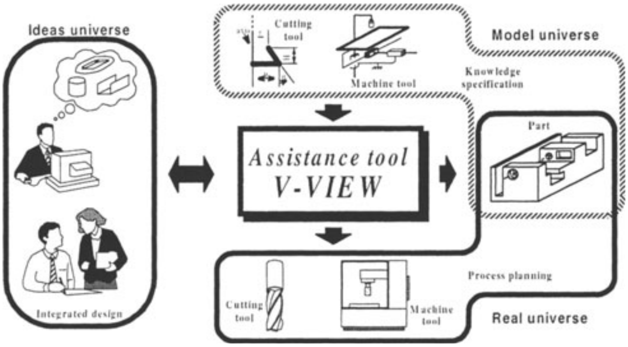

Figure 1. Environment of the assistance tool V-VIEW.

The application V-VIEW is used to quickly verify the manufacturability of the parts and then to identify the shapes which are not manufacturable or manufacturable with difficulty. The means are simply represented by their models. When the manufacturability of a given part is ensured, the real means are defined in the process planning stage.

The CAD model of the part and the models of the means presented in the model universe (see Figure 1) form the basis of V-VIEW. From these models, our approach consists in defining the constraints which associate the geometric elements of the part model to the parameters identified in the models of the means (the simplified model of cutting tools and the simplified model of machine tools). In terms of the determination of the means, we seek to satisfy the constraints thus elaborated. Procedures for the application of the constraints are created to improve response time of the V-VIEW application.

3. BASIC MODELS

3.1. Simplified Model of Cutting Tools

The cutting tools are revolving tools used in milling of prismatic shapes. For this type of shapes, the tools generally used are drills, 2 or 3 flat end-mill tools and tee slot mills or dovetails. With these tools, surfaces can be machined in point milling and flank milling with a side or an axial plunge. These types of tools and machining modes form the framework of the simplified model. In this model a tool is represented by one axis to which we associate flat ends (a main end and possibly a secondary end) and/or a generator. The schematic representation of this simplified model comprises the axis (half right-hand line), flat ends (segment of lines) and the generator (segment of lines).

The functional surfaces of the tool which can be with three are indicated in the following order by BGB (main end B, generator G and secondary end B). In the designation of the type of cutting tools, the defect of each of the three functional surfaces is specified by the letter X.

This simplified model which includes 4 tool classes (see Figure 2) is used for the specification of the cutting tools. It is quite obvious that for the choice of cutting tools in the development stage of the machining process, the parameters (in a very reduced number here) must correspond to those defined in the catalogues provided by the cutting tool manufacturers. It is for this reason that the simplified model has to integrate constraints defined either explicitly or not as the case may be by the cutting tool manufacturers.

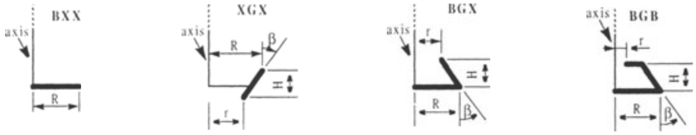
BXX
axis
R
XGX
axis
R
β
r
BGX
axis
r
R
β
axis
BGB
r
R
β

Figure 2. Cutting tool classes

3.2. Machining Feature Model

From the CAD model of a given part, we seek to identify the machined faces in order to evaluate their manufacturability. This set of machined faces created according to the process planner's point of view corresponds to the concept of machining feature largely described in several works (Tassel et al., 1997; Salomons, 1995).

In our approach, the set of machined faces (machining feature) is determined on the basis of the concavity of their common edge (see Figure 3a). Indeed, when the material angle α between two faces (along their common edge) is equal to or higher than 180°, the machining of the one face cannot be done independently of the other ones (Deneux et al., 1994).

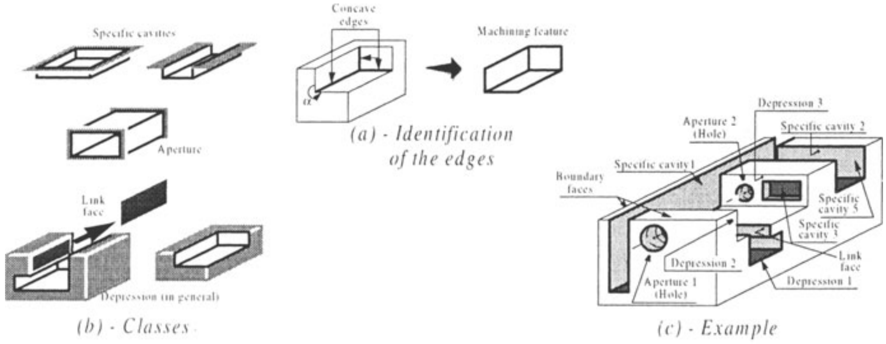
Concave edges
α
Machining feature
Specific cavities
Aperture
Link face
Depression (in general)
Depression 3
Aperture 2 (Hole)
Specific cavity 2
Specific cavity 1
Boundary faces
Specific cavity 5
Specific cavity 3
Link face
Depression 2
Depression 1
Aperture 1 (Hole)

(a) - Identification of the edges

(b) - Classes

(c) - Example

Figure 3. Representation of the machining feature

A classification of the machining features can be made by analysing the adjacency graph of the set of faces identified. In this classification, we distinguished three main classes (see Figure 3b): cavity (a face is linked to all the other faces), aperture (each face is linked to two others thus forming a loop) and depression which is the general case of adjacency.

When a cavity is identified, we can seek to associate to it a cutting tool of the type BGX whose end B will machine the face related to all the others. In the case of an aperture, a cutting tool of the type XGX can be specified. The association of the cutting tools to the machining features supposes checking the compatibility of the material angle between the different faces. The machining features of this third class called depression require a non-determinist analysis for the association of the cutting tools. When a face on the part does not belong to any machining feature, it can be a link face or a boundary face (see Figure 3c).

3.3. Simplified Model of Machine Tools

A milling machine tool has a mechanical structure with 3 cartesian axes X, Y and Z. On this type of machine, the orientation of some faces (or machining features) can only be obtained when using a specific part holder presenting adjustable supports. The high number of part holders as well as the cost of their manufacturing and adjustment lead us to consider the choice of alternate machines with 4 or 5 axes. The first parameter that must be specified during the choice of a machine tool is thus the number of useful axes. The positioning of a machining feature in the coordinate system of the machine tool requires one to know the orientation of one of the faces of the machining feature and the position of the limit points of the machining feature. The position of the limit points is determined using the kinematic parameters of a machine tool.

The specification of the kinematic parameters of a machine tool has already been presented in several papers (Tassel et al., 1997; Méry, 1997). Two models are generally used for this specification. The first model is the Denavit-Hartenberg model largely used in robotics (Khwaja et al., 1998). It is based on the description of the articular parameters of the machine tool. The second model is defined using the parameters controlled by the Numerical Controler (NC) unit of the machine tool (Méry, 1997). In our approach, we chose to include the parameters controlled by the NC unit (Xm, Ym, Zm, Am and Bm) in the simplified model of machine tools. The transition from these parameters to the model of Denavit-Hartenberg is carried out once the complete kinematics of the machine tool is determined.

In the case of the milling machines, the axes of the coordinate system correspond to the directions of three basic translations X, Y and Z in the simplified model of machine tools (see Figure 4). A and B are two rotation parameters which can be associated to the directions X, Y or Z. To the parameter "axis of machine (ABXYZ)" we added two others: the capacity according to the machine spindles and the types of machining operation performed.

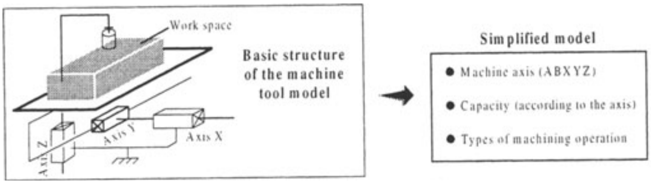
Work space
Basic structure of the machine tool model
Axis Z
Axis Y
Axis X
Simplified model
● Machine axis (ABXYZ)
● Capacity (according to the axis)
● Types of machining operation

Figure 4. Simplified model of machine tool

4. DETERMINATION OF THE MEANS

4.1. Determination of the Cutting Tools

The parameters defined in the simplified model of cutting tools can be determined when the type of one tool is given. According to the arrangement of the faces in the cavity and aperture classes of machining feature, their identification leads to the direct determination of the BGX and XGX cutting tool types respectively. In our approach, all the information required for the determination of the cutting tools are attached to the new concept of Minimal Machining Configuration (MMC) developed. Thus, an MMC is defined by:

- the type of the cutting tool (BXX, XGX, BGX or BGB), the position of its axis (direction and side defined according to the characteristics of the machining feature) and the parameters R, r, H and β defined in the simplified model,
- the faces of the machining feature machined by the cutting tool.

To determine the MMC of the machining features identified in the CAD model of the parts, we seek to satisfy the constraints defined for the cutting tools. 26 constraints, 9 for the XGX tool type, 9 for the BGX and 8 for the BGB have been defined (Duong et al., 1999). As their presentation here would be too long, we thus limit the presentation to the constraints related to the MMC of the type BGB.

4.2. Constraints and Procedure

Theoretically, a BGB cutting tool can be used to machine at least two faces and at most five faces. To identify an MMC of this type, let us take two sets of faces $B=\{f_i, f_j\}$ and $F=\{g_k \ / \ k=1 \text{ to } n\}$. The faces f_i and f_j are machined respectively (unless otherwise stated) by the two ends B1 and B2 of the cutting tool. The faces g_k of the set F are machined by the generator G of the cutting tool.

Let us consider P_i one point of the face f_i and P'_i the image of P_i by orthogonal projection on the face f_j. The 3 following constraints express that both faces are opposite each other and also specify the position of the faces of the set F (see Figure 5a).

.Constraint C1: f_i and f_j are plane faces.

.Constraint C2: $\overrightarrow{P_i P'_i} \cdot \vec{n_i} > 0$ and $\vec{n_i} = -\vec{n_j}$.

.Constraint C3: All the faces of the set F have a concave link with the faces f_i and f_j.

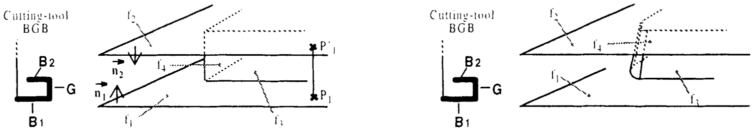

(a) Facing faces *(b) Faces orientation*

(c) Division of the set F in islands

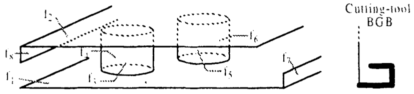

Figure 5. Arrangement of the faces in the machining features

In the example presented in Figure 5b, the faces f_1 and f_3 have the material angle equal to 90° whereas that of the faces f_1 and f_4 is different from 90°. In this case it is impossible to machine both faces with only one MMC of the type BGB. In addition the fact that the axis of the conical blending face is not perpendicular to the face f_1 makes it impossible to machine it with an MMC of the type BGB. The 2 following constraints can be used to validate all these situations.

.Constraint C4: All the faces of the set F have the same out-of-material angle (as opposed to the material angle) with the face f_i.

.Constraint C5: The axis of any cylindrical or conical face belonging to the set F is perpendicular to the face f_i.

In the example presented in Figure 5c, the set F consists of two islands of cylindrical faces. The machining of these two islands by an MMC of the type BGB is impossible, at least in terms of the space which separates them. Moreover, as the face f_7 is concave to the face f_1 we can consider the machining of f_1 by surface B1 of the cutting tool expect that the dimensions and position of the face f_2 give accessibility. According to this observation, the simultaneous presence of the faces f_7 and f_8 makes it impossible to machine the feature by an MMC of the type BGB. The constraints C6 and C7 presented below are defined for these situations. The last constraint C8 expresses the fact that the use of such an MMC can only be justified if the set F is not empty.

.Constraint C6: Whatever the pair of faces of the set F considered, there will always be a path allowing to go from one to the other by gradually traversing the faces of set F.

.Constraint C7: At least one of the faces of B is not concave to faces not belonging to F.

.Constraint C8: The set F is not empty.

According to the procedure used for the application of constraints, one must start by seeking the potential faces f_i and f_j of the machining feature which satisfy the constraints C1 and C2. Then, we create the set F by applying the constraint C3 to the other faces of the machining feature. Finally, after the elimination of some B sets which not satisfy the constraint C8, we apply in order constraints C7, C5, C6 and C4.

The parameter β is computed starting from the material angle obtained during the application of constraint C4. The limit value Hmax of parameter H corresponds to the distance between faces f_i and f_j. Its determination leads to the specification of an interval [Hmin, Hmax]. Hmin is a constant value fixed by the manufacturers of cutting tools. For the determination of the parameters R and r, we have developed a method based on the calculation of the minimal distance between the concave edges (Mawussi et al., 2000).

4.3. Determination of the machine tools

For a given machining feature, the determination of the parameters of the simplified model consists of the following tasks. The identification of the boundary faces for their use as the leading plane of the set up of the part, the analysis of the orientation of the axes of the cutting tools defined in the various MMC and the evaluation of the accessibility to the faces of the machining feature by the cutting tools.

For the identification of the boundary faces, we seek for faces which are perpendicular to the axis of the cutting tools and which satisfy the accessibility constraints. The evaluation of the size of the boundary faces leads to the choice of the face (or the set of faces belonging to the same surface) which provides the greatest stability of the part. In the example presented in Figure 6, the face f_4 will be selected for the machining of the hole.

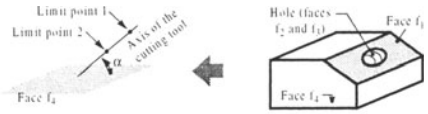

Figure 6. Position of the machining feature

In the example presented in the Figure 6, the analysis of the orientation of the tool axis leads to the determination of the angle α. The controlled limit points of the cutting tools are computed at the level of the evaluation of the accessibility of the faces of the machining feature.

The change from the data defined at the end of the three tasks presented below to the determination of the parameters of the simplified model of machine tool requires the classification of the machining features based on the different directions of the axes of the cutting tools. From this classification, we can define the directions of the three basic axes X, Y and Z. For any other axis which is non parallel to X, Y or Z, we determine its orientation angles λ and δ in the coordinate system created from XYZ. These orientation angles correspond to the rotation angles around the defined A and B axes of the machine tool. When a machine tool is identified, its capacity is determined by evaluating the limit points associated to the manufacturing of the machining features. Finally. the types of machining operations are defined according to the type of MMC resulting from the determination of the cutting tools.

5. CONCLUSION

In this paper, we have presented a part of our work related to the determination of cutting tools and machine tools. The approach presented is based on constraints associating the parameters of the simplified models of these means to the geometric characteristics of the faces composing the machining features identified on a given part. The simplified models of the means are derived from their virtual representation.

This approach is currently being validated through industrial case studies. The average response time (3 minutes) recorded during the validation experiments lead us to consider a new optimization of the application developed using CATGEO and IUA (development tools) associated with the CAD/CAM software CATIA provided by DASSAULT SYSTEMS.

6. REFERENCES

Bhuiyan N. and Thomson V. Simulation of concurrent engineering process. Proceedings of the international conference on industrial engineering and production management FUCAM 99, Glasgow, July 12-15, 1999: 211-221.

Brissaud D., Martin P. Process planning: from automation to integration. IFAC Symposium on Information Control Problems in Manufacturing, Nancy-Metz, june 1998: 231-236,.

Deneux D., Maranzana R. and Soenen R. The material angle: A part-level criterion for tool-feature extraction. Proceedings of the IFIP WG5.3 Conference on Feature Modeling and Recognition in Advanced CAD/CAM Systems, Valenciennes, France, 1994: 357-369.

Duong V. H., Mawussi K. V_VIEW: un outil pour la spécification des outils de coupe en conception intégrée. Colloque international sur la Conception et Production Intégrée CPI'99, Tanger - MAROC, 1999: 142-151.

Gayretli A., Abdalla H. S. An object-oriented constraints-based system for concurrent product development. Robotics and Computer-Integrated Manufacturing, Vol. 15, 1999: 133-144.

Huang G. Q., Lee S. W., Mak K. L. Web-based product and process data modelling in concurrent «design for X. Robotics and Computer-Integrated Manufacturing, Vol. 15, 1999: 53-63.

Khwaja A.A., Rahman M.O. and Wagner M.G. "Inverse Kinematics of Arbitrary Robotic Manipulators Using Genetic Algorithms" in *Advances in Robot, Kinematics: Analysis and Control*, Kluwer Academic Publishers (Lenarcic, J., and Husty, M.L. editions), 1998: 375-382.

Mawussi K., Duong V. H., Kassegne K. Determination of the parameters of cutting tools in integrated design of products. Proceedings of CE2000, Lyon - France, 2000: ???

Méry B., *Machines à commande numérique*. Editions Hermès, Paris 1997

Salomons, O.W. *Computer support in the design of mechanical products. Constraint specification and satisfaction in feature-based design for manufacturing*. Ph.D. Thesis, University of Twente, The Netherlands, 1995.

Tassel S., Villeneuve F. Analyse de l'aptitude à la fabrication d'un produit au plus tôt: adéquation moyen de production, produit. Proceedings of the GRP conference on Product process procedures , 16-17 October 1997, ENS de Cachan.

Vandenbrande J.H., Requicha A.A.G. Spatial reasoning for the automatic recognition of machinable features in solid models. IEEE Trans. Pattern Analysis and Machine Intelligence, 15 (12), 1993: 1269-1285.

P. DE LIT, T. L'EGLISE, J. DANLOY, B. REKIEK,
A. DELCHAMBRE

SELECTING MATERIAL HANDLING EQUIPMENT WITH PROMETHEE

Abstract. The authors present a comprehensive approach to select material handling equipment (MHE) at assembly line design stage. They defined a two-level MHE typology, namely generic types and specific equipment, to describe the numerous available systems. Based on this description, the system identifies the most suitable equipment in two stages. At the primary stage the performances of basic types are evaluated for the considered problem. Having chosen one (or more) generic equipment, specific information is used to evaluate and select the appropriate specific one. The main originality of this work is the application of a multicriteria decision-aid method, called PROMETHEE II, embedded into a decision tree. At each selection stage (node of the tree), eligible solutions are ranked according to a global evaluation of their performance for the considered parameters. The ranking is computed thanks to criteria and weights, allowing the user to accurately describe the selection process. Industrial case studies, which validate the approach, are presented.

1. INTRODUCTION

Material handling equipment (MHE) selection implies choosing handling equipment that best meets the requirements in terms of production (respect of the cycle time [CT]), material (weight, shape), moves (available space), etc. As material handling usually intervenes for an important part of the production costs, the choice of an efficient conveying system is an important step in the line design. Examples of spectacular productivity improvements thanks to a redesign of the material handling strategy (see for instance (Witt, 1996)) show that this issue cannot be neglected. Ideally, MHE selection and product design should be performed concurrently as proposed by (Atmani and Dutta, 1996) who advocated for the adaptation of the product design to the capabilities of available MHE.

There is not always a clear answer to the best way to handle material. In some cases there are a number of different methods which satisfy the requirements. This is why MHE selection is an important stage in facilities planning or in assembly line design, which is the authors' field of investigation. Choosing the right method does not only involves cut-and-dry mathematical techniques, but also relies on personal judgement and expertise. As it is necessary to take several parameters into account, some being crucial and other being more design sensitive, one needs to provide the designer with an interactive method, allowing him to easily trace the effects of his choices on the proposed solutions.

In this study, the authors present a new methodology to help the assembly line designer to choose the right MHE to convey the product from station to station in assembly lines. The system is based on a multicriteria decision-aid method embedded in a decision-tree. The system outputs a quantitative ranking of the most suitable solutions out of a set of 21 standard systems, widely used in paced assembly lines.

P. Chedmail et al. (eds.), Integrated Design and Manufacturing in Mechanical Engineering, 331-338.
©2002 *Kluwer Academic Publishers.*

This paper is organised as follows: previous work on material handling selection is first described in section 2; section 3 explains the selection methodology; the possible solutions for the problem and the criteria taken into account are presented in section 4; the application of the selection algorithm to industrial case studies is then reported in section 5 before conclusions are drawn.

2. LITERATURE OVERVIEW

As the MHE selection process highly depends on the evaluation of solutions, expert systems (ESs) have widely found their way into this problem. (Cole et al., 1987) presented one of the first selection ESs, called MOVE. It addresses only six kinds of equipment, which is quite limited in scope, but includes the basics of ES, namely IF-THEN rules, to describe the selection process. (Fisher et al., 1988) presented an ES, MATHES, which deals with 24 types of equipment (not especially assembly focused) and uses eight parameters to accomplish the selection. MATHES computes a certainty factor CF for each eligible equipment, resulting from expert selection, to rank the solutions. Unsuited resources are eliminated during the selection if their CF is too low. So a solution considered to be poor according to one criteria will *a priori* be eliminated. (Bookbinder and Gervais, 1992) developed an ES using filters to select a basic equipment type, and a multiple attribute decision-making methodology to select and rank the best solutions out of 30 potential ones. The system takes six attributes (pertinent parameters) into account and computes an evaluation of the alternatives to determine their performance. The global performance of an equipment is computed by evaluating its distance to an ideal fictitious one. This distance is altered by weights, allowing the user to define the relative importance of each attribute. This methodology introduces the idea of multicriteria ranking, but the evaluation of the solutions is computed with a weighted sum. ADVISOR is another ES described by (Chu et al., 1995). On the basis of IF-THEN rules, ADVISOR computes a value called normalised accumulated rating (NAR) to rank the suitable solutions out of 77 equipment types. This NAR is computed using an arithmetic mean of the scores obtained by an equipment for the selected factors (each equipment having a different score for all the discrete values of the parameters). This technical ranking is followed by a filtering: a minimal acceptance level is to be reached for an equipment to be considered as a candidate solution. The final choice is made on the basis of an economical analysis taking into account operating costs, investments, resale value and payback period. ADVISOR is certainly the most complete approach to the MHE problem. Unfortunately it suffers on the previously mentioned drawback: the ratings are computed using an aggregation method. In the field of assembly, (Boothroyd and Dewhurst, 1991) proposed a classification of the assembly systems and selection charts based on the annual production, the average number of parts in a product variant, and the total number of components in the product family. (Sinzinkayo et al., 2000) later refined the selection using fuzzy logic to avoid the abrupt transitions between solutions in Boothroyd's charts. Possible solutions are given a confidence level, which permits to rank them.

3. SELECTION METHODOLOGY

The MHE selection problem as stated in the introduction naturally leads to a methodology reproducing a human's expertise. As shown in the literature overview, ESs have been widely applied to that problem, leading to an *a priori* classification of the equipment but to a poor relative evaluation of the suitable solutions. The authors propose to state the problem as a multicriteria decision-aid one.

An originality of the proposed approach is that the selection is performed by going through a decision tree which branches are developed according to the results of a multicriteria decision-aid problem. Each node constitutes an independent decision problem. The idea is to cluster the potential solutions and to perform a multi-level selection. At each selection stage the possible solutions are ranked and each promising one yields a node being further developed in the solution tree. This node contains a new multicriteria decision-aid problem, with its own criteria and its own possible solutions.

In order to develop such a tool, it is necessary to describe the problem as a hierarchical one. The methodology is indeed based on the idea that it is possible to find a clustering of equipment, in terms of criteria and solutions, allowing the multi-level approach. As further discussed in the next section, MHE has been classified into several generic categories, allowing to propose a two-level typology. The multicriteria decision tree will consequently have two selection levels.

In order to solve the multicriteria decision-aid problem, the authors opted for the PROMETHEE II method because of its ease of application, its efficiency and its interactivity (thanks to a transparent influence of each criterion on the proposed ranking). A complete description of the theory related to the PROMETHEE II method is out of the scope of this study. For more details about it, the reader is invited to refer to (Brans and Mareschal, 1994). It is however important to know that it computes a "net flow" ϕ associated to each solution. This flow yields a ranking, called the PROMETHEE II complete ranking, between the different solutions of the problem. The rules defining this ranking are:

$$\begin{cases} aP^{II}b \Leftrightarrow \phi(a) > \phi(b) \\ aI^{II}b \Leftrightarrow \phi(a) = \phi(b) \end{cases} \tag{1}$$

It means that solution a is preferred to solution b if and only if $\phi(a) > \phi(b)$, and that solutions a and b are indifferent if and only if $\phi(a) = \phi(b)$. The main advantage of this evaluation methodology is that it is based on the importance of a performance difference between two solutions, which best describes whether a solution should be preferred to another. It is also important to know that a weight is associated to each criterion. These weights are involved in the computation of the ϕ flows and represent the relative influence of one criterion with respect to the other ones. PROMETHEE II allows to compare completely different criteria and avoids inconsistencies arising with the use of a weighted sum.

An important feature of the developed selection tool is that the application of PROMETHEE II can be preceded by an optional filtering stage, which eliminates MHE completely unsuitable according to some criteria. The ranking is then performed on the remaining solutions.

4. MHE TYPOLOGY AND EVALUATION CRITERIA

On the basis of general definitions of MHEs (Tompkins et al. 1996; CICMHE; Peters et al., 1998), the authors defined a classification system for 21 standard equipment, commonly used to transfer the product from station to station in assembly lines (both manual and automated ones). Five generic categories are defined as follows:

- synchronous system with indexing device (SSID): rotary table, linear system;
- synchronous system without indexing device (SSWID): slat conveyor, trolley conveyor;
- asynchronous system with active conveyor (ASAC): roller conveyor, band belt conveyor, belt conveyor, chain conveyor, skate-wheel conveyor, power and free system, inverted power and free system, monorail;
- asynchronous with autonomous pallet (ASAP): autodrive pallet, Montrack, automated guided vehicle (AGV), automated electrified monorail (AEM);
- non powered system (NPS): "nothing", NP rollers, NP skate-wheels, NP ball table, NP chariot.

This classification is essential in the methodology, as it defines the eligible solutions for each node of the selection tree.

Table 1. MHE selection criteria by type.

Product and components	
Mass [kg]	Shape [cyl/paral]
External envelope [cm]	Number of variants [number]
Number of components [number]	Component quality [% good parts]
Abrasive component [y/n]	Dirty components [y/n]
Greasy component [y/n]	Fragile components [y/n]
Product type [mechanical, electrical, electro-mechanical, automotive]	
Handling	
Long distances [y/n]	Position accuracy [y/n]
High temperatures [y/n]	End of line [y/n]
Up- and download at same point [y/n]	Access from below [y/n]
Need for a pallet [y/n]	Working level [on-ground, overhead]
Distance [one station, several stations]	Several products at same time [y/n]
Production	
Cycle time [s]	Planned automation [high, low]
Product accumulation [y/n]	Antistatic ambiance [y/n]

Parameters relevant for MHE selection are classified into three categories: product and components, handling and production. This classification is commonly used to collect information in industry. Table 1 shows the parameters considered for the selection, with their value types.

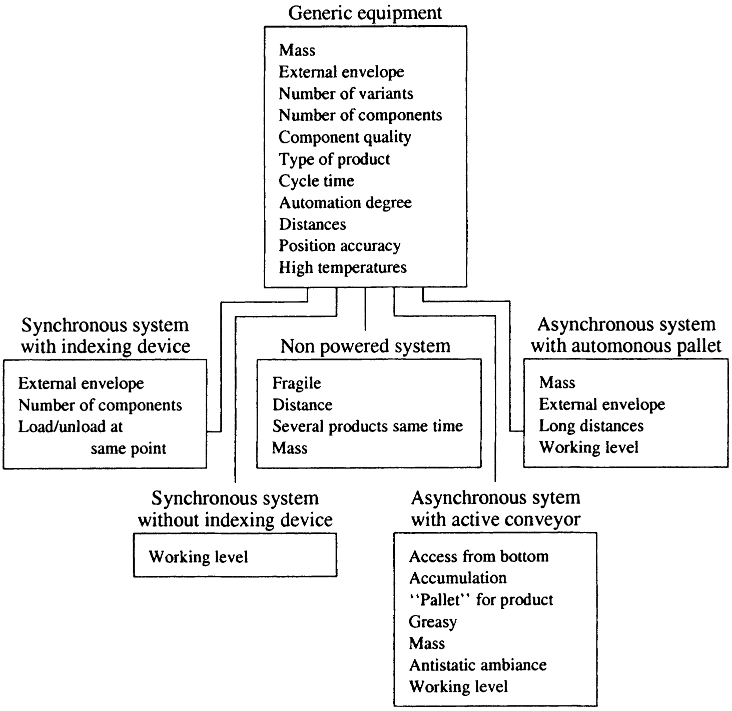
Generic equipment
Mass
External envelope
Number of variants
Number of components
Component quality
Type of product
Cycle time
Automation degree
Distances
Position accuracy
High temperatures
Synchronous system with indexing device
External envelope
Number of components
Load/unload at same point
Non powered system
Fragile
Distance
Several products same time
Mass
Asynchronous system with automonous pallet
Mass
External envelope
Long distances
Working level
Synchronous system without indexing device
Working level
Asynchronous sytem with active conveyor
Access from bottom
Accumulation
"Pallet" for product
Greasy
Mass
Antistatic ambiance
Working level

Figure 1.Tree structure of the problem and associated criteria

As mentioned in the previous section, the multi-level selection is based on a hierarchical description of the problem, but also on a sharing of the criteria among the different equipment categories. The criteria considered in a node of the tree are those that are discriminating in the associated problem. For instance in Figure 1, which presents the MHE typology in a tree view, with the associated criteria, the fact that components are fragile is discriminating in the choice of an NPS, but is not in an SSID. Note that some criteria appear in several nodes in the tree; for instance, the number of components is a criterion in the choice of both a generic category and an SSID.

The PROMETHEE II method evaluates the performances of each possible solution for the current node in the tree. This evaluation leads to the exploration of one or more child nodes, depending on the results and the choice of the user. Indeed, even if one supposes that the criteria related to each node allow the system to find out the most suitable solution, this process is not exclusive. As the PROMETHEE II complete ranking only describes the relative differences between the performances of the solutions, there are several cases in which those differences are not important enough to distinguish the best solution. Several child nodes may then be developed for a given parent. This unfortunately leads to a delicate selection process, as each node owes an independent selection problem, with its own criteria and its own possible solutions. Consider the following example: at the upper level, the results of the evaluation report the SSID and the ASAC as eligible solutions. The child nodes for those two generic families will be exploited, but have to be considered independently. Indeed, looking at the criteria involved in the SSID, one shall notice that they are mainly linked to the shape and the weight of the variant to transport. The ASACs are more distinguished by the production environment: the choice between band belt or chain is indeed based on environmental conditions, while the shape of the product is rather indifferent in that selection. It would thus make no sense to compare all the specific SSIDs with the specific ASACs. The solution proposed is to evaluate the two problems separately and to compare if necessary the best solutions with an economical criterion. The evaluation and preference functions used in the proposed problem formulation and the weight of the criteria are presented in (DeLit, 2000).

5. CASE STUDIES

To illustrate the selection process, the authors propose three industrial case studies: an electrical safety-switch, a car alternator and a car. The description of those three problems is reported in Table 2.

Table 2. Values of the parameters related to the first stage of the MHE selection.

Parameter	Switch	Alternator	Car
Mass (kg)	0.1	3	1000
Shape	parallelepiped	cylinder	parallelepiped
Dimensions (cm)	10 x 6 x 2	20 x 20	450 x 150 x 145
Number of variants	2	5	> 100
Number of components	10	22	> 1000
Component quality (%)	99	99	98
Product type	EM	EM	automotive
Cycle time (s)	2	7	120
Planned automation	high	high	high
Position accuracy	yes	yes	yes
Long distances	no	no	yes
High temperatures	no	no	no

The results of PROMETHEE II for the first level of selection are reported in Table 3. One type of transfer system (SSID) is best suited for the safety switch. However, ASACs and ASAPs are not considered to be bad options. The CT strongly favours the SSID, but the number of variants and the number of components suggest the use of the two other solutions. As a matter of fact, when the CT is very low, it nearly becomes impossible to use another system than an SSID. This criteria has been completed with an optional filter that eliminates all solutions but the SSID if the CT is lower than 5 seconds. If it is activated, the ASAC and ASAP will be eliminated.

Table 3. Flow values for the basic equipment types.

	Switch	Alternator	Car
SSID	0.217	-0.167	-0.767
SSWID	-0.517	-0.533	0.442
ASAC	0.180	0.333	0.067
ASAP	0.185	0.433	0.400
NPS	-0.065	-0.067	-0.142

Two equipment types could be used for the alternator: the ASAC or the ASAP. Because of the automation degree and the low CT, NPSs were discarded. For the car, two systems could be chosen: ASAP or SSWID.

Let us further proceed in the selection, by exploring the SSID node for the safety switch. The criteria involved in the selection between rotary table or linear system are the dimensions, the number of components and the need to up- and unload the product at the same point. It has here been supposed that the up- and unloading of the products happen at different places. The values from the PROMETHEE II computation then suggest the linear system as best suitable. The actual assembly line for the switch assembly is composed of rotary tables for the assembly of some subassemblies and of a linear conveying system for the final assembly of the product. The dimensions of these subassemblies make them well suited to a conveying by the rotary tables.

The car is a complex case study because of the size of the product or the number of components or product variants, but also because of its evolution in the assembly line (welding, painting, manual assembly operations are performed along the line). These various conditions lead to several MHE possibilities. The AGV is a well performing ASAP in this case. It gets a excellent ranking in the evaluation, while the others are poorly performing, mainly due to the size and weight of the product. This solution has been chosen by some automotive constructors. Among SSWIDs, the slat conveyor is an good candidate. This solution has also been adopted by some industrials.

As mentioned in the previous section, it is not always possible to clearly identify a unique solution at a given problem level, which leads to the exploration of several child nodes. In the case of the alternator, ASAC and ASAP are well adapted generic solutions. Those two nodes will thus be further developed. For the ASAC, there are two conveyors that emerge from the other systems (chains and belts). This is mainly due to the access from below needed in the case of the alternator (in order to avoid a reorientation, it is preferred to access the product from below). Autodrive pallets from Fabricom and Montrack from Montech are well suited ASAPs in this case.

This car alternator, whose line was designed by Fabricom, is a product built for several car companies, and the actual conveying system used is an autodrive pallet.

6. CONCLUSIONS

An original MHE selection tool for paced assembly lines is presented in this paper. Its main originality is the use of the multicriteria decision-aid tool PROMETHEE II embedded in a selection tree, which permits a two-level selection: generic equipment and a further refinement yielding the actual type of equipment to be used. The proposed methodology is highly interactive, and the effects of changes in the user's answers are easily traced, so that he can check the influence of each of his inputs on the proposed solutions. This avoids the "black box" effect proper to ESs. The results obtained show that the proposed methodology is coherent, and suited to the selection of MHE for assembly lines. In further works the comparison of several equipment proposition thanks to economical criteria will be investigated.

Pierre De Lit, Université libre de Bruxelles, CAD/CAM Department, 50 av F. D. Roosevelt, CP 165/14, B-1090 Brussels, Belgium. e-mail: pdelit@ulb.ac.be.

7. REFERENCES

Atmani, A. and Dutta, S. P. (1996). Product design and material handling selection – A concurrent engineering approach. *International Journal of Industrial Engineering*, 3(1):40–50.

Bookbinder, J. H. and Gervais, D. (1992). Material handling equipment selection via an expert system. *Journal of Business Logistics*, 13(1):149–172.

Boothroyd, G. and Dewhurst, P. (1991). *Product Design for Assembly*. Boothroyd Dewhurst, Inc., Wakefield, Rhode Island.

Brans, J.-P. and Mareschal, B. (1994). The PROMCALC & GAIA decision support system for multicriteria decision aid. *Decision Support Systems*, 12:297–310.

Chu, H.-K., Egbelu, P. J., and Wu, C.-T. (1995). ADVISOR: A computer-aided material handling equipment selection system. *International Journal of Production Research*, 33(12):3311–3330.

Cole, J. H. (1987). MOVE: A planning assistant for material handling. Engineering Costs and Production Economics, 12:134–152.

College-Industry Council on Material Handling Education (CICMHE). MH taxonomy. www.mhia.org/et/mhe tax.htm.

De Lit, P. (2000). *A Comprehensive and Integrated Approach for the Design of a Product Family and its Assembly System*. PhD thesis, Université libre de Bruxelles, Brussels, Belgium.

Fisher, E. L., Farber, J. B., and Kay, M. G. (1988). MATHES: An expert system for material handling equipment selection. Engineering Costs and Production Economics, 14:297–310.

Peters, B. A., Malmborg, C., Petrina, G., Pratt, D., and Taylor, D. (1998). An introduction to material handling equipment selection. Technical report, College-Industry Council on Material Handling Education (CICMHE).

Sinzinkayo, A., Mascle, C., and Balazinski, M. (2000). Application de la logique floue pour le choix d'une méthode d'assemblage. In *Proceedings of the 3rd International Conference on Integrated Design and Manufacturing in Mechanical Engineering*, Montreal, Canada. Presses Internationales Polytechnique. Paper VA-46.2.

Tompkins, J. A., White, J. A., Bozer, Y. A., Frazelle, E. H., Tanchoco, J. M. A., and Trevino, J. (1996). *Facilities Planning*. John Wiley and Sons, Inc., New York, second edition.

Witt, C. E. (1996). Repairing equipment: The material handling way. *Material Handling Engineering*, July, pages 37–40.

George DRAGOI, Daniel BRISSAUD

A METHODOLOGY FOR COST AND QUALITY OPTIMIZATION IN A DESIGN SYSTEM BY LINKING QUALITY METHODS

Abstract. A fierce competition and high customer expectations force manufacturing business to improve quality, to lower selling prices and to shorten delivery time. This also pressures into introducing new products in the market. This paper highlights linkages among QFD, SPC and Taguchi's methods for a complete design process to be achieced: a global and integrative methodology is presented. Weaknesses of QFD is bottleneck engineering and optimization. The five-step model of QFD (as a customer-driven product design, the process starts with customer analysis) are extended by extra tools: SPC and Taguchi. The impacts of SPC and Taguchi on QFD have been studied and recorded. QFD provides with the customer's input and Taguchi provides with the process to determine the best parameters of a robust design or SPC combinations. The voice of the customer is prioritized and expressed by functions, demanded quality, performances measures, failure modes, concepts and manufacturing. This paper discusses the linkages among three powerful quality tools. The sinergy among QFD, SPC and Taguchi's methods becomes an ideal design process able to perform concurrent engineering and integrated design. A methodological view is focused on here and particularly an integrated tool for cost and quality optimization within a design system.

Résumé. Aujourd'hui la compétitivité d'une entreprise se traduit par sa capacité à offrir à ses clients des produits ou des services de haute qualité au prix le plus bas possible. Il n'est pas difficile d'admettre des idées ou des concepts tels que 'la qualité c'est l'affaire de tous', 'la qualité c'est la prévention', le 'zéro défaut', le zéro stocks, le zéro délais, le zéro papier, le zéro panne, etc. Ce qui est vraiment difficile et peut être le plus important est de dire 'comment faire' pour réaliser bien dès la première fois. Chaque outil qualité possède ses spécificités et ses applications: aucun outil ne peut vraiment remplacer un autre. Nous proposons une méthodologie d'intégration de plusieurs outils qui nous permet de construire un système cohérent et pertinent qui peut s'adapter et permet de déployer la stratégie de l'entreprise en visant à assurer que ses ambitions sont cohérentes avec ses ressources. A l'issue du projet de conception, on propose une solution de valeur adaptée aux besoins, explicites ou non, présents ou futurs, des utilisateurs (point de vue externe - valeur d'usage), et réalisable à un coût admissible par le fabricant (point de vue interne - valeur productive ou ajoutée) et vendu à un prix admissible par le client (point de vue externe - valeur d'échange).

1. INTRODUCTION

A fierce competition and high customer expectations are forcing manufacturing business to improve quality, to lower selling prices and to shorten delivery time [2, 3, 6]. This also pressures into introducing new products in the market. There is a realization in the manufacturing efficiency for improving quality and reducing costs, but without growing investments in automation and advanced machine tools. Before and after introducing a new technology into the working environment, its impacts on the quality throughout the product life has to be understood and assessed [7, 9]. Once introduced into the working environment most technology can lower job

P. Chedmail et al. (eds.), Integrated Design and Manufacturing in Mechanical Engineering, 339-346.
©2002 *Kluwer Academic Publishers.*

satisfaction, employee morale and occupational safety. Delivering reliable and high quality products and processes at low costs has become the key to survive in today global economy. This reflects the fact that quality cannot economically be achieved by inspection. Driven by the need to compete on cost and performance many enterprises are increasingly focusing on the optimization of product design. Designing with quality is cheaper than trying to inspect and re-engineer after the product under production or worse, at the customer's. The early design phases of a product or process have the greatest impact on life cycle costs and quality [7]. Therefore significant cost savings and quality improvements can be realized by optimizing product designs. Thus, new methodologies, technology and advanced statistical tools must be employed to design high quality products at low cost. Some existing design methodologies tend to reveal a bias towards a particular style of application. In each domain addressed by the project, many tools and methods have been developed to make clear and improve the engineer's work. Those tools and methods increase productivity and reliability of products and processes. Those modules are the basis and the necessary condition of a successful integration. They are not developed here, the topic is how to integrate those modules into a engineering cooperative work to more and more improve product and process developments.

State-of-art on integration of the design techniques

The integration issue has been focussed for numerous years by three main approaches: Design for X, Value Analysis and Integrated System of Design.

Design for X. Design for Manufacturing and Design for Assembly were introduced by Boothroyd and Dewhurst a long time ago. Many other Design for X methods (X=quality, cost, reliability,.) where X represents each professional discipline which is involved in the design activities, have been developed until today and are widely used in industrial product development. The principle is basically the optimization of two professional engineering activities. Considering the whole production system, Design for X addresses only a local issue of the cooperation of two engineers. The limits of Design for X are numerous. It gives greater place to a particular point of view (manufacturing, assembly, cost, reliability, quality) to the detriment of the other participants of the design process; all the points of view have to be considered in an optimal design.

Value Analysis and Quality. For forty years, those methods have been exploring and improving. The principle is to satisfy the customer who has the greater place to the detriment of the manufacturing processes; those methods are external-enterprise based. The integration of the different participants of the design project is realized working in inter-disciplinary groups in which each participant brings his/her knowledge and constraints to build tables and criteria evaluating the design solutions. The limits of those methods come from the exclusive requirements of the customer in the definition of the production system. The internal aspects of the enterprise are disadvantaged compared to the external aspects due to the customer.

Those two aspects have to be well balanced for an optimal system of production to satisfy both the customer and the enterprise.

Integrated System Design. Advanced techniques permitted to develop numerous applications able to help design and control of production systems. Integration is seen as a workflow of data from an upstream application to a downstream application. Data are integrated in databases common and available to all the design participants. Applications specific to disciplines are also integrated into a design process considering a sequence imposed by the availability of input data. The limits of this approach are due to the prominence of computer implementation opposed to the flexibility of the design process itself. The design process able to chain all the applications is rigid, planned and pre-determined for all the problems of production system design and control. It does not enable to perfectly be adapted to each design process, which is obligatory different from the previous one and to innovate easily.

Today, the solution is a cooperative system and a multi-disciplinary approach. The challenge of integration is to enable an effective cooperation among the professionals for an optimal definition or control of production systems. The constraints of each discipline and each professional are as important as others. Product definition, process definition, quality, production management, economical, sociological or organizational constraints are strongly coupled in the development of production systems and cannot be split into different rigid frontiers.

2. QUALITY ISSUES, METHODS AND TOOLS

This paper discusses the linkages among three powerful quality tools to achieve an integrated system design. The sinergy among QFD, SPC and Tagushi's methods becomes an ideal design process able to perform concurrent engineering and integrated design. A methodological view is focused here and particularly an integrated tool for cost and quality optimization within a design system [7, 16]. Among the different schools of design methodology, there are different balances among various design factors. In each domain addressed by the project - product definition, manufacturing processes, quality techniques, production management -, many tools and methods have been developed to make clear and improve the enginers' work. Those tools and methods increase productivity and reliability of products and processes. Those modules are the basis and the necessary condition of a successful integration [4, 10]. They are not developed here, the topic is how to integrate those modules into a cooperative work to more and more improve product and process developments [7]. The quality depends on the view of quality: management view, client view, methods, techniques and tools, standards view. Today, the principle is to satisfy the customer who has the greater place to the detriment of the manufacturing processes; those methods are external-enterprise based. The integration of the different participants of the design project is realized by working in inter-disciplinary groups in which each participant brings his/her knowledge and constraints to build tables and criteria evaluating the design solution.

The principle of QFD

The fundamental principle of QFD is to gather the whole relevant information about the customer and to use this information to drive the design of a product or service. Many tools have been integrated into the QFD process to facilitate the deployment of this information throughout the design and manufacturing processes, and its dissemination to relevant organizational functions. The primary function of QFD is to identify the most significant issues and to link priorities and target values back to the customer. Identifying customers segments to be prioritized in an effective first step. Gathering the desired improvements from the customer and from the context use is a significant second step. The context of use defines the constraints under which the product has to function.

Taguchi view on cost of variability

The basic building system of Taguchi's methods is the idea of reducing the effect of uncontrolled factors to ensure the performance target to be continuously achieved [12, 13-15]. The Taguchi's contributions have developed the target–oriented quality principle (non linear loss function) and experimental design methods for product or process developments. Uncontrolled factors are the internal variations of the components or the external variation of the environment. Taguchi's view on cost of variability can be summarised as: Quality is good within range (conformance-oriented quality); Quality is best when on target; different grades of quality result in different costs. The concept of quality loss function is based on the principle of the electrical engineering signal/noise ratio used to maximize the ratio of useful energy to waste energy [15]. Dynamic applications of Taguchi's into QFD steps are useful for thinking future models of a product [16]. Taguchi methodology assumes that both ideal function and the whole system design are known. The ideal function of a design represents the theoretically perfect relationship between the performance and input signal. Dynamic applications look for design parameters, which increase the linearity of the relationships by making the response independent of the sources of variations.

SPC view

The fundamental principle of QFD is to monitor variation by monitoring causes and effects. The types of variations can be: special variations due to human or machine or design errors (fixable problems); variations due to the nature of the process (non-fixable problems). SPC detects the existence of special variations: reacts when necessary (do not overreact) but SPC does not find the cause of variation (we do that). A variety of statistical analyses can be applied using SPC. It is an integrated system for manipuling, analysing and presenting data. It is a modular system with a large range of modules that can be added to the basic system.

3. COST AND QUALITY OPTIMIZATION BY THE COUPLING OF THE THREE METHODS

We propose to develop a system of integration, which takes into account the advances of the three methods previously seen and keeping the flexibility necessary to the activities of design and control of production systems. Using this methodology it is possible to generate concepts to reduce negative effects and improve performances of existing product designs. The system includes analytical tools used to structure the problem and knowledge base tools used to point to the direction of solution concepts. This methodology realizes the linkages QFD, SPC and Taguchi's methods for a complete design process to be achieved. Weaknesses of QFD is bottleneck engineering and optimization. The five step model of QFD (as a customer driven product design, the process starts with customer analysis) are extended by extra tools: SPC and Taguchi. The impacts of SPC [1, 5, 8, 11] and Taguchi on QFD have been studied and recorded. QFD provides with the customer's input and Taguchi provides with the process to determine the best parameters of a robust design or SPC combinations. The voice of customer is prioritized and expressed by functions, demanded quality, performances measures, failure modes, concepts and manufacturing [17].

The methodology

The methodology is in five steps (Figure 1). The first step is the identification of the customer segments: selecting criteria for ranking client segments; ranking the client segments. It improves both designs which have never been considered possible, and new demands which are possible to satisfy. It builds the database of customer segments and enables a more aggressive attitude because of the possibilities offered by the technical evolutions.

The voice of customer segments and the context of product use are the significant second step. The customer's needs into database are expressed by demanded quality, reliability issues, solutions, functions, failure modes and safety. The voice of customer context should be added to the system resources to the who? What? Where? When? How? information. Because the enterprise thinks resources, it look at the resources available to provide with an ideal design and constraints and useful functions as well. Identifying by Taguchi methods the ideal function and the sources of variation offer another solutions and perspectives.

The third step. The technical step maps the subjective demanded quality information of the customer's segments into the objective performances or measures of performances used by the engineers. In this step it is important to identify conflicts between different performance measures if the product is a upgrade model. This step often calls to QFD, Taguchi and SPC. Many enterprises stop after the house of quality of QFD has been completed and continue own design process. Conflicts are used to establish compromises in performance and to start the analysis of technical contradictions. Those conflicts influence the compromises in the target values set after a technical benchmarking done. Taguchi's method can take advantage of the positive interactions. Taguchi offers the quality loss function – QLF - as an effective evaluation of technical benchmarkings. This step improves manufacturing equipments by looking at conflicts and another problems, the manufacturing process by the view of the process evolution and reduces cost by looking at the systems resources.

The fourth step. The target values, the priorities and the conflicts, the cost, the manufacturability can be inputs for this analysis. The system would generate many alternatives from the performances desired and the resources of the organization. With Taguchi, the best target values for a robust design are determined for each addressed alternative.

The fifth step. This is the step of organizational knowledge system of the manufacturing process. It have concerns with the equipment, the process and the capability of the current technology. It provides with a search of technologies which can improve the product from a manufacturing process given. One can determine Taguchi's robust operating conditions to find the appropriate signal to select the exact desired output of the production process. Within this step, a database upon designed experiments for operating conditions is developed. Additional tools for the product evolution and the problems formulation on products / services have been developed.

4. CONCLUSION

This paper realizes the linkages among QFD, SPC and Taguchi's methods for a complete view of the design process to be achieved. The five steps of QFD are used including additional tools. Weaknesses of QFD are bottleneck engineering and optimization. QFD provides with the customer's inputs and Taguchi provides with the process to determine the best parameters of a robust design or SPC combinations.

We propose a methodology to develop a system of integration, which takes into account the advances of the three methods and includes other tools, and keeps the flexibility necessary to the activities of design and control of production systems. The model follows the general approach of concurrent engineering [6] and it addresses manufacturability, cost and quality at the product design stage. The process capability index is a better indicator for quality level or manufacturing yield than the quality loss coefficient in the quality loss function approach. The manufacturing variability is also addressed as a constraint that replaces the quality loss function, in order to ensure the required level of manufacturing yield [7, 16]. The need to provide with the concept design and the development stages to the market by a product introduction process has been highlighted: carefully structured knowledge about process characteristics and capabilities has to be merged with cost estimating methods. Before leaving the topic of design costing, it is true to say that non-conformance must always be addressed while designing. At each level of details, at each moment and for each component, the process planning has to be organised in order to obtain the desired variability means. It enables to analyze the manufacturability cost and quality at the product design stage [7, 16]. A procedure enables the exploration of design and process combinations for manufacturing cost. For financial control and successful marketing, it is necessary to have cost targets and realizations throughout the product introduction process. Product cost is virtually always a prime element in decision making for manufacturing industry. The main problem in product introduction is the prevision of reliable cost information in the early stages.

The paper has outlined a methodology for the quality based design of new system and product based on the integration of the quality tools addressing how QFD, Taguchi's methods and SPC processes can be used to improve the design quality of products at the conceptual stage. The combined use of those tools to evaluate products, provides with a systematic approach for identifying where design quality can be improved at the conceptual stage (virtual product). Benefits of the system include: shorter development time and reduced time to market, reduced engineering changes, rapid comparison of alternative designs and competition products, systematic component costing, lower component cost...

REFERENCES

[1] Aft L. S. - Statistical Management and Problem Solving – *ASME*, 1990.
[2] Cullen J. and Hollingum J. – Implementing Total Quality, *Springer-Verlag*, New York, 1987.
[3] Davidow W. H., Malone M.S., The Virtual Corporation, *Harper Collins Publishers*, New York, 1992.
[4] Davenport T. - Process Innovation Reengineering work throught Information Technology, *Ernst and Young Harward Business School Press*, 1993.
[5] Dixon W.J., Massey F.J. – An Introduction to Statistical Analysis, *McGraw-Hill*, New York, 1983.
[6] Dragoi G., Guran M. – Sisteme integrate de productie asistate de calculator, *Editura Tehnica*, Bucuresti, 1997, ISBN 973-31-1124-4.
[7] Dragoi G., Brissaud D., Tichkiewitch S. - Analysis of the manufacturabily cost and quality at the product design stage, *Revista Romana de mecanica Fina si Optica*, Supliment nr.2/1998, vol. II, ISSN 1220-6830, pp. 543-547.
[8] Everitt B. S. and Dunn G. – Applied Multivariate Data Analysis, *Edward Arnold*, London, 1991.
[9] Eyes D. D. - Total Quality Management, *Engineering Tims*, oct. 1988.
[10] Hammer M., Champy J., Reengineering the Corporation – A manifesto from business revolution, *Harper Collins Publishers*, New York, 1993.
[11] John, W. M. P. - Statistical Methods in Engineering and Quality Assurance, *Wiley Series in Probability and Mathematical Statistics*, 1990.
[12] Phadke S. M. – Quality Engineering Using Robust Design, *Prentice Hall, Englewood Cliffs*, N.J., 1989.
[13] Pugh S. – Total Design, *Addison Wesley*, England, 1991.
[14] Ross, P. - Taguchi Techniques for Quality Control, *Edition McGraw Hill, Book Company*, New York,1988.
[15] Taguchi, G., Elsayed A., E., Hsiang, C., T. - "Quality Engineering in Production Systems", *Mc.Graw – Hill Book Company*, International Edition, 1989.
[16] Tarcolea C., Dragoi G., Tichkiewitch S. - Multidimensionnal Taguchi's model with dependent variables in quality system, *IDMME'98 – Integrated Design and Manufacturing for Mechanical Engineering*, vol. 4, p. 1211-1219, ISBN – 2-913087-00-0.
[17] Urlichts R, Schreiner T., Chen, P., Design for machining, quality, cost and environment, International Conference on Engineering Design – ICED'99, Munich, 1999, vol.3.

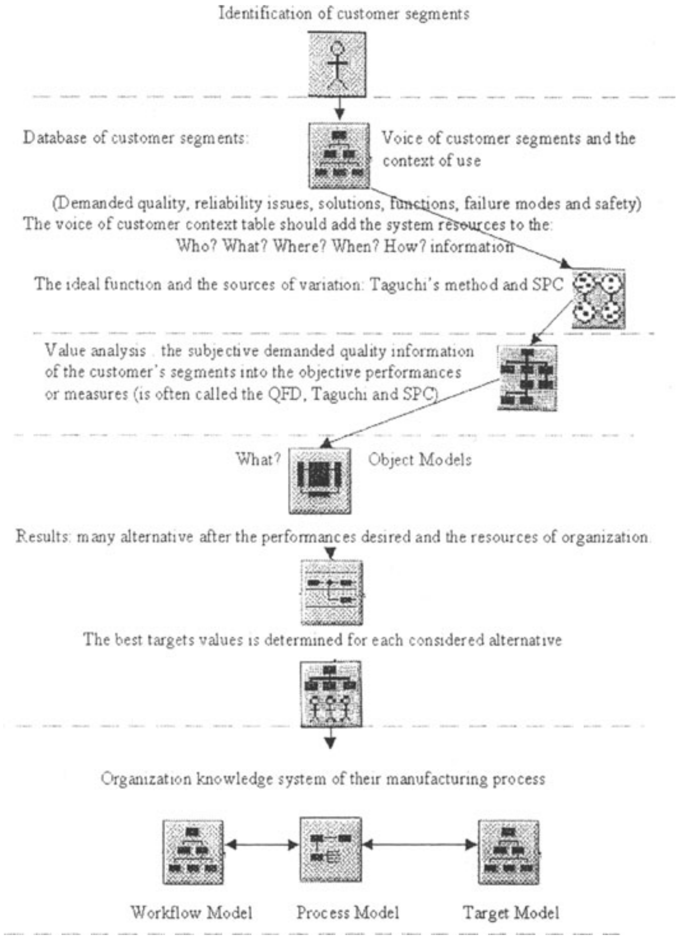
Identification of customer segments
Database of customer segments:
Voice of customer segments and the context of use
(Demanded quality, reliability issues, solutions, functions, failure modes and safety)
The voice of customer context table should add the system resources to the:
Who? What? Where? When? How? information
The ideal function and the sources of variation: Taguchi's method and SPC
Value analysis . the subjective demanded quality information of the customer's segments into the objective performances or measures (is often called the QFD, Taguchi and SPC)
What?
Object Models
Results: many alternative after the performances desired and the resources of organization
The best targets values is determined for each considered alternative
Organization knowledge system of their manufacturing process
Workflow Model
Process Model
Target Model

Figure 1: the five steps of the methodology.

George DRAGOI[*,**], *Daniel BRISSAUD*[**]
[*] *Polytechnical University of Bucarest, 313, Splaiul Independentei, 77206 Bucharest, Romania*
[**] *Laboratoire Sols, Solides, Structure, B.P.53, 38041 Grenoble cedex 9, France*
e-mail addresses: George.Dragoi@hmg.inpg.fr ; Daniel.Brissaud@hmg.inpg.fr

N. REJNERI, J.-C. LEON, G. DEBARBOUILLE

DISASSEMBLY SEQUENCING USING TECHNOLOGICAL DATA

Abstract. In this article, a method is presented which can automatically generate all feasible disassembly sequences of a product both from geometric and technological points of views. The components of the assembly are modelled with accurate B-Rep models and the mobility between them are modelled as effective translations, rotations or helical movements.

In order to reduce the algorithm complexity inherited from such models, i.e. the number of geometrically feasible sequences and the complexity of the movements, this approach is based on technological data associated to the geometric description of components.

The geometric and technological data are taken into account to create associations of components, i.e. the number of components is reduced, and to define criteria for the evaluation and selection of disassembly sequences in order to reduce the number of sequences effectively built and hence the algorithm complexity.

1. INTRODUCTION

The goal of disassembly sequencing is to plan a feasible series of operations to split a product into its individual parts. In the context of assembly, it has been estimated that the assembly process contributes to twenty to sixty per cent of the manufacturing cost and to twenty per cent to the investment of production equipment for the factories.

The assembly sequences are determined by reversing the operations of disassembly. Thus, the assembly sequences are valid without taking into account the application of forces and interference's tools that are generally different in assembly or disassembly contexts.

Previous works show that many researches have been developed to determine [1, 3, 4, 5, 8, 9] and to evaluate [2, 5, 7] assembly-disassembly sequences but most of them are only based on geometric data and constraints, thus a typical product can have several hundreds or thousands of possible disassembly sequences. Furthermore, a significant number of approaches are based on facetted models of components and on models of relative movements relying on sequences of infinitesimal translations [8].

In fact, only the approach defined in [10], introduce technological data in order to complete their physical model of contact and to take into account the fitting constraints. Their model includes two matrixes:

- a functional pseudo-matrix indicating which half degree of freedom is linked or free between the two considered elements,
- a contact pseudo-matrix representing the half degree of freedom between two elements before their possible fitting (gluing, elastic deformation,…).

P. Chedmail et al. (eds.), Integrated Design and Manufacturing in Mechanical Engineering, 347-354.
©2002 *Kluwer Academic Publishers.*

In order to reduce the algorithm complexity of disassembly simulation, the current approach is similar and based on technological information associated to the geometry of components. Such a relationship is critical because the geometry of the components is based on B-Rep models containing cylindrical, free-form surfaces, … rather than facetted representation and the relative mobility of components is modelled with effective translations, rotations, … of finite amplitude rather than infinitesimal translations only.

This paper deals particularly about how technological data are used. The first section describes the initial parameters and the data used by the disassembly model. The second one presents how it is possible to reduce the number of components by creating subsets of components based on technological data. In the third section, we briefly present the criteria defined to eliminate, evaluate and select disassembly sequences among all geometric feasible ones. In the last section, the proposed approach is applied to a mechanical product and the reduction of generated disassembly sequences according to technological parameters and other data is evaluated.

2. PARAMETERS AND DATA FOR DISASSEMBLY

This section is subdivided into four parts. The first one briefly states definitions about disassembly entities. The second one describes the hypotheses and minimal data used in the current approach. The third one is a presentation of the geometric disassembly criterion of a component. The last part is a description of complementary technological data needed.

Definitions: The disassembly simulation process of a product is based on three main entities:

- the product or mechanism as a whole,
- the *component*, representing an elementary part of the product,
- the *contact* between two components, representing a mechanical linkage between a pair of functional surfaces.

A *component* can be either:

- an elementary component, considered as a non decomposable one. Some of its attributes are shown in Figure 1a,
- or a subassembly or a group, i.e. a set of components. Their characteristics are described in the second section.

A *contact* between a pair of components is one among the fifteen possible configurations of contacts, shown in Figure 1b. Each of them allows the algorithm to determine the disassembly mobilities of product components and hence the disassembly sequences of the whole product.

A *mobility* is a possible infinitesimal exact movement (a rotation, a translation, a helical movement) to remove contacts between two functional surfaces of components. Possible motions are translations, rotations and helical movements. These motions are determined using a model based on quaternion formalism and dual algebra for each couple of functional surfaces, i.e. fifteen possible contact types.

Neither this model nor the association of contacts into an equivalent contact to determine the relative mobility between two components is presented in this paper to focus on the presentation of the influence of technological data.

An *equivalent contact* of a component is one among the fifteen possible contacts types. In fact, each combination of contacts must produce a new configuration which fits into an existing contact type.

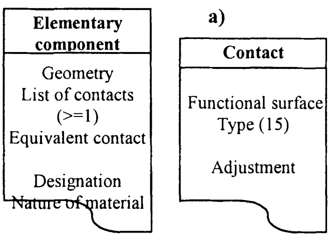

b)

anchorage, pin joint, cylindrical fit, prismatic fit, helical fit, plane, spherical fit, punctual,	linear annular fit, rectilinear fit, cylindrical fit unidirectional, prismatic fit unidirectional., helical fit unidirectional., bilateral plane, n arbitrary planes.

Figure 1 .a) Attributes of elementary components and contacts. b) Fifteen types of contacts.

Hypotheses and minimal data: The proposed approach can only be applied with the following hypotheses:

- initially the relative positions of components are known and coincide with the assembled position of a normal working configuration,
- the geometric model of the functional surfaces representing the contacts are described by an exact Boundary Representation (B-Rep) model. Indeed, most of the mechanical linkages are based on elementary geometric surfaces (planes, cylinders, spheres, ...) which have an exact representation in the actual CAD software. At last, an exact representation at the opposite of a polyhedral one allows the algorithm to take into account the potential finite rotations or helical movements rather than infinitesimal translations only,

Therefore, the minimal data input into the algorithm to generate disassembly sequences are:

- the geometric models of components associated with a global coordinate system of the product,
- the contacts between functional surfaces of components. To locate contacts, the algorithm used here is based on the geometric surface representation of the components and a tolerance value between these surfaces. Some geometric configurations cannot lead to an automatic identification of a contact, hence specific information needs to be added to perform a correct mobility analysis.

Geometric disassembly criterion of a component: From the information described above, it is possible to state the geometric disassembly criterion of a component (see Figure 2 for an example). This dismounting process is defined by the following parameters:

a. the disassembly mobilities of a component with respect to its adjacent ones,

b. the minimal extraction distance to remove contacts along the possible disassembly translation directions, i.e. the finite mobility of a component,

c. the geometric interference between a component and its environment when moved according to the extraction and security distances.

Therefore, a component will be geometrically removable if and only if at least one of its finite translation mobilities exists without geometric interference (intersection and/or contact with the remaining components or its environment).

At each disassembly step of the sequence, the algorithm identifies the list of potential removable components. From this list, geometric and technological criteria are applied to select the best component and hence all feasible disassembly sequences are generated.

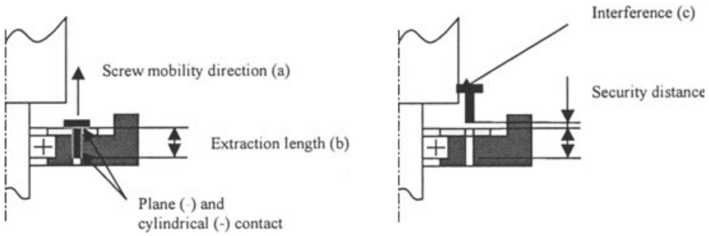
Screw mobility direction (a)
Extraction length (b)
Plane (-) and cylindrical (-) contact
Interference (c)
Security distance

Figure 2. Geometric disassembly criterion of a screw.

Technological data: Technological information is taken into account to enforce the meaning of sequences determined and to reduce the number of disassembly sequences, hence reducing the overall algorithm complexity though geometry and movements are accurately described. Two levels are distinguished:

- firstly, at the component level in order to separate them in accordance with their impact on disassembly sequencing:
  - merge one or more geometric models of components into one only,
  - create components subassemblies or groups,
  - define technological criteria to eliminate, evaluate components which have a relative kinematic mobility with respect to others,
- secondly, at the contact level in order to represent their real behaviour compared to the supposed perfect one.

Information attached to components: Up to now, only two categories of information have been defined, the components designation and their constitutive material. The data are generally defined in the bill of materials associated with the product.

Standard designation: The designation allows the algorithm to identify the standard components. Most of the time, the standard components are defined by an incomplete and partial geometry. So, the distinction between standard components helps inferring one or more geometric models which can be automatically built from their designation and associated with these components. Typically, a standard component can be a retaining ring which requires two distinct representations: one in assembled position and the other one for the disassembly process. Hence, the data structure describing a component should be able to handle multiple geometric models to match with the various geometric configurations encountered during the disassembly simulation process.

Nature of material: The nature of material allows the algorithm to compute the weight of components and to identify for example the possible tools or gripping systems required to perform the disassembly task. The characteristics of materials, i.e. density, are stored in an array into a data structure.

Information attached to contacts: The data attached to the contacts between adjacent components are currently restricted to their fit and set up for a couple of cylindrical surfaces only. The fits are used as qualitative data to express either possible relative movements or uncertainty of such movements or movement without or with damage of the surfaces, i.e. loose fit, uncertain fit, snug fit with or without components damage.

3. HOW TO REDUCE THE NUMBER OF COMPONENTS ?

The number of disassembly sequences increases at most according to the number of components of a product. Therefore, component clusters are desirable in order to reduce the disassembly complexity.

All the data described in the previous section allow the algorithm to define two categories of components: groups and subassemblies.

Groups of components:

a. definition: A group of components is a set of components, generally without contact between them, which must be extracted during the same operation. The components must have the same designation, typically a group of screws.

b. characteristics: The attributes of a group of components are (see Figure 3a):

- the constitutive components,
- the designation which is identical to each component designation,
- the nature of material if all the components share the same data.

Subassemblies:

a. definition: A subassembly is a set of components composed of two or more components that can be handled simultaneously and even turned upside down without separating. The geometric and technological characteristics of its components can be different from each other.

b. characteristics: The subassembly characteristics are similar in nature to those of an elementary component but are obtained by merging the list of its component attributes (see Figure 3b):

- the geometric representation,
- the contacts,
- the equivalent contact,
- the designation according to the components designation,
- the nature of the material, if all components share the same one.

c. rules: Some heuristic rules have been set up to automate the determination of subassemblies according to the geometric and technological characteristics of the components. Three categories of rules, based on the following data, have been generated:

a. the contact fits provide an easy and efficient way to create subassemblies. Such typical subassemblies can be a housing or a shaft with a ball bearing snug fitted onto it,

b. the components designation leads to the definition of one or more clustering rules. Typical assemblies can be a cluster of a screw and all the components in contact with it. The principle of such an algorithm is described in Figure 4,

c. the contacts between the components. It is possible to define a relative equivalent contact for each adjacent component and hence their corresponding relative mobilities. Therefore, if no direction of translation exist between two components, a subassembly is created.

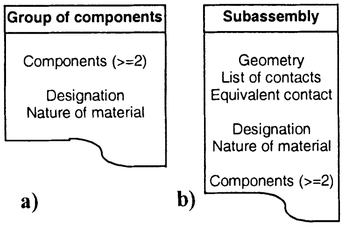

Figure 3. a) Attributes of a group of components. b) Attributes of a subassembly.

How to eliminate and evaluate sequences ? Here, the goal is to define criteria to generate disassembly sequences in order to:

- firstly, eliminate all the sequences identified as non geometrically and/or technologically feasible,
- secondly, evaluate the remaining sequences to select the best one.

Up to now, eight criteria have been defined in the current application and can be divided into two categories ; geometric and technological criteria:

- geometric: the number of contacts, the extraction distance, the volume of components, the mobility direction of components, the accessibility of components, the number of hands to manipulate components,
- technological: the fit of contacts, the designation of components.

4. EXAMPLE AND RESULTS

The proposed product is an alternator composed of seventeen elementary components similar to the one of Kroll [6], as shown in Figure 6a.

Alternator data: The information defined and used for the disassembly sequencing are:

- *contacts* of components,
- components with *standard designation* are described in figure 5a,
- only one *adjustment*, i.e. snug fit, is defined between the rear-bearing and the rotor.

Sequences: Without the technological information, there are more than 1500 possible geometric sequences to disassemble this alternator. Something which could hardly be performed by the application within a reasonable amount of time.

However, using the components designation, the identification of subassemblies and groups of components, the disassembly sequences count is reduced to 248 for 9 components, i.e. three subassemblies and two groups of components have been identified (see Figure 6b their designation and relative positions). The sequences are not shown because of the large size of the tree-browser. Finally, when activating the selection criteria among the feasible sequences, only two disassembly sequences of the product have been kept.

The running times to perform subassemblies and to find all complete disassembly sequences for the alternator assembly are shown in Figure 5b. The application runs on a SGI Indigo2 workstation, MIPS R4400, 96 Mb of memory.

For an entire disassembly process, each subassembly and group of components is then recursively disassembled applying the same rules and criteria.

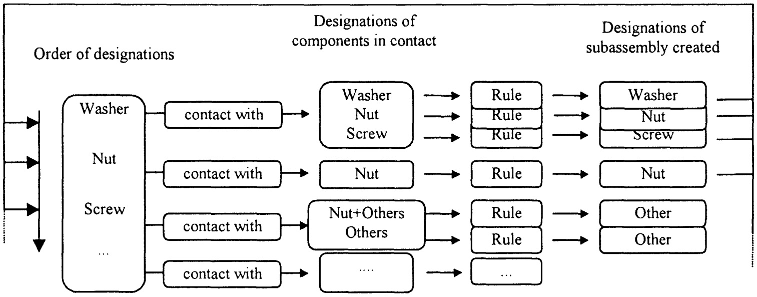
Order of designations
Designations of components in contact
Designations of subassembly created
Washer
Nut
Screw
...
contact with
contact with
contact with
contact with
Washer
Nut
Screw
Nut
Nut+Others
Others
....
Rule
Rule
Rule
Rule
Rule
Rule
...
Washer
Nut
Screw
Nut
Other
Other

Figure 4. Principle of the algorithm used to identify subassemblies using the standard designation of components. Heuristics are based on the functional meaning of the component designation first and then on their contact configuration.

Components	Standard designation
Bolt (3 at 120°), Screw (2 at 180°)	Screw
Lock-washer	Lock-washer
Nut	Nut
Rear-bearing, Rear-housing	Ball-bearing

a)

Alternator	Subassemblies	Subassemblies + selection criteria
Computation Subassemblies	3.86 sec.	3.86 sec.
Number of sequences	248	2
Computation Sequences	2 min. 20.64 sec.	36.45 sec.

b)

Figure 5. a) Standard designation of components. b) Computing times for the alternator.

5. CONCLUSION AND PERSPECTIVES

The application developed is able to perform automatic disassembly sequence generation process and analysis using as input a geometric description of the proposed assembly, technological information about each component and their contacts between them.

The method described here allows to reduce the number of disassembly sequences through two levels of treatments:

- firstly, the reduction of the number of individual components,
- secondly, the elimination and the evaluation of removable components.

Other possible directions of future work include the identification and the organisation of new technological data for the disassembly sequence evaluation and also apply the current method to other areas like maintenance or recycling operations, i.e. to identify a sequence to dismount one component of the product.

CAD data files describing products from industry are also welcomed to perform further tests and enhance the current application.

The research work is performed in cooperation with Matra Datavision. The application is implemented in C++ and uses the object libraries of Cas.Cade.

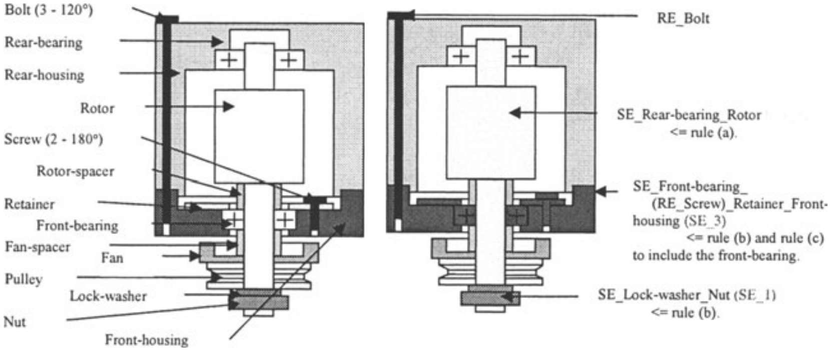
Bolt (3 - 120°)
Rear-bearing
Rear-housing
Rotor
Screw (2 - 180°)
Rotor-spacer
Retainer
Front-bearing
Fan-spacer
Fan
Pulley
Lock-washer
Nut
Front-housing
RE_Bolt
SE_Rear-bearing_Rotor
<= rule (a).
SE_Front-bearing_
(RE_Screw)_Retainer_Front-
housing (SE_3)
<= rule (b) and rule (c)
to include the front-bearing.
SE_Lock-washer_Nut (SE_1)
<= rule (b).

Figure 6. a) Elementary components of the alternator. b) Components of the alternator after subassemblies and groups computation.

6. REFERENCES

1. Baldwin, D. F., Whitney, D. E., An integrated computer aid for generating and evaluating assembly sequences for mechanical product, IEEE Trans. Robotics Automat., 1997: 78-94.
2. Boothroyd, G., Alting, L., Design for Assembly an Disassembly, Annals of the CIRP, vol. 41 (2), 1992: 625-636.
3. Bourjault, A., Contribution à une approche méhodologique de l'assemblage automatisé : Elaboration automatique des séquences opératoires, Ph.D. thesis, University of Franche-Comté, France, 1984.
4. Gottipolu, R. B., Ghosh, K., Representation and selection of assembly sequences in computer-aided assembly process planning, Int. J. Prod. Res., vol. 35 (12), 1997: 3447-3465.
5. Kanai, S., Makino, H., ASPEN : Computer-aided Assembly Sequence Planning and Evaluation system based on predetermined time standard, Annals of the CIRP, vol. 45 (1), 1996: 35-39.
6. Kroll, E., Modeling and reasoning for computer-based assembly planning, in Concurrent Engineering: Automation, Tools and Techniques, Edited by Andrew Kusiak, 1993: 177-205.
7. Laperriere, L., Elmaraghy, H., GAPP : a Generative Assembly Process Planner, J. of Manufacturing Systems, vol. 15 (4), 1996.
8. Latombe, J-C., Wilson, R., Assembly sequencing with toleranced parts, Proc. of Solid modeling 95 Conf., Salt lake city, Utah, USA.
9. Romney, B., Godard, C., An efficient system for geometric assembly generation and evaluation, Proc. ASME Int. Computers in engineering conf., 1995: 699-712.
10. Mascle, C., Maranzana, R., Feature Modeling in Assembly Planning, Int. IFIP Conf. Modélisation et reconnaissance de caractéristiques en CFAO, Valenciennes, France, may 1994.

Jean-Claude LEON
Laboratoire Sols, Solides, Structures UMR CNRS 5521
Domaine Universitaire
BP 53X 38041 Grenoble Cedex 9
France
Jean-Claude.Leon@hmg.inpg.fr

A. SINZINKAYO, C. MASCLE, M. BALAZINSKI

APPLICATION OF FUZZY LOGIC FOR AN ASSEMBLY METHODOLOGY

Abstract. This paper describes an application of fuzzy logic to choose an assembly process. Based on Boothroyd's method, this application improves the reliability of decision-making and eliminates numerous repetitive calculations.

1. INTRODUCTION

In this paper an application of fuzzy logic to Design For Assembly methodology is introduced. The main goal is to show that fuzzy logic is a tool which will help a design engineer make decisions and resolve certain problems related to product assembly. Indeed, the most known decision making methods for this application are only partially satisfactory and could lead engineers to make bad choices. This work is based on the well-known Boothroyd-Dewhurst methodology for design analysis. This well documented methodology incorporates ergonomic measures and economic calculations that have been developed in previous research works. Boothroyd-Dewhurst's methodology is an iterative approach which consists of selecting the most suitable assembly process through analysis of task duration, costs and assembly difficulties. This analysis depends on parameters describing the product and its environment such as the product life-cycle time, the number of parts and sub-assemblies, the total number of parts required to build every configuration of the product, the annual production volume per shift, etc. Regardless of the selected assembly process, manual or automatic, various tables permit the calculation of assembly time and the cost for each part, subassembly or used assembly process. The objective of this paper is to demonstrate that an approach using a decision support system significantly improves the Boothroyd-Dewhurst methodology and helps the engineer make decisions regarding choice of an assembly process for a given product. It also cuts down the number of repeated calculations and should significantly reduce design engineering time for the product.

2. RELATED WORKS

Product design is a complex creative activity which requires experience and knowledge. For this reason it will be presented as several progressive stages. The activity begins with product conception phase (ideas, concepts and functional requirements), which is followed by preliminary design. Next is detailed design

P. Chedmail et al. (eds.), Integrated Design and Manufacturing in Mechanical Engineering, 355-362.

©2002 *Kluwer Academic Publishers.*

(drawings and prototypes) and the activity finishes with first-off production. In this sequence the fit between mating parts is verified using prototypes and first product assembly, after part and product design is completed. This linear and sequential approach does not favour potential error detection as soon as possible in the design process. It is widely accepted that 75-85% of the overall cost of a product is committed during the design and planning stages of its development. Early consideration of manufacturing and assembly problems during the product design stage is therefore the most cost effective way for reducing assembly costs and increasing productivity. Consideration of the assembly process late in the product development sequence leads to very high costs for design modifications made at this point. "When around 20% of design phase is completed, already 80% of manufacturing costs are committed" [5]. To resolve this problem, many companies have adopted simultaneous engineering concepts (Ettlier and Stoll) [9]. This method effectively increases product quality and reduces production time and cost. Using this parallel development approach, potential problems in assembly process can be solved in design stage. Design For Assembly (DFA) is a key element of concurrent engineering, which typically starts the pre-design stage by gathering together a multidisciplinary team of designers, manufacturing engineers, process monitors and marketing personnel to work on the development of a new product. As mentioned before, numerous problems appear when various parts are assembled. A number of design-for-assembly techniques and evaluative mechanisms such as those of Boothroyd-Dewhurst (USA), Lucas (UK) and Hitachi (JP) have been used in industry. Boothroyd-Dewhurst Design-For-Assembly (DFA) methodology [3] was developed in the late 1970s. The Boothroyd-Dewhurst DFA evaluation process centres on establishing the cost of handling and inserting parts. The process can be applied to manual or automated assembly. Regardless of the assembly process, parts are evaluated in terms of ease of handling, ease of insertion and whether or not the part in question is actually necessary. The findings are then compared to proprietary data from which a time and cost is generated for the related assembly operations performed on the part. Finally, an attempt at reducing the number of parts is made by examining each part and identifying whether it exists as a separate part for fundamental reasons. Utilisation of numerous tables is essential to analyse each component (part or subassembly). Since the early implementation of DFA methods, steps have been taken to provide a more integrated approach. Boothroyd-Dewhurst have developed a number of Windows based tools including DFA. Chan and Mo [6] improved the method while extracting the required information automatically from CAD-CAM software. This technology is useful for automatic determination of assembly solutions if this information is integrated into the research method for the assembly solution.

A detailed analysis of the product is realised using the DFA method. In an alternative approach Warnecke and Lörn [14] present a catalogue of assembly solutions permitting the engineer to choose an assembly path, the machinery to use and the constraints that must be respected. . This allows the choice of an assembly solution that best suits the level of the available operations. Value analysis is used to choose a solution for each sub-operation. The major inconveniences of this approach are the manual consultation of the catalogue and the absence of integration to existing computerised systems. It is based on experience rather than on scientific principles. Methods based on a scientific approach offer the advantage of allowing objective decisions in a given situation.

Other researchers analysed the constraints and the rules that must be considered during the automatic scheduling of assembly. Among these, Jones and Wilson [8] enumerated numerous constraints typically encountered during automated assembly. These constraints serve as instructions to the user and guide him toward a final choice for scheduling. The work is interesting because the authors set up the constraints so that they may be easily adapted for use by computer systems, contrary to the information contained in the catalogue of solutions of Warnecke, Lörn and Kiener [14]. Some constraints can be applied to a binary vision of the assembly in the setting of the choice of an assembly solution - as to choose the least expensive solution - but the majority take into account a sequence of assembly operations.

Schraft [13] enumerated further rules to follow in view of a successful automatic assembly. He enumerates six important rules, and contrary to Jones and Wilson, mentions general concepts, which are more complex to program. Several advantages emerge favouring the use of Warnecke and Lörn's catalogue. First, the solutions represent the know-how of a company concerning assembly. While facilitating and optimising its use, it is possible to reduce the previously mentioned inconveniences incurred due to the incorporation of an employee's evaluation into the process. As this method adapts comfortably to data base concepts, it is possible to computerise this catalogue to permit its consultation through a graphic interface.

In order to define the sequence of assembly in view of recycling, several research papers have been published on disassembly (Design For Disassembly or DFD). Brooke [4] discusses the recycling advantages of the disassembly approach, particularly for the automotive industry. Research by Mascle [12] presents the use of disassembly and inverse engineering (reverse engineering) as a means of improving conception of a product to achieve a more efficient assembly sequence. His use of the half degrees of freedom allows identification of the free directions of disassembly, and therefore of assembly. Potential errors of conception are easily detected using this approach.

Hitachi's Assemblability Evaluating Method (A. E. M.) is another imposing alternative for the elaboration of assembly solutions. It is supported using data bases and economic calculations. This method was developed in the late 70s and includes three main stages: the product conception phase(drawing, prototypes, etc.), the phase of assessment of its assemblability (degree of difficulty of the assembly operations, the costs, etc.), and a final product improvement phase based on a comparison (of the concepts, of the other products etc.). This method, developed by the Hitachi Company, is now commercially available but the little support documentation is available for consultation.

3. BOOTHROYD-DEWHURST'S METHODOLOGY

Boothroyd-Dewhurst's methodology is an iterative process which consists in selecting a suitable assembly process, analysing working times and assembly difficulties, and then optimising product redesign. Starting with a redesigned product, each component is analysed until an efficient assembly sequence is developed. This study involves the application of fuzzy logic to improve this methodology, so analysis of its description was the initial focus of the investigation, followed by the review of related research works.

The first step of the process consists in selecting the most suitable assembly process. Boothroyd-Dewhurst elaborated a table that analyses six input parameters: (**NP**): number of products to assemble; (**NA**): number of parts; (**NT**): total number of parts in order to build every configuration of the product; (**ND**): number of parts that will be modified during the life of the product; (**VS**): annual production volume per shift; (**RI**): investment factor. The table provides one or two possible solutions, and their respective confidence factor (%), for each definition interval of the input parameters. Five assembly systems has been taken into consideration: MA: manual assembly; MM: manual assembly with mechanical assistance; AI: automatic indexed assembly; AF: free transfer automated assembly and AP: programmable devices. Regardless of the selected assembly process, the second step aims to analyse each part of a product following chronological steps:

Step1: Taking stock for product data including engineering drawings, used configuration of the product, prototypes, etc.
Step2: Numbering parts and subassemblies by disassembly order.
Step3: Preparing a working sheet.
Step4: Writing the working sheet.
Step5: Determining the estimated assembly time (TM), cost (CM) and minimum number of theoretical parts (NM). This step concerns the manual assembly case. For automatic assembly other geometrical constraints are considered to continue the analysis.
Step6: Estimating assembly efficiency (EM) calculated as:

$$EM = \frac{3xNM}{TM} \qquad (1)$$

Step7: Designing a new product by part number and time reduction.

Utilisation of Boothroyd-Dewhurst's tables is essential for finding an assembly solution, but this becomes heavy and time consuming for user. This is an area where improvement is required. The final decision is still taken with designer know-how. The associated literature review revealed that current computerised DFA applications tend to take advantage of artificial intelligence techniques, used as support systems.. These systems however, are difficult to program and require large amounts of computer memory. The main objective of this work is to show that fuzzy logic can be effectively applied as a relevant tool for decision making in assembly. We will therefore use table data as input and compare our results with those obtained by Boothroyd-Dewhurst's methodology. Figures 1 and 2 show the screen shot of these results. A rule-based approach to decision making using fuzzy logic techniques uses a set of rules linking a finite number of premises and conclusions. The knowledge base of such systems consists of two components: a linguistic terms base and a fuzzy rules base. The former is divided into two parts: the fuzzy premises (or inputs) and the fuzzy conclusions (or outputs). In general, both contain more than one premise and one conclusion. The fuzzy sets theory was introduced by L.A. Zadeh, professor at California University at Berkeley in the 60s. The FUZZY-FLOU Software used in this work is an issue of the collaboration between École Polytechnique de Montréal (Canada) and Technical University of Silese at Gliwice (Poland) [1]. It runs on Windows and Unix systems.

4. FUZZY LOGIC APPLICATION

In this chapter, we study the improvement of Boothroyd-Dewhurst's methodology using fuzzy logic. First, product assembly is carefully examined and then the methodology is used to analyse the assembly process. Using the table, the chosen assembly process can be manual, automatic or programmable mechanisms. Fuzzy logic can be introduced here to find transitional solutions. Comparison between results obtained by both methods permits to validation of the knowledge base used to build the fuzzy sets. For selecting the assembly process, a fuzzy model, representing the assembly system selection table was created. This model consists of 3 premises and 5 conclusions. The premises were:

- Annual production volume (VS) can vary from 0.2 to 0.65 millions.
- Number of parts (NA),
- Investment factor (RI).

The conclusion is the assembly system (manual-MA, manual with mechanical assistance-MM, automatic indexed assembly-AI, free transfer automated assembly-AF, programmable devices-AP). In relationships between the fuzzy sets of the premises and those of the conclusions we have not used all available data because now FUZZY-FLOU system accepts only 5 premises and five conclusions. In this case, considered premises settle the most influential factors. An example of a typical rule is(rule 14):

«**If** (VS is 0.3 millions **and** NA is 6 **and** RI is 1.5) **then** (MM is 10 (100%) **and** MA is 7.5 (75%) **and** AI is 0 **and** AF is 0 **and** AP is 0)».

The results obtained in this example are similar to those using the tables. Boothroyd-Dewhurst's methodology foresees an alternative solution in some cases when the difference from the economic point of view between two solutions doesn't exceed 10%. For the precise case, Fuzzy-Flou provides results that overlap (100% and 75%). Improving the discretisation will be sufficient to obtain the same results. It is important to note that this assessment depends on the quality of the data base used at the beginning. A good data base requires extensive knowledge as supplied by experienced specialists on the subject. We used simple rules that would facilitate the design engineer's task, because there is less risk of error. A big advantage of this application method is that a value can be obtained for each of the assembly processes and it is thus possible to simulate and easily compare results for different cases.

Example. Data input: An assembly consisting of 7 components (NA) according to one model (NT=7). The number of components whose drawing changes (ND) is 4.

The yearly production (VS) is 220000 by shift of work and there are 2 shifts per 24 hour day (SH). The yearly cost of an assembly operator (WA) is 20000 \$. The capital allocated to replace a team's operator in case of automation (QE) is 18000 \$.

Stage 1: The investment factor RI is calculated with the help of the following formula: RI = (SH X QE)/WA. Replacing the values of the parameters in the formula we get RI: RI=2x18000/20000=1.8

Stage 2: Selection of the suitable line: at VS=0.22 and NA=7, line number 7 of the table is chosen..

Stage 3: Selection of the suitable column: The following factors are considered: NA=7, therefore NT < 1.5NA, ND=4; ND > 0.5NA and RI=1.8; column 6 is chosen. The designated cell (7;6), in table 1 [2], contains the MA letters representing an manual assembly line. The results of the figure 1 show that the same choice is achieved using Fuzzy-Flou.

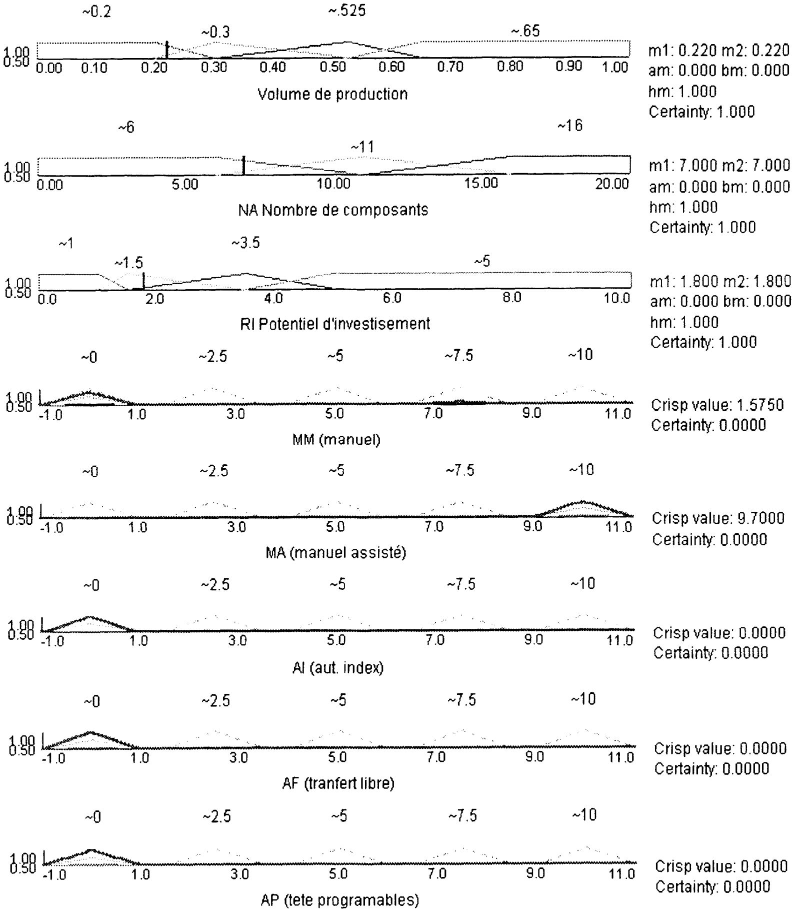

Figure 1. FDSS application results n° 1.

5. CONCLUSION

Use of Boothroyd-Dewhurst's tables permits choice of an assembly process for a given product and in some cases provides an alternative solution. This method however, doesn't allow the possibility of continued transition from one assembly solution to another because the range of the values is set. The application of fuzzy logic increases the number of alternative choices. In many cases, two or three possible solutions are offered. The results of tests made with the Fuzzy Decision Support System FDSS show that it permits the user to observe the transition from one column to another as different parameters are varied. When using different values near the limits of the tables for assembly processes that overlap, one can determine the values of parameters for which both processes are equal and can be directly interchanged. The capability of the fuzzy logic approach to show the transition from one assembly process to another provides the opportunity to refine decision making. Thus, the results of this survey bring us to conclude that Fuzzy-Flou can act as a decision tool for the choice of an assembly process. Application of Fuzzy-Flou to support the Boothroyd method increases confidence in decision making and allows inventors to use this knowledge base for different industrial applications. In the assembly area and especially during the product reconception stage, it reduces the time typically required to perform numerous repetitive calculations.

6. REFERENCES

[1] Balazinski, M., Bellerose, M.; Czogala E., «Application of fuzzy logic techniques to the selection of cutting arameters in machining processes», Fuzzy Sets and Systems, 63 (19940) 307-317.

[2] Boothroyd, G., Dewhurst, P., «Les assemblages- comment optimiser leur conception», Ed. du CETIM, 1986,p.1-96.

[3] Boothroyd, G., Dewhurst, P.," Design for Assembly", 1996.

[4] Brooke, L., "Think DFD, Automotive Industries", p. 71-73

[5] Cambron, M., Ingénierie Simultanée, notes de cours, École Polytechnique de Montréal, 1999.

[6] Chan, D.S.K., Mo, J.P.T., (1993), «Transformation of Product Design Features for Assembly Analysis, Royal Melbourne Institute of Technology», 1993 International Conference on Assembly, 22-24 November, Adelaide, Australie, p.55-60.

[7] Dallaire, D., «Module d'analyse économique LOGAM», Projet de fin d'études, École Polytechnique de Montréal, (1997).

[8] DeGuire, B., «Étude des Systèmes Multi-agents Pour la Recherche De Solutions D'Assemblage», Mémoire de maîtrise, École Polytechnique de Montréal, (1997).

[9] Ettlie, J.E., Stoll, H.W., (1990), "Managing the Design-manufacturing Process,McGraw-Hill Engineering and Technology Management Series, New York, 79-87.

[10] Gabriele, G.A. (N/D)," The application of Design for Assembly Principles to Design of Aerospace Structures", Rensselaer Polytechnic Institute, Department of Mechanical Engineering, Aeronautical Engineering and Mechanics, Troy, New York.

[11] Jones, R.E., Wilson, R.H.(1996), "A survey of constraints in Automated Assembly Planning", Proc. 1996 IEEE Intl. Conf. On Robotics and Automation, 1525-1532.

[12] Mascle C., «Conception et méthodes d'assemblage», Éd. EPM, Montréal, p.31-72.

[13] Shraft, R. D. (N/D) „Assembly-Oriented Design – Condition for Successful Automation“ (Montagegerechte Konstruktion – Die Voraussetzung für eine Erfolgreiche Automatsierung), Fraunhofer Institut für Produktionstechnic und Automatisierung (IPA), Stuttgart, West Germany.

[14] Warnecke, Lörn et Kiener, «Techniques de montage et d'assemblage», Edirep, $1^{\text{ère}}$ Édition, Paris p.129-270.

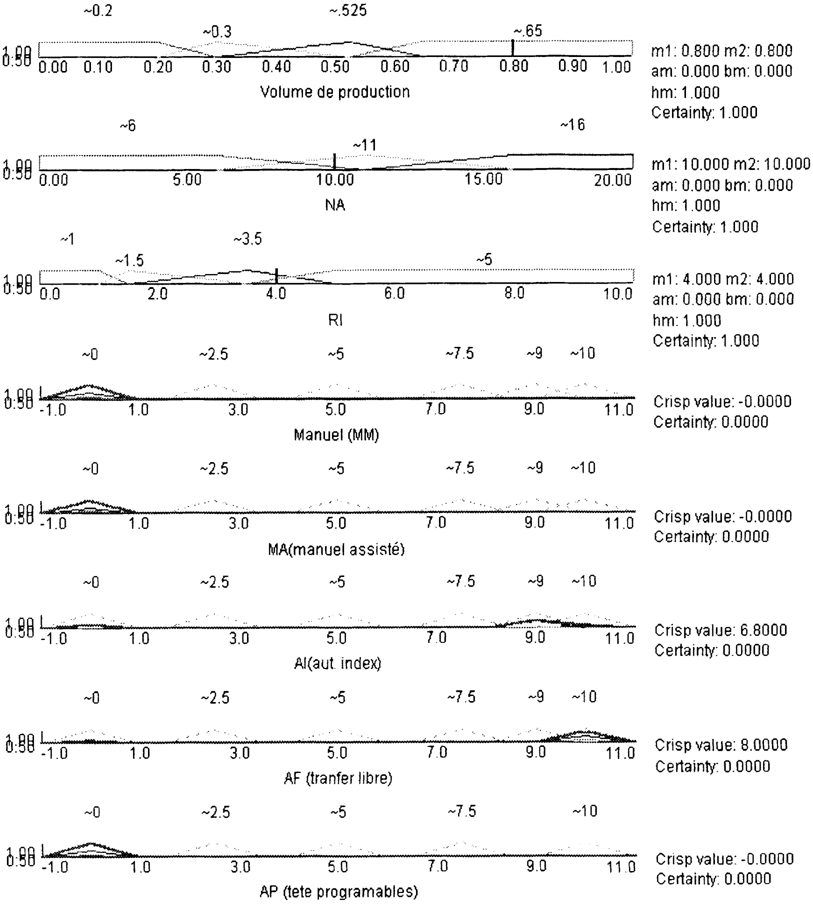

Figure 2. FDSS application results n° 2.

7. AFFILIATIONS

Section fabrication, Département de Génie Mécanique
École Polytechnique
C.P. 6079, succ. Centre-ville, Montréal, Québec, H3C3A7

Chapter 6
OPTIMAL DESIGN OF MACHINES, STRUCTURES AND COMPONANTS

Design of Closed Planar Mechanisms of Grippers to Clutch Flat Parts 365
L. SLUTSKI

Interaction of Gear Epicyclic Planets and the Effect of Web for Internal Gears 373
J.-P. DE VAUJANY, M. GUINGAND, D. PLAY

Kinematics of Robots with Roller-Constrained Ball-Wheels 381
S. OSTROVSKAYA, J. ANGELES

Structural Synthesis of Kinematic Chains and Mechanisms............................. 391
L. NOTASH, J. ZHANG

General Manipulators synthesis for a given workspace.................................... 399
S. GUERRY, F.B. OUEZDOU, S. RÉGNIER

Object Manipulation and Mannequin Driving Based on Multi-Agent Architecture.. 407
P. CHEDMAIL, C. LE ROY, B. MAILLÉ

Isotropic design of a parallel machine-tool mechanism.................................... 415
D. CHABLAT, P. WENGER, J. ANGELES

Application of the Design of Experiments Method to a Transversely Loaded Cylindrical Assembly 423
A. DAIDIÉ, H. LAKISS, D. LERAY, J. GUILLOT

Determination of the Mode Dominance for Model Reduction 431
K. LIU, X. SUN

Development of a New Methodology for Delamination Detection in Laminated Structures 439
J.C. WALRICK, D. COUTELLIER, P. GEOFFROY

Search of Contact in Dynamic Finite Element Code: Presentation of an Analytical Method 447
E. ARNOULT, B. PESEUX, J. BONINI

Recent Progress in Preliminary Design of Mechanical Components with Topology Optimisation 457
P. DUYSINX, M. BRUYNEEL

Finding the Optimal Stock Spring from Optimal Spring Design Characteristics 465
M. PAREDES, M. SARTOR, C. MASCLET

Design Process and Optimisation of an Integrated Electromechanical Battery. 473
C. KERZREHO, J.-Y. COGNARD

A Hybrid Calculation Model for Bolted Assemblies Used for Slewing Bearings 481
A. VADEAN, D. LERAY, H. LAKISS, J. GUILLOT

L. SLUTSKI

DESIGN OF CLOSED PLANAR MECHANISMS OF GRIPPERS TO CLUTCH FLAT PARTS

Abstract. The paper discusses the design and applications of a type of closed planar mechanisms for use in universal gripping devices, to clutch flat parts with different profiles. Various configurations and methods of simulation for these mechanisms are proposed. The method is implemented as a computer program for use by a designer, in an interactive mode. A working prototype was built and tested, while performing an assembly operation.

1. INTRODUCTION

A multitude of existing robotic gripping devices do not satisfy the current needs of different industries. For instance, an important characteristic of grippers, such as adaptability to object shape, has not been adequately analyzed and realized for industrial systems. The development of adaptable devices is stimulated by the need for flexible manufacturing systems, where a wide range of processes require operational changes of gripper properties.

As a basic example, a specific industrial problem, relevant this paper, will be described. In flexible systems, for instance of stamping, a common task is to clutch flat parts of different shapes in turn and place them in stamps. To that end, electromagnets, vacuum cups or other working elements are usually used in robotic grippers. To ensure flexibility, these working elements have to change their positions. A known type of simple suction device with a number of vacuum cups, which are usually used for conventional manipulations [1], does not solve all the problems of this class of operation. Another approach is based on the use of a gripper plate with an array of holes, connected to a vacuum controller [2]. The plate shape usually corresponds to the shape of the part to be manipulated, preventing flexibility. As an illustration of a more universal approach, another design [3] can be mentioned. Four suction elements are used here, which have relative motion, allowing some flexibility of gripping device. However, to implement these motions, three pneumatic cylinders are used to drive working points; that is relatively complex and demands some control means.

A desirable goal then is to build simple, industrially accepted grippers where a programmable device, while allowing fewer available working element positions, facilitates high reliability and low price. The approach used in this research is based on the application of so called high-class mechanisms [4]. Their feature, gripping devices mounted on a mobile structure consisting of rigid pivoting links ensures the above-mentioned property of adaptation. The purpose of this work is to establish a class of new grippers to solve specific problems of robotic grasping, that embody

P. Chedmail et al. (eds.), Integrated Design and Manufacturing in Mechanical Engineering, 365-372.
©2002 *Kluwer Academic Publishers.*

this important practical feature, and to describe methods for the design and development of universal grippers.

2. UNIVERSAL GRIPPER CONFIGURATIONS

In principle, different kinds of high-class mechanisms may be used to design the described type of grippers. However, since many of these are usually rather complicated, let us consider the simplest examples of basic mechanisms.

The first of them is the mechanism of the fourth class [4], with four rigid links providing a movable contour (Fig. 1). On some points of this contour (e.g., in its joints *A* and *B*), the working elements (e.g., electromagnets) are placed. These places may be chosen arbitrarily but when doing this, one has to take into account further problems with the device design. Then, to simplify the solution of these problems, it is better to place the working elements in contour joints and moreover, to place them in alternative joints as it is shown in Fig. 1. In this case, relative freedom of element motion is achieved and a mechanism can be designed which meets the requirements of a basic technological process. In our example, the mechanism motion follows the driving link *ON* rotation but, obviously, an input link may be designed in different ways. This issue will be discussed later.

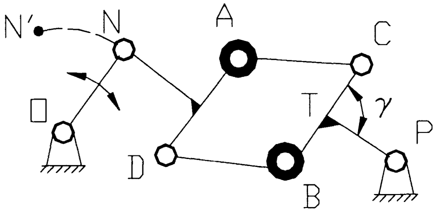

Figure 1. Mechanism with the four-link movable contour and two working elements

Another type of mechanism, which may be used for this purpose, is that with six rigid links forming a movable contour (Fig. 2). As in the previous case, three working elements may be placed in alternative joints *C, D, E* of the contour with the same ability to move them by rotation of the input link *ON*. When placing working elements in alternative joints, symmetry is achieved and the design becomes simpler. It can be seen that in this case, the program motion of three working points is achieved by means of only one driving motor, placed in the joint *O*.

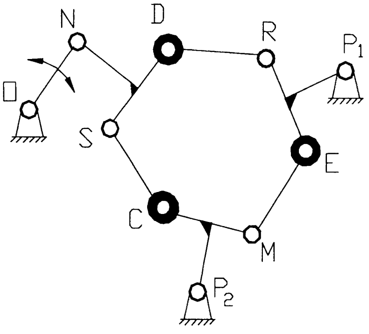

Figure 2. Mechanism with the six-link movable contour and three working elements

It is important that, in principle, not only one driving link can be used in these mechanisms, as it is shown in Figs. 1 and 2, but two, three, etc. Specific problems, which are solved by these mechanisms, require special design techniques that are, however, based on approaches presented below.

3. GRIPPER DESIGN

The design problem for the described mechanisms may be stated differently. For the first presentation of the problem, rather simple approaches to its solutions are proposed here. Another important point to note is that, in principle, a general approach to create design algorithms for both considered mechanisms is the same. It was especially done to ensure standardization of design methods for these types of mechanisms. The difference is in applying some additional procedures for different mechanisms, or in performing standard routines more times. That is why a design algorithm for the simpler mechanism with two working points (Fig. 1) is described first, and second, some special alterations for the design of the next mechanism, with three working elements (Fig. 2), are explained later. Note that almost all formulae used in the design are not shown here due to the limited scope of the paper.

3.1. Mechanism with Two Working Points

The input data to design the mechanism of Fig. 1 are two pairs of Cartesian coordinates, located arbitrarily, for the two working points in the plane. The synthesis algorithm includes the following steps:

Step 3.1.1. It is necessary to match initial 1 and 2 and final 3 and 4 (Fig. 3) positions of working points one to the other. The need in this procedure is because each of the initial points 1 or 2 may be moved to the positions 3 or 4.

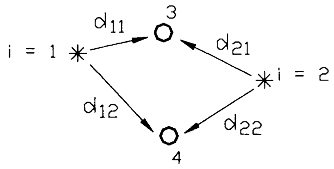

Figure 3. Matching initial (asterisks) and final (circles) positions of working points

This stage of the design can be performed using a computer program, by means of calculations based on a criterion of the proximity of matching points. This index, being calculated for two possible combinations of points, allows the choice of the one that ensures minimum motion of the mechanism, when moving from one configuration to another.

Step 3.1.2. Determination of minimum link lengths of the gripper movable contour. It may be assumed that link lengths of the movable contour are equal; that is, the contour represents a rhombus. This ensures first, the simplification of the design procedure and second, the standardization of gripper parts for their manufacturing. Based on this assumption, a parameter γ is introduced which represents a minimum angle between contour links when they are in a closed state. This angle need not be zero to avoid singular configurations, including dead positions of the mechanism. Then, if the length of contour link is L, its minimum value can be calculated by means of the following expression: $L = d_{imax} / 2cos(\gamma/2)$, $i = 1,2$, where d_{imax} is the maximum distance between pairs of working points for initial and final positions of the gripper found in the previous step.

Step 3.1.3. It is possible now to determine coordinates of all points of the movable contour for each of the two configurations considered. Specifically, the coordinates of points C and D (Fig. 1), for initial and final positions of the gripper have to be calculated now. When determining positions of contour points, a corresponding subroutine in fact solves kinematics of dyads (for instance, AD and DB, Fig. 1) and it is known that these kinematics usually have two solutions. Therefore, using this procedure, several possible configurations of the mechanism are obtained. The designer (or the program) has then to choose configurations of the mechanism for two positions, which will be used in further calculations. For that, a special

Step 3.1.4 determines corresponding configurations of the mechanism. In the case of such a simple mechanism, the intention is to achieve a convex polygon, which is the rhombus.

Step 3.1.5. A center of rotation of the link BC (Fig. 1) can then be found. To that end, in a general case, its start (BC) and final ($B'C'$) positions should be considered and perpendiculars have to be projected from the middles of lines BB' and CC'. Their intersection point corresponds to the location of joint P. Assuming that point T

of the link *BC* (Fig. 1) is in the center, it is possible to determine two parameters of this link: the length *TP* and the angle δ between this part and the link *BC*.

It is necessary to note that the point *P* can be, in principle, determined for each of the contour links. Therefore, to minimize the overall mechanism dimensions, it is worth choosing a minimum |PT| value out of a possible four.

Step 3.1.6. Now, the most complicated stage of the design is performed when a driving unit of the gripper has to be incorporated. This stage allows different approaches to its solution.

First, in order to achieve mechanism simplification and minimum overall dimensions, it is preferable to assume that the joint *N* is located on a perpendicular projected from the middle of link *AD* (Fig. 1). In a particular case, the joint *N* may lay even on the link *AD* itself. Further, different types of input links may be used. For a general form of the mechanism, the input point *N* of the four-class group may be driven by means of either a link with a rotational joint (as it is shown in Fig. 1) or a sliding link which is moved on a guide of rectilinear or nonlinear shape.

When a sliding link is taken as the gripper input, the problem arises on how to obtain a profile of a program curve to move the input point from an initial to a final position. It is quite clear that the problem has many different solutions, but in some cases a straight line connecting these points can be taken as a program curve. However, such a solution is not optimal. Therefore, a straightforward way to an optimal solution of the problem is in introducing an additional criterion, in order to select the best trajectory. To solve this problem, it is necessary to calculate at least all the positions and angle coordinates of the mechanism; that is, to solve its forward kinematics. Besides, some force parameters may be needed (like pressure angles) to ensure smooth motion of the slider on the guide. However, the problem is that the solution of the forward kinematics for this kind of mechanisms is rather difficult. To avoid these complicated calculations, another approach has been used in our study, which considers inverse motion of the mechanism, when its input joint is in the point *P* (Fig. 1). Then, the problem is reduced to the solution of kinematics of the third-class group, which is much simpler. Its solution is rather well known and described, for instance, in [6]. In our study, a simplified numerical procedure was used, when an additional function of the change of the angle between links *BC* and *AC* was introduced. In particular, in our calculations, this angle change was specified as uniform. Then, coordinates of the points *B* and *C* were calculated for some of their discrete positions. In accordance with this, the angle between links *BC* and *AC* was also changed. Thus, a sequence of point *N* positions from the initial known position to the final one was calculated. These points were used to approximate a smooth curve.

The final **Step 3.1.7** allows the mechanism simulation by showing the designer the results of synthesis. The operator can introduce some corrections in the design process based on the simulation results.

3.2. Mechanism with Three Working Points

The input data to design the mechanism of Fig. 2 are two triple sets of coordinates of arbitrary positions of working elements *D, C* and *E*. Then, as previously, the first procedure finds which initial position a working point moves from, to which final one. In other words,

Step 3.2.1 is intended to match initial and final positions of working points. Here, the procedure is performed based on the criterion similar to that of **Step 3.1.1**.

Step 3.2.2. Determination of minimum link lengths of the gripper movable contour. With the same assumption, as previously, that link lengths of the mechanism movable contour are equal, link length calculations are based here on the consideration of maximum distances between working positions. Thus, link lengths are found similarly to the procedure of **Step 3.1.2**.

Step 3.2.3. As for the previous mechanism, the mechanism under discussion is designed by means of a corresponding subroutine to solve kinematics of dyads (like *CM, ME* and *RE, RD* - Fig. 2). Solutions for several possible configurations of the mechanism; that is gripper assemblies, are then obtained.

Step 3.2.4 is used to define the contour configuration. When doing this, an important point follows.

It is clear that in certain cases of working point positions, the mechanism in motion may reach its singular configurations. In most cases, the problem can be solved by choosing the movable contour configuration as a convex polygon (as it was done for the first mechanism). For this, special procedures are required. They consist of determining a middle point of the contour and then choosing those configurations of dyads that are most removed from the middle point. This approach is workable for the majority of possible contour configurations. However, in some special cases supplemental actions have to be performed. An example of this situation is when all the working points are located in a straight line. Then, the above procedure does not work and some additional rules are required. However, to avoid software complexity, in the computer program, a link was used in this situation to the interactive mode, where the designer could choose preferable positions of dyads.

Step 3.2.5. The problem solved here is to find contour points that are passively connected to the base. Note again that such a point may be, in principle, determined for each of the contour links. Therefore, to maintain minimum overall dimensions, it is worth choosing minimum radii connecting these links to the base.

Step 3.2.6. Now gripper drive selection is made. The approach based on the use of inverse motion described in **Step 3.1.6** could be applied. However, the feature here is that there are two passive joints (P_1 and P_2 - Fig. 2) connected to the base and one of them is supposed to be an input link in inverse motion. It forms a four-bar mechanism, all positions of which can be determined. After that, the problem is reduced again, like in **Step 3.1.6**, to the determination of motion of a dyad between joints *C* and *D* (Fig. 2), including the input point *N*, which is connected to the base by a corresponding kinematic chain. This last group is of the third class and its motion analysis can be performed according to the approach stated in **Step 3.1.6**.

Step 3.2.7. Final stage of the designed mechanism simulation and verification of the solution.

4. IMPLEMENTATION

The computer program implementing the above-presented algorithm includes a main program presenting a menu to the designer where one of the two mechanisms considered may be chosen (according to the number of working points). Subsequently, one of two secondary subprograms is then run. The designer is asked to introduce into the subprogram required coordinates of working points and then continues interactively with the computer. The program is structured so that both subprograms use the same routines to calculate mechanism parameters.

The second of the two mechanisms presented, namely, with three working points, has been built. The program trajectory in this prototype is chosen as a straight line. In the driving unit, a DC motor is attached to a feed screw that is connected, in turn, to a nut rigidly attached to a pin. When the motor turns the feed screw, the pin (guided in a slot) pushes (or pulls - depending on the motion direction) the input point. The slot is located in a program plate, which is used also as a mechanism base.

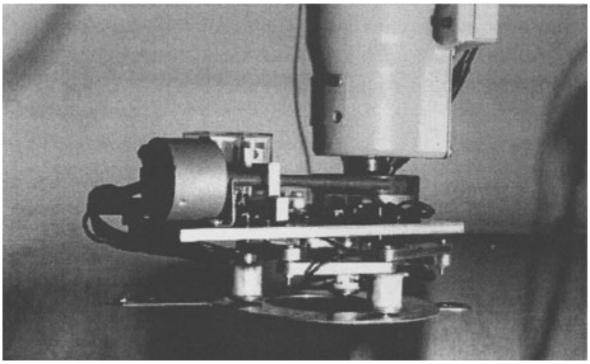

Figure 4. A view of the gripper mechanism with a driving unit

The control unit includes limit switches, placed on extreme ends of the program plate slot, and relays that change the sign of voltage supplied to the DC motor. Its operation is based on the limit switch signals, which are produced when the pin reaches its extreme positions. The gripper testing was performed while attached to a KAREL A-300 industrial robot (Fig. 4). All voltages used in the gripper control unit are taken from the robot control cabinet.

For gripper testing, a simple assembly operation was designed and implemented: two flat parts with different profiles were placed in corresponding magazines located in different positions within the robot workspace. The task was to take each part in turn and place it within two vertical beams used as guides. So, to take each part, the robot had to change electromagnet gripper element positions. The tests showed that the gripper works effectively and allows fast repositioning of working elements.

5. CONCLUSION

The presented approach to building programmable gripper can serve as a basis for developing grippers not only to clutch flat parts, but also those with parallel surfaces. Moreover, grippers for more complicated types of surfaces can be designed through changes in devices.

Proposed techniques allow different kinds of construction improvements. For example, the program plate can be interchangeable, so program trajectories may be changed as required. Optionally, the inverse motion approach used in Steps **3.1.6** and **3.2.6** can be implemented in actual devices.

There are ways to further improve device performance by developing methods of their synthesis. For instance, it is practical in industrial applications to develop the presented approach to create grippers with an increased number of clutching elements and with more, than the two, working positions of clutching elements, used in this study. The latter is theoretically attractive since it requires further development of the synthesis methods presented here. It is also important in different industrial applications of the presented grippers, because their use can be more universal.

Novatronics Inc., Stratford, Canada

6. REFERENCES

1. Fan Yu Chen. Gripping mechanisms for industrial robots. *Mechanism and Machine Theory* 1982; 17: 299-311.
2. Kolluru R, Valavanis KP, Stewart A, Sonnier MJ. A flat surface robotic gripper for handling limp materials. *IEEE Robotics & Automation Magazine* 1995; 2: 19-26.
3. Simada Y, Kadovaki K., Murata H., Teruo I. Robot gripper. *Japan Patent Application* 1984; No. 59 - 97886.
4. Djoldasbekov UA, Slutski LI, Baigunchekov JJ. Manipulation devices based on high-class mechanisms. In: *Theory and Practice of Robots and Manipulators, Proceedings of RoManSy'84, 5-th CISM-IFToMM Simposium*; 1985; Udine, Italy.
5. Merlet J-P. Direct kinematics of planar parallel manipulators. *Proceedings of the IEEE International Conference on Robotics and Automation*; Minneapolis, Minnesota, 1996.

J.P. DE VAUJANY, M. GUINGAND and D. PLAY

Laboratoire CASM - INSA de Lyon
20 av. Albert Einstein
69621 Villeurbanne Cedex
Phone: 33 4 72 43 85 46 - Fax: 33 4 72 43 63 86

INTERACTION OF GEAR EPICYCLIC PLANETS AND THE EFFECT OF WEB FOR INTERNAL GEARS

Abstract. In aeronautics, internal gears have small rim thicknesses, howeverthough these rims are subjected to considerable deformation. Stresses in tooth roots appear outside meshing zones. The study presented in this paper deals with possible interactions between planets. The increase of stresses localized between two meshing planets is quantified by using a numerical model (Finite Prism Method). Furthermore, the influence of web position on the distribution of contact pressure is examined. For a spur gear, the presence of a web displaces the tooth contact zone. Peaks of pressure appear at the edge of the tooth. Web position can be determined in relation with the misalignments and, with a stiffer structure, a uniform contact pressure distribution can be obtained along the width of the tooth.

1. INTRODUCTION

When designing gearboxes for helicopter power transmissions, one of the constraints that must be taken into account is the need to reduce the weight of mechanical elements. Consequently, the ring thickness of planet gears is small, which in turn leads to considerable deformation of the structure. It is possible to use these deformations in the gear meshing zone to even the distribution of efforts between the planets of a planetary train. However, they lead to considerable stresses in tooth roots. It has been shown that for small rim thicknesses, the increase of stresses is considerable in tooth roots even when far from the meshing zone [1, 2, 4, 6]. It is therefore necessary to study the interaction of meshing between different planets. In parallel, the influence of the position of a web placed on the rim was analyzed. This numerical study was performed in order to calculate contact pressure distributions as a function of axis misalignments.

2. NUMERICAL MODEL

A numerical model for simulating quasi-static behavior of internal gears was developed [3, 7]. This model facilitates the design of planetary gears supported by webs. It takes into account tooth geometry, the general geometry of the gear, the

P. Chedmail et al. (eds.), Integrated Design and Manufacturing in Mechanical Engineering, 373-380.
©2002 *Kluwer Academic Publishers.*

assembly and the relative position of elements. In particular it calculates the load sharing between the teeth in contact, stresses in tooth roots and meshing stiffness. Tooth deflection and surface deformations (Boussinesq's theory) are considered. Models are much used in design offices, thus computation times and computer memory have been optimized by integrating the Finite Prism Method [7], derived from the Finite Element Method [3, 5]. The principle consists in making mechanical and geometrical conversions of an entity in 3D into an equivalent 2D problem (transversal section of the prism). After resolution, 3D displacement, stress and results are obtained. Tooth meshing is simulated in the transversal plane for a toothed sector with at least 5 teeth. Tooth meshing is defined in 2D by using eight node quadrilateral elements (Fig. 1). This meshing is done automatically by the CATIA software.

The model uses different steps to simulate the behavior of an epicyclic gear internal ring for several kinematic positions in the line of action:
- definition of the profile of teeth for the pinion and the toothed ring,
- kinematics simulation,
- study of elastic bending and contact behavior,
- calculation of load sharing and instantaneous contact pressures,
- calculation of loaded transmission error and 3D stresses in tooth roots.

3. INTERACTION BETWEEN TWO GEAR PLANETS

3.1. Load sharing

Loads applied by the pinion on the ring can lead to deformation of the entire toothed sector. It has been shown that these deformations occur for a rim thickness less than 5 times the pitch module [4]. Thus, if the angle between two planets is less than that which separates two fixing points of the rim, the deformations of the structure interact with each other during gear meshing. In the example processed, each planet applies an input torque of 481 N.m. The model of the ring is defined by a sector of 19 teeth (angle of approximately 131,5°). The geometrical characteristics of the gear are presented in table 1. Figure 1 shows the position of two meshing planets. The two planets are considered in phase for this kinematic position and each of them has two couples of teeth in contact.

Table 1. Gear characteristics

	Pinion	Gear
Number of the teeth	16	52
Pitch module: m (mm)	4	4
Pressure angle (°)	20	20
Face width (mm)	45	45
Rim thickness (mm)	5*m	2*m

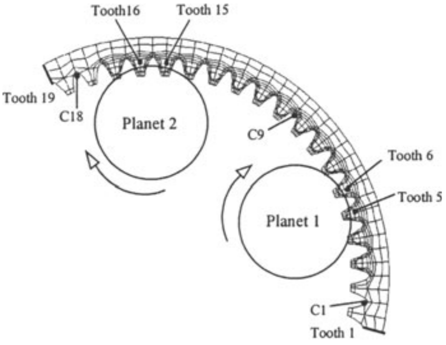

Figure 1. Definition of roots, teeth and two planets.

Initially, the meshing of each planet is studied separately. The analysis is carried out to determine the load sharing between the couple of teeth in contact and the distribution of stresses in the tooth roots. Afterwards, computation is carried out by taking into account the two meshings simultaneously. Table 2 presents loads calculated for the three cases studied. Load sharing is slightly influenced by the proximity of two meshings for most loaded teeth (teeth nos. 6 and 16). The gap between efforts calculated with one and two planets is considerable only for teeth nos. 5 and 15, which are less loaded.

Table 2. Loads on the teeth in contact

	Condition of the meshing			
	Planet 1	Planet 2	Planet 1 and 2	ratio %
tooth 5 (N)	139	-	215	55
tooth 6 (N)	1461	-	1385	-5
tooth15 (N)	-	407	469	15
tooth16 (N)	-	1192	1130	-5

3.2. Stresses in tooth roots

Figures 2 and 3 present deformations of the external circle of the ring for cases with one (pinion 1) and two planets respectively. The figures permit visualization of ring displacement with comparison to its initial position. The meshing of pinion 2 limits rim deformation in the area of its meshing and thus decreases the effect of rotation of the deformed line due to pinion 1. For the section near the meshing of planet 1, the deformation is very similar whatever the number of planets participating in the meshing.

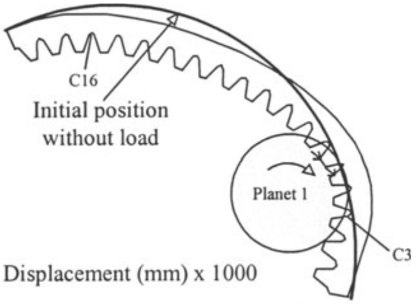
C16
Initial position without load
Planet 1
C3
Displacement (mm) x 1000

Figure 2. Deformation with one planet.

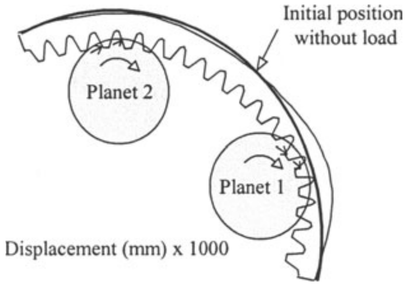
Initial position without load
Planet 2
Planet 1
Displacement (mm) x 1000

Figure 3. Deformation with two planets.

Figures 4, 5 and 6 show the distribution of stresses for 14 roots C3 to C16 defined in figure 1. Figures 4 and 5 illustrate the case of a single planet (1 or 2). In figure 6, the two pinions participate in the meshing with the ring.

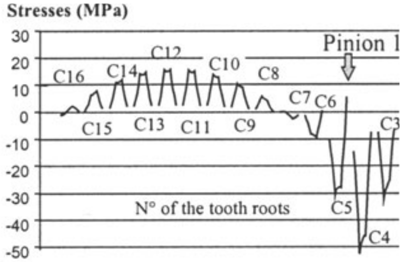

Figure 4. Stresses with one planet (pinion 1).

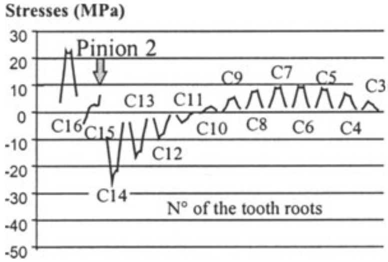

Figure 5. Stresses with one planet (pinion 2).

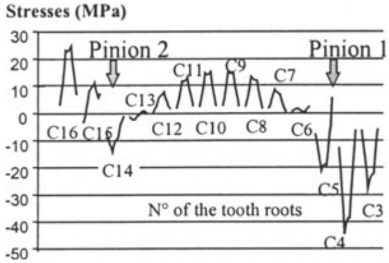

Figure 6. Stresses in the tooth roots with two planets together.

For meshing with planet 1 (Fig. 4), the deformation of the rim limits tensile stress in roots 5 and 6 due to the loadings of the 2 teeth. On the other hand, compressive stresses are much higher (Fig. 4: $\sigma_c = -50$ MPa in root 4) than those obtained in the case of the meshing of planet 2 (Fig. 5: $\sigma_c = -25$ MPa in root 14). The roots far from the loaded teeth located before and after the meshing zone are subjected to tensile stress. Thus, when the two planets are close to each other, tensile stresses are superposed and consequently stress increased (cases of roots 8, 9 and 10 in figure 6). On the contrary, for the roots subjected to compressive stress (Fig. 4: roots 3 to 6 and Fig. 5: roots 11 to 14), the stress values decrease during the interaction of the two planets (12% for the maximal compressive stress in root 4 and 40% in root 14). Elsewhere, for the intermediate roots (roots 6, 7, 11 and 12), the stresses become positive due to the effect of rim deformation.

4. EFFECT OF WEB POSITION

The previous study shows that it is not possible to analyze the meshing zone alone. When designing a product, it is necessary to consider the mode defined for clamping the gear. In the gearboxes of helicopter transmissions, internal toothed rings are fixed via webs that connect the rim to the casing. Standard calculation methods do not take into account the location and the dimension of these webs. A preliminary study [5] identified and quantified the influence of the web on the distribution of stresses in tooth roots and contact pressures on active tooth flanks. This study shows that the geometry of the web limits the effects of axis misalignment for the spur gear.

4.1 Contact pressure

In order to visualize the effect of a web on distributions of contact pressure, three types of web setting (Fig. 7) are studied for the internal spur gear. Geometrical characteristics are presented in Table 3. Only the ring has a web while the edges of the rim and the pinion are fixed. The driving torque is equal to 100 daN.m for all the calculations.

Table 3. Gear characteristics

	Pinion	Ring
Number of the teeth	51	195
Pitch module (mm)	2.53	2.53
Pressure angle (°)	20	20
Face width (mm)	58	58

After the kinematics simulation and the analysis of elastic behavior, the contact pressures on the flanks of the teeth are calculated. With 9 positions during the meshing period, the pressure distribution is presented in Figure 8 for kinematics position 4 and for the three types of web: web centered over the rim (a), on the edge (b), and web on one side in extension from the rim (c). Only the contact pressure on the couple of tooth 4 is indicated but in this position, tooth 3 also participates in the meshing. In all cases, the maximal pressure is situated exactly at the location of the web along the width of the tooth. With a centered web (a), few differences appear between the maximal value and the pressures distributed over the rest of the contact zone. On the other hand, for the web of type (b), a significant pressure peak is obtained on the side of the tooth (80% difference in comparison to the other side). As for the position of the web (c), the value of the maximal pressure (484 N/mm²) is situated between those of the two other cases (a) and (b) (420 and 528 N/mm²).

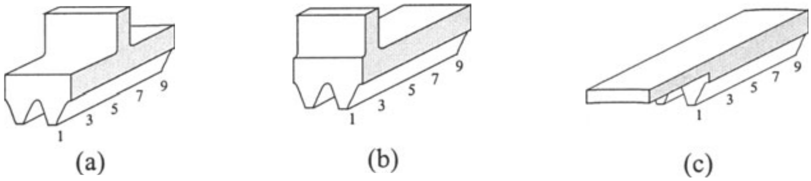

Figure 7. Position of the web on the ring.

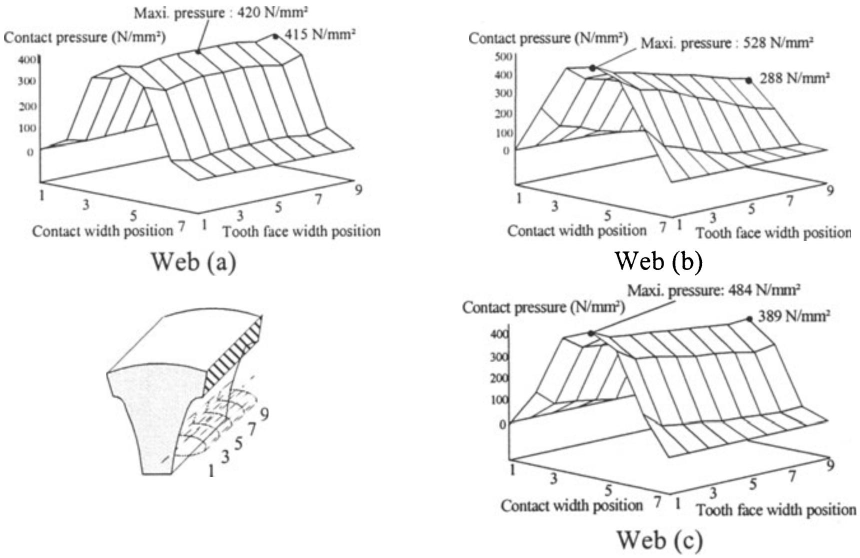

Figure 8. Distribution of the contact pressure on a tooth.

Distributions of stresses in the tooth root were also studied, though they are not presented in this text. However, the same distribution as those of the contact pressures is obtained. Obviously, this can be explained by the fact that the stress in a root is directly linked to pressure distribution. Nonetheless, in the area of tooth roots close to the intersection between the web and the rim, the stresses also depend on the thickness of the rim. Thus for the web (b), the maximal stress located at the level of the web is three times higher than that calculated on the other side. This value (300 N/mm²) is 50% higher than those obtained for the other cases (a) and (c) (approximately 200 N/mm²).

4.2 Misalignments

The study of the distribution of contact pressures and stresses in tooth roots shows that the position of the web (b) permits obtaining a structure that is stiffer on one side of the tooth than on the other. The displacement of contact pressures on one side of the tooth can help to offset certain faults. The inclination is almost neglected. However, it has been shown [3, 4] that inclination has an influence in the case of deviation. Taking into account the most unfavorable coupling misalignment case (deviation and inclination) (Fig. 9), distributions of contact pressure were calculated with a model of type (b) (Fig. 7). They are presented in Figure 10 on the flank of tooth 4, and for the case of a ring without a web but with fixing around the entire rim.

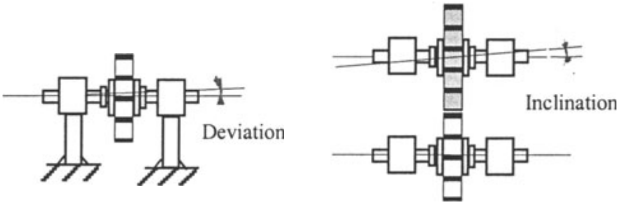

Figure 9. Definition of misalignments.

Deviation and inclination angles of one minute each were applied to obtain comparisons with the initial position of the pinion. The maximal value of the pressure obtained was always located at the web position, but the difference between the two sides is only 16%. When comparing this result to the case without a web, the contact zone is not wholly located on one side of the tooth and more uniform distribution is obtained with the side web. The influence of the position of the web therefore compensates the effects of misalignment. For wider misalignment angles, it is thus possible to couple the influence of the web and a crown along the width of tooth.

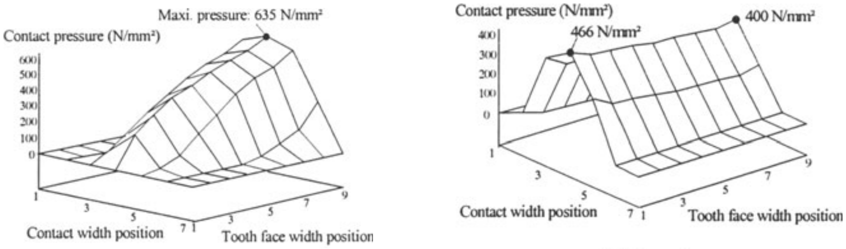

Without web   *With web*

Figure 10. Distribution of the contact pressure with misalignments: Deviation (1') and inclination (1').

5. CONCLUSION

Decreasing the rim thickness of the ring leads to significant deformations. The numerical model developed permits quantifying the interaction of the two meshing planets. Load sharing between teeth in contact is influenced less. On the other hand, stresses in the tooth roots are modified. Regarding the example processed, tensile stresses increase in the roots far from the teeth in contact. Compressive stresses decrease (40%) in the presence of the two planets. The web used to fix the gear on the casing modifies the distribution of contact pressure. It is therefore shown that the web offsets faults in the case of misalignment. Indeed, peaks of pressure on the side of the tooth are eliminated and more uniform distribution is obtained.

Acknowledgments: The initial research program was financed by the EUROCOPTER France Company.

References

1. Chong, T.H. and Kubo, A., Simple stress formulae for a thin-rimmed spur gear. Part 3, Journal of Mechanisms, Transmissions and Automation in Design, Transactions of the ASME, Sept. 1985, Vol. 107, 418-423.
2. Chong, T.H., Suzuki, T., Aida, T. Et Fujio, H., Bending stresses of internal spur gear, Bulletin of the JSME, April 1982, Vol.25, N°202, 679-686.
3. De Vaujany J.P., Comportement d'engrenage cylindrique intérieur. Effets de jante et de voile, 1996, INSA de Lyon, N°96 ISAL 0128, 178 p.
4. De Vaujany, J.P., Kim, H.C., Guingand, M. et Play, D, Effect of Rim and Web on Stresses of Internal Cylindrical Gears, 7th International Power Transmission and Gearing Conference, ASME, San Diego, Calif., Oct. 1996, p. 73-80.
5. Kim, H.C., De Vaujany, J.P., Guingand, M. et Play, D. Stress analysis of cylindrical webbed gears. Parametric study, Journal of Mechanical Design, ASME, Juin 1998, Vol.120, 349-357.
6. Oda, S., Miyachika, K. and Sayama, T., Effects of rim and web thicknesses on bending fatigue strength of internal gear, Bulletin of JSME, Feb. 1986, Vol. 29, N° 248, 586-592.
7. Olakorede, A.A., Répartition de charges et résistance en conception d'engrenages cylindriques - Application de la Méthode des Prismes Finis en CAO, 1990, INSA de Lyon, N°90 ISAL 0049.

Svetlana OSTROVSKAYA, Jorge ANGELES

KINEMATICS OF ROBOTS WITH ROLLER-CONSTRAINED BALL-WHEELS

Abstract. We report on the kinematics of wheeled mobile robots (WMR) with ball-wheels, and highlight their functional properties. To meet the fundamental requirements for the functioning of ball-wheels, the translational form-closure should be imposed on each ball to capture the ball without relying upon the ground. A set of symmetrical configurations of contact points is proposed. The relation between the twist of the platform of the WMR and the independent joint rates is obtained.

1. INTRODUCTION

Wheeled mobile robots (WMR) equipped with conventional wheels are classical examples of nonholonomic systems. They have a lower number of independent velocities (mobility) than the number of positional degrees of freedom (dof) [1]. This means that, being able to reach an arbitrary position and orientation on the plane (three dof), WMRs cannot have arbitrary angular and translational velocities simultaneously (a mobility of two). As a result, the real-time control of WMR entails many theoretical and practical problems [2], [3]. Moreover, the nonholonomy of WMRs with conventional wheels causes complexities in trajectory planning and in the design of control algorithms, making standard planning and control algorithms developed for robotic manipulators inapplicable. To deal with these problems, WMRs with a mobility of three, called omnidirectional mobile robots, or full-mobility robots, have been developed. Full mobility is achieved by equipping the WMR with different kinds of wheels: offset-steered driving wheels; omnidirectional wheels; spherical wheels; etc.

The most maneuverable wheel is a ball which possesses three dof without slip” [4]. The ball-wheel omnidirectional mechanism consists of a spherical tire supported by rollers [1, 5]. The WMR equipped with such wheels possesses three dof without slip and provides a smooth motion with constant Jacobian, and hence, without singularities [6].

A detailed analysis of WMRs with the different aforementioned wheels was reported in [4]. WMRs with conventional and omnidirectional wheels were analyzed in [2] but without considering ball-wheels. The most recent overview analysis of the development and classification of different kinds of wheeled mobile robots can be found in [7].

P. Chedmail et al. (eds.), Integrated Design and Manufacturing in Mechanical Engineering, 381-390.
©2002 *Kluwer Academic Publishers.*

In this paper we discuss the kinematics of WMRs with ball-wheels in roller-type bearings, and highlight their properties.

2. KINEMATICS OF ROLLER-CONSTRAINED BALL-WHEELS

We introduce a velocity-level analysis which is needed in the dynamics analysis.

2.1. General Considerations

We assume that the WMR is a mechanical system composed of rigid bodies connected by ideal joints, which operates on a regular horizontal surface, free of obstacles. In this work we deal with WMRs equipped with ball-wheels, driven by identical rollers. We also assume that the wheel-ground and wheel-roller contacts are point contacts, and that the translational friction at such contacts is large enough to prevent slippage.

Arrays of ball-wheels must satisfy two fundamental requirements for functioning [6]:

1. Each ball-wheel must be free to rotate with respect to the platform without sliding; and

2. The ball centre should be fixed with respect to the platform.

To meet these requirements, the translational form-closure should be imposed on the balls [6, 8]. Translational form-closure means that the ball centre is fixed to the platform without imposing any constraint on rotation of the ball. This form-closure may be provided by ball contacts with the wheel mechanism and with the ground. The ball-ground contact is not reliable and can be broken any time during the platform motion. Therefore, the ball mechanism should be able to capture the ball without relying upon the ground.

A single ball rolling on a surface without sliding has a mobility of three. Since “a minimum of seven contacts are needed to fix a body in space” [8], the number of contacts needed for a translational form-closure for a ball is $7 - 3 = 4$. On the other hand, from a geometric point of view, the general equation of the sphere contains four arbitrary constants; therefore, the sphere should satisfy four specific independent conditions. Moreover, to guarantee form-closure, the four contact points must not lie within a single hemisphere of the ball, including its boundary, so that there will be always at least one contact point on an arbitrary hemisphere of the ball.

The configuration of a WMR platform can be described by a three-dimensional array of generalized coordinates, corresponding to the three dof (two for position and one for orientation), which can be chosen as $\mathbf{q} \equiv \begin{bmatrix} \mathbf{c}^T & \psi \end{bmatrix}^T$ where $\mathbf{c}$ is the 2-dimensional position vector of the platform centre of mass, while ψ is the angle of the platform orientation with respect to a reference frame. Then, the twist $\mathbf{t}$ of this platform can be expressed as: $\mathbf{t} = \begin{bmatrix} \dot{\mathbf{c}}^T & \dot{\psi} \end{bmatrix}^T$. Needless to say, if the WMR is composed of several bodies, it has more dof than the platform itself and, therefore, needs additional generalized coordinates to describe its configuration.

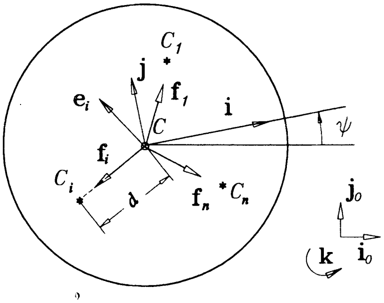

Figure 1: Unit vectors for the ith ball-wheel.

If the layout of the platform of a WMR with s wheels is symmetric with respect to its mass center C, then (Fig. 1)

$$\sum_{i=1}^{s} \mathbf{e}_i = 0 \ , \quad \sum_{i=1}^{s} \mathbf{f}_i = 0 \tag{1}$$

where $\mathbf{e}_i$ and $\mathbf{f}_i$ are unit vectors of a frame fixed to the platform with the origin at the platform centre of mass and with $\mathbf{f}_i$ oriented toward the centre of the ith wheel. Moreover, if $\mathbf{c}_i$ is the position vector of the centre C_i of the ith wheel in the reference frame, while d is the common horizontal distance between the mass centre C of the platform and that of the wheel, then

$$\mathbf{c}_i = \mathbf{c} + \mathbf{f}_i d \ , \quad i = 1, \ \dots \ , s \ . \tag{2}$$

Upon differentiation of both sides of eq.(2) with respect to time, we have

$$\dot{\mathbf{c}}_i = \dot{\mathbf{c}} - \dot{\psi}\mathbf{e}_i d \ . \tag{3}$$

From eq.(3), using eq.(1), we derive the kinematic relations which hold if the wheel layout is symmetric with respect to the centre of the WMR platform, namely,

$$\dot{\mathbf{c}} = \frac{1}{s}\sum_{i=1}^{s} \dot{\mathbf{c}}_i \ , \quad \dot{\psi} = -\frac{1}{sd}\sum_{i=1}^{s} \mathbf{e}_i^T \dot{\mathbf{c}}_i \ . \tag{4}$$

2.2. Actuation Scheme

It is clear that the platform, as a rigid body under planar motion, has a mobility of three; each single ball has also a mobility of three but, being fixed to the platform by the translational form-closure, each ball is subjected to two kinematic constraints (3). Then, the mechanical system of the platform with s ball-wheels, fixed to this platform by the translational form-closure, has a mobility of $3 + 3s - 2s = 3 + s$ and should be driven by $3 + s$ actuators.

The velocity of the ball centre of the ith wheel is

$$\dot{\mathbf{c}}_i = \boldsymbol{\omega}_i \times (R\mathbf{k}) = R\boldsymbol{\omega}_i \times \mathbf{k} \tag{5}$$

where $\boldsymbol{\omega}_i$ is the ith ball angular velocity: $\boldsymbol{\omega}_i = \begin{bmatrix} u_i & v_i & w_i \end{bmatrix}^T$. Now, if we note that $\boldsymbol{\omega}_i \times \mathbf{k} = \begin{bmatrix} v_i & -u_i & 0 \end{bmatrix}^T$, we can rewrite eq.(5) in 2-dimensional form:

$$\dot{\mathbf{c}}_i = -R\mathbf{E}\mathbf{w}_i = R\mathbf{E}^T\mathbf{w}_i \tag{6}$$

where we have introduced the notation

$$\mathbf{E} \equiv \begin{bmatrix} 0 & -1 \\ 1 & 0 \end{bmatrix}, \quad \mathbf{w}_i \equiv \begin{bmatrix} u_i \\ v_i \end{bmatrix}. \tag{7}$$

Then, eq.(3) can be written in the form

$$R\mathbf{E}^T\mathbf{w}_i = \dot{\mathbf{c}} - \dot{\psi}\mathbf{e}_i d .$$

It is clear from eqs.(6) and (7) that one component of the angular velocity vector $\boldsymbol{\omega}_i$, namely, w_i, which is normal to the ground, is not constrained; therefore, the platform motion does not depend on this component, and vice versa. Hence, w_i $(i = 1, 2, 3)$ can have arbitrary values regardless of the platform motion. Actuation or constraint of this component of the wheel angular velocity is left to the discretion of the designer. For example, the ball motion can be controlled in such a way as to maintain a certain desired (zero or non-zero) magnitude of w_i. Therefore, s of the $3 + s$ actuators should be employed to control w_i, for $i = 1, \cdots, s$, leaving us with three actuators needed to define the WMR platform motion.

Two possibilities to connect the last three actuators to the wheels arise: (i) one actuator per each of three wheels or (ii) two actuators for one wheel and one actuator for one more wheel. This means that the number of non-redundant driving wheels for a platform undergoing a planar motion is three (i) or two (ii), while the total number of wheels can be arbitrary. For symmetry, we can recommend connecting one actuator to each of the three driving wheels to define the twist $\mathbf{t}$ of the platform and choosing the number of ball-wheels equal to three or multiples of three.

2.3. Optimum Location of the Rollers

2.3.1. Velocity Analysis of Roller-Constrained Ball-Wheels

Let a roller be mounted on a roller-carrier as shown in Fig. 2. The ith roller-carrier can rotate with respect to the platform about an axis parallel to the

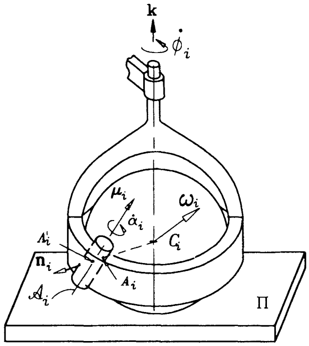

Figure 2: Ball-wheel with a roller fixed to the roller-carrier

unit vector $\mathbf{k}$ (normal to the ground) and passing through the centre C_i of the ith ball (Fig. 2). Let A_i be the contact point between the ball and the roller whose axis of rotation, $\mathcal{A}_i$, is parallel to the unit vector $\boldsymbol{\mu}_i$, with R being the radius of the ball and r the radius of the roller. Let $\dot{\phi}_i\mathbf{k}$ be the angular velocity of the roller-carrier (Fig. 2) and $\mathbf{a}_i$, $\mathbf{a}_i'$ denote the position vectors of points A_i and A_i', where A_i' is a point of the roller-carrier which coincides with the centre of the roller. Hence, the velocity of point A_i' is

$$\dot{\mathbf{a}}_i' = \dot{\mathbf{c}}_i + \dot{\phi}_i\mathbf{k} \times (\mathbf{a}_i' - \mathbf{c}_i) \ . \tag{8}$$

Besides, the velocity of the contact point A_i on the roller is

$$\dot{\mathbf{a}}_i = \dot{\mathbf{a}}_i' + \dot{\alpha}_i\boldsymbol{\mu}_i \times (\mathbf{a}_i - \mathbf{a}_i') \ , \tag{9}$$

where $\dot{\alpha}_i$ is the angular velocity of the roller rotation around its axis. Substituting eq.(8) into eq.(9), we obtain

$$\dot{\mathbf{a}}_i = \dot{\mathbf{c}}_i + \dot{\phi}_i\mathbf{k} \times (\mathbf{a}_i' - \mathbf{c}_i) + \dot{\alpha}_i\boldsymbol{\mu}_i \times (\mathbf{a}_i - \mathbf{a}_i') \ . \tag{10}$$

Let $\mathbf{n}_i$ denote the unit vector normal to the sphere at point A_i, pointing outwards. Then,

$$\mathbf{a}_i' - \mathbf{c}_i = (R + r)\mathbf{n}_i \ , \quad \mathbf{a}_i - \mathbf{a}_i' = -r\mathbf{n}_i \tag{11}$$

and eq.(10) can be written in the form:

$$\dot{\mathbf{a}}_i = \dot{\mathbf{c}}_i + \dot{\phi}_i(R + r)\mathbf{k} \times \mathbf{n}_i - \dot{\alpha}_i r\boldsymbol{\mu}_i \times \mathbf{n}_i \ . \tag{12}$$

Moreover, we have

$$\dot{\mathbf{a}}_i - \dot{\mathbf{c}}_i = \boldsymbol{\omega}_i \times R\mathbf{n}_i \ . \tag{13}$$

Substituting eq.(13) into eq.(12), we derive

$$R\boldsymbol{\omega}_i \times \mathbf{n}_i = \dot{\phi}_i(R + r)\mathbf{k} \times \mathbf{n}_i - \dot{\alpha}_i r\boldsymbol{\mu}_i \times \mathbf{n}_i \ . \tag{14}$$

By dot-multiplying eq.(14) with $\mathbf{k}$ we obtain, after simplification,

$$\dot{\alpha}_i = -\frac{R}{r}\frac{\mathbf{k}\times\mathbf{n}_i\cdot\boldsymbol{\omega}_i}{\mathbf{k}\times\mathbf{n}_i\cdot\boldsymbol{\mu}_i} . \tag{15}$$

For robustness, we must maximize $|\mathbf{k}\times\mathbf{n}_i\cdot\boldsymbol{\mu}_i|$. To this end, $\{\mathbf{n}_i, \boldsymbol{\mu}_i, \mathbf{k}\}$ must be an orthonormal triad, and hence, $\mathbf{k}\times\mathbf{n}_i\cdot\boldsymbol{\mu}_i = 1$. This means that we need $\mathbf{n}_i$, as well as $\boldsymbol{\mu}_i$, to lie in a plane perpendicular to $\mathbf{k}$ or parallel to the rolling plane. This is possible only if the location of the roller axis is chosen on the equatorial plane of the ball (Fig. 3). In this case, we obtain from eq.(15):

$$\dot{\alpha}_i = -\frac{R}{r}\boldsymbol{\mu}_i\cdot\boldsymbol{\omega}_i . \tag{16}$$

The vertical component w_i of the ball angular velocity $\boldsymbol{\omega}_i$ can be found by dot-multiplying eq.(14) by $\boldsymbol{\mu}_i$:

$$\dot{\phi}_i(R+r) = Rw_i$$

where, obviously, $w_i = \mathbf{k}\cdot\boldsymbol{\omega}_i$. Hence, we have

$$w_i = \frac{R+r}{R}\dot{\phi}_i .$$

We have thus shown that w_i, the vertical component of the angular velocity of the ball, is fully defined by the roller-carrier rotation. Hence, to define this component, the roller-carrier should be actuated. To define the remaining two components of $\boldsymbol{\omega}_i$, which determine $\dot{\mathbf{c}}_i$, the velocity of the centre of the wheel, a single ball-wheel should be driven by two rollers . Let the angular velocity of these rollers around their axes, of unit vectors $\boldsymbol{\mu}_i$ and $\boldsymbol{\nu}_i$, be $\dot{\alpha}_i$ and $\dot{\beta}_i$,

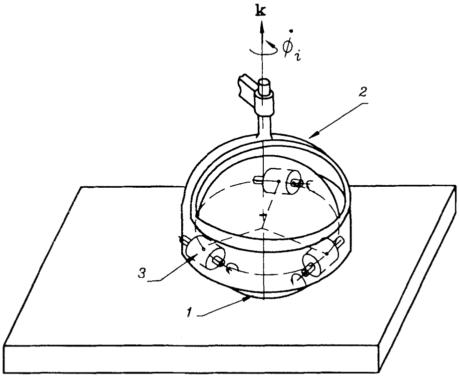

Figure 3: Ball-wheel with its rollers: 1, the ball; 2, the roller-carrier; 3, one roller

correspondingly. We assume henceforth that the axes of the rollers are located in a plane parallel to the ground. Hence, these unit vectors are considered *two-dimensional* from now on. Then, we write eqs.(16) for the two rollers in the form

$$\dot{\alpha} = \boldsymbol{\mu}_i \cdot \mathbf{w}_i \ , \quad \dot{\beta} = \boldsymbol{\nu}_i \cdot \mathbf{w}_i \tag{17}$$

The two components of $\boldsymbol{\omega}_i$ can now be expressed in terms of $\dot{\alpha}_i$ and $\dot{\beta}_i$:

$$\mathbf{w}_i = \begin{bmatrix} u_i \\ v_i \end{bmatrix} = \frac{r}{R\Delta_i}\mathbf{E}(\dot{\alpha}_i \boldsymbol{\nu}_i - \dot{\beta}_i \boldsymbol{\mu}_i) \tag{18}$$

where Δ_i is defined as $\Delta_i = \boldsymbol{\nu}_i^T \mathbf{E} \boldsymbol{\mu}_i$. Finally, we can write the ball angular velocity vector in the form:

$$\boldsymbol{\omega}_i = \frac{1}{R}\begin{bmatrix} \mathbf{E}(\dot{\alpha}_i \boldsymbol{\nu}_i - \dot{\beta}_i \boldsymbol{\mu}_i)(r/\Delta_i) \\ (R+r)\dot{\phi}_i \end{bmatrix} . \tag{19}$$

2.3.1. *Optimum Location of the Roller Bearings*

As discussed above, to meet the translational form-closure requirements for a ball, at least four rollers must contact the ball. Moreover, all points of contact between ball and rollers must not be contained within any single hemisphere and its boundary. Nevertheless, if three rollers are located in the equator, as shown in Fig. 3, the points of contact with these rollers are contained on the boundary of the corresponding hemispheres. Therefore, there must be another set of rollers located in such a way that there will be always at least one contact point on an arbitrary hemisphere of the ball, i.e., at least, one above and one below the equator. These roller axes must be fixed by revolute joints to a frame which is capable of rotating around an axis normal to the ground. The kinematic relations for these rollers should also obey eq.(14). After dot-multiplying eq.(14) by $\boldsymbol{\mu}_i$, we obtain

$$\{[\dot{\phi}_i(R+r)\mathbf{k} - R\boldsymbol{\omega}_i] \times \mathbf{n}_i\} \cdot \boldsymbol{\mu}_i = 0 \tag{20}$$

from which follows that vector $\boldsymbol{\mu}_i$, that defines the roller axis orientation, should be normal to $\mathbf{l}_i \equiv [\dot{\phi}_i(R+r)\mathbf{k} - R\boldsymbol{\omega}_i] \times \mathbf{n}_i$. On the other hand, $\boldsymbol{\mu}_i$ is normal to $\mathbf{n}_i$ itself. Therefore, $\boldsymbol{\mu}_i$ should be parallel to $\mathbf{l}_i \times \mathbf{n}_i$. Hence, to satisfy the non-slipping conditions we cannot have more than two contact points with supporting rollers in one horizontal non-equatorial plane (Fig. 4). But if the contact point between the ball and the roller lies in the equatorial plane of the ball, then $\mathbf{n}_i$ is horizontal. If the roller axis is also horizontal, then vector $\dot{\phi}_i(R+r)\mathbf{k} - R\boldsymbol{\omega}_i$ should be horizontal as well and $\mathbf{l}_i$ vertical. In this case any horizontal direction for $\boldsymbol{\mu}_i$ will satisfy eq.(20).

Then, to complete the form-closure for the ball, a set of symmetrical configurations of contact points is proposed in Fig. 5. In Case 1 we have seven rollers; in Case 2 we have six rollers (in both cases the ball is supported without

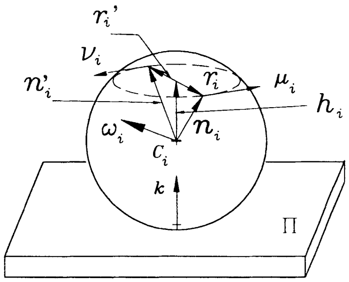

Figure 4: Contact points with supporting rollers

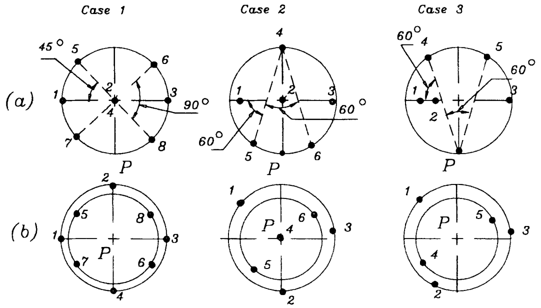

Figure 5: Cases of roller locations: (*a*) front view; (*b*) top view

relying upon ground contact). Case 3 requires only five rollers, but relies upon ground contact to support the ball-wheel.

2.3.2. Velocity Analysis of Roller-Constrained Ball-Wheels

From eqs.(6) and (18) we derive

$$\dot{\mathbf{c}}_i = R\mathbf{E}^T\mathbf{w}_i = \frac{r}{\Delta_i}(\dot{\alpha}_i\boldsymbol{\nu}_i - \dot{\beta}_i\boldsymbol{\mu}_i) \ . \tag{21}$$

Hence, using eqs,(4),

$$\mathbf{t} \equiv \begin{bmatrix} \dot{\mathbf{c}} \\ \dot{\psi} \end{bmatrix} = \frac{r}{3d}\sum_{i=1}^{3}\frac{1}{\Delta_i}\begin{bmatrix} d\mathbf{1} \\ -\mathbf{e}_i^T \end{bmatrix}\mathbf{u}$$

where $\mathbf{1}$ denotes the 2×2 identity matrix and $\mathbf{u}$ is the two-dimensional vector defined as $\mathbf{u} \equiv \dot{\alpha}_i\boldsymbol{\nu}_i - \dot{\beta}_i\boldsymbol{\mu}_i$. Let us now introduce the notation $\mathbf{M} \equiv \begin{bmatrix} \boldsymbol{\mu}_1 & \boldsymbol{\mu}_2 & \boldsymbol{\mu}_3 \end{bmatrix}$, $\mathbf{N} \equiv \begin{bmatrix} \boldsymbol{\nu}_1 & \boldsymbol{\nu}_2 & \boldsymbol{\nu}_3 \end{bmatrix}$, and

$$\boldsymbol{\mu}_e \equiv \begin{bmatrix} \mathbf{e}_1^T\boldsymbol{\mu}_1 \\ \mathbf{e}_2^T\boldsymbol{\mu}_2 \\ \mathbf{e}_3^T\boldsymbol{\mu}_3 \end{bmatrix}, \ \boldsymbol{\nu}_e \equiv \begin{bmatrix} \mathbf{e}_1^T\boldsymbol{\nu}_1 \\ \mathbf{e}_2^T\boldsymbol{\nu}_2 \\ \mathbf{e}_3^T\boldsymbol{\nu}_3 \end{bmatrix}, \ \dot{\boldsymbol{\xi}} \equiv \begin{bmatrix} \dot{\alpha} \\ \dot{\beta} \end{bmatrix},$$

where

$$\dot{\boldsymbol{\alpha}} \equiv \begin{bmatrix} \dot\alpha_1/\Delta_1 \\ \dot\alpha_2/\Delta_2 \\ \dot\alpha_3/\Delta_3 \end{bmatrix}, \quad \dot{\boldsymbol{\beta}} \equiv \begin{bmatrix} \dot\beta_1/\Delta_1 \\ \dot\beta_2/\Delta_2 \\ \dot\beta_3/\Delta_3 \end{bmatrix}.$$

Then we can express the twist of the platform in the form

$$\mathbf{t} = \frac{r}{3}\begin{bmatrix} \mathbf{N} & -\mathbf{M} \\ -\boldsymbol{\nu}_e^T/d & \boldsymbol{\mu}_e^T/d \end{bmatrix}\dot{\boldsymbol{\xi}}\,.$$

In case (i) we connect one actuator to one roller for each of the three wheels. Then, the angular velocity of only one of the rollers connected to each of three driving wheels is independent. Without loss of generality, we choose all $\dot\alpha_i$ independent, and hence, $\dot\beta_i$ can be expressed in terms of $\dot\alpha_i$ upon noticing that the wheels are fixed to the platform by translational form-closure. We can, therefore, write:

$$\mathbf{e}_i^T\dot{\mathbf{c}}_{i+1} = \mathbf{e}_i^T\dot{\mathbf{c}}_{i+2}, \qquad i = 1, 2, 3\,.$$

This forms a system of three equations linear in $\dot\alpha_i$ and $\dot\beta_i$ if we consider eqs.(21). Hence, we can express $\dot\beta_i$ in terms of $\dot\alpha_i$ in the form $\mathbf{D}_M\dot{\boldsymbol{\beta}} = \mathbf{D}_N\dot{\boldsymbol{\alpha}}$ where we have introduced the notation

$$\mathbf{D}_M \equiv \begin{bmatrix} -\mathbf{e}_2^T\boldsymbol{\mu}_1 & 0 & \mathbf{e}_2^T\boldsymbol{\mu}_3 \\ \mathbf{e}_3^T\boldsymbol{\mu}_1 & -\mathbf{e}_3^T\boldsymbol{\mu}_2 & 0 \\ 0 & \mathbf{e}_1^T\boldsymbol{\mu}_2 & -\mathbf{e}_1^T\boldsymbol{\mu}_3 \end{bmatrix}, \quad \mathbf{D}_N \equiv \begin{bmatrix} -\mathbf{e}_2^T\boldsymbol{\nu}_1 & 0 & \mathbf{e}_2^T\boldsymbol{\nu}_3 \\ \mathbf{e}_3^T\boldsymbol{\nu}_1 & -\mathbf{e}_3^T\boldsymbol{\nu}_2 & 0 \\ 0 & \mathbf{e}_1^T\boldsymbol{\nu}_2 & -\mathbf{e}_1^T\boldsymbol{\nu}_3 \end{bmatrix}.$$

Hence, $\dot{\boldsymbol{\beta}} = \mathbf{D}_M^{-1}\mathbf{D}_N\dot{\boldsymbol{\alpha}}$, where $\mathbf{D} \equiv \mathbf{D}_M^{-1}\mathbf{D}_N$, and

$$\dot{\boldsymbol{\xi}} \equiv \begin{bmatrix} \dot\xi_1 \\ \dot\xi_2 \\ \dot\xi_3 \end{bmatrix} = \begin{bmatrix} \dot{\boldsymbol{\alpha}} \\ \mathbf{D}\dot{\boldsymbol{\alpha}} \end{bmatrix} = \begin{bmatrix} \mathbf{1}_{3\times 3} \\ \mathbf{D} \end{bmatrix}\dot{\boldsymbol{\alpha}}$$

Then, we have

$$\mathbf{t} = \frac{r}{3}\begin{bmatrix} \mathbf{N} - \mathbf{M}\mathbf{D} \\ -\boldsymbol{\nu}_e/d + \boldsymbol{\mu}_e\mathbf{D}/d \end{bmatrix}\dot{\boldsymbol{\alpha}}\,.$$

To derive the inverse kinematic relations we note, from eq.(17), that we have $\dot{\boldsymbol{\alpha}}_i = \boldsymbol{\mu}_i^T\mathbf{w}_i$ and from eqs.(3) and (6),

$$\mathbf{w}_i = \frac{1}{R}\mathbf{E}\dot{\mathbf{c}}_i = \frac{1}{R}\mathbf{E}(\dot{\mathbf{c}} - \dot\psi\mathbf{e}_i d) = \frac{1}{R}\mathbf{E}\begin{bmatrix} \mathbf{1}_{2\times 2} & -\mathbf{e}_i d \end{bmatrix}\mathbf{t}\,.$$

We finally obtain

$$\dot\alpha_i = \frac{1}{R}\boldsymbol{\mu}_i^T\mathbf{E}\begin{bmatrix} \mathbf{1}_{2\times 2} & -\mathbf{e}_i d \end{bmatrix}\mathbf{t}\,, \quad i = 1, 2, 3$$

or using relation $\mathbf{E}\mathbf{e}_i = \mathbf{f}_i$

$$\dot{\boldsymbol{\alpha}} = \frac{1}{R}\begin{bmatrix} \boldsymbol{\mu}_1^T\mathbf{E}/\Delta_1 & -\boldsymbol{\mu}_1^T\mathbf{f}_1(d/\Delta_1) \\ \boldsymbol{\mu}_2^T\mathbf{E}/\Delta_2 & -\boldsymbol{\mu}_2^T\mathbf{f}_2(d/\Delta_2) \\ \boldsymbol{\mu}_3^T\mathbf{E}/\Delta_3 & -\boldsymbol{\mu}_3^T\mathbf{f}_3(d/\Delta_3) \end{bmatrix}\mathbf{t}$$

which are the inverse kinematic relations sought.

ACKNOWLEDGMENTS

Prof. Manfred Husty, Innsbruck University, is gratefully acknowledged for his help in deriving the optimum location of the roller bearings. The support of both Quebec's *Fonds pour la formation de chercheurs et l'aide à la recherche* and Canada's Natural Science and Engineering Research Council is duly acknowledged.

References

[1] S. Ostrovskaya and J. Angeles, "Nonholonomic systems revisited within the framework of analytical mechanics", *Applied Mechanics Reviews*, 1998; 51(7):415–433.

[2] G. Campion, G. Bastin, and B. D'Andréa-Novel, "Structural properties and classification of kinematic and dynamic models of wheeled mobile robots", *IEEE J. Robotics and Automation*, 1996; 12(1):47–62.

[3] G. Oriolo, S. Panzieri, and G. Ulivi, "An iterative learning controller for nonholonomic mobile robots", *The Int. J. Robotics Research*, 1998; 17(9):954–970.

[4] P. F. Muir and C. P. Neuman, "Kinematic modeling of wheeled mobile robots", *J. Robotic Systems*, 1987; 4(2):281–340.

[5] M. West and H. Asada, "Design and control of ball wheel omnidirectional vehicles", *Proc. IEEE Int. Conf. Robotics and Automation*, 1995; vol. 2, 1931–1938.

[6] M. West and H. Asada, "Design of ball wheel mechanisms for omnidirectional vehicles with full mobility and invariant kinematics", *ASME J. Mechanical Design*, 1997; 119(2):153–161.

[7] G. Dudek and M. Jenkin, *Computational Principles of Mobile Robotics*, Cambridge University Press, Cambridge, U.K, 2000.

[8] K. Lakshminarayana, "Mechanics of form closure", *ASME 78-DET-32*, 1978; 32:2–8. vol.

LEILA NOTASH AND JINGQIU ZHANG

STRUCTURAL SYNTHESIS OF KINEMATIC CHAINS AND MECHANISMS

Abstract. This study deals with the generation of kinematic chains with a given number of links and degree of freedom, as well as the derivation of the structurally distinct mechanisms from a specified kinematic chain by fixing a link of the kinematic chain as a frame link. Algorithms for determining the number of binary links and polygonal links of a chain, as well as the number of binary links that are connected to each other and their combinations, are developed. In order to eliminate isomorphic kinematic chains and mechanisms, a modified Degree Code method is proposed. Moreover, computer programs using Matlab are developed to computerize the whole procedure.

1. INTRODUCTION

At the initial design process of the mechanism design, it would be very helpful to have all possible kinematic chains for a given number of links and degree of freedom (DOF). To properly select the frame link for the design, all possible structurally distinct mechanisms derived from a specified kinematic chain should be investigated as well. For these purposes, the structural synthesis of chains and mechanisms is needed and it has been the subject of a number of studies for a long time. The methods employed in these studies are based on pure intuition and inspection, Franke's notation, graph theory, transformation of binary chains, and so on (Davies and Crossley, 1966; Manolescu 1973; Raicu, 1974; Mruthyunjaya and Raghavan, 1984).

In this study, the algorithm of Hwang and Hwang (1992) is used for generating non-degenerate and non-isomorphic chains with a given number of links and DOF. A method for deriving structurally distinct mechanisms from a specified chain is proposed. To detect isomorphic chains and mechanisms, a modified Degree Code method, based on an algorithm proposed by Tang and Liu (1993) is introduced. Computer programs using Matlab are developed, and the results are validated.

2. GENERATION OF KINEMATIC CHAINS

The two main steps of generating chains are as follows: (i) determination of the connection between links and joints, and detection of degenerate chains with rigid sub-chains; (ii) detection of isomorphic chains. The connection between links and joints could be presented by the contracted link adjacency matrix (*CLAM*) of Hwang and Hwang (1992) and the isomorphic chains could be identified utilising the Degree Code method of Tang and Liu (1993).

P. Chedmail et al. (eds.), Integrated Design and Manufacturing in Mechanical Engineering, 391-398.
©2002 *Kluwer Academic Publishers.*

A chain consists of two kinds of links: binary links and polygonal links. Each string of binary links, called a contracted link, is regarded as a unit. Each polygonal link is also regarded as a unit. The *CLAM* of a chain with n units is an $n \leftrightarrow n$ symmetric matrix with diagonal element $e_{ii} = f$ (if unit i is a polygonal link with f joints), and $e_{ii} = -m$ (if unit i is a contracted link with m binary links), for $i = 1, \ldots, n$. The largest value of the diagonal elements is placed in the left top element of the first column of the *CLAM*, and other elements are arranged in sequence, i.e., the smallest value of the diagonal elements is put in the right bottom element of the last column. The off-diagonal element e_{ij} of the *CLAM* is defined as $e_{ij} = t$ if unit i and unit j are connected by t joints, and $e_{ij} = 0$ otherwise (Hwang and Hwang, 1992). For example, there are 3 polygonal and 4 contracted links in the chain shown in Figure 1*b* (same chain as in Figure 1*a*, with different numberings to specify the units). The *CLAM* of the chain is a $7 \leftrightarrow 7$ matrix as given in equation (1).

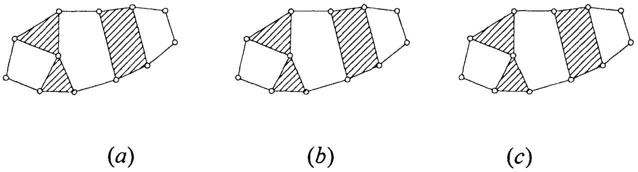
(*a*) (*b*) (*c*)

Figure 1. A ten-link chain with "B" representing the base link.

$$CLAM = \begin{matrix} 4 & 0 & 0 & 1 & 1 & 0 & 2 \\ 0 & 3 & 1 & 1 & 0 & 1 & 0 \\ 0 & 1 & 3 & 0 & 1 & 1 & 0 \\ 1 & 1 & 0 & -1 & 0 & 0 & 0 \\ 1 & 0 & 1 & 0 & -1 & 0 & 0 \\ 0 & 1 & 1 & 0 & 0 & -2 & 0 \\ 2 & 0 & 0 & 0 & 0 & 0 & -3 \end{matrix} \quad (1)$$

2.1. Algorithm for Enumerating Chains

The chains could be enumerated for a required number of links and DOF by constructing all the possible *CLAM*s that satisfy the given requirements. For this purpose, the algorithm presented in Hwang and Hwang (1992) is used and modified. The algorithm includes three steps: the determination of diagonal elements with positive values for polygonal links; the determination of diagonal elements with negative values for the contracted links; and the determination of off-diagonal elements, which represent the connectivity between the links. For implementing the procedure, link assortments, contracted-link assortments, and off-diagonal elements of the *CLAM* are generated.

2.1.1. Determination of Link Assortments

The link assortment of a chain is a set of numbers consisting of the number of binary links n_2 , ternary links n_3 , and *i*-nary links n_i , in order respectively, in the chain; i.e., $\{n_2 , n_3 , \ldots, n_i , \ldots, n_p \}$, in which the subscript p is the number of joints of the polygonal link with the largest number of joints. The value of p in a chain with l links and F DOF is determined as (Hwang and Hwang, 1992):

$$p = \begin{cases} (l-F+1)/2 & if\ F = 0\ or\ 1 \\ min \begin{matrix} l-F-1 \\ (l+F-1)/2 \end{matrix} ? & if\ F\ ?\ 2 \end{cases} \qquad (2)$$

An algorithm is introduced to determine all the possible link assortments with l links and F DOF. After the link assortments of a chain are determined, the diagonal elements with positive values and the absolute value of the sum of the diagonal elements with negative values can be obtained. The link assortment algorithm is:

Step 1: Compute p for the given number of links l and DOF F using equation (2), noting that p must be an integer number for any chain.

Step 2: For any $\{n_2 , n_3 , \ldots, n_i , \ldots ,n_p \}$ in which n_i $(i = 2 , \ldots, p)$ is from 0, …, l, calculate the number of links $l^* = n_2 + n_3 + \cdots + n_p$ and the number of joints $j^* = (2n_2 + 3n_3 + \cdots + pn_p)/2$ for a chain with F^* DOF, in which F^* can be determined utilising Grübler's equation for 1 DOF joints as $F^* = 3(l^* - 1) - 2j^*$.

Step 3: If the DOF F^* satisfies the given DOF of the chain, $F^* = F$, and the number of links l^* is equal to l, $l^* = l$, the link assortment $\{n_2 , n_3 , \ldots, n_i , \ldots, n_p \}$ is one of the assortments which satisfy the specified requirements.

Step 4: Repeat the procedure from step 2 to get all of link assortments that satisfy the requirements.

As an example, chains with ten links and 3 DOF are considered. Using equation (2), the value of p is 6. All the possible link assortments are generated using Matlab and are given in Table 1. The chain in Figure1*b* has 7 binary links, 2 ternary links and 1 quaternary link. Its link assortment is $n_2 = 7$, $n_3 = 2$ and $n_4 = 1$ (third row in Table 1). Therefore, the first three diagonal elements of its corresponding *CLAM* are 4, 3 and 3. The sum of absolute value of the remaining diagonal elements is 7.

2.1.2. Determination of Contracted-Link Assortments

The contracted-link assortment of a chain is a set of numbers consisting of the number of contracted links with one, two, and *i*-binary links, in order respectively, i.e., $\{ b_1, b_2, \ldots, b_i, \ldots, b_q \}$ in which q is the largest number of binary links in the

Table 1. Link assortments of 3 DOF ten-link chains

n_2	n_3	n_4	n_5	n_6
6	4	0	0	0
7	**2**	**1**	**0**	**0**
8	0	2	0	0
	1	0	1	0
9	0	0	0	1

contracted links of the chain. The maximum value of q for an F DOF chain is $q = F + 1$, and the following equations can be derived (Hwang and Hwang, 1992):

$$b_1 + b_2 + b_3 + \cdots + b_q = b \tag{3}$$

$$b_1 + 2b_2 + 3b_3 + \cdots + qb_q = n_2 \tag{4}$$

where b is the number of contracted links, and n_2 is the total number of binary links in the chain. The possible range of b ($b_{min} \leq b \leq b_{max}$) has to be determined first to list all of the possible contracted-link assortments for a given link assortment. If l_x represents the number of polygonal links and $2j_x$ gives the total number of joints of the polygonal links, the following relationships hold (Hwang and Hwang, 1992):

$$n_3 + n_4 + \cdots + n_p = l_x \tag{5}$$

$$3n_3 + 4n_4 + \cdots + pn_p = 2j_x \tag{6}$$

The maximum value of b, b_{max}, could occur when the polygonal links are not adjacent to one another, which means that each contracted link is connected to two joints of two polygonal links. Hence, a possible maximum value for b_{max} could be equal to j_x. Also, b_{max} is limited by the total number of binary links n_2. Therefore, $b_{max} = min\{n_2, j_x\}$. The minimum value of b, b_{min}, could occur when the polygonal links are connected, as close together as possible, without forming a rigid chain so as to reduce the number of the contracted links b. Therefore, the polygonal links must form a chain with 1 or 2 DOF if the number of polygonal links l_x is even or odd. Hence, using Grübler's equation, b_{min} is defined as $b_{min} = j_x - j_x^*$, where:

$$2j_x^* = \begin{array}{ll} 0 & if\ l_x = 1 \\ 3(l_x - 1) - 1, & if\ l_x = 2,\ 4,\ 6,\ \ldots \\ 3(l_x - 1) - 2, & if\ l_x = 3,\ 5,\ 7,\ \ldots. \end{array}$$

An algorithm is developed to generate all the possible contracted-link assortments for a given link assortment. Thus, the diagonal elements with negative values in the *CLAM* are determined. The algorithm consists of the following steps:

Step 1: Calculate $q = F + 1$.

Step 2: Get n_2 from one of the link assortments (determined in Section 2.1.1).

Step 3: Determine b_{max} and b_{min}.

Step 4: For any $\{b, b_1, b_2, \ldots, b_i, \ldots, b_q\}$ in which b is from b_{min} to b_{max}, and $b_i(i=1, \ldots, q)$ is from $0, \ldots, n_2$, calculate $b^* = b_1 + b_2 + b_3 + \cdots + b_q$, and $n_2^* = b_1 + 2b_2 + 3b_3 + \cdots + qb_q$.

Step 5: If n_2^* and b^* satisfy $n_2^* = n_2$ and $b^* = b$ respectively, a contracted-link assortment $\{b, b_1, b_2, \ldots, b_i, \ldots, b_q\}$ is obtained. Repeat from step 4 to generate different sets of $\{b, b_1, b_2, \ldots, b_i, \ldots, b_q\}$.

Step 6: After all the possible contracted-link assortments for one of the link assortments are computed, move to the next link assortment by going to step 2 until all the possible contracted-link assortments are generated.

Using this algorithm, all the possible contracted-link assortments for the link assortment $\{7, 2, 1\}$ are obtained by running a Matlab program, and the results are listed in Table 2. It can be seen that the chain shown in Figure 1*b* is one of the chains with the fifth contracted-link assortment $\{2, 1, 1\}$ given in Table 2.

If the generated chain contains a degenerate sub-chain, the corresponding *CLAM* will contain a degenerate sub-matrix. Therefore, the degenerate chains could be detected by inspecting the *CLAM*s. The steps for systematic generation of all the possible *CLAM*s and discussion on identifying degenerate sub-matrix of the *CLAM*s, are given in Hwang and Hwang (1992) and will not be repeated here.

Table 2. Contracted-link assortments for the link assortment {7, 2, 1}

b	b_1	b_2	b_3	b_4
3	0	2	1	0
	1	0	2	0
	1	1	0	1
4	1	3	0	0
	2	**1**	**1**	**0**
	3	0	0	1
5	3	2	0	0
	4	0	1	0

2.2. Detection of Isomorphic Chains

Based on graph theory, a mechanism (chain) can be converted into its equivalent graph by considering nodes and edges corresponding to links and joints of the mechanism respectively, and edge connection between nodes corresponding to the kinematic pairing between the links of the mechanism. Nodes of the graph are labeled with link numbers. If there exists more than one type of kinematic pairs in the mechanism, it is necessary to label the edges of the graph distinctly.

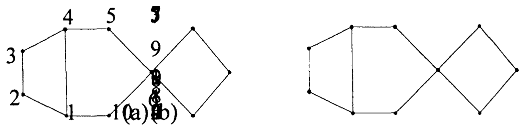

(*a*) (*b*)

Figure 2. (a) Graph representation of the chain in Figure 1a; (b) The graph after relabeling.

The degree of a node of a graph is defined as the number of edges incident to it. For instance, in Figure 2*a* which is a graph representation of the chain given in Figure 1*a*, the degrees of the nodes of the graph in the numerical order of the nodes (starting from node 1) are (3,2,2,3,2,4,2,2,2,2). The nodes could be rearranged so that their degrees are in descending order, and the nodes with the same degree could be permuted to get a new relabeling. The degrees of the nodes could be used to arrange the adjacency matrix (*AM*) of the chains. For an *l*-link chain, the *AM* is an $l \leftrightarrow l$ symmetric matrix with its entry $a_{ij} = 1$, if link *i* is adjacent to link *j*, and $a_{ij} = 0$ otherwise. Thus, all diagonal elements of the *AM* are zero. The proposed modified Degree Code method represents the chains by the *CLAM*, rather than by the *AM* as was proposed by Tang and Liu (1993), since for a given chain the size of the *CLAM* is smaller than that of the *AM*. The algorithm is as follows:

Step 1: Determine the degrees of the nodes in the graph.
Step 2: Rearrange the nodes so that their degrees are in descending order.
Step 3: Permute the nodes with the same degree to get a new relabeling.
Step 4: For each relabeling, concatenate the absolute values of the diagonal elements and the upper right triangular elements of the corresponding *CLAM*, and form a number with a base, which is the greatest absolute value of elements in the *CLAM* plus one. Covert this number into a decimal integer.
Step 5: Find the maximum value of these integer numbers, i.e., the Degree Code.

To avoid the precision problem in Matlab, the Degree Code of the *CLAM* could be composed of two parts. The first part is the string of the absolute values of the diagonal elements of the *CLAM*, which is not converted to a decimal integer. The second part is the elements in the upper right triangle of the *CLAM*, except for all "0" elements on the rows corresponding to negative diagonal elements. The second part is then converted to a decimal integer. In identifying isomorphic chains, the first parts of Degree Codes of two chains are compared firstly. If they are identical, the second parts will be compared; otherwise, these two chains are non-isomorphic, i.e., the first and second parts of the Degree Codes of isomorphic chains are equal.

The Degree Code of the chain in Figure 1*b*, with the corresponding *CLAM* given in equation (1), is formed by two parts. The absolute values of the diagonal elements give the first part (4331123); and the upper right triangle of the *CLAM,* except for all "0" elements on the rows corresponding to negative diagonal elements, give the second part (001102110100110, which can be represented in base ten as 756957).

3. GENERATION OF STRUCTURALLY DISTINCT MECHANISMS

When a link of a chain is fixed, it becomes a mechanism. In general, *n* mechanisms can be derived from an *n*-link chain. However, all these mechanisms may not be distinct. If any two links of a chain are structurally equivalent, the mechanisms derived by making them the fixed links are the same. Thus, the number of structurally distinct mechanisms that can be derived from a given chain is equal to the number of structurally dissimilar links in the chain. The Degree Code is used to be the invariant to discriminate among the links of a chain. The relative disposition of a link in a chain is reflected in the Degree Code. The Degree Codes for all mechanisms derived from the given chain are determined and compared. If any two fixed links have the same Degree Code, they are isomorphic, otherwise not. If the number of structurally distinct fixed links are known, the number of structurally dissimilar mechanisms of the chain are determined.

Based on the Degree Code method, the only need for generating structurally distinct mechanisms from a specified chain is to label the ground link with a symbol. If the *i*th link of the chain is selected as the base, every non-zero element of the *i*th row and *i*th column in the *AM* or *CLAM* corresponding to a given chain needs to be added with a number to make the chain with a specified frame different from the original chain. So as to avoid element repetition in the *AM* (*CLAM*), the number added has to be equal to or greater than the largest element in the *AM* (*CLAM*).

For example, if link 3 of the chain given in Figure *1a* is chosen as the base (labelled with "B"), with its corresponding link relabeling shown in Figure 1*c*, its Degree Code is string "00111100011000200010001000000000000000001001200"using the *AM.* By fixing links 1 to 10 one at a time, six structurally distinct mechanisms with ground links 1, 3, 5, 6, 7 and 8 are derived from the chain given in Figure 1*a*.

4. COMPUTER PROGRAM

A Matlab program is developed for generating all of the possible chains for a specified number of links and DOF. The program first permutes all the possible link and contracted-link assortments, and generates all the possible connections between polygonal and contracted links for each combination of link and contracted-link assortments. Then the degenerate chains are detected and eliminated, and the isomorphic chains are identified and removed using the Degree Code method. The non-degenerate and non-isomorphic chains that could be generated with 6 to 13 links and DOF from 1 to 8, respectively, are generated (Zhang et al., 2000). The results are consistent with the published data by Mruthyunjaya (1984), and Hwang and Hwnag (1992). Another Matlab program is developed to generate all of the possible structurally distinct mechanisms for a given chain, based on the Degree Code of the chain when the links of the chain are fixed one at the time, after eliminating the isomorphism. All of the structurally distinct mechanisms for several chains have been determined and the results are concordant with Manolescu (1973).

5.CONCLUSIONS

The method proposed by Hwang and Hwang (1992) was used to generate chains with a specified number of links and DOF. Algorithms for obtaining the link assortments and contracted-link assortments, which are not available in their article, were proposed and also proved to be reliable after testing with the published cases. Although the Degree Code method proposed by Tang and Liu (1993) was utilized to eliminate the isomorphic chains, the method was modified to adapt to chains represented by the *CLAM*, rather than by the *AM*. The proposed method of deriving structurally distinct mechanisms from a given chain is simple and reliable. Furthermore, in order to solve the precision problem of Matlab in detecting isomorphism, the modification of the Degree Code method was conducted in the structural synthesis. The input allocation of a chain which was discussed in Zhang et al. (2000) is not reported here because of space limitation.

6. REFERENCES

[1] Davies, T. H. and Crossley, F. E. (1966) Structural analysis of plane linkages By Franke's condensed notation. J. Mechanisms, 1, 171-183.

[2] Manolescu, N. I. (1973) A method based on Baranov trusses, and using graph theory to find the set of planar jointed kinematic chains and mechanisms. Mech. Mach. Theory, 8, 3-22.

[3] Hwang, W. M. and Hwang, Y. W. (1992) Computer-aided structural synthesis of planar kinematic chains with simple joints. Mech. Mach. Theory, 27(2), 189-199.

[4] Mruthyanjaya, T. S. (1984) A computerized methodology for structural synthesis of kinematic chains: Part 2 - Application to several fully or partially known cases. Mech. Mach. Theory, 19(6), 497-505.

[5] Mruthyunjaya, T. S. and Raghavan, M. R. (1984) Computer-aided analysis of the structure of kinematic chains. Mech. Mach. Theory, 19(3), 357-368.

[6] Raicu, A. (1974) Matrices associated with kinematic chains with from 3 to 5 members. Mech. Mach. Theory, 9(2), 123-129.

[7] Tang, C. S. and Liu, T. (1993) The Degree Code - A new mechanism identifier. Trans. ASME, J. Mechanical Design, 115, 627-630.

[8] Yan, H. S. and Hall, A. S. (1981) Linkage characteristic polynomials: Definitions, coefficients by inspection. Trans. ASME, J. Mechanical Design, 103, 578-584.

[9] Zhang, J., Notash, L. and Wu, C. (2000) Structural synthesis of kinematic chains and mechanisms. Proc. CSME/IDMME Conference, 10 pages, Montreal.

7. AFFILIATIONS

Leila Notash is an Associate Professor with the Department of Mechanical Engineering, Queen's University, Kingston, Ontario, Canada.
Jingqiu Zhang is a design engineer with Avon Automotive, Farmington Hills, Michigan, USA.

GENERAL MANIPULATORS SYNTHESIS FOR A GIVEN WORKSPACE

F.B. Ouezdou, S. Guerry and S. Régnier
Laboratoire de Robotique de Paris,
U.P.M.C-U.V.S.Q., CNRS 1778,
10-12 Avenue de l'Europe, 78140 Vélizy (France)
ouezdou@robot.uvsq.fr

Abstract

This paper deals with the kinematic synthesis of manipulators. A discusion of the problem of determining the kinematic parameters of a manipulator is based on the assumption that the locus of its end-effector has to cover a region which is as close as possible to the shape of a desired volume. The approach centers on the identification of intrinsic parameters of a volume to define an error between the two volumes. Furthermore, an efficient method to determine six degrees of freedom manipulator workspace is developed. Then, the synthesis problem is formulated as an optimization problem where the manipulator which minimize the error between its workspace and the desired volume is looked for. The determination of a planar and a spatial serial manipulator able to reach a given region will illustrate the approach suggested here.

1. INTRODUCTION

The aim of kinematic synthesis of manipulators is to find a starting solution for an iterative design process. Numerous criteria are proposed in the literature to help designers to choose manipulator kinematic parameters. A geometric criterion requires the manipulator end-effector to reach a set of points [1], [2] or to follow a trajectory [3]. In order to reduce the number of solutions, kinematic [4] or static [5] criteria are added, constraining the manipulator under other physical aspects. More general critera such as isotropy [6] or dexterity [7] require minimal performance on a whole region of space rather than on a few points.

The present paper deals with another criterion, namely the shape of the manipulator workspace. The aim is to determine the kinematic dimensions of the links of a manipulator for a prescribed workspace. This will ensure that the manipulator is able to reach some particular region in space or make sure that known obstacles are out of the manipulator's reach. The problem can be stated as follows : to specify the kinematic parameters of a manipulator in such a way that the locus of the end-effector covers a region whose shape is as close as possible to the shape of a desired volume. Hence, the synthesis problem

P. Chedmail et al. (eds.), Integrated Design and Manufacturing in Mechanical Engineering, 399-406.
©2002 *Kluwer Academic Publishers.*

is formulated as an optimization problem where the manipulator parameters which minimize the error between the two volume shapes are looked for.

The optimization problem formulation raises two major difficulties: measuring the error between two volumes and determining the workspace of general manipulators. As will be shown in section 2, the first problem is solved through a normalization process based on identifying a set of intrinsic parameters describing the given volume shape. The error is then defined as an euclidian distance between two vectors. Section 3 will look at the general manipulator workspace determination method. This method takes advantage of the serial structure of the manipulators studied in this paper to build intermediate workspace from the end effector to the manipulator base. Section 4 explains in detail the synthesis process which is based on an optimization technique to determine the manipulator parameters. The objective function uses the volume error to evaluate manipulators.

2. COMPARISON OF VOLUMES

The optimization formulation of this problem concerns the fundamental issue of measuring the error between two volumes. A well known approach consists in computing the volume of the mismatch region. This is difficult because any translation, rotation and scaling of one volume relative to the other involve a modification of the mismatch region. Although there is clearly an optimal transformation which makes the error minimal, determining such transformation is a long and difficult process, making the error estimation impractical in the context of kinematic synthesis of manipulators.

2.1 Normalization process

The approach suggested here is a three-dimensional extension of the one proposed by Dibakar and Mruthyunjaya [8] for planar trajectories. It reduces the two volumes (i.e. the desired one and the current manipulator workspace) to their shape representation by performing a *normalization transformation*. The *shape* of an object is defined in relation to all its aspects which are independent of its size and coordinate system.This leads to the identification of those aspects which are invariant under the translation, rotation, scaling and reflection operators. For example, a sphere with a center at $(0, 0, 0)$ and a radius of 1 and another sphere with a center at $(1, 6, 2)$ and a radius of 0.5 represent two different volumes but both have a spherical shape. The normalization process takes advantage of the fact that every volume has an intrinsic coordinate frame located at the center of gravity of the volume and its axes are the principal inertia axes of the volume (i.e. assuming a unitary density of the workspace). The aim of the normalization is to rotate the volume so as to make its principal inertia axes parallel to reference frame axes, and then to scale the volume so as it fits within an edge unit cube without deforming it. Figures 1(a) to 1(d) show the different steps involved in the process :

1. Rotation: the initial volume $\mathcal{V}$ (figure 1(a)) is rotated in order to make its principal inertia axes parallel with the reference frame axes (figure 1(b)). Parameters for this rotation are found from the coordinates of the eigenvector of the inertia matrix of the volume. Eigenvectors are stored in ascending order of eigenvalues.
2. Translation: the rotated volume is then translated in such a way that it is contained in the first quadrant and one corner of its axes-aligned bounding box is on the reference frame origin (figure 1(c)).

   The translation parameters are found from the coordinates of the "lower far left" corner of the bounding box, i.e. the corner with the smallest coordinates.
3. Scaling: the rotated and translated volume is scaled to fit in an edge unit cube (with corner at position $(0, 0, 0)$ and $(1, 1, 1)$)(figure 1(d)). The parameter of the scaling is computed from the greatest length of the bounding box. The resulting volume is named the *normalized volume* $\tilde{\mathcal{V}}$.

The last step in the normalization process is carried out by computing the greatest length of the axes aligned parallelepedic bounding box of the rotated volume. This leads to the identification of a *characteristic length* (L_c) of the volume.

2.2 Global parameters

A normalized volume is independent of translation, rotation and scale. Hence, the extraction of some global parameters which are specific to the shape of the volume is made possible. The global parameters considered for shape representation are as follows:

- the volume of the normalized volume: $\tilde{V} = V/L_c^3$,
- the surface of the normalized volume: $\tilde{S} = S/L_c^2$,
- the position of the center of gravity of the normalized volume (first moment): $\tilde{c}_x = c_x/L_c$, $\tilde{c}_y = c_y/L_c$ and $\tilde{c}_z = c_z/L_c$
- the principal moments of inertia of the normalized volume (second moment): $\tilde{I}_{xx} = I_{xx}/L_c^3$, $\tilde{I}_{yy} = I_{yy}/L_c^3$ and $\tilde{I}_{zz} = I_{zz}/L_c^3$.

where c_x, c_y, c_z are the center of gravity coordinates of the rotated and translated volume, V, S and I_{xx}, I_{yy}, I_{zz} are respectively volume, surface and the principal moment of inertia of the volume before the normalization process.

The normalized volume is then represented by a seven dimensional vector, called normal vector and given by the following relation:

$$\tilde{\mathcal{V}}_n = \left(\tilde{V}, \tilde{S}, \tilde{c}_x, \tilde{c}_y, \tilde{c}_z, \tilde{I}_{xx}, \tilde{I}_{yy}, \tilde{I}_{zz}\right)^T \qquad (1)$$

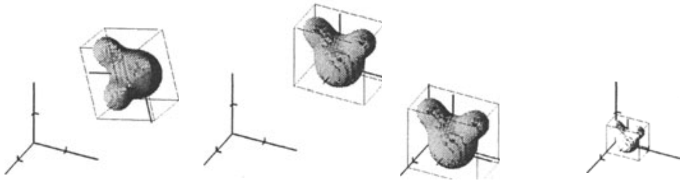

(a) Initial vol. (b) Rotation (c) Translation (d) Scaling

Figure 1. Normalization process

2.3 Distance between two volumes

The error between two volumes (i.e $\mathcal{V}^1$ & $\mathcal{V}^2$) is determined as follows: in the first step, the normalized volume $\tilde{\mathcal{V}}^1$ and $\tilde{\mathcal{V}}^2$ are computed. Then, their normal vectors $\tilde{\mathcal{V}}_n^1$ and $\tilde{\mathcal{V}}_n^2$ are extracted. Hence, The error between the two volumes is defined as the euclidian distance between the normal vectors shown as:

$$d(\mathcal{V}^1, \mathcal{V}^2) = \|\tilde{\mathcal{V}}_n^1 - \tilde{\mathcal{V}}_n^2\| \tag{2}$$

3. MANIPULATOR'S WORKSPACE

The second issue to be solved in the workspace synthesis procedure is the determination of the volume of the workspace of a given manipulator.

The workspace determination problem has drawn a lot of work from many researchers in the past years, but it has been solved analytically only for simple manipulators with a few degrees of freedom. No analytical formulation of the workspace for serial manipulators with a general architecture exists. Hence, for our purpose, a numerical representation has to be used.

As will seen in the next section, the workspace determination method is used to assess all manipulators proposed by the optimization technique. As such, the method should be fast, efficient and general enough to deal with different manipulator architecture. Furthermore, the workspace determination method must make it possible to take into account joint limits due to the fact that they deeply influence the workspace shape.

3.1 Intermediate workspace:

The workspace determination method uses the concept of intermediate workspace introduced by Ebert-Uphoff and Chirikjian [9]. Manipulators are represented as a serial chain of $n+1$ elements connected by n joints. Elements are numbered from 0 (base) to n (end-effector). The i^{th} *(upper) intermediate manipulator* $\mathcal{M}_i$ is the sub-manipulator made up of element i to the end-effector ($\mathcal{M}_n$ represents the end-effector and $\mathcal{M}_0$ represents the whole manipulator). The i^{th} *(upper) intermediate workspace* W_i^I is then the workspace of the i^{th} intermediate manipulator $\mathcal{M}_i$. Hence, W_i^I denotes the workspace of the manipulator from the i^{th} element to the end-effector and W_{i+1}^I denotes the workspace of the manipulator from the $(i+1)^{th}$ element to the end-effector. These two workspaces are related to each other by the i^{th} joint. Hence, W_i^I is computed as the locus of the points in W_{i+1}^I when the i^{th} joint variable steps from its lower limit to its upper limit.

The workspace determination technique iterates from the end-effector to the base of the manipulator computing intermediate workspace for all intermediate manipulators. The end-effector intermediate workspace W_n^I consists of a single point located at the end-effector position.

3.2 Workspace representation:

In order to contain all points generated for each intermediate workspace, an efficient workspace representation is needed. The latter should have several properties : fast access to each point, the smallest memory storage requirement and a suitable description form for the normalization process.

As manipulator joints are continuous devices, computing one intermediate workspace from another will create an infinite number of points. Due to the fact that it is impossible to store all these points for all intermediate workspace, an approximation scheme is needed.

For each intermediate workspace W_i^I, a parallepipedic bounding box is determined in such a way that its edges are parallel to the axes of the intermediate workspace frame. This bounding box is discretized into a set of elementary cubes with an edge length equal to ϵ_i (ϵ_i is a real giving the resolution of discretization). This discretization needs the computing of a number of grid elements in each direction $nb = (nb_x, nb_y, nb_z)$. The "lower far left" corner (i.e the corner with the smallest coordinates) of the bounding box is used as a reference point P_0 to place the workspace in the frame. So there are nb_x elementary cubes along the x axis, nb_y elementary cubes along the y axis and nb_z elementary cubes along the z axis. A three-dimensional array $D_i(i, j, k)$, $1 \leq i \leq nb_x$, $1 \leq j \leq nb_y$, $1 \leq k \leq nb_z$ of boolean represents whether the corresponding elementary cube intersects (i.e true for intersecting cubes) the intermediate workspace W_i^I or not. Figure 2(a), 2(b) and 2(c) show the representation method. Figure 2(a) gives the volume to be approximated while 2(b) and 2(c) show the resulting representation with and without empty cube emphasized.

3.3 Workspace mapping algorithm

The algorithm constructing the intermediate workspace W_i^I from the previous one W_{i+1}^I process can be split into three steps :

1 Estimating the size and location of the intermediate workspace W_i^I, deducing the number of elementary cubes needed along each axis, building the array D_i and then setting all its elements at false.

2 Mapping W_{i+1}^I to W_i^I: For all indices (i, j, k) for which $D_{i+1}(i, j, k)$ is true:
  - Finding $P = (x(i), y(j), z(k))^T$ the center of the corresponding elementary cube.
  - For each possible value of joint variable i (i.e. Δ_i discretization parameter):
    - Computing $P' = (x', y', z')^T$ the image of point P by the transformation of link i.
    - Finding (i', j', k') indices of the elementary cube in which lie P'.
    - Setting $D_i(i', j', k')$ at true.

3 Often the first step overestimates the size of W_i^I. So in this step, the algorithm looks for the smallest bounding box and updates D_i with the smallest array.

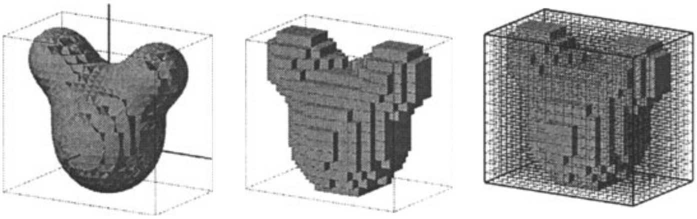

P. Chedmail et al. (eds.), *Integrated Design and Manufacturing in Mechanical Engineering*, 407-414.
©2002 *Kluwer Academic Publishers. Printed in the Netherlands.*

Figure 2. Volume Representation

This algorithm uses two discretization parameters. While the first step deals with the parameter ϵ_i which is the elementary cube edge length, the second one uses the parameter Δ_i to step through the i^{th} joint range. These two parameters are chosen as a tradeoff between computing speed, memory requirement and accuracy.

3.4 Extracting the global parameters

For each manipulator proposed by the optimization technique, its workspace is computed as W_0^I. The normalization process is then carried out by using the information contained in the D_0 array, considering only the marked cubes. Hence the volume is the sum of all elementary cube volumes, the center of gravity is the barycentre of the center of all elementary cubes (with equal weight) and the inertia matrix is the sum of all elementary inertia matrices.

4. SYNTHESIS PROCESS

The synthesis process is defined as an optimization problem whose aim is to find the manipulator parameters which minimize the error between manipulator workspace and a desired volume. Manipulators are parameterized according to the Khalil-Kleifinger parameters [10]. The design vector is made up of all parameters which influence the manipulator workspace and can be split in two main groups: a set of dimensional parameters $(3 * n)$ and a set of joint limits $(2 * n)$(where n is the number of joints). The set of dimensional parameters describes the manipulator kinematics and the set of joint parameters gives the manipulator configuration.

An objective function uses the workspace determination process and the error measure previously defined in Eq. (2) to evaluate a given manipulator. The synthesis process then uses an optimization technique based on an adaptive simulated annealing technique [11] to find the best manipulator's parameters. This approach is illustrated with 2R planar and 3R spatial manipulators (i.e. R means rotational joints). The first one concerns the determination of a planar manipulator with two rotational joints which should reach a given planar region. The design vector X is following as shown here:

$$X = \left[l_1, l_2, q_1^{min}, q_1^{max}, q_2^{min}, q_2^{max}\right]^T \tag{3}$$

where l_1, l_2 are the link length, q_i^{max} and q_i^{min} are the upper and lower bounds for the value of the i^{th} joint. The desired reachable region is given in figure 3(a). The results obtained for a cost function value about 5×10^{-4} are given in table 1

Table 1. Solution parameters for 2R manipulator (in centimeters and degrees)

i	l_i	q_i^{min}	q_i^{max}
1	100	-5.69	84.15
2	19.07	-195.21	167.42

The second example deals with the determination of three rotational spatial manipulator. The desired workspace region which should be reached by the manipulator is given in figure 3(c). The results obtained are indicated in table 2.

Table 2. Solution parameters for 3R spatial manipulator (in centimeters and degrees)

i	0	1	2	4
α_i	0	-91.86	8.84	-1.25
d_i	0	100	50.14	21.12
r_i	0	-1.65	0.95	-0.12
θ_i^{min}	-2.27	-55.39	-189.97	0
θ_i^{min}	46.08	50.75	205.31	0

5. CONCLUSION

This paper has presented a kinematic synthesis process whereby a manipulator whose workspace is as close as possible to a desired volume is found. An error function has been built to measure the distance between the two volumes.

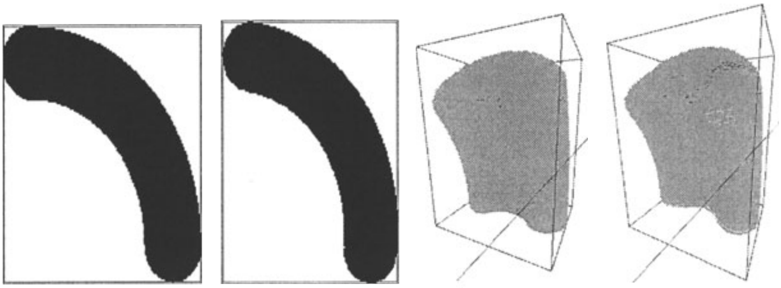

(a) 2R shape (b) 2R Results (c) 3R shape (d) 3R Results

Figure 3. 2R planar and 3R spatial manipulators examples

It uses a normalization transformation so as to avoid rotation, position and scaling dependencies and extract shape-intrinsic parameters from the normalized volume. A general method has been presented to determine the workspace of a serial manipulator. The approach has been illustrated with a 2R planar and a 3R spatial serial manipulator.

REFERENCES

[1] FC. Park and JE. Bobrow, *"Geometric Optimization Algorithms for Robot Kinematic Design"*, Journal of Robotic Systems, 1995, Vol 12, Nb 6, pp 453–463.

[2] FB. Ouezdou and S. Regnier, *"General method for kinematic synthesis of manipulators with task specifications"*, Robotica,, 1997, Vol 15, pp 653–661.

[3] J. Han and WK. Chung and Y. Youm and SH. Kim, *"Task Based Design of Modular Robot Manipulator using Efficient Genetic Algorithm"*, International Conference on Robotics and Automation, April 1997, pp 507–512.

[4] S. Guerry and S. Regnier and FB. Ouezdou, *"Kinematic Design of manipulators"*, Ro.Man.Sy, 1998.

[5] M. Raghavan and B. Roth, *"Kinematic analysis of the 6R manipulator of general geometry"*, International symposium on robotics research, August 1989, pp 263–269.

[6] J. Angeles and C. Lopez-Cajun, *"Kinematic isotropy and the conditioning index of serial robotic manipulators"*, The international journal of Robotics Research, Vol 11, Nb 6, 1992.

[7] K.A. Abdel-Malek and H.J. Yeh, *"Local Dexterity Analysis for Open Kinematic Chains"*, Mechanism and Machine Theory, 2000, Vol 35, pp 131–154.

[8] Sen Dibakar and T. S. Mruthyunjaya, *"Synthesis of workspaces of planar manipulators with arbitrary topology using shape representation and simulated annealing"*, Mechanism and Machine Theory, Vol 34, 1999, pp 391-420.

[9] Imme Ebert-Uphoff and Gregory S. Chirikjian, *"Generation of binary manipulator workspaces and work envelopes"*, Proceedings of the third IASTED International conference on Robotics and Manufacturing, Cancun, Mexico, June 1995.

[10] W. Khalil and J. F. Kleinfinger, *"A new geometric notation for open and closed loop robots"*, IEEE conference Robotics and Automation, pp 75–79, 1986.

[11] Lester Ingber, *"Adaptive Simulated Annealing (ASA)*, `http://www.ingber.com`, 1999, Lester Ingber Research, 1020 S Wabash Ave Ste 5D, Chicago, IL 60605

P. CHEDMAIL, C. LE ROY, B. MAILLE

OBJECT MANIPULATION AND MANNEQUIN DRIVING BASED ON MULTI-AGENT ARCHITECTURE

Abstract: Digital mock-ups, path planners and virtual reality tools are increasingly used within the industrial framework, allowing accessibility and maintainability checks without physical mock-ups. For this, it is necessary to simulate an object moving without collision. Two methods are commonly proposed: automatic path planning approach and direct simulation through robotic or virtual reality tools. In order to use the potential and avoid the drawbacks of these two methods, we settled for a mixed approach using local algorithm abilities and the global view ability of a human operator. To achieve this co-operation, we use a multi-level tree architecture composed by multi-agent "blackboard" systems. The different agents acts to nullify the collisions between the manipulated object and the cluttered environment, attract it towards its target, allow human operator's actions on the path, and provide the mannequin with a coherent behavior. Thanks to our system we manage to perform an accessibility task for object and mannequin with more than 20 degrees of freedom in a cluttered environment.

1. INTRODUCTION

For twenty years path planners for mobile objects in cluttered environments have been developed in the framework of robotics. Meanwhile, virtual reality tools are increasingly used within the industrial framework. These tools allow the use of digital mock-ups for accessibility or maintainability checks between mechanical parts. To establish mounting/dismounting sequences it is necessary to simulate an object moving without collision. For object manipulation we intend to use human synthesis and global view abilities. Consequently, we couple software abilities with human operator capabilities. Our architecture for this co-operation is based on multi-agent principles.

We recall the state of the art for accessibility checks in the next paragraph. Next, we introduce the multi-agent principles as they are used in our architecture. Then we describe principles for co-operation between artificial and human agents. By the end, we focus on the performances of our approach.

2. STATE OF THE ART FOR ACCESSIBILITY CHECKS

One of the design office activities is the validation of the designed parts. For assemblability, accessibility or maintainability two main different methods are commonly proposed. The first one concerns automatic path planning approach. The second one concerns simulation through robotic or virtual reality tools.

P. Chedmail et al. (eds.), Integrated Design and Manufacturing in Mechanical Engineering, 407-414.
©2002 *Kluwer Academic Publishers.*

2.1. Automatic path planners

2.1.1 Classical path planners

Collision-free trajectory research approaches are mainly based on two principles. Some methodologies need a global perception of the environment ([13], [15], [2]), others consider the moves of the object only in its close or local environment ([11], [1]). All these techniques are limited either by the computation cost or the existence of local minima as explained by Namgung [14]. Figure 2 sums up these approaches.

2.1.2 Path planner with specific approaches

For highly cluttered environments, it can be useful to be helped by human global view of the environment. Hwang [8] has settled for such an approach. Within Hwang's method, the designer can define a sequence of sub-goals in the environment. These sub-goals lead to the partition dividing of the problem in several simpler path-planning problems. This approach is a sequential mix between Figure 2 and Figure 3. Kavraki and Latombe [10] propose a similar approach by placing sub-goals defined in a randomised manner. These methods confirm that human abilities or stochastic approach greatly enhance path planners, even if these methods act sequentially.

2.2. Accessibility with direct simulation

Another approach is based on robotic CAD systems that allow the designer to manipulate robots, mechanisms or even mannequins. For this approach, the designer uses his or her global perception to achieve the task, but this manipulation is usually sequential and long. Classical virtual reality tools enhance the robotic on-line manipulation with the use of immersion devices. This technique only invokes the virtual environment and an immersed operator. Some drawbacks are the lack of kinematics constraints and the fact that collisions between objects are not automatically avoided, although they are usually detected. Figure 3 sums up this approach.

2.3. Conclusion

Important potentials of automatic path planners and direct simulation have been pointed out. Nevertheless, the algorithmic approaches are long and lead to local minima. The approaches with on-line manipulation are too long with robotic CAD systems or need a high number of expensive devices for virtual reality immersion. In order to avoid these drawbacks, we intend to settle for a mixed approach of the presented methodologies, using local algorithm abilities and global view ability of a human operator.

3. MULTI-AGENT SYSTEMS

The above chapter clearly points out the local abilities of several path planners and the global abilities of human vision. We intend to manage simultaneously these local and global abilities. The main purpose is to know how to build an interaction between human and algorithms in order to have an efficient path planner [3]. For this, we have built a path planner based on multi-agent principles proposed by Ferber [7] with a human interactive integration between algorithmic processes rather than on a sequential integration as proposed by Hwang [8].

3.1. Retained multi-agent theory

3.1.1 Elementary agent definition

Several workgroups have established rules for the definition of the agents and their interactions. Within these research groups it is important to point out the contributions of Ferber [7] and Jennings [9]. We keep the definition of an elementary agent definition from these analyses.

3.1.2 Considered multi-level architecture

For our purpose we have no direct communication between agents. This kind of architecture can be compared to "blackboard" systems. This principle is described in [7], [6] and [9]. Each agent acts with a period of activity that expresses priority between the agents. With this method, similar to the use of tokens, each agent has enough time to process its contribution. For this architecture we have a main process which collects elementary agents' contributions (normalised by a predetermined step) and updates the database.
Figure 1 is composed of different basic "blackboard" levels, which allow a partition dividing of our software construction.

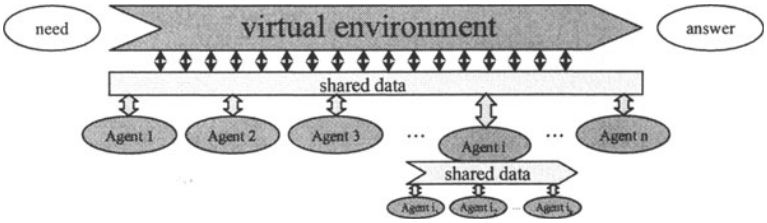

Figure 1: Blackboard principle with co-operating agents

4. ACCESSIBILITY AND MAINTAINABILITY CHECK WITH MULTI-AGENT SYSTEM IN VIRTUAL REALITY

Our purpose is to validate new CAD/CAM solutions based on a distributed approach using a virtual reality environment. To enhance assemblability, accessibility or maintainability we try to manage simultaneously the local abilities of algorithms and the global view ability of an operator, as suggested in figure 4. We build a coupled approach using multi-agent and distributed principles. These principles were defined by Chedmail and described accurately in [3]. The virtual site enables graphic visualisation of the database for the human operator, and communicates positions of the virtual objects to external processes.

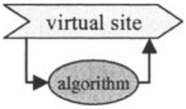

Figure 2: algorithmic approach

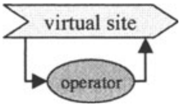

Figure 3: direct simulation approach

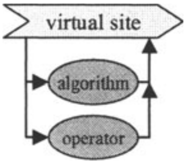

Figure 4: Co-operation principles

4.1. Object manipulation

For object manipulation we use former principles defined by Chedmail and Le Roy in [4]. Here-after we summarise this approach for elementary agents definition. Beside variables of position and orientation of all parts of the cluttered environment we consider the six degrees of freedom of the manipulated object and the degrees of freedom of the kinematics of the objects. The global vector position and orientation of the manipulated object is $\mathbf{X_{po}} = {}^t(x, y, z, R, Y, P)$, the vector for the degrees of freedom of this object is $\mathbf{X_q} = {}^t(q_1, q_2, , .., q_n)$.

4.1.1 Elementary agents

- *Attraction* agent:

The *attraction* agent affects the manipulated object with elementary moves toward its target. This *attraction* agent is similar to the attraction force introduced by Khatib [11]. It's aim is to minimize the distance between the manipulated object and its target. Its action only affects $\mathbf{X_{po}}$.

- *Collision* agent:

The *collision* agent is composed by two elementary agents:

- The *repulsion* agent acts on the position and orientation of the manipulated object to minimize the length of the collision line thanks to the gradient of this length according to the Cartesian environment frame. Its contribution only affects $\mathbf{X_{po}}$.

- The *kinematics* agent: For an object built with internal degrees of freedom, a specific *kinematics* agent is used. The *kinematics* agent acts on these degrees of freedom in order to minimize the length of the collision line thanks to the gradient of this length according to these degrees of freedom. Its contribution only affects $\mathbf{X_q}$.

- *Human operator*, *operator* agent.

The *human operator* agent has a global view of the cluttered environment displayed by the way of the virtual reality software. We use a SpaceMouse, which allows object manipulation with six degrees of freedom. Its contribution only affects $\mathbf{X_{po}}$.

4.1.2 Sum-up of agents' contributions

In table 1 hereunder, we consider the variables that permit to define a trajectory out of collision. Each agent uses the database (environment position, orientation, parameters, etc.) in order to act in a relevant way according to its aim.

Table 1: Agents' contribution on process variables

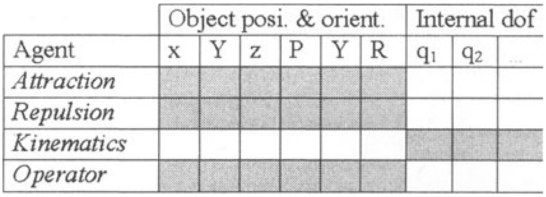

	Object posi. & orient.						Internal dof		
Agent	x	Y	z	P	Y	R	q_1	q_2	...
Attraction	▨	▨	▨	▨	▨	▨			
Repulsion	▨	▨	▨	▨	▨	▨			
Kinematics							▨	▨	▨
Operator	▨	▨	▨	▨	▨	▨			

4.2. Mannequin manipulation

Our mannequin is composed with several geometric parts defining limbs and links. These geometrical parts are considered like mechanical parts of a kinematics object and we have ergonomic constraints. This approach for our software architecture for mannequin driving leads to the decomposition in different multi-agent levels. For the moment we only consider one arm and the body for the mannequin manipulation.

4.2.1 Elementary agents

First level for our mannequin driving is similar than the one defined for the manipulation of an object. Consequently, we first consider our mannequin like a classical kinematics chain. So, we use an *attraction* agent for the mannequin hand move toward the manipulated object, a *repulsion* agent for the mannequin body collision avoidance and a *kinematics* agent for its different links. We do not use an *operator* agent, which is only devoted to the object manipulation. Our mannequin is composed of an articulated arm, an unarticulated body, and a head with an articulated neck.

- *Ergonomics* agent: The three agents defined above for mannequin driving do not respond to common human behavioural requirements. Consequently we included a new agent interacting with the others and aiming at ergonomic behaviour. This agent is separated into three elementary agents.
  - *Altitude* agent: In order to maintain a coherent body altitude we use an *altitude* agent. This agent acts on the degrees of freedom of the arm up to the shoulder in order to assure a nice body placement for altitude.
  - *Verticality* agent: An agent that ensures the *verticality* of the body is added the *altitude* agent. This agent acts on the three degrees of freedom of the mannequin shoulder.
  - *Visualisation* agent: The *visualisation* agent has to ensure that the mannequin can see the target where he has to put the manipulated object. This agent acts on two degrees of freedom for the head moves.

4.2.2 Sum-up of agents' contributions for the mannequin

Table 2 hereunder shows agents' contribution on the mannequin. We can notice the high coupling level for shoulder's degrees of freedom. The number of degrees of freedom for the arm can change according to moves we want to perform.

Table 2: Agents' contribution for the mannequin

		Hand posi. & orient.						Arm dof			Shoulder			Head		
Agent		X	y	z	P	Y	R	q_1	…	q_i	q_{s1}	q_{s2}	q_{s3}	q_{h1}	q_{h2}	q_{h3}
Attraction		▨	▨	▨	▨	▨	▨									
Repulsion		▨	▨	▨	▨	▨	▨									
Kinematics								▨	▨	▨	▨	▨	▨	▨	▨	▨
Ergonomics	*Altitude*							▨	▨	▨	▨	▨	▨			
	Vertical.										▨	▨	▨			
	Visualis.													▨	▨	▨

4.3. Global multi-agent architecture

While gathering the different systems for object and mannequin manipulation we obtain the multi-level schema of our global software architecture, which is presented in Figure 5.

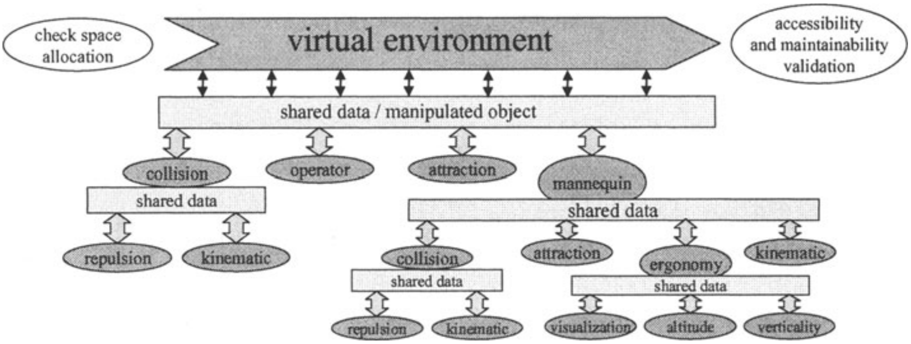
check space allocation
virtual environment
accessibility and maintainability validation
shared data / manipulated object
collision
operator
attraction
mannequin
shared data
repulsion
kinematic
shared data
collision
attraction
ergonomy
kinematic
shared data
repulsion
kinematic
shared data
visualization
altitude
verticality

Figure 5: Global multi-agent architecture [12]

4.4. Global process optimisation

4.4.1 Variations of the periods of activity

Former studies from Chedmail and Le Roy [5] expose principles for optimisation of a single object manipulation. The results for the object manipulation correspond to what it was possible to expect: the *collision* agent must be the most important agent (rate 1) to avoid collision and the *operator* agent must be stronger (rate 4) than the *attraction* agent (rate 8) in order to allow the operator to act significantly on the trajectory. For the mannequin manipulation agents, the most important agents (rate 1) are *repulsion*, *kinematics*, *altitude* and *verticality*, in order to have a coherent behavior for the mannequin while avoiding collisions. The *visualization* agent's rate is 2 because this agent is less important than the *collision* agent.

4.4.2 Results

These results are used and moderated after several experiments on different databases, with different initial configurations and with different predetermined steps. Eventually, we assert the reliability of periods defined previously. Thanks to our system we manage to perform an accessibility task for our object and mannequin with 20 degrees of freedom in a cluttered environment. These experiments are performed in real time with a human *operator* who has to act punctually in order to avoid local minima.

5. CONCLUSIONS AND FURTHER WORK

Our innovative architecture enables objects driving with a mannequin. Moreover, we manage to couple heterogeneous constraints like collision avoidance, human operator contribution and mannequin ergonomics in the same architecture.

The main drawback of our system is that we need a highly simplified model for our *repulsion* agent in order to support real time moves. Nevertheless, our limitations are due to hardware capabilities whereas on line manipulation limitations are due to human capabilities which are unfortunately not likely to increase as much as those of hardware during the coming years.

6. ACKNOWLEDGEMENTS

We address our acknowledgements to the European Community that supported this study in the framework of the CEDIX project [16].

7. AFFILIATIONS

P. Chedmail, C. Le Roy, Institut de Recherche en Communications et Cybernétique de Nantes - U.M.R. CNRS 6597, 1, rue de la Noë - B.P. 92101 - 44321 Nantes Cedex 3 – France. Email : Patrick.Chedmail@irccyn.ec-nantes.fr

B. Maillé, SNECMA Moteurs, Intégration - Maquette Numérique, Centre de Villaroche, 77550 Moissy-Cramayel, France. Email : Bruno.Maille@snecma.fr

8. REFERENCES

[1] Barraquand, J., and Latombe, J.C., "Robot Motion Planning : A Distributed Representation Approach", *The International Journal of Robotics research*, December 1991.

[2] Boissonnat, J.D., Faverjon, B., and Merlet, J.P., "Perception et planification", *Traité des nouvelles technologies*, Série Robotique. Hermès, Paris, France, 1988.

[3] Chedmail, P., Damay, T., and Rouchon, C., "Integrated design and artificial reality : accessibility and path planning", *ASME Engineering System Design and Analysis (ESDA'96)*, vol. 8, pp. 149-156, ISBN 0-7918-1503-X, July 1-4, 1996, Montpellier.

[4] Chedmail, P. and Le Roy, C. "A Distributed Approach For Accessibility And Maintainability Check With A Manikin". DAC-8677, ASME Design Engineering Technical Conferences, Las vegas, Névada, USA, September 12-15, 1999.

[5] Chedmail, P. and Le Roy, C. "Multi-agent architecture for an interactive path-planner". Advances in computational multibody dynamics, IDMEC/IST, Lisbon, Portugal, September 20-23, 1999.

[6] Ferber, J., and Ghallab, M., "Problématique des univers multi-agents intelligents", *Actes des journées nationales PRC-IA*, 1988, pp.295-320.

[7] Ferber, J., 1995, "Les systèmes multi-agents, vers une intelligence collective", InterEditions, 1995.

[8] Hwang, Y. K., Cho, K. R., Lee, S., Park, S. M., and Kang, S., "Human Computer Cooperation in Interactive Motion Planning", *ICAR'97*, Monterey, CA, July 7-9, pp. 571-576, 1997.

[9] Jennings, N. R., Sycara, K. and Wooldridge, M., "Roadmap of agent research and development", *Autonomous agents and multi-agent systems*, Vol. 1, pp. 7-38, 1998.

[10] Kavraki, L. E., Latombe, J.-C., Motwani, R. and Raghavan, P., "Randomized Query Processing in Robot Path Planning", *Journal of Computer and System Sciences*, 57(1):50-60, August 1998.

[11] Khatib, O., 1986, "Real time obstacle avoidance for manipulators and mobile robots", *International Journal Robotics Research*, Vol. 5, no. 1, pp.90-98, 1986.

[12] Le Roy C., "Accessibilité et aptitude au montage, réalité virtuelle et approche multi-agent", thèse de doctorat de l'Université de Nantes, 5 janvier 2000.

[13] Lozano-Pérez, T., and Wesley, M. A., "An algorithm for planning collision-free paths among polyhedral obstacles", Comm. ACM, 22 (10), pp. 560-570, 1979.

[14] Namgung, I., and Duffy, J., "Two Dimensional Collision-Free Path Planning Using Linear Parametric Curve", *Journal of Robotic Systems 14(9)*, pp. 659-673, 1997.

[15] Tournassoud, P., "Géométrie et intelligence artificielle pour les robots", Hermès, Paris, France, 1990.

[16] CEDIX, contract BRPR-CT96-0151, project BE95-1461, "Concurrent Engineering based design for integrated X-methodologies"

D. CHABLAT, PH. WENGER, J. ANGELES

ISOTROPIC DESIGN OF A PARALLEL MACHINE-TOOL MECHANISM

Abstract: The subject of this paper is the isotropic design of a hybrid mechanism intended for three-axis machining applications. Parallel mechanisms are interesting alternative designs in this context. We compare machine-tool mechanism, with a hybrid serial parallel structure, of which we optimize the first two-axis subsystem, i.e. the table of the machine tool. The comparative study is conducted on the basis of a prescribed workspace and given kinetostatic performance. The two-degree-of-freedom mechanisms analyzed in this paper can be extended to three-axis machines by adding a third axis in series with the first two.

1. PRELIMINARIES

1.1 Serial Mechanism with Three Degrees of Freedom

Most industrial machine tools use a simple PPP serial kinematic chain with three orthogonal prismatic joint axes (Figure 1).

In this case, the motion in the *XY* plane and the motion along the *Z*-axis, where the axis of rotation of the tool is located.

The problem of the *PPP* mechanism is that the actuator controlling the *Y*-axis supports at the same time the workpiece and the actuator controlling the displacement of the *X*-axis, which affects the dynamic performance.

To solve this problem, it is possible to use more suitable architectures like parallel or hybrid mechanisms. For a PPP mechanism, the kinematic model takes the form

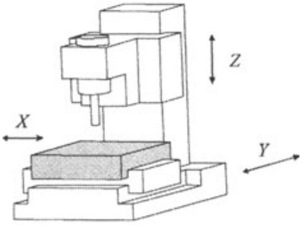

Figure 1: Traditional mechanism of three-axis machine tool

$$\mathbf{J}\,\dot{\boldsymbol{\rho}} = \dot{\mathbf{p}}, \text{ with } \mathbf{J} = \mathbf{1}_{3\times 3}$$

where $\dot{\mathbf{p}} = [\dot{x}\ \dot{y}\ \dot{z}]^T$ is the velocity-vector of the tool center P and $\dot{\boldsymbol{\rho}} = [\dot{\rho}_1\ \dot{\rho}_2\ \dot{\rho}_3]^T$ is the velocity-vector of the prismatic joints.

The Jacobian matrix **J** being the identity matrix, the manipulability and force [Yoshikawa 85] ellipsoids are both a unit sphere for all configurations in the Cartesian workspace. The aim of this paper is to replace this structure by a hybrid serial-parallel mechanism.

1.2 Planar Parallel Mechanisms with Two Degrees of Freedom

We focus on a two-DOF parallel mechanism, Figure 2, for the motion of the table

P. Chedmail et al. (eds.), Integrated Design and Manufacturing in Mechanical Engineering, 415-422.
©2002 *Kluwer Academic Publishers.*

of the machine tool depicted in Figure 1.

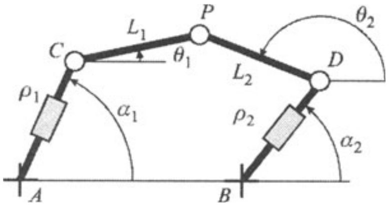

Figure 2: Parallel mechanism with two degrees of freedom

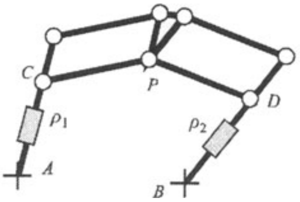

Figure 3: Parallel mechanism with two degrees of freedom with control of the orientation

The joint variables are ρ_1 and ρ_2 associated with the two prismatic joints and the output variables are the Cartesian coordinates of the tool center $P=[x\ y]^T$. The mechanism can be parameterized by the lengths L_1 and L_2, the angles α_1 and α_2, the position of points A and B, and the actuated joint ranges $\Delta\rho_1$ and $\Delta\rho_2$. To reduce the number of design variables, we set $L_1 = L_2$ and $\Delta\rho_1 = \Delta\rho_2$ This simplification also provides symmetry and, in turn, reduces the manufacturing costs.

To control the orientation of the reference frame attached to the tool center point P, two parallelograms can be used, which also increases the rigidity of the structure, Figure 3. The dimensioning of the parallelogram links is outside of the scope of the paper. However, the rigidity of the structure as well as the joint limits of the passive joints depends on the technological solutions adopted for their design.

To produce the third motion of the machine tool, it is possible to place orthogonally a third prismatic joint on top of the first two. This one can be located as in the case of Figure 1.

1.3 Kinematics of Planar Parallel Mechanisms

The velocity $\dot{\mathbf{p}}$ of point P can be expressed in two different ways. By traversing the closed loop (ACP-BDP) in the two possible directions, we obtain

$$\dot{\mathbf{p}} = \dot{\mathbf{c}} + \dot{\theta}_1\, \mathbf{E}\,(\mathbf{p} - \mathbf{c}) \text{ and } \dot{\mathbf{p}} = \dot{\mathbf{d}} + \dot{\theta}_2\, \mathbf{E}\,(\mathbf{p} - \mathbf{d}), \text{ with } \mathbf{E}=\begin{bmatrix} 0 & -1 \\ 0 & 1 \end{bmatrix} \tag{1}$$

where $\mathbf{E}$ is a matrix of rotation through 90°, $\mathbf{c}$ and $\mathbf{d}$ representing the position vectors of the points C and D, respectively. Moreover, the velocities $\dot{\mathbf{c}}$ and $\dot{\mathbf{d}}$ of the points C and D are given by

$$\dot{\mathbf{c}} = \frac{\mathbf{c} - \mathbf{a}}{\|\mathbf{c} - \mathbf{a}\|}\dot{\rho}_1 = \begin{bmatrix} \cos(\alpha_1) \\ \sin(\alpha_1) \end{bmatrix}\dot{\rho}_1,\ \dot{\mathbf{d}} = \frac{\mathbf{d} - \mathbf{b}}{\|\mathbf{d} - \mathbf{b}\|}\dot{\rho}_2 = \begin{bmatrix} \cos(\alpha_2) \\ \sin(\alpha_2) \end{bmatrix}\dot{\rho}_2$$

where the angles α_1 and $\alpha_2$are the orientations of the prismatic actuators from line AB of Figs. 2 and 3. We would like to eliminate the two idle joint rates θ_1 and θ_2 from equations (1), which we do upon dot-multiply the former by $(\mathbf{p} - \mathbf{c})^T$ and the latter by $(\mathbf{p} - \mathbf{d})^T$, thus obtaining

$$(\mathbf{p}-\mathbf{c})^T \dot{\mathbf{p}} = (\mathbf{p}-\mathbf{c})^T \frac{\mathbf{c}-\mathbf{a}}{\|\mathbf{c}-\mathbf{a}\|} \dot{\rho}_1 \text{ and } (\mathbf{p}-\mathbf{d})^T \dot{\mathbf{p}} = (\mathbf{p}-\mathbf{d})^T \frac{\mathbf{d}-\mathbf{b}}{\|\mathbf{d}-\mathbf{b}\|} \dot{\rho}_2 \qquad (2)$$

Equations (2) can now be cast in vector form, namely, $\mathbf{A}\,\dot{\mathbf{p}} = \mathbf{B}\,\dot{\rho}$, with **A** and **B** denoted, respectively, as the parallel and serial Jacobian matrices, $\dot{\rho}$ defined as the vector of actuated joint rates and $\dot{\mathbf{p}}$ is the velocity of point P, i.e.,

$$\mathbf{A} \equiv \begin{bmatrix} (\mathbf{p}-\mathbf{c})^T \\ (\mathbf{p}-\mathbf{d})^T \end{bmatrix}, \mathbf{B} \equiv \begin{bmatrix} (\mathbf{p}-\mathbf{c})^T \frac{\mathbf{c}-\mathbf{a}}{\|\mathbf{c}-\mathbf{a}\|} & 0 \\ 0 & (\mathbf{p}-\mathbf{d})^T \frac{\mathbf{d}-\mathbf{b}}{\|\mathbf{d}-\mathbf{b}\|} \end{bmatrix}, \dot{\rho} = \begin{bmatrix} \dot{\rho}_1 \\ \dot{\rho}_2 \end{bmatrix}, \dot{\mathbf{p}} = \begin{bmatrix} \dot{x} \\ \dot{y} \end{bmatrix}$$

When **A** and **B** are not singular, we obtain the relations,

$$\dot{\mathbf{p}} = \mathbf{J}\dot{\rho} \text{ with } \mathbf{J} = \mathbf{A}^{-1}\mathbf{B} \text{ and } \dot{\rho} = \mathbf{K}\,\dot{\mathbf{p}} \text{ with } \mathbf{K} = \mathbf{B}^{-1}\mathbf{A} \qquad (3)$$

We base our design on the Jacobian matrix **K**.

1.4 Parallel Singularities

Parallel singularities occur when the determinant of **A** vanishes [Chablat 98], i.e. when det(**A**) = 0. In the presence of such a singularity, the tool center P can move with the actuators locked.

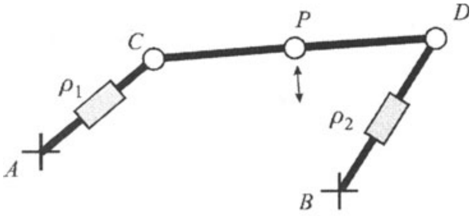

Figure 4: Parallel singularity

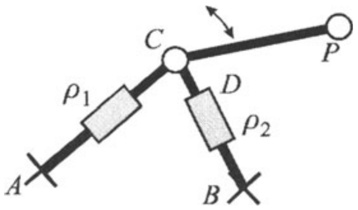

Figure 5: Structural singularity

These singularities are to be avoided, because the structure cannot resist any force, and control is lost. To avoid any performance deterioration, it is necessary to limit the range of the actuated joints. For the mechanism under study, parallel singularities occur whenever the points C, D, and P are aligned (Figure 4), i.e. when $\theta_1 - \theta_2 = k\,\pi$, for $k = 1,2,\ldots$. These singularities are located inside the Cartesian workspace and form the boundaries of the joint workspace. Moreover, structural singularities can occur when $L_1 = L_2$ (Figure 5). In these configurations, the control of point P is lost.

1.5 Serial Singularities

Serial singularities occur when det(**B**) = 0. In the presence of theses singularities, there is a direction along which no Cartesian velocity can be produced. Serial singularities define the boundary of the Cartesian workspace [Merlet 97]. For the mechanism under study, serial singularities occur whenever $\theta_1 - \alpha_1 = \pi / 2 + k\,\pi$, or $\theta_2 - \alpha_2 = \pi / 2 + k\,\pi$, for $k = 1, 2, \ldots$, i.e. whenever AC is orthogonal to CP or BD is orthogonal to $D\,P$.

1.6 Application to Machine-Tool Design

For a three-axis machine tool, as that in Figure 1, the table moves along two perpendicular axes. The joint limits of each actuator determine the dimension of the Cartesian workspace. For the parallel mechanisms under study, this transformation is not direct. The resulting Cartesian workspace is more complex and its size smaller for equal strokes of the actuators. We want to have a Cartesian workspace which will be close to the Cartesian workspace of an industrial serial machine tool. For our two-DOF mechanism, we prescribe a rectangular Cartesian workspace. In addition, the workspace must be reduced to a t-connected region, i.e. a region free of serial and parallel singularities. Finally, we want to prescribe relatively stable kinetostatic properties in the workspace.

2. ISOTROPIC DESIGN

2.1 Matrix Condition Number

During our process of design, we will define the loci of equal condition number of the Jacobian matrices. To do this, we first recall the definition of the condition number $\kappa(\mathbf{M})$ of an $m \times n$, matrix $\mathbf{M}$ with $m \leq n$. This number can be defined in various ways; for our purposes, we define $\kappa(\mathbf{M})$ as the ratio of the largest, σ_1, to the smallest, σ_s singular values of $\mathbf{M}$ [Golub 89]. The singular values $\{\sigma_k\}_1^m$ of matrix $\mathbf{M}$ are defined as the square roots of the nonnegative eigenvalues of the positive semi-definite $m \times m$ matrix $\mathbf{M}\,\mathbf{M}^T$.

2.2 Conditioning of the Parallel Jacobian Matrix

To calculate the condition number of $\mathbf{A}$, we need the product $\mathbf{A}\mathbf{A}^T$, which we calculate below:

$$\mathbf{A}\mathbf{A}^T = L_1^2 \begin{bmatrix} 1 & \cos(\theta_1 - \theta_2) \\ \cos(\theta_1 - \theta_2) & 1 \end{bmatrix}$$

The eigenvalues η_1 and η_2 of the above product are given by $\eta_1 = L_1^2\,(1 + \cos(\theta_1 - \theta_2))$ and $\eta_2 = L_1^2\,(1 - \cos(\theta_1 - \theta_2))$. Upon simplification, the condition number of matrix $\mathbf{A}$ is:

$$\kappa(\mathbf{A}) = 1 / |\tan((\theta_2 - \theta_1) / 2)|$$

In light of the above equation, it is apparent that $\kappa(\mathbf{A})$ attains its minimum of 1 when $|\theta_1 - \theta_2| = \pi / 2 + k\,\pi$ for k=1, 2, ... At the other end of the spectrum, $\kappa(\mathbf{A}) \to\infty$ when $|\theta_1 - \theta_2| = k\,\pi$, for k=1, 2, ... The configurations for which $\kappa(\mathbf{A}) = 1$ are called *isotropic* (Figure 7), whereas configurations for which $\kappa(\mathbf{A}) \to\infty$ are the parallel singularities of the manipulator (Figure 4). The study of the conditioning of **A** enables us to find a set of configurations for which **A** is isotropic. These conditions, however, do not give to the orientations α_1 and α_2 of the actuated joints.

2.3. Conditioning of the Serial Jacobian Matrix

By virtue of the diagonal form of **B**, its singular values, β_1 and β_2, are simply the absolute values of it diagonal entries. The condition number $\kappa(\mathbf{B})$ of **B** is thus

$$\kappa(\mathbf{B}) = \sqrt{\frac{\beta_{\max}}{\beta_{\min}}} \text{ with } \mathbf{B} \equiv L_1 \begin{bmatrix} \cos(\theta_1 - \alpha_1) & 0 \\ 0 & \cos(\theta_2 - \alpha_2) \end{bmatrix}$$

where, if $|\cos(\theta_1 - \alpha_1)| < |\cos(\theta_2 - \alpha_2)|$ then $\beta_{\min} = |\cos(\theta_1 - \alpha_1)|$ and $\beta_{\max} = |\cos(\theta_2 - \alpha_2)|$, else, $\beta_{\min} = |\cos(\theta_2 - \alpha_2)|$ and $\beta_{\max} = |\cos(\theta_1 - \alpha_1)|$. It is apparent that $\kappa(\mathbf{B})$ attains its minimum of 1 when $|\cos(\theta_1 - \alpha_1)| = |\cos(\theta_2 - \alpha_2)| \neq 0$. At the other end of the spectrum, $\kappa(\mathbf{B}) \to\infty$ when $|\cos(\theta_1 - \alpha_1)| = 0$ or $|\cos(\theta_2 - \alpha_2)| = 0$. The configurations for which $\kappa(\mathbf{B})$=1 are the isotropic configurations and the configurations for which $\kappa(\mathbf{B}) \to\infty$ are the serial singularities. As for the study of the conditioning of matrix **B**, the isotropy conditions of the matrix B do not give the orientations α_1 and α_2 of the actuators.

2.4. Conditioning of the Kinematic Jacobian Matrix

To define the orientation of the prismatic joints, we study the conditioning of the Jacobian matrix **K** given in the equation (3b). In this case, matrices $\mathbf{B}^{-1}$ and **K** are written simply,

$$\mathbf{B}^{-1} = \frac{1}{L_1} \begin{bmatrix} (1/c_1) & 0 \\ 0 & (1/c_2) \end{bmatrix}, \mathbf{K} = \begin{bmatrix} (1/c_1)\,(\mathbf{p} - \mathbf{c})^T \\ (1/c_2)\,(\mathbf{p} - \mathbf{d})^T \end{bmatrix} \text{with } c_i = \cos(\theta_i - \alpha_i)\ , i = 1, 2$$

The isotropy conditions of the matrix **K** are,

$$(1/c_1)\,\|\mathbf{p} - \mathbf{c}\| = (1/c_2)\,\|\mathbf{p} - \mathbf{d}\| \text{ and } (\mathbf{p} - \mathbf{c})^T\,(\mathbf{p} - \mathbf{d}) = 0$$

Now, we set $\alpha_1 = 0$ and $\alpha_2 = \pi / 2$ in order to have $\mathbf{K} = \mathbf{1}_{2\times2}$ in the isotropic configuration when $\theta_1 = 0$ and $\theta_2 = \pi / 2$. In this configuration, a motion of the prismatic joint ρ_1 produces a motion along X (Figure 7), and a motion of the prismatic joint ρ_2 produces a motion along Y as a machine tool with a *PP* architecture.

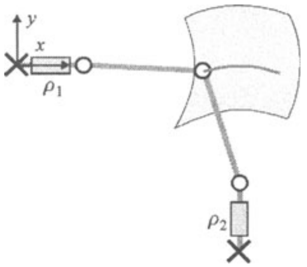

Figure 6: Motion of the point P generated by the motion of the joint $\boldsymbol{\rho}_1$

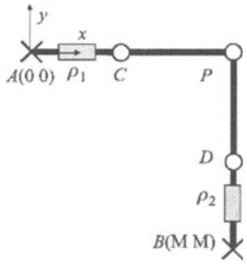

Figure 7: Isotropic configuration

Moreover, if we place point A at the origin and B at $(M\ M)$ (Figure 7), the values of ρ_1 and ρ_2 are equal when the manipulator reaches its isotropic configuration. This remark enables us to study the problem of velocity amplification due to the parallel mechanism. Indeed, in the case of a serial mechanism with three linear axes of motion, a motion of an actuated joint yields the same motion of the tool (or of the workpiece). For parallel mechanisms, these motions are not equivalent. When the manipulator is close to a parallel singularity, there is an amplification of motion (or velocity), i.e. a unit motion of one actuated joint can produce a motion of the tool which is several times larger. Thus, to move the tool with a constant accuracy, the precision of the actuated joints must be very high.

2.5. Study of the Joint and Cartesian Workspaces

In this study, we will see that isotropy conditions give very interesting properties for the manipulator under study. To this end, we study two mechanisms, one with coaxial actuators, of the biglide type (Figure 8), i.e. the mechanism most usually found, and the other with actuator axes at right angles, as shown in Figure 9.

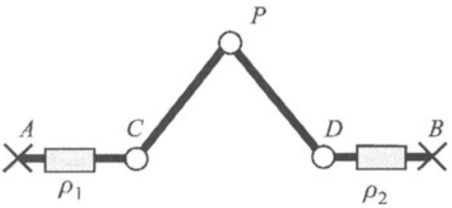

Figure 8: Biglide mechanism

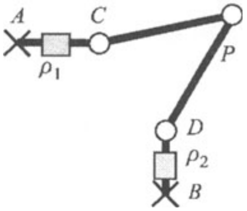

Figure 9: Isotropic mechanism

To define the joint limits, we will study the manipulability ellipsoids of matrix **K** [Yoshikawa 85]. By using equation (3), we can write a relation between the velocity $\dot{\mathbf{p}}$ of point P and the joint velocity $\dot{\rho}$ vector. With $\|\dot{\rho}\| \leq 1$, we have $\dot{\mathbf{p}}^T\ \mathbf{K}\mathbf{K}^T\ \dot{\mathbf{p}} \leq 1$. Equation (4) defines the range of variation of $\dot{\mathbf{p}}$. The transformation of a unit circle of the whole joint workspace by matrix $\mathbf{K}\mathbf{K}^T$ gives an ellipse in the Cartesian workspace [Lallemand 94]. The square roots γ_1 and γ_2 of the eigenvalues of matrix

$\mathbf{KK}^T$ are the values of the semi-axes of the ellipse which define the two velocity-amplification factors, $\lambda_1 = 1 / \gamma_1$ and $\lambda_2 = 1 / \gamma_2$, according to these principal axes.

To limit the variations of this factor in the Cartesian workspace, we set the constraints

$$1/3 < \lambda_i < 3. \tag{4}$$

This means that for a given joint velocity, the output velocity is at most three times larger or, at least, three times smaller than the velocity of P. This constraint also permits us to limit the loss of rigidity (velocity amplification lowers rigidity) and of accuracy (velocity amplification also amplifies the encoder resolution). The values in equation (4) were chosen as an example and should be defined precisely depending on the type of machining tasks.

To be able to compare the two mechanisms studied here, the distance between points A and B is the same in two cases, as well as the lengths L_1 and L_2. Likewise, the scale factors of the joint and the Cartesian workspaces are also equal.

In our design, we do not want any singular configuration in the Cartesian workspace. Also, the velocity-amplification factors are bounded in the Cartesain workspace when using the constraints introduced in equation (4). Thus, a *useful joint workspace* of a square shape is defined in the joint workspace as well as its image in the Cartesian workspace, which is the *useful Cartesian workspace.* In the case of the isotropic mechanism, the definition of a zone without singularities in the joint workspace, in the presence of constraints (4), leads to smaller joint limits than in the case of the biglide mechanism (Figures 10a and 11a). Moreover, the useful Cartesian workspace of the isotropic mechanism is better for machining because the registered square is seven times larger than that of the biglide mechanism (Figures 10b and 11b).

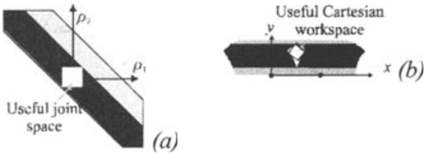

Figure 10: Joint and Cartesian workspaces for the biglide mechanism

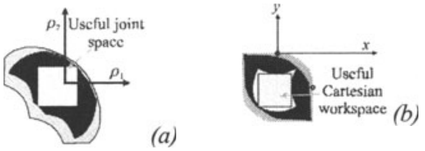

Figure 11: Joint and Cartesian workspaces for the isotropic mechanism

For the isotropic mechanism, we show in Figure 12 the curves of iso-values of the velocity-amplification factors. It is noted that velocity amplification λ_i varies within [0.4 , 1.6]. Moreover, if one limits a square zone in the useful Cartesian workspace, one observes that the constraints are reached only in one small zone (noted I), placed on the boundary.

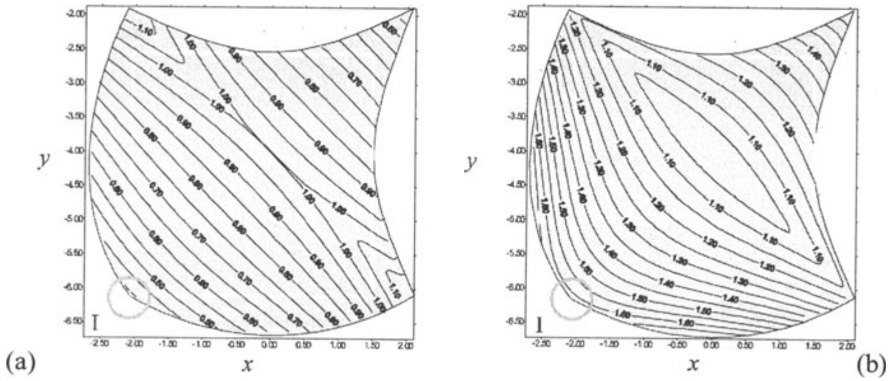

Figure 12: Curves of iso-values of the factor of velocity amplification factor (a) λ_1 and (b) λ_2, in the useful Cartesian workspace of the isotropic mechanism

3. CONCLUSIONS

Introduced in this paper is the isotropic design of a parallel mechanism with two degrees of freedom. The optimum design, based on the conditioning of the Jacobian matrices, led simultaneously to, good kinematic performance and a simple, regular Cartesian workspace free of singular configurations. The velocity amplification factor is used to define joint ranges. Its values are bounded by reasonably values in the workspace. Future work will aim at generalizing this mechanism to the spatial case, to obtain a parallel mechanism with three degrees of freedom.

12. REFERENCES

[Chablat 98]: Chablat D., " Domaines d'unicité et parcourabilité pour les manipulateurs pleinement parallèles ", Thèse de Doctorat, Nantes, Novembre, 1998.

[Lallemand 94]: Lallemand, J.P. et S. Zeghoul, Robotique: Aspects fondamentaux, Masson, Paris, 1994.

[Merlet 97]: Merlet J.P., Les robots parallèles, 2$^{\text{ème}}$ édition, Hermes, Paris, 1997.

[Yoshikawa 85]: Yoshikawa T., " Manipulability and redundant control of mechanisms", Proc. IEEE, Int. Conf. Rob. And Aut., pp. 1004-1009, 1985.

[Daniali 95]: Daniali M., " Contributions of the Kinematics Synthesis of Parallel Manipulators ", Thèse de doctorat, McGill, 1995.

[Gosselin 88]: Gosselin C., " Kinematic Analysis, Optimisation and Programming of Parallel robotic Manipulators ", Thèse de doctorat, McGill, 1988.

[Golub 89]: Golub G.H. et Van Loan C.F., *Matrix Computations,* The John Hopkins University Press, Baltimore, 1989.

13. AFFILIATIONS

D. Chablat, Ph. Wenger, Institut de Recherche en Communication et Cybernétique de Mantes, 1 rue de la Noë, 44321 Nantes, France.

J. Angeles, McGill Centre for Intelligent Machines, McGill University, 817 Sherbrooke Street West, Montreal, Quebec, Canada H3A 2K6.

DAIDIÉ A., LAKISS H., LERAY D., GUILLOT J.

APPLICATION OF THE DESIGN OF EXPERIMENTS METHOD TO A TRANSVERSELY LOADED CYLINDRICAL ASSEMBLY

Abstract: this article deals with bolted assemblies subjected to transverse loading. The design of experiments (DOE) method is applied to this type of assembly in order to analyse the behaviour of the various design parameters. The results of observation come from a finite elements model which was preliminarily validated by an experimental study. A factorial design with six factors and three levels, makes it possible to draw interesting conclusions about the various factors likely to influence the design of this type of connection.

1. INTRODUCTION

At present, the usual models for the computation of bolted assemblies only take axial loading into account [4]. In order to improve these models, we will focus on the behaviour of transversely loaded assemblies.

This type of assembly is in frequent use, particularly, in the automotive industry. The search for computational tools to be used from the preliminary design stage leads us to develop specific models of pre-sizing.

In order to reduce costs, experimental tests are limited to the setting of a numerical three-dimensional finite elements model. This model is based on the assumption that bolt bending is circular and has been validated by an experimental study [5].

After introducing the model from a mechanical point of view, the DOE method will be applied using the results of numerical simulations.

The DOE methodology is often applied in the experimental field of products or industrial processes. As for the present study, it will be used to analyse results of numerical simulations. This procedure should help us to exploit computing capabilities more fully and to carry out experiments only as checks.

2. ASSEMBLY PARAMETERS (FIGURE 1)

The assembly chosen for this study is composed of a cylindrical part, considered as a rigid body, resting against a frame and bolted by a high-strength screw. The study will only treat cases when the height dimension "h" is much greater than the screw shank diameter "d".

Depending on the position of the load application point, it can be observed that the model exhibits two stress types i.e. bending or shearing.

P. Chedmail et al. (eds.), Integrated Design and Manufacturing in Mechanical Engineering, 423-430.
©2002 *Kluwer Academic Publishers.*

2.1. Boundary conditions

- Displacements
  $U_A \neq 0$ (slip)
  $\mu = 0{,}2$ (friction coefficient)
- Normal stresses
  $\sigma_i \leq \sigma_{yield} = 650$ MPa (Plasticity)
  $\sigma_A \leq P_{yield} = 1000$ MPa (caulking)

2.2. Study parameters

- Factors
  d : Screw diameter
  Dp : Part diameter
  lp : Height of the part
  h : Position of load FT
  Q : Preload
  F_T : Transverse load
- Responses
  σ_i : Screw shank stress
  σ_A : Stress at point A of the part
  U_A : Displacement along the contact surface at point A

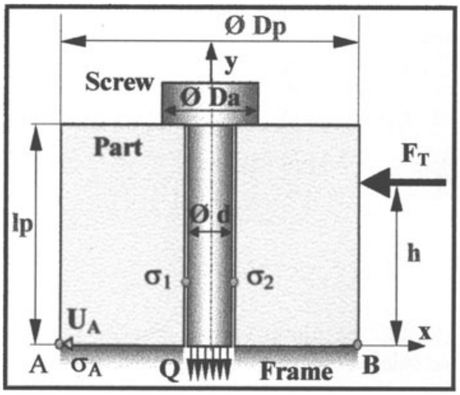

Figure 1. The assembly to be studied.

When bending is the dominant behaviour, the part may rock around point A. In the case of shearing, the part may slip relative to the mounting. Thus, slip occurs between the part and the mounting, when the shear stress τ_{XY} at point A reaches the limit value for the friction stress.

Apart from the phenomena of tilt and slip, limits have to be taken into account in order to avoid shank failure or caulking of the part at point A.

3. OBJECTIVES

The aim of this study is to size the assembly by controlling the six design parameters (or Factors). Acting on the variables enables us to observe the various behaviours of the structure.

The procedure used in this study, is based on the DOE method [1] [2] [6] [8] [9], which takes as responses the results of numerical simulations, in particular those of stresses and displacements. All finite element simulations have been carried out with I-DEAS and its SIMULATION application [7].

4. DESIGN FACTORIAL

Our problem comprises 6 design variables which can be varied at 3 levels in order to ascertain the effect of each parameter.

Within the scope of a complete study of the assembly, it would be necessary to carry out no less than 729 runs (36). This figure shows the physical difficulty in making a complete study. In order to remedy this problem, we have decided to use a fractional design. The BPEW Software proposes a minimum plan of 27 runs for three-levels of study.

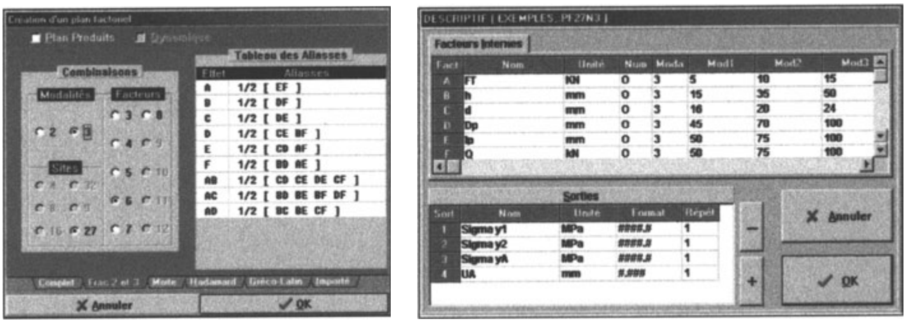

Combinaisons

Modalités: ○ 2 ● 3

Facteurs: ○ 3 ○ 4 ○ 5 ● 6 ○ 7 ○ 8 ○ 9 ○ 10 ○ 11 ○ 12

Sites: ○ 4 ○ 8 ○ 16 ○ 32 ○ 9 ● 27

Tableau des Aliasses

Effet	Aliasses
A	1/2 [EF]
B	1/2 [DF]
C	1/2 [DE]
D	1/2 [CE BF]
E	1/2 [CD AF]
F	1/2 [BD AE]
AB	1/2 [CD CE DE CF]
AC	1/2 [BD BE BF DF]
AD	1/2 [BC BE CF]

Fact	Nom	Unité	Num	Moda	Mod1	Mod2	Mod3
A	FT	kN	0	3	5	10	15
B	h	mm	0	3	15	35	50
C	d	mm	0	3	16	20	24
D	Dp	mm	0	3	45	70	100
E	lp	mm	0	3	50	75	100
F	Q	kN	0	3	50	75	100

Sorties

Sort	Nom	Unité	Format	Répét
1	Sigma y1	MPa	####.#	1
2	Sigma y2	MPa	####.#	1
3	Sigma yA	MPa	####.#	1
4	UA	mm	#.###	1

Figure 2. BPEW software design of experiments with 27 runs of 6 factors at 3 levels.

For the development of the numerical experimental tests, all factors are considered as continuous variables that vary within the experimental study. Choosing this type of variables will make it possible to build ideal models relating to the behaviour of the assembly (search for predictor). Figure 2 gathers together the different levels for each factor. For each test, 4 responses (σ_{Y1}, σ_{Y2}, σ_{YA}, U_A) are examined.

The choice of test values for each factor depends on the coherence of the expected results for the various responses. If all these results are to be within the field of solutions, it is necessary to seek the most constraining combinations of factors to find the extreme values suitable for each factor. The values for each factor are steadily spaced to ensure homogeneous coverage of the field of study.

This type of design makes it possible to process three interactions which are: AB (F_T.h), AC (F_T.d), AD (F_T.Dp). For these interactions, analysing the responses will enable us to examine their influence on assembly behaviour. Like most fractional designs, this type of design generates level 3 and 4 aliasings, i.e. there exist aliasings between actions and interactions as well as between different interactions. Thus, errors will certainly be found when estimating the effects of the factors, unless the interactions they are "aliased" to are negligible.

From the preceding remarks, a theoretical response Y~ can be established for each test. For the considered design, this theoretical response will have the following shape:

$$Y \sim = \overline{M} + A + B + C + E + F + AB + AC + AD \qquad (1)$$

Where the various parameters of this expression represent:

$\overline{M}$: general mean of responses
A, B... F: mean factor effect
AB, AC, AD: interaction between two factors.

5. VALIDATION OF THEORETICAL MODEL RESPONSE Y~

By comparing the theoretical responses to the numerical responses obtained with I-DEAS, notice the close correlation between the two results. By assuming that the residual represents the difference between the numerical value and the value calculated by the model, notice that, for the first three responses, they are very low; on the other hand for the displacement response, the value of the residual is higher than the acceptable displacement value.

This response analysis may already be considered to be difficult to apply. Table 1 summarises the maximum values obtained by this experiment.

Table 1: Summary of residuals for stress and displacement responses.

Response	σ_{Y1}	σ_{Y2}	σ_{YA}	U_A
Maximum residual	0,27	-0,37	2,26	0,03

6. FOR THE PURPOSES OF COMPARISON

The effects of the various factors may be represented on a common graph (Figures 3, 4 and 5). These graphs simply represent the tables of mean values. Note that the behaviour of σ_{Y1} is similar to that of σ_{Y2} (Figure 3). This shows the two main factors (d and Q) acting on the value of stress in the screw shank. The other factors do not change the response.

In the caulking response analysis (Figure 4), factor Dp is the dominating parameter when considering response σ_{YA}. In order to minimise caulking, it is best to choose the largest possible part diameter. However, it is to be noticed that some other factors have an impact, although less significantly, on caulking. Essentially F_T, h and Q have a significant impact. In the case of Q, this because additional preload implies additional normal force through the contact surface between the part and the mounting. In the case of F_T and h, the torque they generate is also transmitted via the contact surface.

The analysis of response U_A is much more difficult than the preceding ones. From Figure 5, notice that three factors seem crucial (F_T, lp, Q) in the study of slip U_A. The prevalence of F_T is logical insofar as it is the disturbing factor which must be controlled by the conditions of contact between the part and the rigid body. The intensity of factor Q influences the effectiveness of tightening and acts directly on contact behaviour. Raising the preload lessens the risk of slipping.

The last dominating factor, lp, is more difficult to understand. Reducing part height also lessens slipping. That can be explained by the fact that the influence of the preload is distributed correctly within the part. In addition, F_T.h interaction does not induce any bending.

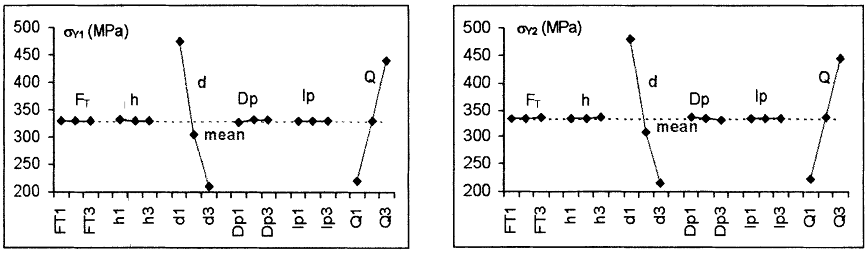

Figure 3. Graph of mean effects for σ_{Y1} and σ_{Y2}.

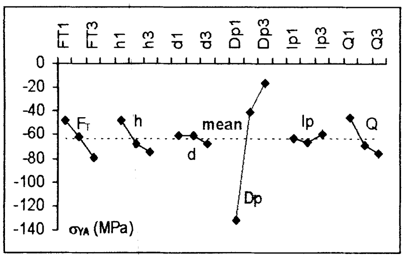

Figure 4. Graph of mean effects for σ_{YA}.

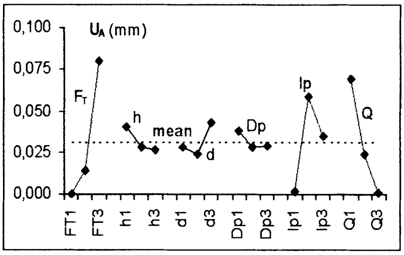

Figure 5. Graph of mean effects for U_A.

7. DETERMINING THE MOST INFLUENTIAL FACTORS

The method of variance analysis as been used after a DOE intended to identify the influential factors on a response. The variance of each factor and each interaction can be calculated. The analysis of variance (ANOVA) consists in comparing those variances with the residual variance using Snedecor's test. In order to reveal the significant factors, an analysis of variance, when possible, can be made with 99% confidence, i.e. $\alpha = 1\%$ risk of error.

7.1. Stresses σ_{Y1}, σ_{Y2}

Notice that the stresses in the screw shank (σ_{Y1}, σ_{Y2}) are comparable. For these responses, the ANOVA selected the five most significant factors, including two interactions. The screw diameter d and preload intensity Q are the two most important factors. This is not surprising as: the stress in the shank depends essentially on the diameter and on the preload.

The ANOVA also gives two interactions (F_T.h and F_T.Dp) as significant, but it must be noticed that their contribution is as low as 2%. It is interesting to investigate the cause of their influence, however. Indeed, considering the ANOVA or the graphs of mean effects, the aliases that are linked to the interactions are thought of as not having any significant influence on assembly behaviour. The only explanation for their significant presence would be found by examining each alias they are attached to (Figure 2). Notice that for the two interactions which interest us (AB and AD), the interaction d.Q appears in their alias.

In fact, it is the effect of this interaction which dominates compared to the other interactions. The analysis of σ_{Y1} is similar to that of σ_{Y2}. The same factors and interactions can be found to effect the assembly.

7.2. Caulking σ_{YA}

For this study, an ANOVA with a reliability of 99% revealed only one significant factor: D (Dp). To build an a useable model, it is necessary to increase the risk of error a to 5%. The ANOVA now reveals the significant influence of four factors ($A = F_T$, B = h, D = Dp, F = Q) and one interaction ($AD = F_T.Dp$). Among these principal factors, notice that the contribution of the effect of D (Dp) is highly significant since it represents 79 % of the sum of the effects. Once again, this result seems logical as caulking depends on the pressure distribution at the contact surface. The lower the area of contact surface, the higher the pressure.

The other factors, as well as the interaction, have the same level of contribution i.e. close to 5 % of the sum of the effects. In the analysis of interaction AD it is the effects of factors F_T and Dp that are actually measured and cleanly not the effects of aliased interactions. This shows that the interactions h.d and d.Q have little influence and thus do not disturb the interaction $F_T.Dp$. In addition, the aliasing of this interaction also implies the interaction h.lp. However, the latter is present in the aliasing of the interaction AC, which is not significant. We may consider that the influence of h.lp is not significant. In the study of stress responses, the reliability of results obtained is confirmed by Wilk-Shapiro test.

7.3. Slip U_A

Note that running the test of Wilk-Shapiro rejects the assumption of normality. In this case, the statistical results are less reliable. We erroneous interpretations of the various influences obtained by an ANOVA are likely. Consequently, this response will not be taken into account in the design of experiments.

8. CALCULATION OF THE PREDICTORS

Taking into consideration the preceding remarks, numerical models will be established for σ_{Y1}, σ_{Y2}, σ_{YA}. Only the most significant factors will be taken into account (Table 3).

For this approach, the values of the various factors will be limited to the value of one level. To define the "discrete Predictor", the model is written in a matrix form [10]. The factors are represented by vectors whose active level is 1 and the two others are taken at 0. The effects of each factor as well as the interactions are modelled by matrices.

The results obtained for the models σ_{Y1}, σ_{Y2} are very satisfactory since error compared to the bench-mark data of I-DEAS does not exceed 1.5%.

Concerning response σ_{YA}, the comparisons show more important variations than the other responses. The highest differences are close to 20 MPa. Looking at the tests as a whole, only four of them give errors higher than 10% with a maximum of 23%. However, we note that the most important errors are for low values of caulking stresses. When using a sizing approach, extreme limits are usually considered ; in this case, our model remains reliable.

Table 3. Model calculated for response σ_{Y2}, σ_{YA}.

$$\boldsymbol{\sigma}_{Y2}\ \tilde{}_{cal} = 334{,}21 + \begin{bmatrix}145{,}81 & -26{,}20 & -119{,}61\end{bmatrix}\mathbf{C} + \begin{bmatrix}-111{,}72 & 0{,}70 & 111{,}02\end{bmatrix}\mathbf{F} + \mathbf{A}^t\begin{bmatrix}-20{,}48 & 30{,}11 & -9{,}63\\ -10{,}73 & -18{,}74 & 29{,}48\\ 31{,}21 & -11{,}37 & -19{,}84\end{bmatrix}\mathbf{D}$$

$$+\mathbf{A}^t\begin{bmatrix}-28{,}83 & 9{,}94 & 18{,}89\\ 19{,}08 & -29{,}64 & 10{,}57\\ 9{,}76 & 19{,}70 & -29{,}46\end{bmatrix}\mathbf{B} + \begin{bmatrix}3{,}09 & -1{,}20 & -1.89\end{bmatrix}\mathbf{D}$$

$$\boldsymbol{\sigma}_{YA}\ \tilde{}_{cal} = -63{,}16 + \begin{bmatrix}-68{,}71 & 21{,}85 & 46{,}86\end{bmatrix}\mathbf{D} + \begin{bmatrix}15{,}26 & 0{,}91 & -16{,}17\end{bmatrix}\mathbf{A} + \begin{bmatrix}17{,}51 & -5{,}38 & -12{,}13\end{bmatrix}\mathbf{F}$$

$$+\begin{bmatrix}15{,}66 & -4{,}36 & -11{,}30\end{bmatrix}\mathbf{B} + \mathbf{A}^t\begin{bmatrix}18{,}85 & -5{,}99 & -12{,}86\\ 0{,}60 & -0{,}26 & -0{,}34\\ -19{,}45 & 6{,}25 & 13{,}20\end{bmatrix}\mathbf{D}$$

9. CHECK TESTS

After establishing the different behavioural models of the bolted assembly, it is necessary to carry out additional tests to check their quality. It is imperative that these new tests should be different from those that were already carried out for the design, but they must be contained within the domain of validity of the design.

In the shaded boxes, Table 4 recapitulates this information. Some factors (in italics), are not taken into account in the model but are essential for a calculation with I-DEAS.

Table 4. Comparison of responses from I-DEAS and BPEW discrets models.

	A	B	C	D	E	F	σ_{Y1} (MPa)		σ_{Y2} (MPa)		σ_{YA} (MPa)	
	F	**h**	**d**	**Dp**	**lp**	**Q**	**Response**		**Response**		**Response**	
	(kN)	(mm)	(mm)	(mm)	(mm)	(kN)	**IDEAS**	**BPEW**	**IDEAS**	**BPEW**	**IDEAS**	**BPEW**
$\sigma_{Y1\,max}$	10	15	M16	100	*50*	100	636,07	636,64	636,36	637,71	-12,62	-12,2
					100		636,81	636,64	637,08	637,71	-13,55	-12,2
$\sigma_{Y2\,max}$	15	35	M16	45	*50*	100	631,06	631,06	646,20	645,04	-195,25	-183,98
					100		633,42	631,06	641,26	645,04	-171,87	-183,98
$\sigma_{YA\,min}$	15	50	*M24*	45	*100*	100	291,54	317,42	305,59	330,46	-205,62	-190,92
			M16				630,31	582,50	644,48	595,88	-202,47	-190,92
	15	15	M16	100	*75*	100	580,03	580,29	580,04	579,07	-17,09	-15,74
					60		579,97	580,29	579,98	579,07	-14,47	-15,74

The values of these factors in the code to are varied in order to check that their contribution remains insignificant.

Simulation results and the results from the predictor models correlate closely. Assuming that the numerical values obtained by I-DEAS can be used as a reference, note that the error of the predictor models does not exceed 10%.

Within the scope of search for a solution, these results are definitely acceptable.

10. CONCLUSION

On the one hand, we have highlighted the most important parameters for various responses. Although for some of the responses these factors were intuitively obvious (d, Q for the stress in the screw shank), the method of DOE made it possible to confirm these influences in a more objective way. On the other hand, when dealing with caulking and slipping, the most significant parameters have been detected, but operating the mathematical model has proved difficult in the case of (U_A).

Results may be more coherent if the range of different factors is varied, and the field of investigation widened. For instance, the preload (Q) could correspond to 30%, 60% and 90% of the yield stress in the screw. The assembly could then be set with parameters of no dimension, enabling assemblies with other screw dimension to be studied.

11. AFFILIATION

DAIDIÉ Alain, LAKISS Hassan, LERAY Dimitri, GUILLOT Jean
Laboratoire de Génie Mécanique de Toulouse – INSA
135 avenue de Rangueil 31077 Toulouse (France)
e-mail: alain.daidie@insa-tlse.fr

12. REFERENCES

[1] Benoist, D., Tourbier, Y, "Plans d'expériences : Construction et analyse", Editions Lavoisier Techniques et Documents, PARIS, France, pp 700, 1995.

[2] Box, G. E. P., Hunter W.G., Hunter J.S., "Statistics for experimenters: an introduction to design, data, analysis, and model building", John Wiley & Sons, New York, 1978.

[3] BPEW Software, Promostar, Sarl BP 2132, 69603 Villeurbanne Cedex, France.

[4] Guillot J., "Assemblages par éléments filetés - Calculs-.Technique de l'ingénieur", Tome 1 B5560 à B5562, 21 rue cassette, 75006, Paris, 1987.

[5] Lakiss, H., "Etude des assemblages boulonnés chargés transversalement par des efforts dynamiques avec prise en compte des conditions de contact", Ph.D.Thesis, INSA Toulouse, France, 2000.

[6] Sado, G., Sado, M.-C., "Les plans d'expériences : De l'expérimentation à l'assurance qualité", Afnor technique, pp 266, 1996.

[7] SDRC (Structural Dynamic Research Corporation), I-DEAS MS7 software, 2000 Eastman Drive, Milford, Ohio 45150, Printed in the U.S.A, 1999.

[8] Tagushi, G., "On-line quality control during production", American Supplier Institute, Dearborn, Michigan, USA, 1981.

[9] Tagushi, G., "System of experimental Design", Vol 1 et 2, Kraus, 1987.

[10] Viguier, M., "Pratique des plans d'expériences : Méthodologie Taguchi et compléments", Les Editions d'organisation, Paris, France, 1988.

DETERMINATION OF THE MODE DOMINANCE FOR MODEL REDUCTION

Kefu Liu[1] and Xiaodong Sun
Department of Mechanical Engineering, Lakehead University
Thunder Bay, Ontario, Canada P7B 5E1

Abstract. When time domain state-space identification algorithms are employed, identified models may need to be overparameterized due to system nonlinearity or measurement errors. After an initial oversized model is obtained, model reduction must be conducted. An important step in model reduction is to determine those significant modes. Several commonly used model reduction methods such as the balanced realization (BR) technique select significant modes by minimizing the impulsive response error between the original model and reduced model. This study proposes an alternative method. The method is based on modal approximation. Two indices are devised to determine significant and insignificant modes. The parameter matrices expressed in the modal realization are reduced by eliminating the terms corresponding to the insignificant modes. Experimental modeling of a flexible manipulator system is used to demonstrate the effectiveness of the proposed method. The results using the BR technique are also given as a comparison.

1. Introduction

State-space model is a popular model used to represent linear time-invariant systems. For computer control systems, discrete-time state-space model is often employed. Identification of a discrete-time state-space model determines the parameter matrices using experimental input/output data. Some well-known time domain state-space identification algorithms are the Eigensystem Realization Algorithm (ERA) [1], the Observer/Kalman Filter System Identification algorithm (OKID) [2], and the Observability Range Space Extraction identification algorithm (ORSE) [3]. The methods can achieve high accuracy when a model is properly overparameterized. An overparameterized model contains significant modes and insignificant modes. Insignificant modes include less important system modes and computational modes caused by nonlinearity and measurement noise. Model reduction intends to obtain a lower-order model by eliminating insignificant modes. The reduced-order model should capture the essential characteristics of the underlying physical system.

An important issue for model reduction is how to distinguish between significant modes and insignificant modes. Several commonly used model reduction methods such as the balanced realization (BR) technique determine significant modes by minimizing the error of the impulsive responses between an original model and reduced one. The experience with the BR technique has revealed some limitations of the technique. First, to apply the BR technique, models must be asymptotically stable [4]. For systems that contain rigid modes or lightly damped modes, identified models may not be stable. Second, the measure of minimizing the impulsive response error tends to overemphasize lightly

---

[1] Tel.: (807) 343-8634; Fax: (807) 343-8928
Email: kefu.liu@lakeheadu.ca

P. Chedmail et al. (eds.), Integrated Design and Manufacturing in Mechanical Engineering, 431-438.
©2002 *Kluwer Academic Publishers.*

damped modes. Third, the BR technique involves determination of a threshold for small Hankel singular values and the choice of a threshold value is more or less a matter of subjective judgement. From the controllability point of view, a mode with a small Hankel singular value means that it requires a large control effort, not necessarily is insignificant.

In this study, we propose to employ the modal approximation concept for model reduction. With the parameter matrices expressed in modal coordinates, it is easy to determine the model stability. An unstable model can be forced to be stable by modifying the eigenvalues that are outside the unit circle [5]. We suggest to judge the model accuracy in terms of the error between the actual response and the simulated response generated by the reduced-order model. This criterion is consistent with system identification, i.e., the best fit between the measured output of the system and the simulated output of the model used. Because the total response is the sum of individual modal responses, modal responses can be used to quantify the contribution of individual modes to the total response. Based on this rationale, two indices are proposed. The first index is referred to as the Modal Response Magnitude (MRM) as it intends to measure the magnitude of an individual modal response. The second index is referred to as the Modal Response Coherence (MRC) as it intends to measure the degree of correlation between an individual modal response and the actual response. We use a single-link flexible manipulator as an example to illustrate the application of the proposed technique. Initial models with different orders are identified using the ORSE algorithm. The models reduced using the proposed technique are compared with the models reduced using the BR algorithm. The observations are drawn.

2. Indices of the Mode Dominance

A linear time-invariant system can be represented by a discrete-time state-space mode as

$$\begin{aligned} x(k+1) &= \mathbf{A}x(k) + \mathbf{B}u(k) \\ y(k) &= \mathbf{C}x(k) + \mathbf{D}u(k) \end{aligned} \tag{1}$$

where $u(k) \in R^{r\times 1}$ is the system input vector, $x(k) \in R^{n\times 1}$ the system state vector, $\mathbf{A} \in R^{n\times n}$ the state transition matrix, $\mathbf{B} \in R^{n\times r}$ the input influence matrix, $\mathbf{C} \in R^{m\times n}$ the output influence matrix, $\mathbf{D} \in R^{m\times r}$ the direct transmission matrix, $\mathbf{y}(t) \in R^{m\times 1}$ the output vector, r the number of the inputs, n the number of the state variables or the model order, m the number of the outputs, and the notation $R^{i\times j}$ represents the $i \times j$ real matrix space. In this study, it is assumed that the output is not directly related to the input, i.e., $\mathbf{D} = \mathbf{0}$.

In experiment, the output $y(k)$ is contaminated by measurement noise $w(k)$ giving the measured output $\tilde{y}(k)$

$$\tilde{y}(k) = y(k) + w(k). \tag{2}$$

The input $u(k)$ for $k = 0, 1, \cdots, K-1$, is assumed to be noise free as it is generated by computer. With experimental data samples $\tilde{y}(k)$ and $u(k)$ for

$k = 0, 1, \cdots, K-1$, system identification finds the parameter matrices in the following equations

$$\begin{aligned} z(k+1) &= \bar{\mathbf{A}}z(k) + \bar{\mathbf{B}}u(k) \\ \hat{y}(k) &= \bar{\mathbf{C}}z(k) \end{aligned} \tag{3}$$

where

$$z(k) = \mathbf{T}^{-1}x(k),\ \bar{\mathbf{A}} = \mathbf{T}^{-1}\mathbf{A}\mathbf{T},\ \bar{\mathbf{B}} = \mathbf{T}^{-1}\mathbf{B},\ \bar{\mathbf{C}} = \mathbf{C}\mathbf{T}, \tag{4}$$

and $\mathbf{T} \in R^{n\times n}$ is any nonsingular matrix. Equation (3) is another realization of equation (1). The response $\hat{y}(k)$ is named as the simulated or predicted response. The ORSE algorithm achieves this goal in the two steps. First, the $\bar{\mathbf{A}}$ and $\bar{\mathbf{C}}$ matrices are determined by solving the following least-squares problem

$$\min_{\bar{\mathbf{A}},\,\bar{\mathbf{C}}} \|\tilde{y}(k) - \hat{y}(k)\|_2\,. \tag{5}$$

Then, the $\bar{\mathbf{B}}$ matrix is found by solving the following least squares problem

$$\min_{\bar{\mathbf{B}}} \|\tilde{y}(k) - \hat{y}(k)\|_2\,,\ \text{subject to } \bar{\mathbf{A}},\ \bar{\mathbf{C}} \text{ given by (5).} \tag{6}$$

With an overparameterized model $(\bar{\mathbf{A}}, \bar{\mathbf{B}}, \bar{\mathbf{C}})$, model reduction finds a reduced-order model $(\bar{\mathbf{A}}_R, \bar{\mathbf{B}}_R, \bar{\mathbf{C}}_R)$ according to a pre-chosen criterion. The model reduced using the BR technique is closest to the original model in the sense of the minimum error between the impulse responses or the frequency responses of the two models, i.e.,

$$\min \|G(J\omega) - G_R(J\omega)\|_2 \tag{7}$$

where $\mathbf{G}(J\omega) = \bar{\mathbf{C}}(e^{J\omega\Delta t}\mathbf{I} - \bar{\mathbf{A}})^{-1}\bar{\mathbf{B}}$ and $\mathbf{G}_R(J\omega) = \bar{\mathbf{C}}_R(e^{J\omega\Delta t}\mathbf{I} - \bar{\mathbf{A}}_R)^{-1}\bar{\mathbf{B}}_R$ are the frequency response functions for the initial and reduced-order models, respectively, $J = \sqrt{-1}$, ω is the frequency variable, and Δt is the sampling interval. The criterion assumes that impulse is used as input to the system. The minimum impulse response error may not guarantee the minimum response error if the system excitation is not impulse. As the objective of system identification is to minimize the prediction error between the actual response and simulated one, we propose to judge the model closeness in terms of the minimum error between the actual response and the simulated one. The problem becomes to determine those modes that contribute significantly to the total response. This can be done by using the modal approximation concept.

The simulated response consists of n modal responses which can be obtained in the following way. An eigendecomposition is conducted on the identified transition matrix

$$\bar{\mathbf{A}} = \mathbf{\Psi}\Lambda\mathbf{\Psi}^{-1} \tag{8}$$

where

$$\Psi = \begin{bmatrix} \psi_1 & \cdots & \psi_{n_1} & \psi_{n_1+1} & \cdots & \psi_n \end{bmatrix} \in C^{n\times n} \tag{9}$$

is the eigenvector matrix and

$$\Lambda = \mathrm{diag}\begin{bmatrix} \lambda_1 & \cdots & \lambda_{n_1} & \lambda_{n_1+1} & \cdots & \lambda_n \end{bmatrix} \in C^{n\times n} \tag{10}$$

is the eigenvalue matrix. The notation $C^{i\times j}$ represents the $i \times j$ complex matrix space. It is assumed that there are $n_1/2$ pairs of complex eigenvalues and eigenvectors, i.e., $\lambda_{j+1} = \lambda_j^*$, $\psi_{j+1} = \psi_j^*$ for $j = 1, 3, \cdots, n_1 - 1$ where the superscript '*' denotes complex conjugate. The remaining $n - n_1$ eigenvalues and eigenvectors are real. Defining a set of new states in modal coordinates as

$$\eta(k) = \mathbf{\Psi}^{-1} z(k) \tag{11}$$

then equation (3) becomes

$$\begin{aligned} \eta(k+1) &= \mathbf{\Lambda}\eta(k) + \hat{\mathbf{B}}u(k) \\ \hat{y}(k) &= \hat{\mathbf{C}}\eta(k) \end{aligned} \tag{12}$$

where

$$\hat{\mathbf{B}} = \mathbf{\Psi}^{-1}\bar{\mathbf{B}} = \left[\begin{array}{cccccc} \hat{b}_1^T & \cdots & \hat{b}_{n_1}^T & \hat{b}_{n_1+1}^T & \cdots & \hat{b}_n^T \end{array}\right]^T \in C^{n\times r} \tag{13}$$

$$\hat{\mathbf{C}} = \bar{\mathbf{C}}\mathbf{\Psi} = \left[\begin{array}{cccccc} \hat{c}_1 & \cdots & \hat{c}_{n_1} & \hat{c}_{n_1+1} & \cdots & \hat{c}_n \end{array}\right] \in C^{m\times n}. \tag{14}$$

It is noted that complex quantities appear in pairs, i.e., $\hat{b}_{j+1} = \hat{b}_j^*$ and $\hat{c}_{j+1} = \hat{c}_j^*$ for $j = 1, 3, \cdots, n_1 - 1$. The system response is a sum of the modal responses, i.e.,

$$\hat{y}(k) = \sum_{j=1,3}^{n_1-1} \hat{y}_j(k) + \sum_{j=n_1+1}^{n} \hat{y}_j(k) \tag{15}$$

where $\hat{y}_j(k) \in R^{m\times 1}$ is the response of the jth mode or the jth modal response. Modal approximation assumes that the response can be approximated by a summation of dominant modal responses. For a pulse input, i.e., $u(0) = 1$ and $u(k) = 0$ for $k \neq 0$, the modal response of a pair of complex modes is given by

$$\hat{y}_j(k) = \hat{c}_j\lambda_j^{k-1}\sum_{l=1}^{r}\hat{b}_{jl} + \hat{c}_j^*(\lambda_j^*)^{k-1}\sum_{l=1}^{r}\hat{b}_{jl}^*,\ j = 1, 3, \cdots, n_1 - 1, \tag{16}$$

and the modal response of a real mode is given by

$$\hat{y}_j(k) = \hat{c}_j\lambda_j^{k-1}\sum_{l=1}^{r}\hat{b}_{jl},\ j = n_1 + 1, \cdots, n. \tag{17}$$

As it can be seen that the pulse responses depend on the input influence coefficients, output influence coefficients, and eigenvalues. For an asymptotically stable mode, i.e., $|\lambda_j| < 1$, $\hat{y}_j(k)$ approaches zero when k approaches infinity. If the modal responses to a pulse input are used to judge the mode dominance, the modes with a small magnitude of λ_j such as heavily-damped modes, may be considered less significant than the modes with a large magnitude of λ_j as the former vanishes faster than the latter. This shows that the use of pulse responses or impulsive responses to measure the mode dominance is problematic as it tends to overemphasize lightly-damped modes. Therefore it is important that the modal responses to the actual input used in identification be used in the proposed indices.

To determine the mode dominance, a Modal Response Magnitude (MRM) is defined to measure the average magnitude of the jth modal response:

$$MRM_j = \frac{\sum\limits_{i=1}^{m}\Big(\sum\limits_{k=0}^{K-1} \left|\hat{y}_{ij}(k)\right| / K\Big)}{\sum\limits_{i=1}^{m}\Big(\sum\limits_{k=0}^{K-1} \left|\tilde{y}_{i}(k)\right| / K\Big)},\ j = 1, 3, \cdots, n_1 - 1, n_1 + 1, \cdots, n. \qquad (18)$$

A mode with a large MRM is considered to be significant. However, the MRM only reflects one aspect of the modal responses as it is based only on the response magnitude. To measure the correlation between an individual modal response and the actual response, a Modal Response Coherence (MRC) is defined as

$$MRC_j = \max_i\Bigg(\frac{\sum\limits_{k=0}^{K-1} \hat{y}_{ij}(k)\tilde{y}_i(k)}{\sum\limits_{k=0}^{K-1} \tilde{y}_i(k)\tilde{y}_i(k)}\Bigg),\ j = 1, 3, \cdots, n_1 - 1, n_1 + 1, \cdots, n. \qquad (19)$$

3. Application of the Proposed Technique

In this section, reduction of identified models for a single-link flexible manipulator is used as an example. The identification of initial models using the ORSE algorithm has been reported in [6]. The system consists of a flexible arm, a bevel gear set, a direct current (DC) motor, the current amplification and signal conditioning circuitry, and PC computer. The arm is made of 6061-T6 aluminum with the dimension of 1 × 0.051 × 0.003 m. The motor used in this experimental setup is a permanent magnet DC motor with a rated stall torque of 2.938 N-m. The control input is a voltage signal generated by the computer. A linear amplifier circuitry converts the input voltage to motor current. The DC motor has an integral tachometer to measure motor shaft speed. A potentiometer is attached to the arm hub to measure its angular position. Vibrations of the arm are measured using two Wheatstone bridges. The first bridge is located near the clamped end of the arm. The second bridge is placed in the middle of the arm. The computer used to control the system is a Pentium II with a speed of 200 MHz. A National Instruments PCI-MIO-16E-4 data acquisition board is used for real time control. LabWindows by National Instruments is used for programming. Totally, there are four system outputs, namely, the potentiometer signal, the tachometer signal, the base strain gauge signal, and the middle strain gauge signal. The experimental setup is, therefore, a system with a single input and four outputs, i.e., $r = 1$ and $m = 4$. It is also noted that the direct transmission matrix **D** is zero.

A prior knowledge of the system dynamics is useful for determination of a proper order for the model. The motion of the system consists of the rigid motion of the arm hub and flexible/vibratory motion of the arm. Depending on the modeling extent, the rigid motion may be represented using two or three modes. If the system is perfectly linear and the measurement is free of noise, a state-space model that includes up to the third vibratory mode should have a minimum order of 8 or 9. However, a first-order low-pass filter is used for the tachometer signal. Presence of Coulomb friction in the rigid body motion is noticeable. It was also noted that depending on operation condition, the beam may behave close to a clamped-free beam (the first three natural frequencies are 2.6, 16.2, and 45.5 Hz) or a pinned-free beam (the first two natural frequencies are 11.4 and 36.9 Hz) or somewhere in between. All these irregularities require that an initial model be overparameterized.

$n = 13$			$n = 21$		
modes	f_j	ζ_j	modes	f_j	ζ_j
1/2	23.64	.0289	1/2	46.61	.0324
3/4	20.90	.0568	3/4	23.58	.0075
5/6	9.968	.0215	5/6	22.44	.0523
7/8	7.466	.0864	7/8	19.97	.0321
9/10	2.537	.3415	9/10	10.64	.0184
11/12	.4542	.7319	11/12	9.424	.0192
13	real, $\lambda_{13} > 1$		13/14	7.383	.0623
			15/16	4.369	.0796
			17/18	1.852	.3644
			19/20	.4338	.6150
			21	real, $\lambda_{21} > 0$	

Table 1. Modal information of the initial models.

$n = 13$		$n = 21$	
MRM	MRC	MRM	MRC
11/12	11/12	19/20	19/20
3/4	7/8	21	21
7/8	13	13/14	13/14
13	9/10	5/6	17/18
9/10	3/4	17/18	5/6
5/6	5/6	1/2	11/12
1/2	1/2	7/8	1/2
		11/12	7/8
		15/16	15/16
		9/10	9/10
		3/4	3/4

Table 2. Ranking of the mode dominance.

Table 1 lists the modal information for two initial models identified using the same data. The exciting signals used were a series of square waveforms with varying periods. The sampling interval was chosen to be $\Delta t = 1/300$ sec. and the data length was $K = 3000$. Both the initial models are unstable and have one real eigenvalue that is outside the unit circle. Using the proposed technique, the models were transformed into modal coordinates. To force the models to become stable, the eigenvalue that is greater than one was forced to be 0.9999. The modal responses of the individual modes were generated using the actual inputs. The proposed indices were evaluated using the simulated modal responses. Table 2 ranks the mode dominance in a descending order, i.e., from the most significant to the least significant. Table 3 gives the prediction errors defined by

$$\bar{\delta} = \sum_{i=1}^{4} \delta_i/4,\ \delta_i = \frac{\mathrm{RMS}(\tilde{y}_i - \hat{y}_i)}{\mathrm{RMS}(\tilde{y}_i)},\ i = 1, \cdots, 4. \tag{20}$$

where RMS denotes root-mean-square error. In Table 3, $\bar{\delta}_0$ denotes the errors of the initial models, $\bar{\delta}_{MRM}$ the errors of the models reduced according to the MRM ranking, $\bar{\delta}_{MRC}$ the errors of the models reduced according to the MRC ranking, and $\bar{\delta}_{BR}$ the errors of the models reduced according to the BR technique. For brevity, in the following discussion, the models reduced according to the MRM, MRC ranking, and BR technique are referred to as the MRM, MRC, and BR models, respectively.

initial models	n'	$\bar{\delta}_{MRM}$	$\bar{\delta}_{MRC}$	$\bar{\delta}_{BR}$
$n = 13$, $\bar{\delta}_0 = .3126$	9	.3629	.3629	.3920
as above	7	.4637	.5179	.6233
$n = 21$, $\bar{\delta}_0 = .3096$	11	.4006	.3975	.6090
as above	7	.4974	.4993	.6418

Table 3. Prediction errors of the reduced-order models.

If the 13rd-order model is reduced to a 9th-order model, the MRM and MRC models are slightly better than the BR model. However, if the 13rd-order model is reduced to a 7th-order model, the MRM and MRC models are much better than the BR model. Model reduction for the initial 21st-order model gives a similar result.

$n = 13$, $n' = 8$			$n = 21$, $n' = 12$		
$\bar{\delta}_{BR} = .4996$			$\bar{\delta}_{BR} = .5065$		
modes	f_j	ζ_i	modes	f_j	ζ_i
1/2	21.12	.0553	1/2	46.59	.0331
3/4	9.961	.0210	3/4	22.20	.0618
5/6	7.419	.1043	5/6	19.32	.0290
7, 8	real		7/8	9.396	.0236
			9/10	7.557	.0757
			11, 12	real	

Table 4. Modal information of the minimum-order BR models.

With the BR technique, a proper model order should be determined using the Hankel singular value ranking. Table 4 gives the modal information of the BR models reduced in such a way. It should be pointed out that, in both the cases, the quality of the reduced-order models is not as good as that of the lower-order models reduced by the proposed technique. It is also noted that the representation of those vibratory modes is redundant.

4. Conclusion

This study has been motivated by overcoming some shortcomings of the balanced realization technique. A technique based on modal approximation has been developed. An initial model is transformed into its modal representation. Individual modal responses to the actual input are generated using the identified model in the modal realization. The modal response magnitude (MRM) measures the magnitude of individual modal response. The modal response coherence (MRC) measures the correlation between the simulated modal responses and the measured responses. A lower-order model is obtained by eliminating those terms in the parameter matrices corresponding to the insignificant modes. The reduced-order model is an approximation of the initial model in the sense that its simulated responses are close to the measured responses.

Based on the study, the following conclusions can be drawn. (1) The models reduced according to the MRM or MRC ranking have better model accuracy than those reduced by the BR technique. (2) When the model order is not large enough, the BR technique tends to miss some modes associated with the rigid body motion while it can capture the vibratory modes. (3) In general, the models reduced using the BR technique still contain some computational modes.

5. References

1. Juang J. -N. and Pappa R. S. An eigensystem realization algorithm for modal parameter identification and model reduction. Journal of Guidance 1985;8(5):620-627.

2. Juang J. -N. Applied System Identification. Englewood Cliffs, New Jersey: Prentice Hall, 1994.

3. Liu K. and Miller D. W. Time domain state space identification of structural systems. ASME Journal of Dynamic Systems, Measurement, and Control. 1995;117:608-618.

4. Moore B. Principal component analysis in linear systems: controllability, observability, and model reduction, IEEE Trans. on Automatic Control. 1981:26(1):17-31.

5. Bauer R. J. and Hughes P. C. Three approaches to balanced order reduction of unstable models; 1999, Proceedings of the SEM annual conference on theoretical, experimental and computational mechanics, 1999 June 7-9; Cincinnati. Ohio.

6. Liu K. and Sun X. System identification and model reduction for a single-link flexible manipulator. Journal of Sound and Vibration, 2001;242(5):867-891.

DEVELOPMENT OF A NEW METHODOLOGY FOR DELAMINATION DETECTION IN LAMINATED STRUCTURES.

J.C. WALRICK[1], D. COUTELLIER[1], P. GEOFFROY[2]
[1]LAMIH- UMR CNRS 8530, 59313 Valenciennes Cedex 9
[2]O.N.E.R.A - DMSE. 5, Boulevard Paul-Painlevé, 59045 Lille Cedex.
Daniel.Coutellier@univ-valenciennes.fr

Abstract: A new methodology to study the behaviour of delaminated composite structures has been developed. This study can be split up into two parts:

- The first one is about the detection of delamination in damaged laminated thin structures. In the finite element computational code, those laminated structures are modelled using shell elements. The methodology uses post-process criteria based on fracture mechanics linked with damage mechanics of computational code by the effective stress tensor.
- In the second place, the influence of delamination over the overall behaviour of the structure is taken into account. This influence is introduced by locally changing the material characterisation, progressively during the loading phase. These integrated effects change the numerical behaviour on loading and energy curves.

Experimental validation studies are carried out in static tension tests, static and dynamic tests and low velocity impact with a spherical tool. The comparison between experimental and numerical results allows us to conclude to a good correlation and to the validation of this methodology. Many perspectives appeared at completion of this work.

INTRODUCTION

The composite laminate structures are being used to an increasing extent in the transportation domain, specially developed for aeronautical design. Actually, continuous fibre reinforced resins plies give significant weight gain, efficient load carrying capabilities and a good strength fracture.

Unfortunately, those laminates have a relative sensitivity to the low velocity impact damage. So, crashworthiness is one of the foremost goals of aircraft design and certification, especially for strength fracture assessment and mechanical behaviour prediction under damage. Accurate analyses of different damage modes are complex and different kinds of damage mechanics are distinguished within a ply: matrix-cracking, fibre fracture and shear cracks in fibre-matrix interface. This damage has lead to an inter-plies damage: the delamination, which has a major influence on structure overall behaviour under loading. To that aim, the delamination effects must be taken into account in order to provide as accurate a representation as might be of all the damaging processes. The objective of this research was to develop a numerical methodology to follow up the delamination growth in the finite element (F.E.) modelling of composite laminate.

P. Chedmail et al. (eds.), Integrated Design and Manufacturing in Mechanical Engineering, 439-446.
©2002 *Kluwer Academic Publishers.*

Delamination mechanisms are linked to the stacking sequence. We distinguish the damage behaviour: the first stable, leading to a progressive overall failure, the second, unstable with a brutal collapse.

Thanks to the methodology, a new computation, introducing delamination, is applied to bring more accurate mechanical behaviour prediction, until total fracture. Some experimental programmes have been undertaken to validate numerical observations from methodology. We achieved three point bending tests with two kinds of laminate and a localised low velocity impact test on clamped plates.

FINITE ELEMENT MODEL USED

In finite element simulation, more often than not, the thin laminated structures are modelled using shell elements. Most models are made with several shells in the thickness with particular attention to produce the stacking sequence of plies. Thus, the approach of this work is different: in a dynamic computational code, a single multi-layer element shell has been developed [1] for this kind of structures with uni-directional long fibre composite plies.

For delamination location, we define an epoxy interface between different direction plies (figure 1). The interface is thinner than the other plies.

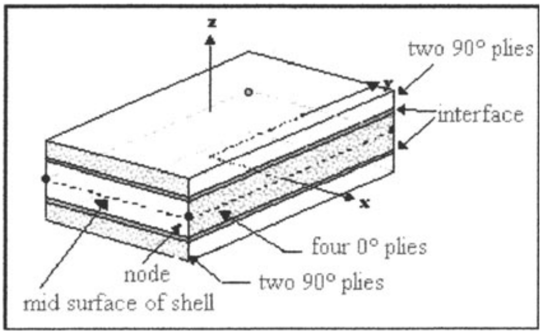

Figure 1. Single multi-layer element.

However, this element does not allow any physical representation of inter-layer cracks opening displacements (i.e. Mode I of fracture mechanics) associated with delamination. So, this study deals only with the shear fracture effects (Mode II and III), whose stress components are already available. The ply model available in the code is defined as a homogenous orthotropic material; this means there is no distinction between fibre and matrix characteristics. The mechanical behaviour ply corresponds to damage-elasticity. Damage growth in the composite ply is introduced thanks to two variables d_{12} and d_{22} whose values can increase from 0 (no damage) to 1 (total failure) [2]. d_{22} is linked with the transverse crack in the matrix under tension and is applied to transverse Young's Modulus E_{22} by :

$$E_{22} = E_{22}^{0}.(1-d_{22}) \text{ if } \sigma_{22} > 0 \qquad (1)$$

with E_{22}^0 initial modulus for undamaged ply.

d_{12} controls the shear cracks in fibre/matrix interface with the G_{12} shear modulus.
$G_{12} = G_{12}^0.(1\text{-}d_{12})$ (2)

with G_{12}^0 representing initial shear modulus for undamaged ply.

In addition to that, fibre fracture is given by the critical fracture strain of fibre ε_{11r}. Rising damage, given by d_{12} and d_{22}, intrinsically depends on internal strain energy within ply. This notion of stored energy is taken for the development of a delamination detection methodology.

DELAMINATION DETECTION AND FOLLOW-UP

Numerical methodology together with fibre fracture, matrix cracking in plies and a delamination growth in interface are the most common damage mechanisms. The further growth of delamination can be predicted on the basis of fracture mechanics. The methodology uses several fracture criteria for each interface and associated plies [3]. The criteria are applied in post-processing of explicit code, using the stress tensor for each layer. For the interface, the criteria are twofold:

The first is the follow-up of strain energy density growth within the interface [4]. This density is computed with the principal stresses σ_1, σ_2, σ_3 by:

$$\frac{dW}{dv} = \frac{1+\nu}{6E} \cdot \left[(\sigma_1-\sigma_2)^2 + (\sigma_2-\sigma_3)^2 + (\sigma_3-\sigma_1)^2\right] + \frac{1-2\nu}{6E}(\sigma_1+\sigma_2+\sigma_3)^2 \qquad (3)$$

with E the Young's modulus, ν Poisson's ratio for epoxy interface. The damage variables d_{12} and d_{22} are included in the corresponding effective stress components.

The second is a Tsai-Hill failure criterion. It is a quadratic stress criterion for ply. The ply is specified as an anisotropic material, using the effective stress tensor as follows:

$$f^2 = \frac{\sigma_1^2}{X^2} + \frac{\sigma_2^2}{Y^2} - \frac{\sigma_1 * \sigma_2}{X^2} + \frac{\tau_{12}^2}{U^2} + \frac{\tau_{23}^2}{S^2} + \frac{\tau_{31}^2}{S^2} \qquad (4)$$

X, Y, U and S are respectively longitudinal, transverse and shear fracture threshold stresses. For the interface used, X and Y are equal to 130 Mpa, U and S to 30 Mpa. f^2 value grow from 0 (no failure) to 1 (total failure).

Both criteria are used for delamination detection like filter factors at the interface of each element. An assessment of interfacial fracture can be given by a decrease in the energy density at interface, combined with a sufficiently high value of the associated Tsai-Hill criterion (figure 2).

Tsai-Hill acts like a filter on the too low energy fluctuation in the meshing elements far away from the loading area. This fluctuation is taken for failure sign if associated Tsai-Hill value is significant enough.

In addition, methodology uses specific Chang criterion [5] for associated plies fracture. This criterion distinguishes tension and compression matrix failures, which initiates delamination to the interface:

$$\left(\frac{\sigma_{22}}{S_2}\right)^2 + \left(\frac{\sigma_{12}}{S_{12}}\right)^2 \geq 1 \qquad (5)$$

$$\left(\frac{\sigma_{22}}{2S_{12}}\right)^2 + \left[\left(\frac{C_2}{2S_{12}}\right)^2 - 1\right]\frac{\sigma_{22}}{C_2} + \left(\frac{\sigma_{12}}{S_{12}}\right)^2 \geq 1 \qquad (6)$$

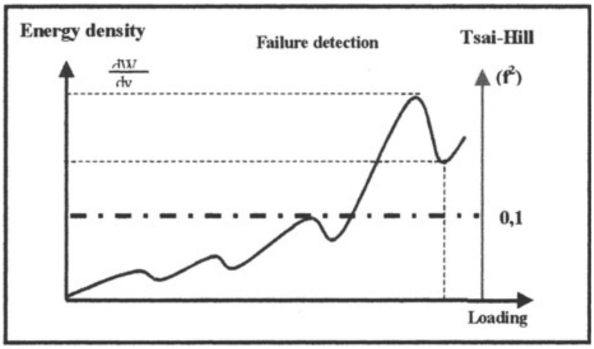

Figure 2. Criteria used for each interface.

EXPERIMENTAL ADJUSTMENT

An interface damage parameter adjustment is realized by static tensile test. So, Composite samples are made of the Prepreg (glass E/epoxy with 55% volume fibre ratio). Some stacking sequence $[\pm\theta]_{ns}$ are selected with $10° \leq \theta \leq 30°$ to give priority to shear fracture in the interface. This experimental test allows the strength values identification (X,Y,S for equation 4) or damage parameters linked with d_{12} and d_{22} law evolution. The figure 3 below presents an example of delamination location for numerical and experimental tests with [±25].

For those configurations delamination is sudden and extended in the interface, leading to structure failure. Delamination locations at failure are comparable between experimental and numerical methodologies, for similar critical strains. We carried out tensile tests with $[\pm15]_s$, $[0/\pm15]_s$, $[\pm15/0]_s$ laminates, providing the same results.

DYNAMIC BENDING TESTS

Rectangular laminated plate samples (50*200mm) undergo three point bending tests with an hydraulic jack device (figure 4).

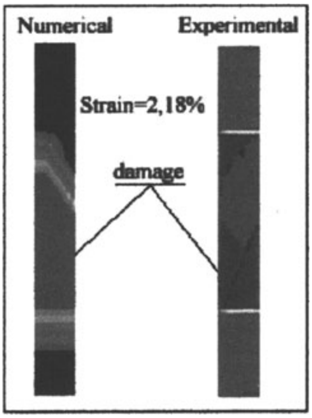
Numerical
Experimental
Strain=2,18%
damage

Figure 3. Delamination for $[\pm25]_s$.

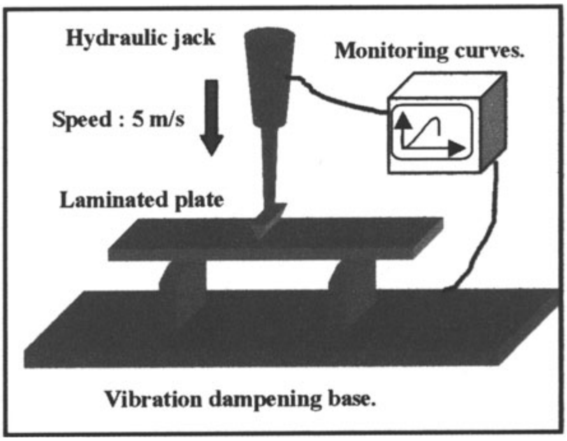
Hydraulic jack
Monitoring curves.
Speed : 5 m/s
Laminated plate
Vibration dampening base.

Figure 4. Three point bending test.

Two kinds of samples are chosen for the tests:

The first, $[90_2/0_4/90_2]$, presents a bottom interface 90/0 delamination, initiated by several transverse matrix cracks within the bottom 90° plies. Cracks propagating in this 90° plies thickness appear from the bottom tensile plate's surface. When they reach 0° plies, they are deflected in the interface plane and start in several delamination fronts (figure 5).

The second, $[0_2/90_4/0_2]$, gives brutal failure and is initiated by several matrix cracks in the middle 90° plies.They give one single delamination front, extended in the bottom 0/90 interface and reach the edge of plate. So, this delamination causes brutal structure failure.

We apply the methodology to the laminated models of finite element test simulation. For each model, the criteria are applied within the interface (strain energy density decrease and Tsai-Hill failure criterion) and Chang criterion for composite plies. We sum up the delamination location by damage interface cartography given by the application of a detection methodology. For the second stage, we define an integration process of delamination effects in a 'sequential' computation, which integrates delamination within laminated thin structure. Those effects over modelling are included in a code by locally weakening the mechanical features of the damaged plies and delaminated interface. For $[90_2/0_4/90_2]$ those weakening are applied on the 90 sublaminated plies and associate bottom 90/0 interface. For $[0_2/90_4/0_2]$, they take effect on the damaged 90° middle plies, where several matrix failures are detected and on large areas on bottom interface.

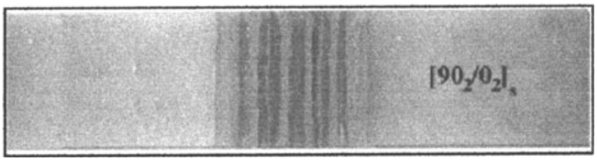

Figure 5. Transverse stripes delamination (in red) of $[90_2/0_4/90_2]$ (top view).

To compare the provision of sequential computation, we also give "direct" computation, without any delamination effect integration. There are no modifications of the mechanical features during the loading phase. Figures give an example of delamination distribution of experimental tests. Methodology and resulting 'sequential' computational codes are applied on a quater plate equivalent model (with symmetrical boundary conditions). The views of figure 6 display some integrated damage distribution in a quarter bending platemodel due to sequential computation. In the model, the delamination area is associated. With shell, whose interface features damage values (d_{12} and d_{22}) close to 1. We must notice that d_{12} and d_{22} for interface are given with the same evolution law. The sequential computation gives a similar delamination distribution (figure 6). Direct computation is not able to give this restitution, where delamination is not detected until reaching important loading values. Therefore, damage is only like a single transverse delamination front reaching from the middle of the plate interface to a small area, regarding sequential computation.

The delamination distribution accuracy depends on meshing: minimum step of delamination growth is directly linked to the shell length. Actually, this damage step cannot be any lower than the element size. So, there is an accurate low limit for delamination detection in the model given by the shell length, which must abide by a height/length ratio.

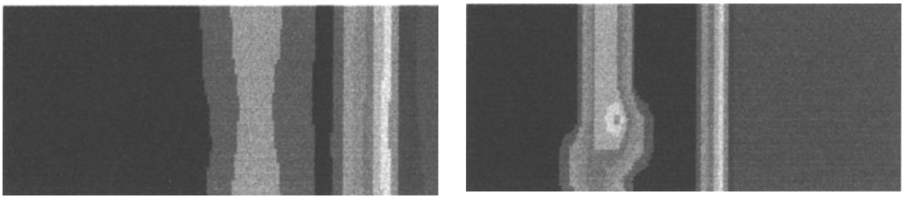

Figure 6. Quarter plate delamination growth at 2 and 6 mm of bending

Laminated global behaviour is given by evolution energy for two computational types (direct and sequential) and experimental measures. These evolutions are displayed as a function of displacement.

For $[90_2/0_4/90_2]$, damage effects, particularly multi-front delamination leading to progressive failure of laminate. The experimental energy curve (figure 7) takes into account this progressive failure by a slow decrease as a function of displacement in the middle of plate. Sequential computation gives a better prediction of energy evolution than direct computation.

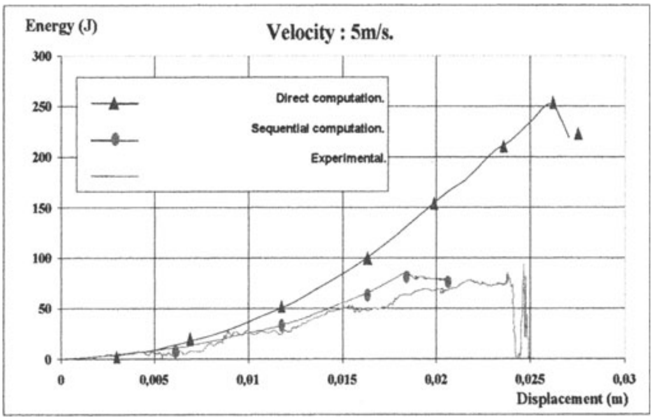

Figure 7. Energy evolution curves comparison for $[90_2/0_4/90_2]$.

The same observations are made for the brutal failure case with $[0_2/90_4/0_2]$ laminated bending (figure 8).

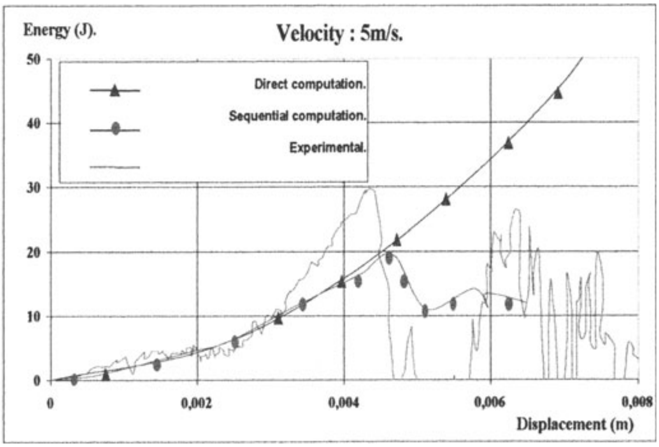

Figure 8. Energy evolution curves comparison for $[0_2/90_4/0_2]$.

A failure level as shown for experimental curve to 4.5 mm, is predicted by sequential computation. A sliding phenomenon of plate between supports is observed in experimental tests, due to unsymmetrical distribution in the sample length. However, this phenomenon is difficult to take into account in numerical simulation. So, a difference in fracture energy level is found for sequential computation at global failure.

CONCLUSION

A numerical methodology is suggested for delamination prediction and the restitution of mechanical effects in multi-layered shell element. The delamination is defined like a strain energy decrease phenomenon linked to crack propagation. Energy evolution and specific quadratic stress criteria are applied in post-treatment of explicit finite elements code for composite plies and interface. It was able to follow both the initiation and delamination growths.

The validation are carried out with experimental tests in low velocity impact. A good consistency is shown for damage mechanisms and delamination shapes, in different examples. The methodology developed is recognized a predictive process for several studied laminates. It can be used like a potential tool to size laminated structures at the design stage.

In future prospects, we can foresee :

A validation for crash studies in complex structures to predict behaviour until total failure.

The methodology integration in the finite element code saves amount of time and entails a better synergy between failure detection and restitution of effects due to damage.

REFERENCES

1 Coutellier D., Rozycki P., "Multi-layered multi-material finite element for crashworthiness studies." Composites Part A: applied science and manufacturing, 2000.

2 Ladevèze P., Le Dantec E., "Damage modelling of the elementary ply for laminated composites." Composite science and technology, vol. 43, pp. 257-267, 1992.

3 Walrick J.C., "Contribution au développement d'une nouvelle méthodologie pour l'étude du délaminage dans les structures stratifiées composites." Ph D, Valenciennes university, 1999.

4 Usik L., Lesieutre G.A., Fang L., "Anisotropic damage mechanics based on strain energy equivalence and equivalent elliptical microcracks.", International Journal of Solids Structures, Vol. 34, pp. 4377-4397, 1997.

5 Choi H.Y., Chang F.K., A model for predicting damage in graphite/epoxy laminated composites resulting from low velocity point impact., Journal of Composite Materials, Vol 26, pp 2134-2169, 1992.

E. ARNOULT - B. PESEUX - J. BONINI

SEARCH OF CONTACT IN DYNAMIC FINITE ELEMENT CODE : PRESENTATION OF AN ANALYTICAL METHOD

Abstract : The purpose of this communication is to develop a method of analytic contact search applied to a finite element code and to present the first numerical results. This method is based on the construction of geometrical entities being sufficiently continuous to get rid off the facetisation problems due to the spatial discretisation of the studied structure by finite elements. These geometrical entities are built up using the mathematical notion of spline applied to some nodes of the mesh. The search of contact is then realised with these entities, and then the obtained results are projected on the initial mesh.

Our method, developed in the particular context of contact studies between casing and blades of turbojet engine, has been implemented in two finite element codes of different nature: Samcef (implicit formulation) and Plexus (explicit formulation), and then tested on some configurations.

1. CONTEXT OF THE STUDY

Dynamical contacts in turbojets are dealt with in many studies, on both experimental and numerical plans. For this last point, different research and processing algorithms of the contact have been developed. These algorithms can be integrated in finite element codes capable to describe the global evolution of a complex structure during a movement.

However, within a code, it sometimes happens that the numerical tool performance is decreased due to their utilisation in a not - optimal environment. Limitations can have external explanations, as it is the case when the processor in charge of calculation is not enough powerful; but these limitations can also be a consequence of internal problems, when there is interaction between the use of several numerical tools for instance.

In the case of tools dedicated to the processing of the contact, the facetisation (which is a direct consequence of the discretisation of structures) stands for a good example of this last kind of problems. During dynamic studies, especially when contact phenomena arises, two situations particularly underline the generated difficulties: discontinuity of the normal vector between elements (see figure 1a) and bad estimation of curvatures of the real geometry (see figure 1b).

Usually, these difficulties are got round using the following artifices: the problem of the indetermination of the normal vector is solved by attributing to node B a normal vector reached by the sum of the normal vectors of adjacent elements; as for effects of the second difficulty, they can be lessened by adding supplementary nodes.

P. Chedmail et al. (eds.), Integrated Design and Manufacturing in Mechanical Engineering, 447-456.
©2002 *Kluwer Academic Publishers.*

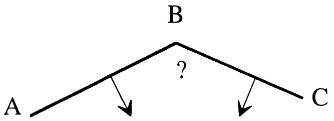

Figure 1a : Discontinuity of normal vector

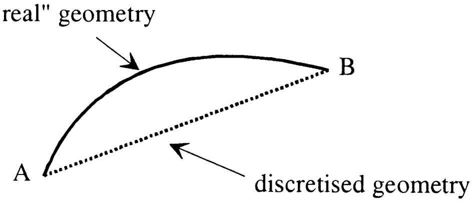

Figure 1b : Bad curvature approximation

However, these solutions are only mid-terms: in the first case, the normal vector, although defined in every point of the mesh, remains discontinuous when crossing element boundaries, which is not a sufficient condition in some configurations (for example: rotation of a transmission shaft in a bearing support). In the second case, the addition of nodes decreases the relative size of the elements and increases the size of the mesh. So it globally increases the time of calculation, particularly in rapid dynamics where the value of the time step depends directly on the element size.

The method we suggest in this paper has been motivated by the study of the search of intersection points of two geometrical entities in the particular framework of studies of blades/casing contacts in turbojet engines. In this configuration indeed, problems of facetisation involve a very bad simulation of the rotation of the bladed disk in the casing, and can lead to a "numerical" break of the two parts due to the fact that the number of nodes generally retained for the model is too small.

2. GENERAL OVERVIEW

The suggested method takes place in the stage of research of contact points. More exactly, it is fully related to the determination of the nodes of the mesh that have not filled a given criterion. The next stage, that corresponds to the calculation of efforts to apply to the structure to take into account the contact, is modified only by data that are provided at the end of the detection of the contact (normal vector, local coordinates of the involved nodes...).

Therefore, our process includes first of all a stage of identification of potential contact areas on the two structures in movement. Geometrical entities are then constructed with nodes contained in each area. As part of the studies of contact between blades and casing, the constructed entities will be therefore on the one hand a surface (the casing) and on the other hand a skew curve (profile of the blade tip). A research of intersection is then realised on these geometrical entities by following a recursive process. Finally, once contact points are identified, it remains to project the results on the initial mesh, that is to say to attribute to each impacted shell and to each impacting node some values that will allow the calculation of the contact force. Later on, we will suppose that the first stage (identification of potential contact areas) has been undertaken. We therefore dispose of a group of nodes upon which we are going to construct some geometrical entities presenting a sufficient character of continuity to get rid off problems of facetisation. The flexibility given by the theory of splines is a great argument that justify its use.

3. SOME RESULTS ABOUT SPLINES

Some results about spline functions and about methods generally used to build spline curves and spline surfaces are briefly described here (for more information, see [1], [2]).

Skew curves are represented using parametric coordinates. Each point P of the curve is therefore determined by its three coordinates x, y and z that depend on a same parameter t whose interval of variation is to be defined with care [3].

The data set of the problem is a group of *npt* points P_i, and a degree n of modelisation. The principle of construction of a spline function is the following: within the interval of definition of the parameter t, the vectorial expression of the skew curve approaching the group of points P_i is:

$$c(t) = \sum_{i=0}^{N} Q_i B_{ni}(t) \tag{1}$$

where B_{ni} are basis functions of the space of the splines of degree n called B-splines (these basis functions are in fact polynomials of degree n defined within the parametric interval), and the $N+1$ points Q_i are called control points of the curve. Three methods are frequently used to determine these control points:

- take for the Q_i the points of the data set (P_i): it is called the direct method;
- calculate Q_i in order that the resulting curve passes exactly through points P_i for some particular values of the parameter t: it is therefore an interpolation;
- calculate Q_i so that the sum of squares of distances from each point P_i to the resulting curve is minimal: it is called the least square smoothing method.

An important spline function property consists of their location inside the convex polygon defined by their control points. As a consequence, for the direct method, the spline curve is generally far from the points of the data set. This is why only the two other methods (smoothing and interpolation) will be used.

As for curves, surfaces will be represented using parametric coordinates, and control points can be determined with one of the three methods presented above. The data set of the problem is a group of $nptu \times nptv$ points P_{ij}. The parametrisation is therefore undertaken in two preferential directions we will note u and v. The group of data points will be therefore approached by a surface whose vectorial equation is:

$$s(u,v) = \sum_{i=0}^{N_u} \sum_{j=0}^{N_v} Q_{ij} B_{nu,i}(u) B_{nv,j}(v) \tag{2}$$

where Q_{ij} are the $(Nu+1) \times (Nv+1)$ control points of the surface. As shown in this formulation, the modelisation of a surface is equivalent to the crossed modelisation of several skew curves: those defined by point Q_{ij}, j being constant, and those defined by point Q_{ij}, i being constant. It is thus possible to use B-splines of different degrees in the two directions (these degrees are noted nu and nv in the expression above).

4. SEARCH OF INTERSECTION

Methods commonly used in finite element codes (Lsdyna [4], Plexus [5]...) generally begin by dividing nodes into two groups called "masters" and "slaves". Then a first stage consists in undertaking a loop on the totality or part of slave elements: for each of them, a test is realised on the totality or on a part of the master elements so as to determine whether some of them can match a predefined criterion. Afterwards, if some group of master/slave nodes have satisfied the first criterion, a second test is realised to precisely confirm or invalidate the existence of contact. The stage of search of master/slave nodes couples can be made in a global way (hierarchical approach) or in a local way (vicinity approach) [6].

In the suggested method, the first stage of classification is retained: the curve is chosen to be the slave entity; the other stage is realised by using the spline formulation. Due to the non - linearity of this formulation, an analytic solution can not be found in the general case. A numerical iterative process has therefore to be set.

5. PRINCIPLE OF THE METHOD

The result of the search of intersection is defined for a given precision ε. The result given by the algorithm should be understood as follows: inside a sphere of radius ε, it exists at least two points, one belonging to the curve and the other to the surface. Each of the involved parameters, that is t for the curve, and u and v for the surface, is then discretised. The obtained increments dt, du and dv depend on the precision ε [7]. The boundaries of the parameterised areas can be determined after a first rough sorting using a hierarchical approach for example.

Subsequently, P_t will designate the point of the curve associated to the parameter t, and P_{uv} the point of the surface associated to the parameters (u, v). The curve is used as a support for the search (see figure 2).

For each discretised value of the parameter t, the surface is swept, and to each couple (u, v), the distance P_tP_{uv} is calculated (see figure 3). If this distance becomes smaller than the precision ε , parameters t, u and v are stored in memory (these are told "initial parameters").

Values of parameters are then increased. As soon as the distance becomes bigger than ε , parameters are stored again in memory (these are told "terminal parameters"). Thus, some potential intersection areas between the two geometrical entities can be exhibited (see figure 4). It is then possible to proceed to a new scanning of these areas, with a new precision smaller than ε . The operation is repeated until a required precision is reached.

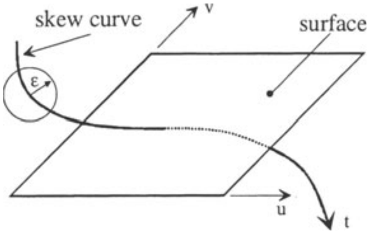

Figure 2 : Initial situation

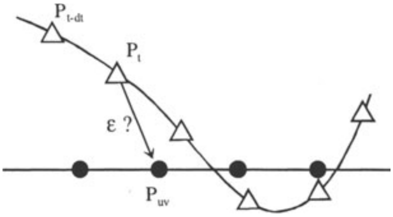

Figure 3 : Principle of the method

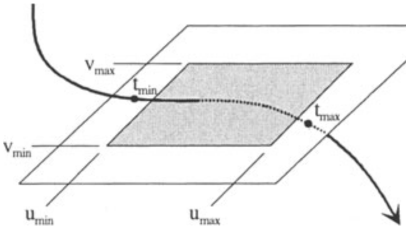

Figure 4 : Final situation

6. IMPLEMENTATION IN SAMCEF

First of all, the method of search of contact with the use of spline functions has been implemented in the finite element code Samcef [8].

It was not possible to develop directly within the source files of the code. So our developments have been realised via the user element which is a fortran routine compiled with the totality of the code. The user element allows the user to include in the code some elements he can set all the characteristics (number of nodes, degrees of freedom, constitutive law).

In the present case, the user element developed by I. Guilloteau [9] has been used: it concerns a simplified element of contact, using a modified penalty method. In its formulation, the search of contact uses geometrical entities of degree 1 built on finite elements. These entities are parts of the shells approximating plans for the casing, and segments for the blades. Thereafter, this method will be designated under the term "classic method". This classic search is therefore replaced by the method of search with spline modelisation. The test we use consists to simulate the rotation of an unbalanced blade inside a casing. The blade is represented by a generalised spring, and the casing (part of a cylinder clamped at its basis) is modelised by shells of Mindlin. The mesh is represented on figure 6.

This test is used to observe the value of the normal force on the blade tip during the contact, and the CPU time to simulate 5 rotations of the blade. The varying parameters are on the one hand the choice of the method of search of the contact (classic, splines of interpolation and by smoothing splines) and on the other hand the number of elements used to discretise the circumference of the casing (three configurations have been studied: 72, 36 and 18 elements).

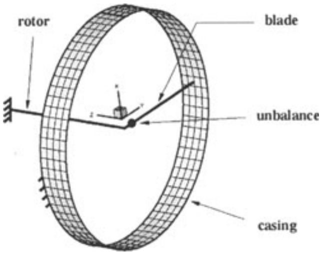

Figure 6 : General view of the mesh

7. SAMCEF RESULTS

The first presented results concern the contact force : these results are normalised with respect to the maximal amplitude of the first contact force obtained with a method of interpolation in the 72 element configuration. It can be observed on figure 7 (72 elements in the circumference of the casing) that spline methods give very similar results with regard to the maximal amplitude of the force of the first contact (the difference between the methods is approximately 3%).

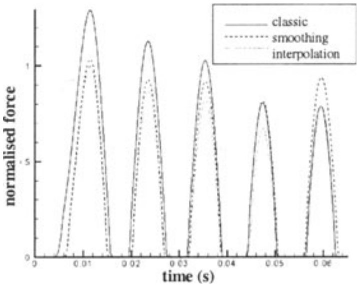

Figure 7 : Configuration with 72 ***elements***

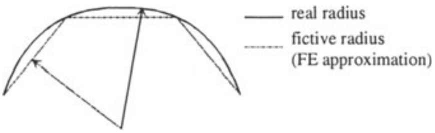

Figure 8 : Finite element approximation

With a classic method, the radius of the casing is systematically underestimated (see figure 8). As a consequence the contact force whose calculation depends here on the radial penetration is always overestimated. In the present case, the contact force is about 30% bigger than the force given by a spline method. Moreover, the finite element approximation involves an early detection of the instant of the first contact (t = 4 ms for the classic method and t = 6 ms with a spline interpolation).

When the number of elements used to define the circumference of the casing decreases, these two problems greatly emphasize. When just 18 elements are used for example (see figure 9), the classic method detects a strong initial penetration that induces an amplitude of the first contact force twice bigger than the one obtained with a spline interpolation.

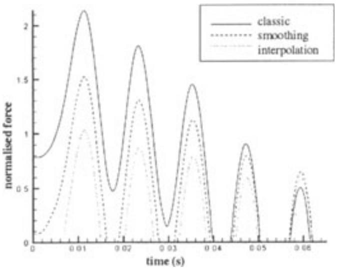

Figure 9 : Configuration with 18 *elements*

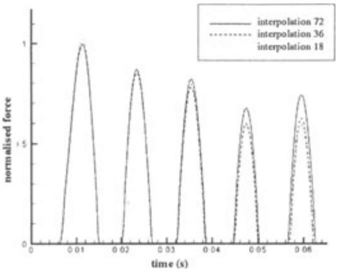

Figure 10 : Interpolation method

By representing on a same figure the results given by the three configurations (72, 36 and then 18 elements in the circumference of the casing), it is interesting to note that the interpolation spline method is very little sensitive to the fineness of the mesh concerning the amplitude of the first contact force peaks (see figure 10).

The second series of results focuses on the required CPU time to simulate 5 revolutions of the blade. All CPU times presented on figure 11 are normalised with respect to the required CPU time with 72 elements and the classic method.

It appears that spline methods are more expensive than the classic method (approximately 25% of supplementary time in the configuration with 72 elements), what was expected due to the iterative scheme that is used for the search of contact. However, it is important to note that a spline interpolation method with 36 elements requires less CPU time (approximately 30%) than the classic method with 72 elements, while providing a comparable result.

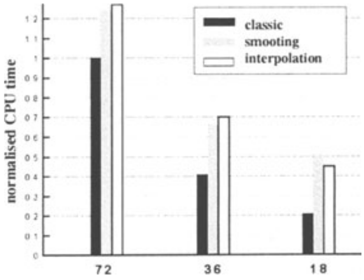

Figure 11 : CPU time comparison

8. IMPLEMENTATION IN PLEXUS

The method of contact search with splines functions has then been implemented in a rapid dynamic finite element code named Plexus [5] which uses an explicit formulation. In this code, it has been possible to develop directly in source files of the code (a specific instruction has been created that allows, in the data set, the selection of this kind of contact search).

The test we use for this code was selected to underline the way the two problems of facetisation we are concerned with were faced, namely the problem of taking into account the curvatures of the structures, and the problem of discontinuity of the normal vector.

This test consists of a plate (the blade) sent with an initial translation velocity V_0 onto the wall of a cylinder (the casing) clamped to its extremities (see figure 13). No particular boundary condition is attributed to the blade (all the dofs are free), and the problem is thus symmetric.

Elements used to mesh the blade and the casing are shells Q4GS [10]. The mesh is realised such that the blade is directed to impact a ridge of a shell (see figure 14).

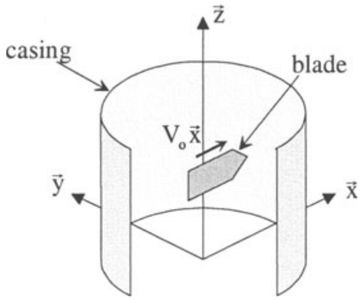

Figure 13 : General view of the test

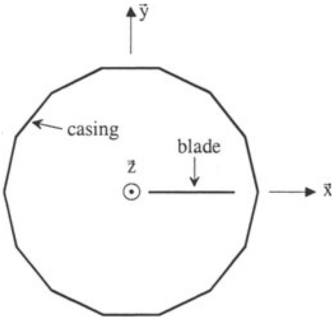

Figure 14 : Mesh top view

The result which is observed is the evolution of the contact force. In this explicit formulation, the contact force is calculated according to the relative position (local coordinates) of impacting nodes within impacted facets. The search of contact existing in Plexus is a slipping line and surface method [11]: slave nodes and master elements are matched, and the contact force is calculated with a kinematic formulation involving the local coordinates of nodes transgressing the criterion of contact in impacted elements. This method will be later on designated as the "classic method".

The results we present are related to the amplitude of the contact force in the two directions $\vec{x}$ and $\vec{y}$. First of all in the direction $\vec{x}$ of impact (called "normal force"), it can be observed that the force given by the classic method is quite perturbed (see figure 15) while the force given by the spline method is quite regular.

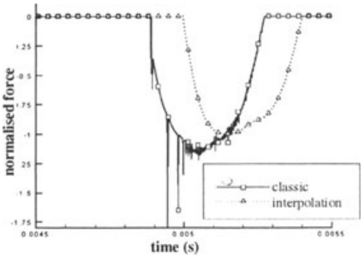

Figure 15 : Normal force

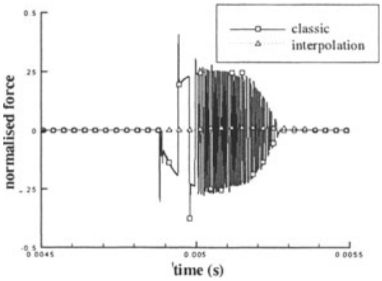

Figure 16 : Tangential force

Due to the symmetry of the problem, no force is expected in the tangential direction $\vec{y}$. However one can observe a non-zero force (called "tangential force") with a classic method, since it has an amplitude hardly three times smaller than the one in the normal direction (see figure 16). A spline method also provides a non-zero force, but with a very weak amplitude (more than 100 times smaller than the normal force).

The very perturbed results provided by the classic method can be explained by the difficulty that exists to choose the reprojecting element when contact occurs: depending on the time step, and with the notations of figure 17, the reprojection will be made sometimes on the facet 1 and sometimes on the facet 2. The normal vectors of these two facets being very different, the values of contact forces are also very distinct.

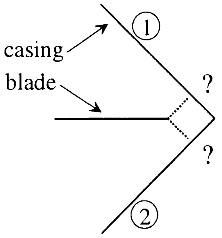

Figure 17 : Problem of reprojection

This problem does not exist with the spline interpolation, since the normal vector is perfectly continuous in all the area of definition of the surface.

9. CONCLUSION AND PROSPECTS

The presented method aims at dealing with problems of facetisation when finite element codes are used to simulate some non-linear movements between structures.

The developments realised in two different finite element codes show that the time required for the search of contact points is bigger than the time required when using a classic method, but can be compensated by the given possibility to work with a reduced size mesh.

Under way developments aim at testing this method on some more complex problems (rotation of a transmission shaft in a bearing support for example) for which some programming difficulties will have to be faced (management of strong tangency areas that can considerably increase the time of calculation for example).

Applications of this method to other configurations except that of blade/casing contact studies are considered such as the use for stamping problems and the simulation of thermoforming (studies are being proceeded in our laboratory).

Acknowledgements : The authors would like to deeply acknowledge the CEA (the French Nuclear Department), and especially H. Bung for the help provided in the Plexus implementation.

10. AFFILIATIONS

Etienne ARNOULT
Université de Technologie de Compiègne
Laboratoire Roberval – UMR UTC CNRS 6066
Rue Personne de Roberval
60200 COMPIEGNE - FRANCE
Etienne.Arnoult@utc.fr

Bernard PESEUX
Ecole Centrale Nantes
Laboratoire Mécanique et Matériaux
BP 92101
44321 NANTES Cedex 03 - FRANCE
Bernard.Peseux@ec-nantes.fr

Jérôme BONINI
SNECMA
Centre de Villaroche
Département Méthodes
77550 MOISSY CRAMAYEL - FRANCE
Jerome.Bonini@snecma.fr

11. REFERENCES

[1] De Boor C., "A practical guide to Splines", vol. 27 of Applied Mathematical Sciences. Springer Verlag, 1978.
[2] Nurnberger G., "Approximation by spline functions", Springer Verlag, 1989.
[3] Daniel M., "Modélisation de courbes et surfaces par des B-splines – Application à la conception et à la visualisation de formes", PhD Thesis, Ecole Nationale Supérieure de Mécanique, Nantes, May 1989.
[4] Hallquist J., "LS-DYNA3D, Theoritical manual", Dynalis, 1995.
[5] CEA, "PLEXUS: Theoritical manual", 1997.
[6] Cescotto S., "Contact quasi-statique: résolution avec régularisation", in Modélisation mécanique et numérique du contact et du frottement, IPSI, pp. 251-256, Paris, 15-17 oct. 1996.
[7] Arnoult E., "Modélisation numérique et approche expérimentale du contact en dynamique: Application au contact aubes/carter de turboréacteur", PhD Thesis, University of Nantes, January 2000.
[8] Samtech, "SAMCEF, User manual", version 7.1, 1997.
[9] Guilloteau I., "Modélisation du contact en dynamique: construction d'un élément simplifié de contact et application à l'interaction rotor/stator", PhD Thesis, University of Nantes, November 1999.
[10] Batoz J. & Dhatt G., "Modélisation des structures par éléments finis", vol. 3 –"Coques", Hermès, 1990.
[11] Bonini J. & Bung H., "Modélisation des problèmes de contact-impact avec frottement en explicite par la méthode des multiplicateurs de Lagrange", in Actes du Troisième Colloque National en Calcul des Structures, vol. 1, pp 411-416, CSMA, Giens (France), 20-23 May 1997.

PIERRE DUYSINX AND MICHAEL BRUYNEEL

RECENT PROGRESS IN PRELIMINARY DESIGN OF MECHANICAL COMPONENTS WITH TOPOLOGY OPTIMIZATION

1. INTRODUCTION

Since 10 years topology optimization has been trying to bring an efficient answer to the automatic choice of the morphology of mechanical components, i.e. the number and the relative positions of the holes in the structural domains, the number and the nature of the structural members, their connectivity and the character of the connecting joints. This problem is one of the main questions to be addressed during the preliminary design phase of mechanical and structural components. Up to now, the selection of the mechanical morphology has been let to engineers' experience or to their intuition (which is even worse sometimes). With topology optimization the choice of the morphology can now rely on rational arguments and can be driven with the help of mathematical tools. This has two advantages. At first topology optimization can facilitate the automation of the preliminary design, but it can also improve substantially the performance of new mechanical products, that is, topology optimization can propose original and innovative solutions to engineering problems.

For a long time topology optimization has been based on 'compliance type' arguments as in the pioneer paper of Bendsøe and Kikuchi (1988). This kind of formulation has produced quite interesting results in many problems especially because controlling the displacements under the loads is generally good for deflection control and because, *for one load case*, compliance minimization leads to a fully stressed design nearly everywhere in the structure (Rozvany and Birker, 1994, Rozvany, 1996 and 1998). However recently new results showed that topology predictions can not always be reduced to a compliance minimization. For example Rozvany and Birker (1994) have demonstrated that, for trusses, topology optimization can lead to different results when there are several load cases, different stress limits in tension and compression, or when there are several materials involved.

This key role of stress constraints has to be demonstrated in the framework of topology optimization of continuum structures, for several load cases and when unequal stress limits in tension and compression are considered.

The present developments continue along the work that was done in Duysinx and Bendsøe (1998) to introduce stress constraints in topology optimization of continuum structures. At first an integrated (i.e. global) relaxed stress constraint is

P. Chedmail et al. (eds.), Integrated Design and Manufacturing in Mechanical Engineering, 457-464.
©2002 *Kluwer Academic Publishers.*

introduced. A second contribution is the generalization of the von Mises equivalent stress to other quadratic criteria that are able to cope with unequal stress limits.

In addition to these mechanical constraints, one can also introduce geometric constraints on the material distribution. Besides the very classic area/volume constraint, the perimeter constraint offers an elegant way to control the complexity of the geometry that comes out from the optimization procedure. A first contribution has been made to cope with this difficult constraint in the mathematical programming solution procedure. A second development aimed at extending the existing perimeter measure to 3-D and axisymmetric problems.

2. FORMULATION OF TOPOLOGY PROBLEM

Shape optimization of structures without any a priori on the structural topology can be achieved by formulating the problem as an optimal material distribution on a given design domain (see Bendsøe, 1995). In order to solve numerically the optimal material distribution problem, the design domain is divided into finite elements and a density variable is attached to each element. The optimal material distribution problem could be solved as a discrete valued problem, but this approach is very complicated because of its highly combinatorial nature. Here a simplified formulation is considered. We allow the density parameter to run continuously from void to solid via all intermediate densities. The modeling of effective intermediate densities properties is based on a power-law model (also called SIMP model as in Rozvany et al., 1992). This model is extremely popular for solving industrial applications because of its simplicity. If the script * denotes effective properties of the porous material and the index 0 is relative to the solid material properties, the effective Young's modulus E^* is given in term of the density ρ by $E^* = \rho^p E^0$. The exponent $p > 1$ is introduced to penalize the intermediate densities in order to end up with ‘black and white’ designs.

This continuous formulation presents the advantage to allow the use of sensitivity analysis and mathematical programming algorithms to solve the problem in an efficient way (see for example Duysinx, 1997). However because the power law model is an approximation of composite materials the design problem is ill-posed, i.e. the numerical solutions are mesh-dependent. To overcome the difficulty, we use here a restriction method of the design space based on a bound over the perimeter (Haber et al., 1996).

In addition to stiffness properties, if one wants to consider stress constraints in continuous topology optimization, one also needs the definition of a relevant stress measure in the porous composites. Modeling of strength properties can be made by following the approach developed in Duysinx and Bendsøe (1998). An overall stress measure controls the stress state in the microstructure. In the framework of the SIMP model, Duysinx and Bendsøe (1998) showed that a power-law model with the same power p is a consistent model for the micro-stresses σ_{ij} . Therefore if the failure is predicted by a quadratic overall failure criterion like von Mises equivalent criterion, the first failure in the microstructure of the porous composites is predicted by the following criterion in terms of effective stresses:

$$\sigma_{ij} = \sigma^*_{ij} / \rho^p \qquad \Rightarrow \qquad \| \sigma^{eq}(\rho) \| = {}^*\sigma^{eq} / \rho^p \leq T \tag{1}$$

3. PERIMETER CONSTRAINT

The perimeter constraint was originally introduced by Haber et al. (1996) to assure the regularization of topology problems (even with 0/1 variables and with intermediate density penalization). In addition to that property it was shown that the perimeter method is a very elegant solution to control the complexity of topology solutions, and thereby, to introduce an indirect control over the manufacturability of the solution (Figure 1). When working with distributions of porous materials, the intuitive geometric measure of perimeter can be replaced by the total variation of the density, which is just the density jumps across the finite element edges when density discretization is constant on each element.

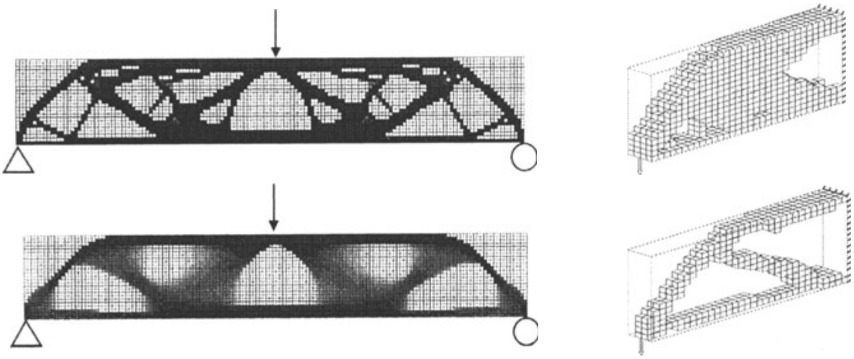

Figure 1. Using perimeter constraint for the control of the complexity of topology solutions.

Perimeter constraints showed to be very difficult to control within the mathematical programming solution procedure. A first contribution was realized to cope with this type of constraint (Duysinx, 1997). Another part of the work has been devoted to extend the existing measure, which was restricted to planar geometries, to 3-D (Bruyneel, 1998) and axisymmetric structures (Figure 1b).

4. STRESS CONSTRAINTS

At first it is interesting to remind the reader with a very important difficulty that arises when dealing with stress constraints in topology optimization. As it has been shown in Kirsch (1990) and in Cheng and Jiang (1992), topology optimization with stress constraints is subject to the *'singularity phenomenon'*. At short the paradox comes from the fact that the optimization procedure is often unable to remove or to add some vanishing members without violating the stress constraints although one would end up with a perfectly feasible design if they were removed or added. From a mathematical point of view, the classical algorithms are unable to reach some optimum configurations because of the degeneracy of the design space. In order to turn around the difficulty, one has to use a perturbation technique of the stress constraints, generally known as the ε-relaxation technique (Cheng and Guo, 1997) that results in a relaxation of the stress limits in the low-density regions. In this paper we use the following ε-relaxed formulation of the overall stress criterion:

$$\frac{1}{T}\frac{{}^{*}\sigma^{eq}}{\rho^{p}} - \frac{\varepsilon}{\rho} + \varepsilon \le 1 \tag{2}$$

This relaxed formulation of the stress constraints is considered in the numerical solution of the topology optimization problem with stress constraints. The solution procedure requires the solution of a sequence of perturbed problems with decreasing values of the parameter ε.

5. INTEGRATED STRESS CONSTRAINTS

In Duysinx and Bendsøe (1998) the stress is treated as a local constraint, i.e. for every finite element. This formulation offers a full control of the stress state, but it also dramatically increases the size of the optimization problem and thus the computation time of the solution. Here we propose an alternative approach based on an integrated version of the ε-relaxed failure criterion. The global stress constraint (i.e. integrated constraint) simplifies the computational complexity of the optimization problem at the expense of a weaker control of the local stress state. A key issue is to take into account the 'singularity phenomenon' of the stress constraints. So an original aspect is to include simultaneously the ε-relaxation technique that alleviates the singularity phenomenon and the use of effective stress criteria into the global stress constraint.

We propose to consider two global measures of the relaxed distributed stress criterion. The first global constraint is the '*q-norm*' of the relaxed stress criterion (3); the second one is the '*q-mean*' of the relaxed stress criterion (4).

$$\left[\sum_{e=1}^{N}\left(\max\left\{0, \frac{1}{T}\frac{({}^{*}\sigma^{eq})_{e}}{\rho_{e}^{p}} - \frac{\varepsilon}{\rho_{e}} + \varepsilon\right\}\right)^{q}\right]^{1/q} \le 1 \tag{3}$$

$$\left[\frac{1}{N}\sum_{e=1}^{N}\left(\max\left\{0, \frac{1}{T}\frac{({}^{*}\sigma^{eq})_{e}}{\rho_{e}^{p}} - \frac{\varepsilon}{\rho_{e}} + \varepsilon\right\}\right)^{q}\right]^{1/q} \le 1 \tag{4}$$

To prevent negative valued relaxed criteria from contributing to the norms, one must consider the maximum value of the relaxed stress criterion and zero. Negative values of the relaxed criterion appear only for low stressed elements and thus can be truncated without influencing the global constraint. Furthermore, the function remains continuous up to derivative '*q-1*', so that the constraint remains sufficiently smooth. A major advantage of '*q-norm*' and '*q-mean*' functions comes from the fact that they make possible to bound the maximum value of the relaxed criterion by upper or by lower values. The '*q-norm*' is an upper bound of the maximum value of the criterion while the '*q-mean*' is a lower bound of the maximum local value of the criterion. In addition this gap closes to 0 when '*q*' value is going to infinity. So sharp bounding needs to take high values of '*q*' parameter. However in practice, we take *q=4* because it allows to control weakly the maximum value of the stress criterion while avoiding ill-conditioned optimization problems.

6. TREATMENT OF UNEQUAL STRESS CONSTRAINTS

Up to now topology optimization with stress constraints was based on the quadratic von Mises criterion. This criterion is very usual, because it predicts very precisely failure for ductile materials and metals, which are commonly used in mechanical engineering. However von Mises criterion is unable to predict real-life designs when the structure is made of materials with unequal stress limits like concrete or composite materials. One can also remember that thin structural members, like cables or thin sheets, are not able to sustain high compressive loads because of buckling. An indirect procedure to take into account this buckling constraint in the preliminary design phase consists in restricting the compressive loads by reducing the stress limit in compression. From a practical point of view these different behaviors in tension and compression result in quite specific designs. In order to predict layouts that take into account different behaviors in tension and compression, one requires particular failure criteria that are able to cope with unequal stress limits.

To this end, two quadratic criteria have been selected and implemented. They both introduce a dependency on the first invariant of the stresses. The first equivalent failure criterion is the *Raghava criterion* (5a), which is generally used with adhesive materials. An interesting alternative to Raghava is the *Ishai criterion* (5b). These stress criteria and the related equivalent stress can be written as:

$$\sigma_{RAG}^{eq} = \frac{J_1(s-1) + \sqrt{J_1^2(s-1)^2 + 12 J_{2D} s}}{2s} \le T \qquad \sigma_{ISH}^{eq} = \frac{(s+1)\sqrt{3 J_{2D}} + (s-1) J_1}{2s} \le T \qquad (5)$$

T and C are the stress limits (in absolute value) respectively in tension and compression, and 's' is the ratio between the stress limits in compression and in tension: $s = C/T$. The criteria are written in terms of the first stress invariant $J_1 = \sigma_{ii}$ and the second deviator stress invariant $J_{2D} = 0.5 s_{ij} s_{ij}$. The presence of the second invariant is obvious because the criteria have to render the von Mises criterion when the stress limits are equal. The first invariant is related to the hydrostatic pressure and its presence in the criteria is essential to introduce the dependence upon the sign of the stress state and so the different behaviors in tension and compression.

7. THE 3-BAR TRUSS EXAMPLE

Despite its extreme simplicity, the 3-bar truss problem is very well suited to illustrate several concepts related to topology optimization with stress constraints. The geometry of the problem is given in Figure 2. The sizes and material data of the benchmark are normalized: L=1 m, W=2.5 m, E=100N/m^2, ν=0.3. Three load cases (with different magnitudes and orientations) are applied at the center of the free edge. The design domain is meshed with 50 x 20 finite elements. This means that for local stress constraints one has to deal with 3 x 1000 restrictions. The volume bound is set to 25% of the design domain area.

At first the minimum compliance design is studied (Figure 3a). The optimal topology is a 2-bar truss. Compliances for the 3 load cases are 73.3 Nm, but stress level is quite high. Using von Mises criterion, maximum value of the local criterion varies from 228 N/m^2 to 571 N/m^2 per load case. In a second optimization run one consider local von Mises stress constraints with a stress limit of 150 N/m^2 and one gets the topology of Figure 3b which is a 3-bar truss. The compliances of the minimum stress design solution are a bit bigger than minimum compliance solution (91.2 Nm, 45.6 Nm and 45.0 Nm for load cases 1, 2 and 3).

The conclusion that can be drawn from the comparison of these two optimization runs is that compliance design and minimum stress design can lead to different topology solutions when there are several load cases.

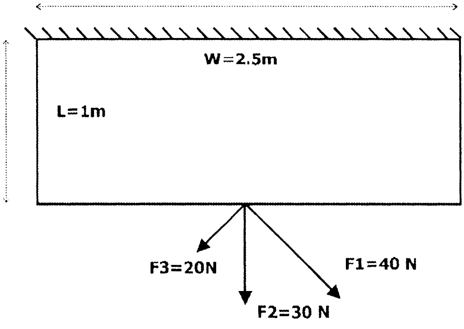

Figure 2. Geometry of the '3-bar truss' problem.

One can further compare the local stress constraint formulation and the alternative approaches based on global restrictions ('*q-mean*' and '*q-norm*') with optimization runs presented in Figures 4. One has the solution when minimizing the volume of material with a (heuristic) bound of 92 N/m^2 over *the 'q-mean*' of von Mises stresses (Figure 4a). The optimal area is 0.56 m^2. In Figure 4b, the bound over '*q-norm*' is set to 500 N/m^2 and the optimal area is 0.62 m^2. Topology results, which are 2-bar truss designs, look more like the compliance design, because we lose the control over the local stress state. However maximum local stress values are much lower than in compliance design. For '*q-mean*' one has the following maximum von Mises stresses: 237 N/m^2, 215 N/m^2, and 207 N/m^2 for the first, second and third load cases. For the '*q-norm*' on has a maximum von Mises stresses of 230 N/m^2, 235 N/m^2, and 231 N/m^2 respectively for the three load cases. The weaker control over stress level allows to save one or two orders of magnitude in the optimizer solution time compared to the local stress approach. Finally one can appreciate the effect of unequal stress limits in tension and compression and Ishai criterion with results presented in Figures 5. The two results exhibit globally a 2-bar truss topology as for minimum compliance design, even though the geometry is quite different. When material is very resistant to compressive stresses, the middle and the left bars merge. In the opposite way when material is very good in tension, the optimal structure looks like a cable structure. This shows that real characteristics of the problem, here the unequal properties in tension and compression, may strongly influence topology results.

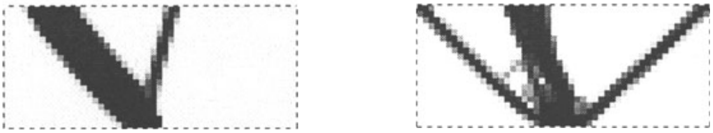

Figure 3. a) Min. compliance solution and b) Min. of the max. of the local von Mises stress.

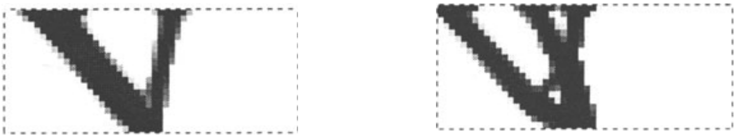

Figure 4. a) Min. of 'q-mean' of stress criteria and b) Min. of 'q-norm' of stress criteria.

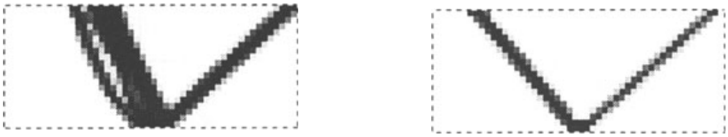

Figure 5. Minimum of maximum of local Ishai criteria
a) $T=150\ N/m^2$, $C=450\ N/m^2$ and b) $T=450\ N/m^2$, $C=150\ N/m^2$.

8. CONCLUSIONS

Our work has extended the number of mechanical criteria, which can be considered in topology optimization design. For static analysis, we can consider compliance and deformation energy criteria, displacements constraints and stress constraints. Of course these constraints can be considered for one or several load cases. Because of their local character, the treatment of stress constraints in every finite element can be very cumbersome. So local stress constraints can be replaced by integrated (global) constraints with a certain success. Different stress criteria can also be taken into account. The classic von Mises criterion can be substituted by Raghava or Isaï criteria for unequal stress limits in tension and compression.

In addition to mechanical constraints, one can also introduce geometric constraints on the material distribution: area/volume and perimeter constraint. Perimeter constraints are very interesting because they offer an elegant way to control the complexity of the geometry that comes out from the optimization procedure. Several works were realized to extend the 2-D perimeter measure for plane structure to 3-D and axisymmetric problems.

As illustrated in the numerical application of this paper, the optimal structural morphology can be sensitive to the design criteria that are considered in the optimization. More generally the experience gained while solving optimization problems with the different design criteria presented herein leads to reconsider the general idea that topology optimization, as a preliminary design tool, can be based on a restricted number of design criteria, especially compliance. On the contrary we believe that a larger set of criteria like stress constraints have to be introduced in topology design in order to predict really optimal morphologies of structural components.

9. AFFILIATIONS

University of Liège, Mechanical Institute B52, B-4000, Liège, Belgium.

10. REFERENCES

Bendsøe M.P. & Kikuchi N. (1988). Generating optimal topologies in structural design using a homogenization method. Comp. Meth. in Appl. Mech. and Eng.,71, 197-224.

Bendsøe M.P. (1995). Optimization of structural topology, shape, and material. Berlin: Springer Verlag.

Bruyneel M. (1998). Le périmètre en optimisation topologique de structures tridimensionnelles. University of Liège, Aerospace Laboratory. Report OF50.

Cheng G.D. & Jiang Z. (1992). Difficulties in truss topology optimization with stress constraints. Eng. Optim., 20, 129-148.

Cheng G.D. & X. Guo. (1997). ε-relaxed approach in structural topology optimization. Struct. Opt., 13, 258-266.

Duysinx P. (1997). Layout optimization: a mathematical programming approach. Danish Center for Applied Mathematics and Mechanics. DCAMM Report No 540.

Duysinx P. & M.P. Bendsøe. (1998). Topology optimization of continuum structures with local stress constraints. Int. J. Num. Meth. Engng., 43, 1453-1478.

Haber R.B, Jog C.S. & M.P. Bendsøe. (1996). A new approach to variable-topology shape design using a constraint on perimeter. Struct. Opt., 11, 1-12.

Kirsch U. (1990). On singular topologies in optimum structural design. Struct. Opt., 2, 133-142.

Rozvany G.I.N,. Zhou M. & Birker T. (1992). Generalized shape optimization without homogenization. Struct. Opt., 4, 250-252.

Rozvany G.IN. & Birker T. (1994). On singular topologies in exact layout optimization. Struct. Opt., 8, 228-235.

Rozvany G.I.N. (1996). Some shortcomings in Michell's truss theory. Struct. Opt., 12, 244-250.

Rozvany G.I.N. (1998). Exact analytical solutions for some popular benchmark problems in topology optimization. Struct. Opt., 15, 42-48.

PAREDES M., SARTOR M., MASCLET C.

FINDING THE OPTIMAL STOCK SPRING FROM OPTIMAL SPRING DESIGN CHARACTERISTICS

Abstract. This paper presents two methods for selecting the best stock spring from within a database. A way of calculating the optimal custom spring design which takes into account the database properties is described and two methods that explore the neighbourhood of the optimal continuous solution are detailed. Two methods for exploring the neighbourhood of the optimal continuous solution are discussed. The first, called the "expanding" method explores the database in successive layers, and stops once a solution has been found which cannot be improved upon. The second method also uses the "expanding" technique but stops once a spring which matches the specifications has been found. The algorithm then performs a "sliding" operator, whereby the immediate neighbourhood of the existing solution is explored. When no better spring can be found, this process stops. Two examples are shown. They demonstrate the effectiveness for our approach in selecting a stock spring without exploring the whole database. The most time-consuming stage is the calculation of the optimum custom-made spring design. Both these methods are particularly useful when applied to large database.

1. INTRODUCTION

The creation of mechanical objects is often the end result of a long design process where standard component selection is perhaps the simplest, but nonetheless frequent class of design decision problems. As catalogues become increasingly common and voluminous, this process can be time-consuming. Text-only assistance is not an efficient means for designers to find a stock spring which respects not only certain geometrical properties stored in a database but also several operating characteristics. Thus, optimal operating points have to be calculated for each potential stock spring depending on the requirements.

Finding the best stock spring and calculating its associated operating parameters is a Mixed Discrete Optimization problem. The most common mathematical solution is first to approximate an optimum by treating all variables as continuous and then to use algorithms to find the best feasible discrete point in the region of the continuous variable optimum. Optimization procedures dealing with continuous variables are numerous and well known. Technical literature provides mathematical methods which calculate design parameters corresponding to an optimal custom spring design (Sandgren (1990), Kannan and Kramer (1994), Deb and Goyal (1998)). To help designers select stock springs, Yuyi et al (1995) and Motz and Haghighi (1990)] have implemented methods that propose some stock springs close to the optimal custom spring design. But, in every case, the designer has to calculate the operating parameters for each proposed spring by hand, in order to select the one that best fit his specifications. Moreover, as the best stock spring is not necessarily close to the custom-designed optimum, the designer is never sure he has selected the best spring.

P. Chedmail et al. (eds.), Integrated Design and Manufacturing in Mechanical Engineering, 465-472.
©2002 *Kluwer Academic Publishers.*

To find the discrete optimum, many algorithms have been developed such as the optimal discrete search by Pappas and Allentuch (1974), the sequential linearization approach by Han Tong and Papalambros (1991) or the Boolean logic method by Peng and Siddall (1993). These methods explore the discrete neighbourhood of the continuous optimum but are difficult to implement. When there is a high number of discrete variables, they can however help to find the discrete optimum without enumerating the total neighbourhood of the continuous point. Considering that spring catalogues give a maximum of four discrete variables in the optimization problem, our objective is to find methods that would extract the most suitable solution by just testing a few springs. Thus two methods have been developed. They use a particular optimal spring as a starting point to explore the database.

2. STARTING FROM A PARTICULAR OPTIMAL SPRING

Usually, optimal spring design is calculated by solving a conventional optimisation problem: Minimise or Maximise F($\boldsymbol{x}$) where $\boldsymbol{x}$ is a vector of continuous variables and F($\boldsymbol{x}$) is either the mass, or the fatigue life, or the operating load P2, or the operating length L2...

In addition to the objective function, a large set of constraints is considered, so as to express design specifications (operating length limits, operating load limits…), the standards (fatigue life, buckling length…) and the technical capability limits of the spring manufacturer (maximum outside diameter, minimum outside diameter, maximum wire diameter…).

But catalogues often provide a much smaller exploration domain than the hyper cube generally considered in the continuous optimisation process. The global optimum can therefore be a long way from the discrete approach. To match catalogue properties and decrease the gap between the two optima, constraints related to the database limits can be added to the initial optimisation problem. The augmented formulation will lead to a particular optimal spring which can be retained as an appropriate starting point for a catalogue search. The first task is thus to model the catalogue data in order to obtain the boundaries of the exploration domain.

2.1 Modelling the database

For this study, the catalogue of the «Ressort Vanel» company, comprising 5050 springs, has been used. For each spring, the characteristics detailed in the catalogue are stored in a table as shown in Figure 1. A spring reference can be for instance the index of the associated line in the table.

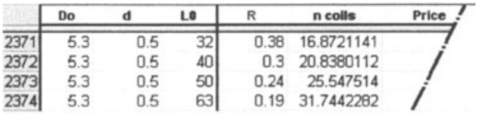

	Do	d	L0	R	n coils	Price
2371	5.3	0.5	32	0.38	16.8721141	
2372	5.3	0.5	40	0.3	20.8380112	
2373	5.3	0.5	50	0.24	25.547514	
2374	5.3	0.5	63	0.19	31.7442282	

Figure 1. Spring table

Table 1. Link between parameters

De	X	De	X	d	Y	d	Y	L0	Z
1,6	1	11	23	0,16	1	2	23	3,2	1
2	2	11,7	24	0,18	2	2,2	24	4	2
2,5	3	12,5	25	0,2	3	2,5	25	5	3
2,8	4	13,2	26	0,22	4	2,8	26	6,3	4
3,2	5	14	27	0,25	5	3,2	27	8	5
3,6	6	15	28	0,28	6	3,6	28	10	6
4	7	16	29	0,32	7	4	29	12,5	7
4,5	8	17	30	0,35	8	4,5	30	16	8
5	9	18	31	0,4	9	5	31	20	9
5,3	10	19	32	0,45	10	5,5	32	25	10
5,6	11	20	33	0,5	11	6	33	32	11
5,9	12	21	34	0,55	12			40	12
6,3	13	22	35	0,6	13			50	13
6,6	14	23,5	36	0,7	14			63	14
7	15	25	37	0,8	15			80	15
7,5	16	26,5	38	0,9	16			100	16
8	17	28	39	1	17			125	17
8,5	18	30	40	1,1	18			160	18
9	19	32	41	1,25	19			200	19
9,5	20	36	42	1,4	20				
10	21	40	43	1,6	21				
10,5	22	45	44	1,8	22				

Within this catalogue, springs are classified using three parameters : Do (outside diameter), d (wire diameter) and L0 (free length). Each spring can be represented by a point in the [Do, d, L0] space. Our suggestion is to add a matrix M[X, Y, Z] to this discrete space. The table 1 show the link between Do and X, d and Y, L0 and Z. Matrix dimensions are thus : M[44, 33, 19]. This matrix will contain only the spring references.

Note that M[] is not fulfilled by the database references. Some points of the discrete space have associated spring references, but not the others. For example M[10,11,11] = 2371 (see Fig 1) but M[1,33,19] = 0, as no spring exists with the dimensions Do = 1.6 mm, d = 6 mm, L0 = 200 mm.

2.2 Analysing the database limits

Figure 2 shows rectangles that surround the catalogue springs. The objective is to find the database limits in the three following planes : d/L0, Do/d and Do/L0. In each of these planes, a curve is sought that minimises the distance from the database (in number of cells within M[]) while staying outside the database limits.

Equations of the curves detailed in Figure 3 are:

$$dmax = 0.246\ Do^{0.9108},\ dmin = 0.07066\ Do^{0.9949}$$
$$L0max = 23.1\ Do^{0.6677},\ L0min = 1.4177\ Do^{0.8301}$$
$$L0max = 175.56\ d^{1.098},\ L0min = 0.07066\ d^{0.9049}$$

These equations are added to the initial optimisation problem in order to find an optimal custom spring design within the catalogue limits. In this study, x is defined with Do (outside diameter), d (wire diameter), L0 (free length), R (spring rate), L1 (maximum operating length), L2 (minimum operating length). From the result obtained, the values of Do, d, L0 are retained as starting point coordinates. Then, two exploration methods to select the most suitable spring from the database are presented.

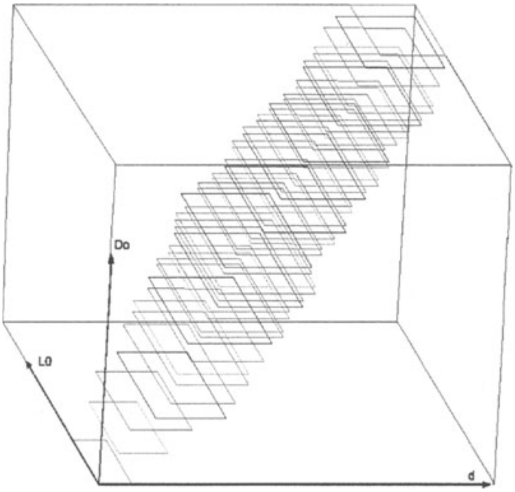

Figure 2. Do, d, L0 space

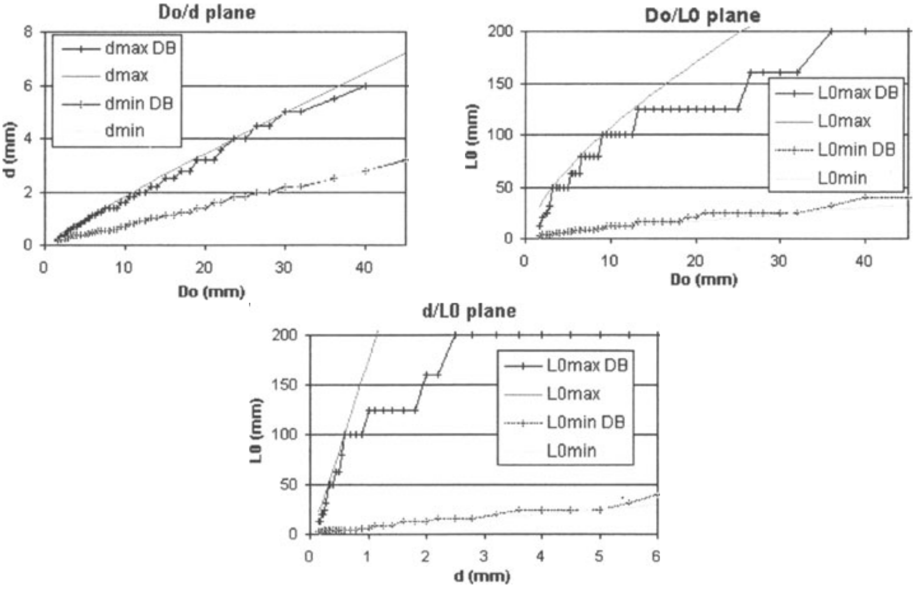

Figure 3. Limit curves

2. EXPLORATION METHODS

The optimal stock solution is not necessarily close to the custom-designed optimum. The following exploration methods test points on the matrix M[]. When a point is tested, the associated spring is evaluated in 5 steps (provided that the spring exists : $M[X,Y,Z]\neq 0$).

1 - Read the characteristics stored in the spring table
2 - Calculate the optimum operating points according to the specifications, the objective function and the standards (fatigue life, buckling length...) as described by Paredes (2000)
3 - Calculate the whole range of characteristics
4 - Calculate the objective function value
5 - Evaluate how the spring satisfies the requirements.

2.1 First exploration method : «Expanding»

The proposed method tests points that surround the starting point in successive layers, beginning with the points closest to the starting point (first layer), the others being gradually tested as described in Figure 4.

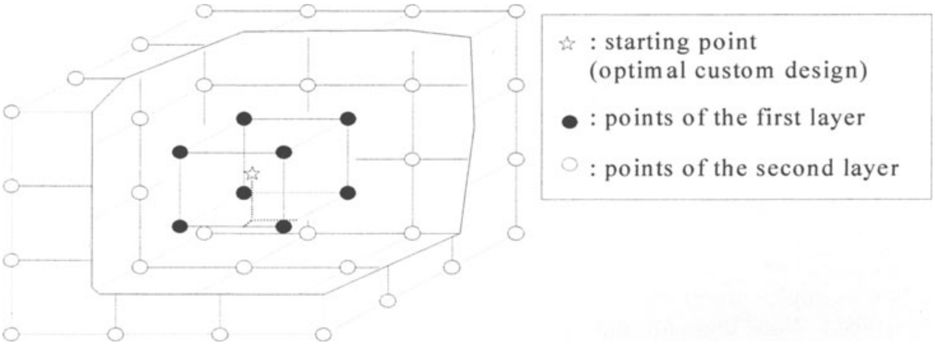
☆ : starting point (optimal custom design)
● : points of the first layer
○ : points of the second layer

Figure 4. Expanding

In a n dimension space, a continuous point is surrounded by 2^n discrete points. In our case n=3, the first layer contains 8 points. The Nth layer contains the points located on the faces of a cube with sides 2N long. Thus, it contains $[6\ (2N-2)^2 + 24N - 16]$ points.

The progression is stopped when the exploration of a layer does not improve the solution obtained on the preceding layer. The stop criterion selected is thus as follows : the algorithm stops when, at the end of the exploration of the Nth layer, the optimal stock spring still belongs to the (N-1)th layer.

2.2 Second exploration method : "Expanding, then sliding a window"

When the dimensions of the database spatial model are large ($n>2$), the exploration of numerous layers results in the testing of a large number of points. An alternative approach can then be used : "Expanding, then sliding a window". The exploration starts as defined previously but when at least one spring matching the specifications has been found on a layer, the expansion is stopped and the process continues by sliding a window.

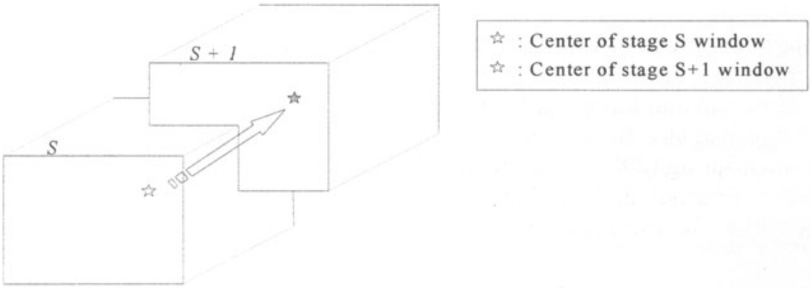

Figure 5. Sliding a window

At this stage, the algorithm only tests the points from within a window that surrounds the optimal point previously found as shown in Figure 5 (discrete neighbourhood). For an n dimension space and a R window radius, a discrete point is surrounded by $(1+2R)^n-1$ points. In our case, the unit-neighbourhood is tested inducing $n = 3$ and $R = 1$: 26 points are thus evaluated. If a better point is found, the window is slid onto that new point. The algorithm is stopped when the stage has not improved the preceding solution.

3. EXAMPLES

Two examples are given below to illustrate and compare the efficiency of the two methods. Note that, all the springs in the database have been simultaneously evaluated in order to control the results. Both these examples deal with, steel springs with closed and ground ends.

3.1 Minimum mass

In this example, the spring with the smallest mass value and a spring travel of 10 mm, a minimum inside diameter (Di) of 4 mm, F1 equal to 15 N and a maximum L1 of 35 mm is sought. The optimal custom spring design within the database limits induces Do = 6.42 mm, d = 0.75 mm, L0 = 39.69 mm. Thus, according to table 1, the first layer cube coordinates are [13, 14, 11], [14, 15, 12] (points of the diagonal). Results obtained with both methods are shown in Table 2.

Table 2. Minimum mass

Method	Expanding	Exp. then sliding
Nb of layers	5	2
Nb of windows	-	3
Nb of springs	656	**142**
Result coordinates	17, 15, 13	17, 15, 13

The algorithm proposes in every case [17, 15, 13] as a solution, i.e.
Do = 8.0 mm, d = 0.8 mm, L0 = 50 mm, R = 0.68 N/mm, working between L1 = 27.94 mm and L2 = 17.94 mm.
Checking procedure: the evaluation of the entire database (5050 springs) leads to the same stock spring (298 springs match the specifications). In this example, the best method is "Expanding, then sliding a window". In this case, the optimal stock spring can be found after evaluating only 142 springs.

3.2 Minimum operating length

Prototype design specifications are : Do ≤ 38mm, Di ≥ 27mm, L1 ≤ 50mm, spring travel equal to 11mm. 5N ≤ P1 ≤ 15N and 50N ≤ P2 ≤ 100N (spring loads). The spring with the smallest operating length is sought. Using the optimal design in continuous variables obtained without adding the database constraints induces first layer coordinates of : [40, 22, 10], [41, 23, 11]. When these constraints are added to the optimization problem, the first layer coordinates become [40, 23, 9], [41, 24, 10]. The results obtained are detailed in Table 3.

Table 3. Minimum operating length

Starting point	without adding constraints		when adding constraints	
Method	Expanding	Exp. Then sliding	Expanding	Exp. then sliding
Nb of layers	3	2	2	1
Nb of windows	-	1	-	1
Nb of springs	43	**20**	15	**10**
Result coordinates	41, 24, 10	41, 24, 10	41, 24, 10	41, 24, 10

In every case, [41, 24, 10] is proposed as a solution, i.e. Do = 32 mm, d = 2.2 mm, L0 = 25 mm, R = 5.78 N/mm, working between L1 = 22.4 mm and L2 = 11.4 mm.
Checking procedure : the evaluation of the entire database leads to the same stock spring from the 12 springs that match the specifications. Once again, it shows the efficiency of the "Expanding, then sliding a window" method. It also shows the importance of adding the database constraints to the initial optimization problem in order to reduce the number of springs evaluated.

4. CONCLUSION

This paper presents two methods for selecting stock springs from within a catalogue. These methods are less time consuming than that which tests all the springs, especially for large catalogues. The first method consists in testing the springs that surround the optimal custom spring design. The algorithm called "Expanding" tests springs by successive layers, moving away gradually until the exploration of a layer no longer improves the solution selected on the preceding layer. The second method starts with a similar expansion process and stops as soon as a spring that satisfies the specifications is found. Then the springs from within a window that surrounds that spring are tested. If a better spring is found, the window is slid onto this point and a new step is carried out until no better solution remains. The results obtained are satisfactory and have a high "result" VS "number of tested springs" ratio. This ratio can be increased by adding the database limit constraints to the initial optimization problem of finding the optimal custom spring design. As it reduces calculation time, this method is particularly useful for large data-bases. It can also help in selecting a temporary stock spring to replace a broken custom-made spring, as here the starting characteristics are already known. In addition, it is particularly important to reduce operating time in integrated design procedures.

5. AFFILIATION

PAREDES Manuel, SARTOR Marc, MASCLET Cédric
LGMT - INSA, 135 avenue de Rangueil 31077 Toulouse (France)
Tel : 33 5 61 55 97 18 Fax : 33 5 61 55 97 00
email: manuel.paredes@insa-tlse.fr
web: http://www.meca.insa-tlse.fr/lgmt

6. REFERENCES

Deb, K. & Goyal, M. (1998). A Flexible Optimisation Procedure for Mechanical Component Design Based on Genetic Adaptive Search. *Journal of Mechanical Design*, *120*, 162-164.

Han Tong, L. & Papalambros, P.Y. (1991). Computational Implementation and Test of a Sequential Linearization Algorithm for Mixed-discrete Nonlinear Design Optimization. *Journal of Mechanical Design*, *113*, 335-345.

Kannan, B. K. & Kramer, S. N. (1994). An Augmented Lagrange Multiplier Based Method for Mixed Integer Discrete Continuous Optimisation and its Applications to Mechanical Design. *Journal of Mechanical Design*, *116*, 405-411.

Motz, D. S. & Haghighi, K. (1990). An Integrated Approach to Knowledge-Aided Design and Optimisation of Mechanical Springs. *Transactions of the ASAE*, *33(5)*, 1729-1735.

Pappas, M. & Allentuch, A. (1974). Mathematical Programming Procedures for Mixed-Continuous Design Problems. *Journal of engineering for Industry*, 201-209.

Paredes, M., Sartor, M. & Fauroux J.C. (2000). Stock Spring Selection Tool. *SPRINGS*, *winter*, 53-67.

Peng, L. & Siddall, J.N.(1993). A Boolean Local Improvement Method for General Discrete Optimization Problems. *Journal of Mechanical Design*, *115*, 776-783.

Sandgren, E.(1990). Nonlinear Integer and Discrete Programming in Mechanical Design Optimisation. *Journal of Mechanical Design*, *112*, 223-229.

Yuyi, L., Kok-Keong, T. & Liangxi, W. (1995). Application of Expert System for Spring Design and Procurement. *SPRINGS*, *march*, 66-80.

C. KERZREHO & J.-Y. COGNARD

DESIGN PROCESS AND OPTIMISATION OF AN INTEGRATED ELECTROMECHANICAL BATTERY

Abstract : As part of an electromechanical battery design project using flywheels, we present here the results of a research on solutions with low cost price and high energy density. The energetic characteristics formalisation helps us to choose and design a suited structure integrating a motor-generator and magnetic bearings. The rotor design requires to take into account the mechanical and electromechanical coupling as a function of the assembly technology. The converter optimisation is based on geometric modification and optimised numerical models.

1. THE PROJECT

There is no need to prove how important the electrical energy storage stake is. Currently, the electrochemical batteries give the best performances in words of energy density and specific energy density. However, those storage mediums have two major drawbacks which are a life term bound to some thousand charge/discharge cycles and a maximum specific power value of around 150W/kg for the lithium based battery [1]. The electromechanical batteries store energy in a flywheel as kinetic energy. Therefore, they can push back those limits and offer other opportunities. For example, they are used in building high power uninterruptable power supply and regenerative breaking systems. As part of a multidisciplinary project gathering together mechanical and electromechanical specialists, we work to define a household electromechanical battery. The aims are, on the one hand, to secure and regulate the home current supplies and consumption by providing energy from this device during short current failure and high power request. On the other hand, it could be used in conjunction with alternative electric generators, as wind turbines and photovoltaic panels, to improve their availability and durability [2]. The accumulation capacity for the considered module is a couple of kilowatts-hours with a minimal time for the charge or the discharge of around one hour. To be profitable, the materials of the rotor constituents should be used at the maximum. Also, a specific structure has to be found, fitted and optimised for this specific application, integrating the different functions into a coherent system, particularly, the motor-generator and the bearings. The acceptable energy lost after a few days, coming from various drags, do not represent more than 20% of the whole capacity. It requires the use of some cheap magnetic bearings and a vacuum housing. In this article, we present the results ending in a prototype design defined to validate the concepts and the technological choices carried out. It will be fit into an experimental system including alternative power supplies and chemical batteries.

P. Chedmail et al. (eds.), Integrated Design and Manufacturing in Mechanical Engineering, 473-480.

©2002 *Kluwer Academic Publishers.*

2. GENERAL STRUCTURE DESIGN OF THE BATTERY

In order to choose the structure of the system, a study as been performed to define the potentialities of different configuration classes and materials in terms of energy specific density, energy density and manufacturing cost per stored energy unit. For our application, the charge or discharge time is quite a long one, more than several minutes. On the one hand, the stresses coming from the accelerations are small compared to the ones associated to the rotation. Thus, during the pre-design phase, the rotor is supposed to rotate at a stationary speed. On the other hand, as the accumulation function is dominating, the flywheel nearly defines the rotor shape and, at this stage, only its characteristics are taken into account for energetic evaluations. In the case of small displacement assumption, the stress and strain field distributions of two homothetic flywheels are the same if the running conditions are identical. This property allows us to define flywheel families which mechanical and energetic behaviour are characterised by shared values. In the case of linear elastic behaviour materials, the stress field, for a given family, can be depict by a unique non-dimensional stress field $\overline{\overline{C}}$ from (1), where V is the flywheel peripheral outer velocity and ρ the material density. The application of a design criterion, Von-Mises for the metals and Tsaï-Hill for the composite materials [3], leads us to define a stress coefficient k_σ, characterising the structure resistance. This coefficient governs the maximal flywheel outer peripheral speed with respect to the material equivalent yield stress R_p.

$$s(M) = \rho V^2 \,\overline{\overline{C}}(M) \quad ; \; k_\sigma = \underset{M \in \text{Flywheel}}{\text{Max}} \left\| \overline{\overline{C}}(M) \right\| \tag{1}$$

$$V_{\max} = \sqrt{\frac{1}{k_\sigma}\frac{R_p}{\rho}} \quad ; \; V^s_{\max} = \sqrt{\frac{s}{k_\sigma}\frac{R_p}{\rho}} \tag{2}$$

To fix the limits of the battery life in terms of charge-discharge cycle number, fatigue criterion must be used. For steels, one use a Dang-Van criterion to define a fatigue coefficient s ($s<1$) [4]. Among other things, it depends on the ratio r of the maximal outer speed to the minimal one (3) which is also used to define the battery energy recovery rate through (4). The fatigue coefficient sets another maximal outer speed associated with the cycling life limit.

The sensibility of those coefficients to shape details is particularly high and therefore dominates the design and optimisation processes. They are also used to define, through relations (4), the specific energy density, the energy density and the associated energetic shape coefficients K and K_{dim}. E_u is the useful energy with safety fatigue coefficient and E_e the effective maximal rotor kinetic energy. Their ratio defines the battery energy recovery rate. A r value of 3 sets it up to around 90%. The non-dimensional values i and m are defined by (4) from the mass M, the inertia I and the outer radius R of the rotating parts.

$$r = V_{\max} / V_{\min} = \omega_{\max} / \omega_{\min} \quad ; \quad \frac{E_e}{M} = K \frac{sR_p}{\rho} \quad ; \quad K = \frac{1}{2} \frac{i}{m} \frac{1}{k_\sigma} \tag{3}$$

$$E_u = \frac{r^2 - 1}{r^2} E_e \quad ; \quad \frac{E_u}{V_{dim}} = K_{dim} sR_p \quad ; \quad K_{dim} = \frac{1}{2\pi} \frac{i}{k_\sigma} i = \frac{I}{\rho R^5} \quad ; \quad m = \frac{M}{\rho R^4} \tag{4}$$

Table 1 : Basic structures with flywheel, electric machine and bearings

	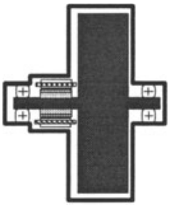	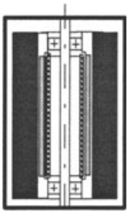	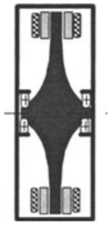
Shape	Solid cylinder	Hollow cylinder	Constant stress disk
Electric machine shape	Cylindrical	Cylindrical	Flat
Magnetic field	Radial	Radial	Axial

Table 2 : Studied material data

Material class	**Designation**	**Elastic modulus (Gpa)**	**Density**	**Yield strength (Mpa)**	**Equivalent energetic specific density (Wh/K)**	**Equivalent energetic density (Wh/litre)**	**Base material price (•/kg)**	**Manufactured cost estimation (•/kg)**
Steel	36NiCrMo16	210	7,8	880	31	244	3,50	4
	Maraging steel 300	210	7,8	1950	69	542	28,50	12
Titanium allow	TA6V	110	4,42	868	55	241	33,00	11
	IMI550	110	4,42	1025	64	285	47,00	15
	10-2-3	110	4,42	1228	77	341	58,00	18
Aluminium	2017	73	2,79	280	28	78	5,00	4
	2618	73	2,76	390	39	108	7,00	5
	7049	73	2,8	570	57	158	7,00	7
	AU5GT	73	2,8	395	39	110	7,00	5
Unidirectionnal composite (60% of fiber)	E Glass - epoxy	46	2,04	1400	191	389	8,50	22
	HM Graphite - epoxy	230	1,65	800	135	222	*83,00*	28
	HR Graphite - epoxy	159	1,55	1380	247	383	50,00	35
	Kevar - epoxy	84	1,37	1400	284	389	*50,00*	39

A battery price estimation has been performed for three basic configurations : solid cylinder, hollow cylinder and constant stress type disk [5] (table 1) for metal materials and composite ones with epoxy matrix (table 2). As a result, due to the relatively long discharge time and the very high rotational angular velocity, around 20000 rev/min, the costly components are the flywheel, the electronic power converter and the vacuum housing. Figure 1 illustrates the flywheel energetic capabilities and cost estimations for the materials listed table 2. For this component, various energy density to energy specific density ratio may be considered for nearly the same price. The raw material prices per kilogram have been defined with suppliers for one ton quantity. The specific price, the density and the tensile strength are used to estimate the manufacturing process cost. As the flywheel rotating stresses are nearly only of traction type, we have calculated that massive realisations in ceramic materials are inadequate for a reliable device in strength term. If the ceramic-ceramic composite materials have much better capabilities [6], their costs are unacceptable for this application. The fatigue coefficient is set to 0.5 and is compatible with a high number of cycles for the metal rotor. It has not been evaluated for the composite structures. Realisations with various materials do not really improve the energetic effectiveness and lead to higher cost. In particular, the difference between the stress coefficient values of the solid and hollow shapes is a limit. However, in [7,8], we find studies resulting in composite structures obtained by sticking with interference pipes of various materials. The energetic specific density is then increased as the energetic density is not too disrupted. But we believe the benefits are lost by the manufacturing and reliability problems.

The choice and design of the structure has been made as a compromise including the simultaneous studies on the electric machine and on the magnetic bearings. We have considered also the magnitude of the overall dimensions, the realisation cost, and the easiness of realisation. As a result, we defined an original architecture (figure 2) based on a solid cylindrical flywheel and an integrated electric machine, specifically designed for the application [9]. To simplify the manufacturing, the different parts are currently realised in magnetic steel. This is also a necessary property for the flywheel to integrate the electric machine and bearings.

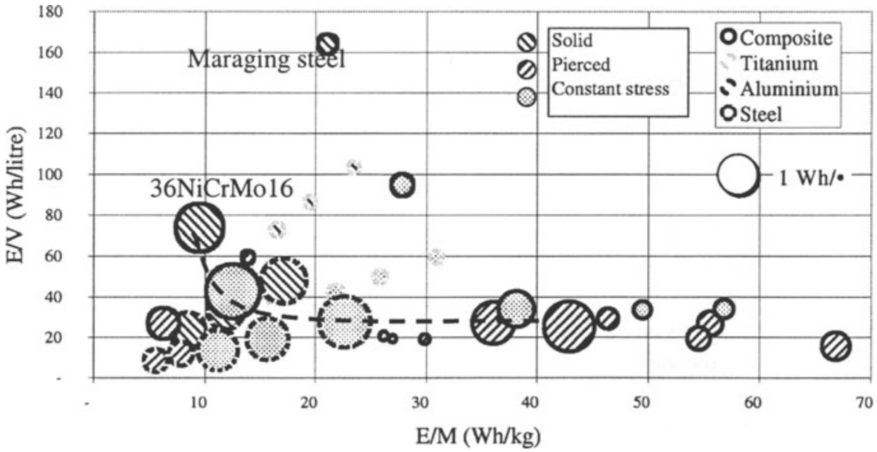

Figure 1 : Flywheel energetic characteristic estimations for basic shapes

3. THE COMPONENT DESIGN, CONSTRAINTS AND INTERACTIONS

The main components (the flywheel, the motor-generator and the bearings) are integrated into a single structure. Its design, in terms of stored energy, working power and stability is therefore a global process taking into account the interactions between the different components (specific design and technological constraints).

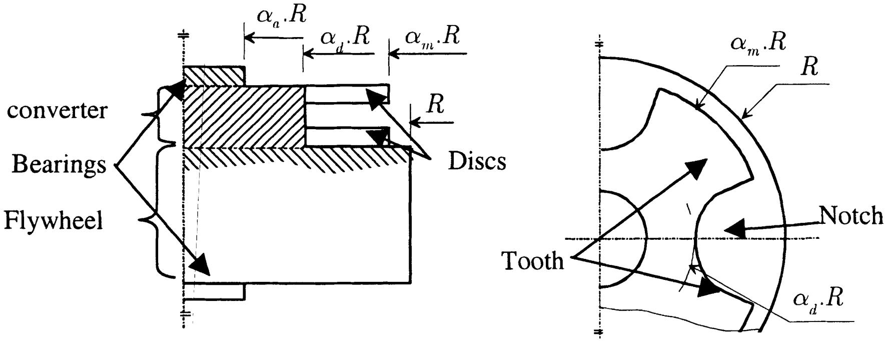

Figure 2 : Rotor configuration and converter's parameters

The electric machine, specifically designed for our application by the electrotechnical team (figure 2) has the general shape of a disk, around 5 centimetres high, connected to the flywheel [9]. The rotor consists of two disks modified by radial notch and manufactured in magnetic steel. The running characteristics (angular velocity range, efficiency, maximum power) and his shape characteristics (own inertia, outer radius, notch depth) are closely linked to the flywheel characteristics. In this way, the battery has to provide a constant maximum power over the whole velocity range. Due to this condition, a minimal velocity has to be defined in association with the maximal torque. This velocity is also defined through the battery energy recovery rate and the r ratio. It's therefore a data of the flywheel design. The r ratio is an important parameter of the electric machine too. The storage optimisation aspects lead to define the maximal rotating velocity through the material strength and outer radius. One more time, those points are closely linked with energetic accumulation and dynamic stability. Another point is that the notches decrease the converter mechanical strength. Therefore, to be able to support the maximal flywheel velocity, its external radius should not exceed a certain value. If one names α_m the ratio of the motor-generator rotor external radius to the flywheel one, its maximal value is defined by the strength coefficient of both components for a yield criterion and for a fatigue criterion by relations (5).

$$\alpha_m = \frac{\text{Converter radius}}{\text{Flywheel radius}} \leq \sqrt{\frac{k_{\sigma,\text{flywheel}}}{k_{\sigma,\text{converter}}}} \; ; \; \alpha_m \leq \sqrt{\frac{s_{\text{converter}} / k_{\sigma,\text{converter}}}{s_{\text{flywheel}} / k_{\sigma,\text{flywheel}}}} \qquad (5)$$

The flywheel's coefficients are assumed to be fixed for given geometry and materials values. The converter coefficients depend, in particular, of the tooth number and of the radius at the notch bottom. This last parameter, defined by the α_d coefficient, is also a crucial data for the electric machine design. More generally, the converter strength depends on the shape details of its constitutive parts and on the assemblage technology used. Between all the different solutions studied, the one retained consists of one disk directly machined on the flywheel. So, this main component is a part of the electric machine too. The other disk is brought back on a common axis, assembled with interference to cancel the gap induced by the rotation and the stiffness differences between the axis and the converter disk. This axis must resist to the efforts induced by the magnetic bearings and, above all, by the security bearings. It must insure the continuity of the magnetic field at high speed and its size (α_a) is another main parameter of the electric machine. Thus, the converter design depends, among other things, on the size and strength of the flywheel. The flywheel's design depends on the running characteristics of the motor-generator, and to a lesser extend, of its inertia. Therefore, the optimisation is an iterative process.

High tensile-steels lead to very high angular velocity, around 20000 rev/min. It requires, for our low self-discharge application, the use of vacuum housing and magnetic bearings. The propounded solution is based on the use of permanent magnets since they create levitation force without any power consumption [10]. As completely passive magnetic bearings lead to unstable systems, a second levitation force, created by an axial coil, is used to stabilise the whole system. It is controlled by a quick continuous control around the equilibrium axial position, which coincides with a zero consumption state. The radial centring is passive and is realised by reluctant bearings positioned on both side of the rotor. These bearings are well suited in terms of manufacture simplicity and cost. But they impose constraints on the inertial matrix of the rotor to assure a steady state over the whole speed range. During power transfer, the converter creates little non-controlled efforts. According to their numerical evaluations, they may be neglected. However, as we want the converter and the bearings to be independent, separation of their magnetic flows must be considered during design. Also, the solution should limit the magnetic leak due to the secure bearing presence, without altering the overall dimensions.

4. STRUCTURE OPTIMISATION

For a global optimisation of the propounded structure and taking into account all the component characteristics, we have worked to improve and characterise the converter's strength and the material used. The first one is needed because of the technological assemblage choice we have made. For one of the converter's disks, the notches and the axis hole reduce its strength significantly. As a result of the relations (5), α_m is small. It defines a converter with a little outer radius compared to the flywheel dimensions, resulting in poor energetic capacities. The necessary definition of the disk section shape is made by geometric optimisation using a finite element software, CASTEM 2000 [11], in conjunction with the MATLAB non-linear optimisation module. The optimisation target value is linked to the motor-generator performances, particularly the efficiency, and depends a lot on the stress coefficient k_σ. Constraints on the shape of the air gap surface, the disks interval and the non-magnetic saturation conditions are integrated into the optimisation process. Also, it takes into account the minimal assemblage interference value defined to avoid gap presence at full speed between the disk and the axis. A non-breaking criterion is used to check the values of the induced stresses at stationary state. If the disk radius is not the target value, as the converter performance is closely linked to it, the good solutions have a stress coefficient around the flywheel coefficient (5).

The converter electrotechnical optimisation has been done at the same time [9] and is linked to the previous point as it needs the maximum disk radius value for each given converter shape. This optimisation procedure allows us to find the optimal values of some geometrical parameters linked to the mechanical – electrotechnical coupling. Computations have been made around flywheels which have the same diameter and height, manufactured in 36NiCrMo16 and working with a 90% energy recovery rate. One have find that manufacturing a disk into the flywheel does not change its strength and does not reduce the maximal outer peripheral velocity linked to its fatigue strength.

As we previously saw, the other disk needs to be geometrically optimised to get the minimal strength compatible with the expected converter characteristics. As optimisation process is difficult to drive directly in 3D, we first simplify the experimental plane and keep only the main parameters α_d and α_a. The optimisation process at each point has been done in two stages [12,13]. The first stage starts with the previously defined optimised sections for all the studied area. The second stage uses those shapes as the starting points for 3D optimisations. This is done through the design software IDEAS using the stress coefficient k_σ as target value and a non magnetic saturation condition.

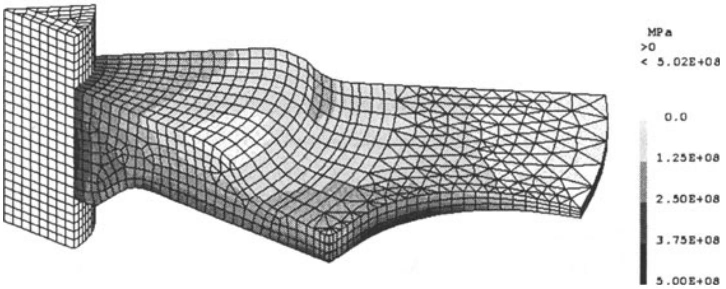

Figure 4 : Von-Mises stresses at full speed (1/8 of the optimised components)

Figure 3 presents the optimised disk and the Von-Mises equivalent stress distribution at full velocity V_{max}. The most stressed areas are the disk inner surface and the notch's bottoms. At this velocity, pressure between the axis and the disk vanishes. The fatigue coefficient is calculated afterwards. On the one hand, if the fatigue coefficient decreases as the stress coefficient is improved, the s/k_σ ratio still increases, reflecting a better fatigue strength for the component. On the other hand, the α_m coefficient is better when calculated with the fatigue criterion.

It is possible to optimise the battery energetic characteristics using adapted materials and shapes, another way is to maximise the material use by pre-stressing the flywheel. The adopted process has been presented in [14] and is close to the one used to improve the fatigue strength of pressurised vessels [15]. The idea is to rotate the rotor at a higher angular velocity that the one defined by the yield strength through (2). When one stop the disk, the plastic strains induce residual stresses which are opposite to those induced by the rotation. Therefore, the energetic capability is increased.

5. CONCLUSION

Having defined the study of electromechanical batteries, we have, for a maximal component integration, set up a specific system suited to our application. It's global study is based on numeric results and on model of both converter and magnetic bearings. A prototype using the different components is under development. It will allow us to detail the characterisation of the elements and to study the interactions, and dynamic behaviour of the system.

6. REFERENCES

[1] Multon B, Peter JM. Stockage d'énergie électrique, Revue de l'Electricité et de l'Electronique. 1996.
[2] Wind-diesel fares well, Modern Power Systems. 1988.
[3] Berthelot JM. Matériaux composites: comportement mécanique et analyse des structures. Masson, 1992.
[4] Lemaitre J, Chaboche JL. Mécanique des matériaux solides. Dunod, 1996.
[5] Berger M, Porat I. Optimal Design of a Rotating Disk for Kinetic Energy Storage. ASME J. Applied Mech., 1988; Vol. 55, N° 1: 164-170.
[6] Hild F. Ultimate strenght of structures made of Fiber - reinforced ceramic - matrix - composites , University of California, Santa Barbara, 1993.
[7] Ha SK,Tsai SW. Structural Analysis of a Composite Multi-Ring Flywheel for Energy Storage System. Composite Science and Technology / ICCST 1, S. Adali et V.E. Verijenko, Durban, South Africa ; 1996: 179-187.
[8] Flanagan RC. Design, Manufacture and Test Results for four High Energy Density Fibre Composite Rotors. IECEC'86, 1986: 901-907.
[9] Bernard N, Multon B, Ben Ahmed H. Open Loop Position with Current Control of a Synchronous Motor / Generator for Flywheel Accumulator. European Power Electronic, Lausanne, 1999.
[10] Delamare, J, Faure F. Les paliers magnétiques. Revue 3EI, 1998: 2-9
[11] Verpeaux P, Charras T, Millard A. CASTEM 2000, une approche moderne du calcul des strutures. Pluralis, Calcul des structures et intelligence artificielle, 1988:261-271.
[12] Clamagirand S, Pariset B, Kerzreho C. Etudes sur un prototype de batterie électromécanique. research project, INSA de Rouen, France, 1999.
[13] Kerzreho C, Cognard JY, Dumont G. Définition et optimisation de la structure d'une batterie électromécanique intégrée. 14ème Congrès Français de Mécanique, AUM-AFM, N° 695, 1999.
[14] Timoshenko S. Résistance des Matériaux. Dunod, Vol. 2, 1968.
[15] Mughrabi H, Donth B, Vetter G. Low-Temperature Autofrettage: an Improved Technique to Enhance the Fatigue Resistance of Thick-Walled Tubes against Pulsating Internal Pressure. Fatigue fract. eng. mater. struct., 1997; Vol. 20, N°4: 595-604.

7. AFFILATIONS

INSA de Rouen, Avenue de l'Université, 76800 St Etienne de Rouvray
E.N.S. de Cachan - Antenne de Bretagne, campus de Ker Lann, 35170 Bruz

VADEAN A., LERAY D., LAKISS H., GUILLOT J.

A HYBRID CALCULATION MODEL FOR BOLTED ASSEMBLIES USED FOR SLEWING BEARINGS

Abstract: slewing bearings are bearings of very large diameter used for cranes, radar dishes, tunnel boring machines, etc. The two bearing rings are clamped to the structure by preloaded high-strength screws or bolts. The connection is like a thick and narrow cylindrical flange, which includes a large number of fasteners. It is subjected to extreme loading, which is variable in time. Given the low fatigue resistance of threaded elements, they must be sized with a great accuracy. This article presents a simple and efficient numerical model specially developed for the sizing of these connections. The originality of the modelling process lies in the use of a hybrid finite element. This element has the general behaviour of a ring (cylindrical shell element), except for the axial direction where its stiffness is the local stiffness that governs the behaviour of the bolted assembly. By discretising the ring in several elements, this formulation can take into account non-linear stiffness distribution in the assembly and in particular the effect of the load application height. This model was then validated via several 3D finite elements simulations and gives excellent results.

1. INTRODUCTION

This article deals with the development of a simplified finite elements model allowing fast and precise calculation of the fastening bolts for very large diameter bearings (400 mm to 14m). These bearings are mainly slewing bearings used for shipyard and tower cranes, tunnel boring machines, radars, offshore equipment, etc. They transmit combined loads and one or both rings are provided with gear teeth to enable the swing drive to operate. The rings are attached to other structural elements by means of screws or bolts. The three types of bearings studied are presented in Figure 1: ball bearings, crossed roller bearings and three row roller bearings.

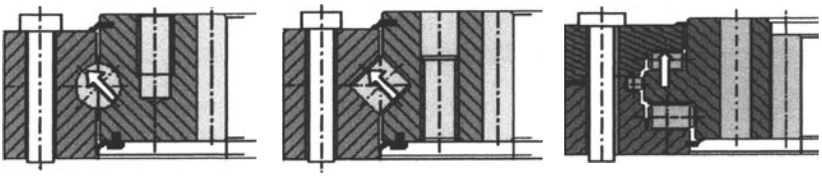

Figure 1. The study domain.

Note that each ring is higher than its thickness and is subjected to complex loading having axial and radial components of same importance. The traditional models, VDI 2230 [7] or the non-linear model of GUILLOT [1] are not appropriate. We proposed another model [6] using special plate elements, which takes into account the rigidity loss due to the hole clearance. The results obtained were

P. Chedmail et al. (eds.), Integrated Design and Manufacturing in Mechanical Engineering, 481-488.
©2002 *Kluwer Academic Publishers.*

satisfactory, but the model required a different setting for each bearing geometry. In order to improve on this, a new model has been developed that takes into account simultaneous the bending stiffness in the axial direction with plate elements and in radial direction with tube elements. The tube elements were modified to consider the characteristics related to the behaviour of preloaded bolted assemblies.

2. PRESENTATION OF THE NEW MODELLING

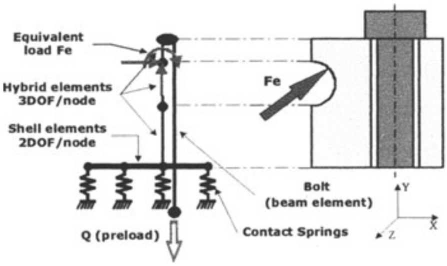

Figure 2. The modelling principle.

As Figure 2 shows, the bearing ring model consists of three types of elements:

– the plate elements that keep the same expression as for the circular-plate model [6]. Their role is to characterize displacements (and boundary separation) of the ring from its elastic foundation, as well as the bending according to axial direction OY.

– the so-called hybrid elements which make it possible to take into account part compression stiffness during prestressing, as well as the specific bending of a tube along radial direction OX. The 3DOFs per node enable the structure to be loaded with a torque equivalent to the outer load Fe.

– the springs that model the contact with the mounting and characterize the elastic behaviour of the interface and the unilateral contact. Springs stiffness will be a parameter affecting the setting of the model.

The bolt has the same formulation as an equivalent beam, used in the former models. The modelling of the bolted assembly was reduced to a sector of bearing associated with the most loaded bolt. The loading, as well as the formulation of the hybrid elements, are axisymmetric and represent a simplifying assumption for the model.

3. HYBRID ELEMENTS

The number of hybrid elements is directly related to bearing geometry. One element for the structure between the load application point and the highest surface of the ring is thus assigned; a second element for the reduced section determined by the bearing runway and a third for the lower part between the runway and the mounting.

4. DETERMINING THE AXIAL STIFFNESS OF THE BEARING SECTOR

In order to calculate the axial stiffness of the bearing sector we have used the improvement made by MASSOL [2] to the formulation of RASMUSSEN [4] for a cylindrical elementary assembly.

5. HYBRID ELEMENT STIFFNESS MATRIX

Due to the relatively low radial width compared to the outer diameter and the height, the behaviour of the outer ring is similar to an interior loaded tube. It is important to take into account the specific bending of a cylindrical shell [5], as well as the radial displacements, produced by a radial force (or radial component). The stiffness matrix of the hybrid element is based on the formulation of cylindrical shell element. In order to take into account accurately the axial stiffness as well as the prestressing strains, in the matrix of the tube element, the lines and the columns corresponding to the tensile terms (degrees of freedom v_i) have been replaced by the corresponding terms from a beam formulation of equivalent stiffness.

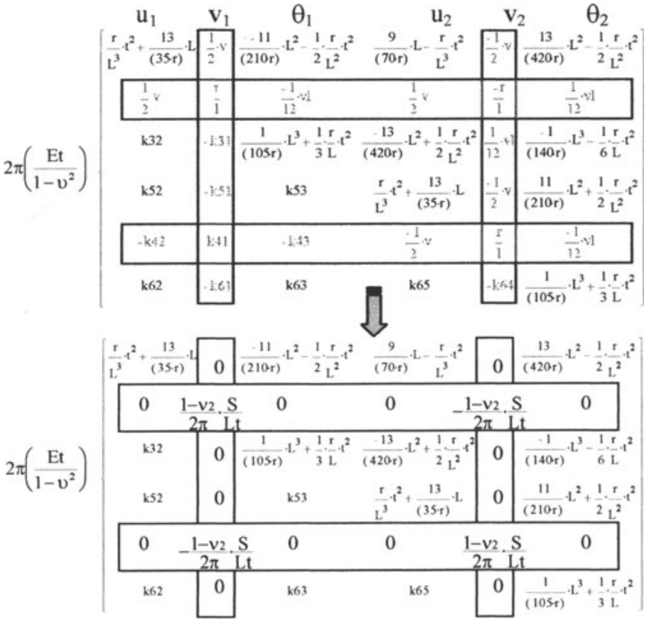

Figure 3. Transformation of the tube element matrix into the hybrid element matrix.

The S section present in the new terms is the equivalent cross-section obtained from the improved Rasmussen's formulation, presented above. Furthermore, in order to consider the height of the load application, the total flexibility must be distributed among elements in the real non-uniform pattern.

6. CONSIDERING THE APPLICATION POINT OF THE EXTERNAL LOAD

The height application of the external load, as shown in [1], has a major influence on the bolted assembly behaviour and on the resulting values of the supplements of tensile force and bending moment in the threaded element. For an axial load, a bolted assembly can be represented schematically according to Figure 4.

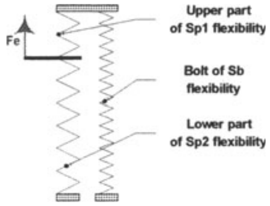

Figure 4. Schematic diagram of a bolted assembly.

What complicates the computation is that the part flexibility is not uniformly distributed across the thickness. In fact, the image of the compressed zone under the head of bolt, up to the mating plane, appears as a volume approaching the shape of a truncated cone (Figure 5).

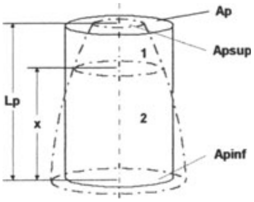

Figure 5. The real zone of compression.

To approximate the real situation, an appropriate algorithm is used to calculate the flexibility of a compressed part, shared in two or multiple segments. This calculation uses the Rasmussen's formulation of the equivalent section as described in [7].

The lower part can be discretized into as many segments as necessary, without repeating this computation algorithm, since it is sufficient to preserve the sum of the elements flexibilities (Sp_2) constant, as these act in the same way during loading. So, our bearing ring modelling is made up of three segments corresponding to the hybrid elements:

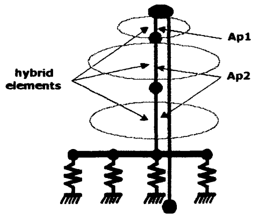

Figure 6. Cross-section of hybrid elements.

The length L_1 of the first segment is directly related to the height of the application of the external force, defined by the bearing geometry. In order to refine the distribution flexibility, a correction factor "γ" has been introduced. It will be a multiplier of the calculated cross-section Ap_1, to obtain the corrected equivalent cross-section: $Ap_{1c} = \gamma . Ap_1$

Obviously, the introduction of this factor will also affect the value of the second equivalent section Ap_2, since the sum of the Sp flexibilities has to remain constant.

The force application height factor γ will be the first setting factor of our model.

7. CONTACT STIFFNESS AND THE DISTRIBUTION OF THE AXIAL STIFFNESS

Axial stiffness brings simultaneously into play the hybrid elements and the contact springs. However, the total axial flexibility will be equal to the sum of the springs' flexibility *Srt* and that of the part (the three hybrid elements Sp_i). The hybrid elements have flexibility:

$$Sph = Sp_1 + Sp_2 + Sp_3;$$

and the contact springs have total stiffness:

$Krt = \sum Kri$; (springs in series) giving flexibility: $Srt = \frac{1}{Krt}$

Total part flexibility, obtained by using the improved Rasmussen's formulation (contact springs included) will be consequently:

$$Sp = Sph + Srt = cte;$$

By affecting a factor of distribution, "*rep*" to the part flexibility Sp, the following are recalculated:

- springs flexibility: $Srt = rep * Sp$;
- hybrid elements flexibility: $Sph = (1-rep) * Sp$.

The stiffness distribution factor ***rep*** *will be the second and the last setting factor of the model.*

8. MODELLING THE FASTENING BOLT

The modelling of the threaded element is that of an equivalent beam. The *Seq* section and the *Ibeq* quadratic moment of this beam are equivalent quantities with the same axial and bending stiffness as a real bolt (or screw) [1].

9. THE LOADING

The inclined external loading can be replaced in our modelling by an equivalent torque (Figure 1), composed of an axial load and a bending moment for the axial component, and a radial force for the radial component of the load.

10. THE TOTAL STIFFNESS MATRIX AND THE SYSTEM RESOLUTION

The assembly of the stiffness matrix is carried out in respect of the finite elements method. However, in order to reduce the size of this matrix the unused DOFs have been eliminated. The calculation is carried out in two steps:

1. The first consists in calculating the necessary displacement $\mathbf{y}_q$ of the bolt end that induces the preload force.
2. In the second step, by imposing the displacement y_q and applying the external load *Fe*, the tensile force supplement and the bending moment supplement can be calculated. Thus, the system resolution was carried out using a method of penalization, as described in [3].

11. COMPARISON BETWEEN THE RESULTS OF THE HYBRID MODEL AND THOSE OF THREE-DIMENSIONAL FINITE ELEMENTS SIMULATIONS

The direction of the equivalent external force associated to a bolt sector is inclined in respect of the axial direction for the first two bearings, and axial for the three rows roller bearings. To validate our modelling, a search has been carried out for values for the setting factors valid for each loading component, axial or radial. Numerous finite elements simulations have enabled us to classify the bearings studied into two categories, according to their behaviour and their geometry characteristics and loading. The first category is composed of the ball bearings and the crossed roller bearings – inclined loading, similar relationship between dimensions – and the second category by the three row roller bearings – significant ring height, axial loading, two parts outer ring, etc. The comparison of the two models, the hybrid model versus the three-dimensional finite elements simulations, has been carried out by considering the characteristic curves of tensile effort and bending moment supplements due to the external force.

For the first category of bearings, the values of the two setting factors are: the application force height factor $\gamma = 1$ and the stiffness distribution factor **rep** = 0.06.

The value of γ illustrates the high degree of accuracy of our model. Although for the first category the γ factor can be suppressed, it will be necessary for the second category of bearings.

The model performs very well in different loading conditions. When the bearing is subjected to the total inclined load and using the same values of the setting factors, the following curves are obtained:

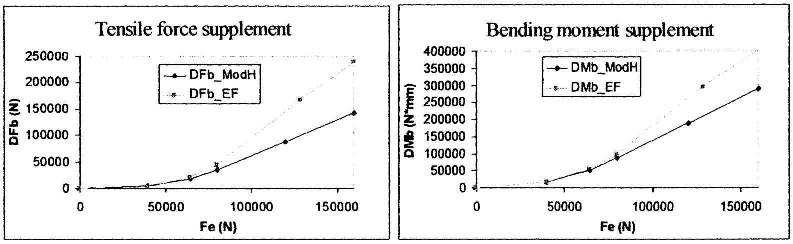

Figure 7. Crossed rollers bearing. Total inclined force supplements.

The gap between the curves of the two models remains within an acceptable margin of error of 20% for the load interval defined by the manufacturer (the upper limit of the external force on bolt sector is Femax = 32 kN).

For the second category of bearings, the three rows roller bearing, the comparison is presented in Figure 8.

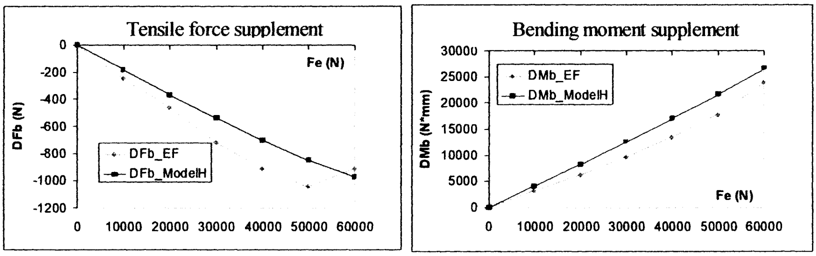

Figure 8. Three row roller bearing. Total force supplements.

The values of the two setting factors for the three rows roller bearing are: γ = 0.38 for the application force height factor, and ***rep*** = 0.32 for the stiffness distribution factor.

While for the first category of bearings, the setting was made directly on the values of supplements, for the three row roller bearing the method was different due to the particular behaviour of the bearing. Thus, finite elements analysis highlighted a significant bending moment when the bolt was preloaded and that phenomenon was accentuated by the application of the external force. This is explained by the position of the bolt near the outer diameter resulting in a weaker support surface on the mounting. Consequently, the setting has to be carried out on the value of the initial bending moment generated by the preloading. The curves show the model's ability to illustrate accurately the particular aspect of the decreasing tensile force in the bolt, giving negative values for the force supplement. The dominating phenomenon for this second category of bearing is the ring bending, which develops as early as the preloading. The values of the bending moment variation are calculated by the hybrid model with high level of accuracy.

12. CONCLUSION

Using the potential of hybrid modelling, the following advantages have been obtained:

↳ the model can be easily adjusted using only two setting factors;

↳ these factors can have the same values for all bearings of the same category, which makes the model suitable for a wide range of bearing dimensions;

↳ the particular phenomenon of average tensile stress decrease in the case of the three row roller bearing was taken into account.

In conclusion, we can affirm that the numerical model with hybrid elements is satisfactory for the modelling of bolted assembly of the slewing bearings. Static dimensioning can be very accurate and a suitable fatigue check can be implemented in very short time and for low costs.

13. AFFILIATION

VADEAN Aurelian, LERAY Dimitri, LAKISS Hassan, GUILLOT Jean
Laboratoire de Génie Mécanique de Toulouse – INSA
135 avenue de Rangueil 31077 Toulouse (France)
e-mail: aurelian.vadean@insa-tlse.fr

14. REFERENCES

1. Guillot J. Assemblages par éléments filetés: calculs. Article B5-560. Techniques de l'ingénieur; Paris, 1987, 21 rue Cassette
2. Marty D. Etudes des brides boulonnées précontraintes soumises à des chargements de fatigue. Mémoire de DEA, INSA Toulouse, 1994.
3. Massol J. Etudes des brides boulonnées précontraintes soumises à des chargements de fatigue. Thèse de doctorat, INSA Toulouse, 1994.
4. Rasmussen J. A two body contact problem with friction. Euromech Colloquium NR 110. Rimforsa . 27-29 September, 1978: 115-120
5. Rockey L. et al. Introduction à la méthode des éléments finis. Paris: Editions Eyrolles, 61, Bd. Saint-Germain, 75005, 1979.
6. Vadean A, Guillot J. Modèle plaque axisymétrique pour les fixations des roulements. 4ème Congrés de Mécanique, Mohammadia, Maroc. Avril 1999.
7. Vadean, A. Modélisation et simulation du comportement des liaisons par éléments filetés de roulements de très grand diamètre. Thèse de doctorat, INSA Toulouse, 2000.
8. VDI Richtlinien, VDI 2230, Blatt 1. Systematische Berechnung hochbeanspruchter Schraubenverbindungen. Avril, 1983